

MOLECULAR, CELLULAR AND MODEL ORGANISM APPROACHES FOR UNDERSTANDING THE BASIS OF NEUROLOGICAL DISEASE

EDITED BY: Robert J. Harvey and Kirsten Harvey
PUBLISHED IN: Frontiers in Molecular Neuroscience





frontiers

Frontiers Copyright Statement

© Copyright 2007-2017 Frontiers Media SA. All rights reserved.

All content included on this site, such as text, graphics, logos, button icons, images, video/audio clips, downloads, data compilations and software, is the property of or is licensed to Frontiers Media SA ("Frontiers") or its licensees and/or subcontractors. The copyright in the text of individual articles is the property of their respective authors, subject to a license granted to Frontiers.

The compilation of articles constituting this e-book, wherever published, as well as the compilation of all other content on this site, is the exclusive property of Frontiers. For the conditions for downloading and copying of e-books from Frontiers' website, please see the Terms for Website Use. If purchasing Frontiers e-books from other websites or sources, the conditions of the website concerned apply.

Images and graphics not forming part of user-contributed materials may not be downloaded or copied without permission.

Individual articles may be downloaded and reproduced in accordance with the principles of the CC-BY licence subject to any copyright or other notices. They may not be re-sold as an e-book.

As author or other contributor you grant a CC-BY licence to others to reproduce your articles, including any graphics and third-party materials supplied by you, in accordance with the Conditions for Website Use and subject to any copyright notices which you include in connection with your articles and materials.

All copyright, and all rights therein, are protected by national and international copyright laws.

The above represents a summary only. For the full conditions see the Conditions for Authors and the Conditions for Website Use.

ISSN 1664-8714

ISBN 978-2-88945-173-9

DOI 10.3389/978-2-88945-173-9

About Frontiers

Frontiers is more than just an open-access publisher of scholarly articles: it is a pioneering approach to the world of academia, radically improving the way scholarly research is managed. The grand vision of Frontiers is a world where all people have an equal opportunity to seek, share and generate knowledge. Frontiers provides immediate and permanent online open access to all its publications, but this alone is not enough to realize our grand goals.

Frontiers Journal Series

The Frontiers Journal Series is a multi-tier and interdisciplinary set of open-access, online journals, promising a paradigm shift from the current review, selection and dissemination processes in academic publishing. All Frontiers journals are driven by researchers for researchers; therefore, they constitute a service to the scholarly community. At the same time, the Frontiers Journal Series operates on a revolutionary invention, the tiered publishing system, initially addressing specific communities of scholars, and gradually climbing up to broader public understanding, thus serving the interests of the lay society, too.

Dedication to Quality

Each Frontiers article is a landmark of the highest quality, thanks to genuinely collaborative interactions between authors and review editors, who include some of the world's best academicians. Research must be certified by peers before entering a stream of knowledge that may eventually reach the public - and shape society; therefore, Frontiers only applies the most rigorous and unbiased reviews.

Frontiers revolutionizes research publishing by freely delivering the most outstanding research, evaluated with no bias from both the academic and social point of view.

By applying the most advanced information technologies, Frontiers is catapulting scholarly publishing into a new generation.

What are Frontiers Research Topics?

Frontiers Research Topics are very popular trademarks of the Frontiers Journals Series: they are collections of at least ten articles, all centered on a particular subject. With their unique mix of varied contributions from Original Research to Review Articles, Frontiers Research Topics unify the most influential researchers, the latest key findings and historical advances in a hot research area! Find out more on how to host your own Frontiers Research Topic or contribute to one as an author by contacting the Frontiers Editorial Office: researchtopics@frontiersin.org

MOLECULAR, CELLULAR AND MODEL ORGANISM APPROACHES FOR UNDERSTANDING THE BASIS OF NEUROLOGICAL DISEASE

Topic Editors:

Robert J. Harvey, UCL School of Pharmacy, London, UK

Kirsten Harvey, UCL School of Pharmacy, London, UK

The advent of next-generation sequencing technologies has resulted in a remarkable increase our understanding of human and animal neurological disorders through the identification of disease causing or protective sequence variants. However, in many cases, robust disease models are required to understand how changes at the DNA, RNA or protein level affect neuronal and synaptic function, or key signalling pathways. In turn, these models may enable understanding of key disease processes and the identification of new targets for the medicines of the future. This e-book contains original research papers and reviews that highlight either the impact of next-generation sequencing in the understanding of neurological disorders, or utilise molecular, cellular, and whole-organism models to validate disease-causing or protective sequence variants.

Citation: Harvey, R. J., Harvey, K., eds. (2017). Molecular, Cellular and Model Organism Approaches for Understanding the Basis of Neurological Disease. Lausanne: Frontiers Media. doi: 10.3389/978-2-88945-173-9

Table of Contents

- 05 Editorial: Molecular, Cellular and Model Organism Approaches for Understanding the Basis of Neurological Disease**
Robert J. Harvey and Kirsten Harvey
- 07 Missense Mutation R338W in ARHGEF9 in a Family with X-linked Intellectual Disability with Variable Macrocephaly and Macro-Orchidism**
Philip Long, Melanie M. May, Victoria M. James, Simone Grannò, John P. Johnson, Patrick Tarpey, Roger E. Stevenson, Kirsten Harvey, Charles E. Schwartz and Robert J. Harvey
- 15 Novel Missense Mutation A789V in IQSEC2 Underlies X-Linked Intellectual Disability in the MRX78 Family**
Vera M. Kalscheuer, Victoria M. James, Miranda L. Himelright, Philip Long, Renske Oegema, Corinna Jensen, Melanie Bienek, Hao Hu, Stefan A. Haas, Maya Topf, A. Jeannette M. Hoozeboom, Kirsten Harvey, Randall Walikonis and Robert J. Harvey
- 25 Rare Variants in Neurodegeneration Associated Genes Revealed by Targeted Panel Sequencing in a German ALS Cohort**
Stefanie Krüger, Florian Battke, Andrea Sprecher, Marita Munz, Matthis Synofzik, Ludger Schöls, Thomas Gasser, Torsten Grehl, Johannes Prudlo and Saskia Biskup
- 43 Protective LRRK2 R1398H Variant Enhances GTPase and Wnt Signaling Activity**
Jonathon Nixon-Abell, Daniel C. Berwick, Simone Grannó, Victoria A. Spain, Craig Blackstone and Kirsten Harvey
- 56 A Recombinant Human Pluripotent Stem Cell Line Stably Expressing Halide-Sensitive YFP-I152L for GABA_AR and GlyR-Targeted High-Throughput Drug Screening and Toxicity Testing**
Katharina Kuenzel, Oliver Friedrich and Daniel F. Gilbert
- 70 Generation of Functional Inhibitory Synapses Incorporating Defined Combinations of GABA_(A) or Glycine Receptor Subunits**
Christine L. Dixon, Yan Zhang and Joseph W. Lynch
- 80 The Intracellular Loop of the Glycine Receptor: It's not all about the Size**
Georg Langlhofer and Carmen Villmann
- 94 Utility of Induced Pluripotent Stem Cells for the Study and Treatment of Genetic Diseases: Focus on Childhood Neurological Disorders**
Serena Barral and Manju A. Kurian
- 105 Precision Medicine in Multiple Sclerosis: Future of PET Imaging of Inflammation and Reactive Astrocytes**
Pekka Poutiainen, Merja Jaronen, Francisco J. Quintana and Anna-Liisa Brownell

- 128** *Function Over Form: Modeling Groups of Inherited Neurological Conditions in Zebrafish*
Robert A. Kozol, Alexander J. Abrams, David M. James, Elena Buglo, Qing Yan and Julia E. Dallman
- 143** *Defects of the Glycinergic Synapse in Zebrafish*
Kazutoyo Ogino and Hiromi Hirata
- 161** *Age-Dependent Degeneration of Mature Dentate Gyrus Granule Cells Following NMDA Receptor Ablation*
Yasuhito Watanabe, Michaela K. Müller, Jakob von Engelhardt, Rolf Sprengel, Peter H. Seeburg and Hannah Monyer
- 171** *Molecular Mechanisms Regulating LPS-Induced Inflammation in the Brain*
Olena Lykhmus, Nibha Mishra, Lyudmyla Koval, Olena Kalashnyk, Galyna Gergalova, Kateryna Uspenska, Serghiy Komisarenko, Hermona Soreq and Maryna Skok



Editorial: Molecular, Cellular and Model Organism Approaches for Understanding the Basis of Neurological Disease

Robert J. Harvey* and Kirsten Harvey

Department of Pharmacology, UCL School of Pharmacy, London, UK

Keywords: next-gen sequencing, genetics, cell line, zebrafish, mouse

Editorial on the Research Topic

Molecular, Cellular and Model Organism Approaches for Understanding the Basis of Neurological Disease

Next-generation sequencing technologies have resulted in remarkable increases in our understanding of human neurological disorders through the identification of disease-causing or protective sequence variants. However, in many cases, new molecular, cellular, and whole-organism models are required to understand how changes at the DNA, RNA, or protein level affect neuronal and synaptic function. In turn, these models may enable understanding of key disease processes and the identification of new targets for the medicines of the future. What is also evident is the high quality and impact of the research conducted in this field. This is reflected in the reviews and research articles in this Special Issue entitled “*Molecular, cellular and model organism approaches for understanding the basis of neurological disease.*”

Mutation and gene discovery in neurological diseases has recently been transformed by large-scale DNA sequencing approaches coupled with stringent variant filtering. This is particularly true of intellectual disability, characterized by significantly impaired intellectual and adaptive function. Long et al. and Kalscheuer et al. highlight the utility of this methodology by resolving two families with X-linked intellectual disability caused by mutations in *ARHGEF9* and *IQSEC2*, which both encode neuronal GDP–GTP exchange factors. One important aspect of these studies was functional validation of the pathogenic variants using molecular modeling, phosphoinositide binding, gephyrin clustering, or GDP–GTP exchange activity. By contrast, Krüger et al. reported on the use of panel sequencing to study a cohort of 80 German patients with Amyotrophic lateral sclerosis (ALS), a rapidly progressive, fatal neurological disease that causes degeneration of motor neurones. This approach allowed deep sequencing of 39 confirmed ALS genes and candidate genes, as well as 238 genes associated with other neurodegenerative diseases. They identified 79 rare potentially pathogenic variants in 27 ALS-associated genes, as well as pathogenic hexanucleotide repeats in *C9orf72*. Based on this study, the authors recommend two-staged genetic testing for ALS in patients with familial and sporadic ALS, comprising *C9orf72* repeat analysis followed by comprehensive panel sequencing.

It is also important to remember that not all rare genetic variants are disease causing. Nixon-Abell et al. reported the detailed molecular and cellular characterization of a protective variant in *LRRK2*, encoding leucine-rich repeat kinase 2 (*LRRK2*) which is intimately associated with the pathogenesis of Parkinson’s disease. Importantly, the p.R1398H variant affects GTPase function, axon outgrowth, and Wnt signaling in a manner opposite to pathogenic *LRRK2*

OPEN ACCESS

Edited and reviewed by:

Nicola Maggio,
The Chaim Sheba Medical Center,
Israel

*Correspondence:

Robert J. Harvey
r.j.harvey@ucl.ac.uk

Received: 14 February 2017

Accepted: 03 March 2017

Published: 20 March 2017

Citation:

Harvey RJ and Harvey K (2017)
Editorial: Molecular, Cellular and
Model Organism Approaches for
Understanding the Basis of
Neurological Disease.
Front. Mol. Neurosci. 10:74.
doi: 10.3389/fnmol.2017.00074

mutations. The authors concluded that LRRK2-mediated Wnt signaling and GTPase function are fundamental in conferring disease susceptibility, and that this has clear implications for future therapeutic interventions in Parkinson's disease.

Sophisticated cellular models of disease are increasingly vital as high-throughput screening tools for recreating events at normal and disrupted synapses *in vitro*. Kuenzel et al. reported a new tool for screening of *in vitro* neurotoxicity (NT) and developmental neurotoxicity (DNT) mediated by inhibitory γ -aminobutyric acid type A (GABA_A) and glycine receptors (GlyRs). They generated a human pluripotent stem cell line (NT2) that stably expresses YFP^{I152L}, a halide-sensitive variant of YFP, which allows for fluorescence-based functional analysis of Cl⁻ channels. Importantly, upon stimulation with retinoic acid, these NT2 cells undergo neuronal differentiation, allowing pharmacological and toxicological evaluation of native GABA_ARs and GlyRs at different developmental stages. By contrast, Dixon et al. reported an "artificial synapse" system—a neuron-HEK293 cell co-culture technique for generating inhibitory synapses incorporating defined combinations of wild-type or mutant GABA_AR or GlyR subunits. As well as allowing control over the subunit composition of the GlyRs under study, the electrotonically compact shape of HEK293 cells combined with rapid agonist application allows IPSC waveforms to be resolved with high fidelity using electrophysiology.

The role of the GlyR M3-M4 intracellular domain in health and disease was also reviewed by Langlhofer and Villmann who comprehensively documented molecular determinants of phosphorylation, intracellular sorting, protein-protein interactions, subunit topology, and modulation by G proteins, ethanol, and cannabinoids. Barral and Kurian also reviewed the current and future potential of patient-derived induced pluripotent stem cells (iPSCs) in the field of childhood neurological disorders. Importantly, iPSCs can now be routinely differentiated into specific neuronal subtypes which represent valuable *in vitro* models of disease. They are also vital tools for testing existing drugs with repurposing potential, or novel compounds and gene therapies, which then can be translated to clinical practice. Imaging also has a key role to play in diagnosis of disease. Poutiainen et al. reviewed advances in non-invasive imaging techniques such as positron emission tomography (PET) and prospective biomarkers for the diagnosis of multiple sclerosis.

Whole-organism *in vivo* models also continue to make an impact in this field. Kozol et al. and Ogino and Hirata

reviewed the many advantages of zebrafish in the study of neurological disease. Validation of new disease genes and mutations is now possible through CRISPR/Cas9 mutagenesis of zebrafish gene orthologs, which rapidly creates new disease models which are amenable to phenotyping and high-throughput drug screening. Watanabe et al. also highlighted the use of sophisticated mouse models, showing how doxycycline-sensitive, Cre-mediated gene ablation of NMDA receptors in hippocampal excitatory neurons results in neurodegeneration in aging mice. This study highlighted the potentially damaging effects of long-term administration of NMDAR antagonists for therapeutic purposes. Lykhmus et al. used an acute model of LPS-induced neuroinflammation in mice and an *in vitro* model in cultured glioblastoma U373 cells to study neuroinflammation, which accompanies and often precedes the development of neurodegenerative pathologies such as Parkinson's and Alzheimer's diseases. They found that acute LPS-induced inflammation induced the cholinergic anti-inflammatory pathway in the brain, with down-regulation of $\alpha 7$ subunit-containing nAChRs limiting these effects. Curiously, nAChR $\alpha 7$ subunit-specific antibodies aggravated neuroinflammation, by inducing the pro-inflammatory interleukin-6 and dampening anti-inflammatory miRNAs. However, the authors also highlighted that nAChR $\alpha 7$ -specific antibodies may protect brain mitochondria and decrease the levels of pro-apoptotic miRNAs, preventing LPS-induced neurodegeneration.

We thank all contributors for their interesting and informative articles and the reviewers for their constructive and thoughtful suggestions.

AUTHOR CONTRIBUTIONS

KH and RJH wrote the manuscript and both authors approved the final version for publication.

Conflict of Interest Statement: The authors declare that the research was conducted in the absence of any commercial or financial relationships that could be construed as a potential conflict of interest.

Copyright © 2017 Harvey and Harvey. This is an open-access article distributed under the terms of the Creative Commons Attribution License (CC BY). The use, distribution or reproduction in other forums is permitted, provided the original author(s) or licensor are credited and that the original publication in this journal is cited, in accordance with accepted academic practice. No use, distribution or reproduction is permitted which does not comply with these terms.



Missense Mutation R338W in *ARHGEF9* in a Family with X-linked Intellectual Disability with Variable Macrocephaly and Macro-Orchidism

Philip Long¹, Melanie M. May², Victoria M. James^{1†}, Simone Grannò¹, John P. Johnson³, Patrick Tarpey⁴, Roger E. Stevenson², Kirsten Harvey¹, Charles E. Schwartz^{2*} and Robert J. Harvey^{1*}

¹ Department of Pharmacology, UCL School of Pharmacy, London, UK, ² JC Self Research Institute, Greenwood Genetic Center, Greenwood, SC, USA, ³ Department of Medical Genetics, Shodair Children's Hospital, Helena, MT, USA, ⁴ Wellcome Trust Sanger Institute, Wellcome Trust Genome Campus, Hinxton, UK

OPEN ACCESS

Edited by:

Jean-Marc Taymans,
UMR1172, Jean-Pierre Aubert
Research Center, France

Reviewed by:

Angel L. De Blas,
University of Connecticut, USA
Silvia Bassani,
CNR Institute of Neuroscience, Italy

*Correspondence:

Charles E. Schwartz
ceschwartz@ggc.org;
Robert J. Harvey
r.j.harvey@ucl.ac.uk

†Present address:

Victoria M. James,
Wellcome Trust, London, UK

Received: 16 October 2015

Accepted: 14 December 2015

Published: 20 January 2016

Citation:

Long P, May MM, James VM, Grannò S, Johnson JP, Tarpey P, Stevenson RE, Harvey K, Schwartz CE and Harvey RJ (2016) Missense Mutation R338W in *ARHGEF9* in a Family with X-linked Intellectual Disability with Variable Macrocephaly and Macro-Orchidism. *Front. Mol. Neurosci.* 8:83. doi: 10.3389/fnmol.2015.00083

Non-syndromal X-linked intellectual disability (NS-XLID) represents a broad group of clinical disorders in which ID is the only clinically consistent manifestation. Although in many cases either chromosomal linkage data or knowledge of the >100 existing XLID genes has assisted mutation discovery, the underlying cause of disease remains unresolved in many families. We report the resolution of a large family (K8010) with NS-XLID, with variable macrocephaly and macro-orchidism. Although a previous linkage study had mapped the locus to Xq12-q21, this region contained too many candidate genes to be analyzed using conventional approaches. However, X-chromosome exome sequencing, bioinformatics analysis and segregation analysis revealed a novel missense mutation (c.1012C>T; p.R338W) in *ARHGEF9*. This gene encodes collybistin (CB), a neuronal GDP-GTP exchange factor previously implicated in several cases of XLID, as well as clustering of gephyrin and GABA_A receptors at inhibitory synapses. Molecular modeling of the CB R338W substitution revealed that this change results in the substitution of a long electropositive side-chain with a large non-charged hydrophobic side-chain. The R338W change is predicted to result in clashes with adjacent amino acids (K363 and N335) and disruption of electrostatic potential and local folding of the PH domain, which is known to bind phosphatidylinositol-3-phosphate (PI₃P/PtdIns-3-P). Consistent with this finding, functional assays revealed that recombinant CB CB2_{SH3}-^{R338W} was deficient in PI₃P binding and was not able to translocate EGFP-gephyrin to submembrane microaggregates in an *in vitro* clustering assay. Taken together, these results suggest that the R338W mutation in *ARHGEF9* is the underlying cause of NS-XLID in this family.

Keywords: *ARHGEF9*, collybistin, gephyrin, PH domain, XLID

INTRODUCTION

Intellectual disability (ID) is characterized by significantly impaired intellectual and adaptive function, and is often defined by an IQ score below 70 in addition to deficits in two or more adaptive behaviors (e.g., social skills, problem solving) that affect everyday life. ID is also subdivided into syndromal ID, where ID is associated with other clinical, morphological, or behavioral symptoms or non-syndromal ID, where intellectual deficits appear without other associated defects (Stevenson et al., 2012). X-linked intellectual disability (XLID) refers to forms of ID typically associated with X-linked recessive inheritance. Mutations in monogenic XLID have been reported in >100 genes, many of which are now used in routine diagnostic screening panels (Basehore et al., 2015). Despite screening for mutations in selected known XLID genes by conventional linkage/candidate gene analysis or array CGH for examining copy number variants (CNVs), large number of families mapping to the X-chromosome remained unresolved (Lubs et al., 2012). These cases either represent undiscovered disease-relevant mutations in known genes, or causal mutations in novel XLID loci that remain to be identified.

Mutation and gene discovery in XLID has recently been transformed by large-scale DNA sequencing approaches coupled with stringent variant filtering (Tarpey et al., 2009; Rauch et al., 2012; Gilissen et al., 2014; Redin et al., 2014; Hu et al., 2015; Niranjana et al., 2015; Tzschach et al., 2015). For example, a recent study in a large cohort of unresolved families with XLID revealed that 20% of families carried pathogenic variants in established XLID genes (Hu et al., 2015), as well as revealing seven novel XLID genes (*CLCN4*, *CNKSRR2*, *FRMPD4*, *KLHL15*, *LAS1L*, *RLIM*, and *USP27X*) and two candidates (*CDK16* and *TAF1*). Another strategy, known as Affected Kindred/Cross-Cohort Analysis (Niranjana et al., 2015) has also identified variants in known and novel XLID genes including *PLXNA3*, *GRIPAP1*, *EphrinB1* and *OGT*. However, analysis of next-generation data sets has also highlighted a number of XLID genes where truncating variants or previously published “mutations” are observed at a relatively high frequency in normal controls, calling into question whether certain single nucleotide variants (SNVs) are indeed causal (Tarpey et al., 2009; Piton et al., 2013). This highlights the need for integrating structure-function based approaches into the analysis pipeline for validating potentially disease-causing variants.

In this study, we have combined next-generation sequencing, variant filtering and structure-function assays to resolve the cause of XLID in a large family (K8010) with NS-XLID, with variable macrocephaly and macro-orchidism (Johnson et al., 1998). The previous clinical study in this family revealed ten affected males and two affected females in two generations, as well as four obligatory carriers. Most affected males exhibited macrocephaly and macro-orchidism, which are typical signs of the fragile X syndrome. However, cytogenetic testing and analysis of *FMR1* indicated they did not have this syndrome. It was also notable that some normal males in the family

also exhibited macro-orchidism and macrocephaly. Linkage analysis suggested that the causative gene was located on Xp11-q21 (Johnson et al., 1998). We present compelling evidence that the likely cause of XLID in this family is a missense mutation in *ARHGEF9*, encoding a neuronal RhoGEF known as collybistin (CB) involved in both inhibitory synaptic organization and mammalian target of rapamycin complex 1 (mTORC1) signaling pathways (Machado et al., 2015).

MATERIALS AND METHODS

Subjects

Family K8010 was previously reported by Johnson et al. (1998). Briefly, the males resembled those with fragile X syndrome in that they had macrocephaly (abnormally large head, typically 2.5 standard deviations above normal for weight and gender), macro-orchidism (abnormally large testes), blue eyes, prominent jaw and long facies. Additionally, one carrier female was described as being “slow”. However, using linkage analysis, the locus was mapped to Xq12-q21 rather than Xq27.3. Additionally, *FMR1* gene analysis was negative (Johnson et al., 1998).

Exon Capture and DNA Sequencing

Next generation sequencing was conducted as a partial follow-up of 15 probands from a large scale sequencing of 718 X-chromosome genes in 208 XLID probands (Tarpey et al., 2009). The deep sequencing was conducted using the Agilent SureSelect Human X chromosome kit (Takano et al., 2012). A novel and unique mutation in *ARHGEF9*, c.1012C>T, was noted in K8010. Segregation analysis was conducted using Sanger sequencing.

Polymorphism Analysis

Screening of 566 normal individuals (420 males, 146 females) for the *ARHGEF9* c.1012C>T variant was carried out using allele-specific amplification. Primers used were: *ARHGEF9*-ASOF 5'-TACGGCCGCAACCAGCtGt 3' and *ARHGEF9*-ASOR 5'-CCCATCAGTATTTGCCCACT-3'. The ASOF primer recognized the mutation, which is indicated by the “t” at the 3' end of the primer. The third base from the 3' end was also changed from an “a” to a “t” to increase the specificity of the PCR. The ASOR primer was designed so that the T_m of both primers were similar and to generate a PCR product of above 500 bp. Gradient duplex PCR analysis was conducted using mutation and normal samples to choose the optimum annealing temperature. High-throughput duplex PCR analysis with a mutation and normal sample as positive and negative controls.

Molecular Modeling of the Collybistin R38W Mutation

The non-synonymous R38W substitution was modeled into the structure of rat CB (PDB 2DFK; Xiang et al., 2006) using the *swapaa* command in Chimera (Pettersen et al., 2004) using the Dunbrack backbone-dependent rotamer library

(Dunbrack, 2002). This took into account the lowest clash score, highest number of H-bonds and highest rotamer probability. Electrostatic potential of wild-type and R338W mutant CB was calculated using the Adaptive Poisson-Boltzmann Solver (APBS) web server (Baker et al., 2001; <http://www.poissonboltzmann.org/>).

Site-Directed Mutagenesis and Expression Constructs

Full-length human CB cDNAs were cloned into the vector pRK5 as previously described (Kalscheuer et al., 2009). Mutations were introduced into pRK5myc-hCB3_{SH3}- construct using the QuikChange site-directed mutagenesis kit (Agilent) and confirmed by Sanger DNA sequencing of the entire coding region.

PI₃P Pull-Down Assays

Human embryonic kidney (HEK293) cells were grown in DMEM supplemented with 10% (v/v) fetal bovine serum at 37°C, 5% CO₂ and transfected with 4 µg pRK5myc-hCB3_{SH3}- wild-type or R338W mutants using FuGENE (Roche). After 24 h, transfected cells were solubilized in a buffer containing Triton X-100 (Sigma-Aldrich), 1%; 150 mM NaCl; 50 mM Tris, pH 7.4, with protease inhibitor cocktail (Roche, Sussex, UK). Insoluble material was removed by centrifugation at 16, 100× g for 20 min. Phosphatidylinositol-3-phosphate (PI₃P/PtdIns-3-P) agarose beads (40 µl; Eschelon Biosciences) were incubated with cell lysates for 2 h at 4°C. Beads were washed four times in buffer. Proteins were eluted from beads by heating at 98°C for 3 min in 2 × sample loading buffer and then subjected to SDS-PAGE. Proteins binding to beads were detected by Western blotting using mouse anti-c-myc antibody (Sigma, 1:1000) and HRP-conjugated goat anti-mouse (Santa Cruz, 1:2000). Immunoreactivity was visualized using West Pico Chemiluminescent Substrate (Pierce). Expression levels of hCB3_{SH3}- and hCB3_{SH3}-R338W, and PI₃P pulldown assay results were assessed using an unpaired, two-tailed Student's *t*-test.

Gephyrin Clustering Assays

These were performed essentially as previously described (Harvey et al., 2004). HEK293 cells were co-transfected with pRK5myc-hCB3_{SH3}- wild-type, pRK5myc-hCB3_{SH3}+ wild-type, pRK5myc-hCB3_{SH3}- R338W, pRK5myc-hCB3_{SH3}- R290H or pRK5myc-hCB3_{SH3}- R356N/R357N constructs at a 1:1 ratio with pEGFP-gephyrin using electroporation (Gene Pulser II, Bio-Rad). Cells were fixed after 24 h for 2 min in 4% (w/v) PFA in PBS. Immunostaining to detect CB was performed using a mouse anti-c-myc antibody (1:200, Sigma) and detected using an AlexaFluor 546 goat anti-mouse secondary antibody (1:600; Invitrogen). Counterstaining for cell nuclei was performed with DAPI (1:500; Life Technologies). Confocal microscopy was performed using a Zeiss LSM 710 META. All images were taken with a × 63 objective.

RESULTS

Identification of a R338W Mutation in ARHGEF9 in Family K8010

X-chromosome exome sequencing of an individual male in family K8010 followed by bioinformatics analysis and filtering against publicly-available datasets revealed a novel missense change in *ARHGEF9*, chrX:62,885,810G>A, c.1012C>T; p.R338W, predicted as probably damaging (PolyPhen-2, score 1.000), damaging (SIFT) and a Combined Annotation Dependent Depletion (CADD) score of 19.37 (possibly pathogenic). This suggested that this missense mutation could be responsible for XLID, macrocephaly and macro-orchidism in this family. Subsequent segregation analysis using Sanger DNA sequencing indicated that the *ARHGEF9* c.1012C>T variant co-segregated with the phenotype in all individuals tested (Figures 1A,B).

Collybistin Mutation R338W is Predicted to Disrupt PH Domain Folding

CB belongs to the Dbl family of guanine nucleotide exchange factors, occurs in multiple splice variants (Kins et al., 2000; Harvey et al., 2004) and is specific for Cdc42, a small GTPase belonging to the Rho family (Xiang et al., 2006). CB has a multi-domain structure consisting of a regulatory SH3 domain, a catalytic RhoGEF domain and a pleckstrin homology (PH) domain (Figure 1C). Residue R338W is the first reported *ARHGEF9* missense mutation affecting a highly conserved residue in the PH domain (Figure 1D). Previous nonsense and missense mutations in CB have affected residues in the N-terminus (p.Q2X; Shimojima et al., 2011), regulatory SH3 domain (p.G55A; Harvey et al., 2004) and catalytic RhoGEF domain (p.R290H; Lemke et al., 2012; Papadopoulos et al., 2015). To assess how the R338W substitution might disrupt CB function, molecular modeling was performed using the structure of rat CB (PDB 2DFK; Xiang et al., 2006), which has a sequence identity of 85.5% to human CB [aligned using HAlign algorithm (Söding, 2005) within Clustal-Omega (Sievers et al., 2011)]. The R338W change replaces a long, electropositive side-chain (arginine) with a large non-charged, hydrophobic side-chain (tryptophan). Positively-charged residues are thought to be critical for interaction of the PH domain with the membrane (Xiang et al., 2006) and R338W clearly changes the electrostatic potential of the PH domain, as visualized using APBS (Figures 2A–C). R338W is also predicted to introduce a number of clashes with surrounding residues (e.g., N335, K363; Figures 2D,E), which is also predicted to affect interactions with membrane and the fold of the PH domain.

Mutation R338W in Collybistin Disrupts Phosphatidylinositol-3-Phosphate Binding

The CB PH domain has previously been shown to play a key role in binding PI₃P/PtdIns-3-P, a phosphoinositide with an emerging role in membrane trafficking and signal

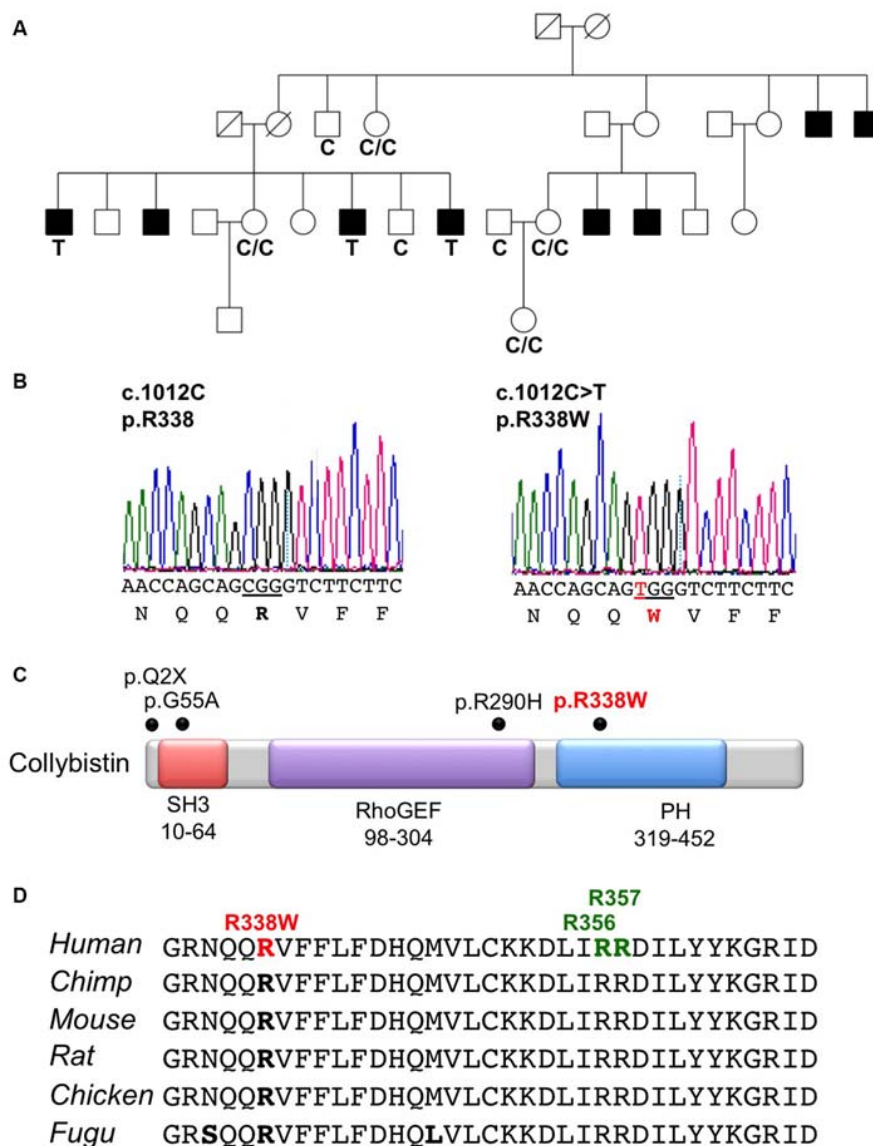
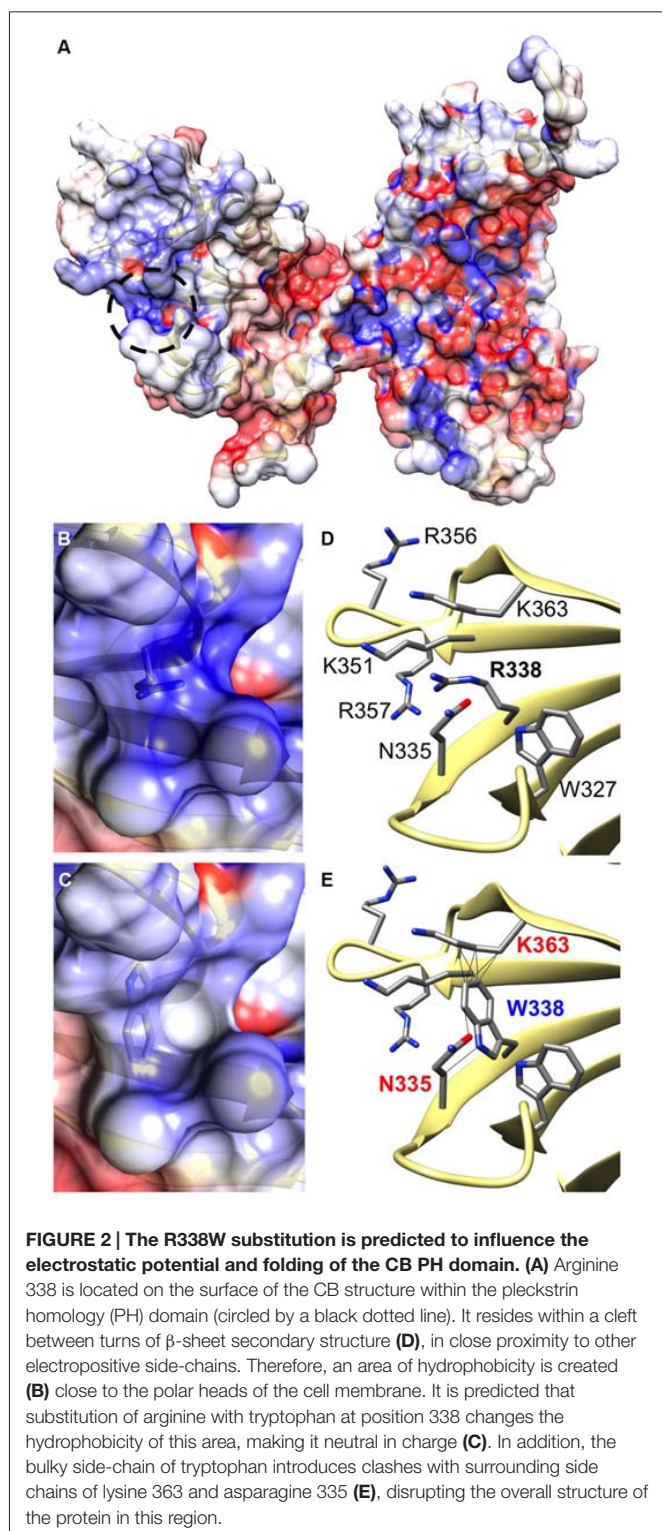


FIGURE 1 | Identification of a R338W mutation in *ARHGEF9* in family K8010. (A) Pedigree of the K8010 family, which has been updated. Open symbols represent normal individuals, filled squares represent affected males. Individuals tested for the nucleotide substitution in each family are indicated with either a T (mutant allele) or a C (normal allele). **(B)** DNA sequence electropherograms for the c.1012C>T mutation reported in this study. **(C)** Schematic of the human collybistin (CB) protein with a regulatory SH3 domain, a catalytic RhoGEF domain and a pleckstrin homology (PH) domain. The relative locations of known missense and nonsense mutations in *ARHGEF9* are shown. **(D)** Sequence alignments of CB proteins from various species showing the high conservation of R338W in the PH domain. Note that R338W is not one of the known PI_3P binding residues (R356 and R357, green).

transduction. Deletion of the CB PH domain, or mutation of two key arginine residues (R356/R357) involved in PI_3P binding has been demonstrated to abolish CB-mediated gephyrin clustering in functional assays (Harvey et al., 2004; Kalscheuer et al., 2009; Reddy-Alla et al., 2010). In order to determine whether the R338W mutation affected CB binding to PI_3P , we performed pull-down assays using PI_3P immobilized on agarose beads incubated with lysates of HEK293 cells transfected with either wild-type CB variant $\text{CB}_{\text{SH3-}}$ or mutant $\text{CB}_{\text{SH3-}}^{\text{R338W}}$. Total expression of

$\text{CB}_{\text{SH3-}}^{\text{R338W}}$ was not significantly different to wild-type $\text{CB}_{\text{SH3-}}$ when normalized to β -actin expression (**Figure 3A**, left and right panels, wild-type $\text{CB}_{\text{SH3-}}$ 1.00 ± 0.23 vs. R338W 1.16 ± 0.33 ; normalized to wild-type \pm SEM, $n = 5$). However, when the PI_3P pull-down fraction was expressed as a percentage of raw input, a significant reduction of PI_3P binding was observed for the R338W variant (**Figure 3A**, middle and right panels, wild-type 100 ± 13.5 vs. R338W 38 ± 8.6 ; pull-down fraction \pm SEM, $n = 5$, $p < 0.006$).



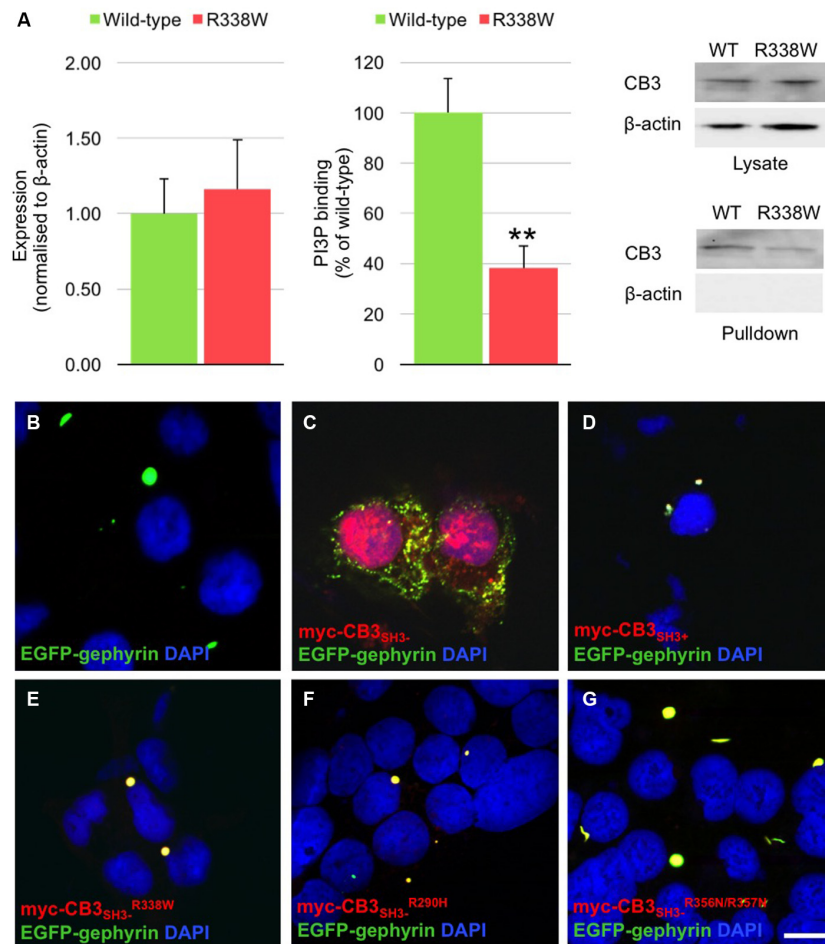
Mutation R338W Disrupts Collybistin-Mediated Gephyrin Clustering

Given the key role of CB in mediating gephyrin clustering at inhibitory synapses, we also investigated whether the R338W substitution affected the ability of CB to translocate gephyrin

to submembrane microaggregates in a cellular clustering assay (Harvey et al., 2004; Kalscheuer et al., 2009). This involved co-expression of myc-tagged human CB (myc-CB_{SH3-}; Kalscheuer et al., 2009) with EGFP-gephyrin in HEK293 cells. CB variants containing the regulatory SH3 domain (CB_{SH3+}) typically co-localize with EGFP-gephyrin in large intracellular aggregates (**Figures 3B,D**; Kins et al., 2000; Harvey et al., 2004; Kalscheuer et al., 2009) and require neuroligins, GABA_A α 2 or the small Rho-like GTPase TC10 for activation (Pouloupoulos et al., 2009; Saiepour et al., 2010; Mayer et al., 2013). However, variants lacking the regulatory SH3 domain (e.g., CB_{SH3-}) typically result in the formation of EGFP-gephyrin submembrane clusters (**Figure 3C**). However, the CB_{SH3-}^{R338W} variant did not result in the formation of submembrane microaggregates with EGFP-gephyrin, but rather co-localized with EGFP-gephyrin in large intracellular aggregates (**Figure 3E**) similar to the distribution previously observed for CB_{SH3+} or CB mutants that disrupt PI₃P binding, such as R290H and the double mutant R356N/R357N (**Figures 3F,G**; Reddy-Alla et al., 2010; Papadopoulos et al., 2015). This demonstrates that the R338W substitution disrupts CB-mediated accumulation of gephyrin in submembrane microclusters.

DISCUSSION

This study reports the identification and functional characterization of a novel mutation (p.R338W) in *ARHGEF9* that is likely to represent the cause of XLID in family K8010. Using next-generation X-exome sequencing, Affected Kindred/Cross-Cohort Analysis and inheritance testing, we found a novel SNV (c.1012C>T; p.R338W) in *ARHGEF9* that segregated with the disease phenotype. Using molecular modeling and functional assays for CB PI₃P binding and gephyrin clustering, we were able to establish the likely pathomechanism for p.R338W: a local disruption in the PH domain structure, leading to a reduction in PI₃P binding and/or PH domain folding, and consequent loss in the ability of CB to mediate gephyrin clustering in an *in vitro* assay. The identification of *ARHGEF9* as the causative gene for family K8010 is consistent with previous studies that have identified CB as a neuronally-expressed RhoGEF with a key role in inhibitory synaptic transmission (Kins et al., 2000; Harvey et al., 2004). At selected inhibitory synapses, CB interacts with gephyrin (Kins et al., 2000; Harvey et al., 2004), a scaffolding protein with dual roles in inhibitory receptor clustering and molybdenum co-factor synthesis (Feng et al., 1998). CB knockout mice show increased anxiety and impaired spatial learning associated with a selective loss of GABA_ARs in the basolateral amygdala and hippocampus (Papadopoulos et al., 2007). Unsurprisingly, loss of CB clearly leads to significant changes in GABAergic inhibition, network excitability and synaptic plasticity (Jedlicka et al., 2009). Recent studies have also implicated CB in mTOR signaling: CB physically interacts with mTOR and inhibits mTORC1 signaling pathway and protein synthesis (Machado et al., 2015). This suggests that disruption of mTORC1 signaling pathways could also contribute to ID in patients with *ARHGEF9* loss-of-function mutations.



A number of mutations in *ARHGEF9* have been identified in patients encompassing missense and nonsense mutations, deletions and complex rearrangements (**Table 1**). Curiously, the associated phenotypes vary quite substantially. For example, Harvey et al. (2004) reported a p.G55A missense mutation in *ARHGEF9* associated with hyperekplexia, early infantile epileptic encephalopathy and severe psychomotor retardation (p.G55A, SH3 domain). By contrast, Shimojima et al. (2011) identified an *ARHGEF9* nonsense mutation (p.Q2X) in an individual with refractory seizures, right frontal polymicrogyria and severe psychomotor retardation. Lemke et al. (2012) also reported a p.R290H missense mutation in the CB RhoGEF

domain associated with epilepsy and ID. Furthermore, large *de novo* deletions affecting *ARHGEF9* as well as neighboring genes *SPIN4* and *LOC92249* have been reported to be associated with complex phenotypes that include features such as partial seizures, delayed psychomotor development and generalized overgrowth (**Table 1**; Lesca et al., 2011; Shimojima et al., 2011). Lastly, a balanced chromosomal translocation (Kalscheuer et al., 2009) and a paracentric inversion (Marco et al., 2008) have been reported with yet more clinical features, including disturbed sleep-wake cycle, increased anxiety and aggressive behavior or hyperarousal, respectively.

TABLE 1 | ARHGEF9 mutations and associated phenotypes.

Mutation type	Nucleotide	Protein	Reported phenotype	Reference
Missense and nonsense mutations	c.4C>T	p.Q2X	Refractory seizures, right frontal polymicrogyria, severe psychomotor retardation, ataxia	Shimojima et al. (2011)
	c.869G>A	p.G55A	Hyperekplexia, early infantile epileptic encephalopathy and severe psychomotor retardation	Harvey et al. (2004)
	c.869G>A	p.R290H	Epilepsy and intellectual disability	Lemke et al. (2012)
	c.1012C>T	p.R338W	Intellectual disability with variable macrocephaly and macro-orchidism	This study
Deletions	<i>De novo</i> 737 kb deletion including <i>ARHGEF9</i> , <i>SPIN4</i> , <i>LOC92249</i>		Complex partial seizures, severely delayed psychomotor development, generalized overgrowth and trigonocephaly	Kalscheuer et al. (2009)
	<i>De novo</i> 1.29 Mb deletion of Xq11.11 including <i>ARHGEF9</i> , <i>SPIN4</i> , <i>LOC92249</i>		Delayed psychomotor development, loss of consciousness, hypotonia, cyanosis, generalized overgrowth, mild dysmorphic features, hyperactivity with attention deficit, limited social interaction	Marco et al. (2008)
Complex rearrangements	Balanced translocation 46, X, t(Xq11.1;18q11.21)		Disturbed sleep-wake cycle, late-onset epileptic seizures, increased anxiety, aggressive behavior and intellectual disability	Kalscheuer et al. (2009)
	Balanced <i>de novo</i> paracentric inversion (X)(q11.1;q27.3)		Hyperarousal (noise and social situations), global developmental delay, dysarthric speech, difficulty with smooth eye pursuit, bilateral lower extremity spasticity, brisk reflexes and extensor plantar responses, wide-based gait	Marco et al. (2008)

The exact reasons behind this clinical variability remains unknown, but are likely to be linked to several factors. Firstly, certain CB mutations (e.g., p.G55A, p.R290H, C-terminal truncations) clearly cause dominant-negative effects on gephyrin and GABA_A receptor clustering in neuronal systems (Harvey et al., 2004; Kalscheuer et al., 2009; Papadopoulos et al., 2015). Secondly, for female patients with CB mutations, the clinical features observed may depend on the degree of X-inactivation skewing. At least two studies involving a translocation or inversion in *ARHGEF9* have indicated skewed X inactivation in favor of the abnormal X chromosome (Marco et al., 2008; Kalscheuer et al., 2009). However, one emerging theme in functional studies of CB missense mutations appears to be loss of PI₃P binding. Our own functional analysis suggests that the p.R338W variant causes a local disruption in the PH domain structure, leading to a reduction in PI₃P binding and/or PH domain folding, and consequent loss in the ability of CB to mediate gephyrin clustering. Similar findings have recently been reported for the p.R290H mutation linked to epilepsy and ID, which appears to alter the strength of intramolecular interactions between the RhoGEF and PH domains, also leading to a loss of PI₃P binding affinity (Papadopoulos et al., 2015). These results highlight the key role of phosphoinositide binding and correct

localization of CB for synaptic function. However, given the variability in clinical phenotypes associated with CB mutations, it is also evident that next-generation sequencing diagnostics have a pivotal role to play in the diagnosis of X-linked disorders.

AUTHOR CONTRIBUTIONS

RJH and CES designed the experiments; JPJ contributed DNA samples; RES provided clinical evaluation; PL, SG, MMM, VMJ, PT and KH performed the experiments; CES, SG, PT, KH and RJH analyzed the data; CES and RJH wrote the paper. All authors were involved in revising the paper for important intellectual content, and gave final approval of the version to be published.

FUNDING

This work was supported by the Medical Research Council (J004049 to RJH and KH), a NINDS grant (R01NS073854 to CES) and in part by the South Carolina Department of Disabilities and Special Needs (SC DDSN). The funders had no role in study design, data collection and analysis, decision to publish, or preparation of the manuscript. Dedicated to the memory of Ethan Francis Schwartz (1996–1998).

REFERENCES

- Baker, N. A., Sept, D., Joseph, S., Holst, M. J., and McCammon, J. A. (2001). Electrostatics of nanosystems: application to microtubules and the ribosome. *Proc. Natl. Acad. Sci. U S A* 98, 10037–10041. doi: 10.1073/pnas.181342398
- Basehore, M. J., Michaelson-Cohen, R., Levy-Lahad, E., Sismani, C., Bird, L. M., Friez, M. J., et al. (2015). Alpha-thalassemia intellectual disability: variable phenotypic expression among males with a recurrent nonsense mutation - 109C>T (p.R37X). *Clin. Genet.* 87, 461–466. doi: 10.1111/cge.12420
- Dunbrack, R. L., Jr. (2002). Rotamer libraries in the 21st century. *Curr. Opin. Struct. Biol.* 12, 431–440. doi: 10.1016/s0959-440x(02)00344-5
- Feng, G., Tintrup, H., Kirsch, J., Nichol, M. C., Kuhse, J., Betz, H., et al. (1998). Dual requirement for gephyrin in glycine receptor clustering and molybdoenzyme activity. *Science* 282, 1321–1324. doi: 10.1126/science.282.5392.1321

- Gilissen, C., Hehir-Kwa, J. Y., Thung, D. T., van de Vorst, M., van Bon, B. W., Willemsen, M. H., et al. (2014). Genome sequencing identifies major causes of severe intellectual disability. *Nature* 511, 344–347. doi: 10.1038/nature13394
- Harvey, K., Duguid, I. C., Alldred, M. J., Beatty, S. E., Ward, H., Keep, N. H., et al. (2004). The GDP-GTP exchange factor collybistin: an essential determinant of neuronal gephyrin clustering. *J. Neurosci.* 24, 5816–5886. doi: 10.1523/jneurosci.1184-04.2004
- Hu, H., Haas, S. A., Chelly, J., Van Esch, H., Raynaud, M., de Brouwer, A. P., et al. (2015). X-exome sequencing of 405 unresolved families identifies seven novel intellectual disability genes. *Mol. Psychiatry* doi: 10.1038/mp.2014.193 [Epub ahead of print].
- Jedlicka, P., Papadopoulos, T., Deller, T., Betz, H., and Schwarzacher, S. W. (2009). Increased network excitability and impaired induction of long-term potentiation in the dentate gyrus of collybistin-deficient mice *in vivo*. *Mol. Cell. Neurosci.* 41, 94–100. doi: 10.1016/j.mcn.2009.02.005
- Johnson, J. P., Nelson, R., and Schwartz, C. E. (1998). A family with mental retardation, variable macrocephaly and macro-orchidism and linkage to Xq12–q21. *J. Med. Genet.* 35, 1026–1030. doi: 10.1136/jmg.35.12.1026
- Kalscheuer, V. M., Musante, L., Fang, C., Hoffmann, K., Fuchs, C., Carta, E., et al. (2009). A balanced chromosomal translocation disrupting ARHGEF9 is associated with epilepsy, anxiety, aggression and mental retardation. *Hum. Mutat.* 30, 61–68. doi: 10.1002/humu.20814
- Kins, S., Betz, H., and Kirsch, J. (2000). Collybistin, a newly identified brain-specific GEF, induces submembrane clustering of gephyrin. *Nat. Neurosci.* 3, 22–29. doi: 10.1038/71096
- Lemke, J. R., Riesch, E., Scheurenbrand, T., Schubach, M., Wilhelm, C., Steiner, I., et al. (2012). Targeted next generation sequencing as a diagnostic tool in epileptic disorders. *Epilepsia* 53, 1387–1398. doi: 10.1111/j.1528-1167.2012.03516.x
- Lesca, G., Till, M., Labalme, A., Vallee, D., Hugonenc, C., Philip, N., et al. (2011). De novo Xq11.11 microdeletion including ARHGEF9 in a boy with mental retardation, epilepsy, macrosomia and dysmorphic features. *Am. J. Med. Genet. A* 155A, 1706–1711. doi: 10.1002/ajmg.a.34004
- Lubs, H. A., Stevenson, R. E., and Schwartz, C. E. (2012). Fragile X and X-linked intellectual disability: four decades of discovery. *Am. J. Hum. Genet.* 90, 579–590. doi: 10.1016/j.ajhg.2012.02.018
- Machado, C. O., Griesi-Oliveira, K., Rosenberg, C., Kok, F., Martins, S., Rita Passos-Bueno, M., et al. (2015). Collybistin binds and inhibits mTORC1 signaling: a potential novel mechanism contributing to intellectual disability and autism. *Eur. J. Hum. Genet.* 24, 59–65. doi: 10.1038/ejhg.2015.69
- Marco, E. J., Abidi, F. E., Bristow, J., Dean, W. B., Cotter, P., Jeremy, R. J., et al. (2008). ARHGEF9 disruption in a female patient is associated with X linked mental retardation and sensory hyperarousal. *J. Med. Genet.* 45, 100–105. doi: 10.1136/jmg.2007.052324
- Mayer, S., Kumar, R., Jaiswal, M., Soykan, T., Ahmadian, M. R., Brose, N., et al. (2013). Collybistin activation by GTP-TC10 enhances postsynaptic gephyrin clustering and hippocampal GABAergic neurotransmission. *Proc. Natl. Acad. Sci. U S A* 110, 20795–20800. doi: 10.1073/pnas.1309078110
- Niranjan, T. S., Skinner, C., May, M., Turner, T., Rose, R., Stevenson, R., et al. (2015). Affected kindred analysis of human X chromosome exomes to identify novel X-linked intellectual disability genes. *PLoS One* 10:e0116454. doi: 10.1371/journal.pone.0116454
- Papadopoulos, T., Korte, M., Eulenburg, V., Kubota, H., Retiounskaia, M., Harvey, R. J., et al. (2007). Impaired GABAergic transmission and altered hippocampal synaptic plasticity in collybistin-deficient mice. *EMBO J.* 26, 3888–3899. doi: 10.1038/sj.emboj.7601819
- Papadopoulos, T., Schemm, R., Grubmüller, H., and Brose, N. (2015). Lipid binding defects and perturbed synaptogenic activity of a collybistin R290H mutant that causes epilepsy and intellectual disability. *J. Biol. Chem.* 290, 8256–8270. doi: 10.1074/jbc.M114.633024
- Pettersen, E. F., Goddard, T. D., Huang, C. C., Couch, G. S., Greenblatt, D. M., Meng, E. C., et al. (2004). UCSF Chimera—A visualization system for exploratory research and analysis. *J. Comput. Chem.* 25, 1605–1612. doi: 10.1002/jcc.20084
- Piton, A., Redin, C., and Mandel, J. L. (2013). XLID-causing mutations and associated genes challenged in light of data from large-scale human exome sequencing. *Am. J. Hum. Genet.* 93, 368–383. doi: 10.1016/j.ajhg.2013.06.013
- Poulopoulos, A., Aramuni, G., Meyer, G., Soykan, T., Hoon, M., Papadopoulos, T., et al. (2009). Neuroligin 2 drives postsynaptic assembly at perisomatic inhibitory synapses through gephyrin and collybistin. *Neuron* 63, 628–642. doi: 10.1016/j.neuron.2009.08.023
- Rauch, A., Wieczorek, D., Graf, E., Wieland, T., Ende, S., Schwarzmayr, T., et al. (2012). Range of genetic mutations associated with severe non-syndromic sporadic intellectual disability: an exome sequencing study. *Lancet* 380, 1674–1682. doi: 10.1016/S0140-6736(12)61480-9
- Reddy-Alla, S., Schmitt, B., Birkenfeld, J., Eulenburg, V., Dutertre, S., Böhringer, C., et al. (2010). PH-domain-driven targeting of collybistin but not Cdc42 activation is required for synaptic gephyrin clustering. *Eur. J. Neurosci.* 31, 1173–1184. doi: 10.1111/j.1460-9568.2010.07149.x
- Redin, C., Gérard, B., Lauer, J., Herenger, Y., Muller, J., Quartier, A., et al. (2014). Efficient strategy for the molecular diagnosis of intellectual disability using targeted high-throughput sequencing. *J. Med. Genet.* 51, 724–736. doi: 10.1136/jmedgenet-2014-102554
- Saiepour, L., Fuchs, C., Patrizi, A., Sassoè-Pognetto, M., Harvey, R. J., and Harvey, K. (2010). Complex role of collybistin and gephyrin in GABAA receptor clustering. *J. Biol. Chem.* 285, 29623–29631. doi: 10.1074/jbc.M110.121368
- Shimajima, K., Sugawara, M., Shichiji, M., Mukaida, S., Takayama, R., Imai, K., et al. (2011). Loss-of-function mutation of collybistin is responsible for X-linked mental retardation associated with epilepsy. *J. Hum. Genet.* 56, 561–565. doi: 10.1038/jhg.2011.58
- Sievers, F., Wilm, A., Dineen, D. G., Gibson, T. J., Karplus, K., Li, W., et al. (2011). Fast, scalable generation of high-quality protein multiple sequence alignments using Clustal Omega. *Mol. Syst. Biol.* 7:539. doi: 10.1038/msb.2011.75
- Söding, J. (2005). Protein homology detection by HMM-HMM comparison. *Bioinformatics* 21, 951–960. doi: 10.1093/bioinformatics/bti125
- Stevenson, R. E., Schwartz, C. E., and Rogers, R. C. (2012). *Atlas of X-linked Intellectual Disability Syndromes*. 2 Edn. New York: Oxford Univ Press
- Takano, K., Liu, D., Tarpey, P., Gallant, E., Lam, A., Witham, S., et al. (2012). An X-linked channelopathy with cardiomegaly due to a CLIC2 mutation enhancing ryanodine receptor channel activity. *Hum. Mol. Genet.* 21, 4497–4507. doi: 10.1093/hmg/dds292
- Tarpey, P. S., Smith, R., Pleasance, E., Whibley, A., Edkins, S., Hardy, C., et al. (2009). A systematic, large-scale resequencing screen of X-chromosome coding exons in mental retardation. *Nat. Genet.* 41, 535–543. doi: 10.1038/ng.367
- Tzschach, A., Grasshoff, U., Beck-Woedl, S., Dufke, C., Bauer, C., Kehrer, M., et al. (2015). Next-generation sequencing in X-linked intellectual disability. *Eur. J. Hum. Genet.* 23, 1513–1518. doi: 10.1038/ejhg.2015.5
- Xiang, S., Kim, E. Y., Connelly, J. J., Nassar, N., Kirsch, J., Winking, J., et al. (2006). The crystal structure of Cdc42 in complex with collybistin II, a gephyrin-interacting guanine nucleotide exchange factor. *J. Mol. Biol.* 359, 35–46. doi: 10.1016/j.jmb.2006.03.019

Conflict of Interest Statement: The authors declare that the research was conducted in the absence of any commercial or financial relationships that could be construed as a potential conflict of interest.

Copyright © 2016 Long, May, James, Grannò, Johnson, Tarpey, Stevenson, Harvey, Schwartz and Harvey. This is an open-access article distributed under the terms of the Creative Commons Attribution License (CC BY). The use, distribution and reproduction in other forums is permitted, provided the original author(s) or licensor are credited and that the original publication in this journal is cited, in accordance with accepted academic practice. No use, distribution or reproduction is permitted which does not comply with these terms.



Novel Missense Mutation A789V in *IQSEC2* Underlies X-Linked Intellectual Disability in the MRX78 Family

Vera M. Kalscheuer^{1,2*}, Victoria M. James³, Miranda L. Himmelright⁴, Philip Long³, Renske Oegema⁵, Corinna Jensen¹, Melanie Bienek¹, Hao Hu¹, Stefan A. Haas⁶, Maya Topf⁷, A. Jeannette M. Hoogeboom⁵, Kirsten Harvey³, Randall Walikonis⁴ and Robert J. Harvey^{3*}

¹ Department of Human Molecular Genetics, Max Planck Institute for Molecular Genetics, Berlin, Germany, ² Research Group Development and Disease, Max Planck Institute for Molecular Genetics, Berlin, Germany, ³ Department of Pharmacology, UCL School of Pharmacy, London, UK, ⁴ Department of Physiology and Neurobiology, University of Connecticut, Storrs, CT, USA, ⁵ Department of Clinical Genetics, Erasmus MC University Medical Center Rotterdam, Rotterdam, Netherlands, ⁶ Department of Computational Molecular Biology, Max Planck Institute for Molecular Genetics, Berlin, Germany, ⁷ Department of Biological Sciences, Institute for Structural and Molecular Biology, Birkbeck College, London, UK

OPEN ACCESS

Edited by:

Nicola Maggio,
The Chaim Sheba Medical Center,
Israel

Reviewed by:

HiroYuki Sakagami,
Kitasato University School of
Medicine, Japan
Cheryl Shoubridge,
University of Adelaide, Australia

*Correspondence:

Vera M. Kalscheuer
kalscheu@molgen.mpg.de;
Robert J. Harvey
r.j.harvey@ucl.ac.uk

Received: 23 October 2015

Accepted: 14 December 2015

Published: 11 January 2016

Citation:

Kalscheuer VM, James VM,
Himmelright ML, Long P, Oegema R,
Jensen C, Bienek M, Hu H, Haas SA,
Topf M, Hoogeboom AJM, Harvey K,
Walikonis R and Harvey RJ (2016)
Novel Missense Mutation A789V in
IQSEC2 Underlies X-Linked
Intellectual Disability in the MRX78
Family.
Front. Mol. Neurosci. 8:85.
doi: 10.3389/fnmol.2015.00085

Disease gene discovery in neurodevelopmental disorders, including X-linked intellectual disability (XLID) has recently been accelerated by next-generation DNA sequencing approaches. To date, more than 100 human X chromosome genes involved in neuronal signaling pathways and networks implicated in cognitive function have been identified. Despite these advances, the mutations underlying disease in a large number of XLID families remained unresolved. We report the resolution of MRX78, a large family with six affected males and seven affected females, showing X-linked inheritance. Although a previous linkage study had mapped the locus to the short arm of chromosome X (Xp11.4-p11.23), this region contained too many candidate genes to be analyzed using conventional approaches. However, our X-chromosome exome resequencing, bioinformatics analysis and inheritance testing revealed a missense mutation (c.C2366T, p.A789V) in *IQSEC2*, encoding a neuronal GDP-GTP exchange factor for Arf family GTPases (ArfGEF) previously implicated in XLID. Molecular modeling of *IQSEC2* revealed that the A789V substitution results in the insertion of a larger side-chain into a hydrophobic pocket in the catalytic Sec7 domain of *IQSEC2*. The A789V change is predicted to result in numerous clashes with adjacent amino acids and disruption of local folding of the Sec7 domain. Consistent with this finding, functional assays revealed that recombinant *IQSEC2*^{A789V} was not able to catalyze GDP-GTP exchange on Arf6 as efficiently as wild-type *IQSEC2*. Taken together, these results strongly suggest that the A789V mutation in *IQSEC2* is the underlying cause of XLID in the MRX78 family.

Keywords: ArfGEF, BRAG1, IQ-ArfGEF, *IQSEC2*, MRX78, XLID

INTRODUCTION

Intellectual disability (ID) is a developmental brain disorder characterized by impaired intellectual and adaptive functions, and can be defined by an IQ below 70 and limitations in intellectual functioning and adaptive behaviors. As a result of the excess in males affected by ID, and the identification of families where ID shows clear X-linked segregation, significant attention has focused on the genetics of X-linked intellectual disability (XLID)—a common, clinically and genetically complex disorder often arising from mutations in one of >100 genes on the X chromosome. XLID may be associated with other clinical, morphological, or behavioral symptoms (syndromic XLID) or appear without other associated defects (non-syndromic XLID). However, despite extensive genetic studies using conventional linkage/candidate gene analysis or analysis of copy number variants (CNVs), for a significant number of families, the underlying cause of XLID has remained unclear. Fortunately, the genetics of XLID has recently been accelerated by next-generation DNA sequencing and novel bioinformatics approaches for variant filtering (de Ligt et al., 2012; Rauch et al., 2012; Redin et al., 2014; Hu et al., 2015; Tzschach et al., 2015). However, analysis of large exome data sets from the general population has also revealed a number of “XLID genes” where truncating variants or previously published “mutations” are observed at a relatively high frequency in normal controls, calling into question whether they are indeed causal. For example, recent studies questioned the implication of *AGTR2*, *MAGT1*, *ZNF674*, *SRPX2*, *ATP6AP2*, *ARHGEF6*, *NXF5*, *ZCCHC12*, *ZNF41*, *ZNF81* and *RAB40AL* in XLID (Piton et al., 2013; Otdak et al., 2014). This highlights the vital importance of structure-function analyses for validating potentially disease-causing variants.

In this study, we have combined next-generation sequencing, variant filtering and structure-function assays to resolve the cause of XLID in a large family known as MRX78 (de Vries et al., 2002). A previous investigation of the MRX78 family revealed linkage to the short arm of chromosome X (Xp11.4-p11.23; de Vries et al., 2002). We present compelling evidence that the likely cause of XLID in the extended MRX78 pedigree with six affected males and seven affected females in four generations is a missense mutation in the known XLID gene *IQSEC2* (MIM*300522; Shoubbridge et al., 2010) encoding a neuronal ArfGEF (known as IQSEC2, BRAG1 and IQ-ArfGEF) involved in cytoskeletal organization, dendritic spine morphology and excitatory synaptic organization, along with a review of previously published *IQSEC2*-related XLID patients.

MATERIALS AND METHODS

Genetic Analysis

Written informed consent was obtained from the legal guardians of patients III-5 and III-8 regarding next-generation sequencing. This study was declared exempt from approval by the medical ethics committee of the Erasmus MC University Medical Center (decision MEC-2012-387). Confirmation of the mutation in the additional family members was performed on DNA

previously obtained and used for diagnostic purposes and was carried out according to Erasmus MC University Medical Center regulations for secondary use of tissue after diagnostic procedures. In addition, patients or legal guardians were informed and gave verbal consent to use remaining samples for scientific research. X-chromosome exome resequencing and bioinformatics analysis was performed as recently described (Hu et al., 2014, 2015). DNA from the affected male individual III-8 was used for constructing the sequencing library using the Illumina Genomic DNA Single End Sample Prep kit (Illumina, San Diego, CA, USA). Enrichment of the X-chromosomal exome was then performed using the Agilent SureSelect Human X Chromosome Kit (Agilent, Santa Clara, CA, USA), which contains 47,657 RNA baits for 7591 exons of 745 genes of the human X chromosome. Single-end deep sequencing was performed on the Illumina Genome Analyzer GAIIX (Illumina, San Diego, CA, USA). Reads were subsequently mapped to the human reference genome (hg18 without random fragments) with RazerS (Weese et al., 2009) tolerating a sequence difference up to 5 bp per read. We applied the split mapping tool SplazerS (version1.0; Emde et al., 2012) in order to detect short insertions (<30 bp) and larger deletions (<50 kb) from unmapped and indel-containing reads. In addition, large insertions/deletions were predicted using ExomeCopy (Love et al., 2011) by analysing changes in depth of coverage along the targeted regions. Single-nucleotide polymorphisms (SNPs) and short indels (<5 bp) were called with snpStore. In parallel, we used the Medical Resequencing Analysis Pipeline (MERAP; Hu et al., 2014). Here, the mapping was performed using SOAP2 allowing at most two mismatches, and requiring at least four reads for single-nucleotide variant (SNV) and indel detection. For both approaches all sequence variants were screened against public databases [dbSNP138, 1000 Genomes project, Exome Variant Server (ESP6500)], and the in-house database of the Max Planck Institute, Berlin for annotating likely non-pathogenic and previously reported neutral variants. In addition, the OMIM catalog and the Human Gene Mutation Database (HGMD) were used as a filter to identify all previously described mutations. PCR primers for mutation confirmation and segregation analysis were IQSEC2-D221F 5'-cctcttgctgtccttttcca-3' and IQSEC2-D221R 5'-tgggcccaaaattagttcaa-3'.

Building a Homology Model of Human IQSEC2

Structural templates for homology modeling of IQSEC2 were determined using HHPred¹ (Söding et al., 2005). Homology modeling of the Sec7 and PH domains of IQSEC2 relied on three template crystal structures. The human BIG1 SEC7 domain (PDB ID: 3LTL, sequence identity 42%) was used to model the SEC7 domain, human GEP100 IQ motif (PDB ID: 3QWM, sequence identity 70%) was used to model the PH domain and finally, the mouse Grp1 Arf GTPase exchange factor (PDB ID: 2R0D; DiNitto et al., 2007) was used to model parts of both the Sec7 and PH domains and to guide the orientation of the domains

¹<http://toolkit.tuebingen.mpg.de/hhpred>

relative to each other (overall sequence identity of 38%). A model of the 24 amino acid linker between the SEC7 and PH domains (residues 942–966) was calculated using I-TASSER² (Zhang, 2008; Roy et al., 2010, 2012), which predicts proteins structure from sequence using multiple threading alignments via LOMETS (Wu and Zhang, 2007) and iterative assembly simulations based on structural templates or by *ab initio* modeling. For this linker, I-TASSER built a model with a straight α -helix, based on structural coordinates from various homologous structures in PDB (PDB IDs: 3CC2G, 2KEGA, 1K73I, 1S72G, 1M90I, 1QVFG) with sequence similarities of 21–28% [confidence score (C-score) of -0.9]. This was consistent with secondary structure prediction methods; PSIPRED³ (Jones, 1999) and RaptorX⁴ (Källberg et al., 2012), which predicted residues 948–960 to form a helix with a high confidence ($>80\%$). Single pairwise, sequence-structure alignments were calculated using HHpred, then the alignments were combined manually to generate one multiple alignment of the entire IQSEC2 sequence with the four template structure sequences (three PDB structures and one model of the linker). Based on this alignment, 30 models were generated using MODELLER-9.10 and assessed with the Discrete Optimized Protein Energy (DOPE) statistical potential score (Shen and Sali, 2006). The model with the lowest DOPE score was selected as representative. The p.A789V mutation was modeled with the *swapaa* command in Chimera (Pettersen et al., 2004) using the Dunbrack backbone-dependent rotamer library (Dunbrack, 2002) and taking into account the lowest clash score, highest number of H-bonds and highest rotamer probability.

Site-Directed Mutagenesis and Expression Constructs

The missense mutation c.C2366T, p.A789V was introduced into full-length human pCAGGS-IQSEC2 using the QuikChange site-directed mutagenesis kit (Agilent) and the primers hIQSEC2-A789V1 5'-accggtgggagtggtcactctcatctgg-3' and hIQSEC2-A789V2 5'-ccaggatgaagtgaacctccaccggt-3'. Expression constructs were verified by Sanger DNA sequencing of the entire coding region.

Arf Activation Assay

Golgi-localized, ear-containing ARF-binding protein 3 (GGA3) pull-down of activated ARF GTPases was performed as previously described in Shoubridge et al. (2010). Plasmids encoding HA-ARF6 in pXS and FLAG-tagged wild-type IQSEC2, IQSEC2^{A789V} or IQSEC2^{E849K} in pCAGGS were co-transfected into HEK293 cells with Lipofectamine 2000 (Invitrogen, Carlsbad, CA, USA). Cells were harvested in lysis buffer (50 mM Tris-HCl, pH 7.5, 100 mM NaCl, 2 mM MgCl₂, 0.1% SDS, 0.5% sodium deoxycholate, 1% Triton X-100, 10% glycerol, and HALT protease inhibitor cocktail (Pierce, Rockford, IL, USA), and lysates were incubated with GST:GGA3 coupled to glutathione beads. Beads were washed in lysis buffer without protease

inhibitors and boiled in SDS-PAGE buffer. Samples were run on SDS-PAGE gels and transferred to PVDF membranes. The membranes were probed with primary antibodies against HA (Covance, Princeton, NJ, USA) or FLAG (Sigma, St. Louis, MO, USA) and IRDye secondary antibodies and visualized and quantified with the use of a LiCor Odyssey Infrared Imaging System. The fluorescence intensity of each of the bands was quantified with Image Studio Lite. ARF6-GTP bands were normalized to total ARF6 expression for each of the conditions, and then the ratio of normalized ARF6-GTP to normalized ARF6 was calculated for wild-type IQSEC2, IQSEC2^{A789V} and IQSEC2^{E849K}. The GGA pull-down assay was assessed by one-way ANOVA followed by Tukey's Multiple Comparison Test for *post hoc* analysis.

RESULTS

Clinical Re-assessment of Family MRX78

The revised pedigree of the MRX78 family is depicted in **Figure 1A** and a summary with clinical findings is presented in **Table 1**. Individual I-2 had mild ID and was illiterate. She had a stroke at age 71 and developed dementia thereafter. She passed away at age 80. She gave birth to 15 children; two were stillborn. Two sons and a daughter died in childhood, they were said to be “handicapped”, one son had spina bifida. All children were placed in foster homes. She had two brothers with normal cognition and three sisters. II-2 had mild ID with difficulty reading and writing. II-6 has ID. II-8 has learning difficulties and is unable to read or write. Her chromosome studies were normal and urine analysis was negative for MAO-A deficiency. Her husband (II-7) also had learning difficulties/ID. II-9 has severe ID, intractable epilepsy and does not speak, or interact socially. He does like physical contact (e.g., holding hands) and responds to his name. He developed walking difficulties in his fifties, with unstable gait (“as a drunk person”) and is now wheelchair bound. There is no tremor and his vision and hearing are good. III-1 and III-2: These brothers both have severe ID. They do not seem to recognize a familiar person and have no speech. They can be physically aggressive towards caretakers, and both are on levomepromazine therapy. Vision and hearing are normal. Urine metabolic investigations were normal, and there was no MAO-A deficiency. Subject III-1 has had one seizure as a teenager. III-3 has moderate ID and no seizures. His height is 176.5 cm, occipital frontal circumference (OFC) 55 cm, and he has no dysmorphic features. Urine metabolic investigations were normal, and MAO-A deficiency was excluded. III-4 had learning difficulties. III-5 was born at term after an uncomplicated pregnancy with birth weight 4400 grams. Developmental delay was evident from early age. At age 12 extensive investigations were performed. At this time he had a moderate to severe ID and severe behavioral problems, refractory to treatment, including Haldol and valproic acid. An EEG showed a diffuse encephalopathy, without epileptic discharges, a brain CT-scan was normal (data not shown). IQ testing age 16 years showed verbal IQ (VIQ) compatible to age 4.7 years, and performance IQ (PIQ) compatible to 4.1 years. He showed minor regression when he was retested at 28 years with the Wechsler Intelligence

²<http://zhanglab.ccmb.med.umich.edu/I-TASSER>

³<http://bioinf.cs.ucl.ac.uk/psipred/>

⁴<http://raptorx.uchicago.edu/>

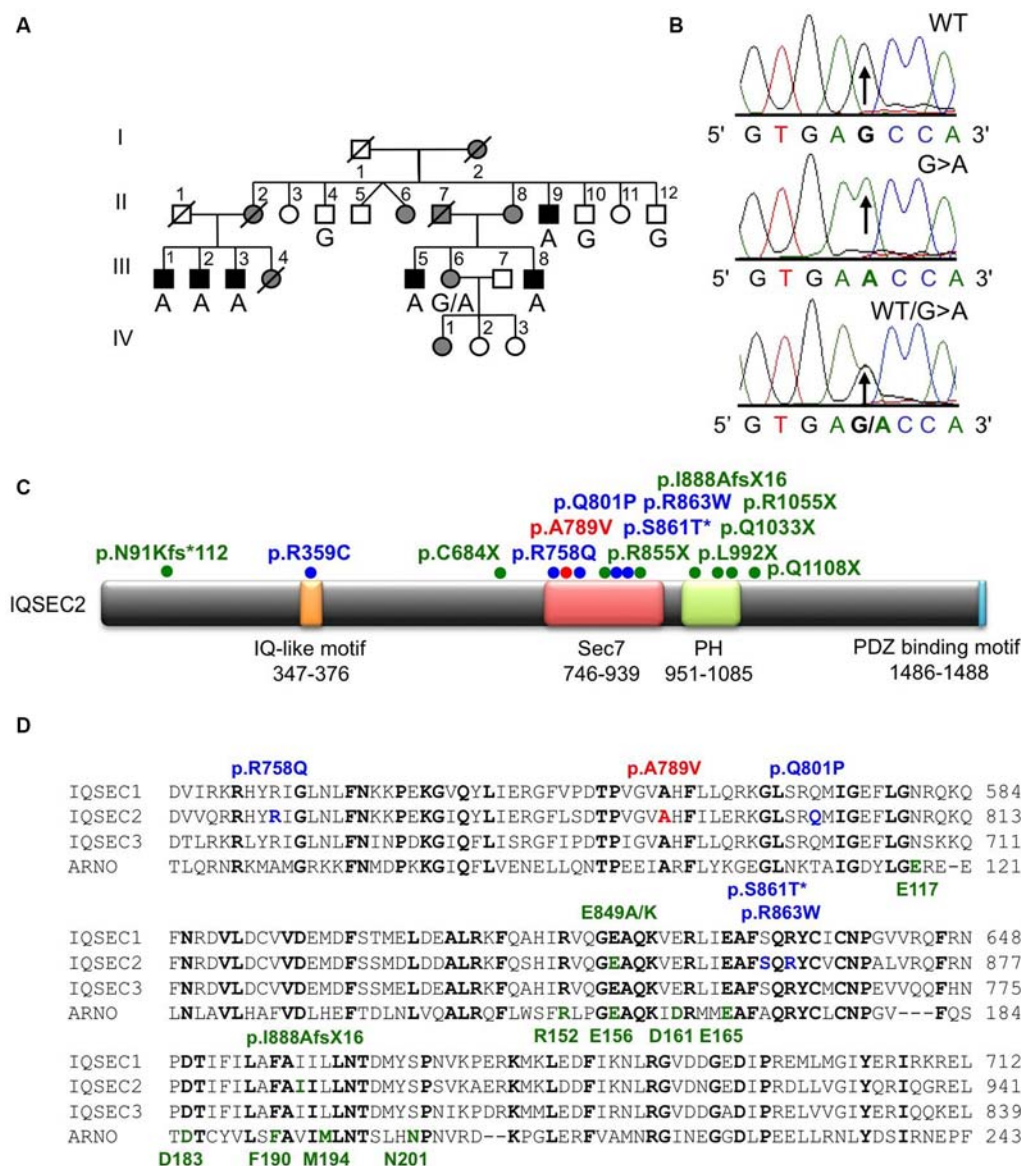


FIGURE 1 | Identification of an A789V mutation in *IQSEC2* in family MRX78. (A) Pedigree of the MRX78 family, which has been updated. Open symbols represent normal individuals, filled gray square represents a male with learning disabilities, filled black squares represent more severely affected males, filled gray circles represent affected females. Individual generations are numbered with Roman numerals on the left of each pedigree. Individuals tested for the nucleotide substitution in each family are indicated either A (mutant allele) or G (normal allele). **(B)** DNA sequence electropherograms for the chrX:53277996 G>A mutation reported in this study. **(C)** Schematic of the human *IQSEC2* protein with a regulatory IQ-like motif, a catalytic Sec7 domain, a pleckstrin homology (PH) domain and a PDZ binding motif. The relative locations of all currently known mutations in *IQSEC2* are shown (see also **Table 2**), * indicates that p.S861T is predicted to abolish a splice site. **(D)** Sequence alignments of *IQSEC1*, *IQSEC2* and *IQSEC3* showing the location of missense mutations in the Sec7 domain. Note that *IQSEC2* Sec7 domain mutations do not affect predicted GTPase binding residues (bold green type below alignments) as defined in the structure of the related Sec7 domain in the ArfGEF ARNO. Bold type indicates amino acids that are identical in all four sequences.

Scale (WISC) when his cognitive abilities were compatible to a 3.5 year-old. His social-emotional functioning was lower, at the level of a 6–18-month-old. Currently, at age 43 years, he is physically healthy, height is 181 cm and weight 90 kg. Neurological examination showed no abnormalities. He has good hearing and vision, with only mild hypermetropia (1.25 dpt). He is independent in basic daily activities such as dressing

and eating, but needs incentive. He is on risperidone treatment (0.5 mg twice daily) and laxantia. He communicates mostly through pictograms. He is quiet and introverted, with occasional verbal aggression, but not physical. He likes puzzles. He is easily distracted. He is suspected of autism spectrum disorder but has not been formally tested. Laboratory investigations in the past, including metabolic screen, Fragile X and chromosome studies

TABLE 1 | Summary of clinical features present in affected males and females in the MRX78 family.

Subject	Gender	Intellectual disability	Epilepsy	Behavioral problems
I-2	F	Mild, illiterate	–	–
II-2	F	Mild	–	–
II-6	F	Present	–	–
II-7	M	Learning difficulties*	–	–
II-8	F	Mild	–	–
II-9	M	Severe, does not speak	Present	Does not interact socially
III-1	M	Severe, does not speak	One seizure as a teenager	Aggressive against others
III-2	M	Severe, does not speak	–	Aggressive against others
III-3	M	Moderate	–	–
III-4	F	Learning difficulties	–	–
III-5	M	Moderate-severe	Diffuse encephalopathy without epileptic discharge	Occasional verbal aggression, suspected of ASD but not formally tested
III-6	F	Learning difficulties	–	–
III-8	M	Severe	–	Pervasive developmental disorder, ASD, severe aggressive outbursts against objects
IV-1	F	Learning difficulties	–	–

*Cause unknown.

were normal. III-6: During pregnancy her mother had several hospital admissions due to vaginal bleeding and premature contractions. Chromosome studies in chorion villi biopsy were normal (46, XX). She was born at term, with cleft lip/palate, her birth weight was 2785 grams and length 50 cm. She has mild learning difficulties, her OFC is 54 cm. She has three daughters, in whom no molecular testing was performed. She has had two first trimester miscarriages. The eldest daughter (IV:1) was born at 38 weeks of gestation, BW 2900 gram. She has learning difficulties and receives special education, her OFC is 57 cm. She is overweight. Her second daughter (IV:2) was born with ventricular septal defect, her BW was 2700 grams after 38 weeks of gestation. She has normal development, and no learning difficulties. Chromosome studies in chorion villi biopsy in the middle and youngest daughter were normal (46, XX). The youngest is still too young to assess her development. III-8: the pregnancy was complicated with episodes of vaginal bleeding and premature contractions. Developmental delay became evident in the first year of life. He had psychiatric consultation at age 11, due to problematic and aggressive behavior. Two years later he was diagnosed with a pervasive developmental disorder. Currently, at age 36, he has severe ID and autism spectrum disorder. He has a fixation on mirrors and sunshades, and will go around and close them. He has shown severe aggressive outbursts with destructive behavior towards furniture and other objects. He receives risperidone 2.5 mg daily. WISC testing age 20 years showed VIQ compatible to age 4.7 years, and PIQ compatible to 4.1 years. He was last tested at age 34 (Vineland Adaptive Behavior Scale) and he had shown mild regression over a 3-year period. His adaptive skills are now at a level for communication of a 1 year 7 month old, for daily activities at a 3-year-old level, for motor skills at a 1 year 5 month old level, and socialization skills compatible to a 10 month old. He is physically in good health. He underwent adenotomy, strabismus surgery, and excision of a follicular jaw cyst. His current height is 177 cm, and weight 82 kg. Neurological examination showed only brisk reflexes of the lower extremities. He has normal hearing

and myopia, with normal media and fundi. Fragile X testing was negative.

Identification of a p.A789V Mutation in IQSEC2 in Family MRX78

X-chromosome exome sequencing followed by bioinformatics analysis and filtering against publicly available datasets revealed three novel missense changes: *IQSEC2*, chrX:53277996G>A, p.A789V, consensus score 4.06, predicted as probably damaging (PolyPhen-2) and damaging (SIFT) with a CADD score of 19; *TXLNG*, chrX:16859571G>C, p.E423D with a low conservation score (0.02) and predicted as benign (Polyphen-2) and tolerated (SIFT) and CADD of 16; *WAS*, chrX:48542814T>G, donor, conservation score 3.69, and CADD of 12. This strongly suggested that the novel missense mutation identified in *IQSEC2* could be responsible for XLID in this family. Subsequent segregation analysis using Sanger DNA sequencing indicated that the *IQSEC2* chrX:53277996G>A variant co-segregated with the XLID phenotype in all individuals tested (Figures 1A,B).

IQSEC2 p.A789V Mutation is Predicted to Disrupt SEC7 Domain Folding

IQSEC2 has a multi-domain structure consisting of a regulatory IQ-like motif, a catalytic Sec7 domain, a pleckstrin homology (PH) domain and a PDZ binding motif (Figure 1C). Residue A789 is located in the catalytic Sec7 domain of *IQSEC2* and is highly conserved within *IQSEC1–3* (Figure 1D), whereas seven out of nine rare missense variants identified in this domain in normal controls (ExAC database⁵) are mostly present in single individual, and are not conserved residues between *IQSEC1–IQSEC3*. It is also notable that 3 of 4 previously reported *IQSEC2* missense mutations identified in XLID families are located in the Sec7 domain (Figure 1C; Shoubridge et al., 2010), including the previously investigated R863W mutation

⁵<http://exac.broadinstitute.org/gene/ENSG00000124313>

present in the large family MRX1. This R863 residue is the only highly conserved amino acid that is substituted to R863Q in a single normal female. To visualize the potential structural consequences of the p.A789V change, we built a comparative model of the IQSEC2 Sec7 and PH domains using the structures of three sequence-related ArfGEFs: BIG1, GEP100 and Grp1 (PDB ID: 3LTL, 3QWM). The resulting model revealed that A789 is located on the third short helix of nine in the Sec7 domain, although it is not one of the residues predicted to interact with Arf GTPases, GDP or Zn^{2+} binding (**Figures 1D, 2A**). The third and fourth helices come together closely and appear to form a hydrophobic pocket. The residues on these two helices are highly conserved and form a very similar structure in all Sec7-containing crystal structures in PDB, suggesting that the interaction between these helices may be of importance for proper folding of the Sec7 domain. Substitution of alanine at residue 789 with valine introduces a larger side-chain into this packed hydrophobic pocket between helices, which is predicted to cause numerous clashes with surrounding side-chains and/or backbones of residues V818, C821 and V822 (**Figure 2B**).

Mutation p.A789V in IQSEC2 Disrupts ArfGEF Activity

We also tested the GEF activity of full-length IQSEC2 and the IQSEC2^{A789V} mutant in a cellular model using a pull-down assay

using the adaptor protein Golgi-localized, ear-containing ARF-binding protein 3 (GGA3; **Figure 3A**). GGAs specifically interact with active, GTP-bound ARF but do not interact with inactive ARF GTPases. As a control, we used the IQSEC2^{E849K} dominant-negative mutation, which reduces the exchange activity of the IQSEC2 Sec7 domain by several orders of magnitude (Shoubridge et al., 2010). Co-transfection of ARF6 with wild-type IQSEC2 resulted in a ~ 5 -fold increase (5.5 ± 0.91 , mean \pm SEM, $n = 3$) in GTP-bound ARF6, but only a 2.5- to 1-fold increase when expressed with IQSEC2^{A789V} (2.5 ± 0.19) or IQSEC2^{E849K} (1.2 ± 0.19) respectively (**Figures 3B,C**). This is consistent with a significant loss of ArfGEF activity in the IQSEC2^{A789V} mutant. It is also noteworthy that the IQSEC2^{A789V} mutation does not appear to affect protein stability (**Figure 3B**), at least in cellular models.

DISCUSSION

This study reports the identification and functional characterization of a novel mutation (c.C2366T, p.A789V) in *IQSEC2* that based on variant filtering and segregation analysis likely presents the cause of XLID in the large family MRX78. A previous analysis in this family revealed X-linked inheritance with linkage to a 15.16 cM region on Xp11 (de Vries et al., 2002). Using molecular modeling of wild-type and mutant protein and assays for ArfGEF activity, we were

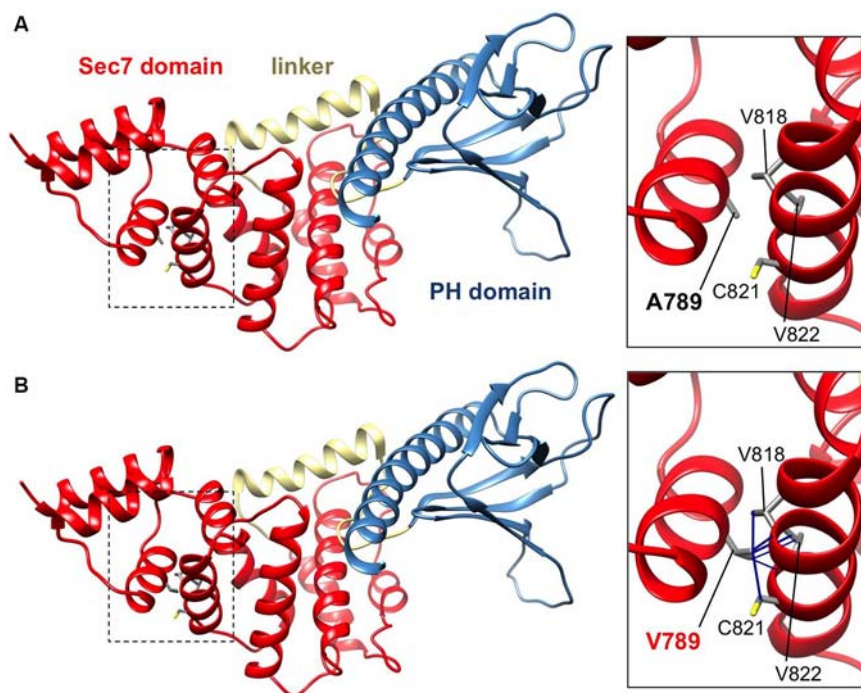
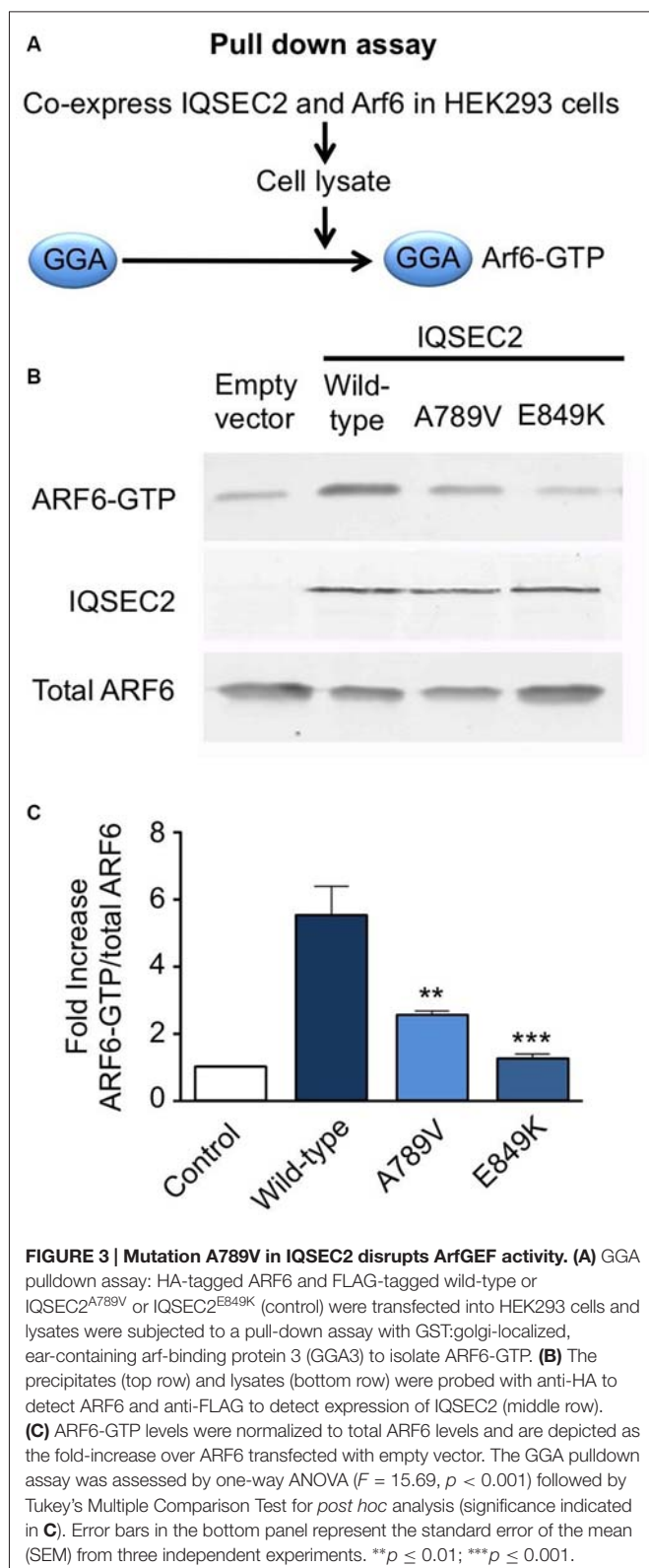


FIGURE 2 | IQSEC2 A789V mutation is predicted to disrupt SEC7 domain folding. Side views of the molecular models of IQSEC2 Sec7 and PH domains, with the Sec7 domain in red, the PH domain in blue and the linker between them in gold. Boxed areas show the areas expanded in the inserts to the right. **(A)** Normal IQSEC2 structure, and **(B)** mutant IQSEC2 harboring the p.A789V mutation. Note that the larger valine side-chain in the packed hydrophobic pocket between helices is predicted to cause numerous clashes with surrounding side-chains and/or backbones of residues V818, C821 and V822, indicating a potential disruption of the local fold in this region.



able to establish the likely pathomechanism for p.A789V: a disrupted hydrophobic pocket in the Sec7 domain structure, leading to loss of IQSEC2 ArfGEF activity. The identification

of *IQSEC2* as the causative gene for MRX78 is consistent with previous studies that have identified *IQSEC2* as a neuronally-expressed ArfGEF with a key role in excitatory synaptic transmission. At excitatory synapses, *IQSEC2* interacts with multivalent postsynaptic density (PSD) proteins such as IRSp53 (Sanda et al., 2009) and PSD-95 (Sakagami et al., 2008), forming a complex with *N*-methyl-D-aspartate (NMDA) receptors.

A recent reassessment of the MRX78 family by one of the co-authors (RO) revealed that except for one all affected males presented with moderate to severe ID, several affected males did not acquire speech skills and presented with behavioral disturbances. Females from this family who carry the mutation on one of her X-chromosomes presented with learning difficulties or mild ID. A summary with genetic findings and clinical presentations of other affected individuals who carry missense, nonsense, deletions, insertions and complex rearrangements is given in (Table 2). Shoubbridge et al. (2010) initially reported four missense mutations in *IQSEC2* associated with non-syndromic XLID (IQ domain p.R359C, Sec7 domain p.R758Q, p.Q801P and p.R863W). However, seizures, autistic traits, psychiatric problems and delayed early language skills were noted in different male individuals in this study. Furthermore, several *de novo* deleterious *IQSEC2* mutations have been reported in males and females who presented with seizure disorders, including Rett-like syndrome and Lennox-Gastaut syndrome: a frameshift mutation (p.N91Kfs*112) and a truncating chromosome breakpoint in intron 1 [46, X(tX;20)(p11.2;q11.2)] in the N-terminal part of *IQSEC2* (Morleo et al., 2008; Olson et al., 2015), a two base pair deletion resulting in p.C684X (region between IQ-like motif and Sec7 domain) (Gandomi et al., 2014), two additional mutations affecting the Sec7 domain (p.R855X and p.S861T that is predicted to abolish the native splice donor site; Rauch et al., 2012; Gandomi et al., 2014; Tran Mau-Them et al., 2014), and one *de novo* mutation (p.Q1108X) C-terminal to the PH domain (Allen et al., 2013). Additionally, Tran Mau-Them et al. (2014) reported two severely affected males with Rett-like features who carried *de novo* intragenic duplications, both of which were thought to disrupt *IQSEC2*. Furthermore, a p.I888Afs followed by a subsequent premature stop codon has been identified in a male with severe non-syndromic ID (Tzschach et al., 2015). *IQSEC2* mutations in ID patients which affect the PH domain of the protein have also been reported, including a p.L992X change in a patient with schizophrenia (Purcell et al., 2014), a *de novo* p.Q1033X mutation in a male with severe ID, epilepsy, strabismus and autistic features (Redin et al., 2014), and a *de novo* mutation (p.R1055X) in a female with severe ID, epilepsy and borderline macrocephaly (Tzschach et al., 2015). A partial *de novo* duplication of *TENM3* inserted into *IQSEC2* and subsequent formation of an in-frame *IQSEC2*-*TENM3* fusion gene was also recently reported. The resulting disruption of *IQSEC2* was thought to contribute to ID, epilepsy, progressive spasticity, and microcephaly in that patient (Gilissen et al., 2014). Furthermore, three maternally inherited duplications with disrupted *IQSEC2* in five males who presented with ID and behavioral disturbances were reported

TABLE 2 | IQSEC2 mutations and associated phenotypes.

Missense and nonsense mutations				
Nucleotide	Protein	Gender of affected and inheritance	Reported phenotype	Reference
c.1075C>T	p.R359C	4M and 1F, maternally inherited	Mild to moderate ID in males, non-syndromic [†] , female with learning difficulties	Shoubridge et al. (2010)
c.2273G>A	p.R758Q	8M, maternally inherited	Mild ID, non-syndromic [†]	Shoubridge et al. (2010)
c.C2366T	p.A789V	6M and 7F (MRX78), maternally inherited	Moderate to severe ID and behavioral disturbances in males, mild ID and learning difficulties in females	This study
c.2402A>C	p.Q801P	8M and 2F (MRX18), maternally inherited	Moderate to severe ID in males, non-syndromic [†] , carrier females with learning difficulties	Gedeon et al. (1994) and Shoubridge et al. (2010)
c.2563C>T	p.R855X	1M, <i>de novo</i>	ID, epilepsy, stereotypic hand movements, strabismus, language partially acquired but delayed, both language and motor skills regressed, behavioral disturbances including self-injury, abnormal MRI	Rauch et al. (2012) and Tran Mau-Them et al. (2014)
c.2582G>C	p.S861T, predicted to abolish splice site	1M, <i>de novo</i>	ID, developmental delay, seizures, hypotonia, vision impairments, plagiocephaly, autistic-like features, absent language skills, abnormal MRI	Suthers et al. (1998) and Gandomi et al. (2014)
c.2587C>T	p.R863W	12M (MRX1), maternally inherited	Moderate ID, non-syndromic [†]	Turner et al. (1971), Suthers et al. (1998), and Shoubridge et al. (2010)
c.2975T>A	p.L992X	1, gender not reported	Schizophrenia	Purcell et al. (2014)
c.3097C>T	p.Q1033X	1M, <i>de novo</i>	Severe ID, no speech, motor developmental delay, severe epilepsy, strabismus, autistic features	Redin et al. (2014)
c.3322C>T	p.Q1108X	1F, <i>de novo</i>	Lennox-Gastaut syndrome, global developmental delay	Allen et al. (2013)
c.3163C>T	p.R1055X	1F, <i>de novo</i>	Severe ID, epilepsy, borderline macrocephaly	Tzschach et al. (2015)
Small deletions/insertions				
Nucleotide	Protein	Gender and Inheritance	Reported phenotype	Reference
c.273_282del	p.N91KfsX112	1F, <i>de novo</i>	ID, features of Rett syndrome, no epilepsy, gait abnormalities, stereotypic hand movements, regression but did not lose purposeful hand skills, cranial MRI showed delayed myelination.	Olson et al. (2015)
c.2052_2053delCG	p.C684X	1M, <i>de novo</i>	ID, hypotonia, strabismus, astigmatism, cortical vision impairment, hypoplastic corpus callosum, myoclonic seizures, positional plagiocephaly with mild relative microcephaly, stereotypic hand movements	Gandomi et al. (2014)
c.2662dup	p.I888AfsX16	1M, <i>de novo</i>	Severe ID, non-syndromic	Tzschach et al. (2015)
Gross deletions and insertions without <i>HUWE1</i> gene involvement				
Nucleotide		Gender and Inheritance	Reported phenotype	Reference
Deletion 400 kb also including <i>KDM5C</i>		1F, <i>de novo</i>	Severe ID and autistic-behavior	Fieremans et al. (2015)
Duplication 22 kb incl. ex. 3		1M, <i>de novo</i>	Severe ID, language partially acquired, midline stereotypic hand movements, partial epilepsy, regression of language and motor skills, behavioral disturbances	Tran Mau-Them et al. (2014)
Duplication 42 kb incl. ex. 3–7		1M, <i>de novo</i>	Severe ID, postnatal microcephaly, no speech, no purposeful hand skills, seizures, behavioral disturbances	Tran Mau-Them et al. (2014)
62 kb insertion of <i>TENM3</i> sequence, fusion gene		1F?, <i>de novo</i>	Severe ID, microcephaly, epilepsy, progressive spasticity, small hands and feet, poor vision	Gilissen et al. (2014)
Duplication 361 kb with disrupted <i>IQSEC2</i> long isoform		1M, maternally inherited	Language delay and behavioral problems	Moey et al. (2015)
Duplication 403 kb with short <i>IQSEC2</i> isoform duplicated		3M, maternally inherited	Mild-moderate ID, mild learning difficulties in one male, autism spectrum disorder, obsessive behavior	Moey et al. (2015)
Duplication 579 kb, including <i>TSPYL</i> , <i>KDM5C</i> and <i>IQSEC2</i>		1M, maternally inherited	Global delay, severe expressive speech delay, behavioral disturbances	Moey et al. (2015)

(Continued)

TABLE 2 | (Continued).

Complex rearrangements		
Description	Reported phenotype	Reference
Balanced 46, X, t(X;20) (p11.2;q11.2) <i>de novo</i>	Severe ID, delayed language and motor development, infantile spasms, regression	Morleo et al. (2008)

[†]seizures, autistic traits, psychiatric problems and delayed early language skills were noted in different individuals in this study, although none of these additional phenotypes were consistent in all affected male individuals in the families studied.

by Moey et al. (2015), and a *de novo* deletion of *IQSEC2* and the XLID gene *KDM5C* (MIM*314690; Jensen et al., 2005) has been identified in a girl with severe ID and autistic behavior (Fieremans et al., 2015). Although originally described as non-syndromic XLID, newly acquired clinical data from the MRX78 family suggests that additional features might be associated with the *IQSEC2* p.A789V mutation, including variable seizures in males, which is consistent with other reports, and behavioral disturbances in five out of six affected males. By contrast, heterozygous female have learning disabilities. As *IQSEC2* is one of the few genes that escape X-inactivation in females with an expression level similar in males and females (Moey et al., 2015) we hypothesize that, in these female carriers, the missense mutation is sufficient to produce symptoms but that the mutant protein has residual function and in addition that there is some compensation from the normal allele. This is in contrast to early truncating mutations in *IQSEC2*, which in females are associated with a more severe phenotype including infantile spasms, epilepsy, autistic features, Lennox Gastaut syndrome and Rett-like syndrome. Given that in several severely affected females *IQSEC2* is either deleted on one of the X-chromosomes or the truncating change is located early in the N-terminus and therefore can be assumed to result in protein degradation due to nonsense-mediated mRNA decay, it is unlikely that in these cases the mutations produce a dominant negative effect. Thus, it is very likely that *IQSEC2* is a dosage-sensitive gene that needs to be tightly regulated for

normal cognitive function in males and females and that *IQSEC2* mutations can cause a spectrum of clinical features in both sexes.

AUTHOR CONTRIBUTIONS

VMK, RW and RJH designed the experiments; AJMH and RO contributed DNA samples and clinical evaluation; VMJ, MLH, PL, CJ, MB, MT and KH performed the experiments; VMK, HH, SAH, MT, KH, RW, and RJH analyzed the data; VMK, RW and RJH wrote the paper. All authors were involved in revising the paper for important intellectual content, and gave final approval of the version to be published.

FUNDING

This work was supported by the Medical Research Council (J004049 to RJH and KH) and the EU FP7 project GENCODYS, grant number 241995 (to HH and VMK) and the Whitehall Foundation (grant number 2010-08-68 to RSW). The funders had no role in study design, data collection and analysis, decision to publish, or preparation of the manuscript. The authors would like to thank the Exome Aggregation Consortium and the groups that provided exome variant data for comparison. A full list of contributing groups can be found at <http://exac.broadinstitute.org/about>.

REFERENCES

- Allen, A. S., Berkovic, S. F., Cossette, P., Delanty, N., Dlugos, D., Eichler, E. E., et al. (2013). *De novo* mutations in epileptic encephalopathies. *Nature* 501, 217–221. doi: 10.1038/nature12439
- de Ligt, J., Willemsen, M. H., van Bon, B. W., Kleefstra, T., Yntema, H. G., Kroes, T., et al. (2012). Diagnostic exome sequencing in persons with severe intellectual disability. *N. Engl. J. Med.* 367, 1921–1929. doi: 10.1056/NEJMoa1206524
- de Vries, B. B., Breedveld, G. J., Deelen, W. H., Breuning, M. H., Niermeijer, M. F., and Heutink, P. (2002). Another family with nonspecific X-linked mental retardation (MRX78) maps to Xp11.4–p11.23. *Am. J. Med. Genet.* 111, 443–445. doi: 10.1002/ajmg.10576
- DiNitto, J. P., Delprato, A., Gabe Lee, M. T., Cronin, T. C., Huang, S., Guilherme, A., et al. (2007). Structural basis and mechanism of autoregulation in 3-phosphoinositide-dependent Grp1 family Arf GTPase exchange factors. *Mol. Cell* 28, 569–583. doi: 10.1016/j.molcel.2007.09.017
- Dunbrack, R. L. Jr. (2002). Rotamer libraries in the 21st century. *Curr. Opin. Struct. Biol.* 12, 431–440. doi: 10.1016/s0959-440x(02)00344-5
- Emde, A. K., Schulz, M. H., Weese, D., Sun, R., Vingron, M., Kalscheuer, V. M., et al. (2012). Detecting genomic indel variants with exact breakpoints in single- and paired-end sequencing data using SplazerS. *Bioinformatics* 28, 619–627. doi: 10.1093/bioinformatics/bts019
- Fieremans, N., Van Esch, H., de Ravel, T., Van Driessche, J., Belet, S., Bauters, M., et al. (2015). Microdeletion of the escape genes *KDM5C* and *IQSEC2* in a girl with severe intellectual disability and autistic features. *Eur. J. Med. Genet.* 58, 324–327. doi: 10.1016/j.ejmg.2015.03.003
- Gandomi, S. K., Farwell Gonzalez, K. D., Parra, M., Shahmirzadi, L., Mancuso, J., Pichurin, P., et al. (2014). Diagnostic exome sequencing identifies two novel *IQSEC2* mutations associated with X-linked intellectual disability with seizures: implications for genetic counseling and clinical diagnosis. *J. Genet. Couns.* 23, 289–298. doi: 10.1007/s10897-013-9671-6
- Gedeon, A., Kerr, B., Mulley, J., and Turner, G. (1994). Pericentromeric genes for non-specific X-linked mental retardation (MRX). *Am. J. Med. Genet.* 51, 553–564. doi: 10.1002/ajmg.1320510453
- Gilissen, C., Hehir-Kwa, J. Y., Thung, D. T., van de Vorst, M., van Bon, B. W., Willemsen, M. H., et al. (2014). Genome sequencing identifies major causes of severe intellectual disability. *Nature* 511, 344–347. doi: 10.1038/nature13394

- Hu, H., Haas, S. A., Chelly, J., Van Esch, H., Raynaud, M., de Brouwer, A. P., et al. (2015). X-exome sequencing of 405 unresolved families identifies seven novel intellectual disability genes. *Mol. Psychiatry*. doi: 10.1038/mp.2014.193 [Epub ahead of print].
- Hu, H., Wienker, T. F., Musante, L., Kalscheuer, V. M., Kahrizi, K., Najmabadi, H., et al. (2014). Integrated sequence analysis pipeline provides one-stop solution for identifying disease-causing mutations. *Hum. Mutat.* 35, 1427–1435. doi: 10.1002/humu.22695
- Jensen, L. R., Amende, M., Gurok, U., Moser, B., Gimmel, V., Tzschach, A., et al. (2005). Mutations in the JARID1C gene, which is involved in transcriptional regulation and chromatin remodeling, cause X-linked mental retardation. *Am. J. Hum. Genet.* 76, 227–236. doi: 10.1086/427563
- Jones, D. T. (1999). Protein secondary structure prediction based on position-specific scoring matrices. *J. Mol. Biol.* 292, 195–202. doi: 10.1006/jmbi.1999.3091
- Källberg, M., Wang, H., Wang, S., Peng, J., Wang, Z., Lu, H., et al. (2012). Template-based protein structure modeling using the RaptorX web server. *Nat. Protoc.* 7, 1511–1522. doi: 10.1038/nprot.2012.085
- Love, M. I., Myšičková, A., Sun, R., Kalscheuer, V., Vingron, M., and Haas, S. A. (2011). Modeling read counts for CNV detection in exome sequencing data. *Stat. Appl. Genet. Mol. Biol.* 10:52. doi: 10.2202/1544-6115.1732
- Moey, C., Hinze, S. J., Brueton, L., Morton, J., McMullan, D. J., Kamien, B., et al. (2015). Xp11.2 microduplications including IQSEC2, TSPYL2 and KDM5C genes in patients with neurodevelopmental disorders. *Eur. J. Hum. Genet.* doi: 10.1038/ejhg.2015.123 [Epub ahead of print].
- Morleo, M., Iaconis, D., Chitayat, D., Peluso, I., Marzella, R., Renieri, A., et al. (2008). Disruption of the IQSEC2 transcript in a female with X;autosome translocation t(X;20)(p11.2;q11.2) and a phenotype resembling X-linked infantile spasms (ISSX) syndrome. *Mol. Med. Rep.* 1, 33–39. doi: 10.3892/mmr.1.1.33
- Oldak, M., Ścieżyńska, A., Mlynarski, W., Borowiec, M., Ruszkowska, E., Szulborski, K., et al. (2014). Evidence against RAB40AL being the locus for Martin-Probst X-linked deafness-intellectual disability syndrome. *Hum. Mutat.* 35, 1171–1174. doi: 10.1002/humu.22620
- Olson, H. E., Tambunan, D., LaCoursiere, C., Goldenberg, M., Pinsky, R., Martin, E., et al. (2015). Mutations in epilepsy and intellectual disability genes in patients with features of Rett syndrome. *Am. J. Med. Genet. A* 167, 2017–2025. doi: 10.1002/ajmg.a.37132
- Pettersen, E. F., Goddard, T. D., Huang, C. C., Couch, G. S., Greenblatt, D. M., Meng, E. C., et al. (2004). UCSF Chimera – A visualization system for exploratory research and analysis. *J. Comput. Chem.* 25, 1605–1612. doi: 10.1002/jcc.20084
- Piton, A., Redin, C., and Mandel, J. L. (2013). XLID-causing mutations and associated genes challenged in light of data from large-scale human exome sequencing. *Am. J. Hum. Genet.* 93, 368–383. doi: 10.1016/j.ajhg.2013.06.013
- Purcell, S. M., Moran, J. L., Fromer, M., Ruderfer, D., Solovieff, N., Roussos, P., et al. (2014). A polygenic burden of rare disruptive mutations in schizophrenia. *Nature* 506, 185–190. doi: 10.1038/nature12975
- Rauch, A., Wiczorek, D., Graf, E., Wieland, T., Ende, S., Schwarzmayr, T., et al. (2012). Range of genetic mutations associated with severe non-syndromic sporadic intellectual disability: an exome sequencing study. *Lancet* 380, 1674–1682. doi: 10.1016/S0140-6736(12)61480-9
- Redin, C., Gérard, B., Lauer, J., Herenger, Y., Muller, J., Quartier, A., et al. (2014). Efficient strategy for the molecular diagnosis of intellectual disability using targeted high-throughput sequencing. *J. Med. Genet.* 51, 724–736. doi: 10.1136/jmedgenet-2014-102554
- Roy, A., Kucukural, A., and Zhang, Y. (2010). I-TASSER: a unified platform for automated protein structure and function prediction. *Nat. Protoc.* 5, 725–738. doi: 10.1038/nprot.2010.5
- Roy, A., Yang, J., and Zhang, Y. (2012). COFACTOR: an accurate comparative algorithm for structure-based protein function annotation. *Nucleic Acids Res.* 40, W471–W477. doi: 10.1093/nar/gks372
- Sakagami, H., Sanda, M., Fukaya, M., Miyazaki, T., Sukegawa, J., Yanagisawa, T., et al. (2008). IQ-ArfGEF/BRAG1 is a guanine nucleotide exchange factor for Arf6 that interacts with PSD-95 at postsynaptic density of excitatory synapses. *Neurosci. Res.* 60, 199–212. doi: 10.1016/j.neures.2007.10.013
- Sanda, M., Kamata, A., Katsumata, O., Fukunaga, K., Watanabe, M., Kondo, H., et al. (2009). The postsynaptic density protein, IQ-ArfGEF/BRAG1, can interact with IRSp53 through its proline-rich sequence. *Brain Res.* 1251, 7–15. doi: 10.1016/j.brainres.2008.11.061
- Shen, M. Y., and Salí, A. (2006). Statistical potential for assessment and prediction of protein structures. *Protein Sci.* 15, 2507–2524. doi: 10.1110/ps.062416606
- Shoubridge, C., Tarpey, P. S., Abidi, F., Ramsden, S. L., Rujirabanjerd, S., Murphy, J. A., et al. (2010). Mutations in the guanine nucleotide exchange factor gene IQSEC2 cause nonsyndromic intellectual disability. *Nat. Genet.* 42, 486–488. doi: 10.1038/ng.588
- Söding, J., Biegert, A., and Lupas, A. N. (2005). The HHpred interactive server for protein homology detection and structure prediction. *Nucleic Acids Res.* 33, W244–W248. doi: 10.1093/nar/gki408
- Suthers, G. K., Turner, G., and Mulley, J. C. (1998). A non-syndromal form of X-linked mental retardation (XLMR) is linked to DXS14. *Am. J. Med. Genet.* 30, 485–491. doi: 10.1002/ajmg.1320300151
- Tran Mau-Them, F., Willems, M., Albrecht, B., Sanchez, E., Puechberty, J., Ende, S., et al. (2014). Expanding the phenotype of IQSEC2 mutations: truncating mutations in severe intellectual disability. *Eur. J. Hum. Genet.* 22, 289–292. doi: 10.1038/ejhg.2013.113
- Turner, G., Turner, B., and Collins, E. (1971). X-linked mental retardation without physical abnormality: renpenning's syndrome. *Dev. Med. Child Neurol.* 13, 71–78. doi: 10.1111/j.1469-8749.1971.tb03033.x
- Tzschach, A., Grasshoff, U., Beck-Woedl, S., Dufke, C., Bauer, C., Kehrer, M., et al. (2015). Next-generation sequencing in X-linked intellectual disability. *Eur. J. Hum. Genet.* 11, 1513–1518. doi: 10.1038/ejhg.2015.5
- Weese, D., Emde, A. K., Rausch, T., Döring, A., and Reinert, K. (2009). RazerS—fast read mapping with sensitivity control. *Genome Res.* 19, 1646–1654. doi: 10.1101/gr.088823.108
- Wu, S., and Zhang, Y. (2007). LOMETS: a local meta-threading-server for protein structure prediction. *Nucleic Acids Res.* 35, 3375–3382. doi: 10.1093/nar/gkm251
- Zhang, Y. (2008). I-TASSER server for protein 3D structure prediction. *BMC Bioinformatics* 9:40. doi: 10.1186/1471-2105-9-40

Conflict of Interest Statement: The authors declare that the research was conducted in the absence of any commercial or financial relationships that could be construed as a potential conflict of interest.

Copyright © 2016 Kalscheuer, James, Himelright, Long, Oegema, Jensen, Bienek, Hu, Haas, Topf, Hoozeboom, Harvey, Walikonis and Harvey. This is an open-access article distributed under the terms of the Creative Commons Attribution License (CC BY). The use, distribution and reproduction in other forums is permitted, provided the original author(s) or licensor are credited and that the original publication in this journal is cited, in accordance with accepted academic practice. No use, distribution or reproduction is permitted which does not comply with these terms.



Rare Variants in Neurodegeneration Associated Genes Revealed by Targeted Panel Sequencing in a German ALS Cohort

Stefanie Krüger¹, Florian Battke¹, Andrea Sprecher¹, Marita Munz^{1,2}, Matthias Synofzik^{2,3}, Ludger Schöls^{2,3}, Thomas Gasser^{2,3}, Torsten Grehl⁴, Johannes Prudlo^{5,6†} and Saskia Biskup^{1,2*†}

¹ CeGaT GmbH, Center for Genomics and Transcriptomics, Tübingen, Germany, ² Department of Neurodegenerative Diseases, Hertie-Institute for Clinical Brain Research, University of Tübingen, Tübingen, Germany, ³ German Research Center for Neurodegenerative Diseases, Tübingen, Germany, ⁴ Department of Neurology, BG-Kliniken Bergmannsheil GmbH, Ruhr-University Bochum, Bochum, Germany, ⁵ Department of Neurology, University of Rostock, Rostock, Germany, ⁶ German Research Center for Neurodegenerative Diseases, Rostock, Germany

OPEN ACCESS

Edited by:

Robert J. Harvey,
UCL School of Pharmacy, UK

Reviewed by:

Margaret M. DeAngelis,
University of Utah, USA
Stephane Pelletier,
St. Jude Children's Research
Hospital, USA

*Correspondence:

Saskia Biskup
saskia.biskup@cegat.de

[†] These authors have shared last
author.

Received: 16 May 2016

Accepted: 20 September 2016

Published: 13 October 2016

Citation:

Krüger S, Battke F, Sprecher A,
Munz M, Synofzik M, Schöls L,
Gasser T, Grehl T, Prudlo J and
Biskup S (2016) Rare Variants
in Neurodegeneration Associated
Genes Revealed by Targeted Panel
Sequencing in a German ALS Cohort.
Front. Mol. Neurosci. 9:92.
doi: 10.3389/fnmol.2016.00092

Amyotrophic lateral sclerosis (ALS) is a progressive fatal multisystemic neurodegenerative disorder caused by preferential degeneration of upper and lower motor neurons. To further delineate the genetic architecture of the disease, we used comprehensive panel sequencing in a cohort of 80 German ALS patients. The panel covered 39 confirmed ALS genes and candidate genes, as well as 238 genes associated with other entities of the neurodegenerative disease spectrum. In addition, we performed repeat length analysis for *C9orf72*. Our aim was to (1) identify potentially disease-causing variants, to (2) assess a proposed model of polygenic inheritance in ALS and to (3) connect ALS with other neurodegenerative entities. We identified 79 rare potentially pathogenic variants in 27 ALS associated genes in familial and sporadic cases. Five patients had pathogenic *C9orf72* repeat expansions, a further four patients harbored intermediate length repeat expansions. Our findings demonstrate that a genetic background of the disease can actually be found in a large proportion of seemingly sporadic cases and that it is not limited to putative most frequently affected genes such as *C9orf72* or *SOD1*. Assessing the polygenic nature of ALS, we identified 15 patients carrying at least two rare potentially pathogenic variants in ALS associated genes including pathogenic or intermediate *C9orf72* repeat expansions. Multiple variants might influence severity or duration of disease or could account for intrafamilial phenotypic variability or reduced penetrance. However, we could not observe a correlation with age of onset in this study. We further detected potentially pathogenic variants in other neurodegeneration associated genes in 12 patients, supporting the hypothesis of common pathways in neurodegenerative diseases and linking ALS to other entities of the neurodegenerative spectrum. Most interestingly we found variants in *GBE1* and *SPG7* which might represent differential diagnoses. Based

on our findings, we recommend two-staged genetic testing for ALS in Germany in patients with familial and sporadic ALS, comprising *C9orf72* repeat analysis followed by comprehensive panel sequencing including differential diagnoses that impair motor neuron function to meet the complexity of ALS genetics.

Keywords: amyotrophic lateral sclerosis, neurodegeneration, next generation sequencing, genetic heterogeneity, polygenic inheritance

INTRODUCTION

Amyotrophic lateral sclerosis (ALS) is a devastating multisystemic neurodegenerative disorder characterized by degeneration of upper and lower motor neurons in the motor cortex, brain stem, and spinal cord (Peters et al., 2015). ALS can be inherited in an autosomal dominant, autosomal recessive or X-linked manner. About 10% of cases are considered as being familial (fALS), whereas the remaining 90% seem to occur sporadically (sALS) with no family history of ALS. Since the first discovery of *SOD1* mutations being causative for ALS1 in 1993 (Rosen et al., 1993), researchers all over the world have made great effort to further delineate the genetic basis underlying ALS. Today, more than 30 confirmed major disease genes are listed by the Amyotrophic Lateral Sclerosis Online genetics Database (ALSO¹), the most frequently affected being *C9orf72* (40% fALS, 5–6% sALS; pathogenic repeat expansion in the non-coding region between exons 1a and 1b, detection by repeat analysis), *SOD1* (20% fALS, 3% sALS), *FUS* (5% fALS, <1% sALS) and *TARDBP* (3% fALS, 2% sALS) (Abel et al., 2012; Su et al., 2014).

Screening of the known ALS genes identifies pathogenic mutations in more than 60% of fALS cases. However, the same genes that can be affected in fALS can also be found mutated in sporadic cases, e.g., due to incomplete penetrance, false paternity, recessive inheritance or *de novo* mutations (Su et al., 2014). Mutations in disease genes affect different molecular pathways which promote motor neuron degeneration and include protein misfolding and subsequent aggregation, mitochondrial dysfunction and oxidative stress, impaired RNA processing, glutamate excitotoxicity and impaired axonal transport (Redler and Dokholyan, 2012; Shaw, 2005). These findings provided fundamental insight into basic underlying pathomechanisms and additionally linked ALS to other disease entities like frontotemporal dementia (FTD) or hereditary spastic paraplegia (HSP).

With the application of genome-wide association studies (GWASs) and high throughput sequencing technologies (next generation sequencing, NGS), a large number of additional disease genes, disease modifiers, and risk factors have been identified especially in sALS. GWASs suggest that genetic factors might contribute to a minimum of 23% of disease risk, whereupon such factors do not necessarily have to be directly causative but instead may act as risk factors or disease modifiers (e.g., age of onset, disease progression) in the interplay with environmental and stochastic factors (Renton et al., 2014; Marangi and Traynor, 2015). Numerous GWASs

have been published which showed associations of various loci with ALS containing potential risk genes such as *FGGY*, *ITPR2* and *UNC13A* (Marangi and Traynor, 2015) but until now, causative variants in most of these genes have not been identified. As GWASs are based on the “common disease – common variant” hypothesis and odds ratios associated with risk alleles are usually low, they are solely suitable for the identification of common disease modifiers with low effect size in complex disorders rather than rare causative variants with large effect sizes. By contrast, NGS represents a powerful, groundbreaking approach to detect rare variants with moderate or high penetrance in Mendelian diseases without having access to large pedigrees (He et al., 2014). ALS and other neurodegenerative diseases which are characterized by great genetic heterogeneity and sometimes overlapping symptoms or even atypical phenotypes benefit to a great extent from NGS and the possibility to analyze all genes implicated in the disease in one approach. During the last years, the use of NGS encompassed and considerably increased the number of identified disease genes and risk factors for ALS, generating further insight into underlying pathomechanisms at the same time. One example is the recent discovery of the mitochondrial protein CHCHD10 as being implicated in ALS which for the first time proves a direct impact of mitochondria in the pathogenesis of the disease, a result obtained by exome sequencing in several families affected by ALS (e.g., Bannwarth et al., 2014; Müller et al., 2014; Kurzwelly et al., 2015). As sequencing costs and turnaround times substantially decreased during the last years, the broad application of NGS has triggered a fundamental shift not only in clinical genetics but also in research on rare heritable diseases. Additionally, by the analysis of large numbers of genes in parallel, it has become evident that some patients carry potentially pathogenic variants in genes that are associated with other entities of the neurodegenerative spectrum. Besides this, one emerging theme in ALS genetics is the presumption that ALS might be a complex disease. This view arises mainly from the observation of reduced penetrance in pedigrees affected by fALS and the partially missing heritability in sporadic cases (van Blitterswijk et al., 2012; He et al., 2014). In recent studies, the authors applied NGS to identify patients who carried pathogenic or potentially pathogenic variants in more than one disease gene with frequencies ranging from 1.6% to 31.7% in fALS and sALS cohorts (van Blitterswijk et al., 2012; Kenna et al., 2013; Cady et al., 2015). However, these studies additionally point out that the genetic basis underlying ALS in cohorts of different European countries and the US differs due to founder effects and thus should not be assumed to be homogeneous.

¹<http://alsod.iop.kcl.ac.uk/home.aspx>

Here we hypothesize that ALS is caused by polygenic contributions from many disease-causing or disease-modifying gene variants which encompass not only known ALS genes but also other genes from the neurodegenerative disease spectrum. To investigate this hypothesis, we used a high-coverage targeted high-throughput sequencing approach to detect variants in 39 ALS associated genes as well as 238 additional genes that are linked to other neurodegenerative diseases in a German cohort of 80 clinically well characterized ALS patients. We aim at identifying known causative mutations and novel variants, to report on patients who carry multiple potentially disease causing variants or variants in genes which are implicated not only in ALS, but also in other neurodegenerative disorders. To our knowledge, this is the first report on extensive genetic screening in a German ALS cohort including not only confirmed ALS genes but also possible candidate genes, modifiers and risk factors to assess the great genetic heterogeneity of ALS in Germany.

MATERIALS AND METHODS

Study Participants

Our cohort includes 80 unrelated clinically diagnosed ALS patients (55% male, 45% female; 7.5% familial, 92.5% sporadic; 82.5% ALS, 6.25% ALS-FTD, 2.5% flail leg, 2.5% flail arm, 6.25% primary lateral sclerosis (PLS)). Mean age of disease onset was 60.1 years (range 29–88 years). Patients were recruited consecutively in ALS outpatient clinics at the university hospitals Rostock and Bochum (Germany). Relationship was excluded by evaluation of family history. Only one affected individual per family was included in this study and there was no evidence of relationship between any study participants. Informed written consent was obtained from all participants. The study was approved by the local medical ethics committee of Rostock University (A2009-10 and A2011-56) and conducted in accordance with the Declaration of Helsinki.

DNA Extraction

Genomic DNA was extracted from EDTA blood using the QIAamp DNA Blood Mini Kit (Qiagen, Hilden, Germany) according to the manufacturer's protocol.

C9orf72 Repeat Analysis

All subjects were screened for a pathological repeat expansion in the *C9orf72* gene (GenBank NM_018325.3, NM_145005.5) using fragment length analysis of fluorescence labeled PCR products as repeat expansions cannot be detected by NGS (method according to DeJesus-Hernandez et al., 2011). Based on a repeat primed PCR we determined the size of GGGGCC repeats (method according to Renton et al., 2011). Repeat lengths of ≥ 30 units were considered as being pathogenic, whereas repeat lengths of 20 to 29 units are considered as intermediate.

Targeted Resequencing

Genomic DNA was enriched using a custom design Agilent SureSelect in solution kit. The design of our diagnostic panel for neurodegenerative diseases (277 genes in total) included 14 genes which were classified as disease genes when this study was initiated, 25 putative candidate genes, modifiers, and risk factors identified by literature research as being most presumably implicated in ALS (e.g., by GWAS, experimental evidence, or connected pathways; **Table 1**), as well as 238 genes associated with other neurodegenerative diseases (for example genes associated with FTD, HSP and others; see Supplementary Data, 763 kb in total). Sequencing was performed using barcoded libraries on the SOLiD 5500xl platform according to the manufacturer's instructions (Fragment Library Preparation 5500 Series SOLiD™ Systems, User Guide, Applied Biosystems by Life Technology). Approximately 2.3 million on target reads were generated per sample and the mean coverage on target was 184.2 sequencing reads with a mean mapping quality of 85.3. On average 89.4% of bases were covered by ≥ 10 reads/base per sample. The primary data analysis was performed using Lifescape (versions v2.5-r0 and v2.5-r2.5.1).

Variant Filtering

Only variants (SNVs/small indels) with a minor allele frequency (MAF) of $\leq 1\%$ in coding and flanking intronic regions (± 8 base pairs) and the UTR regions were evaluated. Known disease causing mutations which are listed in the HGMD database were evaluated in coding and flanking intronic regions up to ± 30 base pairs and up to a MAF of $\leq 5\%$. Population frequencies are adapted from the following databases: 1000 Genomes, dbSNP, Exome Variant Server, ExAC and an internal database. Our quality criteria required coverage of ≥ 10 quality reads per base and a novel allele frequency (NAF) of ≥ 0.3 . Detected variants were assessed based on their MAF, current literature and widely used Online databases [e.g., OMIM (McKusick-Nathans Institute of Genetic Medicine, Johns Hopkins University, Baltimore, MD, USA), HGMD (Stenson et al., 2014), Uniprot (UniProt Consortium, 2015), locus or disease specific databases] and prediction tools [MutationTaster (Schwarz et al., 2014), PolyPhen2 (Adzhubei et al., 2010), SIFT (Choi et al., 2012), NetGene2 Server (Brunak et al., 1991) and Splice Site Prediction by Neural Network (Reese et al., 1997)].

Comparison of Observed Frequencies

We compared the observed frequencies of affected genes in ALS cohorts from the US (Couthouis et al., 2014), Ireland (Kenna et al., 2013), Italy (Chiò et al., 2012) and Great Britain (Morgan et al., 2015) with detected frequencies in our cohort.

Generation of a Protein–Protein Interaction Network

To visually link candidate genes and possible modifiers to ALS, and to put them in relation to each another and to confirmed ALS genes, we created a protein–protein interaction network containing 21 disease genes and 13 candidate genes, possible

TABLE 1 | Genes analyzed in this study.

Gene	Transcript	Genetic subtype
<i>SOD1</i>	NM_000454.4	ALS1
<i>ALS2</i>	NM_020919.3	ALS2
<i>SETX</i>	NM_015046.5	ALS4
<i>SPG11</i>	NM_025137.3	ALS5
<i>FUS</i>	NM_004960.3	ALS6
<i>VAPB</i>	NM_004738.4	ALS8
<i>ANG</i>	NM_001145.4	ALS9
<i>TARDBP</i>	NM_007375.3	ALS10
<i>FIG4</i>	NM_014845.5	ALS11
<i>OPTN</i>	NM_021980.4	ALS12
<i>ATXN2</i>	NM_002973.3	ALS13
<i>VCP</i>	NM_007126.3	ALS14
<i>CHMP2B</i>	NM_014043.3	ALS17
<i>C9orf72</i>	NM_018325.3	FTDALS1
<i>APEX1</i>	NM_001641.3	
<i>ATXN1</i>	NM_000332.2	
<i>CCS</i>	NM_005125.1	
<i>DAO</i>	NM_001917.4	
<i>DCTN1</i>	NM_004082.4	
<i>DPP6</i>	NM_001936.4	
<i>FGGY</i>	NM_001113411.1	
<i>GLE1</i>	NM_001003722.1	
<i>GRN</i>	NM_002087.2	
<i>HEXA</i>	NM_000520.4	
<i>HFE</i>	NM_000410.3	
<i>ITPR2</i>	NM_002223.2	
<i>KIFAP3</i>	NM_014970.3	
<i>LIF</i>	NM_002309.4	
<i>NAIP</i>	NM_004536.2	
<i>NEFH</i>	NM_021076.3	
<i>PON1</i>	NM_000446.5	
<i>PON2</i>	NM_000305.2	
<i>PON3</i>	NM_000940.2	
<i>RNF19A</i>	NM_183419.3	
<i>SLC1A2</i>	NM_004171.3	
<i>SPAST</i>	NM_014946.3	
<i>UNC13A</i>	NM_001080421.2	
<i>VEGFA</i>	NM_001025366.2	
<i>VPS54</i>	NM_001005739.1	

The top 14 genes were classified as disease genes when this study was initiated; a further 25 candidate genes, modifiers and risk factors were also included. Gene names are HGNC symbols, transcripts are identified by RefSeq accessions.

risk factors, and modifiers covered by our sequencing panel (Figure 2). The protein-protein interaction network was created using the STRING database v10² by searching for multiple proteins: ALS2, ANG, ATXN1, ATXN2, C9orf72, CHCHD10, CHMP2B, DPP6, ERBB4, FGGY, FIG4, FUS, GBE1, GLE1, GRN, HNRNPA1, ITPR2, KIFAP3, MATR3, NEFH, OPTN, PFN1, PON3, SETX, SIGMAR1, SLC2A1, SOD1, SPG11, SPG7, TARDBP, UBQLN2, UNC13A, VAPB, VCP. Standard settings

were used, network edges set to show confidence, and structural previews inside network bubbles were disabled.

RESULTS

Identification of Variants in ALS Associated Genes

By analyzing 39 ALS associated genes (Table 1), we were able to detect 79 rare variants (European-American MAF \leq 1% in dbSNP, EVS or ExAC) in 27 genes which passed defined filter criteria (see Variant Filtering) and manual assessment in the Integrated Genome Viewer (IGV, v2.1.28 rev release 175, Robinson et al., 2011; see Table 2). Of these, 34 variants have been published previously whereas 45 have not been described before and therefore are considered as being novel. Excluding synonymous substitutions, we identified 54 rare variants in 23 male and 25 female patients (48 patients representing 60% of our cohort). We found that 20 patients of whom 95% (19 out of 20 patients) are considered as sporadic cases carry variants in 14 known disease genes. Additionally we identified variants in candidate genes, modifiers or risk factors in 28 patients (see Figure 1).

Pathogenic repeat expansions in the *C9orf72* gene were identified in five (6.25%) sporadic patients (mean age of onset: 67.6 years, range 49–76 years). Two of these patients carried additional variants in *FIG4* and *UNC13A* (pat #10), and *ITPR2* (pat #373), respectively (see Table 3). Furthermore, we identified four patients carrying intermediate length repeat expansions (mean age of onset: 57 years, range 40–68 years). Of these, two individuals carried additional missense and splice variants in *ALS2* and *UNC13A* (pat #26), and *SPG11* (pat #729) respectively (see Table 2). Given the size of this sample, the remarkable difference in mean age of onset between the patients with intermediate length expansions and carriers of pathogenic repeat expansions is not statistically significant ($p = 0.11$, Wilcoxon–Mann–Whitney test).

By focusing on candidate genes, modifiers, and risk factors, one interesting finding is the identification of four missense variants in the *GRN* gene (see Table 2). Of these variants, three have already been described as being probably benign in FTD cases (p.T182M), of unknown clinical relevance in FTD and progressive non-fluent aphasia (p.A324T), or as being potentially pathogenic in FTD spectrum disease (p.V77I), respectively (Guerreiro et al., 2008; Pickering-Brown et al., 2008; Yu et al., 2010). Besides this, we detected seven missense variants in the *ITPR2* gene which was linked to ALS by several GWASs in the past (van Es et al., 2007), eight variants in *FGGY*, and three variants in *UNC13A*, as well as variants in *ATXN1*, *DPP6*, *GLE1*, *KIFAP3*, *NEFH*, *PON3* and *SLC1A2* (see Table 2).

Co-occurrence of Variants in ALS Associated Genes

Earlier studies supported a complex genetic basis for ALS, which is also supported by protein–protein interactions between known ALS-associated genes, candidate genes, risk factors, and possible

²<http://string-db.org/>

TABLE 2 | Identified variants in ALS associated genes.

Gene	cDNA	Protein	Zygosity	MAF_EA (%)	MAF (%) in this study	dbSNP	Pat-ID	Gender	Subtype	AAO (years)	Reference	MT	PolyPhen2	SIFT	NG2	NN
ALS disease genes																
ALS2	c.4119A > G	p.I1373M	het	0.52	0.63	rs61757691	#422	f	sALS	61	Kenna et al., 2013	Disease causing	benign	tolerated	-	-
ALS2	c.1816-8C > T	p.?	het	0.25	1.25	rs185911369	#26**	m	PLS	66	-	Polymorphism	-	-	no effect	no effect
ALS2	c.1816-8C > T	p.?	het	0.25	1.25	rs185911369	#524	f	sALS	60	-	Polymorphism	-	-	no effect	no effect
ALS2	c.1127_1129 delAAG	p.E375del	het	-	0.63	-	#45	f	sPLS	43	-	Disease causing	-	-	-	-
ATXN2	c.2049A > T	p.L683F	het	-	0.63	-	#34	f	ALS-FTD	54	-	Disease causing	possibly damaging	damaging	-	-
C9orf72	c.956C > A	p.P319Q	het	-	0.63	-	#37a	m	sALS	50	-	Disease causing	probably damaging	tolerated	-	-
FIG4	c.1940A > G	p.Y647C	het	0.01	0.63	rs150301327	#10*	m	sALS	71	Chow et al., 2009	Disease causing	benign	damaging	-	-
FIG4	c.1910C > A	p.P637Q	het	-	0.63	-	#44	f	ALS	88	-	Polymorphism	benign	tolerated	-	-
SETX	c.3229G > A	p.D1077N	het	0.14	0.63	rs145097270	#571	m	sALS	49	Kenna et al., 2013	Polymorphism	possibly damaging	damaging	-	-
SETX	c.7358A > G	p.K2453R	het	-	0.63	-	#29	f	sALS	73	-	Polymorphism	benign	tolerated	-	-
SPG11	c.6950G > A	p.G2317D	het	<0.01	0.63	rs79186522	#23	f	flail leg	69	-	Polymorphism	benign	tolerated	-	-
SPG11	c.5381T > C	p.L1794P	het	<0.01	0.63	rs201689565	#729**	m	sALS	40	-	Disease causing	probably damaging	damaging	-	-
SPG11	c.3577A > G	p.I1193V	het	0	0.63	-	#747	f	sALS	69	-	Polymorphism	benign	tolerated	-	-
TARDBP	c.931A > G	p.M311V	het	-	0.63	rs80356725	#741	f	sALS	64	Lemmens et al., 2009	Disease causing	benign	tolerated	-	-
VAPB	c.166C > T	p.P56S	het	-	0.63	rs74315431	#3	m	fALS	41	Nishimura et al., 2004; Allaga et al., 2013	Disease causing	probably damaging	damaging	-	-
VAPB	c.390T > G	p.D130E	het	0.15	0.63	rs146459055	#22	f	sALS	67	Suzuki et al., 2009	Disease causing	benign	tolerated	-	-
VAPB	c.479_481 delCTT	p.S160del	het	0.28	0.63	rs566283411	#677	f	sALS	72	Landers et al., 2008	Disease causing	-	-	-	-
VCP	c.1194+3G > A	p.?	het	0.05	0.63	rs183223259	#20	f	ALS-FTD	70	-	Disease causing	-	-	no effect	effect
ALS candidate genes, modifiers, risk factors																
ATXN1	c.1117C > T	p.R373C	het	<0.01	0.63	-	#34	f	ALS-FTD	54	-	Disease causing	Probably damaging	Damaging	-	-
ATXN1	c.511C > A	p.R171S	het	0	0.63	-	#38	f	ALS-FTD	70	-	Disease causing	Probably damaging	Damaging	-	-
DPP6	c.746C > T	p.T249M	het	-	0.63	-	#428	m	sALS	64	-	Disease causing	Possibly damaging	Tolerated	-	-
FGGY	c.1221 + 2T > C	p.?	het	0.45	3.13	rs41287704	#5	m	sALS	58	Kenna et al., 2013	Disease causing	-	-	Effect	Effect
FGGY	c.1221 + 2T > C	p.?	het	0.45	3.13	rs41287704	#21	f	sALS	61	Kenna et al., 2013	Disease causing	-	-	Effect	Effect
FGGY	c.1221 + 2T > C	p.?	het	0.45	3.13	rs41287704	#732	m	sALS	61	Kenna et al., 2013	Disease causing	-	-	Effect	Effect
FGGY	c.1221 + 2T > C	p.?	het	0.45	3.13	rs41287704	#739	m	sALS	72	Kenna et al., 2013	Disease causing	-	-	Effect	Effect

(Continued)

TABLE 2 | Continued

Gene	cDNA	Protein	Zygosity	MAF _{EA} (%)	MAF (%) in this study	dbSNP	Pat-ID	Gender	Subtype	AAO (years)	Reference	MT	PolyPhen2	SIFT	NG2	NN
FGGY	c.1221 + 2T > C	p.?	het	0.45	3.13	rs41287704	#33	m	sALS	63	Kenna et al., 2013	Disease causing	–	–	–	Effect
FGGY	c.1435T > C	p.C479R	het	<0.01	0.63	–	#703	m	fALS	76	–	Disease causing	Probably damaging	Damaging	–	–
FGGY	c.979A > C	p.N327H	het	0.13	1.25	rs34026954	#28	f	ALS	67	Kenna et al., 2013	Disease causing	Probably damaging	Damaging	–	–
FGGY	c.979A > C	p.N327H	het	0.13	1.25	rs34026954	#38	f	ALS-FTD	70	Kenna et al., 2013	Disease causing	Probably damaging	Damaging	–	–
GLE1	c.398G > A	p.R133Q	het	<0.01	0.63	–	#37b	m	sALS	74	–	Disease causing	Benign	Tolerated	–	–
GRN	c.545C > T	p.T182M	het	0.03	0.63	rs63750479	#16	m	sALS	67	Guerreiro et al., 2010	Polymorphism	Benign	Tolerated	–	–
GRN	c.229G > A	p.V77I	het	0.01	0.63	rs148531161	#749	m	sALS	46	Yu et al., 2010	Polymorphism	Benign	Tolerated	–	–
GRN	c.361G > A	p.V121M	het	0	0.63	–	#28	f	ALS	67	–	Polymorphism	Benign	Damaging	–	–
GRN	c.970G > A	p.A324T	het	0.12	0.63	rs63750541	#36	m	flail arm	39	Sleegers et al., 2008; Kenna et al., 2013	Polymorphism	Benign	Tolerated	–	–
ITPR2	c.2831C > T	p.P944L	het	<0.01	0.63	rs377598368	#22	f	sALS	67	–	Disease causing	Benign	Tolerated	–	–
ITPR2	c.3485T > G	p.V1162G	het	0.15	0.63	rs61757114	#373*	f	sALS	72	Kenna et al., 2013	Disease causing	Benign	Tolerated	–	–
ITPR2	c.1834G > A	p.A612T	het	<0.01	0.63	rs199523133	#422	f	sALS	61	–	Disease causing	Possibly damaging	Tolerated	–	–
ITPR2	c.8002G > A	p.A2668T	het	0.21	0.63	rs61757116	#677	f	sALS	72	Kenna et al., 2013	Disease causing	Benign	Tolerated	–	–
ITPR2	c.3635C > T	p.A1212V	het	<0.01	0.63	rs368911384	#741	f	sALS	64	Kenna et al., 2013	Disease causing	Probably damaging	Tolerated	–	–
ITPR2	c.1447G > A	p.V483I	het	0	0.63	–	#29	f	sALS	73	–	Disease causing	Probably damaging	Tolerated	–	–
ITPR2	c.3539G > A	p.R180Q	het	0.62	0.63	rs35862420	#36	m	flail arm	39	Kenna et al., 2013	Disease causing	Benign	Tolerated	–	–
KIFAP3	c.518-5T > A	p.?	het	–	0.63	–	#419	m	sALS	72	–	Polymorphism	–	–	Effect	No effect
KIFAP3	c.1301T > G	p.F434C	het	0.23	0.63	rs116755924	#52	m	sALS	45	–	Disease causing	Probably damaging	Damaging	–	–
NEFH	c.1235G > A	p.R412Q	het	0.01	0.63	–	#534	m	sALS	58	–	Disease causing	Possibly damaging	Damaging	–	–
PON3	c.217G > T	p.G73C	het	–	0.63	–	#47	m	sALS	78	–	Disease causing	Probably damaging	Damaging	–	–
SLC1A2	c.236C > G	p.A79G	het	0.04	0.63	rs377633002	#524	f	sALS	60	Meyer et al., 1998	Disease causing	Benign	Tolerated	–	–
UNC13A	c.3080C > T	p.P1027L	het	1.83	0.63	rs200328448	#10*	m	sALS	71	Koppers et al., 2013; Kenna et al., 2013	Disease causing	Possibly damaging	Damaging	–	–
UNC13A	c.182C > T	p.T61M	het	0.45	0.63	rs140141294	#26**	m	PLS	66	Koppers et al., 2013; Kenna et al., 2013	Disease causing	Possibly damaging	Tolerated	–	–
UNC13A	c.1073A > G	p.Y358C	het	–	0.63	–	#30	m	sALS	60	–	Polymorphism	Possibly damaging	Tolerated	–	–

(Continued)

TABLE 2 | Continued

Gene	cDNA	Protein	Zygosity	MAF_EA (%)	MAF (%) in this study	dbSNP	Pat-ID	Gender	Subtype	AAO (years)	Reference	MT	PolyPhen2	SIFT	NG2	NN
UTR variants																
APEX1	c.*2A > T	p.?	het	0.5	0.63	rs17112002	#47	m	sALS	78	–					
FUS	c.-37C > T	p.?	het	–	0.63	–	#422	f	sALS	61	–					
FUS	c.*41G > A	p.?	het	0.86	0.63	rs80301724	#741	f	sALS	64	Sproviero et al., 2012					
SOD1	c.-8A > C	p.?	het	–	0.63	–	#46	f	ALS-FTD	75	–					
VAPB	c.-33C > G	p.?	het	–	0.63	rs201547974	#676	f	sALS	51	–					
Synonymous variants																
ATXN2	c.2088C > T	p.(=)	het	–	0.63	–	#22	f	sALS	67	–					
DAO	c.723C > T	p.(=)	het	0.23	1.25	rs149956241	#25**	f	flail leg	54	–					
DAO	c.723C > T	p.(=)	het	0.23	1.25	rs149956241	#41	m	sALS	42	–					
DCTN1	c.3669T > C	p.(=)	het	0	0.63	–	#12	m	sALS	61	–					
DCTN1	c.3474A > G	p.(=)	het	–	0.63	–	#54	f	ALS-FTD	55	–					
DPP6	c.693T > C	p.(=)	het	–	0.63	–	#24*	m	sALS	70	Kenna et al., 2013					
FUS	c.1080C > T	p.(=)	het	0.05	0.63	rs190724342	#35	f	sALS	49	Kenna et al., 2013					
HEXA	c.1216C > T	p.(=)	het	0.02	0.63	rs140482769	#7	m	sALS	71	–					
HEXA	c.744C > T	p.(=)	het	–	0.63	–	#749	m	sALS	46	–					
ITPR2	c.4962G > A	p.(=)	het	0.69	0.63	rs191789657	#16	m	sALS	67	Kenna et al., 2013					
ITPR2	c.5569C > T	p.(=)	het	0.12	1.25	rs191281974	#24*	m	sALS	70	Kenna et al., 2013					
ITPR2	c.5569C > T	p.(=)	het	0.12	1.25	rs191281974	#40	f	sALS	43	Kenna et al., 2013					
ITPR2	c.6162C > T	p.(=)	het	<0.01	0.63	–	#31	f	sALS	47	–					
NEFH	c.2061A > G	p.(=)	het	–	0.63	–	#16	m	sALS	67	–					
NEFH	c.2646C > T	p.(=)	het	0.01	0.63	rs528790943	#422	f	sALS	61	Kenna et al., 2013					

(Continued)

TABLE 2 | Continued

Gene	cDNA	Protein	Zygosity	MAF_EA (%)	MAF (%) in this study	dbSNP	Pat-ID	Gender	Subtype	AAO (years)	Reference	MT	MT	SIFT	NG2	NN
PON1	c.603G > A	p.(=)	het	0.17	0.63	rs148452713	#729**	m	sALS	40	Kenna et al., 2013					
SETX	c.6675C > T	p.(=)	het	<0.01	0.63	rs200382898	#33	m	sALS	63	-					
SLC1A2	c.846C > A	p.(=)	het	<0.01	0.63	rs376593061	#46	f	ALS-FTD	75	-					
SLC1A2	c.450G > A	p.(=)	het	0	0.63	-	#52	m	sALS	45	-					
SPG11	c.6258G > T	p.(=)	het	0.81	0.63	rs150761878	#13	m	sALS	73	Kenna et al., 2013					
UNC13A	c.771C > G	p.(=)	het	3.02	0.63	rs146739681	#3	m	fALS	41	Kenna et al., 2013					
UNC13A	c.4560C > T	p.(=)	het	0.1	0.63	rs141334897	#26**	m	PLS	66	-					
UNC13A	c.4143G > A	p.(=)	het	-	0.63	-	#26**	m	PLS	66	-					
UNC13A	c.2220G > A	p.(=)	het	0.17	0.63	rs201361019	#32	m	sALS	46	-					
VCP	c.832T > C	p.(=)	het	0.04	0.63	rs200670526	#625	m	fALS	53	-					

*Patients carry ≥ 30 C9orf72 repeat units. **Patients carry intermediate length C9orf72 repeats. MAF, minor allele frequency; MAF_EA is the maximum population frequency of the variant observed in the European American population in dbSNP, EVS or ExAC. AAO, age at onset; MT, MutationTaster (<http://www.mutationtaster.org/>); PolyPhen2 (<http://genetics.bwh.harvard.edu/pph2/>); SIFT (http://proceedings.fysli.org/genome_submit_2.php); NG2, NetGene2 (<https://www.cbs.dtu.dk/services/NetGene2/>); NN, Splice Site Prediction by Neural Network (http://www.fruitfly.org/seq_tools/splice.html).

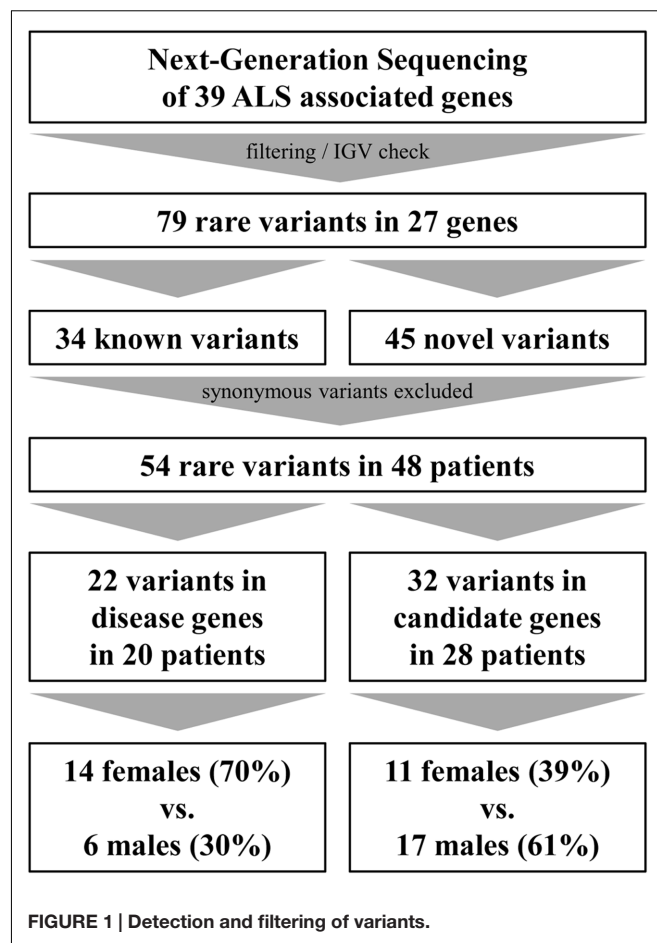


FIGURE 1 | Detection and filtering of variants.

modifiers included in our gene panel (Figure 2). In our example, each of the proteins interacts in the context of key proteins for motor neuron degeneration (except *CHCHD10* and *PON3*), pointing toward possible modifying effects of certain variants.

We searched our cohort for patients who carry multiple variants in ALS-associated genes and could identify 15 individuals carrying at least two variants (18.8%, synonymous variants excluded) in ALS-associated genes (Table 4). For example, missense variants in the *ITPR2* gene were found in co-occurrence with clearly or potentially pathogenic variants in seven (8.75%) individuals. Four of these variants were also detected in an ALS cohort screening by Kenna et al. (2013). In our cohort the mean age of onset in patients who carried a variant in the *ITPR2* gene in co-occurrence was 64.0 years compared to 66.6 years in patients carrying any other variants in co-occurrence (differences are not statistically significant, Wilcoxon–Mann–Whitney test). We detected two additional synonymous variants in *ITPR2* but according to current knowledge we cannot assess their actual impact on the *ITPR2* protein. Four of the 15 patients carried an expanded (Pat #10 and Pat #373) or intermediate (Pat #26 and Pat #729) *C9orf72* repeat expansion in co-occurrence.

The mean age of onset in patients where no variant could be detected was 57.8 years, patients who carried one variant showed

TABLE 3 | Carriers of pathogenic and intermediate C9orf72 repeat expansions.

Pat-ID	Gender	Subtype	AAO (years)	C9orf72	n repeats	Additional variants
#2	m	sALS	49	Positive	30	
#10	m	sALS	71	Positive	35	<i>FIG4</i> c.1940A > G; p.Y647C (het.); <i>UNC13A</i> c.3080C > T; p.P1027L (het.)
#24	m	sALS	70	Positive	31	
#373	f	sALS	72	Positive	34	<i>ITPR2</i> c.3485T > G; p.V1162G (het.)
#673	f	sALS	76	Positive	n.a.	
#6	m	sALS	68	Intermediate	26	
#25	f	flail leg syndrome	54	Intermediate	27	
#26	m	sPLS	66	Intermediate	27	<i>UNC13A</i> c.182C > T; p.T61M (het.); <i>ALS2</i> c.1816-8C > T; p.?
#729	m	sALS	40	Intermediate	27	<i>SPG11</i> c.5381T > C; p.L1794P (het.)

a mean age of onset of 61.3 years and patients carrying two or more variants had a mean age of disease onset of 65.0 years. In comparison, the overall mean age of disease onset in our cohort was 60.1 years. However, these differences in age of onset are not statistically significant (Kruskal–Wallis Rank Sum Test).

Variants in Other NDD Genes

To match the hypothesis of common pathways in different neurodegenerative diseases (NDDs) and to link ALS to other entities of the NDD spectrum, we additionally searched for potentially pathogenic or disease causing variants in 238 genes which are associated with possible differential diagnoses or overlapping phenotypes that are included in our NDD gene panel. We identified 12 patients who carried potentially pathogenic variants in genes that are linked to other entities (Table 5).

In patient #38, we detected two heterozygous variants in the *GBE1* gene (p.S378R and p.P40T, see Table 5). Mutations in *GBE1* can cause autosomal recessively inherited adult Polyglucosan body disease (APBD) which is characterized by upper motor neuron signs similar to ALS, early neurogenic bladder, cognitive impairment and decreased or absent activity of the glycogen branching enzyme (Klein, 2013). APBD is one of the conditions that should be considered when establishing the diagnosis of ALS. Unfortunately, we could not investigate whether both variants occur in the compound-heterozygous state in our patient because samples for segregation analysis could not be obtained. Long-range PCR with mutation-specific primers was impossible due to the large distance of more than 170 kb between the variants.

Another interesting finding is the identification of heterozygous variants in the *SPG7* gene in four sporadic patients (see Table 5). Mutations in *SPG7* can cause autosomal recessively inherited spastic paraplegia type 7, but there are also some published cases of obviously autosomal dominant inheritance (e.g., Sánchez-Ferrero et al., 2013). The disease is mainly characterized by spasticity and weakness of the lower limbs. Additional neurologic symptoms might appear in more complex phenotypes. In our cohort, we identified the truncating mutation p.R213* and the missense mutations p.I743T and p.G349S which are both described as acting disadvantageous on *SPG7* protein function (Brugman et al., 2008; Bonn et al., 2010). None of the four patients had further relevant variants

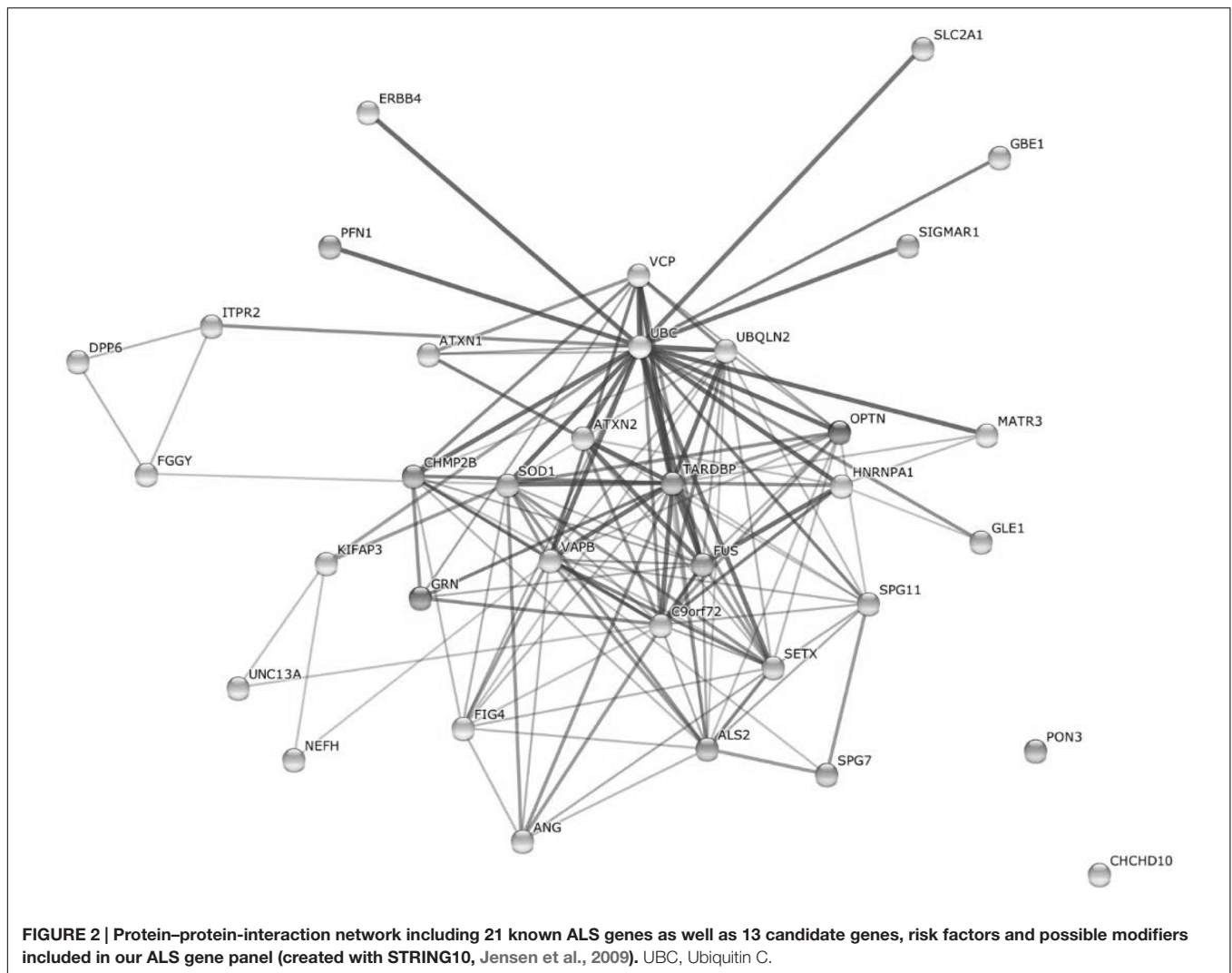
in ALS associated genes (only one patient carries an additional missense variant of unknown clinical relevance in the *FGGY* gene).

We also identified a high number of variants in the *NOTCH3*, *SYNE1*, and *VPS13A* genes as expected in genes of this size. For *SYNE1*, as mainly loss-of-function mutations are considered as being pathogenic in motor neuron disease (Gros-Louis et al., 2007; Izumi et al., 2013; Noreau et al., 2013). Similarly, only variants which result in a loss or gain of one cysteine residue within epidermal growth factor (EGF)-like repeat domains (Dichgans et al., 2001) are considered pathogenic in *NOTCH3*, and for *VPS13A* mostly loss-of-function variants are considered as pathogenic (Tomiyasu et al., 2011). Thus we assume that detected variants in our cohort represent rare polymorphisms. We identified variants in further genes that are included in our gene panel (see Table 5) but are unlikely to be implicated in our patients' phenotypes.

By comparing the number of patients identified to carry potentially pathogenic variants in ALS related genes in our cohort with previously published cohort studies, we show that the frequency of affected genes may vary in different populations (Table 6). For example, in the *VAPB* gene we detected variants in 5% of German patients (four cases) whereas in other populations no variants in *VAPB* were identified at all. Striking differences in frequencies across populations can also be observed for *FIG4*, *FGGY*, *GRN*, *ITPR2*, and *UNC13A*. The studies used vastly different strategies for sequencing and variant evaluation and analyzed different gene sets [from 6 genes, partially hotspots only sequenced by Sanger in Chiò et al. (2012) to 169 genes sequenced by NGS in Couthouis et al. (2014)]. Thus we consider this comparison solely to hint toward possible differences in gene frequencies among populations as a consequence of founder effects.

DISCUSSION

By using next-generation sequencing we analyzed 39 ALS-associated genes in a German cohort of both familial and sporadic ALS patients. In total, we detected 54 rare variants in approved disease genes and possible candidate genes, risk factors, and modifiers (synonymous variants excluded) in 48 patients which represents 60% of our total cohort.



We identified pathogenic or potentially pathogenic variants in 14 analyzed disease genes in 20 patients of whom 19 patients (95%) are affected by sporadic ALS. This finding is unexpected, as it demonstrates that a genetic background can actually be found in a major proportion of seemingly sporadic cases (25%; 19 of 74 patients with sALS). We also would have expected to find more variants in familial cases. Although guidelines and recommendations on how to evaluate unknown variants are published (see for example Richards et al., 2015), the assessment of the actual pathogenicity of detected unknown variants with regard to the patients' phenotypes remains challenging and clear evidence on how a certain variant impairs the phenotype can only be achieved by extensive functional studies.

By focusing on possible candidate genes, risk factors, and modifiers, an interesting finding is the detection of heterozygous missense variants in the *GRN* gene in four patients affected by pure ALS (see **Table 2**). Three of the identified variants (p.V77I, p.V121M and p.A324T) are classified as being potentially pathogenic. Loss-of-function mutations in *GRN* are considered

causative for frontotemporal lobar degeneration with ubiquitin-positive inclusions (Mackenzie et al., 2006). Recent evidence though suggests that missense mutations in *GRN* are also linked to the pathogenesis of ALS, especially as ALS and frontotemporal dysfunction are considered to represent a continuum of overlapping phenotypes, and a large proportion of ALS patients additionally experience frontotemporal dysfunction and vice versa (Sleegers et al., 2008; Cannon et al., 2013). Based on our findings, we recommend that *GRN* gene analysis should be included in routine molecular diagnostic settings and should also be considered in cases of pure ALS without frontotemporal involvement. Further, we detected seven missense variants in the *ITPR2* gene. Although Fernández-Santiago et al. (2011) as well as Chen et al. (2012) could not confirm an association of variants in *ITPR2* with ALS in a German and a Chinese cohort by SNP genotyping, we speculate that variation in the *ITPR2* gene could act as a modulating factor in ALS. A modulating effect might also exist for variants in *FGGY* (eight variants), *GRN* (four variants) and *UNC13A* (three variants).

These findings reflect the overall challenges in assessing the relevance of rare variants with respect to the phenotype as functional studies investigating the actual effect of these variants are largely missing. However, by the implementation

of NGS in clinical genetics, we are now faced with increasing numbers of genes published as being possibly implicated in the pathogenesis of ALS. Such candidate genes gain further support from protein-protein interaction data. As rare variants

TABLE 4 | Co-occurrence of variants in ALS associated genes.

Pat-ID	Gender	Subtype	AAO (years)	Gene	cDNA	Protein	MAF_EA (%)	dbSNP
#10	m	sALS	71	<i>C9orf72</i>	Pathogenic repeat expansion			
#22	f	sALS	67	<i>FIG4</i>	c.1940A > G	p.Y647C	0.02	rs150301327
				<i>UNC13A</i>	c.3080C > T	p.P1027L	0.65	rs200328448
				<i>ATXN2</i>	c.2088C > T	p.(=)	-	-
				<i>ITPR2</i>	c.2831C > T	p.P944L	0.01	rs377598368
				<i>VAPB</i>	c.390T > G	p.D130E	0.1	rs146459055
#26	m	PLS	66	<i>C9orf72</i>	Intermediate repeat expansion			
#422	f	sALS	61	<i>ALS2</i>	c.1816-8C > T	p.?	0.38	rs185911369
				<i>UNC13A</i>	c.4560C > T	p.(=)	0.07	rs141334897
				<i>UNC13A</i>	c.4143G > A	p.(=)	-	-
				<i>UNC13A</i>	c.182C > T	p.T61M	0.2	rs140141294
				<i>ALS2</i>	c.4119A > G	p.I1373M	0.49	rs61757691
				<i>FUS</i>	c.-37C > T	p.?	-	-
				<i>ITPR2</i>	c.1834G > A	p.A612T	0.01	rs199523133
				<i>NEFH</i>	c.2646C > T	p.(=)	-	-
#524	f	sALS	60	<i>ALS2</i>	c.1816-8C > T	p.?	0.38	rs185911369
#677	f	sALS	72	<i>SLC1A2</i>	c.236C > G	p.A79G	0.01	rs377633002
				<i>ITPR2</i>	c.8002G > A	p.A2668T	0.29	rs61757116
#741	f	sALS	64	<i>VAPB</i>	c.479_481delCTT	p.S160del	0.45	rs566283411
				<i>FUS</i>	c.*41G > A	p.?	0.58	rs80301724
				<i>ITPR2</i>	c.3635C > T	p.A1212V	-	rs368911384
				<i>TARDBP</i>	c.931A > G	p.M311V	-	rs80356725
#29	f	sALS	73	<i>ITPR2</i>	c.1447G > A	p.V483I	-	-
#28	f	ALS	67	<i>SETX</i>	c.7358A > G	p.K2453R	-	-
				<i>FGGY</i>	c.979A > C	p.N327H	0.1	rs34026954
#34	f	ALS-FTD	54	<i>GRN</i>	c.361G > A	p.V121M	-	-
				<i>ATXN1</i>	c.1117C > T	p.R373C	-	-
#36	m	flail arm	39	<i>ATXN2</i>	c.2049A > T	p.L683F	-	-
				<i>GRN</i>	c.970G > A	p.A324T	0.14	rs63750541
#38	f	ALS-FTD	70	<i>ITPR2</i>	c.3539G > A	p.R1180Q	0.76	rs35862420
				<i>ATXN1</i>	c.511C > A	p.R171S	-	-
#47	m	sALS	78	<i>FGGY</i>	c.979A > C	p.N327H	0.1	rs34026954
				<i>APEX1</i>	c.*2A > T	p.?	0.66	rs17112002
#373	f	sALS	72	<i>PON3</i>	c.217G > T	p.G73C	-	-
				<i>C9orf72</i>	Pathogenic repeat expansion			
#729	m	sALS	40	<i>ITPR2</i>	c.3485T > G	p.V1162G	0.15	rs61757114
				<i>C9orf72</i>	Intermediate repeat expansion			
#3	m	fALS	41	<i>PON1</i>	c.603G > A	p.(=)	0.12	rs148452713
				<i>SPG11</i>	c.5381T > C	p.L1794P	0.01	rs201689565
				<i>UNC13A</i>	c.771C > G	p.(=)	0.85	rs146739681
#16	m	sALS	67	<i>VAPB</i>	c.166C > T	p.P56S	-	rs74315431
				<i>GRN</i>	c.545C > T	p.T182M	0.03	rs63750479
				<i>ITPR2</i>	c.4962G > A	p.(=)	0.36	rs191789657
				<i>NEFH</i>	c.2061A > G	p.(=)	-	-

(Continued)

TABLE 4 | Continued

Pat-ID	Gender	Subtype	AAO (years)	Gene	cDNA	Protein	MAF_EA (%)	dbSNP
#24	m	sALS	70	<i>C9orf72</i>	pathogenic repeat expansion			
#749	m	sALS	46	<i>DPP6</i>	c.693T > C	p.(=)	-	-
				<i>ITPR2</i>	c.5569C > T	p.(=)	0.17	rs191281974
				<i>GRN</i>	c.229G > A	p.V77I	0.01	rs148531161
#33	m	sALS	63	<i>HEXA</i>	c.744C > T	p.(=)	-	-
				<i>FGGY</i>	c.1221+2T > C	p.?	0.45	rs41287704
#46	f	ALS-FTD	75	<i>SETX</i>	c.6675C > T	p.(=)	0.01	rs200382898
				<i>SLC1A2</i>	c.846C > A	p.(=)	-	-
#52	m	sALS	45	<i>SOD1</i>	c.-8A > C	p.?	-	-
				<i>KIFAP3</i>	c.1301T > G	p.F434C	0.23	rs116755924
				<i>SLC1A2</i>	c.450G > A	p.(=)	-	-

in ALS associated genes according to current knowledge rather represent modifiers with effect on risk of developing the disease, age of onset, severity, or progression rate than disease causing mutations, further effort has to be made to understand how these modulating effects become evident in ALS. Investigating such modulating effects might lead to the identification of pathways that are not yet linked to ALS, enhancing our knowledge of ALS pathogenesis and higher-level neurodegenerative processes.

By performing repeat length analysis we identified five sporadic patients (6.25%) carrying pathogenic repeat expansions in the *C9orf72* gene. This is in line with Majounie et al. (2012) who reported on 5.2% of *C9orf72* repeat expansion carriers amongst German ALS patients. In two carriers of a pathogenic repeat expansion, we detected additional variants in ALS-associated genes. Although van Blitterswijk et al. (2012) suggested that additional genetic factors contribute to ALS pathogenesis in some carriers of a pathogenic *C9orf72* repeat expansion, we cannot assess the impact of additional variants on the patients' phenotypes in our cohort study. We identified four further patients carrying intermediate length repeat expansions. According to recent literature, these might be pathogenic in ALS as patients carrying 20–29 repeats are phenotypically similar to those with more than 30 repeats (Byrne et al., 2014). However, as intermediate length repeats have been detected in both patients and healthy controls, their actual pathogenicity still remains unclear (Rohrer et al., 2015). Of the four individuals with intermediate length repeat expansions, two patients carried additional variants in disease related genes. In our cohort, patients with intermediate length repeats had an earlier age of onset than carriers of a pathogenic repeat expansion (averages of 57.0 and 67.6 years, respectively). This counter-intuitive result leads us to speculate that age of onset was not primarily influenced by the length of repeat expansions but possibly by other factors such as additional variants in other genes. However, we cannot draw a firm conclusion due to our limited cohort size. Surprisingly, we did not detect pathogenic repeat expansions in any of the familial

cases, although this might also be because of the small sample size.

To evaluate the hypothesis that ALS might be of complex genetic origin, we searched our cohort for patients carrying more than one potentially disease-causing variant. We found that 15 patients (18.8% of our cohort, synonymous variants excluded) carry two or more variants in ALS-associated genes and that four of these 15 patients additionally carry an expanded or intermediate *C9orf72* repeat expansion. According to current findings, a complex model of inheritance is used to explain phenomena like reduced penetrance or even intrafamilial phenotypic variability. A hypothesis by Cady et al. (2015) for example implies that disease onset is influenced by the burden of rare variants in ALS-associated genes. The authors reported that 3.8% of 391 study participants harbored two or more variants in 17 analyzed disease genes and that these individuals had disease onset 10 years earlier than patients carrying only one variant. The considerable difference in percentage of patients carrying two or more variants (3.8% in Cady et al., 2015 vs. 18.8% in this study) might be explained by the fact that we included not only variants in approved disease genes but also in candidate genes, modifiers, and risk factors. In contrast, Cirulli et al. (2015) did not report an effect of the number of variants on the age of onset in their cohort of 2869 ALS patients and 6405 controls, but they do not draw a strong conclusion as they did not test for pathogenic *C9orf72* repeat expansions. In our data, we do see a later age of onset in patients carrying two or more variants. However, due to our smaller sample size, we cannot make statistically significant observations on a possible correlation and we cannot exclude that co-occurrence of multiple variants might have a disadvantageous effect on disease onset, severity, disease duration, or site of onset by affecting disease causing variants. As an example, the identification of *ITPR2* variants in co-occurrence in seven patients might hint at a possible negative effect of additional variants in the *ITPR2* gene. Further studies should include both next-generation sequencing and tests for pathogenic repeat expansion in a large cohort to resolve this open question.

TABLE 5 | Detected variants in other NDD genes.

Pat-ID	Gender	Subtype	AAO (years)	Gene	chr. position	cDNA	Protein	Zygosity	MAF_EA (%)	dbSNP	Differential diagnoses (OMIM)	MT	PolyPhen2	SIFT	NG2	NN
#5	m	sALS	58	AR	chrX:66941751	c.2395C > G	p.Q799E	hemi	0.22	rs137852591	#300068, #312300, #300633, #313200	Disease causing	-	Damaging	-	-
#9	m	sALS	66	GBA	chr1:155209737	c.247C > T	p.R83C	het	0.01	rs1141812	#608013, #230800, #230900, #231000, #231005, #127750, #168600	Polymorphism	Probably damaging	Damaging	-	-
#18	m	sALS	42	PLP1	chrX:103043442	c.696+3G > A	p.?	hemi	-	-	#312920, #312080	Disease causing	-	-	No effect	No effect
#24*	m	sALS	70	GARS	chr7:30665930	c.11694T > A	p.L565Q	het	0.02	rs200726600	#601472, #600794	Disease causing	Benign	Damaging	-	-
#385	f	sALS	69	GARS	chr7:306655580	c.1100A > G	p.N367S	het	0.04	rs192443850		Disease causing	Benign	Tolerated	-	-
#780	m	fALS	56	SPG7	chr16:89592755	c.637C > T	p.R213*	het	-	-	#607259	Disease causing	-	-	-	-
				DYNC1H1	chr14:102452918	c.2356C > T	p.R786C	het	-	-	#614228, #614563, #158600	Disease causing	Probably damaging	Damaging	-	-
#34	f	ALS-FTD	54	DYNC1H1	chr14:102508609	c.12259G > A	p.A4087T	het	-	-		Disease causing	Probably damaging	Damaging	-	-
#38	f	ALS-FTD	70	GBE1	chr3:81640290	c.1134T > G	p.S378R	het	0.04	rs36099971	#263570, #232500	Disease causing	Benign	Tolerated	-	-
#41	m	sALS	42	GBE1	chr3:81810551	c.118C > A	p.P40T	het	0.17	rs35196441		Disease causing	Benign	Damaging	-	-
#19	m	sALS	54	SPG7	chr16:89623341	c.2228T > C	p.I743T	het	-	-	#607259	Disease causing	Probably damaging	Damaging	-	-
				SPG7	chr16:89598369	c.1045G > A	p.G349S	het	0.17	rs141659620		Disease causing	Probably damaging	Damaging	-	-
#28	f	sALS	67	SYNE1	chr6:152712567	c.7870C > T	p.R2624W	het	-	-	#612998, #610743	Polymorphism	Probably damaging	Damaging	-	-
				SPG7	chr16:89598369	c.1045G > A	p.G349S	het	0.17	rs141659620		Disease causing	Probably damaging	Damaging	-	-
#32	m	sALS	46	TAF1	chrX:70680560	c.5366A > G	p.N1789S	hemi	0.03	rs147517498	#314250	Disease causing	Benign	Damaging	-	-

*Patient carries a pathogenic C9orf72 repeat expansion.

To genetically and mechanistically link ALS to other pathologies of the NDD spectrum, we searched our cohort for potentially pathogenic variants in 238 genes that are associated with overlapping phenotypes and are covered by our diagnostic panel.

We identified potentially pathogenic variants in neurodegeneration-related genes in 12 patients. Although compound-heterozygosity for the detected variants in *GBE1* in pat #38 is not proven, we speculate that both variants might be at least concurrently causative, especially as the patient revealed UMN-dominant ALS, cognitive impairment, and progressive non-fluent aphasia (PNFA) upon his last

clinical examination in 2012. *GBE1* is a glycogen branching enzyme which is involved in glycogen synthesis. According to Ngo and Steyn (2015), there is a link between the selective degeneration of neurons in ALS and metabolic alterations: Deficits caused by decreased glucose metabolism may trigger hyperexcitability and subsequent selective degeneration of upper and lower motor neurons. Although the underlying mechanisms are still unclear, Wang et al. (2015) could show that the FUS protein (juvenile ALS) interacts to a great extent with mitochondrial enzymes and proteins involved in glucose metabolism. With regard to these presumptions, we speculate that pathogenic variants in *GBE1* might be causative

TABLE 6 | Percentage of patients carrying potentially pathogenic variants in ALS associated genes (missense, splicing, small Indels only) (American: Couthouis et al., 2014; Irish: Kenna et al., 2013; Italian: Chiò et al., 2012; British: Morgan et al., 2015).

Gene	Our cohort (%) <i>n</i> = 80	American (%) <i>n</i> = 242	Irish (%) <i>n</i> = 444	Italian (%) <i>n</i> = 475	British (%) <i>n</i> = 95
<i>SOD1</i>	1.25	1.65	0	2.1	2.11
<i>ALS2</i>	5	1.24	1.35	-	5.26
<i>SETX</i>	2.5	2.07	2.25	-	-
<i>SPG11</i>	3.75	4.13	1.58	-	17.89
<i>FUS</i>	2.5	0.41	0.45	0.21	1.05
<i>VAPB</i>	5	0	0	-	-
<i>ANG</i>	0	0.41	0	0	-
<i>TARDBP</i>	1.25	-	0.45	1.47	2.11
<i>FIG4</i>	2.5	0.83	0	-	-
<i>OPTN</i>	0	0	0.23	0.21	2.11
<i>ATXN2</i>	1.25	1.22	0	-	-
<i>VCP</i>	1.25	0	0.23	-	-
<i>CHMP2B</i>	0	0	0.45	-	-
<i>C9orf72-Repeat</i>	6.25	1.65	8.78	6.74	-
<i>APEX1</i>	1.25	-	-	-	-
<i>ATXN1</i>	2.5	-	-	-	-
<i>CCS</i>	0	-	-	-	-
<i>DAO</i>	0	-	-	-	-
<i>DCTN1</i>	0	2.07	0.45	-	-
<i>DPP6</i>	1.25	1.65	0.23	-	-
<i>FGGY</i>	10	0.41	0.23	-	-
<i>GLE1</i>	1.25	-	-	-	-
<i>GRN</i>	5	0.41	0	-	-
<i>HEXA</i>	0	-	-	-	-
<i>HFE</i>	0	1.65	0.23	-	-
<i>ITPR2</i>	8.75	1.24	0.23	-	-
<i>KIFAP3</i>	2.5	-	-	-	-
<i>LIF</i>	0	-	-	-	-
<i>NAIP</i>	0	-	-	-	-
<i>NEFH</i>	1.25	0.41	0	-	-
<i>PON1</i>	0	0	0	-	1.05
<i>PON2</i>	0	0	0.23	-	1.05
<i>PON3</i>	1.25	0	0	-	-
<i>RNF19A</i>	0	-	-	-	-
<i>SLC1A2</i>	1.25	-	-	-	-
<i>SPAST</i>	0	-	-	-	-
<i>UNC13A</i>	3.75	1.24	0.23	-	-
<i>VEGFA</i>	0	-	-	-	1.05
<i>VPS54</i>	0	-	-	-	-

for ALS or motor neuron degeneration, and that metabolic processes and involved genes must be taken into account in ALS genetics.

We detected known heterozygous variants in *SPG7* (paraplegin) in four patients. Recent evidence suggests that mutations in *SPG7* might be relevant in PLS as Mitsumoto et al. (2015) reported on the identification of a pathogenic heterozygous variant in *SPG7* in a patient affected by PLS. Paraplegin is part of the metalloprotease AAA complex, an ATP-dependent proteolytic complex located on the inner mitochondrial membranes, and functions in controlling protein quality and ribosomal assembly. Ferreira et al. (2004) showed that paraplegin-deficient mice develop axonal swellings as a consequence of accumulation of mitochondria and neurofilaments in the spinal cord which precedes axonal degeneration by impaired anterograde axonal transport. Although further studies are needed to assess the functional role of *SPG7* in human motor neurons, these findings hint at an important role of *SPG7* in motor neuron survival and support our hypothesis, that paraplegin is implicated in the pathogenesis of ALS and those pathogenic mutations in *SPG7* must be taken into account regarding genetic testing in ALS.

In summary, our results support recent observations whereby a genetic background is implicated in the sporadic form of ALS to a higher extent than assumed so far, and strengthen the upcoming hypothesis of ALS being a distinct manifestation of higher-level neurodegenerative processes rather than representing a discrete entity. Further, our results contribute to current discussions on a possible pathogenicity of intermediate repeat expansion in the *C9orf72* gene, especially in the interplay with additional variants in other ALS associated genes. In contrast to previously published studies, we could not prove an earlier age of disease onset in patients carrying multiple variants but speculate that variants in the *ITPR2* gene might act as a modulating factor in ALS. Additionally, our results lead us to assume that variants in *GRN* and *SPG7* might be implicated in the pathogenesis of ALS which is in line with the aforementioned hypothesis of common neurodegenerative processes leading to distinct phenotypes. Surprisingly, we did not detect clearly pathogenic variants in *SOD1* in our cohort, even though this gene is supposed to have a high impact on disease, encouraging us to launch a debate on the actual significance of *SOD1* in Germany.

CONCLUSION

We investigated 39 ALS-associated genes in a German cohort of 80 familial and sporadic ALS patients utilizing next-generation sequencing. We identified 22 variants in disease-causing genes in 20 patients and additionally 32 variants in candidate genes, risk factors, and modifiers in 28 patients. Thus we detected variants in ALS-associated genes in 60% of our study participants, of whom the vast majority are sporadic cases. Surprisingly, pathogenic repeat expansions in *C9orf72* and potentially pathogenic variants in *SOD1* were

both detected at lower frequencies than expected. Instead we identified potentially pathogenic variants in the *GRN* gene in four patients, indicating that the impact of *GRN* mutations is not limited to ALS-FTD and might account for pure ALS, too.

Furthermore, our cohort enabled us to evaluate the hypotheses that ALS is of complex genetic origin. According to this hypothesis, numerous variants have some degree of influence on the clinical phenotype caused by the pathogenic mutation. We did in fact identify patients carrying variants in more than one ALS-associated gene. In contrast to other studies, however, our results do not show that patients with multiple variants have an earlier age of onset.

As ALS should be seen in the context of wider neurodegenerative disorders, we investigated our cohort for potentially pathogenic variants in 238 neurodegeneration related genes. The most interesting findings are the identification of two variants in the *GBE1* gene that might be causative in a patient with UMN-dominant ALS and the detection of heterozygous variants in *SPG7* in four ALS patients. These findings would benefit from extensive high-throughput sequencing in large patient and control cohorts of different ethnic background in order to more accurately assess the overall variability in ALS-associated genes and to better evaluate their impact on the disease.

Our results support the notion that next-generation sequencing could help uncover the genetic heterogeneous basis of ALS and thus argue for the broader application of NGS techniques in routine diagnostic settings. Therefore, our results are of immediate relevance for clinical genetics as we recommend that genetic testing in German patients should be offered not only to those with familial ALS but also to those with apparently sporadic ALS. We propose a two-stage strategy starting with a *C9orf72* repeat analysis, followed by comprehensive gene panel sequencing if *C9orf72* negative. To meet the high number of possible differential diagnoses that mimic ALS, genes causing FTD, HSP, spinal muscular atrophy (SMA) and other entities that impair motor neuron function should be included. Whereas Sanger sequencing focused on a few commonly affected genes such as *SOD1*, panel sequencing offers the opportunity to cover all disease-associated genes in only one approach and thus reveals the genetic heterogeneity of ALS and increases detection rates. Additionally, panel sequencing allows for the detection of multiple variants acting on the individual phenotype which might enable statements for example on disease progression or severity. We hope that our results will contribute to deeper knowledge which will allow the identification of new therapeutic targets for example by interfering with distinct pathways or personalized therapeutic approaches in the future.

It was our aim to broaden the genetic landscape of ALS. We detected previously identified ALS-causing mutations, novel variants within recognized disease-causing genes and candidate genes, in addition to modifiers and risk factors. Assessing the impact of newly detected variants and their potential contribution to the ALS phenotype requires further investigation in order to determine their functional relevance. For several

patients who gave their informed consent, we collected fibroblasts to provide the basis for the necessary functional work up.

AUTHOR CONTRIBUTIONS

Study concept and design: SK, MS, JP, and SB. Acquisition of clinical data and blood sample collection: JP and TGr. Analysis and interpretation of genetic data: SK, FB, AS, and MM. Drafting of manuscript: SK. Critical revision of manuscript: SK, FB, AS, MM, MS, LS, TGr, JP, and SB.

REFERENCES

- Abel, O., Powell, J. F., Andersen, P. M., and Al-Chalabi, A. (2012). ALSoD: a user-friendly online bioinformatics tool for amyotrophic lateral sclerosis genetics. *Hum. Mutat.* 33, 1345–1351. doi: 10.1002/humu.22157
- Adzhubei, I. A., Schmidt, S., Peshkin, L., Ramensky, V. E., Gerasimova, A., Bork, P., et al. (2010). A method and server for predicting damaging missense mutations. *Nat. Methods* 7, 248–249. doi: 10.1038/nmeth0410-248
- Aliaga, L., Lai, C., Yu, J., Chub, N., Shim, H., Sun, L., et al. (2013). Amyotrophic lateral sclerosis-related VAPB P56S mutation differentially affects the function and survival of corticospinal and spinal motor neurons. *Hum. Mol. Genet.* 22, 4293–4305. doi: 10.1093/hmg/ddt279
- Bannwarth, S., Ait-El-Mkadem, S., Chausseuot, A., Genin, E. C., Lacas-Gervais, S., Fragaki, K., et al. (2014). A mitochondrial origin for frontotemporal dementia and amyotrophic lateral sclerosis through CHCHD10 involvement. *Brain* 137(Pt 8), 2329–2345. doi: 10.1093/brain/awu138
- Bonn, F., Pantakani, K., Shoukier, M., Langer, T., and Mannan, A. U. (2010). Functional evaluation of paraplegin mutations by a yeast complementation assay. *Hum. Mutat.* 31, 617–621. doi: 10.1002/humu.21226
- Brugman, F., Scheffer, H., Wokke, J. H., Nillesen, W. M., de Visser, M., Aronica, E., et al. (2008). Paraplegin mutations in sporadic adult-onset upper motor neuron syndromes. *Neurology* 71, 1500–1505. doi: 10.1212/01.wnl.0000319700.11606.21
- Brunak, S., Engelbrecht, J., and Knudsen, S. (1991). Prediction of human mRNA donor and acceptor sites from the DNA sequence. *J. Mol. Biol.* 220, 49–65. doi: 10.1016/0022-2836(91)90380-O
- Byrne, S., Heverin, M., Elamin, M., Walsh, C., and Hardiman, O. (2014). Intermediate repeat expansion length in C9orf72 may be pathological in amyotrophic lateral sclerosis. *Amyotroph. Lateral Scler. Frontotemporal Degener.* 5, 148–150. doi: 10.3109/21678421.2013.838586
- Cady, J., Allred, P., Bali, T., Pestronk, A., Goate, A., Miller, T. M., et al. (2015). Amyotrophic lateral sclerosis onset is influenced by the burden of rare variants in known amyotrophic lateral sclerosis genes. *Ann. Neurol.* 77, 100–113. doi: 10.1002/ana.24306
- Cannon, A., Fujioka, S., Rutherford, N. J., Ferman, T. J., Broderick, D. F., Boylan, K. B., et al. (2013). Clinicopathologic variability of the GRN A9D mutation, including amyotrophic lateral sclerosis. *Neurology* 80, 1771–1777. doi: 10.1212/WNL.0b013e3182919059
- Chen, Y., Zeng, Y., Huang, R., Yang, Y., Chen, K., Song, W., et al. (2012). No association of five candidate genetic variants with amyotrophic lateral sclerosis in a Chinese population. *Neurobiol. Aging* 33, 2721. doi: 10.1016/j.neurobiolaging.2012.06.004
- Chiò, A., Calvo, A., Mazzini, L., Cantello, R., Mora, G., Moglia, C., et al. (2012). Extensive genetics of ALS: a population-based study in Italy. *Neurology* 79, 1983–1989. doi: 10.1212/WNL.0b013e3182735d36
- Choi, Y., Sims, G. E., Murphy, S., Miller, J. R., and Chan, A. P. (2012). Predicting the functional effect of amino acid substitutions and indels. *PLoS ONE* 7:e46688. doi: 10.1371/journal.pone.0046688
- Chow, C. Y., Landers, J. E., Berggren, S. K., Sapp, P. C., Grant, A. E., Jones, J. M., et al. (2009). Deleterious variants of *FIG4*, a phosphoinositide phosphatase, in patients with ALS. *Am. J. Hum. Genet.* 84, 85–88. doi: 10.1016/j.ajhg.2008.12.010
- Cirulli, E. T., Lasseigne, B. N., Petrovski, S., Sapp, P. C., Dion, P. A., Leblond, C. S., et al. (2015). Exome sequencing in amyotrophic lateral sclerosis identifies risk genes and pathways. *Science* 347, 1436–1441. doi: 10.1126/science.aaa3650
- Couthouis, J., Raphael, A. R., Daneshjou, R., and Gitler, A. D. (2014). Targeted exon capture and sequencing in sporadic amyotrophic lateral sclerosis. *PLoS Genet.* 10:e1004704. doi: 10.1371/journal.pgen.1004704
- DeJesus-Hernandez, M., Mackenzie, I. R., Boeve, B. F., Boxer, A. L., Baker, M., Rutherford, N. J., et al. (2011). Expanded GGGGCC hexanucleotide repeat in noncoding region of C9ORF72 causes chromosome 9p-linked FTD and ALS. *Neuron* 72, 245–256. doi: 10.1016/j.neuron.2011.09.011
- Dichgans, M., Herzog, J., and Gasser, T. (2001). NOTCH3 mutation involving three cysteine residues in a family with typical CADASIL. *Neurology* 57, 1714–1717. doi: 10.1212/WNL.57.9.1714
- Fernández-Santiago, R., Sharma, M., Berg, D., Illig, T., Anneser, J., Meyer, T., et al. (2011). No evidence of association of FLJ10986 and ITPR2 with ALS in a large German cohort. *Neurobiol. Aging* 32, 551. doi: 10.1016/j.neurobiolaging.2009.04.018
- Ferreirinha, F., Quattrini, A., Pirozzi, M., Valsecchi, V., Dina, G., Broccoli, V., et al. (2004). Axonal degeneration in paraplegin-deficient mice is associated with abnormal mitochondria and impairment of axonal transport. *J. Clin. Invest.* 113, 231–242. doi: 10.1172/JCI200420138
- Gros-Louis, F., Dupré, N., Dion, P., Fox, M. A., Laurent, S., Verreault, S., et al. (2007). Mutations in SYNE1 lead to a newly discovered form of autosomal recessive cerebellar ataxia. *Nat. Genet.* 39, 80–85. doi: 10.1038/ng1927
- Guerreiro, R. J., Santana, I., Bras, J. M., Revesz, T., Rebelo, O., Ribeiro, M. H., et al. (2008). Novel progranulin mutation: screening for PGRN mutations in a portuguese series of FTD/CBS cases. *Mov. Disord.* 23, 1269–1273. doi: 10.1002/mds.22078
- Guerreiro, R. J., Washecka, N., Hardy, J., and Singleton, A. (2010). A thorough assessment of benign genetic variability in GRN and MAPT. *Hum. Mutat.* 31, E1126–E1140. doi: 10.1002/humu.21152
- He, J., Mangelsdorf, M., Fan, D., Bartlett, P., and Brown, M. A. (2014). Amyotrophic lateral sclerosis genetic studies: from genome-wide association mapping to genome sequencing. *Neuroscientist* 21, 599–615. doi: 10.1177/1073858414555404
- Izumi, Y., Miyamoto, R., Morino, H., Yoshizawa, A., Nishinaka, K., Udaka, F., et al. (2013). Cerebellar ataxia with SYNE1 mutation accompanying motor neuron disease. *Neurology* 80, 600–601. doi: 10.1212/WNL.0b013e3182815529
- Jensen, L. J., Kuhn, M., Stark, M., Chaffron, S., Creevey, C., Muller, J., et al. (2009). STRING 8—a global view on proteins and their functional interactions in 630 organisms. *Nucleic Acids Res.* 37, D412–D416. doi: 10.1093/nar/gkn760
- Kenna, K. P., McLaughlin, R. L., Byrne, S., Elamin, M., Heverin, M., Kenny, E. M., et al. (2013). Delineating the genetic heterogeneity of ALS using targeted high-throughput sequencing. *J. Med. Genet.* 50, 776–783. doi: 10.1136/jmedgenet-2013-101795
- Klein, C. J. (2013). “Adult Polyglucosan Body Disease,” in *GeneReviews [Internet]*, eds R. A. Pagon, M. P. Adam, T. D. Bird, C. R. Dolan, C. T. Fong, R. J. Smith, et al. (Seattle, WA: University of Washington).

FUNDING

Supported by the German Center for Neurodegenerative Diseases (DZNE), Intersite project RO010 to J.P.

SUPPLEMENTARY MATERIAL

The Supplementary Material for this article can be found online at: <http://journal.frontiersin.org/article/10.3389/fnmol.2016.00092>

- Koppers, M., Groen, E. J., van Vught, P. W., van Rheeën, W., Witteveen, E., van Es, M. A., et al. (2013). Screening for rare variants in the coding region of ALS-associated genes at 9p21.2 and 19p13.3. *Neurobiol. Aging* 34:1518.e5–7. doi: 10.1016/j.neurobiolaging.2012.09.018
- Kurzweil, D., Krüger, S., Biskup, S., and Heneka, M. T. (2015). A distinct clinical phenotype in a German kindred with motor neuron disease carrying a CHCHD10 mutation. *Brain* 138(Pt 9), e376. doi: 10.1093/brain/awv014
- Landers, J. E., Leclerc, A. L., Shi, L., Virkud, A., Cho, T., Maxwell, M. M., et al. (2008). New VAPB deletion variant and exclusion of VAPB mutations in familial ALS. *Neurology* 70, 1179–1185. doi: 10.1212/01.wnl.0000289760.85237.4e
- Lemmens, R., Race, V., Hersmus, N., Matthijs, G., Van Den Bosch, L., Van Damme, P., et al. (2009). TDP-43 M31V mutation in familial amyotrophic lateral sclerosis. *J. Neurol. Neurosurg. Psychiatry* 80, 354–355. doi: 10.1136/jnnp.2008.157677
- Mackenzie, I. R., Baker, M., Pickering-Brown, S., Hsiung, G. Y., Lindholm, C., Dwosh, E., et al. (2006). The neuropathology of frontotemporal lobar degeneration caused by mutations in the progranulin gene. *Brain* 129(Pt 11), 3081–3090. doi: 10.1093/brain/awl271
- Majounie, E., Renton, A. E., Mok, K., Doppler, E. G., Waite, A., Rollinson, S., et al. (2012). Frequency of the C9orf72 hexanucleotide repeat expansion in patients with amyotrophic lateral sclerosis and frontotemporal dementia: a cross-sectional study. *Lancet Neurol.* 11, 323–330. doi: 10.1016/S1474-4422(12)70043-1
- Marangi, G., and Traynor, B. J. (2015). Genetic causes of amyotrophic lateral sclerosis: new genetic analysis methodologies entailing new opportunities and challenges. *Brain Res.* 1607, 75–93. doi: 10.1016/j.brainres.2014.10.009
- Meyer, T., Münch, C., Vülkel, H., Booms, P., and Ludolph, A. C. (1998). The EAAT2 (GLT-1) gene in motor neuron disease: absence of mutations in amyotrophic lateral sclerosis and a point mutation in patients with hereditary spastic paraplegia. *J. Neurol. Neurosurg. Psychiatry* 65, 594–596. doi: 10.1136/jnnp.65.4.594
- Mitsumoto, H., Nagy, P. L., Gennings, C., Murphy, J., Andrews, H., Goetz, R., et al. (2015). Phenotypic and molecular analyses of primary lateral sclerosis. *Neurol. Genet.* 1: e3. doi: 10.1212/01.NXG.0000464294.88607.dd
- Morgan, S., Shuai, M., Fratta, P., Sidle, K., Orrell, R., Sweeney, M. G., et al. (2015). Investigation of next-generation sequencing technologies as a diagnostic tool for amyotrophic lateral sclerosis. *Neurobiol. Aging* 36, 1600. doi: 10.1016/j.neurobiolaging.2014.12.017
- Müller, K., Andersen, P. M., Hübers, A., Marroquin, N., Volk, A. E., Danzer, K. M., et al. (2014). Two novel mutations in conserved codons indicate that CHCHD10 is a gene associated with motor neuron disease. *Brain* 137(Pt 12), e309. doi: 10.1093/brain/awu227
- Ngo, S. T., and Steyn, F. J. (2015). The interplay between metabolic homeostasis and neurodegeneration: insights into the neurometabolic nature of amyotrophic lateral sclerosis. *Cell Regen (Lond.)* 4, 5. doi: 10.1186/s13619-015-0019-6
- Nishimura, A. L., Mitne-Neto, M., Silva, H. C., Richieri-Costa, A., Middleton, S., Cascio, D., et al. (2004). A mutation in the vesicle-trafficking protein VAPB causes late-onset spinal muscular atrophy and amyotrophic lateral sclerosis. *Am. J. Hum. Genet.* 75, 822–831. doi: 10.1086/425287
- Noreau, A., Bourassa, C. V., Szuto, A., Levert, A., Dobrzyńska, S., Gauthier, J., et al. (2013). SYNE1 mutations in autosomal recessive cerebellar ataxia. *JAMA Neurol.* 70, 1296–1331. doi: 10.1001/jamaneurol.2013.3268
- Peters, O. M., Ghasemi, M., and Brown, R. H. Jr. (2015). Emerging mechanisms of molecular pathology in ALS. *J. Clin. Invest.* 125, 1767–1779. doi: 10.1172/JCI71601
- Pickering-Brown, S. M., Rollinson, S., Du Plessis, D., Morrison, K. E., Varma, A., Richardson, A. M., et al. (2008). Frequency and clinical characteristics of progranulin mutation carriers in the manchester frontotemporal lobar degeneration cohort: comparison with patients with MAPT and no known mutations. *Brain* 131, 721–731. doi: 10.1093/brain/awm331
- Redler, R. L., and Dokholyan, N. V. (2012). The complex molecular biology of amyotrophic lateral sclerosis (ALS). *Prog. Mol. Biol. Transl. Sci.* 107, 215–262. doi: 10.1016/B978-0-12-385883-2.00002-3
- Reese, M. G., Eckman, F. H., Kulp, D., and Haussler, D. (1997). Improved splice site detection in Genie. *J. Comput. Biol.* 4, 311–323. doi: 10.1089/cmb.1997.4.311
- Renton, A. E., Chiò, A., and Traynor, B. J. (2014). State of play in amyotrophic lateral sclerosis genetics. *Nat. Neurosci.* 17, 17–23. doi: 10.1038/nn.3584
- Renton, A. E., Majounie, E., Waite, A., Simón-Sánchez, J., Rollinson, S., Gibbs, J. R., et al. (2011). A hexanucleotide repeat expansion in C9orf72 is the cause of chromosome 9p21-linked ALS-FTD. *Neuron* 72, 257–268. doi: 10.1016/j.neuron.2011.09.010
- Richards, S., Aziz, N., Bale, S., Bick, D., Das, S., Gastier-Foster, J., et al. (2015). Standards and guidelines for the interpretation of sequence variants: a joint consensus recommendation of the American college of medical genetics and genomics and the association for molecular pathology. *Genet. Med.* 17, 405–424. doi: 10.1038/gim.2015.30
- Robinson, J. T., Thorvaldsdóttir, H., Winckler, W., Guttman, M., Lander, E. S., Getz, G., et al. (2011). Integrative genomics viewer. *Nat. Biotechnol.* 29, 24–26. doi: 10.1038/nbt.1754
- Rohrer, J. D., Isaacs, A. M., Mizielinska, S., Mead, S., Lashley, T., Wray, S., et al. (2015). C9orf72 expansions in frontotemporal dementia and amyotrophic lateral sclerosis. *Lancet Neurol.* 14, 291–301. doi: 10.1016/S1474-4422(14)70233-9
- Rosen, D. R., Siddique, T., Patterson, D., Figlewicz, D. A., Sapp, P., Hentati, A., et al. (1993). Mutations in Cu/Zn superoxide dismutase gene are associated with familial amyotrophic lateral sclerosis. *Nature* 362, 59–62. doi: 10.1038/362059a0
- Sánchez-Ferrero, E., Coto, E., Beetz, C., Gámez, J., Corao, A. I., Díaz, M., et al. (2013). SPG7 mutational screening in spastic paraplegia patients supports a dominant effect for some mutations and a pathogenic role for p.A510V. *Clin. Genet.* 83, 257–262. doi: 10.1111/j.1399-0004.2012.01896.x
- Schwarz, J. M., Cooper, D. N., Schuelke, M., and Seelow, D. (2014). MutationTaster2: mutation prediction for the deep-sequencing age. *Nat. Methods* 11, 361–362. doi: 10.1038/nmeth.2890
- Shaw, P. J. (2005). Molecular and cellular pathways of neurodegeneration in motor neuron disease. *J. Neurol. Neurosurg. Psychiatry* 76, 1046–1057. doi: 10.1136/jnnp.2004.048652
- Sleegers, K., Brouwers, N., Maurer-Stroh, S., van Es, M. A., Van Damme, P., van Vught, P. W., et al. (2008). Progranulin genetic variability contributes to amyotrophic lateral sclerosis. *Neurology* 71, 253–259. doi: 10.1212/01.wnl.0000289191.54852.75
- Sproviero, W., La Bella, V., Mazzei, R., Valentino, P., Rodolico, C., Simone, I. L., et al. (2012). FUS mutations in sporadic amyotrophic lateral sclerosis: clinical and genetic analysis. *Neurobiol. Aging* 33:837.e1–5. doi: 10.1016/j.neurobiolaging.2011.10.005
- Stenson, P. D., Mort, M., Ball, E. V., Shaw, K., Phillips, A., and Cooper, D. N. (2014). The human gene mutation database: building a comprehensive mutation repository for clinical and molecular genetics, diagnostic testing and personalized genomic medicine. *Hum. Genet.* 133, 1–9. doi: 10.1007/s00439-013-1358-4
- Su, X. W., Broach, J. R., Connor, J. R., Gerhard, G. S., and Simmons, Z. (2014). Genetic heterogeneity of amyotrophic lateral sclerosis: implications for clinical practice and research. *Muscle Nerve* 49, 786–803. doi: 10.1002/mus.24198
- Suzuki, H., Kanekura, K., Levine, T. P., Kohno, K., Olkkonen, V. M., Aiso, S., (2009). ALS-linked P56S-VAPB, an aggregated loss-of-function mutant of VAPB, predisposes motor neurons to ER stress-related death by inducing aggregation of co-expressed wild-type VAPB. *J. Neurochem.* 108, 973–985. doi: 10.1111/j.0022-3042.2008.05857.x
- Tomiyasu, A., Nakamura, M., Ichiba, M., Ueno, S., Saiki, S., Morimoto, M., et al. (2011). Novel pathogenic mutations and copy number variations in the VPS13A gene in patients with chorea-acanthocytosis. *Am. J. Med. Genet. B Neuropsychiatr. Genet.* 156B, 620–631. doi: 10.1002/ajmg.b.31206
- UniProt Consortium (2015). UniProt: a hub for protein information. *Nucleic Acids Res.* 43, D204–D212. doi: 10.1093/nar/gku989
- van Blitterswijk, M., van Es, M. A., Hennekam, E. A., Dooijes, D., van Rheeën, W., Medic, J., et al. (2012). Evidence for an oligogenic basis of amyotrophic lateral sclerosis. *Hum. Mol. Genet.* 21, 3776–3784. doi: 10.1093/hmg/dd199
- van Es, M. A., Van Vught, P. W., Blauw, H. M., Franke, L., Saris, C. G., Andersen, P. M., et al. (2007). ITPR2 as a susceptibility gene in sporadic amyotrophic

- lateral sclerosis: a genome-wide association study. *Lancet Neurol.* 6, 869–877. doi: 10.1016/S1474-4422(07)70222-3
- Wang, T., Jiang, X., Chen, G., and Xu, J. (2015). Interaction of amyotrophic lateral sclerosis/frontotemporal lobar degeneration-associated fused-in-sarcoma with proteins involved in metabolic and protein degradation pathways. *Neurobiol. Aging* 36, 527–535. doi: 10.1016/j.neurobiolaging.2014.07
- Yu, C. E., Bird, T. D., Bekris, L. M., Montine, T. J., Leverenz, J. B., Steinbart, E., et al. (2010). The spectrum of mutations in progranulin: a collaborative study screening 545 cases of neurodegeneration. *Arch. Neurol.* 67, 161–170. doi: 10.1001/archneurol.2009.328

Conflict of Interest Statement: The authors declare that the research was conducted in the absence of any commercial or financial relationships that could be construed as a potential conflict of interest.

Copyright © 2016 Krüger, Battke, Sprecher, Munz, Synofzik, Schöls, Gasser, Grehl, Prudlo and Biskup. This is an open-access article distributed under the terms of the Creative Commons Attribution License (CC BY). The use, distribution or reproduction in other forums is permitted, provided the original author(s) or licensor are credited and that the original publication in this journal is cited, in accordance with accepted academic practice. No use, distribution or reproduction is permitted which does not comply with these terms.



Protective LRRK2 R1398H Variant Enhances GTPase and Wnt Signaling Activity

Jonathon Nixon-Abell^{1,2†}, Daniel C. Berwick^{1,3†}, Simone Grannó¹, Victoria A. Spain¹, Craig Blackstone² and Kirsten Harvey^{1*}

¹ Department of Pharmacology, UCL School of Pharmacy, University College London, London, UK, ² Neurogenetics Branch, National Institute of Neurological Disorders and Stroke – National Institutes of Health, Bethesda, MD, USA, ³ Department of Life, Health and Chemical Sciences, The Open University, Milton Keynes, UK

Mutations in *LRRK2* are a common cause of familial and idiopathic Parkinson's disease (PD). Recently, the LRRK2 GTPase domain R1398H variant was suggested in genetic studies to confer protection against PD but mechanistic data supporting this is lacking. Here, we present evidence that R1398H affects GTPase function, axon outgrowth, and Wnt signaling in a manner opposite to pathogenic *LRRK2* mutations. LRRK2 R1398H GTPase domain dimerization and GTP hydrolysis were increased whereas GTP binding was reduced, leading to a decrease in active GTP-bound LRRK2. This protective variant also increased axon length of primary cortical neurones in comparison to wild-type LRRK2, whereas the R1441G LRRK2 pathogenic mutant decreased axon outgrowth. Importantly, R1398H enhanced the stimulatory effect of LRRK2 on canonical Wnt signaling whereas the G2385R risk variant, in accordance with all previously tested pathogenic LRRK2 mutants, had the opposite effect. Molecular modeling placed R1398H in close proximity to PD-causing mutations suggesting that this protective LRRK2 variant, like familial mutations, affects intramolecular RocCOR domain interactions. Thus, our data suggest that R1398H LRRK2 is a *bona fide* protective variant. The opposite effects of protective versus PD associated *LRRK2* variants on GTPase function and canonical Wnt signaling activity also suggests that regulation of these two basic signaling mechanisms is important for neuronal function. We conclude that LRRK2 mediated Wnt signaling and GTPase function are fundamental in conferring disease susceptibility and have clear implications for therapeutic target identification.

Keywords: GTPase activity, LRRK2, Parkinson's disease, protective genetic variant, Wnt signaling

OPEN ACCESS

Edited by:

Joe Lynch,
University of Queensland, Australia

Reviewed by:

Giovanni Piccoli,
Università degli Studi di Trento, Italy
Sunghoe Chang,
Seoul National University,
South Korea

*Correspondence:

Kirsten Harvey
kirsten.harvey@ucl.ac.uk

[†]These authors have contributed
equally to this work.

Received: 09 December 2015

Accepted: 22 February 2016

Published: 08 March 2016

Citation:

Nixon-Abell J, Berwick DC, Grannó S, Spain VA, Blackstone C and Harvey K (2016) Protective LRRK2 R1398H Variant Enhances GTPase and Wnt Signaling Activity. *Front. Mol. Neurosci.* 9:18. doi: 10.3389/fnmol.2016.00018

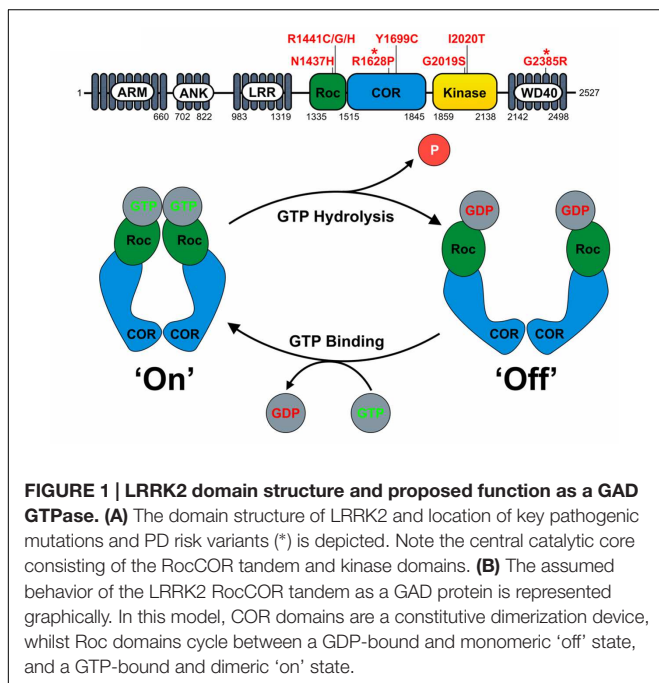
INTRODUCTION

Autosomal-dominant mutations in *LRRK2*, encoding leucine-rich repeat kinase 2 (LRRK2), are the most common known cause of inherited Parkinson's disease (PD; Paisán-Ruiz et al., 2004; Zimprich et al., 2004). Patients with *LRRK2* mutations display symptoms and brain pathologies that are largely indistinguishable from those of individuals with idiopathic PD (Paisán-Ruiz et al., 2004; Zimprich et al., 2004; Ross et al., 2006; Kumari and Tan, 2009). Thus, determining the biological role of LRRK2 is of paramount importance to understanding the etiology of PD, and likely to help uncover new therapeutic strategies.

LRRK2 is a multifunctional protein containing both kinase and GTPase activities and a number of protein–protein interaction domains (**Figure 1**). The ‘catalytic core’ is contained within the Roc (Ras of complex proteins), COR (C-terminal of Roc) and kinase domains (**Figure 1**) and appears essential for LRRK2 function (Berwick and Harvey, 2011). As the only hereditary mutations that are proven to cause PD fall within exons coding for the Roc, COR and kinase domains, the effects of pathogenic mutations on LRRK2 enzymatic activities require further investigation.

The precise extent of the LRRK2 GTPase domain remains controversial. Restricting the LRRK2 GTPase domain to the Roc domain can be justified by the similarity to Ras family small GTPases. Arguing against this are the observations that isolated Roc protein appears to hydrolyse GTP at a greatly reduced rate compared to full-length LRRK2 (Gilsbach and Kortholt, 2014) and that throughout evolution, Roc and COR domains never occur without each other (Bosgraaf and van Haastert, 2003). This supports the definition of a LRRK2 GTPase “RocCOR tandem” domain.

Based on homology to *C. tepidum* Roco protein, the LRRK2 RocCOR tandem is predicted to fall into the GAD (G proteins activated by nucleotide-dependent dimerization) class of molecular switches (Gotthardt et al., 2008; Gasper et al., 2009; Gilsbach and Kortholt, 2014). Under the GAD model, two LRRK2 molecules are expected to dimerize via a constitutive interaction between the COR domains holding the two Roc domains in close proximity (**Figures 1** and **3A,B**). Binding of GTP to the Roc domains results in protein dimerization allowing binding of effector proteins. GTP hydrolysis disrupts Roc dimerization, leading to the dissociation of effector proteins (Gotthardt et al., 2008; Gasper et al., 2009; Gilsbach and Kortholt, 2014).



All known PD-causing mutations located within the LRRK2 RocCOR domain have been reported to increase GTP-binding, decrease GTPase activity, or both (**Table 1**) supporting the idea that shifting LRRK2 to the GTP-bound ‘on’-state promotes neurodegeneration.

A consensus on the cellular role of LRRK2 is still lacking, with numerous competing – though not mutually exclusive – functions reported. Nonetheless, a comprehensive literature review identified cell biological processes involving LRRK2 that appear to be reproducible (Berwick and Harvey, 2013) including effects on membrane trafficking (Piccoli et al., 2011; Ramonet et al., 2011; reviewed by Gómez-Suaga et al., 2014), cytoskeletal function (Parisiadou et al., 2009; Law et al., 2014; reviewed by Gómez-Suaga et al., 2014) and signal transduction pathways including MAPK, Wnt, TLR, and NFAT pathways (Berwick and Harvey, 2011; Boon et al., 2014; reviewed by Gómez-Suaga et al., 2014).

A growing body of data supports the importance of deregulated canonical Wnt signaling in neurodegenerative disease pathogenesis, including PD (Berwick and Harvey, 2014; Inestrosa and Varela-Nallar, 2014). At least six proteins implicated in PD have been described to modulate this pathway, whilst development of the midbrain dopaminergic neurones that are typically lost in PD is acutely dependent on canonical Wnt signaling (Berwick and Harvey, 2014). Furthermore, decreased Wnt signaling has been reported in PD patients (Cantuti-Castelvetri et al., 2007), as well as in various animal models of parkinsonism (L’Episcopo et al., 2011; Gollamudi et al., 2012). Since Wnt ligands are well established as neuroprotective (Berwick and Harvey, 2014; Inestrosa and Varela-Nallar, 2014), the idea that decreased canonical Wnt signaling is involved in PD pathogenesis is an attractive hypothesis. Importantly, evidence for a crucial role of LRRK2 in canonical Wnt signaling is accumulating. Protein–protein interactions between LRRK2 and a number of Wnt signaling components have been reported, including interactions with disheveled (DVL) proteins, the serine/threonine kinase GSK3 β , and LRP6, a Wnt signaling transmembrane receptor (Sancho et al., 2009; Lin et al., 2010; Berwick and Harvey, 2012). Furthermore, over-expressed wild-type LRRK2 enhances the signal strength of activated canonical Wnt signaling (Berwick and Harvey, 2012). Intriguingly, this effect of LRRK2 is weakened by PD-causing mutations in three distinct catalytic domains of LRRK2 – R1441C in the Roc domain, Y1699C in the COR domain, and G2019S in the kinase domain (Berwick and Harvey, 2012) – suggesting that impaired Wnt signaling is a common pathogenic mechanism of familial LRRK2 mutations.

Recently, a number of genetic screens have reported an inherited R1398H *LRRK2* variant in the Roc domain (Chen et al., 2010; Tan et al., 2010; Ross et al., 2011; Heckman et al., 2013, 2014) that appears to confer decreased risk of PD. This could prove extremely informative, since a protective variant can be expected to display the opposite behavior to pathogenic variants in disease-relevant assays. In a single study, R1398H was reported to display decreased kinase activity compared to wild-type LRRK2 (Tan et al., 2010). However, this observation should be treated with caution, as this study also found the G2385R

TABLE 1 | The effect of PD-causing mutations in the LRRK2 RocCOR tandem domain on GTP-binding and GTPase activity.

Mutation	LRRK2 construct	GTP binding	GTP hydrolysis	Prediction	Reference
N1437H	Full length	↑	ns	↑ GTP-bound	Aasly et al., 2010
R1441C	Full length	↑	ns	↑ GTP-bound	West et al., 2007
R1441C	Full length	—	↓	↑ GTP-bound	Li et al., 2007
R1441C	Full length	—	↓	↑ GTP-bound	Lewis et al., 2007
R1441C	Roc	ns	↓	↑ GTP-bound	Deng et al., 2008
R1441C	Full length	ns	↓	↑ GTP-bound	Xiong et al., 2010
R1441C	Roc, COR, kinase	—	—	No change	Xiong et al., 2010
R1441C	970-2527	ns	↓	↑ GTP-bound	Pungaliya et al., 2010
R1441C	Full length	↑	ns	↑ GTP-bound	Stafa et al., 2012
R1441G	Full length	↑	ns	↑ GTP-bound	West et al., 2007
R1441G	Full length	—	↓	↑ GTP-bound	Li et al., 2007
R1441G	Full length	ns	↓	↑ GTP-bound	Xiong et al., 2010
R1441H	Roc	↑	↓	↑ GTP-bound	Liao et al., 2014
"R1441"A	<i>C. tepidum</i> RocCOR	—	↓	↑ GTP-bound	Gotthardt et al., 2008
Y1699C	Full length	↑	ns	↑ GTP-bound	West et al., 2007
Y1699C	Full length	ns	↓	↑ GTP-bound	Xiong et al., 2010
Y1699C	Full length	—	↓	↑ GTP-bound	Daniëls et al., 2011
Y1699C	Full length	↑	ns	↑ GTP-bound	Stafa et al., 2012
"Y1699"C	<i>C. tepidum</i> RocCOR	—	↓	↑ GTP-bound	Gotthardt et al., 2008

Based on published data, the pathogenic N1437H, R1441C, R1441G, R1441H, and Y1699C mutations all elicit an increase in the fraction of GTP-bound LRRK2. Only one construct, an R1441C RocCOR-kinase, displayed no changes in GTP-binding or GTP hydrolysis; however, this mutation decreased GTPase activity in full length LRRK2 in the same publication. Note that mutations at residues equivalent to R1441 and Y1699 in *C. tepidum* Roco protein produce consistent results. Key: up and down arrows represent increases and decreases, respectively; dashes represent no change; 'ns' indicates 'not studied.'

risk variant to have increased kinase activity, in contrast to other reports (Jaleel et al., 2007; West et al., 2007; Nichols et al., 2010; Rudenko et al., 2012). In any case, the need to elucidate the functional relevance of the R1398H experimentally is clear.

Here, we report the behavior of the LRRK2 R1398H variant in five assays for which the effect of a *bona fide* protective mutation in the LRRK2 Roc domain can be predicted: LRRK2 RocCOR tandem domain dimerization, LRRK2 GTP-binding, LRRK2 GTPase assays, axon outgrowth, and canonical Wnt signaling assays. Remarkably, R1398H displays the opposite behavior to pathogenic mutants in all experiments. Furthermore, molecular modeling studies suggest that this amino acid substitution is likely to affect intramolecular RocCOR interactions, consistent with the predicted mode of action for PD-causing mutations in the RocCOR tandem. Thus our data (1) provide strong experimental support for the status of LRRK2 R1398H as a genuine protective variant; (2) increase the weight of evidence that GTP-bound LRRK2 is pathogenic; and (3) provide further data indicating that decreased canonical Wnt signaling is a key pathomechanism underlying PD.

MATERIALS AND METHODS

Molecular Cloning

pDS-BAIT (pDS; Dualsystems Biotech) plasmids containing the LRRK2 Roc and RocCOR domains (encoding amino acids 1330–1515 and 1335–1845, respectively), pACT2 (Clontech) containing the LRRK2 RocCOR domain and pYTH16 containing the intracellular domain of LRP6 (amino acids 1416–1613) have been described previously (Daniëls et al., 2011; Berwick

and Harvey, 2012). pCHMWS vectors expressing 3× FLAG-tagged wild-type LRRK2 and LRRK2-T1348N were a generous gift from Dr. Jean-Marc Taymans (Daniëls et al., 2011). pRK5 myc-LRRK2 has also been described previously (Sancho et al., 2009). R1398H, R1398H/R1441G and G2385R mutations were introduced using the QuikChange Lightning site-directed mutagenesis kit (Agilent) according to the manufacturer's instructions. All constructs were verified by DNA sequencing.

Culture of Immortalized Cell Lines

HEK293 cells and SH-SY5Y cells were grown in Dulbecco's modified Eagle's medium (DMEM) supplemented with 10% (v/v) fetal bovine serum, 100 U/ml penicillin G and 100 µg/ml streptomycin at 37°C and 5% CO₂. Transient transfection was performed using FuGENE HD (Roche) according to the manufacturer's instructions, using a 2.5 µL transfection reagent to 1 µg DNA ratio. In all cases, cells were harvested 24 h after transfection.

Quantitative Yeast-Two Hybrid

The L40 yeast strain (Invitrogen) was co-transformed with pDS Roc or RocCOR bait and pACT2 wild-type or mutant RocCOR prey constructs, and the Y190 yeast strain (Clontech) was co-transformed with the pYTH16 LRP6 intracellular domain bait and pACT2 wild-type or mutant RocCOR prey constructs. Transformations were spread on selective dropout media (Clontech) lacking leucine and tryptophan for transformation controls, or leucine, tryptophan and histidine, supplemented with 0.5 mM 3-aminotriazole (L40 strain) or 10 mM 3-aminotriazole (Y190 strain; for suppression of 'leaky' histidine expression;

Sigma-Aldrich) for nutritional selection. After incubation at 30°C for 3 days, prototrophic colonies were picked and used to inoculate minimal SD (Clontech) media lacking leucine and tryptophan. Samples were subsequently incubated shaking at 30°C overnight. Cell pellets were then resuspended in Z-buffer (60 mM Na₂HPO₄, 40 mM NaH₂PO₄, 10 mM KCl, 1 mM MgSO₄·7H₂O) containing 40 mM β-mercaptoethanol, followed by lysis in 0.1% (w/v) SDS (Sigma-Aldrich) and 0.1% (v/v) chloroform (Sigma-Aldrich). After the addition of chlorophenyl-β-D-galactopyranoside (Sigma-Aldrich), the color change was recorded at 540 nm and readings adjusted for turbidity of the yeast suspension at 620 nm. The background signal (bait plus empty pACT2 vector) was subtracted from each reading and values were normalized to the wild-type RocCOR response, which was set at 100%. All protein interactions were assayed in three to five independent experiments in triplicate.

Molecular Modeling

Molecular modeling was performed on the *C. tepidum* Roc structure (PDB: 3DPU; Gotthardt et al., 2008) using Chimera (Pettersen et al., 2004). Amino acid substitutions were performed with the *swapaa* command using the Dunbrack backbone-dependent rotamer library (Dunbrack, 2002).

GTP-Binding Assay

HEK293 cells were transfected with 3× FLAG-tagged T1348N, R1398H or wild-type LRRK2. The GTP binding assay was performed similarly as described by others (Korr et al., 2006). Briefly, cells were lysed for 10 min on ice in lysis buffer G (100 mM Tris/HCl pH 7.5, 50 mM KCl, 1 mM EDTA, 0.1 mM DTT, 5 mM MgCl₂, 1% Triton X-100, protease inhibitor cocktail, Roche), and lysates were centrifuged for 10 min at 20,000 g and 4°C. Supernatants containing 100 μg protein each, as assessed by QuickStart Bradford assay (Bio-Rad), were incubated for 80 min at 4°C with 30 μl of GTP-Sepharose bead suspension (Sigma) that was pre-treated with 100 μg/ml BSA (Pierce) at 4°C for 1 h. Samples were washed three times with 500 μl lysis buffer G, before bound protein was eluted using 100 μM GTP in lysis buffer G. The resulting eluate was added to 1× NuPAGE sample buffer (Invitrogen) and heated for 6 min at 96°C. The eluates were analyzed by SDS-PAGE and immunoblotting. Initially, protein was loaded into 4–12% (w/v) BisTris pre-cast gels (Invitrogen), prior to transfer to polyvinylidene fluoride membranes (Millipore). Non-specific bands were blocked for 1 h at 37°C with 5% (w/v) skimmed milk in PBS plus 0.1% (v/v) Tween 20. Anti-Calnexin antibody (Abcam) was used at 1:4000, and anti-FLAG antibody (Sigma-Aldrich) was used at 1:3000 at 4°C overnight. For detection, an HRP-conjugated anti-rabbit secondary antibody (Santa Cruz Biotechnology) was used at a final dilution of 1:2000, together with the SuperSignal West Pico Chemiluminescent Substrate (Pierce).

GTPase Assay

GTPase assays were carried out according to Daniëls et al. (2011). Initially, HEK293 cells were transfected with 3× FLAG-tagged T1348N, R1398H or wild-type LRRK2 and lysed after 24 h in GTPase lysis buffer [20 mM Tris/HCl pH 7.5, 150 mM

NaCl, 1 mM EDTA, 1% Triton X-100, 10% Glycerol, protease inhibitor cocktail (Roche), phosphatase inhibitor cocktail 2 (Sigma-Aldrich)]. Cell lysates were clarified as above, added to 40 μl of anti-FLAG M2 affinity gel (Sigma-Aldrich) and incubated overnight at 4°C on a turning disk in order to purify the FLAG-tagged proteins. The affinity gel was subjected to centrifugation (4°C, 100 g, 3 min), followed by two washes in GTPase lysis buffer and a brief rinse in GTPase buffer (20 mM Tris/HCl pH 7.5, 150 mM NaCl, 10 mM MgCl₂, 0.02% Triton X-100). Proteins were eluted from beads with 3× FLAG peptide (Sigma-Aldrich) in GTPase buffer according to manufacturer's instructions. The protein concentration of eluates were calculated from a serial BSA dilution curve, with purity assessed by running a small volume of each sample on an SDS-PAGE gel and staining with GelCode Blue Stain Reagent (Pierce). GTPase assays were performed according to Margalit et al. (2004) using 80 nM LRRK2 protein in GTPase buffer containing 20 U/ml pyruvate kinase (EC 2.7.1.40)/lactate dehydrogenase (EC 1.1.1.27; Sigma-Aldrich), 600 μM NADH (Sigma-Aldrich), 1 mM PEP (Sigma-Aldrich) and 500 μM GTP (Sigma-Aldrich) in a final volume of 200 μl. Reaction mixes were equilibrated to 30°C for 10 min before the reactions were initiated by the addition of GTP and thorough mixing of the contents. Depletion of NADH was measured by monitoring the decrease in absorbance at 340 nm every 5 min across a 50 min period using a VersaMax microplate reader (Molecular Devices).

Primary Cortical Neuronal Cultures

Primary cultures of rat cortical neurones were prepared from E18 embryos obtained from timed-pregnant Sprague-Dawley rats (Taconic Biosciences, Hudson, NY, USA) narcotized with CO₂ (in cylinders) then decapitated using a guillotine. All animal studies were approved by the National Institute of Neurological Disorders and Stroke/National Institute on Deafness and Other Communication Disorders Animal Care and Use Committee (Protocol 1151-12). Neurones were transfected with wild-type and mutant myc-tagged LRRK2 using the Amaxa Rat Neuron Nucleofector Kit, program 0-03, according to the manufacturer's protocol (Lonza Group, Basel, Switzerland). Neurones were then plated at a density of approximately $2.6 \times 10^4/\text{cm}^2$ on cover slips and maintained as described previously (Zhu et al., 2006). At 7 days *in vitro* (DIV) neurones were fixed for 10 min with 4% paraformaldehyde, and permeabilized for 15 min with 0.05% Triton-X (Sigma-Aldrich) prior to a 1 h block in 5% NGS (GIBCO). Slides were then immunostained with primary and Alexa Fluor secondary antibodies, mounted using ProLong gold (Life Technologies), and imaged using a Zeiss LSM710 laser-scanning confocal microscope. Primary antibodies against the following proteins were used: myc-epitope (Santa Cruz Biotechnology), MAP2 (Abcam) and Tau-1 (Abcam). Alexa Fluor 488 (rabbit), 555 (mouse) and 633 (goat) secondary antibodies (Thermo Scientific) were used against myc, tau and MAP-2 epitopes respectively.

Axon Length Measurements

Axon outgrowth properties of neurones were quantified manually. Three to six coverslips from three independent

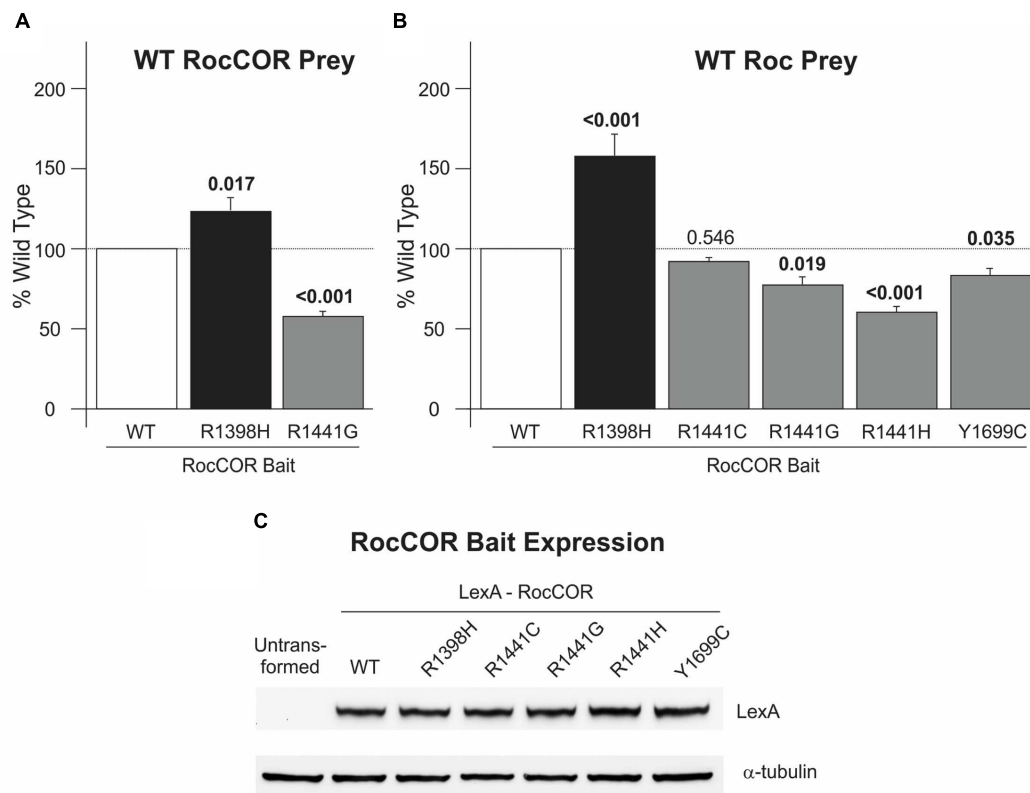


FIGURE 2 | R1398H increases LRRK2 RocCOR dimerization. Quantitative YTH assays reveal that the presence of an R1398H variant in the RocCOR prey constructs **(A)** increases the interaction strength with a RocCOR bait whereas the pathogenic R1441G mutant has the opposite effect (one-way ANOVA for effect of genotype, $F = 39.286$, $p < 0.001$; $n = 5$). Values shown are the means of five independent experiments. **(B)** The R1398H variant also increases the interaction strength with an isolated Roc domain bait whilst the pathogenic R1441G, R1441H, and Y1699C *LRRK2* mutations weaken interaction strength (one-way ANOVA for effect of genotype, $F = 34.729$, $p < 0.001$; $n = 3-6$). **(C)** All LRRK2 mutant constructs express at an equivalent level to wild-type LRRK2. Values shown are the means of at least three independent experiments. p -values for *post hoc* Dunnett's testing relative to wild-type LRRK2 are shown. Error bars represent the standard error of the mean.

experiments for each genotype were analyzed. Axonal outgrowth and branching of dissociated neurones were quantified manually and verified using the NeuronJ plugin for ImageJ. Transfected neurones were identified using the myc-epitope antibody, whilst the length of the longest Tau-1 stained process from each neurone was measured. At least 40 neurones were quantified for each genotype, myc vector control, myc-LRRK2 wild-type, myc-LRRK2 R1398H, myc-LRRK2 R1441G, and myc-LRRK2 R1398H/R1441G from at least three coverslips.

Luciferase Assays

Canonical Wnt activity was measured using the TOPflash reporter plasmid (Veeman et al., 2003) in human dopaminergic SH-SY5Y cells as described previously (Berwick and Harvey, 2012). Cells were extracted 24 h post-transfection using Passive Lysis Buffer (Promega) and assays performed using a Dual Luciferase Reporter Assay kit (Promega) and Turner Instruments 20/20 luminometer. Luciferase values were normalized to co-transfected Renilla plasmid to adjust for

transfection efficiency, and then corrected to values from parallel experiments performed using the FOPflash control plasmid (Veeman et al., 2003).

Statistical Analysis

GTPase assays (Figure 4D) were tested by two-way ANOVA with repeated measures, with the independent variables genotype, time, and time \times genotype, followed by *post hoc* analysis by two-sided Dunnett's testing. Axonal branching was assessed by Kruskal-Wallis (Figure 6B) or Mann-Witney (Supplementary Figure S2A) tests. Axon length was analyzed by one-way ANOVA followed by Bonferroni *post hoc* analysis (Figure 6C) or Student's *t*-test (Supplementary Figure S2B). For axon length analysis, outliers (values defined as differing from the mean by 2 or more standard deviations) were first excluded. All other experiments were analyzed by one-way ANOVA for the effect of genotype followed by a two-sided Dunnett's test with wild-type LRRK2 considered the control. Student's *t*-test was performed using Excel, all other statistics were performed with SPSS software. All error bars represent the standard error of the mean.

RESULTS

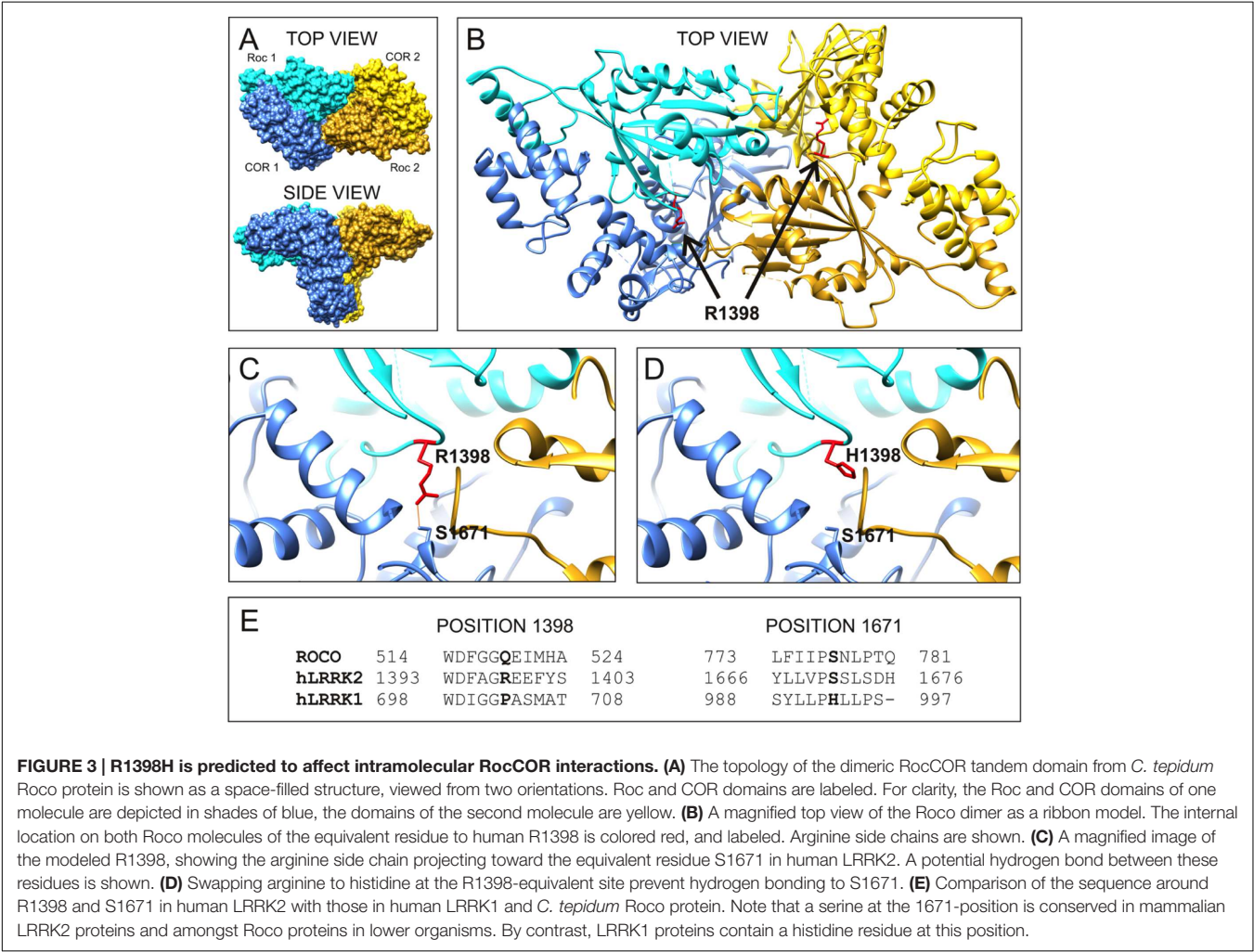
In Contrast to *LRRK2* GTPase Mutants Causing PD, R1398H Increases RocCOR Dimerization

To investigate functional effects of R1398H, we studied this variant in assays of *LRRK2* RocCOR domain dimerization. These sensitive quantitative yeast-two hybrid (Q-YTH) assays have been used previously in our laboratory to show that the PD-causing R1441C, R1441G, R1441H, and Y1699C mutations significantly weaken RocCOR domain dimerization (Daniëls et al., 2011). Intriguingly, R1398H elicited an effect opposite to these pathogenic mutations, with increased RocCOR dimerization observed (Figure 2A). The R1441G mutant was studied as a pathogenic control showing as expected a significant decrease in RocCOR dimerisation (Figure 2A). Consistently, R1398H also strengthened interaction between the *LRRK2* RocCOR tandem domain and an isolated wild-type *LRRK2* Roc domain, whilst the R1441G, R1441H, and Y1699C pathogenic mutations weakened this interaction (Figure 2B). R1441C was also studied in this experiment, displaying a non-significant trend

toward decreased interaction (Figure 2B). These effects were not due to changes in protein expression (Figure 2C). Thus, in contrast to proven PD-causing RocCOR mutations, R1398H enhanced intermolecular dimerization within the *LRRK2* GTPase domain.

Molecular Modeling Suggests that *LRRK2* R1398H Affects Intramolecular RocCOR Interaction

To examine the molecular mechanism underlying altered RocCOR dimerization, the predicted location of R1398 was examined by molecular modeling of the closest available protein structure: the RocCOR tandem domain of *C. tepidum* Roco protein (Gotthardt et al., 2008). Supporting the importance of R1398 in RocCOR dimerization, the equivalent residue in Roco (Q519) resides on the internal face of each Roc domain. To examine the role of human R1398, this amino acid was swapped to arginine in our model (Figure 3C). Using the most probable rotamer conformation, the long basic side chain of arginine projected toward the COR domain of the same molecule. Indeed, R1398 was predicted to bond with the hydroxyl



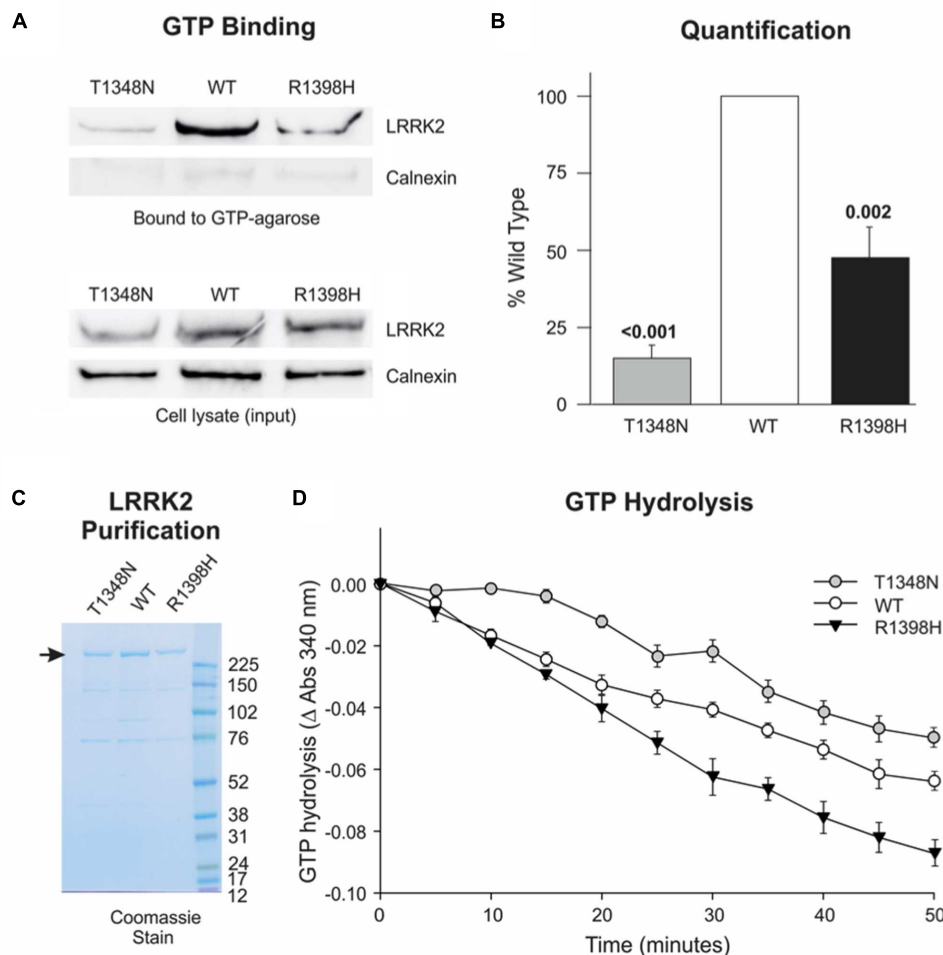
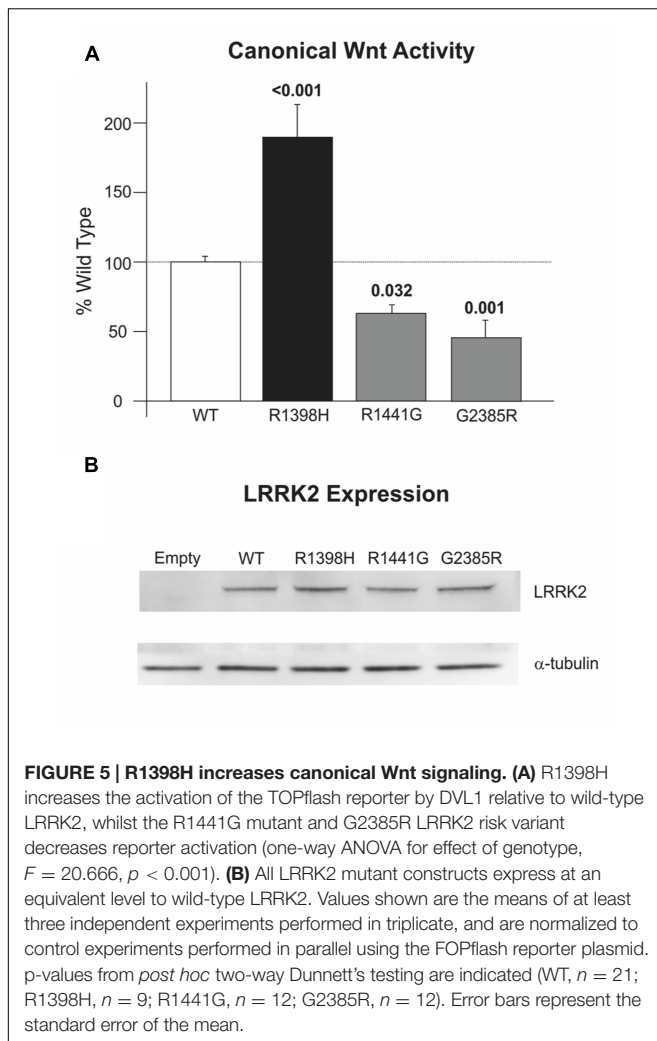


FIGURE 4 | R1398H decreases the fraction of LRRK2 in the GTP-bound 'on'-state and increases GTPase activity. (A,B) GTP binding assays reveal decreased binding of R1398H mutant LRRK2 to GTP-sepharose compared to wild-type. **(A)** Shows a representative experiment; **(B)** the mean of three independent experiments (one-way ANOVA for effect of genotype, $F = 48.475$, $p < 0.001$) with p -values from *post hoc* Dunnett's testing indicated. Values were adjusted to the amount of transfected LRRK2 in cell lysates; gels were re-probed for calnexin to show protein loading and to confirm the purity of GTP-bound protein. **(C)** A protein gel showing the purity and concentration of FLAG-tagged LRRK2 protein to be used in GTPase assays. The masses (kDa) of the molecular weight marker bands are shown. **(D)** GTP hydrolysis assays reveal that the R1398H mutant displays greater GTPase activity than wild-type LRRK2. Two-way ANOVA with repeated measures and a Greenhouse–Geisser correction revealed significant effects of time ($F = 224.221$; $p < 0.001$), genotype ($F = 24.06$; $p < 0.001$) and interaction between time and genotype ($F = 7.021$; $p < 0.001$). p -values from *post hoc* two-sided Dunnett's tests are shown. Value are the means of four independent experiments. Error bars represent the standard error of the mean.

group of a conserved serine in the COR domain (S778 in Roco, S1671 in LRRK2, predicted hydrogen bond distance: 2.776 Å). This is an intriguing possibility, since the R1441C/G and Y1699C pathogenic mutations have also been predicted to modify intramolecular RocCOR interactions (Gotthardt et al., 2008; Daniëls et al., 2011). In agreement, conversion of R1398 to the much shorter histidine – representative of R1398H – prevented bonding with the conserved serine (**Figure 3D**). Taken together, our molecular modeling suggests that the observed increase in *intermolecular* RocCOR dimerization caused by R1398H (**Figure 2**) likely occurs via an indirect mechanism, involving changes to *intramolecular* interactions between Roc and COR domains.

R1398H Decreases the Fraction of GTP-Bound LRRK2

Numerous reports indicate that PD-causing mutations in the LRRK2 RocCOR tandem domain increase the ratio of GTP-bound ('on') LRRK2 to GDP-bound ('off') LRRK2, by weakening GTPase activity and/or facilitating GTP binding (**Table 1**). In principle, a protective amino acid substitution located within this portion of LRRK2 would be expected to have the opposite effect. Thus, the effect of the R1398H variant on LRRK2 GTPase function was examined directly, using full-length human LRRK2 expressed in mammalian cells. Firstly, this variant was studied in GTP binding assays. As reported by others, wild-type LRRK2 bound strongly to immobilized GTP, whilst a



well-characterized mutant, LRRK2 T1348N, had negligible GTP-binding capacity (**Figures 4A,B**). Strikingly, the R1398H variant also displayed weakened GTP binding (~47% of wild-type), although this value was more than threefold greater than for T1348N LRRK2, indicating that GTP binding is not abolished entirely.

We next examined the effect of the LRRK2 R1398H variant on GTP hydrolysis *in vitro*, using steady-state GTPase assays. FLAG-tagged wild-type LRRK2, and LRRK2 containing T1348N and R1398H amino acid substitutions were purified from HEK293 cells (**Figure 4C**), and equimolar amounts were used in subsequent experiments (**Figure 4D**). This protein produced a steady turnover of GTP, confirming that wild-type LRRK2 possesses intrinsic GTPase activity (**Figure 4D**, open circles). Unsurprisingly, since T1348N LRRK2 is almost unable to bind GTP, this mutant possessed very little GTPase activity, with GTP hydrolysis undetectable until the 20 min time point (**Figure 4D**, gray circles). However, R1398H LRRK2 showed a marked increase in GTP hydrolysis relative to wild-type LRRK2 (**Figure 4D**, black triangles). In summary, the protective R1398H LRRK2 variant weakens GTP binding but increases steady-state

GTP hydrolysis, both of which are consistent with a decrease in the proportion of GTP-bound LRRK2.

The Protective R1398H LRRK2 Variant Increases Canonical Wnt Signaling

We have previously reported that PD-causing mutations in the Roc, COR and kinase domains of LRRK2 weaken the activation of canonical Wnt signaling that is elicited by disheveled (DVL) proteins (Berwick and Harvey, 2012). Consistent with this finding, the LRRK2 R1441G pathogenic mutant and importantly the WD40 domain G2385R PD risk variant also reduce pathway activation relative to wild-type LRRK2 in SH-SY5Y cells (**Figure 5A**). By contrast, LRRK2 R1398H enhanced DVL1-driven Wnt activation almost twice as much as wild-type LRRK2 (**Figure 5A**). This opposing effect of the protective LRRK2 variant to that described for pathogenic variants in four distinct LRRK2 domains is notable, and cannot be attributed to altered expression levels (**Figure 5B**). These experiments suggest a strong correlation between PD risk conferred by LRRK2 variants and regulation of canonical Wnt signaling activity.

To further examine a possible causal mechanism that affects canonical Wnt signaling, we investigated the interaction between the LRRK2 R1398H variant and the canonical Wnt co-receptor LRP6 in Q-YTH experiments. Using the LRP6 intracellular domain as bait and the LRRK2 RocCOR tandem domain as prey, we observed a decrease in the interaction strength with the R1398H protective variant relative to wild-type LRRK2 (Supplementary Figures S1A,B). Since pathogenic LRRK2 GTPase mutants also show a decrease in protein-protein interaction (Supplementary Figure S1A, Berwick and Harvey, 2012) altered LRRK2-LRP6 interactions do not explain the increase in canonical Wnt signaling activity of the R1398H protective variant relative to the decrease observed for pathogenic LRRK2 variants.

Protective R1398H LRRK2 Variant Increases Axon Length in Cultured Cortical Neurones

Temporary differences in neurite outgrowth between LRRK2 knockout, mutant and wild-type neurones have been reported in various experimental systems (MacLeod et al., 2006; Dächsel et al., 2010; reviewed by Gómez-Suaga et al., 2014). As LRRK2 GTPase activity and Wnt signaling activity (Salinas, 2012; Gómez-Suaga et al., 2014) affect neurite outgrowth, we decided to examine axon length and branching as a correlate for neurite outgrowth and complexity in rat cortical neurones in primary culture overexpressing LRRK2 wild-type and variants at 7 DIV. Over-expression of wild-type LRRK2 had no effect on mean axonal length ($p = 0.082$) or axon branching ($p = 0.695$) relative to neurones transfected with empty vector control (Supplementary Figure S2). Furthermore, no difference in axon branching was observed between the different LRRK2 genotypes (Kruskal-Wallis $\chi^2 = 0.943$, $p = 0.815$; **Figure 6B**). However, the overexpression of LRRK2 mutants had a marked effect on axon length ($F = 23.52$, $p < 0.001$; **Figure 6C**). In agreement with previous work, neurones overexpressing the pathogenic LRRK2

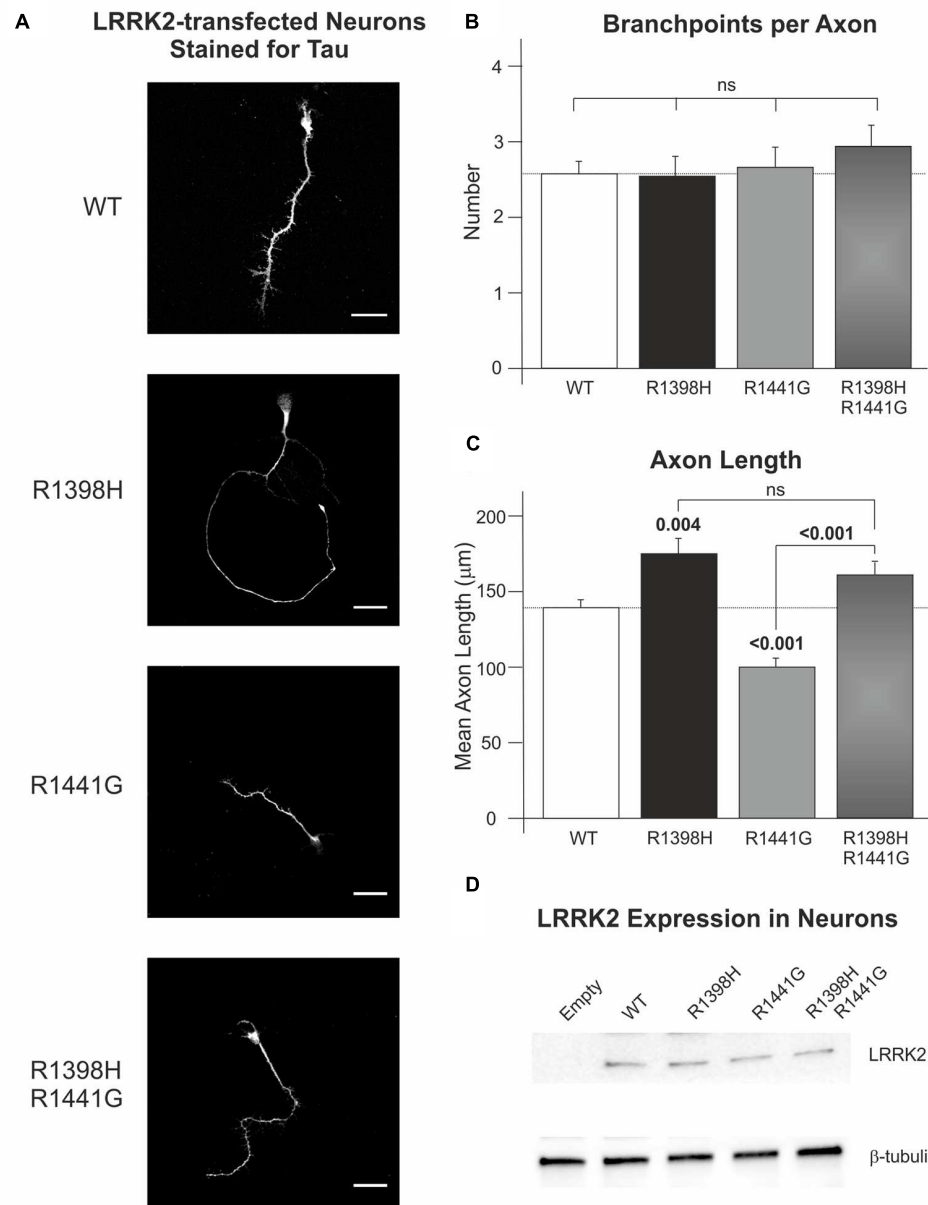
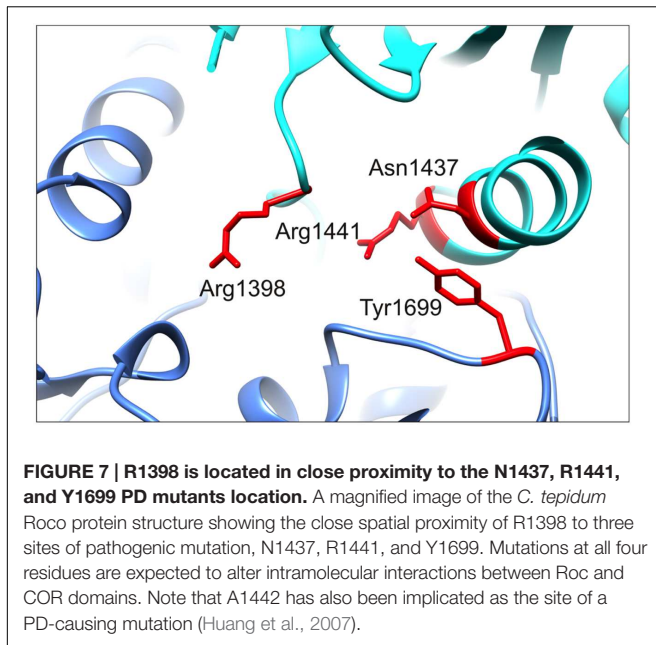


FIGURE 6 | The protective R1398H LRRK2 variant increases axonal length in primary cortical neuronal cultures. Rat primary neurones were transfected with wild-type LRRK2 or the indicated variants prior to fixation and staining for axonal tau protein after 7 DIV. **(A)** Shows representative images of LRRK2-transfected neurones. **(B)** Quantification of the number of axon branches per neurone reveals no effect of R1441G or R1398H mutations (WT, $n = 49$; R1398H, $n = 26$; R1441G, $n = 38$; R1398H/R1441G, $n = 31$). **(C)** By contrast, R1398H increases axonal length and rescues the decrease in length caused by the pathogenic R1441G mutant (WT, $n = 49$; R1398H, $n = 32$; R1441G, $n = 56$; R1398H/R1441G, $n = 39$). **(D)** All LRRK2 mutant constructs were expressed at an equivalent level to wild-type LRRK2. Scale bar: 30 μm . p -values from *post hoc* Bonferroni tests are shown. Error bars represent the standard error of the mean.

R1441G mutant showed a reduction in axon length relative to wild-type LRRK2 (MacLeod et al., 2006; Cho et al., 2013). By contrast, the protective R1398H variant increased axon length in comparison to wild-type overexpressing cells. Remarkably, R1398H was able to rescue the effect of R1441G, as a double R1398H/R1441G mutant phenocopied the effect of the R1398H single mutant (Figure 6).

DISCUSSION

Our data provide robust experimental evidence consistent with the idea that the familial LRRK2 R1398H variant is protective against PD. Firstly, in contrast to the pathogenic R1441C, R1441G, R1441H, and Y1699C variants (Figure 2A; Klein et al., 2009; Daniëls et al., 2011; Law et al., 2014), R1398H



increases LRRK2 RocCOR domain dimerization (**Figure 2**). Secondly, our molecular modeling suggests that this amino acid substitution will affect the interaction between the Roc and COR domains of the same molecule (**Figure 3**). Similarly, the R1441C/G/H and Y1699C mutations, and indirectly the N1437H mutation, have been suggested to affect intramolecular RocCOR interactions and consequently RocCOR dimerization as a proposed molecular pathomechanism (Gotthardt et al., 2008; Klein et al., 2009; Daniëls et al., 2011). Thirdly, our GTP-binding and GTP hydrolysis assays point toward R1398H decreasing the ratio of GTP-bound to GDP-bound LRRK2. This is in direct contrast to PD-causing mutations in the LRRK2 RocCOR tandem domain (**Table 1**). Fourthly, the R1398H protective variant increases axon length in cortical neurones, whereas LRRK2 mutants cause shortening of axons in equivalent assays (**Figure 6**, MacLeod et al., 2006; Dächsel et al., 2010; reviewed by Gómez-Suaga et al., 2014). And fifthly, R1398H has the opposite effect to pathogenic mutations and variants located *throughout* LRRK2 in cellular assays of canonical Wnt activity (**Figure 5**; Berwick and Harvey, 2012). Taken together, we believe our data make a persuasive case in support of the genetic evidence that the R1398H variant is a genuine protective variant.

Curiously, structure-based alterations at the R1398 site have already been studied in assays of LRRK2 GTPase function and produced results that are consistent with our R1398H data. This is encouraging, since mutation of R1398 to any other amino acid can be expected to prevent hydrogen bonding to S1671. The best-studied structure-based LRRK2 R1398 mutant, R1398L, was designed from Ras GTPase homology models, with the expectation that it would behave similarly to the Q61L amino acid substitution that renders Ras proteins ‘GTP-locked.’ However, R1398L had the opposite effect. This change increased GTPase activity, both in full-length LRRK2 and in a deletion construct

containing the Roc, COR and kinase domains of LRRK2 (RocCOR-kinase; Xiong et al., 2010; Stafa et al., 2012; Bioss et al., 2013). R1398L also weakened GTP-binding in RocCOR-kinase constructs, although no effect was seen in full-length LRRK2 (Xiong et al., 2010; Bioss et al., 2013). Although in disagreement with expectations, these data are clearly in accordance with our results for LRRK2 R1398H. An R1398Q mutant was also studied, with the rationale that this mutation would render LRRK2 more like wild-type Ras, but no statistically significant changes to GTP-binding or GTP hydrolysis were detected using full-length LRRK2 (Bioss et al., 2013). However, when R1398Q was introduced into a RocCOR-kinase construct alongside a second Ras-like amino acid substitution, T1343G, GTP-binding was decreased and GTP hydrolysis increased (Xiong et al., 2010).

As mentioned, PD-causing mutations outside the RocCOR tandem domain do not appear to operate via the same mechanism as those affecting GTPase function, i.e., they do not shift LRRK2 GTPase toward the GTP-bound ‘on’-state. This is curious, since logic would dictate that the effects of all PD-causing mutations in *LRRK2* should converge on the same process or processes eventually. By extension, a protective variant would be expected to affect the same process, but in the opposite direction. With this in mind, it is striking that the protective LRRK2 R1398H variant appears to enhance canonical Wnt signaling. This observation is opposite to our data for pathogenic mutations throughout the catalytic core of LRRK2 (Berwick and Harvey, 2012), and a PD risk variant in the C-terminal WD40 domain (**Figure 7**).

Our data add to the growing body of evidence indicating that deregulation of canonical Wnt signaling is involved in LRRK2 PD (Berwick and Harvey, 2014). Previous studies have revealed that LRRK2 interacts with DVL proteins that play a central role in all branches of Wnt signaling: (i) canonical; (ii) planar cell polarity (PCP); and (iii) Wnt/ Ca^{2+} -signaling (Sancho et al., 2009; Berwick and Harvey, 2012). LRRK2 also interacts with multiple components of the β -catenin destruction complex *in vivo* and associates with the Wnt co-receptor LRP6 at membranes. Importantly, expression of familial LRRK2 mutants results in decreased activation of Wnt/ β -catenin signaling (Berwick and Harvey, 2012). Strikingly, in this study we show that the R1398H mutant has the opposite effect.

Our data also have implications beyond LRRK2 PD. Wnt signaling pathways have emerged as essential regulators of neuronal development and maintenance (Inestrosa and Arenas, 2010). Wnt ligands are known to activate signaling pathways that lead to remodeling of the cytoskeleton and promote neurite outgrowth via small GTPases (Inestrosa and Arenas, 2010). Deficiencies in Wnt signaling pathways have been shown to affect synaptic stability in the striatum (Arenas, 2014), whilst antagonism of canonical Wnt signaling in the *substantia nigra* promotes dopaminergic neurone death (L’Episcopo et al., 2014). Wnt signaling is also important in the interplay between the immune system (astrocytes, microglia) and neurones, and deregulation affects adult neurogenesis (SVZ plasticity) with age (L’Episcopo et al., 2014). Furthermore, both aging and neurotoxin exposure are reported to down-regulate canonical Wnt signaling in the adult midbrain, thereby increasing the vulnerability

of dopaminergic neurones. Taken together these observations provide strong evidence that Wnt signaling regulates multiple cell biological functions in the midbrain dopaminergic neurones that degenerate in PD, and that the age-related decrease in canonical Wnt activity may have a central role in the pathogenesis of sporadic forms of PD.

CONCLUSION

Our data support a model where pathogenic RocCOR mutants display altered intramolecular RocCOR interactions, leading to weakened RocCOR dimerization, increased GTP binding and decreased GTP hydrolysis. Together, these effects lead to a greater proportion of LRRK2 molecules existing in the GTP-bound 'on'-state. The protective R1398H Roc domain mutation also affects RocCOR interactions but with the opposite result, leading to more LRRK2 in the 'off'-state. As such, developing small molecules to decrease LRRK2 GTP-binding and/or stimulate LRRK2 GTPase activity seems a promising strategy for the development of PD modifying treatments and has already shown some encouraging results in LRRK2 GTP and kinase domain mutant PD models (Li et al., 2014, 2015).

AUTHOR CONTRIBUTIONS

JN-A, DB, CB, and KH designed the experiments; JN-A, DB, SG, and VS performed the experiments; JN-A, DB, SG, and KH analyzed the data; DB and KH wrote the paper. All authors were involved in revising the paper for important intellectual content, and gave final approval of the version to be published.

REFERENCES

- Aasly, J. O., Vilarinho-Güell, C., Dachselt, J. C., Webber, P. J., West, A. B., Haugarvoll, K., et al. (2010). Novel pathogenic LRRK2 p.Asn1437His substitution in familial Parkinson's disease. *Mov. Disord.* 25, 2156–2163. doi: 10.1002/mds.23265
- Arenas, E. (2014). Wnt signaling in midbrain dopaminergic neuron development and regenerative medicine for Parkinson's disease. *J. Mol. Cell Biol.* 6, 42–53. doi: 10.1093/jmcb/mju001
- Berwick, D. C., and Harvey, K. (2011). LRRK2 signaling pathways. The key to unlocking neurodegeneration? *Trends Cell Biol.* 21, 257–265. doi: 10.1016/j.tcb.2011.01.001
- Berwick, D. C., and Harvey, K. (2012). LRRK2 functions as a Wnt signaling scaffold, bridging cytosolic proteins and membrane-localized LRP6. *Hum. Mol. Genet.* 21, 4966–4979. doi: 10.1093/hmg/ddc342
- Berwick, D. C., and Harvey, K. (2013). LRRK2: an éminence grise of Wnt-mediated neurogenesis? *Front. Cell. Neurosci.* 7:82. doi: 10.3389/fncel.2013.00082
- Berwick, D. C., and Harvey, K. (2014). The regulation and deregulation of Wnt signaling by PARK genes in health and disease. *J. Mol. Cell Biol.* 6, 3–12. doi: 10.1093/jmcb/mjt037
- Biosa, A., Trancikova, A., Civiero, L., Glauser, L., Bubacco, L., Greggio, E., et al. (2013). GTPase activity regulates kinase activity and cellular phenotypes of Parkinson's disease-associated LRRK2. *Hum. Mol. Genet.* 22, 1140–1156. doi: 10.1093/hmg/ddc522
- Boon, J. Y., Dusanochet, J., Trengrove, C., and Wolozin, B. (2014). Interaction of LRRK2 with kinase and GTPase signaling cascades. *Front. Mol. Neurosci.* 7:64. doi: 10.3389/fnmol.2014.00064

FUNDING

This work was supported by The Wellcome Trust [WT088145AIA, WT095010MA to KH], the Medical Research Council [MR/M00676X/1 to KH] and a Vera Down British Medical Association Research Grant [to KH]. CB and JN-A were also supported by the Intramural Research Program of the NINDS, National Institutes of Health. The funders had no role in study design, data collection and analysis, decision to publish, or preparation of the manuscript.

ACKNOWLEDGMENTS

We thank Dr. Jean-Marc Taymans (KU Leuven, Leuven, Belgium) for guidance in performing GTPase assays, Dr. Victoria James (University College London, London, UK) for assistance with molecular modeling, Dr. Peng-Peng Zhu (National Institutes of Health, Bethesda, MD, USA) for instruction on culturing primary neurones and Emma Schul (University College London, London, UK) for use of the microplate reader for GTPase assays.

SUPPLEMENTARY MATERIAL

The Supplementary Material for this article can be found online at: <http://journal.frontiersin.org/article/10.3389/fnmol.2016.00018>

- Bosgraaf, L., and van Haastert, P. J. (2003). Roc, a Ras/GTPase domain in complex proteins. *Biochim. Biophys. Acta* 1643, 5–10. doi: 10.1016/j.bbamcr.2003.08.008
- Cantuti-Castelvetri, I., Keller-McGandy, C., Bouzou, B., Asteris, G., Clark, T. W., Frosch, M. P., et al. (2007). Effects of gender on nigral gene expression and parkinson disease. *Neurobiol. Dis.* 26, 606–614. doi: 10.1016/j.nbd.2007.02.009
- Chen, L., Zhang, S., Liu, Y., Hong, H., Wang, H., Zheng, Y., et al. (2010). LRRK2 R1398H polymorphism is associated with decreased risk of Parkinson's disease in a Han Chinese population. *Parkinsonism Relat. Disord.* 17, 291–292. doi: 10.1016/j.parkreldis.2010.11.012
- Cho, H. J., Liu, G., Jin, S. M., Parisiadou, L., Xie, C., Yu, J., et al. (2013). MicroRNA-205 regulates the expression of Parkinson's disease-related leucine-rich repeat kinase 2 protein. *Hum. Mol. Genet.* 22, 608–620. doi: 10.1093/hmg/ddc470
- Dächsel, J. C., Behrouz, B., Yue, M., Beevers, J. E., Melrose, H. L., and Farrer, M. J. (2010). A comparative study of Lrrk2 function in primary neuronal cultures. *Parkinsonism Relat. Disord.* 16, 650–655. doi: 10.1016/j.parkreldis.2010.08.018
- Daniëls, V., Vancaenenbroeck, R., Law, B. M., Greggio, E., Lobbestael, E., Gao, F., et al. (2011). Insight into the mode of action of the LRRK2 Y1699C pathogenic mutant. *J. Neurochem.* 116, 304–315. doi: 10.1111/j.1471-4159.2010.07105.x
- Deng, J., Lewis, P. A., Greggio, E., Sluch, E., Beilina, A., and Cookson, M. R. (2008). Structure of the ROC domain from the Parkinson's disease-associated leucine-rich repeat kinase 2 reveals a dimeric GTPase. *Proc. Natl. Acad. Sci. U.S.A.* 105, 1499–1504. doi: 10.1073/pnas.0709098105
- Dunbrack, R. L. (2002). Rotamer libraries in the 21st century. *Curr. Opin. Struct. Biol.* 12, 431–440. doi: 10.1016/S0959-440X(02)00344-5
- Gasper, R., Meyer, S., Gotthardt, K., Sirajuddin, M., and Wittinghofer, A. (2009). It takes two to tango: regulation of G proteins by dimerization. *Nat. Rev. Mol. Cell Biol.* 10, 423–429. doi: 10.1038/nrm2689

- Giltsbach, B. K., and Kortholt, A. (2014). Structural biology of the LRRK2 GTPase and kinase domains: implications for regulation. *Front. Mol. Neurosci.* 7:32. doi: 10.3389/fnmol.2014.00032
- Gollamudi, S., Johri, A., Calingasan, N. Y., Yang, L., Elemento, O., and Beal, M. F. (2012). Concordant signaling pathways produced by pesticide exposure in mice correspond to pathways identified in human Parkinson's disease. *PLoS ONE* 7:e36191. doi: 10.1371/journal.pone.0036191
- Gómez-Suaga, P., Fdez, E., Fernández, B., Martínez-Salvador, M., Blanca Ramírez, M., Madero-Pérez, J., et al. (2014). Novel insights into the neurobiology underlying LRRK2-linked Parkinson's disease. *Neuropharmacology* 85, 45–56. doi: 10.1016/j.neuropharm.2014.05.020
- Gotthardt, K., Weyand, M., Kortholt, A., Van Haastert, P. J., and Wittinghofer, A. (2008). Structure of the Roc-COR domain tandem of *C. tepidum*, a prokaryotic homologue of the human LRRK2 Parkinson kinase. *EMBO J.* 27, 2239–2249. doi: 10.1038/emboj.2008.150
- Heckman, M. G., Elbaz, A., Soto-Ortolaza, A. I., Serie, D. J., Aasly, J. O., Annesi, G., et al. (2014). Protective effect of LRRK2 p.R1398H on risk of Parkinson's disease is independent of MAPT and SNCA variants. *Neurobiol. Aging* 35:e5–e14. doi: 10.1016/j.neurobiolaging.2013.07.013
- Heckman, M. G., Soto-Ortolaza, A. I., Aasly, J. O., Abahuni, N., Annesi, G., Bacon, J. A., et al. (2013). Population-specific frequencies for LRRK2 susceptibility variants in the genetic epidemiology of Parkinson's disease (GEO-PD) Consortium. *Mov. Disord.* 12, 1740–1744. doi: 10.1002/mds.25600
- Huang, Y., Halliday, G. M., Vandebona, H., Mellick, G. D., Mastaglia, F., Stevens, J., et al. (2007). Prevalence and clinical features of common LRRK2 mutations in Australians with Parkinson's disease. *Mov. Disord.* 22, 982–989.
- Inestrosa, N. C., and Arenas, E. (2010). Emerging roles of Wnts in the adult nervous system. *Nat. Rev. Neurosci.* 11, 77–86. doi: 10.1038/nrn2755
- Inestrosa, N. C., and Varela-Nallar, L. (2014). Wnt signaling in the nervous system and in Alzheimer's disease. *J. Mol. Cell. Biol.* 6, 64–74. doi: 10.1093/jmcb/mjt051
- Jaleel, M., Nichols, R. J., Deak, M., Campbell, D. G., Gillardon, F., Knebel, A., et al. (2007). LRRK2 phosphorylates moesin at threonine-558: characterization of how Parkinson's disease mutants affect kinase activity. *Biochem. J.* 405, 307–317. doi: 10.1042/BJ20070209
- Klein, C. L., Rovelli, G., Springer, W., Schall, C., Gasser, T., and Kahle, P. J. (2009). Homo- and heterodimerization of ROCO kinases: LRRK2 kinase inhibition by the LRRK2 ROCO fragment. *J. Neurochem.* 111, 703–715. doi: 10.1111/j.1471-4159.2009.06358.x
- Korr, D., Toschi, L., Donner, P., Pohlenz, H. D., Kreft, B., and Weiss, B. (2006). LRRK1 protein kinase activity is stimulated upon binding of GTP to its Roc domain. *Cell Signal.* 18, 910–920. doi: 10.1016/j.cellsig.2005.08.015
- Kumari, U., and Tan, E. K. (2009). LRRK2 in Parkinson's disease. Genetic and clinical studies from patients. *FEBS J.* 276, 6455–6463. doi: 10.1111/j.1742-4658.2009.07344.x
- Law, B. M., Spain, V. A., Leinster, V. H., Chia, R., Beilina, A., Cho, H. J., et al. (2014). A direct interaction between leucine-rich repeat kinase 2 and specific β -tubulin isoforms regulates tubulin acetylation. *J. Biol. Chem.* 289, 895–908. doi: 10.1074/jbc.M113.507913
- L'Episcopo, F., Tirolo, C., Caniglia, S., Testa, N., Morale, M. C., Serapide, M. F., et al. (2014). Targeting Wnt signaling at the neuroimmune interface for dopaminergic neuroprotection/repair in Parkinson's disease. *J. Mol. Cell Biol.* 6, 13–26. doi: 10.1093/jmcb/mjt053
- L'Episcopo, F., Tirolo, C., Testa, N., Caniglia, S., Morale, M. C., Cossetti, C., et al. (2011). Reactive astrocytes and Wnt/ β -catenin signaling link nigrostriatal injury to repair in 1-methyl-4-phenyl-1,2,3,6-tetrahydropyridine model of Parkinson's disease. *Neurobiol. Dis.* 41, 508–527. doi: 10.1016/j.nbd.2010.10.023
- Lewis, P. A., Greggio, E., Beilina, A., Jain, S., Baker, A., and Cookson, M. R. (2007). The R1441C mutation of LRRK2 disrupts GTP hydrolysis. *Biochem. Biophys. Res. Commun.* 357, 668–671. doi: 10.1016/j.bbrc.2007.04.006
- Li, T., He, X., Thomas, J. M., Yang, D., Zhong, S., Xue, F., et al. (2015). A novel GTP-binding inhibitor, FX2149, attenuates LRRK2 toxicity in Parkinson's disease models. *PLoS ONE* 10:e0122461. doi: 10.1371/journal.pone.0122461
- Li, T., Yang, D., Zhong, S., Thomas, J. M., Xue, F., Liu, J., et al. (2014). Novel LRRK2 GTP-binding inhibitors reduced degeneration in Parkinson's disease cell and mouse models. *Hum. Mol. Genet.* 23, 6212–6222. doi: 10.1093/hmg/ddu341
- Li, X., Tan, Y. C., Poulouse, S., Olanow, C. W., Huang, X. Y., and Yue, Z. (2007). Leucine-rich repeat kinase 2 (LRRK2)/PARK8 possesses GTPase activity that is altered in familial Parkinson's disease R1441C/G mutants. *J. Neurochem.* 103, 238–247.
- Liao, J., Wu, C. X., Burlak, C., Zhang, S., Sahm, H., Wang, M., et al. (2014). Parkinson disease-associated mutation R1441H in LRRK2 prolongs the “active state” of its GTPase domain. *Proc. Natl. Acad. Sci. U.S.A.* 111, 4055–4060. doi: 10.1073/pnas.1323285111
- Lin, C. H., Tsai, P. I., Wu, R. M., and Chien, C. T. (2010). LRRK2 G2019S mutation induces dendrite degeneration through mislocalization and phosphorylation of tau by recruiting autoactivated GSK3 β . *J. Neurosci.* 30, 13138–13149. doi: 10.1523/JNEUROSCI.1737-10.2010
- MacLeod, D., Dowman, J., Hammond, R., Leete, T., Inoue, K., and Abeliovich, A. (2006). The familial Parkinsonism gene LRRK2 regulates neurite process morphology. *Neuron* 52, 587–593. doi: 10.1016/j.neuron.2006.10.008
- Margalit, D. N., Romberg, L., Mets, R. B., Hebert, A. M., Mitchison, T. J., Kirschner, M. W., et al. (2004). Targeting cell division: small-molecule inhibitors of FtsZ GTPase perturb cytoskeletal ring assembly and induce bacterial lethality. *Proc. Natl. Acad. Sci. U.S.A.* 101, 11821–11826. doi: 10.1073/pnas.0404439101
- Nichols, R. J., Dзамко, N., Morrice, N. A., Campbell, D. G., Deak, M., Ordureau, A., et al. (2010). 14-3-3 binding to LRRK2 is disrupted by multiple Parkinson's disease-associated mutations and regulates cytoplasmic localization. *Biochem. J.* 430, 393–404. doi: 10.1042/BJ20100483
- Paisán-Ruiz, C., Jain, S., Evans, E. W., Gilks, W. P., Simón, J., van der Brug, M., et al. (2004). Cloning of the gene containing mutations that cause PARK8-linked Parkinson's disease. *Neuron* 44, 595–600. doi: 10.1016/j.neuron.2004.10.023
- Parisiadou, L., Xie, C., Cho, H. J., Lin, X., Gu, X. L., Long, C. X., et al. (2009). Phosphorylation of ezrin/radixin/moesin proteins by LRRK2 promotes the rearrangement of actin cytoskeleton in neuronal morphogenesis. *J. Neurosci.* 29, 13971–13980. doi: 10.1523/JNEUROSCI.3799-09.2009
- Pettersen, E. F., Goddard, T. D., Huang, C. C., Couch, G. S., Greenblatt, D. M., Meng, E. C., et al. (2004). UCSF Chimera: A visualization system for exploratory research and analysis. *J. Comput. Chem.* 25, 1605–1612. doi: 10.1002/jcc.20084
- Piccoli, G., Condliffe, S. B., Bauer, M., Giesert, F., Boldt, K., De Astis, S., et al. (2011). LRRK2 controls synaptic vesicle storage and mobilization within the recycling pool. *J. Neurosci.* 31, 2225–2237. doi: 10.1523/JNEUROSCI.3730-10.2011
- Pungaliya, P. P., Bai, Y., Lipinski, K., Anand, V. S., Sen, S., Brown, E. L., et al. (2010). Identification and characterization of a leucine-rich repeat kinase 2 (LRRK2) consensus phosphorylation motif. *PLoS ONE* 5:e13672. doi: 10.1371/journal.pone.0013672
- Ramonet, D., Daher, J. P., Lin, B. M., Stafa, K., Kim, J., Banerjee, R., et al. (2011). Dopaminergic neuronal loss, reduced neurite complexity and autophagic abnormalities in transgenic mice expressing G2019S mutant LRRK2. *PLoS ONE* 6:e18568. doi: 10.1371/journal.pone.0018568
- Ross, O. A., Soto-Ortolaza, A. I., Heckman, M. G., Aasly, J. O., Abahuni, N., Annesi, G., et al. (2011). Association of LRRK2 exonic variants with susceptibility to Parkinson's disease: a case-control study. *Lancet Neurol.* 10, 898–908. doi: 10.1016/S1474-4422(11)70175-2
- Ross, O. A., Toft, M., Whittle, A. J., Johnson, J. L., Papapetropoulos, S., Mash, D. C., et al. (2006). Lrrk2 and Lewy body disease. *Ann. Neurol.* 59, 388–393. doi: 10.1002/ana.20731
- Rudenko, I. N., Kaganovich, A., Hauser, D. N., Beylina, A., Chia, R., Ding, J., et al. (2012). The G2385R variant of leucine-rich repeat kinase 2 associated with Parkinson's disease is a partial loss-of-function mutation. *Biochem. J.* 446, 99–111. doi: 10.1042/BJ20120637
- Salinas, P. C. (2012). Wnt signaling in the vertebrate central nervous system: from axon guidance to synaptic function. *Cold Spring Harb. Perspect. Biol.* 4:a008003. doi: 10.1101/cshperspect.a008003
- Sancho, R. M., Law, B. M., and Harvey, K. (2009). Mutations in the LRRK2 Roc-COR tandem domain link Parkinson's disease to Wnt signalling pathways. *Hum. Mol. Genet.* 18, 3955–3968. doi: 10.1093/hmg/ddp337
- Stafa, K., Trancikova, A., Webber, P. J., Glauser, L., West, A. B., and Moore, D. J. (2012). GTPase activity and neuronal toxicity of Parkinson's disease-associated LRRK2 is regulated by ArfGAP1. *PLoS Genet.* 8:e1002526. doi: 10.1371/journal.pgen.1002526
- Tan, E. K., Peng, R., Teo, Y. Y., Tan, L. C., Angeles, D., Ho, P., et al. (2010). Multiple LRRK2 variants modulate risk of Parkinson disease: a Chinese multicenter study. *Hum. Mutat.* 31, 561–568. doi: 10.1002/humu.21225

- Veeman, M. T., Slusarski, D. C., Kaykas, A., Louie, S. H., and Moon, R. T. (2003). Zebrafish prickles, a modulator of noncanonical Wnt/Fz signaling, regulates gastrulation movements. *Curr. Biol.* 13, 680–685. doi: 10.1016/S0960-9822(03)00240-9
- West, A. B., Moore, D. J., Choi, C., Andrabi, S. A., Li, X., Dikeman, D., et al. (2007). Parkinson's disease-associated mutations in LRRK2 link enhanced GTP-binding and kinase activities to neuronal toxicity. *Hum. Mol. Genet.* 16, 223–232. doi: 10.1093/hmg/ddl471
- Xiong, Y., Coombes, C. E., Kilaru, A., Li, X., Gitler, A. D., Bowers, W. J., et al. (2010). GTPase activity plays a key role in the pathobiology of LRRK2. *PLoS Genet.* 6:e1000902. doi: 10.1371/journal.pgen.1000902
- Zhu, P. P., Soderblom, C., Tao-Cheng, J. H., Stadler, J., and Blackstone, C. (2006). SPG3A protein atlastin-1 is enriched in growth cones and promotes axon elongation during neuronal development. *Hum. Mol. Genet.* 15, 1343–1353. doi: 10.1093/hmg/ddl054
- Zimprich, A., Biskup, S., Leitner, P., Lichtner, P., Farrer, M., Lincoln, S., et al. (2004). Mutations in LRRK2 cause autosomal-dominant parkinsonism with pleomorphic pathology. *Neuron* 44, 601–607. doi: 10.1016/j.neuron.2004.11.005

Conflict of Interest Statement: The authors declare that the research was conducted in the absence of any commercial or financial relationships that could be construed as a potential conflict of interest.

Copyright © 2016 Nixon-Abell, Berwick, Grannó, Spain, Blackstone and Harvey. This is an open-access article distributed under the terms of the Creative Commons Attribution License (CC BY). The use, distribution or reproduction in other forums is permitted, provided the original author(s) or licensor are credited and that the original publication in this journal is cited, in accordance with accepted academic practice. No use, distribution or reproduction is permitted which does not comply with these terms.



A Recombinant Human Pluripotent Stem Cell Line Stably Expressing Halide-Sensitive YFP-I152L for GABA_AR and GlyR-Targeted High-Throughput Drug Screening and Toxicity Testing

Katharina Kuenzel^{1,2}, Oliver Friedrich^{1,2} and Daniel F. Gilbert^{1,2*}

¹ Department of Chemical and Biological Engineering, Institute of Medical Biotechnology, Friedrich-Alexander-Universität Erlangen-Nürnberg, Erlangen, Germany, ² Erlangen Graduate School in Advanced Optical Technologies, Friedrich-Alexander-Universität Erlangen-Nürnberg, Erlangen, Germany

OPEN ACCESS

Edited by:

Robert J. Harvey,
UCL School of Pharmacy, UK

Reviewed by:

Henry J. Waldvogel,
University of Auckland, New Zealand

Joe Lynch,
The University of Queensland,
Australia

*Correspondence:

Daniel F. Gilbert
daniel.gilbert@fau.de

Received: 10 May 2016

Accepted: 13 June 2016

Published: 28 June 2016

Citation:

Kuenzel K, Friedrich O and Gilbert DF
(2016) A Recombinant Human
Pluripotent Stem Cell Line Stably
Expressing Halide-Sensitive
YFP-I152L for GABA_AR and
GlyR-Targeted High-Throughput Drug
Screening and Toxicity Testing.
Front. Mol. Neurosci. 9:51.
doi: 10.3389/fnmol.2016.00051

GABA_ARs and GlyRs are considered attractive drug targets for therapeutic intervention and are also increasingly recognized in the context of *in vitro* neurotoxicity (NT) and developmental neurotoxicity (DNT) testing. However, systematic human-specific GABA_AR and GlyR-targeted drug screening and toxicity testing is hampered due to lack of appropriate *in vitro* models that express native GABA_ARs and GlyRs. We have established a human pluripotent stem cell line (NT2) stably expressing YFP-I152L, a halide-sensitive variant of yellow fluorescent protein (YFP), allowing for fluorescence-based functional analysis of chloride channels. Upon stimulation with retinoic acid, NT2 cells undergo neuronal differentiation and allow pharmacological and toxicological evaluation of native GABA_ARs and GlyRs at different stages of brain maturation. We applied the cell line in concentration-response experiments with the neurotransmitters GABA and glycine as well as with the drugs strychnine, picrotoxin, flupronil, lindane, bicuculline, and zinc and demonstrate that the established *in vitro* model is applicable to GABA_AR and GlyR-targeted pharmacological and toxicological profiling. We quantified the proportion of GABA_AR and GlyR-sensitive cells, respectively, and identified percentages of approximately 20% each within the overall populations, rendering the cells a suitable model for systematic *in vitro* GABA_AR and GlyR-targeted screening in the context of drug development and NT/DNT testing.

Keywords: YFP-I152L, glycine receptor chloride channel (GlyR), gamma-aminobutyric acid receptor type-A chloride channel (GABA_AR), human pluripotent embryonal teratocarcinoma stem cells, NT2 cells, NT2-N cells

INTRODUCTION

GABA type-A receptors (GABA_AR) and strychnine-sensitive glycine receptors (GlyR) are ligand-gated chloride ion channels that mediate inhibitory neurotransmission in the central nervous system (CNS). In adult neurons, GABA_AR and GlyR ion channels conduct an inhibitory anion current, mainly carried by chloride (Cl⁻) upon activation by γ-aminobutyric acid (GABA) and the amino acid glycine, respectively. In embryonic neurons however, due to a higher intracellular

chloride concentration compared to adult neurons, receptor activation causes an outward directed, depolarizing and excitatory Cl^- flux (Webb and Lynch, 2007). GABA_ARs and GlyRs are both members of the pentameric ligand-gated ion channel (pLGIC) family and require five subunits to form a single functional oligomer. For GABA_ARs there are 19 genes known ($\alpha 1-6$, $\beta 1-3$, $\gamma 1-3$, δ , ϵ , θ , π , and $\rho 1-3$) exhibiting a broad range of heterogeneity and many hundreds of theoretically possible subunit combinations (Olsen and Sieghart, 2009). For GlyRs there are four genes known ($\alpha 1-3$, β) in humans, exhibiting far less diversity compared to GABA_ARs (Lynch, 2009). Each GABA_AR or GlyR isoform as well as each subunit combination has a unique physiological and pharmacological profile. The subunit combination can change during development, in a tissue-specific manner or as a consequence of pathophysiological events (Lynch, 2004; Webb and Lynch, 2007; Esmaeili and Zaker, 2011; Rudolph and Möhler, 2014; Deidda et al., 2015). Genetic or molecular perturbation of the channels' function has been associated with severe neurological disorders including neuropathic pain (Lian et al., 2012; Xiong et al., 2012; Chen et al., 2014), chronic pain sensitization (Harvey et al., 2004; Zeilhofer, 2005; Lynch and Callister, 2006), hyperekplexia (Chung et al., 2010; Bode and Lynch, 2014), epilepsy (Meier et al., 2005; Eichler et al., 2008, 2009; Macdonald et al., 2010), fragile X mental retardation syndrome (D'Hulst et al., 2006), learning and memory deficits (Deidda et al., 2015) as well as neurodegeneration (Kang et al., 2015). In addition, GABA_ARs and GlyRs are increasingly acknowledged in the context of immunomodulation (Stoffels et al., 2011; Gunn et al., 2015), amyotrophic lateral sclerosis (Martin and Chang, 2012) and cancer (Neumann et al., 2004; Cuddapah and Sontheimer, 2011). Therefore, GABA_ARs and GlyRs, including individual isoforms as well as the various subunit combinations in their native neuronal environment are increasingly considered highly attractive drug targets for therapeutic intervention (Alexander et al., 2015). Due to their fundamental role in inhibitory neurotransmission GABA_ARs and GlyRs are increasingly recognized in the context of neurotoxicity (Suñol et al., 1989; Hall and Hall, 1999; Narahashi, 2002; Vale et al., 2003; Mohamed et al., 2004; Islam and Lynch, 2012) and *in vitro* neurotoxicity testing (NT) (Talwar et al., 2013; Tukker et al., 2016).

Although GABA_ARs and GlyRs play fundamental roles during brain development (Avila et al., 2013, 2014), these receptors have only sparsely been associated with developmental neurotoxicity and developmental neurotoxicity (DNT) testing. This is even more surprising as the incidence of neurological diseases including learning and developmental disorders has increased in recent years (May, 2000; Colborn, 2004; Rauh et al., 2006; Herbert, 2010). At the same time, the number and volume of worldwide registered and traded chemical substances has also increased. There is no doubt that developing brain is particularly vulnerable to damage by chemicals (Rice and Barone, 2000) and evaluation of chemicals for developmental neurotoxicity is critical to human health (Grandjean and Landrigan, 2006, 2014). However, only a very small number of chemicals has been tested for developmental toxicity in recent years (Middaugh et al., 2003; Makris et al., 2009), presumably because the current guidelines

for DNT testing exclusively involve animal experiments (OECD, 1997, 2007) that are of poor reproducibility and predictive quality, low in throughput, prohibitively expensive and limited with regard to mechanistic insights into the toxicant's mode of action (Smirnova et al., 2014).

DNT testing is conducted for identification of chemical-induced adverse changes in the structure and function of the developing central nervous system. At present, NT and DNT testing is only officially acknowledged by regulatory authorities when done with standardized *in vivo* animal test methods and when conducted according to guidelines provided by the *Organization for Economic Cooperation and Development* (OECD). For example, NT testing involves daily oral dosing of rats for acute, sub chronic or chronic assessments for 28 days, 90 days, 1 year or longer (OECD, 1997). Primary observations include behavioral assessments and evaluation of nervous system histopathology. DNT testing evaluates *in utero* and early postnatal effects by daily dosing of at least 60 pregnant rats from implantation through lactation. Offspring are evaluated for neurologic and behavioral abnormalities and brain weights and neuropathology are assessed at different times through adulthood (OECD, 2007). The type of exposure (single or repeated dose) and the outcome (lethal or nonlethal; immediate or delayed effects) will result in different classifications for substances under the Globally Harmonized System (GHS).

Since there are various methods available for toxicological profiling of GABA_ARs and GlyRs (Gilbert et al., 2009a,b,d; Talwar et al., 2013) these receptors can serve as valuable molecular targets for *in vitro* developmental neurotoxicity testing (DNT) and provide mechanistic insights into the neurotoxicants or developmental neurotoxicants mode of action.

However, systematic screening for potentiating or inhibiting modulators of GABA_ARs and GlyRs in the context of drug development and NT/DNT testing is hampered due to lack of appropriate *in vitro* models. Recombinant expression systems using e.g., human embryonal kidney-derived (HEK293) cells allow systematic large scale screening for GABA_AR and GlyR modulators in high throughput format (Kruger et al., 2005; Gilbert et al., 2009a,b,d; Talwar et al., 2013; Walzik et al., 2015). Despite recombinant models being successful in the identification of GlyR chloride channel modulators (Balansa et al., 2010, 2013a,b), these systems lack of fundamental neuronal genetic programs and cell intrinsic regulators influencing the functional properties of mature neurons *in vivo* and are restricted to physiological, pharmacological and toxicological analysis of individual GABA_ARs and GlyRs isoforms in isolation. Modulators identified or investigated using recombinant expression systems have been reported to yield contradictory results comparing recombinant systems and native neurons. For example, NV-31 an analog of bilobalide, a major bioactive component of Ginkgo biloba herbal extracts, has been reported to inhibit recombinant GlyRs but to potentiate native hippocampal neuron GlyRs (Lynch and Chen, 2008). Hence, screening data generated using recombinant expression system may be only partially relevant to GABA_ARs and GlyRs expressed *in vivo* and always require time and resource intensive retesting using secondary and individual approaches. Terminally differentiated

neuronal cells of human origin, e.g., primary cells from biopsy samples are rarely available, enable only a limited number of experiments and are typically derived from pathogenic tissue, rendering these cells unsuitable to systematic large-scale screening for modulators of GABA_ARs and GlyRs. Neuronal cells of animal origin such as mouse or rat are widely used for studying mammalian inhibitory neurotransmission in general and the physiological properties of GABA_ARs and GlyRs in particular but are not optimal for identification of human-specific therapeutic leads or pharmacological probes as well as for GABA_AR and GlyR mediated neurotoxicity or developmental neurotoxicity as the physiology of animals may strongly differ from human physiology. Stem cells including induced pluripotent stem cell (iPSC) and pluripotent embryonal carcinoma cells provide an enormous potential for both GABA_AR- and GlyR-targeted drug development and NT/DNT testing as they allow standardized high-throughput *in vitro* screening of a large number of chemicals in maturing and adult human neurons, that is time, cost and resource-effective.

Human pluripotent NTERA-2 (NT2 or TERA2.cl.SP12) stem cells are increasingly considered as a suitable model for *in vitro* NT and DNT studies (Couillard-Despres et al., 2008; Hill et al., 2008; Laurenza et al., 2013; Pallocca et al., 2013; Stern et al., 2014). Upon exposure to retinoic acid, the cells undergo neuronal differentiation, i.e., mimic the process of differentiation in the developing brain, and are potentially suitable to NT/DNT testing at different developmental stages ranging from non-differentiated stem cells, committed neural progenitors to differentiated neuronal, so called NT2-N cells, and glial cells (Lee and Andrews, 1986; Pleasure et al., 1992; Sandhu et al., 2002; Stewart et al., 2003; Ozdener, 2007; Coyne et al., 2011). Electrophysiological studies and extracellular recordings with NT2-N cells have demonstrated voltage-activated calcium, TTX-sensitive sodium and potassium currents, spontaneous synaptic currents as well as glutamate, N-methyl-D-aspartate (NMDA), GABA and strychnine-sensitive glycine-induced currents (Pleasure et al., 1992; Munir et al., 1996; Neelands et al., 1998; Gao et al., 2004; Coyne et al., 2011; Laurenza et al., 2013) demonstrating that these cells exhibit properties similar to those described in native human neurons thus, making them an excellent experimental model for both GABA_AR- and GlyR-targeted drug development and NT/DNT testing. Also, a variety of neuronal markers has been reported to be expressed in differentiated NT2-N cells, including β -tubulin type III, MAP-2 and synapsin I (Pleasure et al., 1992; Stewart et al., 2003; Hsu et al., 2014; Saporta et al., 2014; Stern et al., 2014).

To address the limitations of conventional *in vitro* models for GABA_AR- and GlyR-targeted drug, NT/DNT screening as well as of animal-based *in vivo* NT/DNT testing approaches described above, we aimed to establish a cell line stably expressing YFP-I152L under the control of the human ubiquitin promoter C. The promoter has been reported to drive selective protein expression in principal neurons in the mammalian brain (Wilhelm et al., 2011). NT2 cells have previously been reported to provide a suitable system for expressing exogenous proteins in terminally differentiated neurons (Pleasure et al., 1992).

YFP-I152L, an engineered variant of yellow fluorescent protein (YFP) with greatly enhanced anion sensitivity, is quenched by small anions and is thus suited to reporting anionic influx into cells (Galletta et al., 2001). The fluorescent protein has been successfully applied for structure-function analysis and compound screening with many different chloride channel types (Kruger et al., 2005; Gilbert et al., 2009a,b,d; Balansa et al., 2010, 2013a,b; Chung et al., 2010; Gebhardt et al., 2010; Talwar et al., 2013; Walzik et al., 2015).

We further aimed to apply the cell line in concentration-response experiments with GABA and glycine as well as with a selection of chemicals with known toxicity profiles on GABA_ARs and GlyRs and to compare GABA and glycine EC₅₀ and drug IC₅₀ values with published electrophysiological data and data from fluorescence based functional imaging.

To evaluate the suitability of the *in vitro* model to systematic large-scale functional screening in the context of GABA_AR- and GlyR-targeted drug development and NT/DNT testing, we intended to quantify the proportion of GABA_AR- and GlyR-positive cells.

Our *in vitro* model and methodological approach will be applicable within a framework of various individual strategies assessing NT/DNT at different stages during neuronal differentiation as well as to systematic large-scale *in vitro* neurophysiological, -pharmacological and -toxicological screening with GABA_ARs and GlyRs that is time, cost and resource-effective. Furthermore, in the context of *in vitro*-based experimental and analytical approaches for NT/DNT prediction, our methodology can contribute to reduce or even replace animal experiments and to further promote the concept of the 3Rs in biomedicine (Russell and Burch, 1959).

RESULTS

We have established a recombinant human pluripotent stem cell line, stably expressing halide-sensitive YFP-I152L under the control of the human ubiquitin C promoter. The cell line allows fluorescence-based GABA_AR and GlyR-targeted drug screening and *in vitro* NT/DNT testing at different stages of neuronal maturation. The workflow of cell line generation, stem cell differentiation and functional imaging is shown in **Figure 1**. Images of recombinant non-differentiated NT2-YFP-I152L stem cells and differentiated NT2-N-YFP-I152L cells as well as the principle of functional imaging using the cells are shown in **Figure 2**.

Functional Profiling of GABA_ARs and GlyRs in Recombinant NT2-N-YFP-I152L Cells

To assess whether the generated recombinant stem cell line is suitable to chloride imaging and functional profiling of GABA_ARs and GlyRs, NT2-YFP-I152L cells were differentiated into neuronal NT2-N-YFP-I152L cells as described in the Methods section and were seeded at defined density of 2×10^4 cells in each well of a 96-well plate. Two days later and approximately 1 h prior to fluorescence imaging, the culture

medium was completely removed and was replaced by 50 μ l NaCl control solution. The standard NaCl control solution contained (in mM): NaCl 140, KCl 5, CaCl₂ 2, MgCl₂ 1, HEPES 10, glucose 10, pH 7.4 using NaOH. The 96-well plate was placed onto the motorized stage of a high-content imaging system and cells were imaged in control solution to record cellular YFP fluorescence in unquenched state. Because YFP-I152L is almost insensitive to chloride, its fluorescence intensity is highest in NaCl solution allowing for optimal focussing into the optical layer of cells. Subsequently, cells were perfused with 100 μ l NaI solution containing increasing concentrations of

GABA (0.01–100 μ M, **Figures 3A,B**) or glycine (0.1–1000 μ M, **Figures 3C,D**). The NaI test solution was similar to NaCl control solution except that the NaCl was replaced by equimolar NaI. Cells were imaged throughout the complete procedure of agonist perfusion for a total of 30 seconds and with an acquisition rate of 2 Hz. Fluorescence quench was calculated at single cell level by quantitative analysis as described in the Methods section. The principle of functional profiling of ligand-gated chloride channels is depicted in **Figures 2D–G**. Average time-courses of quench (mean \pm SD, $n = 10$) following the addition of NaI plus the indicated GABA or glycine concentrations are shown in **Figures 3A,C**, respectively and were constructed by pooling results from wells exposed to different solutions with 10 cells per well. Average agonist dose–response curves constructed from the experiments shown in **Figures 3A,C** are shown in **Figures 3B,D**, respectively. Calculated half-maximal activation concentrations (EC₅₀) for GABA (1.1 ± 0.2 μ M) and glycine (4.3 ± 0.5 μ M) are listed in **Table 1** and are overall smaller compared with data from functional Cl[−] imaging and electrophysiology previously reported in the literature (see Discussion). However, Hill coefficients (n_H) for GABA (1.8 ± 0.4) and glycine (1.5 ± 0.2) correspond well with data from the literature. Although EC₅₀ values measured in this study are overall smaller compared to values from the literature, these data demonstrate that the cell line is suitable to chloride imaging and functional profiling of GABA_ARs and GlyRs.

Toxicological Profiling of GABA_ARs and GlyRs in Recombinant NT2-N-YFP-I152L Cells

To evaluate the suitability of the established cell line for systematic screening for GABA_AR and GlyR modulators, we conducted concentration–response experiments with the chemicals strychnine, picrotoxin, fipronil, lindane, bicuculline, and zinc in combination with the neurotransmitters GABA or glycine. To this end, human pluripotent NT2-YFP-I152L cells were differentiated into neuronal NT2-N-YFP-I152L cells as described in the Methods section and were seeded at a density of 2×10^4 cells in each well of a 96-well plate. 48 h later, the culture medium was completely removed and was replaced by 50 μ l NaCl control solution. The cells were imaged in control solution and during perfusion with 100 μ l NaI solution containing 1 μ M GABA or 3 μ M glycine—basically representing half-maximal activation concentrations—and increasing concentrations of the drugs strychnine (100 pM–10 μ M), picrotoxin (1 nM–100 μ M), fipronil (1 nM–100 μ M), lindane (1 nM–100 μ M), bicuculline (1 nM–100 μ M) and zinc (10 nM–1 mM). Average (mean \pm SD,

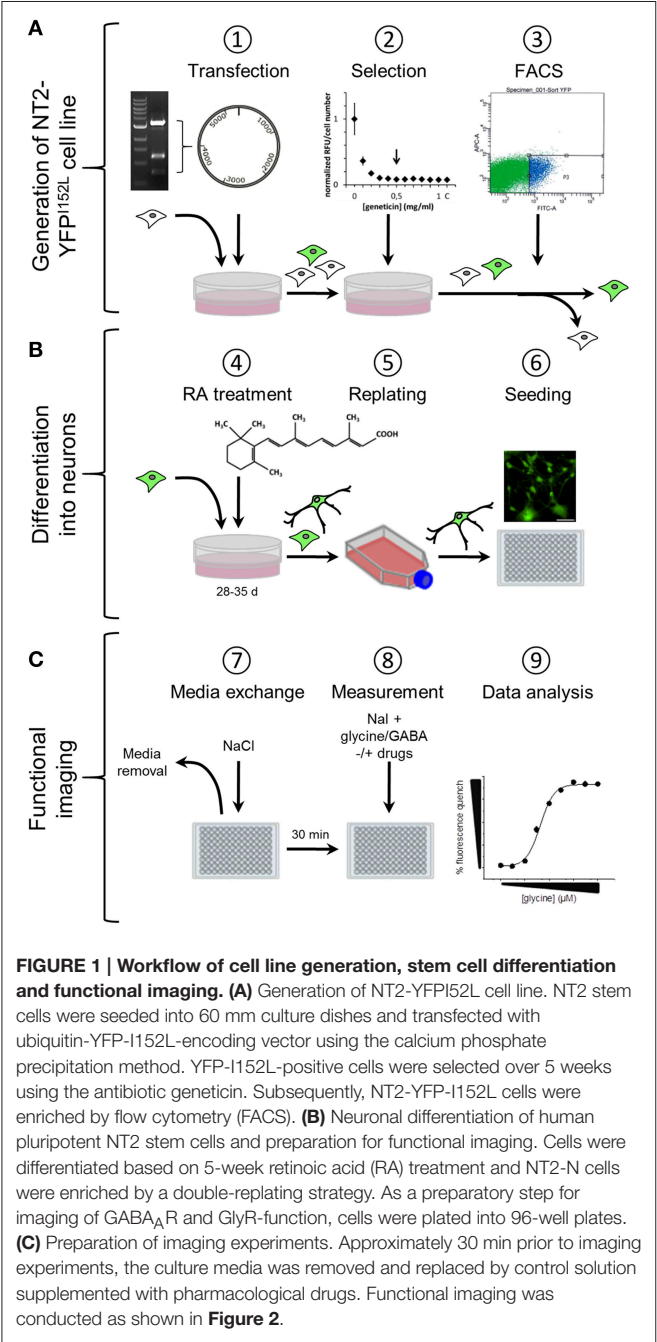
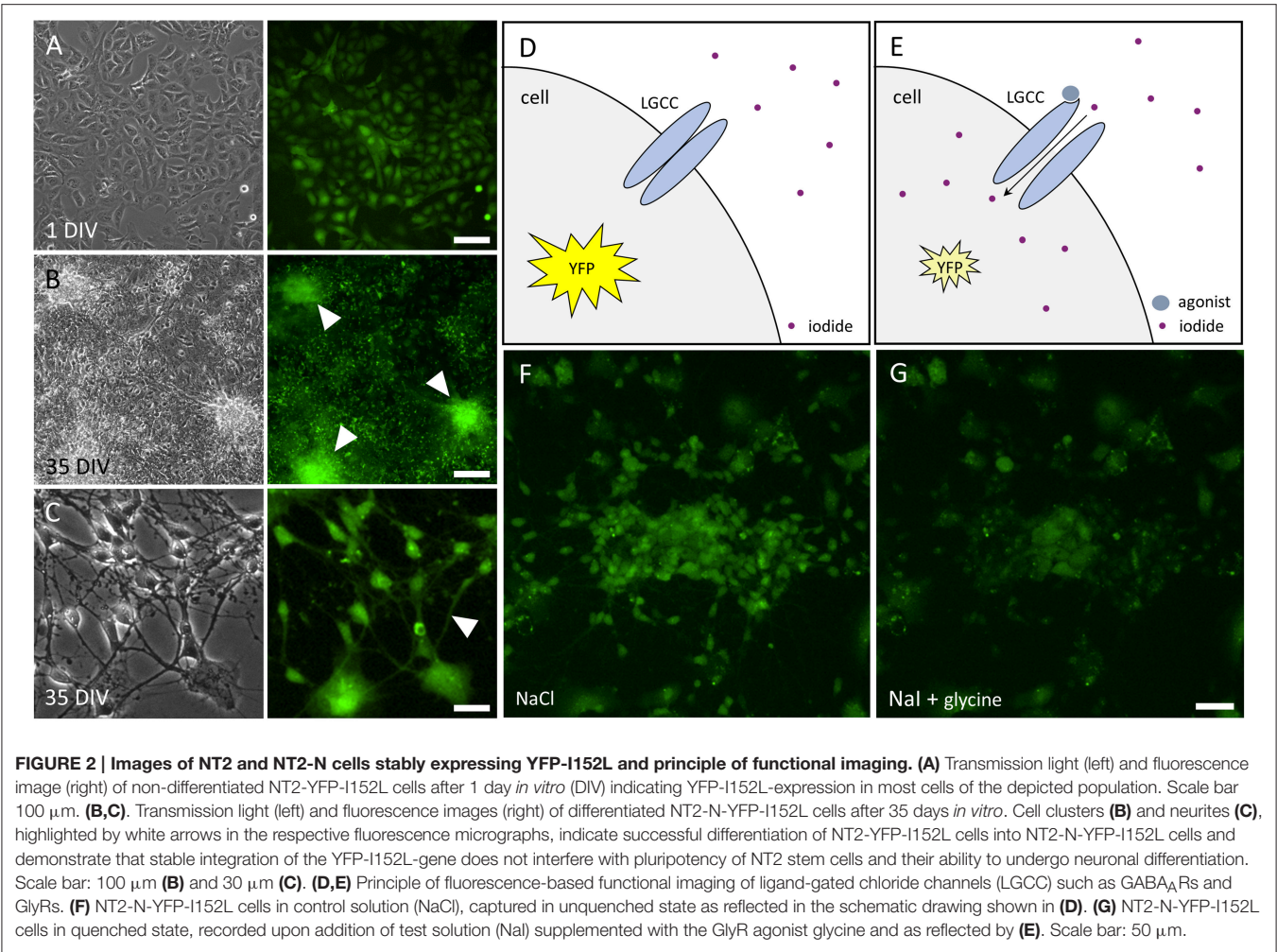


TABLE 1 Calculated half-maximal activation concentration and hill coefficients (EC ₅₀ , n _H) for the used neurotransmitters.							
GABA				Glycine			
EC ₅₀ (μM)	SD	n _H	SD	EC ₅₀ (μM)	SD	n _H	SD
1.1	0.2	1.8	0.4	4.3	0.5	1.5	0.2



$n = 10$) drug dose-responses are shown in **Figures 4, 5**. Calculated half-maximal inhibition concentration (IC_{50}) for the tested chemicals are summarized in **Table 2** and indicate that the recombinant cell line is suitable to GABA_AR and GlyR-targeted toxicological profiling and identification of ion channel-specific drugs.

Quantification of the Proportion of GABA_AR and GlyR Positive NT2-N-YFP-I152L Cells

The applicability of the established recombinant *in vitro* model for high-throughput GABA_AR and GlyR-targeted screening in the context of lead identification and NT/DNT testing strongly depends on the proportion of GABA_AR and GlyR positive NT2-N cells in the whole cell population. A very small percentage of GABA_AR and GlyR expressing NT2-N cells requires a large number of individual experiments including technical and biological replicates to be conducted in order to obtain statistically sound results, potentially compromising the usability of the established cell line for the envisioned application. To obtain a robust estimate of the proportions of GABA_AR and GlyR

TABLE 2 | Calculated half-maximal inhibition concentration (IC_{50}) for the tested chemicals indicating that the recombinant cell line is suitable to GABA_AR and GlyR-targeted toxicological profiling and identification of ion channel-specific drugs.

Drug	GABA		Glycine	
	IC_{50}	SD	IC_{50}	SD
Strychnine (nM)	–	–	17.2	7
Picrotoxin (μM)	5.8	0.9	1.1	0.2
Fipronil (μM)	10.8	5.8	1.5	0.9
Lindane (nM)	–	–	78.1	32.6
Bicuculline (μM)	1.1	0.3	13.4	2.5
Zinc	–	–	–	–

positive NT2-N-YFP-I152L cells in the overall cell population, we calculated the percentage of cells per image indicating a fluorescence quench of at least 20% upon application of saturating GABA or glycine concentration. The threshold of 20% fluorescence quench was chosen because, from our experience, any measured cellular fluorescence change within a range of –20

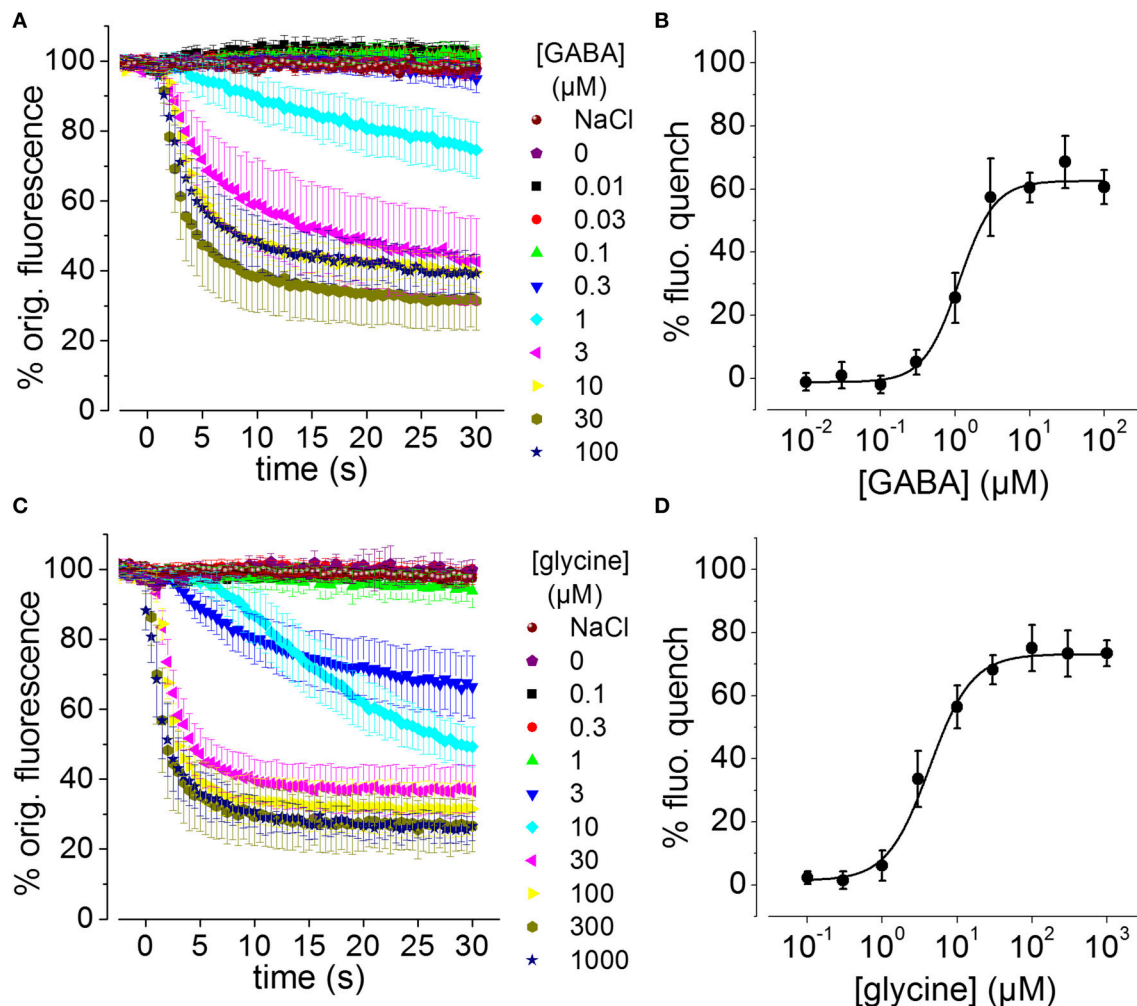
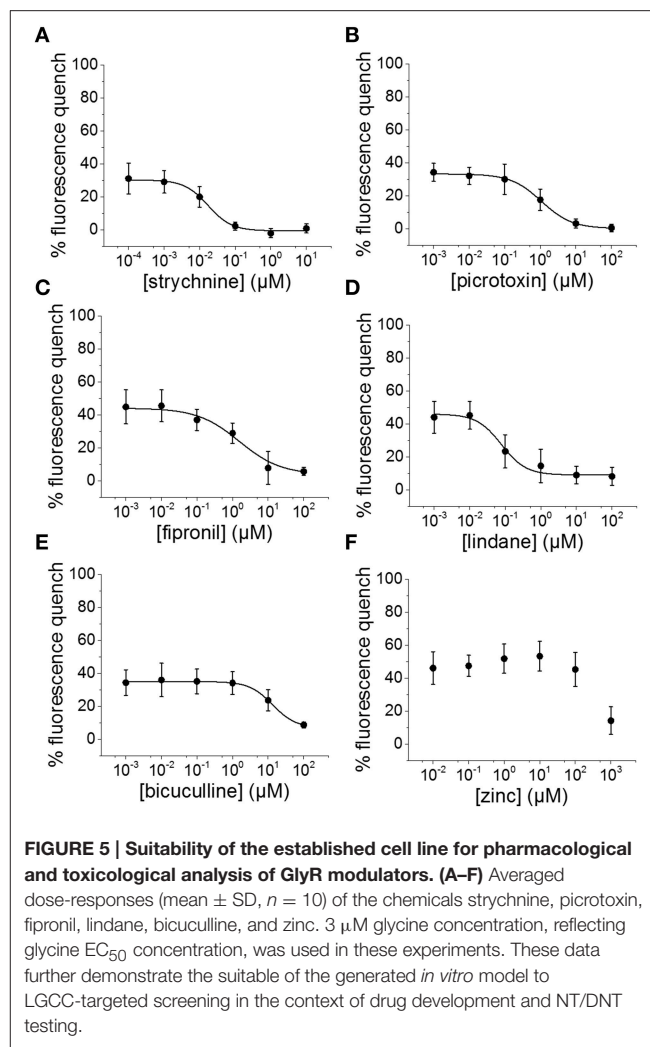
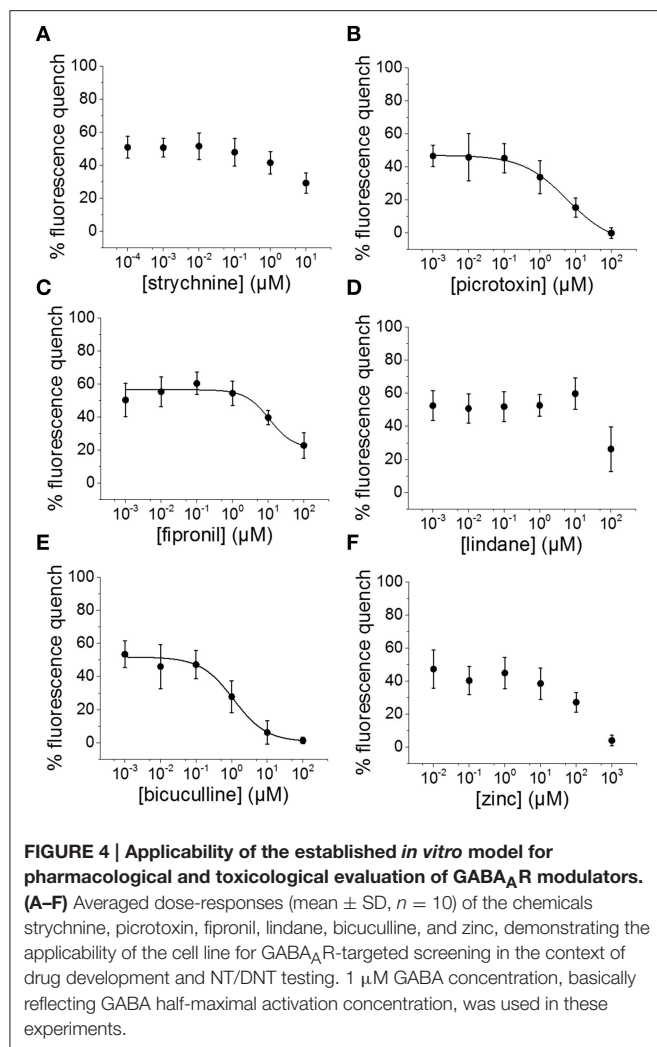


FIGURE 3 | GABA and glycine-induced fluorescence quench in NT2-N cells stably expressing YFP-I152L measured using a fluorescence microscope. (A,C) Averaged time-courses of quench following the addition of NaI plus the indicated GABA or glycine concentrations, respectively. **(B,D)** Averaged GABA and glycine concentration-responses measured from the data in **(A,C)**, respectively, 30 s after receptor activation. In this and the subsequent figures, “% fluorescence quench” is defined as $(F_{\text{init}} - F_{\text{final}}) \times 100 / F_{\text{init}}$, where F_{init} and F_{final} are the initial and final values of fluorescence, respectively. All data are given as mean \pm SD ($n = 10$).

to 20% reflects biological noise typical to the employed assay. As a starting point toward analysing the proportion of GABA_AR and GlyR-positive cells we segmented the images of a total of 24 individual experiments from two different differentiation batches (GABA_AR, batch #1: $n = 7$, batch #2: $n = 6$; GlyR, batch #1: $n = 6$, batch #2: $n = 5$) using a modified version of DetecTIFF[®] software (Gilbert et al., 2009c) employing two individual sets of parameters for the identification of small neuronal NT2-N-YFP-I152L and larger non-neuronal NT2-YFP-I152L cells. **Figure 6A** shows a representative fluorescence micrograph of large NT2-YFP-I152L and small NT2-N-YFP-I152L cells, highlighted with white and gray arrows, respectively. Exemplary segmentation masks created from the image shown in **Figure 6A** for quantitative analysis of fluorescence intensity and calculation of “% fluorescence quench” in small neuronal NT2-N-YFP-I152L cells and large non-neuronal cells are depicted in

Figures 6B,C. The average cell size (in pixel, mean \pm SD) of GABA or glycine-exposed small and large cells calculated from two independent differentiation batches is shown in **Figure 6D** and is as follows: GABA-exposed small cells: 177 ± 94 (batch #1, $n = 1869$) and 152 ± 89 pixel (batch #2, $n = 2560$), GABA-exposed large cells: 1369 ± 760 (batch #1, $n = 1216$) and 1228 ± 709 pixel (batch #2, $n = 1371$); glycine-exposed small cells: 163 ± 93 (batch #1, $n = 1631$) and 158 ± 92 pixel (batch #2, $n = 1071$); glycine-exposed large cells: 1356 ± 757 (batch #1, $n = 1212$) and 1316 ± 752 pixel (batch #2, $n = 828$). In a next step, we calculated the percentage of cells per image indicating a fluorescence quench of at least 20% upon application of saturating GABA and glycine concentration (see histogram in **Figure 6E**) that is as follows: GABA-exposed small cells: 28 ± 13 (batch #1, $n = 7$) and 32 ± 12 % (batch #2, $n = 6$), GABA-exposed large cells: 3 ± 1 (batch #1, $n = 7$) and 6 ± 2 % (batch #2, $n = 6$); glycine-exposed small



cells: 36 ± 14 (batch #1, $n = 6$) and $35 \pm 7\%$ (batch #2, $n = 5$); glycine-exposed large cells: 2 ± 1 (batch #1, $n = 6$) and $4 \pm 2\%$ (batch #2, $n = 5$). Approximately one third of the small cell population is represented by GABA_AR and GlyR-positive cells, equaling 17 ± 8 (GABA, batch #1), 21 ± 9 (GABA, batch #2), 20 ± 9 (glycine, batch #1) and $19 \pm 4\%$ (glycine, batch #2) and rendering $\sim 20\%$ of the overall population GABA_AR and GlyR-positive cells. These data indicate a population of GABA_AR and GlyR-positive cells that is stable between individual experiments and differentiation batches, highlighting the applicability of the established *in vitro* model for systematic GABA_AR and GlyR-targeted high-throughput pharmacological and toxicological screening in the context of drug development and NT/DNT testing.

DISCUSSION

For the sake of feasibility, throughput and cost reasons, GABA_AR and GlyR-targeted screening is typically conducted in non-neuronal recombinant expression systems assessing individual GABA_AR and GlyRs isoforms in isolation. Such expression

systems usually also lack fundamental neuronal genetic programs and cell intrinsic regulators of mature neurons *in vivo*. The initial benefit is often compromised by subsequent time-consuming and cost-intensive re-screens for validation and specificity-evaluation of potential GABA_AR and GlyR-modulators. In the context of neurotoxicity (NT) or developmental neurotoxicity (DNT) testing, GABA_AR and GlyRs can serve as molecular targets and can contribute to deciphering the molecular mechanisms of toxic effects. However, so far there are no suitable *in vitro* models available which comprehensively reflect the complex situation of the central nervous system *in vivo* and NT/DNT testing is still solely based on animal experimentation that is morally questionable, low in throughput, expensive and of rather poor predictive quality. To address these issues, we have established a recombinant human pluripotent stem cell line, stably expressing YFP-I152L that is advantageous for GABA_AR and GlyR-targeted screening in the context of lead identification and drug development as well as for NT/DNT testing for several reasons. First, the recombinant cell line allows functional profiling of GABA_AR and GlyRs in neuronal environment, providing fundamental neuronal genetic programs and cell intrinsic regulators critical to reflecting the functional properties

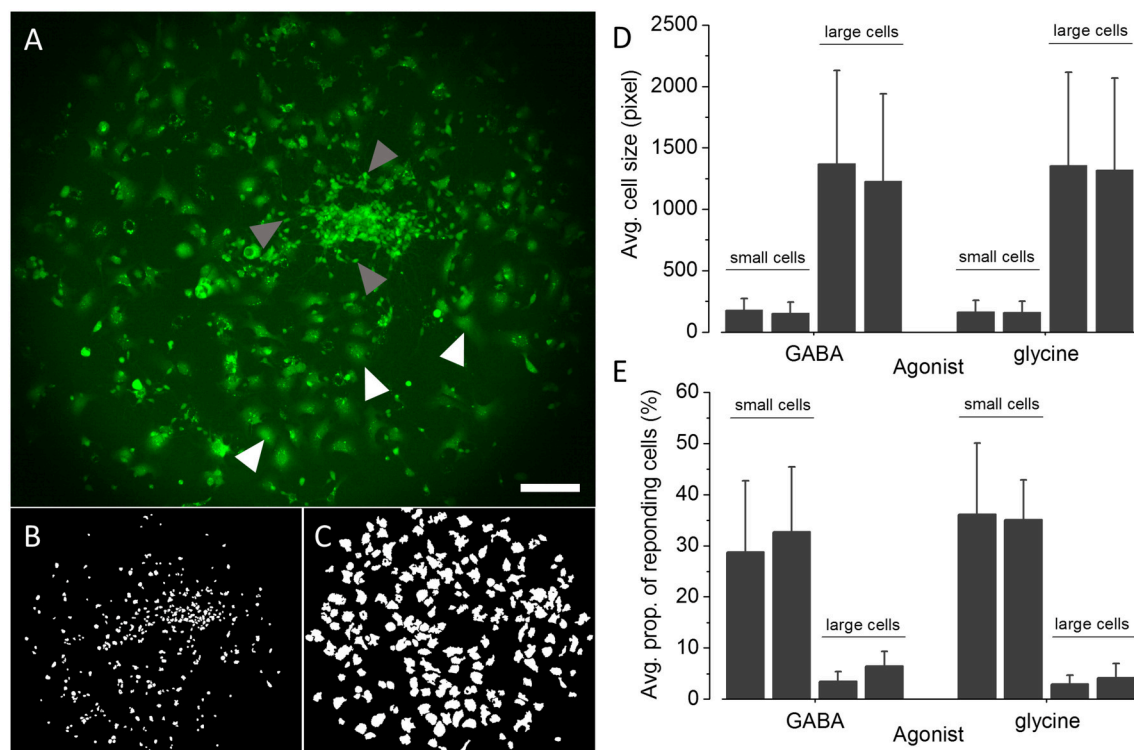


FIGURE 6 | Quantification of the proportions of GABA_AR and GlyR-positive NT2-N-YFP-I152L cells. (A) Representative fluorescence micrograph of NT2-N-YFP-I152L cells in differentiation culture used for functional imaging experiments. **(B,C)** Exemplary segmentation masks created from **(A)** for quantification of “% fluorescence quench” in small NT2-N-YFP-I152L cells (gray arrows, **B**) and large non-neuronal cells (white arrows, **C**), respectively. **(D)** Comparative analysis of the average cell size (in pixel) of GABA_AR and GlyR-positive small neuronal and large non-neuronal cells quantified from two independent differentiation batches each. **(E)** Comparative analysis of the average percentage of small NT2-N-YFP-I152L and large non-neuronal cells, responding with at least 20% fluorescence quench upon exposure to saturating GABA or glycine concentration, respectively. Approximately one third of the small cell population is represented by GABA_AR and GlyR-positive cells, equaling about 20% of the overall population of cells. These data indicate a small proportion of GABA_AR and GlyR-expressing cells that is stable between individual experiments and differentiation batches, further highlighting the applicability of the established *in vitro* model for systematic GABA_AR and GlyR-targeted high-throughput pharmacological and toxicological screening in the context of drug development and NT/DNT testing. Scale bar: 200 μ m.

of mature neurons *in vivo*. Second, the *in vitro* model is of human origin, allowing for GABA_AR and GlyR-targeted screening relevant to human physiology, including identification of leads for therapeutic intervention and toxicity evaluation. Third, as the cell line used in this study mimics brain maturation to a certain extent, it allows analysis of the physiological properties of GABA_AR and GlyR during development of the central nervous system. Fourth, the cell model has been applied over a large range of passages—up to passage number 50 until now—without noticeable loss in YFP-I152L fluorescence intensity, further highlighting its applicability to standardized *in vitro* NT/DNT testing. Finally, differentiation of NT2 cells can be conducted in large scale format allowing for systematic high-throughput experimentation.

We exposed the cell line to GABA or glycine and demonstrated that the *in vitro* model is suitable to functional imaging of both GABA_ARs and GlyRs. Despite the fact that Hill coefficients compare well with data from the literature, the calculated half-maximal activation concentration for GABA and glycine is overall smaller compared to EC₅₀ concentrations previously measured in NT2-N cells using whole cell patch

clamp electrophysiology (Neelands et al., 1998; Gao et al., 2004; Gao and Greenfield, 2005; Coyne et al., 2011). Although it is difficult to isolate the reason for this without directly comparing concentration-response data from the same cells generated with different methodologies, the apparent high GABA and glycine sensitivities may have been caused by the relatively long incubation time in agonist solution, i.e., the time between application of the agonist and quantification of the fluorescence intensity (30 s). Furthermore, we have previously observed differences in glycine EC₅₀, i.e., increased sensitivity for glycine, in recombinantly expressed $\alpha 1$, $\alpha 2$, and $\alpha 3$ GlyR, assessed with the fluorescence-based assay vs. patch clamp electrophysiology (Talwar et al., 2013).

We used the recombinant *in vitro* model in a case study with the drugs strychnine, picrotoxin, flupirtine, lindane, bicuculline and zinc. The imaging data indicate that YFP-I152L-expressing NT2-N cells are applicable to GABA_AR and GlyR-targeted toxicological profiling and identification of ion channel-specific drugs. The drug strychnine specifically inhibited glycine but not GABA-induced anion-influx with average IC₅₀ values that correspond very well with results measured

by either electrophysiological or equilibrium [^3H]-strychnine displacement studies using recombinantly expressed homomeric wildtype $\alpha 1$ GlyRs and variants (Lynch et al., 1997; Vafa et al., 1999). Also, concentration-response experiments with picrotoxin, a standard pharmacological tool for identifying the presence of β -subunits in recombinant and native GlyRs (Lynch, 2004) revealed half-maximal inhibition concentrations and slope values for glycine and GABA-induced anion influxes, that correspond well with results measured by patch clamp electrophysiology in recombinantly expressed homomeric $\alpha 2$ GlyR (Wang et al., 2007) as well as in human pluripotent stem cell-derived neurons (James et al., 2014), respectively. The alkaloid is known to strongly inhibit GABA $_A$ Rs at low micromolar concentrations, whereas GlyRs *in vivo* are considered much less sensitive (Lynch, 2004). However, we observed a reversed sensitivity sequence with a picrotoxin-sensitivity of GlyR that is approximately 5-fold higher compared to GABA $_A$ Rs. As it has been reported that $\alpha\beta$ -heteromeric GlyRs were less sensitive to picrotoxin-inhibition than were α -homomeric GlyRs (Pribilla et al., 1992) we speculate that NT2-N-YFP-I152L cells predominantly express α -homomeric GlyR rather than $\alpha\beta$ -heteromeric GlyRs, although this is no explanation for the reversed picrotoxin-sensitivities of GlyRs and GABA $_A$ Rs. Bicuculline, a purported selective antagonist of the GABA $_A$ receptor, inhibited the GABA-induced fluorescence quench with a half-maximal inhibition concentration similar to values revealed from rat primary neurons by whole cell electrophysiological recordings (Kumamoto and Murata, 1995). Bicuculline also inhibited glycine induced I^- influx in NT2-N-YFP-I152L cells with about 10-fold lower sensitivity compared to GABA-dependent anion influx, highlighting its specificity to GABA $_A$ R on the one hand, but also confirming previous reports on its inhibitory action assessed in both recombinantly expressed (Sun and Machu, 2000) and native glycine receptors (Bhattacharai et al., 2016) on the other hand. The IC_{50} value for glycine-induced fluorescence quench revealed in presence of increasing concentration of the insecticide lindane is about one order of magnitude smaller compared to electrophysiological recordings from recombinantly expressed GlyRs (Islam and Lynch, 2012). These data suggest that NT2-N-YFP-I152L cells predominantly express homomeric GlyRs as lindane has proven to selectively inhibit homomeric but not heteromeric GlyRs (Islam and Lynch, 2012; Talwar et al., 2013). This conclusion is further supported by the above mentioned high picrotoxin-sensitivity of GlyRs. Surprisingly, lindane showed no dose-dependent inhibitory activity on GABA-induced anion influx, although lindane-sensitivity of GABA $_A$ Rs has been reported by many studies conducted in various culture models and cell types (Narahashi, 1996; Ogata et al., 1988; Vale et al., 2003). A study conducted by Belelli et al. (1999) demonstrated no effect on GABA-evoked currents mediated by anesthetic-insensitive wild-type GABA receptors composed of the ($\rho 1$) subunit (Belelli et al., 1999), suggesting expression of GABA $_A$ $\rho 1$ receptor in the examined NT2-N-YFP-I152L cells. Indeed there are a number of studies indicating profound changes in subunit expression and pharmacology during neuronal differentiation—similar to developmental changes in GABA $_A$ R occurring in neurons of

the developing central nervous system—and demonstrating a large variety of neurotransmission phenotypes of non-differentiated NT2 and differentiated NT2-N cell *in vitro* (Neelands et al., 1998, 1999; Guillemain et al., 2000). This question however was not further evaluated in the present study. Fipronil, a broad-spectrum insecticide, inhibited both GABA and glycine induced anion influx in NT2-N cells with sensitivities that correspond very well to results measured by patch clamp electrophysiology in recombinantly expressed GlyRs and GABA $_A$ R (Ratra et al., 2001; Li and Akk, 2008; Islam and Lynch, 2012). Zinc is widely recognized as a modulator of both, GABA $_A$ R and GlyR (Smart et al., 1994). For GlyRs, potentiation as well as inhibition of glycine-activated currents by low ($<10\ \mu\text{M}$) and high concentrations ($>100\ \mu\text{M}$) of zinc, respectively has been reported (Harvey et al., 1999). For GABA $_A$ Rs, inhibition has been shown at concentrations $>10\ \mu\text{M}$ (Kumamoto and Murata, 1995). Although we observed a minor increase of a glycine-induced fluorescence quench (Approximately 10%) in presence of 1 and $10\ \mu\text{M}$ zinc, this effect is not significant. In contrast, zinc-dependent inhibition was observed at concentrations $>100\ \mu\text{M}$ for both GABA and glycine-induced anion influx, confirming previous reports on zinc-sensitive GABA-induced currents recorded from NT2-N cells (Gao et al., 2004). The zinc IC_{50} could not be calculated due to a too small range of applied concentrations but presumably exceeds $1\ \text{mM}$, suggesting the presence of γ subunits which have shown to confer zinc insensitivity to $\alpha\beta$ GABA $_A$ Rs (Smart et al., 1991).

We quantified the proportion of GABA $_A$ R and GlyR positive NT2-N-YFP-I152L cells based on images of the cells and we identified a percentage of approximately 20% of cells expressing GABA $_A$ Rs and GlyRs, respectively. Despite the fact that the proportion of glycine and GABA sensitive cells are comparable, it cannot be concluded from our data whether the cells are simultaneously sensitive to both glycine and GABA or respond to either of the neurotransmitters. Although the calculated proportions have proven stable between different batches of differentiation cultures, the total percentage of GABA $_A$ R and GlyR positive NT2-N-YFP-I152L cells is not optimal for plate reader, i.e., photomultiplier or cell population-based screening, that typically requires a high number of reacting, e.g., GlyR or GABA $_A$ R-positive cells and allows experimentation in high-throughput screening mode. If desired or required, the proportion of NT2-N-YFP-I152L cells may be increased by size-exclusion filtering using e.g., a simple nylon filter of defined mesh size or even more sophisticated cell sorting approaches. As highlighted by gray and white arrows in the fluorescence micrograph depicted in **Figure 6A** and the histogram shown in **Figure 6D**, NT2-N cells are much smaller compared to non-neuronal cells, presumably facilitating size-dependent population-increase of NT2-N cells. Despite the fact that plate reader-based screening allows experimentation in high or even ultra-high-screening mode it is disadvantageous with regard to cellular heterogeneity. Cultures of NT2 cells have been reported to express a large variety of non-neuronal and neuronal phenotypes (Guillemain et al., 2000), as we have shown in the case study using drugs with known and partly GABA $_A$ R and

GlyR-specific pharmacological and toxicological profiles. Besides their neuronal properties and human origin, the heterogeneity of NT2-N cell cultures is probably one of the most important advantages over homogeneous, e.g., recombinant expression systems, as it reflects the *in vivo* situation to a much higher extent than simplifying *in vitro* models. Thus, microscopy-based high-content imaging of NT2-N cells, evaluating the physiological pharmacological and toxicological properties at single cell level, and in the context of cellular heterogeneity, is likely to be the optimal approach for systematic GABA_AR and GlyR-targeted drug screening as well as NT/DNT testing.

To confirm the validity of the morphology or size-based selection criterion, we conducted functional imaging experiments with non-treated NT2-YFP-I152L stem cells and quantified the average cell size as well as the percentage of stem cells, responding with at least 20% fluorescence quench upon exposure to saturating GABA or glycine concentration, respectively (see Supplementary Figure S1). The average cell size (pixel), calculated from two individual experiments each (see Supplementary Figure S1C) is comparable between experiments (GABA, replicate #1: 397 ± 254 pixel, $n = 650$ cells, replicate #2: 385 ± 252 pixel, $n = 547$ cells; glycine, replicate #1: 403 ± 243 pixel, $n = 589$, replicate #2: 400 ± 256 pixel, $n = 654$) and differs from the size of small and large cells, respectively, as indicated in **Figure 6D**. The percentage of non-treated NT2-YFP-I152L stem cells, responding with at least 20% fluorescence quench upon exposure to 1 mM saturating GABA (replicate #1: 0.62%, replicate #2: 0.37%) or glycine (replicate #1: 0.68%, replicate #2: 0.92%) concentration, respectively (see Supplementary Figure S1D), also differs considerably from data obtained with retinoic acid-exposed NT2-N-YFP-I152L cells. These data clearly demonstrate that the morphology, e.g., the size, as well as the functional properties, i.e., the sensitivity to GABA or glycine, vary between non-treated stem cells and NT2-YFP-I152L differentiation cultures containing small neuronal and large non-neuronal cells and confirming the validity of the employed size-based selection criterion.

We have previously published a method allowing for assessment of ligand-gated ion channels in the context of cellular heterogeneity that is based on progressive receptor activation and iterative fluorescence imaging (Talwar et al., 2013). This method could easily be adapted for application with the established *in vitro* model and has the power to deliver imaging data of unsurpassed functional content presumably outranging any other existing technique for assessing physiological properties of ion channels with regard to throughput.

Due to the fact that our method is based on microscopic evaluation using a single fluorescence indicator, it allows additional fluorescence or luminescence-based markers to be implemented for multiplexing, such as ion or pH-sensitive probes e.g., for parallel analysis of further ion channels or transporters, to assess the activity of intracellular, e.g., toxicity-relevant signaling pathways, or for mapping cellular morphology to functional phenotypes.

It is important to mention that the applicability of the cell line as well as the experimental approach depends on the proteins to be evaluated and targeted, on the individual

experimental setup, the available instrumental infrastructure and the biological question to be assessed. While this work focuses on functional profiling and GABA_AR and GlyR-targeted drug screening as well as neurotoxicity and developmental neurotoxicity, our *in vitro* model and methodological approach could also be adapted for other proteins and strategies, such as RNAi or combined compound and RNAi screening, for single-endpoint or time-resolved functional expression analysis or for approaches using overexpression libraries. Altogether, this work contributes to furthering the applicability of cell-based high-throughput functional screening and provides a means for large-scale characterization of neuronal proteins in the context of *in vitro*-based NT/DNT prediction thus, promoting a systems-level understanding of human physiology in homeostasis and disease.

METHODS

Pharmacological Reagents

Glycine, GABA, strychnine, picrotoxin, fipronil, lindane, zinc chloride and bicuculline were obtained from Sigma. Stock solutions of glycine (1 M), GABA (1 M) and zinc chloride (1 M) were prepared in water, strychnine (10 mM), picrotoxin (100 mM), fipronil (30 mM), lindane (30 mM) and bicuculline (100 mM) were dissolved in dimethylsulphoxide (DMSO). All stocks were frozen at -20°C . From these stocks, solutions for experiments were prepared on the day of recording.

Reagents for Differentiation of NT2 Pluripotent Stem Cells

Retinoic acid and poly-D-lysine (PDL) were obtained from Sigma. Retinoic acid was prepared as 100 mM stock in DMSO. Uridine was prepared as 100 mM stock in water. These stocks were kept at -80 to -20°C . PDL was prepared as 10x stocks in water and stored at 4°C . Solutions for differentiation cultures were prepared freshly at the days of experimentation.

Molecular Constructs

The regulatory region of the human ubiquitin C promoter (1204 bp) was amplified by PCR, the vector pFUGW (Addgene) was used as the template as well as specific primers (Invitrogen). The fragment was then inserted into the promoterless vector pDsRed2-1 (Clontech). PCR of the YFP-I152L gene (720 bp) was performed using vector pcDNA3.1-YFP-I152L (Invitrogen) as a template and specific primers (Invitrogen). The YFP-I152L-coding construct was kindly provided from Prof. Joe Lynch (Queensland Brain Institute, The University of Queensland, Brisbane, Australia). After removing the sequence of the red fluorescent protein from the vector phuUbC-DsRed2, YFP-I152L was sub-cloned into the vector. The expression of YFP-I152L is under the control of the constitutive active human ubiquitin C promoter, the plasmid carries the neomycin resistance gene for the selection with the antibiotic geneticin.

Cell Line

Human pluripotent teratocarcinoma NT2 cells (NTERA-2 cl.D1, CRL-1973TM) were purchased from *The American Type Culture Collection* (ATCC).

Generation of Stable Cell Line

For generating a cell line stably expressing YFP-I152L, NT2 stem cells were seeded into 60 mm culture dishes (TPP) at a density of 5×10^5 cells and were incubated at standard conditions over night. The next day, cells were transfected with ubiquitin-YFP-I152L-encoding vector using the calcium phosphate precipitation method. YFP-I152L-positive cells were selected over 5 weeks with 0.5 mg/ml geneticin (Roth, Germany). The geneticin concentration had previously been examined in a concentration-response experiment with 0.1–1.0 mg/ml geneticin by measuring the fluorescence intensity of Hoechst 33342 stained (1 μ M) cells exposed to geneticin for 48 h in 96-well plate format using a VICTOR X4 plate reader (Perkin Elmer). The kill curve for evaluation of the geneticin concentration is shown in **Figure 1A**, subpanel #2. Geneticin-selected NT2-YFP-I152L cells with strongest fluorescence signal were enriched by flow cytometry (FACS, approximately top 30%, see **Figure 1A**, subpanel #3) in a single step. Enriched cells were maintained in geneticin-supplemented medium at the above mentioned concentration until initiation of the differentiation procedure. Recombinant cells were used over a large range of passages between passage number 15 and 50, without noticeable decline in YFP-I152L fluorescence intensity.

Cell Culture

Cells were maintained in DMEM (Invitrogen) supplemented with 10% fetal bovine serum (FBS, Biochrom) and penicillin (100 U/ml)/streptomycin (100 mg/ml) (Invitrogen) and were cultured in T75 flasks (TPP) at 37°C, 5% CO₂ in a humidified incubator according to standard procedures. Cells were passaged every 2–3 days and used in differentiation cultures when approximately 80–90% confluent.

Differentiation Culture

We have previously developed an optimized method for neuronal differentiation of human pluripotent NT2 stem cells in monolayer cultures. In brief, NT2 cells were seeded at a defined density into PDL coated 60 mm dishes (TPP) in standard culture medium supplemented with 10% FBS and penicillin (100 U/ml)/streptomycin (100 mg/ml) and 10 μ M RA and were cultured for 5 weeks at 37°C, 5% CO₂ in a humidified incubator. In the second week, 10 μ M uridine was added to the media.

Preparation of Cells for Experiments

Following retinoic acid treatment, cells were replated into T25 flasks and cultured overnight at standard conditions. The next day, NT2-N-YFP-I152L cells located on top of non-differentiated cells were removed by tapping and were seeded at a density of 2×10^4 into the wells of a BD Matrigel™ matrix (BD) coated 96-well plate. Cells were used in functional imaging experiments 48 h later.

Preparation of Imaging Experiments

Approximately 1 h prior to commencement of experiments culture media in 96-well plates was removed manually and was replaced by 50 μ l standard control solution, which contained (in mM) NaCl 140, KCl 5, CaCl₂ 2, MgCl₂ 1, HEPES 10, and

glucose 10 (pH 7.4, NaOH) upon washing the cells once in 50 μ l standard control solution. The NaI test solution was similar in composition to NaCl control solution except the NaCl was replaced by equimolar NaI. For imaging experiments the agonist NaI test solution was supplemented with 1 mM glycine or GABA and was serially diluted with NaI test solution to obtain agonist solutions containing 0.01, 0.03, 0.1, 0.3, 1, 3, 10, 30, 100 μ M final GABA or 0.1, 0.3, 1, 3, 10, 30, 100, 300 and 1000 μ M final glycine concentration. For antagonist concentration-response experiments, the control solution was supplemented with 1 μ M GABA or 3 μ M glycine and increasing concentrations of either of the drugs strychnine (100 pM–10 μ M), picrotoxin (1 nM–100 μ M), fipronil (1 nM–100 μ M), lindane (1 nM–100 μ M), bicuculline (1 nM–100 μ M) and zinc (10 nM–1 mM). All drugs were diluted from stocks at the day of the experiment and experiments were conducted at room temperature.

Imaging Infrastructure

The 96-well plate was placed onto the motorized stage of a high-end long-term imaging system (Nikon Eclipse Ti, Nikon, Japan) and was imaged with a 10x objective (CFI Plan Fluor DL 10X Phase, N.A. 0.30, Nikon, Japan). Illumination from a xenon lamp (Lambda LS, Sutter Instruments, USA), passing through a filter block (C-FL Epi-FL FITC, EX 465–495, DM 505, BA 515–555, Olympus, Japan) was used to excite and detect YFP fluorescence signal. Fluorescence was imaged by a sCMOS camera (NEO, Andor, Ireland) and digitized to disk onto a personal computer (Dell Precision T3500, Dell, USA) with Windows 7 operating System (Microsoft Corporation, USA). The primary resolution of the camera was 2560 \times 2160 pixel, although images were binned (2 \times 2), resulting in a resolution of 1280 \times 1080 pixel. Each image typically contained 350–700 cells. The CCD image acquisition rate was 2 Hz.

Imaging Experiments

The experimental protocol involved imaging each well for 30 s at 2 Hz acquisition rate capturing the initial fluorescence intensity in the control situation as well as the test situation upon receptor activation, respectively. Liquid handling was performed manually.

Single Cell-Based Quantitative Image Analysis

Cells depicted in fluorescence micrographs were selected manually based on strongest quench for low and intermediate concentrations and based on cell morphology in experiments where high drug concentrations were applied. Registered images of fluorescent cells were segmented and quantitatively analyzed using NIS-Elements software (Nikon, Japan). The fluorescence signal of identified cells was measured in images acquired before and after the addition of agonist solution as the mean of all pixel values within the area of a cell. “% fluorescence quench” in chloride imaging experiments is defined as

$$\% \text{fluorescence quench} = (F_{\text{init}} - F_{\text{final}}) * 100 / F_{\text{init}}$$

where F_{init} and F_{final} are the initial and final values of fluorescence, respectively.

Calculation of Concentration-Response Relationships

Individual concentration responses were constructed by pooling results from ten cells in one well exposed to agonist solution. Concentration-response relationships were fitted with the following equation:

$$F = F_{\max} + \frac{F_{\min} - F_{\max}}{1 + ([\text{Agonist}]/EC_{50})^{nH}}$$

where F is the fluorescence corresponding to a particular agonist concentration, $[\text{Agonist}]$; F_{\min} and F_{\max} are the minimal and maximal fluorescence values, respectively; EC_{50} is the concentration that elicits half-maximal activation; and nH is the Hill coefficient. Curve fits were performed using a least squares fitting routine (Origin 7G, OriginLab Corporation). All averaged results are expressed as mean \pm SD.

Quantification of the Proportion of GABA_AR and GlyR-Positive Cells

Images of fluorescent cells were segmented and quantitatively analyzed using a modified version of DetecTIFF[®] software (Gilbert et al., 2009c). In brief, images were segmented using an iterative size and intensity-based thresholding algorithm and the fluorescence signal of identified cells was calculated as the mean of all pixel values within the area of a cell.

REFERENCES

- Alexander, S. P. H., Peters, J. A., Kelly, E., Marrion, N., Benson, H. E., Faccenda, E., et al. (2015). The concise guide to PHARMACOLOGY 2015/16: ligand-gated ion channels. *Br. J. Pharmacol.* 172, 5870–5903. doi: 10.1111/bph.13350
- Avila, A., Vidal Pía, M., Dear, T. N., Harvey, R. J., Rigo, J.-M., and Nguyen, L. (2013). Glycine receptor $\alpha 2$ subunit activation promotes cortical interneuron migration. *Cell Rep.* 4, 738–750. doi: 10.1016/j.celrep.2013.07.016
- Avila, A., Vidal, P. M., Tielens, S., Morelli, G., Laguesse, S., Harvey, R. J., et al. (2014). Glycine receptors control the generation of projection neurons in the developing cerebral cortex. *Cell Death Differ.* 21, 1696–1708. doi: 10.1038/cdd.2014.75
- Balansa, W., Islam, R., Fontaine, F., Piggott, A. M., Zhang, H., Webb, T. I., et al. (2010). Ircinialactams: subunit-selective glycine receptor modulators from Australian sponges of the family Irciniidae. *Bioorg. Med. Chem.* 18, 2912–2919. doi: 10.1016/j.bmc.2010.03.002
- Balansa, W., Islam, R., Fontaine, F., Piggott, A. M., Zhang, H., Xiao, X., et al. (2013a). Sesterterpene glycyl-lactams: a new class of glycine receptor modulator from Australian marine sponges of the genus Psammocinia. *Org. Biomol. Chem.* 11, 4695–4701. doi: 10.1039/c3ob40861b
- Balansa, W., Islam, R., Gilbert, D. F., Fontaine, F., Xiao, X., Zhang, H., et al. (2013b). Australian marine sponge alkaloids as a new class of glycine-gated chloride channel receptor modulator. *Bioorg. Med. Chem.* 21, 4420–4425. doi: 10.1016/j.bmc.2013.04.061
- Belelli, D., Pau, D., Cabras, G., Peters, J. A., and Lambert, J. J. (1999). A single amino acid confers barbiturate sensitivity upon the GABA $\rho 1$ receptor. *Br. J. Pharmacol.* 127, 601–604. doi: 10.1038/sj.bjp.0702611
- Bhattarai, J. P., Cho, D. H., and Han, S. K. (2016). Activation of strychnine-sensitive glycine receptors by shilajit on preoptic hypothalamic neurons of juvenile mice. *Chin. J. Physiol.* 59, 39–45. doi: 10.4077/CJP.2016.BAE361

Data Analysis and Visualization

Imaging data were annotated in Microsoft Excel and analyzed using Origin 7G (OriginLab Corporation).

AUTHOR CONTRIBUTIONS

KK, OF, and DG conceived the project. KK conducted experiments. KK and DG analyzed the data. KK and DG wrote the paper. All authors commented and agreed on the manuscript.

ACKNOWLEDGMENTS

The authors gratefully acknowledge funding of the Staedler Stiftung, Bavarian Equal Opportunities Sponsorship—Förderung von Frauen in Forschung und Lehre (FFL)—Promoting Equal Opportunities for Women in Research and Teaching and the Erlangen Graduate School in Advanced Optical Technologies (SAOT) by the German Research Foundation (DFG) in the framework of the German Excellence Initiative. The funders had no role in study design, data collection and analysis, decision to publish, or preparation of the manuscript.

SUPPLEMENTARY MATERIAL

The Supplementary Material for this article can be found online at: <http://journal.frontiersin.org/article/10.3389/fnmol.2016.00051>

- Bode, A., and Lynch, J. W. (2014). The impact of human hyperekplexia mutations on glycine receptor structure and function. *Mol. Brain* 7:2. doi: 10.1186/1756-6606-7-2
- Chen, J. T.-c., Guo, D., Campanelli, D., Frattini, F., Mayer, F., Zhou, L., et al. (2014). Presynaptic GABAergic inhibition regulated by BDNF contributes to neuropathic pain induction. *Nat. Commun.* 5, 5331. doi: 10.1038/ncomms6331
- Chung, S. K., Vanbellinthen, J. F., Mullins, J. G., Robinson, A., Hantke, J., Hammond, C. L., et al. (2010). Pathophysiological mechanisms of dominant and recessive GLRA1 mutations in hyperekplexia. *J. Neurosci.* 30, 9612–9620. doi: 10.1523/JNEUROSCI.1763-10.2010
- Colborn, T. (2004). Neurodevelopment and endocrine disruption. *Environ. Health Perspect.* 112, 944–949. doi: 10.1289/ehp.6601
- Couillard-Despres, S., Quehl, E., Altendorfer, K., Karl, C., Ploetz, S., Bogdahn, U., et al. (2008). Human *in vitro* reporter model of neuronal development and early differentiation processes. *BMC Neurosci.* 9:31. doi: 10.1186/1471-2202-9-31
- Coyne, L., Shan, M., Przyborski, S. A., Hirakawa, R., and Halliwell, R. F. (2011). Neuropharmacological properties of neurons derived from human stem cells. *Neurochem. Int.* 59, 404–412. doi: 10.1016/j.neuint.2011.01.022
- Cuddapah, V. A., and Sontheimer, H. (2011). Ion channels and transporters in cancer. 2. Ion channels and the control of cancer cell migration. *Am. J. Physiol. Cell Physiol.* 301, C541–C549. doi: 10.1152/ajpcell.00102.2011
- Deidda, G., Parrini, M., Naskar, S., Bozarth, I. F., Contestabile, A., and Cancedda, L. (2015). Reversing excitatory GABAAR signaling restores synaptic plasticity and memory in a mouse model of Down syndrome. *Nat. Med.* 21, 318–326. doi: 10.1038/nm.3827
- D'Hulst, C., De Geest, N., Reeve, S. P., Van Dam, D., De Deyn, P. P., Hassan, B. A., et al. (2006). Decreased expression of the GABAA receptor in fragile X syndrome. *Brain Res.* 1121, 238–245. doi: 10.1016/j.brainres.2006.08.115
- Eichler, S. A., Forstera, B., Smolinsky, B., Jüttner, R., Lehmann, T. N., Fahling, M., et al. (2009). Splice-specific roles of glycine receptor $\alpha 3$ in the hippocampus. *Eur. J. Neurosci.* 30, 1077–1091. doi: 10.1111/j.1460-9568.2009.06903.x

- Eichler, S. A., Kirischuk, S., Jüttner, R., Schaefermeier, P. K., Legendre, P., Lehmann, T. N., et al. (2008). Glycinergic tonic inhibition of hippocampal neurons with depolarizing GABAergic transmission elicits histopathological signs of temporal lobe epilepsy. *J. Cell. Mol. Med.* 12, 2848–2866. doi: 10.1111/j.1582-4934.2008.00357.x
- Esmaili, A., and Zaker, S. R. (2011). Differential expression of glycine receptor subunit messenger RNA in the rat following spinal cord injury. *Spinal Cord* 49, 280–284. doi: 10.1038/sc.2010.109
- Galletta, L. J., Haggie, P. M., and Verkman, A. S. (2001). Green fluorescent protein-based halide indicators with improved chloride and iodide affinities. *FEBS Lett.* 499, 220–224. doi: 10.1016/S0014-5793(01)02561-3
- Gao, L., and Greenfield, L. J. (2005). Activation of protein kinase C reduces benzodiazepine potency at GABAA receptors in NT2-N neurons. *Neuropharmacology* 48, 333–342. doi: 10.1016/j.neuropharm.2004.10.010
- Gao, L., Lyons, A. R., and Greenfield, L. J. Jr. (2004). Hypoxia alters GABAA receptor function and subunit expression in NT2-N neurons. *Neuropharmacology* 46, 318–330. doi: 10.1016/j.neuropharm.2003.09.008
- Gebhardt, F. M., Mitrovic, A. D., Gilbert, D. F., Vandenberg, R. J., Lynch, J. W., and Dodd, P. R. (2010). Exon-skipping splice variants of excitatory amino acid transporter-2 (EAAT2) form heteromeric complexes with full-length EAAT2. *J. Biol. Chem.* 285, 31313–31324. doi: 10.1074/jbc.M110.153494
- Gilbert, D., Esmaili, A., and Lynch, J. W. (2009a). Optimizing the expression of recombinant alphabeta gamma GABAA receptors in HEK293 cells for high-throughput screening. *J. Biomol. Screen.* 14, 86–91. doi: 10.1177/1087057108328017
- Gilbert, D. F., Islam, R., Lynagh, T., Lynch, J. W., and Webb, T. I. (2009b). High throughput techniques for discovering new glycine receptor modulators and their binding sites. *Front. Mol. Neurosci.* 2:17. doi: 10.3389/neuro.02.017.2009
- Gilbert, D. F., Meinhof, T., Pepperkok, R., and Runz, H. (2009c). DetecTiff: a novel image analysis routine for high-content screening microscopy. *J. Biomol. Screen.* 14, 944–955. doi: 10.1177/1087057109339523
- Gilbert, D. F., Wilson, J. C., Nink, V., Lynch, J. W., and Osborne, G. W. (2009d). Multiplexed labeling of viable cells for high-throughput analysis of glycine receptor function using flow cytometry. *Cytometry A* 75, 440–449. doi: 10.1002/cyto.a.20703
- Grandjean, P., and Landrigan, P. J. (2006). Developmental neurotoxicity of industrial chemicals. *Lancet* 368, 2167–2178. doi: 10.1016/S0140-6736(06)69665-7
- Grandjean, P., and Landrigan, P. J. (2014). Neurobehavioural effects of developmental toxicity. *Lancet Neurol.* 13, 330–338. doi: 10.1016/S1474-4422(13)70278-3
- Guillemain, I., Alonso, G., Patey, G., Privat, A., and Chaudieu, I. (2000). Human NT2 neurons express a large variety of neurotransmission phenotypes *in vitro*. *J. Comp. Neurol.* 422, 380–395. doi: 10.1002/1096-9861(20000703)422:3<380::AID-CNE5>3.0.CO;2-C
- Gunn, B. G., Cunningham, L., Mitchell, S. G., Swinny, J. D., Lambert, J. J., and Belelli, D. (2015). GABA(A) receptor-acting neurosteroids: a role in the development and regulation of the stress response. *Front. Neuroendocrinol.* 36, 28–48. doi: 10.1016/j.yfrne.2014.06.001
- Hall, R. C. W., and Hall, R. C. W. (1999). Long-term psychological and neurological complications of lindane poisoning. *Psychosomatics* 40, 513–517. doi: 10.1016/S0033-3182(99)71191-6
- Harvey, R. J., Depner, U. B., Wasse, H., Ahmadi, S., Heindl, C., Reinold, H., et al. (2004). GlyR alpha3: an essential target for spinal PGE2-mediated inflammatory pain sensitization. *Science* 304, 884–887. doi: 10.1126/science.1094925
- Harvey, R. J., Thomas, P., James, C. H., Wilderspin, A., and Smart, T. G. (1999). Identification of an inhibitory Zn²⁺ binding site on the human glycine receptor alpha1 subunit. *J. Physiol.* 520(Pt 1):53–64. doi: 10.1111/j.1469-7793.1999.00053.x
- Herbert, M. R. (2010). Contributions of the environment and environmentally vulnerable physiology to autism spectrum disorders. *Curr. Opin. Neurol.* 23, 103–110. doi: 10.1097/WCO.0b013e328336a01f
- Hill, E. J., Woehrling, E. K., Prince, M., and Coleman, M. D. (2008). Differentiating human NT2/D1 neurospheres as a versatile *in vitro* 3D model system for developmental neurotoxicity testing. *Toxicology* 249, 243–250. doi: 10.1016/j.tox.2008.05.014
- Hsu, T. C., Liu, K. K., Chang, H. C., Hwang, E., and Chao, J. I. (2014). Labeling of neuronal differentiation and neuron cells with biocompatible fluorescent nanodiamonds. *Sci. Rep.* 4, 5004. doi: 10.1038/srep05004
- Islam, R., and Lynch, J. W. (2012). Mechanism of action of the insecticides, lindane and fipronil, on glycine receptor chloride channels. *Br. J. Pharmacol.* 165, 2707–2720. doi: 10.1111/j.1476-5381.2011.01722.x
- James, O. T., Livesey, M. R., Qiu, J., Dando, O., Bilican, B., Haghi, G., et al. (2014). Ionotropic GABA and glycine receptor subunit composition in human pluripotent stem cell-derived excitatory cortical neurones. *J. Physiol.* 592, 4353–4363. doi: 10.1113/jphysiol.2014.278994
- Kang, J. Q., Shen, W., Zhou, C., Xu, D., and Macdonald, R. L. (2015). The human epilepsy mutation GABRG2(Q390X) causes chronic subunit accumulation and neurodegeneration. *Nat. Neurosci.* 18, 988–996. doi: 10.1038/nn.4024
- Kruger, W., Gilbert, D., Hawthorne, R., Hryciw, D. H., Frings, S., Poronnik, P., et al. (2005). A yellow fluorescent protein-based assay for high-throughput screening of glycine and GABAA receptor chloride channels. *Neurosci. Lett.* 380, 340–345. doi: 10.1016/j.neulet.2005.01.065
- Kumamoto, E., and Murata, Y. (1995). Characterization of GABA current in rat septal cholinergic neurons in culture and its modulation by metal cations. *J. Neurophysiol.* 74, 2012–2027.
- Laurenza, I., Pallocca, G., Mennecozzi, M., Scelfo, B., Pamies, D., and Bal-Price, A. (2013). A human pluripotent carcinoma stem cell-based model for *in vitro* developmental neurotoxicity testing: effects of methylmercury, lead and aluminum evaluated by gene expression studies. *Int. J. Dev. Neurosci.* 31, 679–691. doi: 10.1016/j.ijdevneu.2013.03.002
- Lee, V. M., and Andrews, P. W. (1986). Differentiation of NTERA-2 clonal human embryonal carcinoma cells into neurons involves the induction of all three neurofilament proteins. *J. Neurosci.* 6, 514–521.
- Li, P., and Akk, G. (2008). The insecticide fipronil and its metabolite fipronil sulphone inhibit the rat alpha1beta2gamma2L GABA(A) receptor. *Br. J. Pharmacol.* 155, 783–794. doi: 10.1038/bjp.2008.309
- Lian, Y., Wang, Y., Ma, K., Zhao, L., Zhang, Z., Shang, Y., et al. (2012). Expression of gamma-aminobutyric acid type A receptor $\alpha(2)$ subunit in the dorsal root ganglion of rats with sciatic nerve injury. *Neural Regeneration Res.* 7, 2492–2499.
- Lynch, J. W. (2004). Molecular structure and function of the glycine receptor chloride channel. *Physiol. Rev.* 84, 1051–1095. doi: 10.1152/physrev.00042.2003
- Lynch, J. W. (2009). Native glycine receptor subtypes and their physiological roles. *Neuropharmacology* 56, 303–309. doi: 10.1016/j.neuropharm.2008.07.034
- Lynch, J. W., and Callister, R. J. (2006). Glycine receptors: a new therapeutic target in pain pathways. *Curr. Opin. Investig. Drugs* 7, 48–53.
- Lynch, J. W., and Chen, X. (2008). Subunit-specific potentiation of recombinant glycine receptors by NV-31, a bilobalide-derived compound. *Neurosci. Lett.* 435, 147–151. doi: 10.1016/j.neulet.2008.02.022
- Lynch, J. W., Rajendra, S., Pierce, K. D., Handford, C. A., Barry, P. H., and Schofield, P. R. (1997). Identification of intracellular and extracellular domains mediating signal transduction in the inhibitory glycine receptor chloride channel. *EMBO J.* 16, 110–120. doi: 10.1093/emboj/16.1.110
- Macdonald, R. L., Kang, J. Q., and Gallagher, M. J. (2010). Mutations in GABAA receptor subunits associated with genetic epilepsies. *J. Physiol.* 588, 1861–1869. doi: 10.1113/jphysiol.2010.186999
- Makris, S. L., Raffaele, K., Allen, S., Bowers, W. J., Hass, U., Allea, E., et al. (2009). A retrospective performance assessment of the developmental neurotoxicity study in support of OECD test guideline 426. *Environ. Health Perspect.* 117, 17–25. doi: 10.1289/ehp.11447
- Martin, L. J., and Chang, Q. (2012). Inhibitory synaptic regulation of motoneurons: a new target of disease mechanisms in amyotrophic lateral sclerosis. *Mol. Neurobiol.* 45, 30–42. doi: 10.1007/s12035-011-8217-x
- May, M. (2000). Disturbing behavior: neurotoxic effects in children. *Environ. Health Perspect.* 108, A262–267. doi: 10.1289/ehp.108-a262
- Meier, J. C., Henneberger, C., Melnick, I., Racca, C., Harvey, R. J., Heinemann, U., et al. (2005). RNA editing produces glycine receptor alpha3(P185L), resulting in high agonist potency. *Nat. Neurosci.* 8, 736–744. doi: 10.1038/nn1467
- Middaugh, L. D., Dow-Edwards, D., Li, A. A., Sandler, J. D., Seed, J., Sheets, L. P., et al. (2003). Neurobehavioral assessment: a survey of use and value in safety assessment studies. *Toxicol. Sci.* 76, 250–261. doi: 10.1093/toxsci/kfg211
- Mohamed, F., Senarathna, L., Percy, A., Abeyewardene, M., Eaglesham, G., Cheng, R., et al. (2004). Acute Human Self-Poisoning with the N-Phenylpyrazole

- Insecticide Fipronil—a GABAA-Gated Chloride Channel Blocker. *J. Toxicol. Clin. Toxicol.* 42, 955–963. doi: 10.1081/clt-200041784
- Munir, M., Lu, L., Wang, Y. H., Luo, J., Wolfe, B. B., and McGonigle, P. (1996). Pharmacological and immunological characterization of N-methyl-D-aspartate receptors in human NT2-N neurons. *J. Pharmacol. Exp. Ther.* 276, 819–828.
- Narahashi, T. (1996). Neuronal ion channels as the target sites of insecticides. *Pharmacol. Toxicol.* 79, 1–14. doi: 10.1111/j.1600-0773.1996.tb00234.x
- Narahashi, T. (2002). Nerve membrane ion channels as the target site of insecticides. *Mini. Rev. Med. Chem.* 2, 419–432. doi: 10.2174/1389557023405927
- Neelands, T. R., Greenfield, L. J. Jr., Zhang, J., Turner, R. S., and Macdonald, R. L. (1998). GABAA receptor pharmacology and subtype mRNA expression in human neuronal NT2-N cells. *J. Neurosci.* 18, 4993–5007.
- Neelands, T. R., Zhang, J., and Macdonald, R. L. (1999). GABA(A) receptors expressed in undifferentiated human teratocarcinoma NT2 cells differ from those expressed by differentiated NT2-N cells. *J. Neurosci.* 19, 7057–7065.
- Neumann, S. B., Seitz, R., Gorzella, A., Heister, A., Doeberitz, M., and v. K., Becker, C.-M. (2004). Relaxation of glycine receptor and onconeural gene transcription control in NRSF deficient small cell lung cancer cell lines. *Mol. Brain Res.* 120, 173–181. doi: 10.1016/j.molbrainres.2003.10.021
- OECD (1997). *Test Guideline 424*. OECD Guideline for testing of Chemicals. Neurotoxicity Study in Rodents.
- OECD (2007). *Test Guideline 426*. OECD Guideline for testing of Chemicals. Developmental Neurotoxicity Study.
- Ogata, N., Vogel, S. M., and Narahashi, T. (1988). Lindane but not deltamethrin blocks a component of GABA-activated chloride channels. *FASEB J.* 2, 2895–2900.
- Olsen, R. W., and Sieghart, W. (2009). GABA A receptors: subtypes provide diversity of function and pharmacology. *Neuropharmacology* 56, 141–148. doi: 10.1016/j.neuropharm.2008.07.045
- Ozdener, H. (2007). Inducible functional expression of Bcl-2 in human astrocytes derived from NTera-2 cells. *J. Neurosci. Methods* 159, 8–18. doi: 10.1016/j.jneumeth.2006.06.008
- Pallocca, G., Fabbri, M., Sacco, M. G., Gribaldo, L., Pamies, D., Laurenza, I., et al. (2013). miRNA expression profiling in a human stem cell-based model as a tool for developmental neurotoxicity testing. *Cell Biol. Toxicol.* 29, 239–257. doi: 10.1007/s10565-013-9250-5
- Pleasure, S. J., Page, C., and Lee, V. M. (1992). Pure, postmitotic, polarized human neurons derived from NTera 2 cells provide a system for expressing exogenous proteins in terminally differentiated neurons. *J. Neurosci.* 12, 1802–1815.
- Pribilla, I., Takagi, T., Langosch, D., Bormann, J., and Betz, H. (1992). The atypical M2 segment of the beta subunit confers picrotoxinin resistance to inhibitory glycine receptor channels. *EMBO J.* 11, 4305–4311.
- Ratra, G. S., Kamita, S. G., and Casida, J. E. (2001). Role of human GABA(A) receptor beta3 subunit in insecticide toxicity. *Toxicol. Appl. Pharmacol.* 172, 233–240. doi: 10.1006/taap.2001.9154
- Rauh, V. A., Garfinkel, R., Perera, F. P., Andrews, H. F., Hoepner, L., Barr, D. B., et al. (2006). Impact of prenatal chlorpyrifos exposure on neurodevelopment in the first 3 years of life among inner-city children. *Pediatrics* 118, e1845–1859. doi: 10.1097/00001648-200611001-00247
- Rice, D., and Barone, S. Jr. (2000). Critical periods of vulnerability for the developing nervous system: evidence from humans and animal models. *Environ. Health Perspect.* 108(Suppl. 3), 511–533. doi: 10.1289/ehp.00108.s3511
- Rudolph, U., and Möhler, H. (2014). GABAA receptor subtypes: therapeutic potential in down syndrome, affective disorders, schizophrenia, and autism. *Annu. Rev. Pharmacol. Toxicol.* 54, 483–507. doi: 10.1146/annurev-pharmtox-011613-135947
- Russell, W. M. S., and Burch, R. L. (1959). *The Principles of Humane Experimental Technique*. London: Methuen.
- Sandhu, J. K., Sikorska, M., and Walker, P. R. (2002). Characterization of astrocytes derived from human NTera-2/D1 embryonal carcinoma cells. *J. Neurosci. Res.* 68, 604–614. doi: 10.1002/jnr.10236
- Saporta, S., Spencer, E., and Shamekh, R. (2014). *Stable Differentiation of NT2 Cells*. Google Patents.
- Smart, T. G., Moss, S. J., Xie, X., and Huganir, R. L. (1991). GABAA receptors are differentially sensitive to zinc: dependence on subunit composition. *Br. J. Pharmacol.* 103, 1837–1839. doi: 10.1111/j.1476-5381.1991.tb12337.x
- Smart, T. G., Xie, X., and Krishek, B. J. (1994). Modulation of inhibitory and excitatory amino acid receptor ion channels by zinc. *Prog. Neurobiol.* 42, 393–441. doi: 10.1016/0301-0082(94)90082-5
- Smirnova, L., Hogberg, H. T., Leist, M., and Hartung, T. (2014). Developmental neurotoxicity - challenges in the 21st century and *in vitro* opportunities. *ALTEX* 31, 129–156. doi: 10.14573/altex.1403271
- Stern, M., Gierse, A., Tan, S., and Bicker, G. (2014). Human Ntera2 cells as a predictive *in vitro* test system for developmental neurotoxicity. *Arch. Toxicol.* 88, 127–136. doi: 10.1007/s00204-013-1098-1
- Stewart, R., Christie, V. B., and Przyborski, S. A. (2003). Manipulation of human pluripotent embryonal carcinoma stem cells and the development of neural subtypes. *Stem Cells* 21, 248–256. doi: 10.1634/stemcells.21-3-248
- Stoffels, B., Türlér, A., Schmidt, J., Nazir, A., Tsukamoto, T., Moore, B. A., et al. (2011). Anti-Inflammatory Role of Glycine In Reducing Rodent Postoperative Inflammatory Ileus. *Neurogastroenterol. Motil.* 23, 76–e78. doi: 10.1111/j.1365-2982.2010.01603.x
- Sun, H., and Machu, T. K. (2000). Bicuculline antagonizes 5-HT(3A) and alpha2 glycine receptors expressed in Xenopus oocytes. *Eur. J. Pharmacol.* 391, 243–249. doi: 10.1016/S0014-2999(00)00083-2
- Suñol, C., Tusell, J. M., Gelpí, E., and Rodríguez-Farré, E. (1989). GABAergic modulation of lindane (γ -hexachlorocyclohexane)-induced seizures. *Toxicol. Appl. Pharmacol.* 100, 1–8.
- Talwar, S., Lynch, J. W., and Gilbert, D. F. (2013). Fluorescence-based high-throughput functional profiling of ligand-gated ion channels at the level of single cells. *PLoS ONE* 8:e58479. doi: 10.1371/journal.pone.0058479
- Tukker, A. M., de Groot, M. W., Wijnolts, F. M., Kasteel, E. E., Hondebrink, L., and Westerink, R. H. (2016). Is the time right for *in vitro* neurotoxicity testing using human iPSC-derived neurons? *ALTEX*. doi: 10.14573/altex.1510091. [Epub ahead of print].
- Vafa, B., Lewis, T. M., Cunningham, A. M., Jacques, P., Lynch, J. W., and Schofield, P. R. (1999). Identification of a new ligand binding domain in the alpha1 subunit of the inhibitory glycine receptor. *J. Neurochem.* 73, 2158–2166.
- Vale, C., Fonfra, E., Bujons, J., Messegue, A., Rodriguez-Farré, E., and Suol, C. (2003). The organochlorine pesticides γ -hexachlorocyclohexane (lindane), α -endosulfan and dieldrin differentially interact with GABAA and glycine-gated chloride channels in primary cultures of cerebellar granule cells. *Neuroscience* 117, 397–403. doi: 10.1016/S0306-4522(02)00875-8
- Walzik, M. P., Vollmar, V., Lachnit, T., Dietz, H., Haug, S., Bachmann, H., et al. (2015). A portable low-cost long-term live-cell imaging platform for biomedical research and education. *Biosens. Bioelectron.* 64, 639–649. doi: 10.1016/j.bios.2014.09.061
- Wang, D. S., Buckinx, R., Lecorronc, H., Mangin, J. M., Rigo, J. M., and Legendre, P. (2007). Mechanisms for picrotoxinin and picrotin blocks of alpha2 homomeric glycine receptors. *J. Biol. Chem.* 282, 16016–16035. doi: 10.1074/jbc.M701502200
- Webb, T. I., and Lynch, J. W. (2007). Molecular pharmacology of the glycine receptor chloride channel. *Curr. Pharm. Des.* 13, 2350–2367. doi: 10.2174/138161207781368693
- Wilhelm, F., Winkler, U., Morawski, M., Jager, C., Reinecke, L., Rossner, M. J., et al. (2011). The human ubiquitin C promoter drives selective expression in principal neurons in the brain of a transgenic mouse line. *Neurochem. Int.* 59, 976–980. doi: 10.1016/j.neuint.2011.07.008
- Xiong, W., Cui, T., Cheng, K., Yang, F., Chen, S.-R., Willenbring, D., et al. (2012). Cannabinoids suppress inflammatory and neuropathic pain by targeting α 3 glycine receptors. *J. Exp. Med.* 209, 1121–1134. doi: 10.1084/jem.20120242
- Zeilhofer, H. U. (2005). The glycinergic control of spinal pain processing. *Cell. Mol. Life Sci.* 62, 2027–2035. doi: 10.1007/s00018-005-5107-2

Conflict of Interest Statement: The authors declare that the research was conducted in the absence of any commercial or financial relationships that could be construed as a potential conflict of interest.

Copyright © 2016 Kuenzel, Friedrich and Gilbert. This is an open-access article distributed under the terms of the Creative Commons Attribution License (CC BY). The use, distribution or reproduction in other forums is permitted, provided the original author(s) or licensor are credited and that the original publication in this journal is cited, in accordance with accepted academic practice. No use, distribution or reproduction is permitted which does not comply with these terms.



Generation of Functional Inhibitory Synapses Incorporating Defined Combinations of GABA(A) or Glycine Receptor Subunits

Christine L. Dixon^{1†}, Yan Zhang¹ and Joseph W. Lynch^{1,2*}

¹ Queensland Brain Institute, University of Queensland, Brisbane, QLD, Australia, ² School of Biomedical Sciences, University of Queensland, Brisbane, QLD, Australia

OPEN ACCESS

Edited by:

Kirsten Harvey,
University College London, UK

Reviewed by:

Jochen C. Meier,
Technical University Braunschweig,
Germany
Piotr Bregestovski,
Aix-Marseille University, France

*Correspondence:

Joseph W. Lynch
j.lynch@uq.edu.au

† Present address:

Christine L. Dixon,
Institute of Neurology,
University College London,
London, UK

Received: 12 November 2015

Accepted: 07 December 2015

Published: 23 December 2015

Citation:

Dixon CL, Zhang Y and Lynch JW
(2015) Generation of Functional
Inhibitory Synapses Incorporating
Defined Combinations of GABA(A) or
Glycine Receptor Subunits.
Front. Mol. Neurosci. 8:80.
doi: 10.3389/fnmol.2015.00080

Fast inhibitory neurotransmission in the brain is mediated by wide range of GABA_A receptor (GABA_AR) and glycine receptor (GlyR) isoforms, each with different physiological and pharmacological properties. Because multiple isoforms are expressed simultaneously in most neurons, it is difficult to define the properties of individual isoforms under synaptic stimulation conditions *in vivo*. Although recombinant expression systems permit the expression of individual isoforms in isolation, they require exogenous agonist application which cannot mimic the dynamic neurotransmitter profile characteristic of native synapses. We describe a neuron-HEK293 cell co-culture technique for generating inhibitory synapses incorporating defined combinations of GABA_AR or GlyR subunits. Primary neuronal cultures, prepared from embryonic rat cerebral cortex or spinal cord, are used to provide presynaptic GABAergic and glycinergic terminals, respectively. When the cultures are mature, HEK293 cells expressing the subunits of interest plus neuroligin 2A are plated onto the neurons, which rapidly form synapses onto HEK293 cells. Patch clamp electrophysiology is then used to analyze the physiological and pharmacological properties of the inhibitory postsynaptic currents mediated by the recombinant receptors. The method is suitable for investigating the kinetic properties or the effects of drugs on inhibitory postsynaptic currents mediated by defined GABA_AR or GlyR isoforms of interest, the effects of hereditary disease mutations on the formation and function of both types of synapses, and synaptogenesis and synaptic clustering mechanisms. The entire cell preparation procedure takes 2–5 weeks.

Keywords: inhibitory postsynaptic current, IPSC, GABAergic, glycinergic, neuropharmacology, synaptogenesis, electrophysiology

INTRODUCTION

The central nervous system is comprised of circuits of interconnected neurons that serve to process specific types of information. These circuits regulate their own output by feedback and feedforward connections. Knowledge of the physiological properties of the inhibitory and excitatory synapses that mediate these connections is crucial for understanding the electrical behavior of circuits and ultimately of brain function. Fast inhibitory neurotransmission in these circuits is mediated by GABA type-A receptor (GABA_AR) and glycine receptor (GlyR) chloride channels.

GABA_ARs exhibit a particularly broad range of heterogeneity. As members of the pentameric ligand-gated ion channel (pLGIC) family, five subunits are required to form a single functional oligomer. There are 19 GABA_AR genes (α 1–6, β 1–3, γ 1–3, δ , ϵ , θ , π , and ρ 1–3) with the most common synaptic isoform comprising α 1, β 2, and γ 2 subunits in a 2:2:1 stoichiometry. Although many hundreds of other subunit combinations are theoretically possible, it is thought that around one hundred exist naturally in the brain (Olsen and Sieghart, 2009). GlyRs exhibit far less diversity with only four genes (α 1–3, β) in humans (Lynch, 2009). They also belong to the pLGIC family and synaptic GlyR isoforms comprise heteromeric assemblies of α and β subunits in a 2:3 or 3:2 stoichiometry (Durisic et al., 2012; Yang et al., 2012).

Each GABA_AR or GlyR isoform has a unique physiological and pharmacological profile and it is the unique properties of a particular isoform that are important for the appropriate functioning of a particular network. Disruptions to these properties can result in neurological disorders. For example, hereditary mutations that affect the function of GABA_ARs or GlyRs can lead to epilepsy (Macdonald et al., 2010) or human hyperekplexia (Bode and Lynch, 2014), respectively. Other disruptive mechanisms are also possible. For example, a post-transcriptional RNA editing mechanism that is upregulated in temporal lobe epilepsy increases the prevalence of α 3 GlyRs incorporating the P185L mutation (Meier et al., 2005; Eichler et al., 2008, 2009). Finally, a range of neurological disorders is known to result from aberrant changes to pLGIC phosphorylation status (Talwar and Lynch, 2014). For example, chronic pain sensitization is caused by prostaglandin-induced phosphorylation of α 3 GlyRs (Harvey et al., 2004; Zeilhofer, 2005; Lynch and Callister, 2006) and ethanol-induced phosphorylation of the γ 2 GABA_AR subunit contributes to alcoholism (Qi et al., 2007).

Thus, characterizing the physiological and pharmacological properties of defined GABA_AR and GlyR isoforms under synaptic activation conditions is essential for understanding how neuronal circuits function in health and disease. However, it is difficult to study individual isoforms in their native neuronal environment due to the multitude of other isoforms present, and the difficulty in pharmacologically or genetically isolating the receptor isoform of interest. The neuron-HEK293 cell co-culture protocols we describe here solve this problem by providing a simple, efficient means of generating functional recombinant inhibitory synapses that selectively incorporate the recombinant GABA_AR or GlyR isoform of interest.

Co-culture approaches have previously been developed to understand the roles of synaptic adhesion molecules (including neuroligin and neuroligin) in the formation of glutamatergic or GABAergic synapses (Scheiffele et al., 2000; Biederer et al., 2002; Dean et al., 2003; Graf et al., 2004; Sara et al., 2005; Kim et al., 2006; Dong et al., 2007; Fuchs et al., 2013) or to investigate the impact of disease-causing neuroligin mutations on GABAergic synaptogenesis (Chubykin et al., 2005; Sun et al., 2011). They have also been employed to characterize the functional properties of inhibitory post-synaptic currents (IPSCs), and have revealed kinetic differences among different GABA_AR isoforms (Wu et al., 2012; Dixon et al., 2014) and GlyR isoforms (Zhang et al., 2014).

The original co-culture protocol, involving postnatal hippocampal neurons and transfected HEK293 cells, was optimized for the immunohistochemical analysis of glutamatergic and GABAergic synapse development (Biederer and Scheiffele, 2007). A more recent protocol outlined an improved procedure for generating recombinant GABAergic synapses between striatal medium spiny GABAergic neurons and transfected HEK293 cells (Brown et al., 2014). However, this was also optimized for monitoring synapse development rather than for recording IPSCs in mature synapses. We have extended the co-culture approach in three ways. First, we describe the first spinal neuron-HEK293 cell co-culture preparation suitable for the efficient generation of recombinant glycinergic synapses. Second, we have simplified the technique for creating GABAergic synapses by using embryonic cortical neurons grown in serum-free media that does not promote the growth of glia (Brewer et al., 1993; Brewer, 1995). We have also optimized the technique to facilitate the electrophysiological analysis of GABAergic and glycinergic IPSCs.

MATERIALS AND METHODS

Overview

Protocols for all procedures described in this study are detailed in the Supplementary Information. Lists of reagents and equipment are also provided. An overview of the co-culture procedure is presented in **Figure 1**. The cerebral cortex contains large populations of GABAergic interneurons that were used to provide presynaptic GABAergic terminals onto HEK293 cells that recombinantly express the GABA_AR subunits of interest. Similarly, spinal neurons contain large populations of glycinergic interneurons that were used to provide glycinergic presynaptic terminals onto HEK293 cells expressing GlyR subunits of interest. The main steps in preparing the neuronal cultures are summarized in **Figure 1** (blue box). The steps involved in HEK293 cell transfection are also described in **Figure 1** (green box). An image of a GABAergic neuron forming synaptic contacts with HEK293 cell is shown in the inset.

Preparation of Neuron Cultures

Euthanasia of timed-pregnant rats was performed via CO₂ inhalation, in accordance with procedures approved by the University of Queensland Animal Ethics Committee. To produce GABAergic interneuron cultures, E18 rat embryos were surgically removed from timed-pregnant rats and placed into chilled Ca-Mg-free Hank's Balanced Salt Solution (CMF-HBSS) under sterile conditions. The cortical neuronal tissue was then pinched off using fine forceps, taking care to peel away the meninges to keep glial cell numbers down. The dissected neurons were then triturated, centrifuged and resuspended in Dulbecco's Modified Eagles Medium supplemented with 10% fetal bovine serum (DMEM-FBS). To produce glycinergic interneuron cultures, E15 rat embryos were surgically removed and placed into ice cold CMF-HBSS under sterile conditions. The spinal cords were then removed and pinned at the wider proximal end while

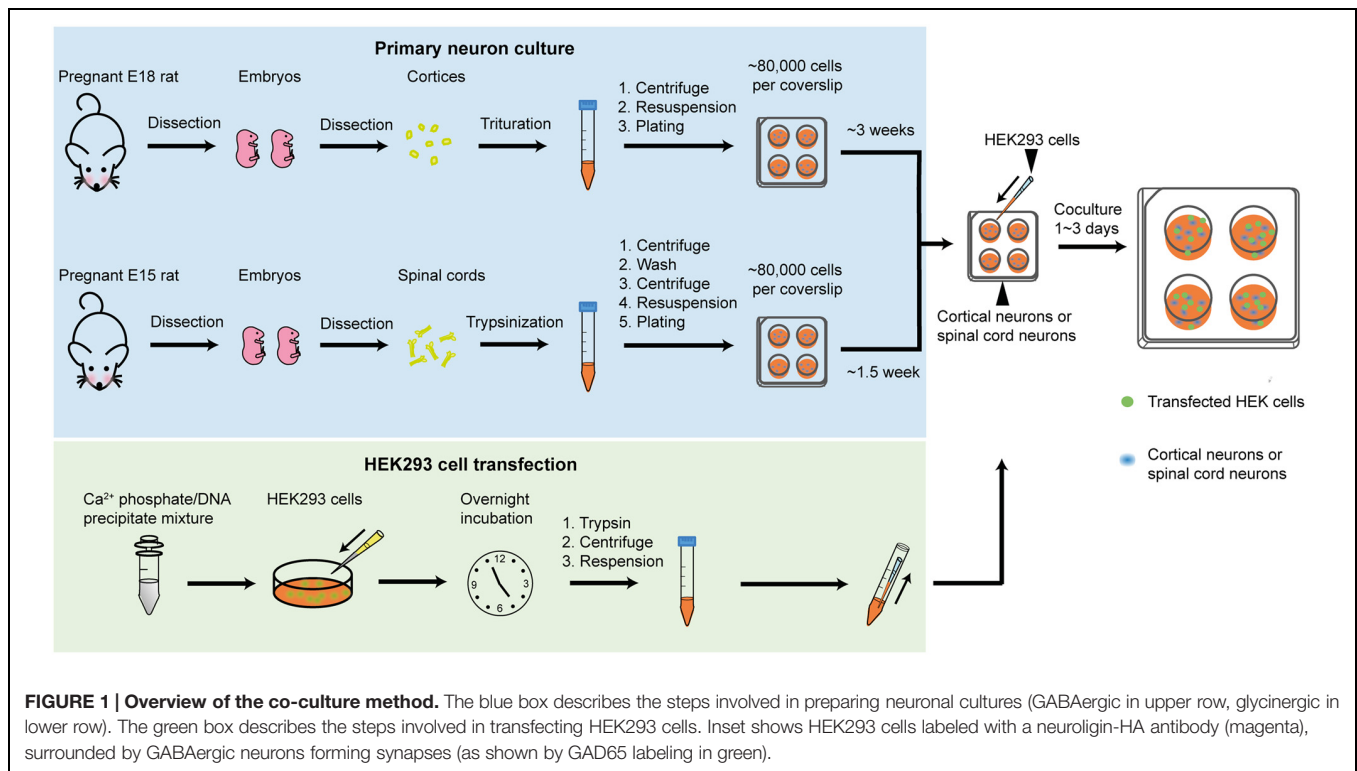


FIGURE 1 | Overview of the co-culture method. The blue box describes the steps involved in preparing neuronal cultures (GABAergic in upper row, glycinergic in lower row). The green box describes the steps involved in transfecting HEK293 cells. Inset shows HEK293 cells labeled with a neuroligin-HA antibody (magenta), surrounded by GABAergic neurons forming synapses (as shown by GAD65 labeling in green).

meninges were carefully detached. The dissected neurons were then triturated, centrifuged and resuspended in DMEM-FBS.

In both cases, the cells were then counted and between 40,000 and 80,000 neurons were plated onto each 12 mm poly-D-lysine-coated coverslip in four-well plates. As previously noted, neuronal density is a key consideration: if it is too low it impairs neuronal survival and if it is too high it encourages neuron clumping (Fuchs et al., 2013). Neuronal cultures were always maintained in a 5% CO₂ incubator at 37°C. After 24 h the entire DMEM-FBS medium was replaced with Neurobasal medium including 2% B27 and 1% GlutaMAX supplements. A second (and final) feed 1 week later replaced half of this medium. In contrast to a previous protocol (Fuchs et al., 2013), we found that antibiotics were unnecessary. Neurons were used in co-culture experiments between 3 and 6 weeks later (for GABAergic co-cultures) or 1–4 weeks later (for glycinergic co-cultures).

Culture and Transfection of HEK293 Cells

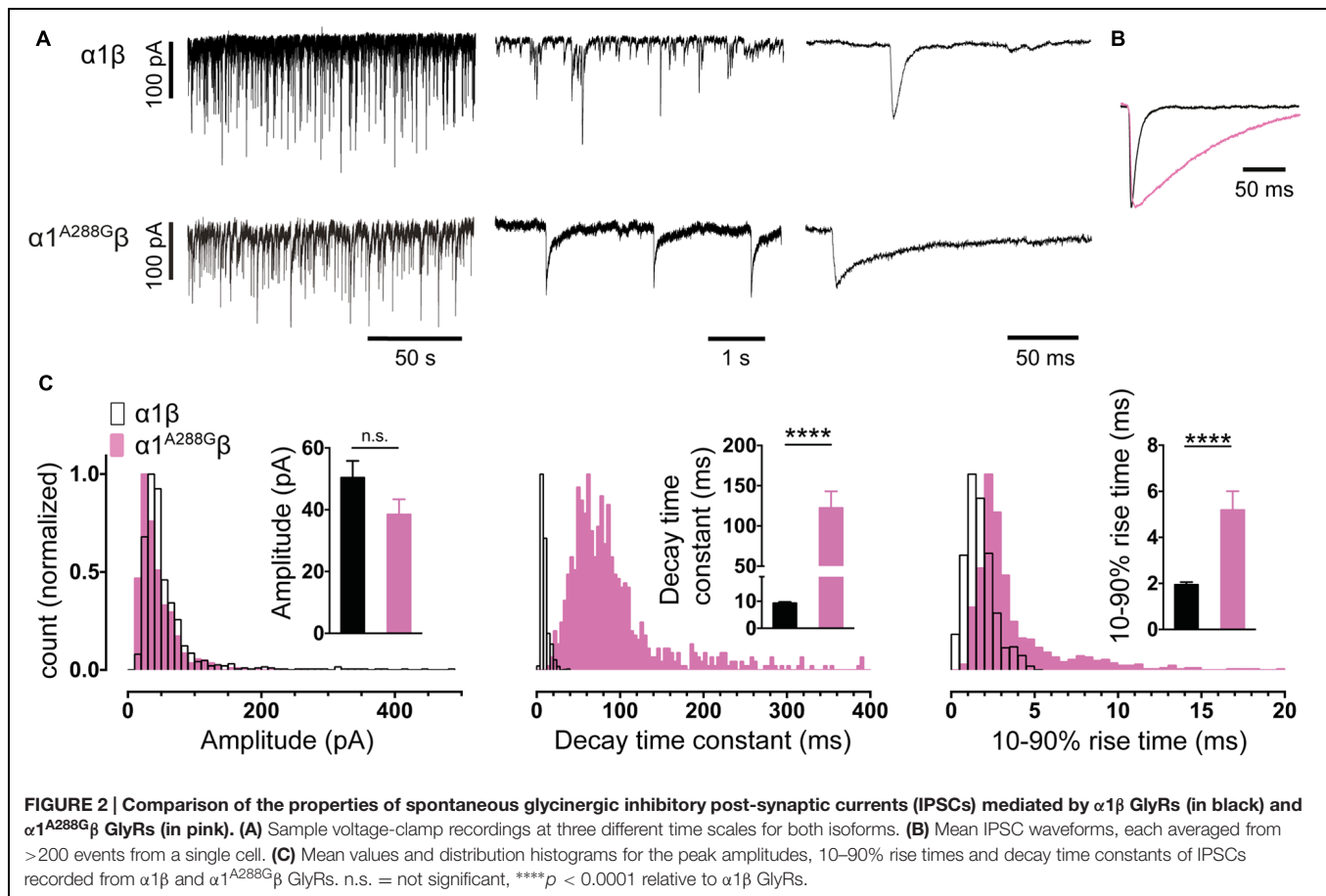
HEK293 cells were cultured in T75 flasks in DMEM-FBS and maintained in a 5% CO₂ incubator at 37°C. The cells were passaged weekly. Prior to transfection, they were trypsinized and plated onto 35 mm culture dishes at a density of 5000 cells/dish. Following overnight incubation, the cells were transfected via a calcium phosphate co-precipitation protocol, using a total of 0.5–2.5 µg DNA per dish. Then, following incubation for 5–20 h in a 3% CO₂ incubator, the transfection was terminated by washing twice with divalent cation-free phosphate buffered saline. The cells were then trypsinized, centrifuged, and resuspended in Neurobasal medium (including 2% B27 and 1% GlutaMAX supplements) then seeded onto the neurons. One 35 mm dish of

HEK293 cells was sufficient to seed four coverslips of neurons. Once seeded with HEK293 cells, the co-cultures were returned to the incubator overnight to allow synapses to form. Cultures were used for patch clamp recording over the following 2–3 days.

Plasmid DNA

A total of 0.5–2.5 µg plasmid DNA should be added to each 35 mm dish of HEK293 cells. This amount may vary according to the individual plasmid expression efficiency, the number and ratios of plasmids to be transfected and the transfection method. When using a calcium phosphate co-precipitation protocol, our recommendations are as follows. When expressing synaptic GlyRs, the total plasmid DNA should comprise: 0.2 µg neuroligin 2A, 0.2 µg gephyrin, 0.1 µg EGFP, with the remainder comprising GlyR subunit DNA that varies according to the number of subunits and the ratio of subunit DNA required. For example, when transfecting GlyR α subunits as homomers, add 0.5 µg DNA. When transfecting α and β GlyR subunits in 1:10 or 1:50 ratios add a total of 2 µg DNA. We recommend transfecting α1:β, α2:β, and α3:β subunits in 1:50, 1:50, and 1:10 ratios, respectively (Zhang et al., 2014). When expressing α1β2γ2 GABA_ARs, the α1, β2, γ2, EGFP and neuroligin 2A plasmid DNAs should be transfected in a 1:1:4:1:1 ratio with a combined total of 0.5 µg DNA.

In experiments described in **Figures 2 and 3** we employed plasmid DNAs encoding the human α1 (pCIS), rat α3L (pcDNA3.1), and human β (pcDNA3.1) GlyR subunits, plus mouse neuroligin 2A (pNice) and rat gephyrin (pCIS). In experiments described in **Figure 4**, we employed human α2 (pcDNA3.1), human α4 (pCIS), β2 (pcDNA3.1), and γ2L



(pcDNA3.1) GABA_AR subunits. Site-directed mutagenesis was performed using the QuikChange mutagenesis kit (Agilent Technologies) according to manufacturers' instructions and the successful incorporation of mutations was confirmed by DNA sequencing.

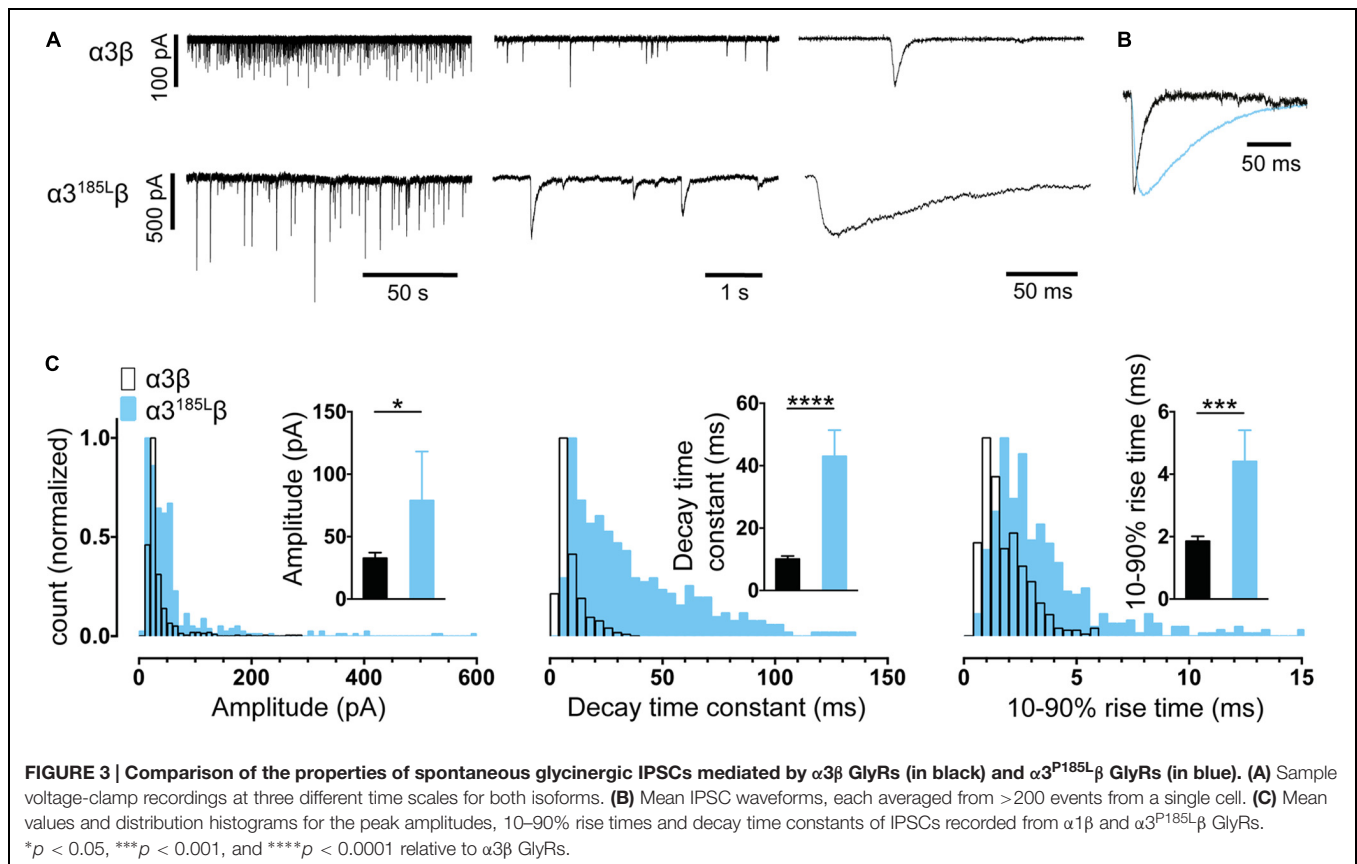
Patch Clamp Electrophysiology and Data Analysis

Standard patch-clamp electrophysiology equipment can be used, with the only specific requirement being a fluorescence microscope for identifying GFP fluorescent cells. Coverslips containing the co-cultured cells were placed gently into the recording chamber on the microscope stage and perfused continuously with an extracellular solution comprising (in mM): 140 NaCl, 5 KCl, 2 CaCl₂, 1 MgCl₂, 10 HEPES, and 10 D-glucose, adjusted to pH 7.4 with NaOH. Patch pipettes were filled with an intracellular solution containing (in mM): 145 CsCl, 2 CaCl₂, 2 MgCl₂, 10 HEPES, 10 EGTA, and 2 MgATP, adjusted to pH 7.4 with NaOH. HEK293 cell selection is largely a matter of trial and error. A good starting point is to select large, strongly fluorescent green cells that are closely surrounded by many neurons, especially small clumps of neurons. Cells with a textured (rather than smooth) appearance often yield abundant IPSCs.

The electrophysiological techniques may vary according to the experimental requirements. For example, if precise quantitation

of rise times is required, it is extremely important that the filtering and digitisation rates are high and that pipette series resistance is low to avoid artefactually slowing down the event. In contrast, testing the effect of a drug on IPSC decay rate is less sensitive to filtering, and it may be necessary to use higher resistance pipettes to obtain a membrane seal that is stable enough to permit recordings that are long enough to apply and wash out the drug.

In all experiments described below, series resistance was compensated to 60% of maximum and was monitored throughout the recording. Spontaneous and action potential-evoked IPSCs in HEK293 cells were recorded at a holding potential -60 mV and currents were filtered at 4 kHz and sampled at 10 kHz. Only cells with a stable series resistance of <25 M Ω throughout the recording period were included in the analysis. Patch pipettes (4–8 M Ω resistance) were made from borosilicate glass (GC150F-7.5, Harvard Apparatus). Analyses of IPSC amplitude, 10–90% rise time, and decay time constant (single-exponential) were performed using Axograph \times (Axograph Scientific). Single peak IPSCs with amplitudes of at least three times above the background noise were detected using a semi-automated sliding template. Each detected event was visually inspected and only well-separated IPSCs with no inflections in the rising or decay phases (suggestive of superimposed events) were included. The respective parameters from all selected events from a single



cell were averaged and are presented as a single data point in **Figures 2–4**. The averages from multiple cells were then pooled to obtain group data. Statistical analysis and plotting were performed on group data with Prism 5 (GraphPad Software). All data are presented as mean \pm SEM. One-way and two-way ANOVA were employed for multiple comparisons. For all tests, the number of asterisks corresponds to level of significance: * $p < 0.05$, ** $p < 0.01$, *** $p < 0.001$ and **** $p < 0.0001$.

RESULTS

Glycinergic IPSCs

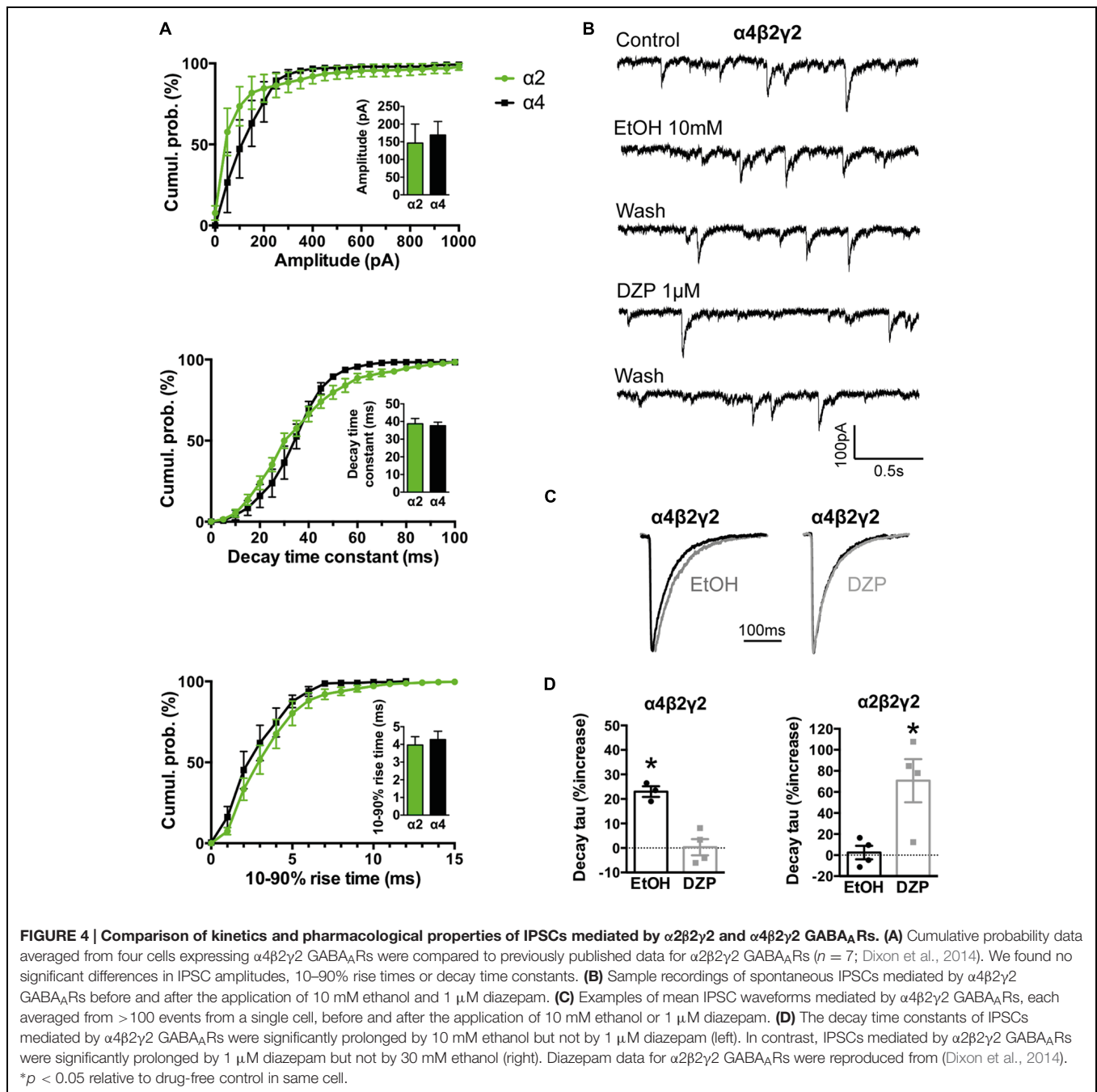
While we found that some co-cultures exhibited spontaneous activity in almost all green fluorescent HEK293 cells, it was more typical to observe spontaneous glycinergic IPSCs in around 20% of cells. This success rate is adequate for most experiments.

It is important to establish that the spontaneous IPSCs produced by the co-culture synapses exhibit similar characteristics to those mediated by native synapses incorporating the same subunits. **Figure 2A** shows sample IPSC recordings from HEK293 cells expressing $\alpha 1\beta$ GlyRs. An IPSC averaged from >200 events recorded from multiple cells is shown in **Figure 2B**. Mean amplitudes, 10–90% rise times and decay time constants are presented in **Figure 2C**. Frequency distributions of IPSC amplitudes, 10–90% rise times and decay time constants all exhibit monotonic distributions suggesting

a single functional population of synapses (**Figure 2C**). In adult hypoglossal motor neurons, where the $\alpha 1\beta$ GlyR isoform predominates (Lynch, 2009), the 10–90% rise times and decay time constants range between 0.6–1.8 and 4.9–7.7 ms, respectively (Singer et al., 1998; Graham et al., 2006; Hirzel et al., 2006; Muller et al., 2006). The mean decay time constant (9.3 ms) and the 10–90% rise time (1.9 ms) recorded in our co-culture synapses correspond well with these results.

We performed a similar analysis on $\alpha 3\beta$ co-culture synapses and found the mean IPSC rise and decay times to be remarkably similar to those mediated by $\alpha 1\beta$ GlyRs (**Figures 3A–C**). These parameters were also distributed monotonically, again suggesting a single population of synapses (**Figure 3C**). Although $\alpha 3\beta$ -mediated IPSCs have yet to be recorded in isolation in native neurons, evidence to date suggests their rise and decay times are indistinguishable from those mediated by $\alpha 1\beta$ GlyRs (Harvey et al., 2004). This fits well with the results from our engineered synapses.

The $\alpha 1$ GlyR subunit D80A and A52S mutations result in startle disease phenotypes in mice (Graham et al., 2006; Hirzel et al., 2006). We previously demonstrated that engineered synapses incorporating $\alpha 1^{D80A}\beta$ and $\alpha 1^{A52S}\beta$ GlyRs exhibited accelerated IPSC decay rates closely resembling those recorded in native synapses from mutant mice homozygous for these mutations (Zhang et al., 2014). This provides an important validation of our technique. In this study we sought to determine whether GlyRs may be located both synaptically



and peri-synaptically in HEK293 cells by introducing mutations that dramatically enhanced the glycine sensitivity. We reasoned that if GlyRs are located peri-synaptically then enhancing their glycine sensitivity may render them susceptible to activation by synaptically released glycine, and if so this should be detectable as an additional slow rise time component (Wu et al., 2012). As noted above, $\alpha 3^{P185L}$ results from a post-transcriptional RNA editing mechanism that is upregulated in (and is causative of) human temporal lobe epilepsy (Eichler et al., 2008, 2009). This mutation reduces the glycine EC₅₀ from 70.9 to 7.4 μ M (Legendre et al., 2009). We also investigated the $\alpha 1^{A288G}$ mutation (which is

not associated with a disease) because it reduces the glycine EC₅₀ from 30.9 to 6.0 μ M (Lynagh and Lynch, 2010).

As shown in **Figures 2A–C**, IPSCs mediated by $\alpha 1^{A288G}\beta$ GlyRs exhibited significantly slower rise times and decay time constants, although additional slow components were never observed on the rising phase of IPSCs. As with unmutated $\alpha 1\beta$ GlyRs, these properties were monotonically distributed (**Figure 2C**) suggesting a single postsynaptic receptor population. Similarly, **Figures 3A–C** shows that IPSCs mediated by $\alpha 3^{P185L}\beta$ GlyRs also exhibited significantly slower rise times and decay time constants that were distributed monotonically. Thus, we

were not able to unequivocally distinguish a putative perisynaptic GlyR population in either case.

GABAergic IPSCs

As with glycinergic IPSCs, we typically observed GABAergic IPSCs in around 20% of HEK293 cells. The rise times and decay time constants of IPSCs recorded from the dominant ($\alpha 1\beta 2\gamma 2$) synaptic subtype (1.2 and 4.0 ms, respectively) are in close accordance with those recorded from neurons known to predominantly express this subtype (Dixon et al., 2014). The co-culture system has revealed that other GABA_AR subunit combinations can yield IPSCs with dramatically different rise and decay times (Wu et al., 2012; Dixon et al., 2014), although it is as yet unclear how these properties relate to those of the same isoforms when expressed in native neuronal synapses.

We have previously demonstrated that the effects of some clinically important drugs on co-culture GABAergic synaptic IPSCs are similar to those recorded at corresponding neuronal synapses. For example, 1 μ M diazepam or 0.1 μ M flunitrazepam significantly increased the decay time constants of IPSCs mediated by $\alpha 2$ -containing GABA_ARs (Dixon et al., 2014) and 1 μ M zolpidem or 1 μ M eszopiclone increased IPSC magnitudes and decay time constants of IPSCs mediated by $\alpha 1$ -containing GABA_ARs (Dixon et al., 2015). Here we extended this characterisation by performing a 'reciprocal' pharmacological comparison of $\alpha 2\beta 2\gamma 2$ and $\alpha 4\beta 2\gamma 2$ GABA_ARs, based the knowledge that $\alpha 4$ -containing GABA_ARs are highly sensitive to ethanol and insensitive to benzodiazepines, whereas $\alpha 2$ -containing GABA_ARs have the opposite profile (Knoflach et al., 1996; Wallner et al., 2006). As shown in **Figures 4A,B**, IPSCs mediated by recombinant $\alpha 2\beta 2\gamma 2$ and $\alpha 4\beta 2\gamma 2$ GABA_ARs exhibit identical amplitudes, 10–90% rise times and decay time constants. A physiologically relevant (10 mM) ethanol concentration significantly increased the IPSC decay time constant in $\alpha 4\beta 2\gamma 2$ GABA_ARs whereas 1 μ M diazepam had no effect (**Figures 4C,D**). On the other hand, 1 μ M diazepam significantly prolonged the IPSC decay time constant in $\alpha 2\beta 2\gamma 2$ GABA_ARs (Dixon et al., 2014), whereas even a very high (30 mM) ethanol concentration had no effect (**Figure 4D**).

DISCUSSION

Applications of the Protocol

We have described protocols for reliably generating recombinant inhibitory synapses that incorporate defined GlyR or GABA_AR isoforms of interest. These are suitable for investigating (1) the kinetics of IPSCs mediated by defined GABA_AR or GlyR isoforms, (2) the effects of drugs on IPSCs mediated by defined GABA_AR or GlyR isoforms, (3) the effect of posttranslational modifications (e.g., phosphorylation) and hereditary disease mutations on the formation and function of both types of synapses, and (4) synaptogenesis and synaptic clustering mechanisms in both types of synapses. We now expand on each of these points.

IPSC Kinetics

Inhibitory post-synaptic currents mediated by different synaptic GABA_AR or GlyR isoforms exhibit unique physiological and pharmacological profiles. It is useful to quantitate these properties because they may help in identifying the presence, or even the role, of a particular isoform in a particular neuron and also because accurate parameters provide key inputs into computational models of neuron or network function. Although studying recombinant receptors in standard heterologous expression systems such as HEK293 cells or *Xenopus* oocytes allows the electrophysiological properties of a single isoform to be studied in isolation, this approach is limited because the neurotransmitter must be applied artificially and it cannot mimic the fast (μ s) dynamic neurotransmitter concentration profile that exists in the synaptic cleft.

Investigating Drug Efficacy and Selectivity

The GABA_AR is an established therapeutic target for clinical indications including epilepsy, anxiolysis, muscle spasms, sedation and anesthesia. GABA_AR-targeted drugs currently in clinical use are not strongly subtype-selective and this can lead to dose-limiting side effects. For example, diazepam produces effective anxiolysis by positively modulating $\alpha 2$ -containing GABA_ARs, although it also elicits the side effect of sedation by modulating $\alpha 5$ -containing GABA_ARs (Trincavelli et al., 2012). Drugs specific for other isoforms are also being sought. For example, selective modulators of $\alpha 5$ -containing GABA_ARs are being developed for a range of indications including stroke, cognitive impairment, and schizophrenia (Soh and Lynch, 2015). Although GlyRs are not currently targeted by clinically useful drugs, molecules that selectively enhance $\alpha 3$ -containing GlyRs are considered promising as new generation treatments for chronic pain (Zeilhofer, 2005; Lynch and Callister, 2006). When evaluating new molecules as potential therapeutic lead compounds for synaptically localized receptors, it is important to test their potency, efficacy and subtype-selectivity under realistic synaptic activation conditions. The system we describe provides the most definitive means available of evaluating drug efficacy and selectivity at IPSCs mediated by defined receptor isoforms.

Investigating Disease Mutations

Engineered synapses have yet to be used to study disease-causing GABA_AR mutations or modifications, and hence, the method has not realized its full potential as a model system for understanding the molecular pathology of neurological disorders. Mutations in GABA_AR $\alpha 1$ and $\gamma 2$ subunits have long been associated with genetic epilepsy syndromes (Macdonald et al., 2010). Thus far, the function and pharmacology of epilepsy-causing mutant GABA_ARs have only been investigated using whole-cell recordings of steady-state GABA-activated currents in heterologous expression systems. The differing approaches that have been used to analyze the effects of these mutations have led to controversy, particularly in the case of the $\gamma 2^{R43Q}$ mutation (Petrou and Reid, 2012). Moreover, of all the identified epilepsy-causing mutant GABA_ARs that exhibit partial or full expression

at the cell membrane, there is an animal knock-in model of only one (Petrou and Reid, 2012). Transgenic animal models are afflicted by compensatory mechanisms that can obfuscate data, especially those involving ion channel genetic manipulations that affect GABAergic transmission (Harris et al., 2011). Because co-culture $\alpha 1\beta 2\gamma 2$ GABA_AR synapses successfully recapitulate the kinetics of neuronal IPSCs (Dixon et al., 2014), they may provide a promising means of investigating the synaptic signaling defects induced by hereditary epilepsy mutations to $\alpha 1$ and $\gamma 2$ subunits.

Glycinergic co-culture synapses incorporating $\alpha 1^{D80A\beta}$ and $\alpha 1^{A52S\beta}$ GlyRs have been shown to exhibit accelerated IPSC decay rates that strongly resemble those recorded in native synapses from mutant mice homozygous for the same mutations (Zhang et al., 2014). This suggests that the co-culture system should be useful for modeling the effects of hyperekplexia mutations to $\alpha 1$ and β subunits (Bode and Lynch, 2014) and autism mutations to $\alpha 2$ subunits (Pilorge et al., 2015). Here we investigated the effect of the $\alpha 3^{P185L}$ mutation that is associated with temporal lobe epilepsy. The mutation resulted in slowing of the IPSC decay rate (Figure 3). However, glycinergic synapses are absent in the temporal lobe and it is thought that the affected receptors are located presynaptically at glutamatergic synapses. In this case, our results suggest the mutant GlyR would remain open for longer during each synaptic event, thus potentiating an excitatory Cl flux leading to enhanced excitatory neurotransmission that could underlie the disorder (Eichler et al., 2008, 2009; Legendre et al., 2009).

Synaptogenesis and Synaptic Clustering Mechanisms

Co-culture synapses have been used extensively to probe the roles of synaptic adhesion molecules in the formation of glutamatergic or GABAergic synapses (Scheiffele et al., 2000; Biederer et al., 2002; Dean et al., 2003; Graf et al., 2004; Sara et al., 2005; Kim et al., 2006; Dong et al., 2007; Fuchs et al., 2013) or to investigate the impact of disease-causing neuroligin mutations on GABAergic synaptogenesis (Chubykin et al., 2005; Sun et al., 2011). The strengths and weaknesses of co-cultures in this respect have recently been reviewed (Fuchs et al., 2013).

CONCLUSION

As the presynaptic terminals of our engineered synapses are provided by real neurons, their function is likely to resemble those of synapses *in vivo*. Indeed, serial electron microscopic reconstructions of GABAergic terminals onto HEK293 cells have confirmed that their ultrastructures are similar to those of native neurons (Fuchs et al., 2013). However, the postsynaptic specializations are less likely to resemble those of

neurons given that HEK293 cells do not endogenously express all necessary postsynaptic clustering proteins at appropriate levels for synaptogenesis. In addition, some proteins that they do express may lack neuron-specific post-translational modifications required for correct synaptic function. These factors could ultimately alter the geometry of the synaptic cleft and the postsynaptic receptor clustering density, leading to non-physiological changes in the neurotransmitter concentration profile that could affect IPSC kinetics. This uncertainty is the main limitation of the technique. We have addressed this as far as possible by comparing the properties of engineered synapses with those of real synapses in cases where we can be reasonably sure about the synaptic subunit composition.

However, due to their non-physiological status, engineered synapses also offer opportunities to investigate new clustering mechanisms. If, for example, substitution of a particular pLGIC subunit results in a drastic, unexpected slowing of the IPSC rise time, it is possible that synaptic receptors have been de-clustered in a manner that may not occur in a neuron. This could in turn lead to the identification of novel clustering molecules and mechanisms. HEK293 cells are ideal for investigating such questions: they do not express all proteins necessary for synaptogenesis, but they do provide a high efficiency of transfection, faithful protein translation and a small, electronically compact shape appropriate for accurate quantitation of IPSC rise and decay times (Thomas and Smart, 2005).

AUTHOR CONTRIBUTIONS

CD, YZ, and JL conceived the project and developed the protocols; CD and YZ performed experiments and analyzed the data; and CD, YZ, and JL wrote the manuscript.

ACKNOWLEDGMENTS

This research was supported by project grants from the Australian Research Council (DP120104373) and the National Health and Medical Research Council (APP1062183). JL is supported by a Principle Research Fellowship from the National Health and Medical Research Council (APP1058542). We thank Dr Nela Durisic for critical review of the manuscript.

SUPPLEMENTARY MATERIAL

The Supplementary Material for this article can be found online at: <http://journal.frontiersin.org/article/10.3389/fnmol.2015.00080>

REFERENCES

- Biederer, T., Sara, Y., Mozhayeva, M., Atasoy, D., Liu, X., Kavalali, E. T., et al. (2002). SynCAM, a synaptic adhesion molecule that drives synapse assembly. *Science* 297, 1525–1531. doi: 10.1126/science.1072356
- Biederer, T., and Scheiffele, P. (2007). Mixed-culture assays for analyzing neuronal synapse formation. *Nat. Protoc.* 2, 670–676. doi: 10.1038/nprot.2007.92
- Bode, A., and Lynch, J. W. (2014). The impact of human hyperekplexia mutations on glycine receptor structure and function. *Mol. Brain* 7, 2. doi: 10.1186/1756-6606-7-2

- Brewer, G. J. (1995). Serum-free B27/neurobasal medium supports differentiated growth of neurons from the striatum, substantia nigra, septum, cerebral cortex, cerebellum, and dentate gyrus. *J. Neurosci. Res.* 42, 674–683. doi: 10.1002/jnr.490420510
- Brewer, G. J., Torricelli, J. R., Evege, E. K., and Price, P. J. (1993). Optimized survival of hippocampal neurons in B27-supplemented Neurobasal, a new serum-free medium combination. *J. Neurosci. Res.* 35, 567–576. doi: 10.1002/jnr.490350513
- Brown, L. E., Fuchs, C., Nicholson, M. W., Stephenson, F. A., Thomson, A. M., and Jovanovic, J. N. (2014). Inhibitory synapse formation in a co-culture model incorporating GABAergic medium spiny neurons and HEK293 cells stably expressing GABAA receptors. *J. Vis. Exp.* 93, e52115. doi: 10.3791/52115
- Chubykin, A. A., Liu, X., Comoletti, D., Tsigelny, I., Taylor, P., and Sudhof, T. C. (2005). Dissection of synapse induction by neuroligins: effect of a neuroligin mutation associated with autism. *J. Biol. Chem.* 280, 22365–22374. doi: 10.1074/jbc.M410723200
- Dean, C., Scholl, F. G., Choih, J., DeMaria, S., Berger, J., Isacoff, E., et al. (2003). Neuroligin mediates the assembly of presynaptic terminals. *Nat. Neurosci.* 6, 708–716. doi: 10.1038/nn1074
- Dixon, C., Sah, P., Lynch, J. W., and Keramidas, A. (2014). GABAA receptor alpha and gamma subunits shape synaptic currents via different mechanisms. *J. Biol. Chem.* 289, 5399–5411. doi: 10.1074/jbc.M113.514695
- Dixon, C. L., Harrison, N. L., Lynch, J. W., and Keramidas, A. (2015). Zolpidem and eszopiclone prime alpha1beta2gamma2 GABAA receptors for longer duration of activity. *Br. J. Pharmacol.* 172, 3522–3536. doi: 10.1111/bph.13142
- Dong, N., Qi, J., and Chen, G. (2007). Molecular reconstitution of functional GABAergic synapses with expression of neuroligin-2 and GABAA receptors. *Mol. Cell. Neurosci.* 35, 14–23. doi: 10.1016/j.mcn.2007.01.013
- Duricic, N., Godin, A. G., Wever, C. M., Heyes, C. D., Lakadamyali, M., and Dent, J. A. (2012). Stoichiometry of the human glycine receptor revealed by direct subunit counting. *J. Neurosci.* 32, 12915–12920. doi: 10.1523/JNEUROSCI.2050-12.2012
- Eichler, S. A., Forstera, B., Smolinsky, B., Jüttner, R., Lehmann, T. N., Fahling, M., et al. (2009). Splice-specific roles of glycine receptor alpha3 in the hippocampus. *Eur. J. Neurosci.* 30, 1077–1091. doi: 10.1111/j.1460-9568.2009.06903.x
- Eichler, S. A., Kirischuk, S., Jüttner, R., Schaefermeier, P. K., Legendre, P., Lehmann, T. N., et al. (2008). Glycinergic tonic inhibition of hippocampal neurons with depolarizing GABAergic transmission elicits histopathological signs of temporal lobe epilepsy. *J. Cell. Mol. Med.* 12, 2848–2866. doi: 10.1111/j.1582-4934.2008.00357.x
- Fuchs, C., Abitbol, K., Burden, J. J., Mercer, A., Brown, L., Iball, J., et al. (2013). GABA(A) receptors can initiate the formation of functional inhibitory GABAergic synapses. *Eur. J. Neurosci.* 38, 3146–3158. doi: 10.1111/ejn.12331
- Graf, E. R., Zhang, X., Jin, S. X., Linhoff, M. W., and Craig, A. M. (2004). Neuroligins induce differentiation of GABA and glutamate postsynaptic specializations via neuroligins. *Cell* 119, 1013–1026. doi: 10.1016/j.cell.2004.11.035
- Graham, B. A., Schofield, P. R., Sah, P., Margrie, T. W., and Callister, R. J. (2006). Distinct physiological mechanisms underlie altered glycinergic synaptic transmission in the murine mutants spastic, spasmodic, and oscillator. *J. Neurosci.* 26, 4880–4890. doi: 10.1523/JNEUROSCI.3991-05.2006
- Harris, R. A., Osterndorff-Kahanek, E., Ponomarev, I., Homanics, G. E., and Blednov, Y. A. (2011). Testing the silence of mutations: transcriptomic and behavioral studies of GABA(A) receptor alpha1 and alpha2 subunit knock-in mice. *Neurosci. Lett.* 488, 31–35. doi: 10.1016/j.neulet.2010.10.075
- Harvey, R. J., Depner, U. B., Wasse, H., Ahmadi, S., Heindl, C., Reinold, H., et al. (2004). GlyR alpha3: an essential target for spinal PGE2-mediated inflammatory pain sensitization. *Science* 304, 884–887. doi: 10.1126/science.1094925
- Hirzel, K., Muller, U., Latal, A. T., Hulsmann, S., Grudzinska, J., Seeliger, M. W., et al. (2006). Hyperekplexia phenotype of glycine receptor alpha1 subunit mutant mice identifies Zn(2+) as an essential endogenous modulator of glycinergic neurotransmission. *Neuron* 52, 679–690. doi: 10.1016/j.neuron.2006.09.035
- Kim, S., Burette, A., Chung, H. S., Kwon, S. K., Woo, J., Lee, H. W., et al. (2006). NGL family PSD-95-interacting adhesion molecules regulate excitatory synapse formation. *Nat. Neurosci.* 9, 1294–1301. doi: 10.1038/nn1763
- Knoflach, F., Benke, D., Wang, Y., Scheurer, L., Luddens, H., Hamilton, B. J., et al. (1996). Pharmacological modulation of the diazepam-insensitive recombinant gamma-aminobutyric acidA receptors alpha 4 beta 2 gamma 2 and alpha 6 beta 2 gamma 2. *Mol. Pharmacol.* 50, 1253–1261.
- Legendre, P., Forstera, B., Jüttner, R., and Meier, J. C. (2009). Glycine Receptors Caught between genome and proteome – functional implications of RNA editing and splicing. *Front. Mol. Neurosci.* 2:23. doi: 10.3389/fnmo.2009.02.023
- Lynagh, T., and Lynch, J. W. (2010). A glycine residue essential for high ivermectin sensitivity in Cys-loop ion channel receptors. *Int. J. Parasitol.* 40, 1477–1481. doi: 10.1016/j.ijpara.2010.07.010
- Lynch, J. W. (2009). Native glycine receptor subtypes and their physiological roles. *Neuropharmacology* 56, 303–309. doi: 10.1016/j.neuropharm.2008.07.034
- Lynch, J. W., and Callister, R. J. (2006). Glycine receptors: a new therapeutic target in pain pathways. *Curr. Opin. Investig. Drugs* 7, 48–53.
- Macdonald, R. L., Kang, J. Q., and Gallagher, M. J. (2010). Mutations in GABAA receptor subunits associated with genetic epilepsies. *J. Physiol.* 588, 1861–1869. doi: 10.1113/jphysiol.2010.186999
- Meier, J. C., Henneberger, C., Melnick, I., Racca, C., Harvey, R. J., Heinemann, U., et al. (2005). RNA editing produces glycine receptor alpha3(P185L), resulting in high agonist potency. *Nat. Neurosci.* 8, 736–744. doi: 10.1038/nn1467
- Muller, E., Le Corrionc, H., Triller, A., and Legendre, P. (2006). Developmental dissociation of presynaptic inhibitory neurotransmitter and postsynaptic receptor clustering in the hypoglossal nucleus. *Mol. Cell. Neurosci.* 32, 254–273. doi: 10.1016/j.mcn.2006.04.007
- Olsen, R. W., and Sieghart, W. (2009). GABA A receptors: subtypes provide diversity of function and pharmacology. *Neuropharmacology* 56, 141–148. doi: 10.1016/j.neuropharm.2008.07.045
- Petrou, S., and Reid, C. A. (2012). *The GABA_Agamma2(R43Q) Mouse Model of Human Genetic Epilepsy*. Parkville VIC: Florey Neuroscience Institute and The Centre for Neuroscience, The University of Melbourne.
- Pilorge, M., Fassier, C., Le Corrionc, H., Potey, A., Bai, J., De Gois, S., et al. (2015). Genetic and functional analyses demonstrate a role for abnormal glycinergic signaling in autism. *Mol. Psychiatry* doi: 10.1038/mp.2015.139 [Epub ahead of print].
- Qi, Z.-H., Song, M., Wallace, M. J., Wang, D., Newton, P. M., McMahon, T., et al. (2007). Protein kinase C ϵ regulates γ -aminobutyrate type A receptor sensitivity to ethanol and benzodiazepines through phosphorylation of γ 2 subunits. *J. Biol. Chem.* 282, 33052–33063. doi: 10.1074/jbc.M707233200
- Sara, Y., Biederer, T., Atasoy, D., Chubykin, A., Mozhayeva, M. G., Sudhof, T. C., et al. (2005). Selective capability of SynCAM and neuroligin for functional synapse assembly. *J. Neurosci.* 25, 260–270. doi: 10.1523/JNEUROSCI.3165-04.2005
- Scheiffele, P., Fan, J., Choih, J., Fetter, R., and Serafini, T. (2000). Neuroligin expressed in nonneuronal cells triggers presynaptic development in contacting axons. *Cell* 101, 657–669. doi: 10.1016/S0092-8674(00)80877-6
- Singer, J. H., Talley, E. M., Bayliss, D. A., and Berger, A. J. (1998). Development of glycinergic synaptic transmission to rat brain stem motoneurons. *J. Neurophysiol.* 80, 2608–2620.
- Soh, M. S., and Lynch, J. W. (2015). Selective modulators of alpha5-containing GABAA receptors and their therapeutic significance. *Curr. Drug Targets* 16, 735–746. doi: 10.2174/1389450116666150309120235
- Sun, C., Cheng, M. C., Qin, R., Liao, D. L., Chen, T. T., Koong, F. J., et al. (2011). Identification and functional characterization of rare mutations of the neuroligin-2 gene (NLGN2) associated with schizophrenia. *Hum. Mol. Genet.* 20, 3042–3051. doi: 10.1093/hmg/ddr208
- Talwar, S., and Lynch, J. W. (2014). Phosphorylation mediated structural and functional changes in pentameric ligand-gated ion channels: implications for drug discovery. *Int. J. Biochem. Cell Biol.* 53, 218–223. doi: 10.1016/j.biocel.2014.05.028
- Thomas, P., and Smart, T. G. (2005). HEK293 cell line: a vehicle for the expression of recombinant proteins. *J. Pharmacol. Toxicol. Methods* 51, 187–200. doi: 10.1016/j.vascn.2004.08.014
- Trincavelli, M. L., Da Pozzo, E., Daniele, S., and Martini, C. (2012). The GABAA-BZR complex as target for the development of anxiolytic drugs. *Curr. Top. Med. Chem.* 12, 254–269. doi: 10.2174/1568026799078787
- Wallner, M., Hancher, H. J., and Olsen, R. W. (2006). Low dose acute alcohol effects on GABA A receptor subtypes. *Pharmacol. Ther.* 112, 513–528. doi: 10.1016/j.pharmthera.2006.05.004
- Wu, X., Wu, Z., Ning, G., Guo, Y., Ali, R., Macdonald, R. L., et al. (2012). gamma-Aminobutyric acid type A (GABAA) receptor alpha subunits play a direct role in synaptic versus extrasynaptic targeting. *J. Biol. Chem.* 287, 27417–27430. doi: 10.1074/jbc.M112.360461

- Yang, Z., Taran, E., Webb, T. I., and Lynch, J. W. (2012). Stoichiometry and subunit arrangement of $\alpha\beta$ glycine receptors as determined by atomic force microscopy. *Biochemistry* 51, 5229–5231. doi: 10.1021/bi300063m
- Zeilhofer, H. U. (2005). The glycinergic control of spinal pain processing. *Cell. Mol. Life Sci.* 62, 2027–2035. doi: 10.1007/s00018-005-5107-2
- Zhang, Y., Dixon, C. L., Keramidas, A., and Lynch, J. W. (2014). Functional reconstitution of glycinergic synapses incorporating defined glycine receptor subunit combinations. *Neuropharmacology* 89C, 391–397.

Conflict of Interest Statement: The authors declare that the research was conducted in the absence of any commercial or financial relationships that could be construed as a potential conflict of interest.

Copyright © 2015 Dixon, Zhang and Lynch. This is an open-access article distributed under the terms of the Creative Commons Attribution License (CC BY). The use, distribution or reproduction in other forums is permitted, provided the original author(s) or licensor are credited and that the original publication in this journal is cited, in accordance with accepted academic practice. No use, distribution or reproduction is permitted which does not comply with these terms.



The Intracellular Loop of the Glycine Receptor: It's not all about the Size

Georg Langhofer and Carmen Villmann*

Institute of Clinical Neurobiology, University of Würzburg, Würzburg, Germany

OPEN ACCESS

Edited by:

Robert J. Harvey,
University College London (UCL), UK

Reviewed by:

Verena Tretter,
Medical University Vienna, Austria
Raphael Lamprecht,
University of Haifa, Israel
Sarah Lummis,
University of Cambridge, UK

*Correspondence:

Carmen Villmann
villmann_c@ukw.de

Received: 13 March 2016

Accepted: 17 May 2016

Published: 03 June 2016

Citation:

Langhofer G and Villmann C (2016)
The Intracellular Loop of the Glycine
Receptor: It's not all about the Size.
Front. Mol. Neurosci. 9:41.
doi: 10.3389/fnmol.2016.00041

The family of Cys-loop receptors (CLRs) shares a high degree of homology and sequence identity. The overall structural elements are highly conserved with a large extracellular domain (ECD) harboring an α -helix and 10 β -sheets. Following the ECD, four transmembrane domains (TMD) are connected by intracellular and extracellular loop structures. Except the TM3–4 loop, their length comprises 7–14 residues. The TM3–4 loop forms the largest part of the intracellular domain (ICD) and exhibits the most variable region between all CLRs. The ICD is defined by the TM3–4 loop together with the TM1–2 loop preceding the ion channel pore. During the last decade, crystallization approaches were successful for some members of the CLR family. To allow crystallization, the intracellular loop was in most structures replaced by a short linker present in prokaryotic CLRs. Therefore, no structural information about the large TM3–4 loop of CLRs including the glycine receptors (GlyRs) is available except for some basic stretches close to TM3 and TM4. The intracellular loop has been intensively studied with regard to functional aspects including desensitization, modulation of channel physiology by pharmacological substances, posttranslational modifications, and motifs important for trafficking. Furthermore, the ICD interacts with scaffold proteins enabling inhibitory synapse formation. This review focuses on attempts to define structural and functional elements within the ICD of GlyRs discussed with the background of protein-protein interactions and functional channel formation in the absence of the TM3–4 loop.

Keywords: GlyR receptors, synaptic inhibition, intracellular domain, interaction partners, posttranslational modifications

INTRODUCTION

Glycine receptors (GlyRs) are the major inhibitory neurotransmitter receptors in adult spinal cord and brainstem. They are important for motor coordination and respiratory rhythm. Disturbances in glycinergic neurotransmission by: (i) mutated genes encoding various GlyR subunits or adjacent proteins of the glycinergic receptor complex; (ii) receptor editing or; (iii) receptor modulation by posttranslational mechanisms lead to neuromotor deficits (hyperekplexia), pain sensitization and autism spectrum disorders (Lynch, 2004; Schaefer et al., 2013; Bode and Lynch, 2014; Pilorge et al., 2015).

Abbreviations: CLRs, Cys-loop receptors; ECD, extracellular domain; ICD, intracellular domain; TM, transmembrane; GlyR, glycine receptor; wt, wild-type.

GlyRs are members of the superfamily of Cys-loop receptors (CLRs) such as nicotinic acetylcholine receptors (nAChR), 5HT₃ receptors, and GABA_{A/C} receptors. They all share a common disulfide bridge in the extracellular N-terminal domain between conserved cysteine residues. GlyRs are pentameric receptors composed of 2 α and 3 β subunits (Grudzinska et al., 2005). Four different α subunits and one β subunit are known. Functional diversity is enhanced by alternative splicing processes, which has been described for all subunits (Kuhse et al., 1991; Malosio et al., 1991; Nikolic et al., 1998; Oertel et al., 2007; Hirata et al., 2013).

Most of the knowledge about GlyR signal processing comes from *in vitro* mutagenesis studies on structure-function relationships. Recently the x-ray structure of GlyR α 3 and the cryo-electron microscopic structure of α 1 were solved (Du et al., 2015; Huang et al., 2015). These structures provided deeper insights into the mechanisms of signal processing and gating. Interestingly, x-ray crystallography of CLR members was only possible when the large intracellular loop between TM3–4 was replaced by a short peptide. The TM3–4 loop harbors the highest variability among all CLRs in terms of length and sequence variations. These loop structures mediate subfamily-specific interactions with intracellular binding partners (Goyal et al., 2011). In GlyRs, the TM3–4 loops interact with the scaffold protein gephyrin important for synaptic anchoring or signal transduction processes. In addition, the TM3–4 loop is modified by posttranslational modifications and binds allosteric modulators that in turn influence functional ion channel properties (Figures 1A–D; Ruiz-Gómez et al., 1991; Kirsch and Betz, 1995; Yevenes et al., 2008; Yevenes and Zeilhofer, 2011). Subdomains of the GlyR TM3–4 loop have been demonstrated to be important for receptor trafficking to the cellular membrane and the nucleus (Sadtlir et al., 2003; Melzer et al., 2010).

IMPORTANCE OF GLYCINE RECEPTORS FOR INHIBITORY NEUROTRANSMISSION

In the nerve muscle circuit, GlyRs control excited motoneurons in spinal cord and brainstem. Motoneuron activation is enabled by released glutamate from dorsal root ganglia. In turn, activated motoneurons fire action potentials towards the neuromuscular endplate where the signal is transmitted via acetylcholine to propagate along muscle fibers resulting in muscle contraction. To balance motoneuron firing, inhibitory GlyRs localized within the motoneuronal membrane are activated by release of glycine from neighboring interneurons. These interneurons are excited by collateral axons of the motoneurons. As a consequence, motoneurons are hyperpolarized and excitation is dampened. This feedback control by GlyRs restores the balance between excitation and inhibition (Schaefer et al., 2012). Using similar mechanisms, GlyRs mediate respiratory rhythms in PreBöt (pre-Böttinger complex) nuclei of the brainstem (Winter et al., 2009; Janczewski et al., 2013). An impaired glycinergic inhibition in the brainstem of the mouse mutant *oscillator* leads to decreased breathing frequency caused by prolongation of expiratory duration. This results in death of affected mice around postnatal day 21 due to respiratory acidosis (Markstahler et al., 2002).

Minor GlyR expression has been determined in the retina, inner ear, and the hippocampus (Harvey et al., 2004; Heinze et al., 2007; Długaiczek et al., 2008; Lynch, 2009; Aroeira et al., 2011).

In the hippocampus, GlyRs are mainly found at extrasynaptic sites pointing to a function in tonic activation processes (Aroeira et al., 2011). These extrasynaptic receptors are formed by homomeric α 2 and α 3 GlyR subunits. A gain of function GlyR α 3 variant (α 3^{P185L}) was previously identified in human hippocampectomies from patients with temporal lobe epilepsy (Meier et al., 2005; Eichler et al., 2008). Additionally, the hippocampus of patients with epilepsy expresses predominantly the long splice isoform of α 3 (α 3L; Eichler et al., 2009). Both findings were used to generate a mouse model with neuron-type specific expressions of the GlyR α 3L^{P185L} to study homeostatic effects that control synaptic neurotransmission. The estimated presynaptic expression of GlyR α 3^{P185L} in glutamatergic terminals facilitated neurotransmitter release (Winkelmann et al., 2014). As a consequence, enhanced hyperexcitability leads to recurrent epileptiform discharge impairing cognitive function and discriminative associative memory (Winkelmann et al., 2014). Changes in cognitive function and discriminative associative memory have been analyzed with the reward-based 8-arm radial maze test that discriminates between working memory (number of entries into an arm that was never baited) and reference memory (re-entries into an arm visited in the ongoing trail).

In contrast, specific expression of GlyR α 3L^{P185L} in parvalbumin-positive interneurons generated hypoexcitability and triggered anxiety-like behavior (Winkelmann et al., 2014). Increased anxiety of GlyR α 3L^{P185L} mice was verified by a preference for the dark using the dark/light test, decreased entries into the center in an open field, and less time spent and decreased numbers of entries into the open arms using the elevated plus maze test (Winkelmann et al., 2014). In conclusion, increased presynaptic function represents a pathogenic mechanism able to alter neural network homeostasis and thereby control neuronal network excitability and trigger neuropsychiatric symptoms (Winkelmann et al., 2014).

Inhibition of postsynaptic GlyR α 3 by PGE2- (prostaglandin E2) induced phosphorylation underlies central inflammatory pain sensitization. This process depends on the activation of protein kinase A that phosphorylates α 3 at residue S346 localized in the TM3–4 loop (Harvey et al., 2004). These findings initiated a series of pharmacological studies with GlyR α 3 as a promising target in pain therapy (Lynch and Callister, 2006).

The involvement of GlyRs in autism spectrum disorders is based on genetic findings and knockout mice although the molecular mechanisms behind their involvement in the excitation/inhibition imbalances are not completely understood (Tabuchi et al., 2007; Pilorge et al., 2015). The analysis of a rare human X-linked *GLRA2* microdeletion (deletion of exons 8 and 9 that refer to the TM3–4 loop) associated with autism exhibited lack of surface GlyR expression *in vitro* and severe axon-branching defects in zebrafish (Pilorge et al., 2015). A knockout of *Gla2* in mice revealed deficits in object recognition memory and impaired long-term potentiation in the prefrontal

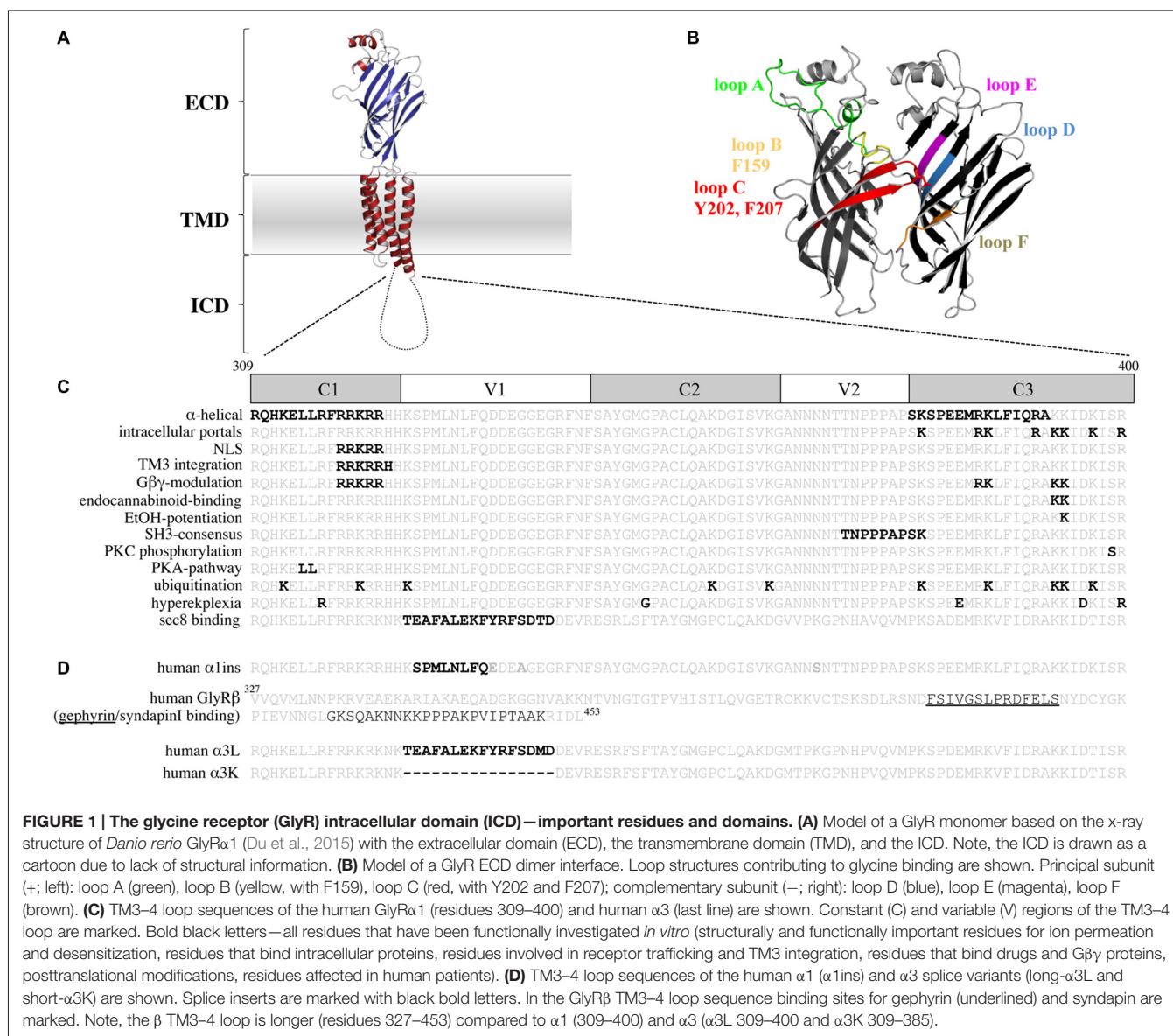


FIGURE 1 | The glycine receptor (GlyR) intracellular domain (ICD)—important residues and domains. (A) Model of a GlyR monomer based on the x-ray structure of *Danio rerio* GlyRα1 (Du et al., 2015) with the extracellular domain (ECD), the transmembrane domain (TMD), and the ICD. Note, the ICD is drawn as a cartoon due to lack of structural information. **(B)** Model of a GlyR ECD dimer interface. Loop structures contributing to glycine binding are shown. Principal subunit (+; left): loop A (green), loop B (yellow, with F159), loop C (red, with Y202 and F207); complementary subunit (−; right): loop D (blue), loop E (magenta), loop F (brown). **(C)** TM3–4 loop sequences of the human GlyRα1 (residues 309–400) and human α3 (last line) are shown. Constant (C) and variable (V) regions of the TM3–4 loop are marked. Bold black letters—all residues that have been functionally investigated *in vitro* (structurally and functionally important residues for ion permeation and desensitization, residues that bind intracellular proteins, residues involved in receptor trafficking and TM3 integration, residues that bind drugs and Gβγ proteins, posttranslational modifications, residues affected in human patients). **(D)** TM3–4 loop sequences of the human α1 (α1ins) and α3 splice variants (long-α3L and short-α3K) are shown. Splice inserts are marked with black bold letters. In the GlyRβ TM3–4 loop sequence binding sites for gephyrin (underlined) and syndapin are marked. Note, the β TM3–4 loop is longer (residues 327–453) compared to α1 (309–400) and α3 (α3L 309–400 and α3K 309–385).

cortex. In summary, these data provide evidence for a link of altered glycinergic inhibition to social and cognitive impairments (Pilorge et al., 2015).

The role of GlyRs detected in non-neuronal tissues, e.g., immune cells, endothelial cells, hepatocytes, renal cells is not completely understood but argues for other functions than a neuronal ion channel (Van den Eynden et al., 2009).

HUMAN AND MURINE MUTATIONS FOUND IN GlyRα1 INTRACELLULAR DOMAIN (ICD)

GlyR mutations can result in the neuromotor disorder hyperekplexia. The most common cause for hyperekplexia are mutations in the *GLRA1* gene which was mapped to the disease in 1993 (Shiang et al., 1993). The second most

common cause for hyperekplexia results from mutations in the *SLC6A5* gene encoding the presynaptic glycine transporter 2 (GlyT2; Rees et al., 2006). Mutant GlyT2 variants represent the presynaptic component of the disease. Rare forms of the disease are generated by mutations in genes encoding other postsynaptic proteins of the inhibitory synapse, e.g., gephyrin and collybistin (CB).

GlyRα1 mutations are distributed over the entire sequence. Among these, most of the dominant inherited mutations are localized in the ion channel domain (TM2) and adjacent loop structures. These mutants are accompanied by functional deficits such as lower maximal currents, reduced single channel conductance, enhanced desensitization or decreased ligand-binding efficacy (Saul et al., 1999; Becker et al., 2008; Chung et al., 2010). In contrast, recessive mutants influence receptor biogenesis, trafficking, and receptor stability (Villmann et al., 2009b; Schaefer et al., 2015).

So far, only five human mutations, R316X, G342S, E375X, D388A, and R392H have been identified in the GlyR α 1 TM3–4 loop (**Figure 1C**). Three of them (R316X, D388A, R392H) are compound heterozygous. Compound heterozygosity refers to two recessive alleles (W68C/R316X, L291P/D388A, and R252H/R392H) that result in hyperekplexia in a heterozygous state (Vergouwe et al., 1999; Rees et al., 2001; Tsai et al., 2004; Chung et al., 2010; Bode and Lynch, 2013). *In vitro* studies on R392H revealed decreased inward currents, reduced expression and less stability as the underlying pathological mechanism. These effects were more pronounced when R392H was coexpressed with R252H. Receptors composed of R252H and R392H were non-functional, arguing for a dominant effect of R252H localized in close proximity to the ion channel pore (Villmann et al., 2009b).

GlyR α 1 variants R316X and E375X lead to truncated α 1 subunits. Truncations of receptor proteins result in significantly decreased surface expression due to protein misfolding and abnormal receptor trafficking (Villmann et al., 2009a; Kang et al., 2015; Schaefer et al., 2015). As a consequence, insufficient receptor densities lead to deficiency of functional ion channels.

A similar TM3–4 loop truncation of the closely related GABA $_A$ γ 2 subunit is associated with generalized epilepsy with febrile seizures plus (GEFS+; Kang et al., 2015).

An *in vitro* analysis of α 1 E375X revealed no surface expression of the truncated α 1 protein when expressed alone to form homomeric receptor complexes. Coexpression of α 1E375X with wild-type (wt) α 1 or α 1 β led to functional ion channel formation. The observed current amplitudes were smaller and EC₅₀ values were increased for GlyRs formed by α 1wt/ α 1E375X/ β in comparison to homomeric α 1 and heteromeric α 1 β wt (**Figure 2A**). This simulation of the *in vivo* configuration constitutes the potential of E375X to integrate into pentamers, its transport to the cell surface and finally its impact on GlyR function (Bode and Lynch, 2013). Similar effects have been observed for the GlyR α 1 ICD variant D388A. Mutant α 1D388A receptors were only recruited to the cellular membrane in presence of either α 1 or α 1 β wt (Bode et al., 2013).

R316X showed impaired trafficking with a small fraction of mutated GlyRs expressed at the cellular surface but insufficient to generate functional ion channels (Schaefer et al., 2015).

A TM3–4 loop truncation in the mouse mutant *oscillator* results in absence of truncated protein from the organism. *Oscillator* carries a 7 bp deletion and depending on the use of an alternative splice acceptor site generates two different transcripts although neither is translated into α 1 protein *in vivo* (Kling et al., 1997). Lack of translation of both transcripts induces severe neuromotor deficits in homozygous *oscillator* mice starting at postnatal day 14. These deficits increase progressively until death at postnatal day 21. During this period GlyRs undergo a subunit switch from homomeric α 2 (embryonic isoform) to heteromeric adult GlyRs (α 1 β , α 3 β). Obviously, there is no compensation by other GlyRs to the lack of functional α 1 β receptors in homozygous *oscillator* mice (Buckwalter et al., 1994; Kling et al., 1997). Thus, *oscillator* represents a GlyR NULL mutation.

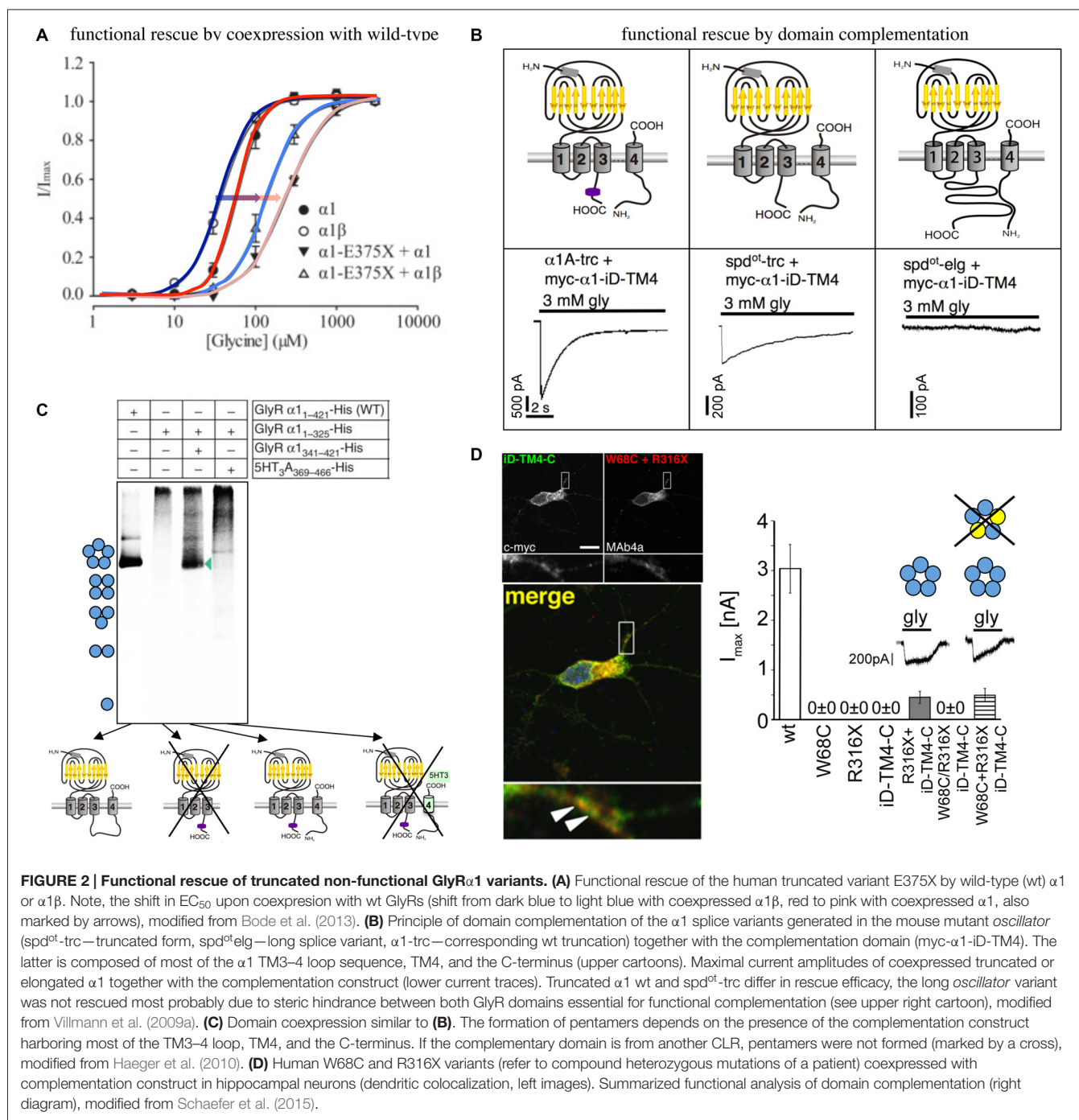
An *in vitro* coexpression of the truncated *oscillator* GlyR α 1 protein (*spd*^{ot}-trc) together with a complementary truncated wild-type α 1 construct (harboring most of the TM3–4 loop sequence, TM4, and the C-terminus = myc- α 1-iD-TM4; **Figure 2B**) restored surface expression of both GlyR domains arguing for lack of precise quality control in the overexpression system (Villmann et al., 2009a). The coexpression of the non-functional truncated GlyR α 1 isoform (*spd*^{ot}-trc) together with the lacking protein portion (myc- α 1-iD-TM4) on a separate plasmid in the same cell regenerated ion channel functionality (GlyR α 1 rescue = functional complementation of an ion channel from for themselves non-functional ion channel domains). These findings suggest that GlyRs are composed of independent folding domains able to interact with each other to complement channel functionality (**Figure 2B**; Villmann et al., 2009a). Using similar GlyR N- and C-terminal domains, it was further shown that non-functionality of truncated GlyRs lacking the TM3–4 loop, TM4 and the C-terminus is due to the inability to form pentameric receptor complexes (**Figure 2C**; Haeger et al., 2010).

How do these independent folding domains interact? An interaction between differently charged residues was analyzed by stepwise truncation of the complementation construct from its N- to the C-terminus. A lack of more than 55 residues from the TM3–4 loop resulted in non-functionality. Interestingly, the coexpression of three GlyR domains regenerated functionality at least to some extent further supporting the finding for independent folding domains of the GlyR (Unterer et al., 2012).

An application of the domain complementation approach to truncated human variants yielded similar results. The human α 1 variant R316X was coexpressed with a corresponding C-terminal complementation construct (iD-TM4-C). The functional restoration of the respective GlyRs achieved 20% of ion channel efficacy compared to the wild-type situation. R316X was identified in a patient concomitant to W68C. The mutant W68C significantly decreased receptor trafficking to the cellular surface. A coexpression of W68C, the complementation construct, and R316X generated functional ion channels indistinguishable from GlyRs lacking W68C (**Figure 2D**). Therefore, it was concluded that the mutant W68C in the extracellular domain (ECD) does not hinder R316X from forward trafficking and integration into the pentameric arrangement (Schaefer et al., 2015).

Hence, GlyRs are able to assemble from independent folding domains and generate functional ion channels. This process does not require the integrity of the GlyR ICD rather subdomain interactions may mediate the efficacy of GlyR ion channel functionality.

In addition to the TM3–4 loop, the ICD also comprises the short intracellular loop connecting TM1 and TM2. The role of the TM1–2 loop in hyperekplexia has been defined by functional studies of the mutant P250T (Saul et al., 1999). Residue P250 is localized in very close proximity to the inner vestibule of the ion channel. The introduction of a threonine at position 250 leads to fast-desensitizing receptors with decreased glycine sensitivity. A mutagenesis series of residue 250 determined side volume and



hydropathy as important mediators in the pathology underlying P250T (Breitinger et al., 2001).

GLYCINE RECEPTOR STRUCTURE

Since 2011, the x-ray structures of several CLR members have been solved. These structures together with electron cryo-microscopy structures revolutionized our current knowledge about conformational rearrangements of the ion channel in the presence of agonists and antagonists leading

to open and closed channel conformations (Unwin, 2005; Hassaine et al., 2014; Miller and Aricescu, 2014; Du et al., 2015). A closer view onto the CLR structure revealed an architecture of two domains: the ECD able to bind the ligand and the transmembrane domain (TMD) encompassing four α -helical transmembrane segments, connected by intra- or extracellular loop structures (Figure 1A). The crystal structures of the large intracellular loops of the GABA_A receptors, the 5HT₃ receptors, and the GlyRs between transmembrane segments 3 and 4 have not been solved yet

most probably due to hindrance of crystal formation when present.

The recently solved structures of GlyR α 1 and GlyR α 3 provided novel insights into GlyR functioning. Conformational rearrangements involve specific loop structures of the ECD as well as the ECD-TMD interface. These rearrangements enable ion channel gating as a consequence of an anti-clockwise outward rotation of TMD during opening of the ion channel pore. A prerequisite for glycinergic signal transduction is agonist-binding to the ligand-binding pocket formed by residues of loops A-F (**Figures 1A,B**). Ligand-binding is stabilized by aromatic residues e.g., F159, Y202, F207 within the pocket. Following binding, the signal is transmitted via extensive interactions near the ECD-TMD interface including the β 1–2 loop, the Cys loop, and the M2–M3 loop at the principal side of the ligand-binding interface with loops β 1–2, β 8–9 and pre-M1/M1 of the complementary side (-) of the pocket (Du et al., 2015). Due to flexibility of loops C and β 8–9, these loop structures initiate the rearrangement of the conformation from the open into the closed form by a backward movement involving the same loop structures and domains (Du et al., 2015). From crystallographic analysis there are so far no hints for an involvement of the intracellular loop between TM3–4 in signal transduction processes due to lack of its presence in constructs used for x-ray crystallography. Voltage-clamp fluorometry experiments however provided evidence for the participation of the TM3–4 loop structure in the rearrangement of M3 and M4 during ion channel opening. In this context it was demonstrated that M3 and M4 undergo large transitions compared to M1 and M2 movements (Han et al., 2013a).

STRUCTURAL DETERMINANTS OF THE GlyR ICD

In contrast to eukaryotic CLRs (nAChRs, GABA_{A/C}Rs, GlyRs, and the 5HT₃ receptors), the prokaryotic CLR-homologs ELIC (*Erwinia chrysanthemi* ligand-gated ion channel) and GLIC (*Gloeobacter violaceus* ligand-gated ion channel) carry very short intracellular loop structures (Hilf and Dutzler, 2008; Nury et al., 2011).

Chimeric CLRs (5HT_{3A}-GLIC, GlyR-GLIC) harboring mainly the short heptapeptide SQPARAA (TM3–4 loop of GLIC) instead of their receptor-specific TM3–4 loop were able to form functional ion channels, which differ in single channel conductances and desensitization compared to wild-type receptors. Their overall properties, such as ion selectivity, efficiency of ligand-binding and current amplitudes were unaffected (Jansen et al., 2008; Papke and Grosman, 2014; Moraga-Cid et al., 2015). Thus, the amino acid sequence of the TM3–4 loop determines subclass-specific ion channel properties. All studies concerning chimeric receptors have been performed in overexpression systems *in vitro* leaving the question for an *in vivo* effect of chimeric proteins unanswered.

Our structural knowledge of the TM3–4 loop is limited to small segments close to TM3 and TM4. The rest of the TM3–4 loop seems to be disordered (Unwin, 2005). The C-terminal end

of the TM3–4 loop of cation-selective CLRs forms an α -helical domain, called the MA stretch (membrane-associated stretch; Unwin, 2005; Hassaine et al., 2014). A large content of charged residues within the MA stretch face a lateral tunnel or portal. These portals enable the permeation of the incoming ions and influence ion channel conductance of the appropriate channel (Kelley et al., 2003).

The structure of the serotonin receptor provided some hints that there is a second α -helical stretch at the beginning of the TM3–4 loop (**Figures 1C, 3A**). The formation of intracellular portals is allocated by the C-terminal MA-stretch and obstructed by the N-terminal helix called MX-helix in a presumably closed channel conformation (Hassaine et al., 2014). The existence of such portals in GlyRs has been proposed due to sequence homology (Carland et al., 2009). Mutations of eight basic residues within the supposed glycinergic portals resulted in non-functional receptors. Moreover, quadruple mutations of positively charged residues (α 1^{R377A/K378A/K385A/K386A} and α 1^{R377E/K378E/K385E/K386E}) reduced ion channel conductance at negative membrane potentials (**Figure 3**). Therefore, these portals are indeed features of an extended glycine receptor permeation pathway (**Figures 1C, 3A,B**). The positive charges surrounding the intracellular portals are assumed to electrostatically attract incoming anions to the intracellular compartment (Carland et al., 2009). CD spectroscopy further revealed the existence of α -helical elements close to TM3 and TM4 in GlyR α 1 (Burgos et al., 2015).

The TM3–4 sequence of GlyRs can be subdivided into variable and conserved regions (Melzer et al., 2010; **Figure 1C**). Basic stretches are highly conserved among various GlyRs. Two other motifs have been determined to the variable region, a poly “NNNN” motif and a proline-rich stretch present in α and β subunits. The role of the asparagine-rich subdomain is completely unsolved.

The existence of a poly-proline helix type II (PPII) within the TM3–4 loop of the GlyR formed by the poly-proline stretch has been proposed by CD-spectroscopy (Cascio et al., 2001; Breiteringer et al., 2004). PPII helices are helical secondary structures with a perfect 3-fold rotation symmetry forming SH3 consensus sequences (*SRC homology 3 domain consensus sequences*, Rath et al., 2005). The recognition motif for the PPII helix xxPxxP is highly conserved among all GlyR subunits and is involved in binding of intracellular partners to the GlyR β loop (**Figure 1D**; Koch et al., 2011; Del Pino et al., 2014). Syndapin was identified as a binding partner of the ³⁸⁴KxxPxxPxxP³⁹⁴ motif in GlyR β . The interaction between syndapin I and GlyR β was greatly diminished when the second proline was exchanged by another residue (Del Pino et al., 2014). A miRNA knockdown of syndapin I in cultured primary spinal cord neurons assigned syndapin I as a mediator in GlyR trafficking or even anchoring (Del Pino et al., 2014). The latter needs further investigations to be proven.

Neurologin 2 or the GABA_A receptors α 2 harbor proline-rich sequences similar to the ³⁶⁵PPPAP³⁶⁹ motif in GlyR α 1 and ³⁸⁵PPPAKP³⁹⁰ GlyR β subunits. The interactions of these proline-rich stretches of neurologin 2 or GABA_A α 2 with the SH3 domain of CB underlie a novel regulatory mechanism for

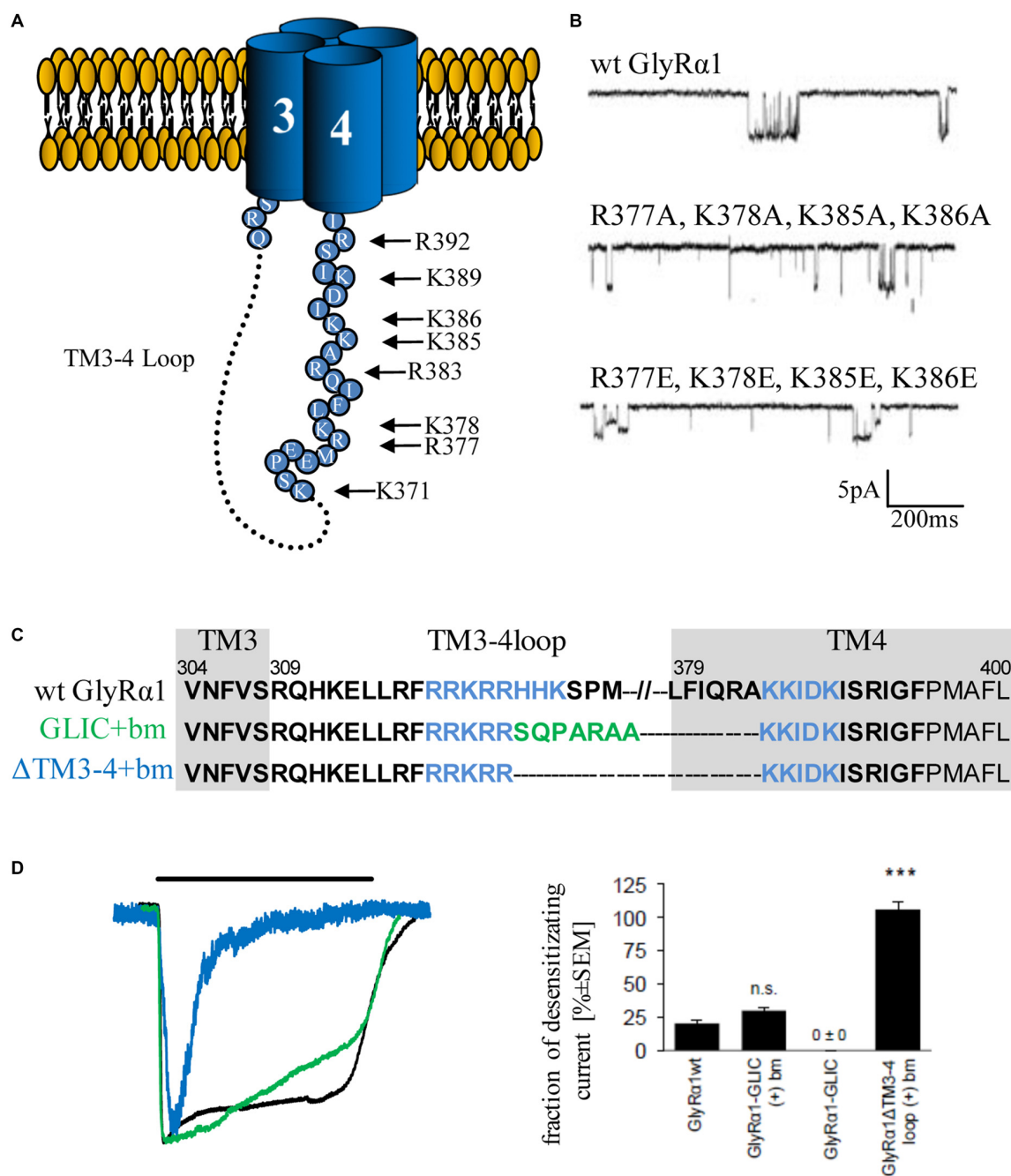


FIGURE 3 | Single channel conductance and desensitization are determined by intracellular portals and TM3–4 loop length. (A) Model of intracellular portals formed by positively charged residues within the membrane-associated (MA) stretch of the TM3–4 loop of the GlyRα1 (modified from Carland et al., 2009). **(B)** Mutations of portal forming residues (quadruple mutations α1^{R377A/K378A/K385A/K386A} and α1^{R377E/K378E/K385E/K386E} have been investigated in comparison to wt) result in reduction of single channel conductance (Carland et al., 2009). **(C)** Truncated GlyRα1 used to investigate the influence of the loop length on receptor desensitization (Langlhofer et al., 2015). The sequence between the basic motifs (blue, bm) has been deleted (ΔTM3–4(+bm)) and replaced by the short *Gloeobacter violaceus* ligand-gated ion channel (GLIC) loop SQPARAA (green, GLIC(+bm)). **(D)** The connection of both basic motifs (blue) resulted in very fast desensitizing GlyRs compared to wt (black). Insertion of the GLIC-loop between the basic motifs had no influence on desensitization (modified from Langlhofer et al., 2015). n.s., not significant. Level of significance, *** $p < 0.001$.

formation and function of inhibitory postsynapses (Soykan et al., 2014). CB has, however, never been shown to directly interact with GlyRs.

A further intracellular protein interaction has been attributed to the 15 residues splice cassette of GlyRα3L in the TM3–4 loop. GlyRα3L binding to the vesicular trafficking protein Sec8 targets

GlyR α 3L to presynaptic sites. Colocalization with the vesicular presynaptic marker VGLUT1 confirmed axonal trafficking of GlyR α 3L towards presynaptic terminals (Winkelmann et al., 2014).

In conclusion, emerging evidences suggest a so far underestimated role of the GlyR TM3–4 loop in the interaction with other intracellular proteins beside gephyrin connecting the receptor to cytoskeletal elements, regulating receptor trafficking and synaptic localization.

MOTIFS IMPORTANT FOR TRAFFICKING AND MODULATION OF CHANNEL PHYSIOLOGY BY PHARMACOLOGICAL SUBSTANCES

Basic residues ³¹⁶RFRRKRR³²² localized within the proposed MX-helix at the N-terminal portal of the TM3–4 loop determine ion channel properties (Figure 1C). The integrity of this positively charged domain is important for proper membrane integration of the apolar TM3 (Sadler et al., 2003). Neutralization of one or two basic residues resulted in translocation to the endoplasmic reticulum (ER).

Furthermore, some residues of the basic motif (³¹⁸RRKRR³²² in GlyR α 1; ³²⁴RRKRR³²⁸ GlyR α 3) are parts of a nuclear localization signal (NLS). Residues of the NLS interact with karyopherins α 3/ α 4 and are actively involved in the nuclear import of GlyRs (Figure 1C; Melzer et al., 2010). Although, the function of GlyRs within the nucleus is unknown, an important function of nuclear import in non-neuronal tissue (Van den Eynden et al., 2009) and brain tumors has been demonstrated (Förster et al., 2014). In glioma, a knockdown of the NLS-containing GlyR α 1 reduced the self-renewal capacity of glioma formation *in vivo* and therefore impaired tumor progression.

Within the basic stretches, residues ³¹⁶RFRRK³²⁰ and ³⁸⁵KK³⁸⁶ are critical for binding cytosolic G-protein subunits (G β γ ; Yevenes et al., 2006) which in turn enhance the glycine-induced chloride currents *in vitro* (Yevenes et al., 2003). It has been further estimated that the interaction of the sequences ³¹⁶RFRRK³²⁰ and ³⁸⁵KK³⁸⁷ with the G-protein subunit G β γ correlates with an allosteric interaction of the same motifs with ethanol (Yevenes et al., 2010). A peptide composed of the motif ³¹⁶RFRRKRR³²² was able to inhibit binding of G β γ to the GlyR α 1 intracellular loop and thus decreased the positive modulation by ethanol (Figure 1C; San Martin et al., 2012). Further determinants for ethanol binding are localized in TM2, the alternative splicing cassette within the TM3–4 loop of the α 1 subunit and within the short extracellular C-terminus (Sánchez et al., 2015). Directly correlated to these data is knowledge from knock-in mice carrying K385A/K386A substitutions which show a reduced sensitivity for ethanol (Aguayo et al., 2014). K385 also plays an important role in the allosteric modulation by endocannabinoids (Yevenes and Zeilhofer, 2011). Although the GlyR α 3 subunit shares sequence similarities with the GlyR α 1 in terms of basic residues, GlyR α 3 subunits have not been modulated by either ethanol or by G β γ proteins. Using a chimeric approach between α 1 and α 3, it was demonstrated

that the 15 residues alternative splice cassette of α 3 and the C-terminus contains modulatory sites for G β γ interaction in addition to the required, but not sufficient residue G254 (Sánchez et al., 2015).

POSTTRANSLATIONAL MODIFICATIONS—UBIQUITINATION AND PHOSPHORYLATION

Residues within the ICD of GlyRs are modulated by posttranslational modifications. Ubiquitination of postsynaptic proteins marks proteins for proteolytic degradation (Christianson and Green, 2004). Many recessive hyperekplexia mutations cause an accumulation of GlyR protein in the ER and within Golgi compartments and influence ubiquitin-mediated receptor degradation (Villmann et al., 2009b; Schaefer et al., 2015). It is proposed that ubiquitination of the GlyR α 1 subunit takes place at 3 out of 10 lysine residues within the TM3–4 loop triggering receptor internalization and proteolytic degradation (Figure 1C). Proteolytic cleavage of the full-length GlyRs generates two fragments of 13 kD and 35 kD (Buttner et al., 2001). These two fragments have never been observed at the cellular surface. Processing of GlyR receptors is therefore a downstream process of ubiquitination within the endocytic degradation pathway.

GlyR subtypes are phosphorylated by protein kinases A and C (PKA and PKC; Figure 1C). Both kinases influence the maximal chloride influx and desensitization (Vaello et al., 1994; Gentet and Clements, 2002). Residue S391 within the TM3–4 loop of GlyR α 1 was identified as a PKC-binding site (Ruiz-Gómez et al., 1991). Phosphorylated α 1 receptors regulate channel activity and modulate the interaction with other intracellular proteins (Changeux et al., 1984). A stimulation of PKC by phorbol 12-myristate (PMA) led to an enhanced GlyR internalization rate via endocytosis. Mutation of a di-leucine motif (L314/L315) within the TM3–4 loop prevented the PMA-stimulated receptor endocytosis (Huang et al., 2007). Phosphorylation of S403 of the GlyR β subunit reduces the affinity between the GlyR β TM3–4 loop and gephyrin resulting in enhanced lateral diffusion of GlyRs and less synaptic GlyR levels (Specht et al., 2011).

Phosphorylation of the GlyR α 3 subunit plays an important role in pain sensitization processes. PGE2 inhibits glycinergic neurotransmission via a PKA-dependent pathway (Harvey et al., 2004). The sequence Arg-Glu-Ser-Arg in the TM3–4 loop of GlyR α 3 represents a strong consensus sequence for PKA. PGE2 receptors activate PKA, which in turn enhances the fraction of phosphorylated GlyR α 3 via residue S346 within the PKA consensus sequence. A decrease in glycinergic signal transduction is a consequence of increased internalization of phosphorylated GlyR α 3. Residue S346 is not conserved in α 1 and therefore α 1 lacks modulation by PKA (Harvey et al., 2004). This study clearly showed the unique role of phosphorylated GlyR α 3 in spinal nociceptive processes, whereas phosphorylation of GlyR α 1 controls spinal motor circuits.

Furthermore, evidence of conformational GlyR modulation by phosphorylation have been obtained in a combined

approach of voltage clamp fluorometry and pharmacological measurements. The GlyR α 3 S346 mutant was unable to induce conformational changes in the extracellular ligand-binding site compared with wild-type α 3. These data showed for the first time that phosphorylation encompasses structural changes in the TM3–4 loop that propagate towards the ECD of the receptor (Han et al., 2013b).

SUMOylation is another type of posttranslational modification influencing receptor endocytosis and ion channel function. Although direct SUMOylation of GlyRs has never been shown, SUMOylation of kainate receptors indirectly influences GlyR endocytosis (Konopacki et al., 2011; Chamberlain et al., 2012). Recently, another kainate-induced mechanism for GlyR endocytosis has been resolved. This process involves a calcium-dependent de-SUMOylation of PKC. Activation of PKC by de-SUMOylation reduced GlyR-mediated synaptic activity concomitant to GlyR endocytosis (Sun et al., 2014). This crosstalk between excitatory and inhibitory receptors may serve to maintain the excitatory–inhibitory balance in the CNS.

ICD INTERACTION WITH SCAFFOLD PROTEINS ENABLES INHIBITORY SYNAPSE FORMATION

The best analyzed interaction between the GlyR and an intracellular binding partner is the interaction of the GlyR β subunit with the scaffold protein gephyrin. This direct interaction involves GlyR β residues 398–410 (Kim et al., 2006).

Gephyrin itself is a cytoplasmic protein, which consists of N-terminal G domains and C-terminal E domains (homologous to *E. coli* proteins MogA and MoeA—molybdenum cofactor biosynthetic proteins, Schwarz et al., 2001) connected by a central linker region. These domains form a hexagonal structure built up by G domain trimers and E domain dimers (Saiyed et al., 2007) anchoring GlyRs at the postsynaptic membrane (Kneussel and Betz, 2000). The binding motifs of the gephyrin E domain to GABA_A receptors (Maric et al., 2014) and the GlyR β TM3–4 loop sequence ³⁹⁸FSIVGSLPRDFELS⁴¹¹ (Figure 1D) have been identified (Meyer et al., 1995). Besides its role as an anchoring protein, gephyrin undergoes interactions with polymerizing tubulin (Kirsch et al., 1991) as well as the microtubuli-associated motor proteins KIF5 and dlc1/2. These interactions are involved in anterograde and retrograde transport mechanisms of GlyRs at inhibitory synapses (Fuhrmann et al., 2002; Maas et al., 2009). Among numerous intracellular proteins bound to gephyrin, the GDP/GTP-exchange factor CB is especially interesting (Kins et al., 2000; Fritschy et al., 2008). Knockout of CB results in a region-specific loss of gephyrin in the hippocampus and gephyrin-binding GABA_A receptor subtypes in the forebrain of knockout mice (Papadopoulos et al., 2007, 2008). Although several attempts have been started to identify novel interaction partners of the GlyR TM3–4 loop using yeast two hybrid screens, mostly gephyrin has been detected due to its high affinity for the GlyR β loop. One might conclude that the affinity between other intracellular binding partners and GlyRs may be

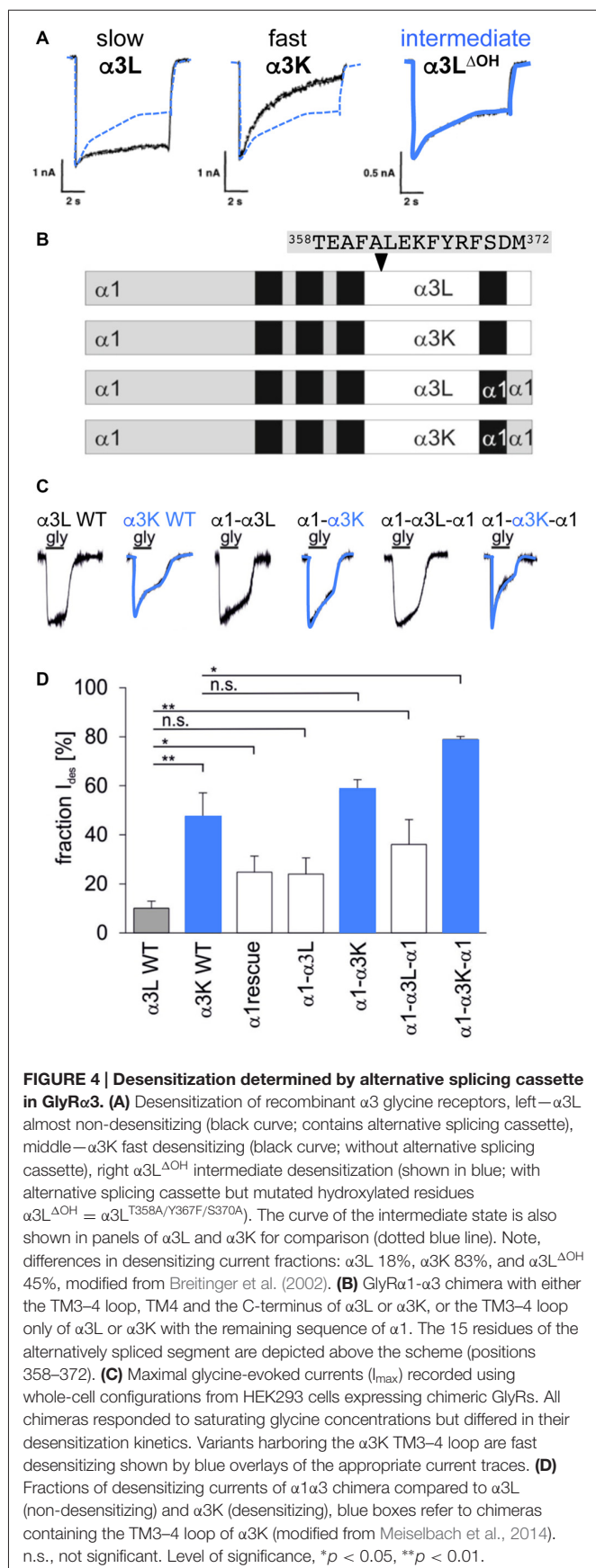
too low with respect to the sensitivity of a yeast two hybrid approach.

Using mass spectrometry, transport proteins Vps35 and neurobeachin (Nbea) and the F-bar protein syndapin I were detected as binding partners of the GlyR β TM3–4 loop (Del Pino et al., 2011, 2014). Syndapines are important for vesicle formation at the cellular membrane, within the trans-Golgi network and the proteasome (Qualmann and Kelly, 2000; Kessels and Qualmann, 2004). Thus, the GlyR β TM3–4 loop acts as an adapter for other intracellular binding partners involved in transport processes of receptor complexes towards the cellular membrane.

DESENSITIZATION

Desensitization is defined as the transition of the agonist-bound open channel into a closed ion channel configuration in the presence of agonist. Wild-type α 1 and α 3 GlyRs show very small portions of desensitizing currents. *In vitro* mutagenesis studies on the TM3–4 loop of various GlyR α subunits revealed single amino acids and grouped residues involved in the desensitization process of GlyR channels (Nikolic et al., 1998; Breitingner et al., 2009; Meiselbach et al., 2014). The human GlyR α 3 carries an alternative-splicing cassette of 15 residues within the TM3–4 loop. The resulting variants α 3L (including the 15 residues) and α 3K (short, lacking the alternative-splicing cassette) differ significantly in their desensitization behavior (Nikolic et al., 1998). These data provided first evidences for the importance of the intracellular TM3–4 loop for ion channel desensitization (Figure 1C). The lack of this alternative-splicing cassette generated fast desensitizing currents in contrast to almost no desensitization observed for the long GlyR α 3 variant (Nikolic et al., 1998). The alternative-splicing cassette of GlyR α 1 subunit does not influence receptor desensitization most probably due to differences in amino acid composition compared to α 3. The α 3 cassette harbors three possible phosphorylation consensus sites. A substitution of residues carrying hydroxyl side chains (α 3L^{ΔOH} = α 3L^{T358A/Y367F/S370A}) within the 15 amino acid insert generated an intermediate state of desensitization between α 3L and α 3K suggesting that hydroxyl groups mediate desensitization processes (Figure 4A; Breitingner et al., 2002). In a follow-up study, the secondary structure analysis of α 3K and α 3L suggested a stabilization of the overall spatial structure of the TM3–4 loop by the α 3 splice cassette (Breitingner et al., 2009). The importance of the alternative-splicing cassette was further supported in an *in vitro* study of α 1 α 3 chimeric proteins. The analysis of α 1 α 3 chimera allocated that desensitization properties are transferable between GlyR subunits (Figures 4B–D; Meiselbach et al., 2014). Chimeras containing the α 3 insert desensitized significantly slower than chimeras lacking the splice cassette.

The TM3–4 loop length differences between prokaryotic and eukaryotic CLRs (Tasneem et al., 2005) posed the following question: Is the TM3–4 loop essential for CLR function? Crystal structures of the prokaryotic channels ELIC and GLIC revealed both the open conformation (GLIC) and the closed channel conformation (Hilf and Dutzler, 2008, 2009;



Bocquet et al., 2009). Although first studies indicated a non-desensitized GLIC in an acidic environment (Bocquet et al., 2007), GLIC desensitization became obvious at a pH lower than 5 (Gonzalez-Gutierrez and Grosman, 2010; Parikh et al., 2011). These data again argue for subtype-specific regulatory elements of desensitization within the CLR superfamily. An exchange of the whole TM3–4 loop of various CLRs (5HT₃ and GABA_C receptor) with the ICD of GLIC (SQPARAA) did not lead to changes in the macroscopic electrophysiological properties of the chimeric ion channels (Jansen et al., 2008; Papke and Grosman, 2014). In a recent study, the full-length loop of GlyRα1 was either replaced completely by the prokaryotic heptapeptide (i), or (ii) basic stretches ³¹⁸RRKRR and ³⁹³KKIDK close to TM3 and 4 have been left intact carrying the heptapeptide in between (GlyRα1-GLIC(+)_{bm}). (iii) A third construct contained a short TM3–4 loop only composed of both basic stretches (GlyRα1-ΔTM3–4(+)_{bm}; Figure 3C). The pure heptapeptide between TM3 and TM4 resulted in intracellular aggregation, lack of surface receptors and non-functionality. Constructs GlyRα1-GLIC(+)_{bm} (ii) and GlyRα1-ΔTM3–4(+)_{bm} (iii) were able to form functional ion channels that differed significantly in their desensitization behavior. The presence of both basic stretches resulted in a fast transition of GlyRα1 channels into a closed conformation. The insertion of SQPARAA between both basic motifs (GlyRα1-GLIC(+)_{bm}) decreased the desensitizing current significantly in comparison to wild-type GlyRα1 (Figure 3D). Thus, the sequence between both basic stretches determines the desensitization behavior of GlyRα1 (Langlhofer et al., 2015). The introduction of the prokaryotic heptapeptide at another position within the GlyRα1 TM3–4 loop between residues Q310 and K385 depicted also differences on the fraction of desensitizing currents (Papke and Grosman, 2014). The common conclusion from studies concerning the length of TM3–4 loop and the determination of desensitization rates revealed that separation of both basic stretches at the N- and C-terminal end of the TM3–4 loop represent a critical determinant of ion channel functionality.

To complete the knowledge on desensitization determined by the GlyR ICD, the human mutation P250T needs to be mentioned. This mutant localized in the M1-M2 loop is associated with very fast desensitization. The original proline introduces conformational rigidity to the short M1-M2 linker. The given higher flexibility by the introduced threonine allows TM2 rearrangements resulting in fast ion channel closure. Thus, fast desensitization underlies the pathology of patients carrying P250T and in turn contributes to enhanced muscle tone delineating a major clinical feature in startle disease patients (Saul et al., 1999; Breiting et al., 2001). Further support for a key role of the M1-M2 loop in desensitization derives from a recent study on the identification of the desensitization gate in CLRs. The TM1–2 loop interacts with the internal end of TM3 determining the desensitization gate. An exchange of GlyR residues with residues from the GABA_C ρ1 subunit elicited the intracellular end of TM3 as the key component for desensitization (Gielen et al., 2015). Further hints for an association of enhanced desensitization and disease were given by studies of the nAChR. The enhanced desensitization of presynaptic nAChRs

at GABAergic terminals generates lower inhibitory input at dopaminergic neurons and concomitantly enhanced activity of the dopaminergic rewards system (Mansvelder et al., 2002). An enhanced desensitization rate of nAChRs has also been described to underlie a special form of frontal lobe epilepsy (Bertrand et al., 2002).

CONCLUSIONS AND OUTLOOK

The ICD of the glycine receptor harbors subdomains important for trafficking and functionality of the inhibitory GlyR. Basic residues are crucial determinants in both processes. Since trafficking is a prerequisite for functional modulation, the basic domains represent key regulators of this receptor family. This is further supported by their involvement in binding of G $\beta\gamma$ proteins and ethanol.

Studies on chimeric proteins have helped us to understand the functional role of the TM3–4 loop. Lack of this large intracellular loop does not lead to non-function, rather to a disruption of ion channel modulation. Except for the cytoplasmic portals that

are proposed to resemble an α -helical structure, the TM3–4 loop is suggested to be unfolded. Unfolding might represent an advantage for the interaction with intracellular proteins important for regulation of receptor recruitment to synaptic sites, ion channel function, and finally degradation initiation. Further research is required to enhance our knowledge on other so far non-identified interactions partners modulating synaptic strength and fine-tuning of GlyR function depending on the surrounding neuronal network.

AUTHOR CONTRIBUTIONS

GL and CV wrote the manuscript.

ACKNOWLEDGMENTS

This work was supported by the Deutsche Forschungsgemeinschaft (DFG VI586 to CV) and the Bayerische Forschungsförderung. GL was further supported by the Graduate School of Life Science Würzburg.

REFERENCES

- Aguayo, L. G., Castro, P., Mariqueo, T., Muñoz, B., Xiong, W., Zhang, L., et al. (2014). Altered sedative effects of ethanol in mice with $\alpha 1$ glycine receptor subunits that are insensitive to G $\beta\gamma$ modulation. *Neuropsychopharmacology* 39, 2538–2548. doi: 10.1038/npp.2014.100
- Aroeira, R. I., Ribeiro, J. A., Sebastião, A. M., and Valente, C. A. (2011). Age-related changes of glycine receptor at the rat hippocampus: from the embryo to the adult. *J. Neurochem.* 118, 339–353. doi: 10.1111/j.1471-4159.2011.07197.x
- Becker, K., Breiting, H. G., Humeny, A., Meinck, H. M., Dietz, B., Aksu, F., et al. (2008). The novel hyperekplexia allele GLRA1(S267N) affects the ethanol site of the glycine receptor. *Eur. J. Hum. Genet.* 16, 223–228. doi: 10.1038/sj.ejhg.5201958
- Bertrand, D., Picard, F., Le Hellard, S., Weiland, S., Favre, I., Phillips, H., et al. (2002). How mutations in the nAChRs can cause ADNFLE epilepsy. *Epilepsia* 43, 112–122. doi: 10.1046/j.1528-1157.43.s.5.16.x
- Bocquet, N., Nury, H., Baaden, M., Le Poupon, C., Changeux, J. P., Delarue, M., et al. (2009). X-ray structure of a pentameric ligand-gated ion channel in an apparently open conformation. *Nature* 457, 111–114. doi: 10.1038/nature07462
- Bocquet, N., Prado De Carvalho, L., Cartaud, J., Neyton, J., Le Poupon, C., Taly, A., et al. (2007). A prokaryotic proton-gated ion channel from the nicotinic acetylcholine receptor family. *Nature* 445, 116–119. doi: 10.1038/nature05371
- Bode, A., and Lynch, J. W. (2013). Analysis of hyperekplexia mutations identifies transmembrane domain rearrangements that mediate glycine receptor activation. *J. Biol. Chem.* 288, 33760–33771. doi: 10.1074/jbc.M113.513804
- Bode, A., and Lynch, J. W. (2014). The impact of human hyperekplexia mutations on glycine receptor structure and function. *Mol. Brain* 7:2. doi: 10.1186/1756-6606-7-2
- Bode, A., Wood, S. E., Mullins, J. G., Keramidas, A., Cushion, T. D., Thomas, R. H., et al. (2013). New hyperekplexia mutations provide insight into glycine receptor assembly, trafficking and activation mechanisms. *J. Biol. Chem.* 288, 33745–33759. doi: 10.1074/jbc.M113.509240
- Breiting, U., Breiting, H. G., Bauer, F., Fahmy, K., Glockenhammer, D., and Becker, C. M. (2004). Conserved high affinity ligand binding and membrane association in the native and refolded extracellular domain of the human glycine receptor $\alpha 1$ -subunit. *J. Biol. Chem.* 279, 1627–1636. doi: 10.1074/jbc.M303811200
- Breiting, H. G., Villmann, C., Becker, K., and Becker, C. M. (2001). Opposing effects of molecular volume and charge at the hyperekplexia site $\alpha 1$ (P250) govern glycine receptor activation and desensitization. *J. Biol. Chem.* 276, 29657–29663. doi: 10.1074/jbc.M100446200
- Breiting, H. G., Villmann, C., Melzer, N., Rennert, J., Breiting, U., Schwarzing, S., et al. (2009). Novel regulatory site within the TM3–4 loop of human recombinant $\alpha 3$ glycine receptors determines channel gating and domain structure. *J. Biol. Chem.* 284, 28624–28633. doi: 10.1074/jbc.M109.043174
- Breiting, H. G., Villmann, C., Rennert, J., Ballhausen, D., and Becker, C. M. (2002). Hydroxylated residues influence desensitization behaviour of recombinant $\alpha 3$ glycine receptor channels. *J. Neurochem.* 83, 30–36. doi: 10.1046/j.1471-4159.2002.01109.x
- Buckwalter, M. S., Cook, S. A., Davisson, M. T., White, W. F., and Camper, S. A. (1994). A frameshift mutation in the mouse $\alpha 1$ glycine receptor gene (Gla1) results in progressive neurological symptoms and juvenile death. *Hum. Mol. Genet.* 3, 2025–2030. doi: 10.1093/hmg/3.11.2025
- Burgos, C. F., Castro, P. A., Mariqueo, T., Bunster, M., Guzmán, L., and Aguayo, L. G. (2015). Evidence for α -helices in the large intracellular domain mediating modulation of the $\alpha 1$ -glycine receptor by ethanol and G $\beta\gamma$. *J. Pharmacol. Exp. Ther.* 352, 148–155. doi: 10.1124/jpet.114.217976
- Buttner, C., Sadler, S., Leyendecker, A., Laube, B., Griffin, N., Betz, H., et al. (2001). Ubiquitination precedes internalization and proteolytic cleavage of plasma membrane-bound glycine receptors. *J. Biol. Chem.* 276, 42978–42985. doi: 10.1074/jbc.M102121200
- Carland, J. E., Cooper, M. A., Sugiharto, S., Jeong, H. J., Lewis, T. M., Barry, P. H., et al. (2009). Characterization of the effects of charged residues in the intracellular loop on ion permeation in $\alpha 1$ glycine receptor channels. *J. Biol. Chem.* 284, 2023–2030. doi: 10.1074/jbc.M806618200
- Cascio, M., Shenkel, S., Grodzicki, R. L., Sigworth, F. J., and Fox, R. O. (2001). Functional reconstitution and characterization of recombinant human $\alpha 1$ -glycine receptors. *J. Biol. Chem.* 276, 20981–20988. doi: 10.1074/jbc.M010968200
- Chamberlain, S. E., González-González, I. M., Wilkinson, K. A., Konopacki, F. A., Kantamneni, S., Henley, J. M., et al. (2012). SUMOylation and phosphorylation of GluK2 regulate kainate receptor trafficking and synaptic plasticity. *Nat. Neurosci.* 15, 845–852. doi: 10.1038/nn.3089
- Changeux, J. P., Devillers-Thiéry, A., and Chemouilli, P. (1984). Acetylcholine receptor: an allosteric protein. *Science* 225, 1335–1345. doi: 10.1126/science.6382611
- Christianson, J. C., and Green, W. N. (2004). Regulation of nicotinic receptor expression by the ubiquitin-proteasome system. *EMBO J.* 23, 4156–4165. doi: 10.1038/sj.emboj.7600436

- Chung, S. K., Vanbellinghen, J. F., Mullins, J. G., Robinson, A., Hantke, J., Hammond, C. L., et al. (2010). Pathophysiological mechanisms of dominant and recessive GLRA1 mutations in hyperekplexia. *J. Neurosci.* 30, 9612–9620. doi: 10.1523/JNEUROSCI.1763-10.2010
- Del Pino, I., Koch, D., Schemm, R., Qualmann, B., Betz, H., and Paarmann, I. (2014). Proteomic analysis of glycine receptor β subunit (GlyR β)-interacting proteins: evidence for syndapin I regulating synaptic glycine receptors. *J. Biol. Chem.* 289, 11396–11409. doi: 10.1074/jbc.M113.504860
- Del Pino, I., Paarmann, I., Karas, M., Kilimann, M. W., and Betz, H. (2011). The trafficking proteins vacuolar protein sorting 35 and neurobeachin interact with the glycine receptor β -subunit. *Biochem. Biophys. Res. Commun.* 412, 435–440. doi: 10.1016/j.bbrc.2011.07.110
- Glugaiczky, J., Singer, W., Schick, B., Iro, H., Becker, K., Becker, C. M., et al. (2008). Expression of glycine receptors and gephyrin in the rat cochlea. *Histochem. Cell Biol.* 129, 513–523. doi: 10.1007/s00418-008-0387-x
- Du, J., Lu, W., Wu, S., Cheng, Y., and Gouaux, E. (2015). Glycine receptor mechanism elucidated by electron cryo-microscopy. *Nature* 526, 224–229. doi: 10.1038/nature14853
- Eichler, S. A., Förster, B., Smolinsky, B., Jüttner, R., Lehmann, T. N., Fähring, M., et al. (2009). Splice-specific roles of glycine receptor $\alpha 3$ in the hippocampus. *Eur. J. Neurosci.* 30, 1077–1091. doi: 10.1111/j.1460-9568.2009.06903.x
- Eichler, S. A., Kirischuk, S., Jüttner, R., Schaefermeier, P. K., Legendre, P., Lehmann, T. N., et al. (2008). Glycinergic tonic inhibition of hippocampal neurons with depolarizing GABAergic transmission elicits histopathological signs of temporal lobe epilepsy. *J. Cell. Mol. Med.* 12, 2848–2866. doi: 10.1111/j.1582-4934.2008.00357.x
- Förster, B., Dzaye, O. D., Winkelmann, A., Semtner, M., Benedetti, B., Markovic, D. S., et al. (2014). Intracellular glycine receptor function facilitates glioma formation *in vivo*. *J. Cell Sci.* 127, 3687–3698. doi: 10.1242/jcs.146662
- Fritschy, J. M., Harvey, R. J., and Schwarz, G. (2008). Gephyrin: where do we stand, where do we go? *Trends Neurosci.* 31, 257–264. doi: 10.1016/j.tins.2008.02.006
- Fuhrmann, J. C., Kins, S., Rostaing, P., El Far, O., Kirsch, J., Sheng, M., et al. (2002). Gephyrin interacts with Dynein light chains 1 and 2, components of motor protein complexes. *J. Neurosci.* 22, 5393–5402.
- Gentet, L. J., and Clements, J. D. (2002). Binding site stoichiometry and the effects of phosphorylation on human $\alpha 1$ homomeric glycine receptors. *J. Physiol.* 544, 97–106. doi: 10.1113/jphysiol.2001.015321
- Gielen, M., Thomas, P., and Smart, T. G. (2015). The desensitization gate of inhibitory Cys-loop receptors. *Nat. Commun.* 6:6829. doi: 10.1038/ncomms7829
- Gonzalez-Gutierrez, G., and Grosman, C. (2010). Bridging the gap between structural models of nicotinic receptor superfamily ion channels and their corresponding functional states. *J. Mol. Biol.* 403, 693–705. doi: 10.1016/j.jmb.2010.09.026
- Goyal, R., Salahudeen, A. A., and Jansen, M. (2011). Engineering a prokaryotic Cys-loop receptor with a third functional domain. *J. Biol. Chem.* 286, 34635–34642. doi: 10.1074/jbc.M111.269647
- Grudzinska, J., Schemm, R., Haeger, S., Nicke, A., Schmalzing, G., Betz, H., et al. (2005). The β subunit determines the ligand binding properties of synaptic glycine receptors. *Neuron* 45, 727–739. doi: 10.1016/j.neuron.2005.01.028
- Haeger, S., Kuzmin, D., Detro-Dassen, S., Lang, N., Kilb, M., Tsetlin, V., et al. (2010). An intramembrane aromatic network determines pentameric assembly of Cys-loop receptors. *Nat. Struct. Mol. Biol.* 17, 90–98. doi: 10.1038/nsmb.1721
- Han, L., Talwar, S., and Lynch, J. W. (2013a). The relative orientation of the TM3 and TM4 domains varies between $\alpha 1$ and $\alpha 3$ glycine receptors. *ACS Chem. Neurosci.* 4, 248–254. doi: 10.1021/cn300177g
- Han, L., Talwar, S., Wang, Q., Shan, Q., and Lynch, J. W. (2013b). Phosphorylation of $\alpha 3$ glycine receptors induces a conformational change in the glycine-binding site. *ACS Chem. Neurosci.* 4, 1361–1370. doi: 10.1021/cn400097j
- Harvey, R. J., Depner, U. B., Wässle, H., Ahmadi, S., Heindl, C., Reinold, H., et al. (2004). GlyR $\alpha 3$: an essential target for spinal PGE2-mediated inflammatory pain sensitization. *Science* 304, 884–887. doi: 10.1126/science.1094925
- Hassaine, G., Deluz, C., Grasso, L., Wyss, R., Tol, M. B., Hovius, R., et al. (2014). X-ray structure of the mouse serotonin 5-HT3 receptor. *Nature* 512, 276–281. doi: 10.1038/nature13552
- Heinze, L., Harvey, R. J., Haverkamp, S., and Wässle, H. (2007). Diversity of glycine receptors in the mouse retina: localization of the $\alpha 4$ subunit. *J. Comp. Neurol.* 500, 693–707. doi: 10.1002/cne.21201
- Hilf, R. J., and Dutzler, R. (2008). X-ray structure of a prokaryotic pentameric ligand-gated ion channel. *Nature* 452, 375–379. doi: 10.1038/nature06717
- Hilf, R. J., and Dutzler, R. (2009). Structure of a potentially open state of a proton-activated pentameric ligand-gated ion channel. *Nature* 457, 115–118. doi: 10.1038/nature07461
- Hirata, H., Ogino, K., Yamada, K., Leacock, S., and Harvey, R. J. (2013). Defective escape behavior in DEAH-box RNA helicase mutants improved by restoring glycine receptor expression. *J. Neurosci.* 33, 14638–14644. doi: 10.1523/JNEUROSCI.1157-13.2013
- Huang, X., Chen, H., Michelsen, K., Schneider, S., and Shaffer, P. L. (2015). Crystal structure of human glycine receptor- $\alpha 3$ bound to antagonist strychnine. *Nature* 526, 277–280. doi: 10.1038/nature14972
- Huang, R., He, S., Chen, Z., Dillon, G. H., and Leidenheimer, N. J. (2007). Mechanisms of homomeric $\alpha 1$ glycine receptor endocytosis. *Biochemistry* 46, 11484–11493. doi: 10.1021/bi701093j
- Janczewski, W. A., Tashima, A., Hsu, P., Cui, Y., and Feldman, J. L. (2013). Role of inhibition in respiratory pattern generation. *J. Neurosci.* 33, 5454–5465. doi: 10.1523/JNEUROSCI.1595-12.2013
- Jansen, M., Bali, M., and Akabas, M. H. (2008). Modular design of Cys-loop ligand-gated ion channels: functional 5-HT3 and GABA $\rho 1$ receptors lacking the large cytoplasmic M3M4 loop. *J. Gen. Physiol.* 131, 137–146. doi: 10.1085/jgp.200709896
- Kang, J. Q., Shen, W., Zhou, C., Xu, D., and Macdonald, R. L. (2015). The human epilepsy mutation GABRG2(Q390X) causes chronic subunit accumulation and neurodegeneration. *Nat. Neurosci.* 18, 988–996. doi: 10.1038/nn.4024
- Kelley, S. P., Dunlop, J. L., Kirkness, E. F., Lambert, J. J., and Peters, J. A. (2003). A cytoplasmic region determines single-channel conductance in 5-HT3 receptors. *Nature* 424, 321–324. doi: 10.1038/nature01788
- Kessels, M. M., and Qualmann, B. (2004). The syndapin protein family: linking membrane trafficking with the cytoskeleton. *J. Cell Sci.* 117, 3077–3086. doi: 10.1242/jcs.01290
- Kim, E. Y., Schrader, N., Smolinsky, B., Bedet, C., Vannier, C., Schwarz, G., et al. (2006). Deciphering the structural framework of glycine receptor anchoring by gephyrin. *EMBO J.* 25, 1385–1395. doi: 10.1038/sj.emboj.7601029
- Kins, S., Betz, H., and Kirsch, J. (2000). Collybistin, a newly identified brain-specific GEF, induces submembrane clustering of gephyrin. *Nat. Neurosci.* 3, 22–29. doi: 10.1038/71096
- Kirsch, J., and Betz, H. (1995). The postsynaptic localization of the glycine receptor-associated protein gephyrin is regulated by the cytoskeleton. *J. Neurosci.* 15, 4148–4156.
- Kirsch, J., Langosch, D., Prior, P., Littauer, U. Z., Schmitt, B., and Betz, H. (1991). The 93-kDa glycine receptor-associated protein binds to tubulin. *J. Biol. Chem.* 266, 22242–22245.
- Kling, C., Koch, M., Saul, B., and Becker, C. M. (1997). The frameshift mutation oscillator (Gla1(sp-dt)) produces a complete loss of glycine receptor $\alpha 1$ -polypeptide in mouse central nervous system. *Neuroscience* 78, 411–417. doi: 10.1016/s0306-4522(96)00567-2
- Kneussel, M., and Betz, H. (2000). Clustering of inhibitory neurotransmitter receptors at developing postsynaptic sites: the membrane activation model. *Trends Neurosci.* 23, 429–435. doi: 10.1016/s0166-2236(00)01627-1
- Koch, D., Spiwoke-Becker, I., Sabanov, V., Sinning, A., Dugladze, T., Stellmacher, A., et al. (2011). Proper synaptic vesicle formation and neuronal network activity critically rely on syndapin I. *EMBO J.* 30, 4955–4969. doi: 10.1038/emboj.2011.339
- Konopacki, F. A., Jaafari, N., Rocca, D. L., Wilkinson, K. A., Chamberlain, S., Rubin, P., et al. (2011). Agonist-induced PKC phosphorylation regulates GluK2 SUMOylation and kainate receptor endocytosis. *Proc. Natl. Acad. Sci. U S A* 108, 19772–19777. doi: 10.1073/pnas.1111575108
- Kuhse, J., Kuryatov, A., Maulet, Y., Malosio, M. L., Schmieden, V., and Betz, H. (1991). Alternative splicing generates two isoforms of the $\alpha 2$ subunit of the inhibitory glycine receptor. *FEBS Lett.* 283, 73–77. doi: 10.1016/0014-5793(91)80557-j
- Langlhofer, G., Janzen, D., Meiselbach, H., and Villmann, C. (2015). Length of the TM3–4 loop of the glycine receptor modulates receptor desensitization. *Neurosci. Lett.* 600, 176–181. doi: 10.1016/j.neulet.2015.06.017

- Lynch, J. W. (2004). Molecular structure and function of the glycine receptor chloride channel. *Physiol. Rev.* 84, 1051–1095. doi: 10.1152/physrev.00042.2003
- Lynch, J. W. (2009). Native glycine receptor subtypes and their physiological roles. *Neuropharmacology* 56, 303–309. doi: 10.1016/j.neuropharm.2008.07.034
- Lynch, J. W., and Callister, R. J. (2006). Glycine receptors: a new therapeutic target in pain pathways. *Curr. Opin. Investig. Drugs* 7, 48–53.
- Maas, C., Belgardt, D., Lee, H. K., Heisler, F. F., Lappe-Siefke, C., Magiera, M. M., et al. (2009). Synaptic activation modifies microtubules underlying transport of postsynaptic cargo. *Proc. Natl. Acad. Sci. U S A* 106, 8731–8736. doi: 10.1073/pnas.0812391106
- Malosio, M. L., Grenningloh, G., Kuhse, J., Schmieden, V., Schmitt, B., Prior, P., et al. (1991). Alternative splicing generates two variants of the $\alpha 1$ subunit of the inhibitory glycine receptor. *J. Biol. Chem.* 266, 2048–2053.
- Mansvelder, H. D., Keath, J. R., and McGehee, D. S. (2002). Synaptic mechanisms underlie nicotine-induced excitability of brain reward areas. *Neuron* 33, 905–919. doi: 10.1016/S0896-6273(02)00625-6
- Maric, H. M., Kasaragod, V. B., Hausrat, T. J., Kneussel, M., Tretter, V., Stromgaard, K., et al. (2014). Molecular basis of the alternative recruitment of GABA_A versus glycine receptors through gephyrin. *Nat. Commun.* 5:5767. doi: 10.1038/ncomms5767
- Markstahler, U., Kremer, E., Kimmina, S., Becker, K., and Richter, D. W. (2002). Effects of functional knock-out of $\alpha 1$ glycine-receptors on breathing movements in oscillator mice. *Respir. Physiol. Neurobiol.* 130, 33–42. doi: 10.1016/S0034-5687(01)00334-6
- Meier, J. C., Henneberger, C., Melnick, I., Racca, C., Harvey, R. J., Heinemann, U., et al. (2005). RNA editing produces glycine receptor $\alpha 3$ (P185L), resulting in high agonist potency. *Nat. Neurosci.* 8, 736–744. doi: 10.1038/nn1467
- Meiselbach, H., Vogel, N., Langlhofer, G., Stangl, S., Schleyer, B., Bahnassawy, L., et al. (2014). Single expressed glycine receptor domains reconstitute functional ion channels without subunit-specific desensitization behavior. *J. Biol. Chem.* 289, 29135–29147. doi: 10.1074/jbc.M114.559138
- Melzer, N., Villmann, C., Becker, K., Harvey, K., Harvey, R. J., Vogel, N., et al. (2010). Multifunctional basic motif in the glycine receptor intracellular domain induces subunit-specific sorting. *J. Biol. Chem.* 285, 3730–3739. doi: 10.1074/jbc.M109.030460
- Meyer, G., Kirsch, J., Betz, H., and Langosch, D. (1995). Identification of a gephyrin binding motif on the glycine receptor β subunit. *Neuron* 15, 563–572. doi: 10.1016/0896-6273(95)90145-0
- Miller, P. S., and Aricescu, A. R. (2014). Crystal structure of a human GABA_A receptor. *Nature* 512, 270–275. doi: 10.1038/nature13293
- Moraga-Cid, G., Sauguet, L., Huon, C., Malherbe, L., Girard-Blanc, C., Petres, S., et al. (2015). Allosteric and hyperekplexic mutant phenotypes investigated on an $\alpha 1$ glycine receptor transmembrane structure. *Proc. Natl. Acad. Sci. U S A* 112, 2865–2870. doi: 10.1073/pnas.1417864112
- Nikolic, Z., Laube, B., Weber, R. G., Lichter, P., Kioschis, P., Poustka, A., et al. (1998). The human glycine receptor subunit $\alpha 3$. Glra3 gene structure, chromosomal localization and functional characterization of alternative transcripts. *J. Biol. Chem.* 273, 19708–19714. doi: 10.1074/jbc.273.31.19708
- Nury, H., Van Renterghem, C., Weng, Y., Tran, A., Baaden, M., Dufresne, V., et al. (2011). X-ray structures of general anaesthetics bound to a pentameric ligand-gated ion channel. *Nature* 469, 428–431. doi: 10.1038/nature09647
- Oertel, J., Villmann, C., Kettenmann, H., Kirchhoff, F., and Becker, C. M. (2007). A novel glycine receptor β subunit splice variant predicts an unorthodox transmembrane topology. Assembly into heteromeric receptor complexes. *J. Biol. Chem.* 282, 2798–2807. doi: 10.1074/jbc.M608941200
- Papadopoulos, T., Eulenburg, V., Reddy-Alla, S., Mansuy, I. M., Li, Y., and Betz, H. (2008). Collybistin is required for both the formation and maintenance of GABAergic postsynapses in the hippocampus. *Mol. Cell. Neurosci.* 39, 161–169. doi: 10.1016/j.mcn.2008.06.006
- Papadopoulos, T., Korte, M., Eulenburg, V., Kubota, H., Retiounskaia, M., Harvey, R. J., et al. (2007). Impaired GABAergic transmission and altered hippocampal synaptic plasticity in collybistin-deficient mice. *EMBO J.* 26, 3888–3899. doi: 10.1038/sj.emboj.7601819
- Papke, D., and Grosman, C. (2014). The role of intracellular linkers in gating and desensitization of human pentameric ligand-gated ion channels. *J. Neurosci.* 34, 7238–7252. doi: 10.1523/JNEUROSCI.5105-13.2014
- Parikh, R. B., Bali, M., and Akabas, M. H. (2011). Structure of the M2 transmembrane segment of GLIC, a prokaryotic Cys loop receptor homologue from *Gloeobacter violaceus*, probed by substituted cysteine accessibility. *J. Biol. Chem.* 286, 14098–14109. doi: 10.1074/jbc.M111.221895
- Pilorge, M., Fossier, C., Le Corrionc, H., Potey, A., Bai, J., De Gois, S., et al. (2015). Genetic and functional analyses demonstrate a role for abnormal glycinergic signaling in autism. *Mol. Psychiatry* doi: 10.1038/mp.2015.139 [Epub ahead of print].
- Qualmann, B., and Kelly, R. B. (2000). Syndapin isoforms participate in receptor-mediated endocytosis and actin organization. *J. Cell Biol.* 148, 1047–1062. doi: 10.1083/jcb.148.5.1047
- Rath, A., Davidson, A. R., and Deber, C. M. (2005). The structure of "unstructured" regions in peptides and proteins: role of the polyproline II helix in protein folding and recognition. *Biopolymers* 80, 179–185. doi: 10.1002/bip.20227
- Rees, M. I., Harvey, K., Pearce, B. R., Chung, S. K., Duguid, I. C., Thomas, P., et al. (2006). Mutations in the gene encoding GlyT2 (SLC6A5) define a presynaptic component of human startle disease. *Nat. Genet.* 38, 801–806. doi: 10.1038/ng1814
- Rees, M. I., Lewis, T. M., Vafa, B., Ferrie, C., Corry, P., Muntoni, F., et al. (2001). Compound heterozygosity and nonsense mutations in the $\alpha(1)$ -subunit of the inhibitory glycine receptor in hyperekplexia. *Hum. Genet.* 109, 267–270. doi: 10.1007/s004390100569
- Ruiz-Gómez, A., Vaello, M. L., Valdivieso, F., and Mayor, F. Jr. (1991). Phosphorylation of the 48-kDa subunit of the glycine receptor by protein kinase C. *J. Biol. Chem.* 266, 559–566.
- Sadtler, S., Laube, B., Lashub, A., Nicke, A., Betz, H., and Schmalzing, G. (2003). A basic cluster determines topology of the cytoplasmic M3–M4 loop of the glycine receptor $\alpha 1$ subunit. *J. Biol. Chem.* 278, 16782–16790. doi: 10.1074/jbc.M213077200
- Saiyed, T., Paarmann, I., Schmitt, B., Haeger, S., Sola, M., Schmalzing, G., et al. (2007). Molecular basis of gephyrin clustering at inhibitory synapses: role of G- and E-domain interactions. *J. Biol. Chem.* 282, 5625–5632. doi: 10.1074/jbc.M610290200
- San Martín, L., Cerda, F., Jimenez, V., Fuentealba, J., Muñoz, B., Aguayo, L. G., et al. (2012). Inhibition of the ethanol-induced potentiation of $\alpha 1$ glycine receptor by a small peptide that interferes with G $\beta\gamma$ binding. *J. Biol. Chem.* 287, 40713–40721. doi: 10.1074/jbc.M112.393603
- Sánchez, A., Yévenes, G. E., San Martín, L., Burgos, C. F., Moraga-Cid, G., Harvey, R. J., et al. (2015). Control of ethanol sensitivity of the glycine receptor $\alpha 3$ subunit by transmembrane 2, the intracellular splice cassette and C-terminal domains. *J. Pharmacol. Exp. Ther.* 353, 80–90. doi: 10.1124/jpet.114.221143
- Saul, B., Kuner, T., Sobetzko, D., Brune, W., Hanefeld, F., Meinck, H. M., et al. (1999). Novel GLRA1 missense mutation (P250T) in dominant hyperekplexia defines an intracellular determinant of glycine receptor channel gating. *J. Neurosci.* 19, 869–877.
- Schaefer, N., Kluck, C. J., Price, K. L., Meiselbach, H., Vornberger, N., Schwarzsinger, S., et al. (2015). Disturbed neuronal ER-golgi sorting of unassembled glycine receptors suggests altered subcellular processing is a cause of human hyperekplexia. *J. Neurosci.* 35, 422–437. doi: 10.1523/JNEUROSCI.1509-14.2015
- Schaefer, N., Langlhofer, G., Kluck, C. J., and Villmann, C. (2013). Glycine receptor mouse mutants: model systems for human hyperekplexia. *Br. J. Pharmacol.* 170, 933–952. doi: 10.1111/bph.12335
- Schaefer, N., Vogel, N., and Villmann, C. (2012). Glycine receptor mutants of the mouse: what are possible routes of inhibitory compensation? *Front. Mol. Neurosci.* 5:98. doi: 10.3389/fnmol.2012.00098
- Schwarz, G., Schrader, N., Mendel, R. R., Hecht, H. J., and Schindelin, H. (2001). Crystal structures of human gephyrin and plant Cnx1 G domains: comparative analysis and functional implications. *J. Mol. Biol.* 312, 405–418. doi: 10.1006/jmbi.2001.4952
- Shiang, R., Ryan, S. G., Zhu, Y. Z., Hahn, A. F., O'Connell, P., and Wasmuth, J. J. (1993). Mutations in the $\alpha 1$ subunit of the inhibitory glycine receptor cause the dominant neurologic disorder, hyperekplexia. *Nat. Genet.* 5, 351–358. doi: 10.1038/ng1293-351
- Soykan, T., Schneeberger, D., Tria, G., Buechner, C., Bader, N., Svergun, D., et al. (2014). A conformational switch in collybistin determines the differentiation of inhibitory postsynapses. *EMBO J.* 33, 2113–2133. doi: 10.15252/emboj.201488143

- Specht, C. G., Grünewald, N., Pascual, O., Rostgaard, N., Schwarz, G., and Triller, A. (2011). Regulation of glycine receptor diffusion properties and gephyrin interactions by protein kinase C. *EMBO J.* 30, 3842–3853. doi: 10.1038/emboj.2011.276
- Sun, H., Lu, L., Zuo, Y., Wang, Y., Jiao, Y., Zeng, W. Z., et al. (2014). Kainate receptor activation induces glycine receptor endocytosis through PKC deSUMOylation. *Nat. Commun.* 5:4980. doi: 10.1038/ncomms5980
- Tabuchi, K., Blundell, J., Etherton, M. R., Hammer, R. E., Liu, X., Powell, C. M., et al. (2007). A neuroligin-3 mutation implicated in autism increases inhibitory synaptic transmission in mice. *Science* 318, 71–76. doi: 10.1126/science.1146221
- Tasneem, A., Iyer, L. M., Jakobsson, E., and Aravind, L. (2005). Identification of the prokaryotic ligand-gated ion channels and their implications for the mechanisms and origins of animal Cys-loop ion channels. *Genome Biol.* 6:R4. doi: 10.1186/gb-2004-6-1-r4
- Tsai, C. H., Chang, F. C., Su, Y. C., Tsai, F. J., Lu, M. K., Lee, C. C., et al. (2004). Two novel mutations of the glycine receptor gene in a Taiwanese hyperekplexia family. *Neurology* 63, 893–896. doi: 10.1212/01.wnl.0000138566.65519.67
- Unterter, B., Becker, C. M., and Villmann, C. (2012). The importance of TM3–4 loop subdomains for functional reconstitution of glycine receptors by independent domains. *J. Biol. Chem.* 287, 39205–39215. doi: 10.1074/jbc.M112.376053
- Unwin, N. (2005). Refined structure of the nicotinic acetylcholine receptor at 4 Å resolution. *J. Mol. Biol.* 346, 967–989. doi: 10.1016/j.jmb.2004.12.031
- Vaello, M. L., Ruiz-Gómez, A., Lerma, J., and Mayor, F. Jr. (1994). Modulation of inhibitory glycine receptors by phosphorylation by protein kinase C and cAMP-dependent protein kinase. *J. Biol. Chem.* 269, 2002–2008.
- Van den Eynden, J., Ali, S. S., Horwood, N., Carmans, S., Bröne, B., Hellings, N., et al. (2009). Glycine and glycine receptor signalling in non-neuronal cells. *Front. Mol. Neurosci.* 2:9. doi: 10.3389/neuro.02.009.2009
- Vergouwe, M. N., Tijssen, M. A., Peters, A. C., Wielaard, R., and Frants, R. R. (1999). Hyperekplexia phenotype due to compound heterozygosity for GLRA1 gene mutations. *Ann. Neurol.* 46, 634–638. doi: 10.1002/1531-8249(199910)46:4<634::AID-ANA12>3.0.CO;2-9
- Villmann, C., Oertel, J., Ma-Högemeier, Z. L., Hollmann, M., Sprengel, R., Becker, K., et al. (2009a). Functional complementation of Glra1(sp-d-ot), a glycine receptor subunit mutant, by independently expressed C-terminal domains. *J. Neurosci.* 29, 2440–2452. doi: 10.1523/JNEUROSCI.4400-08.2009
- Villmann, C., Oertel, J., Melzer, N., and Becker, C. M. (2009b). Recessive hyperekplexia mutations of the glycine receptor $\alpha 1$ subunit affect cell surface integration and stability. *J. Neurochem.* 111, 837–847. doi: 10.1111/j.1471-4159.2009.06372.x
- Winkelmann, A., Maggio, N., Eller, J., Caliskan, G., Semtner, M., Häussler, U., et al. (2014). Changes in neural network homeostasis trigger neuropsychiatric symptoms. *J. Clin. Invest.* 124, 696–711. doi: 10.1172/JCI71472
- Winter, S. M., Fresemann, J., Schnell, C., Oku, Y., Hirrlinger, J., and Hulsman, S. (2009). Glycinergic interneurons are functionally integrated into the inspiratory network of mouse medullary slices. *Pflugers Arch.* 458, 459–469. doi: 10.1007/s00424-009-0647-1
- Yevenes, G. E., Moraga-Cid, G., Avila, A., Guzmán, L., Figueroa, M., Peoples, R. W., et al. (2010). Molecular requirements for ethanol differential allosteric modulation of glycine receptors based on selective G $\beta\gamma$ modulation. *J. Biol. Chem.* 285, 30203–30213. doi: 10.1074/jbc.M110.134676
- Yevenes, G. E., Moraga-Cid, G., Guzmán, L., Haeger, S., Oliveira, L., Olate, J., et al. (2006). Molecular determinants for G protein $\beta\gamma$ modulation of ionotropic glycine receptors. *J. Biol. Chem.* 281, 39300–39307. doi: 10.1074/jbc.M608272200
- Yevenes, G. E., Moraga-Cid, G., Peoples, R. W., Schmalzing, G., and Aguayo, L. G. (2008). A selective G $\beta\gamma$ -linked intracellular mechanism for modulation of a ligand-gated ion channel by ethanol. *Proc. Natl. Acad. Sci. U S A* 105, 20523–20528. doi: 10.1073/pnas.0806257105
- Yevenes, G. E., Peoples, R. W., Tapia, J. C., Parodi, J., Soto, X., Olate, J., et al. (2003). Modulation of glycine-activated ion channel function by G-protein $\beta\gamma$ subunits. *Nat. Neurosci.* 6, 819–824. doi: 10.1038/nn1095
- Yevenes, G. E., and Zeilhofer, H. U. (2011). Molecular sites for the positive allosteric modulation of glycine receptors by endocannabinoids. *PLoS One* 6:e23886. doi: 10.1371/journal.pone.0023886

Conflict of Interest Statement: The authors declare that the research was conducted in the absence of any commercial or financial relationships that could be construed as a potential conflict of interest.

Copyright © 2016 Langlhofer and Villmann. This is an open-access article distributed under the terms of the Creative Commons Attribution License (CC BY). The use, distribution and reproduction in other forums is permitted, provided the original author(s) or licensor are credited and that the original publication in this journal is cited, in accordance with accepted academic practice. No use, distribution or reproduction is permitted which does not comply with these terms.



Utility of Induced Pluripotent Stem Cells for the Study and Treatment of Genetic Diseases: Focus on Childhood Neurological Disorders

Serena Barral¹ and Manju A. Kurian^{1,2*}

¹ Neurogenetics Group, Molecular Neurosciences, UCL Institute of Child Health, University College London, London, UK,

² Department of Neurology, Great Ormond Street Hospital, London, UK

The study of neurological disorders often presents with significant challenges due to the inaccessibility of human neuronal cells for further investigation. Advances in cellular reprogramming techniques, have however provided a new source of human cells for laboratory-based research. Patient-derived induced pluripotent stem cells (iPSCs) can now be robustly differentiated into specific neural subtypes, including dopaminergic, inhibitory GABAergic, motorneurons and cortical neurons. These neurons can then be utilized for *in vitro* studies to elucidate molecular causes underpinning neurological disease. Although human iPSC-derived neuronal models are increasingly regarded as a useful tool in cell biology, there are a number of limitations, including the relatively early, fetal stage of differentiated cells and the mainly two dimensional, simple nature of the *in vitro* system. Furthermore, clonal variation is a well-described phenomenon in iPSC lines. In order to account for this, robust baseline data from multiple control lines is necessary to determine whether a particular gene defect leads to a specific cellular phenotype. Over the last few years patient-derived neural cells have proven very useful in addressing several mechanistic questions related to central nervous system diseases, including early-onset neurological disorders of childhood. Many studies report the clinical utility of human-derived neural cells for testing known drugs with repurposing potential, novel compounds and gene therapies, which then can be translated to clinical reality. iPSCs derived neural cells, therefore provide great promise and potential to gain insight into, and treat early-onset neurological disorders.

Keywords: iPSCs, childhood neurological disorders, *in vitro* disease modeling, gene therapies, drug screening, isogenic control

OPEN ACCESS

Edited by:

Kirsten Harvey,
University College London, UK

Reviewed by:

Erik Maronde,
Goethe-Universität, Germany
Hansen Wang,
University of Toronto, Canada

*Correspondence:

Manju A. Kurian
manju.kurian@ucl.ac.uk

Received: 02 June 2016

Accepted: 15 August 2016

Published: 06 September 2016

Citation:

Barral S and Kurian MA (2016) Utility of Induced Pluripotent Stem Cells for the Study and Treatment of Genetic Diseases: Focus on Childhood Neurological Disorders. *Front. Mol. Neurosci.* 9:78. doi: 10.3389/fnmol.2016.00078

INTRODUCTION

Over the last decade, significant advances such as whole exome and genome sequencing have facilitated genetic screening of patients, resulting in an ever-increasing number of inherited human diseases. Despite this genetic revolution, the molecular mechanisms downstream of a specific gene mutation or genetic variant remain yet to be fully elucidated for the majority of diseases. Future research priorities must therefore lie in studying such disorders in more depth, to not only understand the disease, but also to develop novel therapies for clinical translation.

To date, transgenic animal models and transformed cell lines, have allowed clarification of pathophysiological pathways affected by genetic mutations. Despite their benefits, both methods have a number of limitations, in that they often do not fully mimic human physiology, only partially recapitulate progression of disease, and do not accurately recapitulate human metabolism and homeostasis. It has long been recognized that patient derived cells are a potentially better *in vitro* tool for studying human disease. However, human tissue is often either unavailable or simply not accessible. This is clearly exemplified by neurological disorders, where accessing the brain and neuronal tissue for cell culture and future study is near impossible. Since the first human embryonic stem cells (ESCs) were isolated in 1998 (Thomson et al., 1998), the use of pluripotent stem cells (PSCs) has become a new reality in the study of human diseases, offering a challenging but incredibly useful model to move from clinic to bench and potentially vice versa.

The discovery of cellular reprogramming techniques has been a major step forward in the *in vitro* modeling of human disease, theoretically allowing the study of all genetic disease with specific patient cells as the starting point. Yamanaka and colleagues (Takahashi et al., 2007) elegantly reprogrammed adult dermal fibroblasts to a pluripotent state, by inducing ectopic expression of four factors: Oct4, Sox2, Klf4, and cMyc (Takahashi et al., 2007; Takahashi and Yamanaka, 2016). The induced PSCs generated are highly similar to human ESCs, with the ability to indefinitely proliferate and differentiate in cells derived from the three germ layers. Since publication of Yamanaka's landmark article, reprogramming techniques have been further refined, and many new strategies have been developed to effectively reprogram somatic cells into pluripotency. Integrating retroviruses and lentiviruses have been superseded by the use of non-integrating systems, including adenovirus, Sendai virus, mRNA, episomal vectors, proteins and small molecules (Fusaki et al., 2009; Kim et al., 2009; Zhou and Freed, 2009; Warren et al., 2010; Okita et al., 2011; Bar-Nur et al., 2014).

Neural stem cells (NSCs) have been successfully derived from PSCs and several protocols for PSCs differentiation into a broad variety of mature neurons and glial cell subtypes have been published (Srikanth and Young-Pearse, 2014). Patient-derived neural cells have the specific advantage of retaining the genetic background of the donor and thus offer a unique *in vitro* neuronal disease model. They are an unlimited source of cells that allows the analysis of the cellular mechanisms involved in disease. Furthermore, they provide a novel platform to test new drugs and genetic therapies as well as a source of cells that could potentially be used for cell replacement therapy (Figure 1).

When approaching the study of neurological diseases using human induced pluripotent stem cell (iPSC)-derived neurons as an *in vitro* model system, several considerations need to be taken into account, including the accurate generation of truly pluripotent cells, the relative efficiency of neuronal differentiation, and the strengths, utility and limitations of generated neurons. In this review, we provide a brief overview of what we consider to be the most important

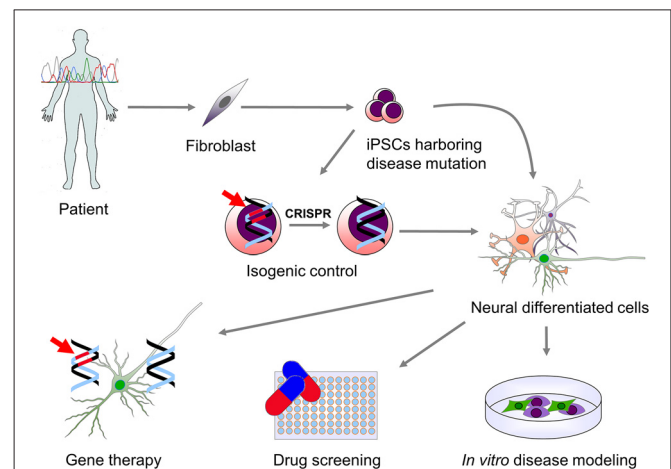


FIGURE 1 | Use of patient-derived induced pluripotent stem cells (iPSCs) for modeling genetic neurological diseases. Genetic screening of patients affected by a neurological disorder may lead to the identification of specific mutations causing disease. Patient-derived somatic cells (fibroblast and other cell types) can be then reprogrammed to a pluripotent state. iPSCs carrying the disease-related mutation (indicated in red) can be then differentiated into the neural cells type (neurons and glial cells) which are affected in the disease. This allows for the *in vitro* study of the molecular mechanisms downstream the genetic mutation. In order to overcome genetic background variability and to validate the effect of the genetic mutation on phenotype observed *in vitro*, isogenic control iPSCs can be generated via genomic correction of the mutation. Moreover, *in vitro* differentiated cells can be used for high-throughput screening of drugs or the validation of specific genetic therapies that can then be translated into clinical practice.

advantages and disadvantages of using human iPSCs to model neurological diseases, and their translational utility at a clinical level. Our main focus will be to evaluate this model system for early-onset genetic neurological disorders (Table 1), although, where relevant and appropriate, we will use examples from other later-onset neurological diseases.

NEURAL DIFFERENTIATION OF HUMAN iPSC: A WIDE VARIETY OF CELL TYPES

Differentiation of iPSCs into neural cells is based on recapitulating embryonic development and relies on the use of specific factors that can promote or inhibit specific signaling pathways. All methods published so far can guarantee high purity of NSCs, but it is more challenging to obtain decent percentages of specific subtypes of desired mature neural cells. To date, it is possible to derive a wide variety of neuronal cell types from PSCs, including forebrain neuronal neurons (Espuny-Camacho et al., 2013; Lancaster et al., 2013); motor neurons (Wada et al., 2009; Nizzardo et al., 2010); dopaminergic neurons (Kriks et al., 2011; Kirkeby et al., 2012); GABAergic neurons (Maroof et al., 2013; Nicholas et al., 2013); medium spiny neurons (Delli Carri et al., 2013); forebrain cholinergic neurons (Wicklund et al., 2010; Hu et al., 2016); serotonergic neurons (Erceg et al., 2008); caudal neurons (Kirkeby et al., 2012); cerebellar neurons (Erceg et al., 2010); astrocytes (Emdad et al., 2012; Juopperi

TABLE 1 | Utility of induced pluripotent stem cells (iPSC) in childhood-onset neurodevelopmental and neurological disorders.

Disease	Gene(s)	Differentiated cell type	Molecular characterization	Compound screening	Gene/RNA therapy
Neurodevelopmental disorders					
Rett syndrome	<i>MECP2</i> <i>CDKL5</i>	Neural progenitor cells Neurons (glutamatergic) Astrocytes	Muotri et al. (2010), Amenduni et al. (2011), Ananiev et al. (2011), Cheung et al. (2011), Kim et al. (2011), Farra et al. (2012), Larimore et al. (2013), Williams et al. (2014), Andoh-Noda et al. (2015), Djuric et al. (2015), Fernandes et al. (2015), Livide et al. (2015), Tang et al. (2016) and Zhang et al. (2016)	Marchetto et al. (2010)	
Fragile X syndrome	<i>FMR1</i>	Neural precursor cells Neurons (forebrain) Glial cells	Urbach et al. (2010), Sheridan et al. (2011), Doers et al. (2014) and Halevy et al. (2015)	Kaufmann et al. (2015) and Kumari et al. (2015)	Park et al. (2015)
Microcephaly	<i>ERCC6</i> <i>CDK5RAP2</i>	Neurons Cerebral organoids	Lancaster et al. (2013) and Vessoni et al. (2016)		
Angelman/Prader-Willi syndromes	<i>UBE3A</i>	Neurons Astrocytes	Chamberlain et al. (2010)		
Timothy syndrome	<i>CACNA1C</i>	Neural progenitor cells Neurons	Krey et al. (2013) and Tian et al. (2014)	Paşca et al. (2011)	
Phelan-McDermid syndrome	Chromosome 22q13 deletion	Neurons (forebrain)		Shcheglovitov et al. (2013)	
Epilepsy					
Dravet syndrome	<i>SCN1A</i>	Neurons (dopaminergic, GABAergic) Forebrain interneurons Glutamatergic neurons Glial cells	Higurashi et al. (2013), Jiao et al. (2013), Liu et al. (2013, 2016) and Maeda et al. (2016)	Jiao et al. (2013)	
Early infantile epileptic encephalopathy	<i>STXBP1</i>	Neurons (glutamatergic, GABAergic)	Yamashita et al. (2016)		
Movement disorders					
Hereditary spastic paraplegia	<i>SPG11</i> <i>ATL1</i> <i>SPAST</i>	Cortical neural progenitor cells Neurons (forebrain glutamatergic)	Denton et al. (2014), Havlicek et al. (2014) and Mishra et al. (2016)	Zhu et al. (2014)	
Ataxia telangiectasia	<i>ATM</i>	Neural progenitor cells Neurons (GABAergic)	Nayler et al. (2012) and Carlessi et al. (2014)	Lee et al. (2013)	
Friedrich's ataxia	<i>FXN</i>	Neural progenitor cells Neural crest cells Neurons (peripheral sensory) Glial cells	Liu et al. (2011), Eigentler et al. (2013), Hick et al. (2013) and Bird et al. (2014)	Shan et al. (2014), Soragni et al. (2014) and Igoillo-Esteve et al. (2015)	Li et al. (2015)
Huntington's disease	<i>HTT</i>	Striatal neural precursor cells Neurons (GABAergic striatal) Astrocytes	Camnasio et al. (2012), Chae et al. (2012), HD iPSC Consortium (2012), Jeon et al. (2012), Juopperi et al. (2012), Mattis et al. (2015) and Szlachcic et al. (2015)	Guo et al. (2013), Hsiao et al. (2014) and Lu et al. (2014)	An et al. (2012) and Cheng et al. (2013)
Metabolic disorders					
Lesch-Nyhan syndrome	<i>HPRT</i>	Neurons	Mastrangelo et al. (2012) and Mekhoubad et al. (2012)		

(Continued)

TABLE 1 | (Continued).

Disease	Gene(s)	Differentiated cell type	Molecular characterization	Compound screening	Gene/RNA therapy
Niemann-Pick type C disease	<i>NPC1</i>	Neurons Astrocytes	Trilck et al. (2013, 2016)	Efthymiou et al. (2015)	
Neuronal ceroid lipofuscinosis disease	<i>TPP1</i> <i>CLN3</i>	Neurons	Lojewski et al. (2014)		
Gaucher's disease	<i>GBA1</i>	Neurons (dopaminergic)	Awad et al. (2015) and Sun et al. (2015)	Tiscornia et al. (2013)	
Metachromatic leukodystrophy	<i>ARSA</i>	Neural stem cells Astroglial progenitor cells	Doerr et al. (2015)		
X-linked Adrenoleukodystrophy	<i>ABCD1</i>	Neurons Astrocytes Oligodendrocytes	Jang et al. (2011) and Baarine et al. (2015)		
Neuromuscular disorders					
Spinal muscular atrophy	<i>SMN1</i>	Neurons (motor neurons, forebrain neurons, sensory neurons) Astrocytes	Ebert et al. (2009), Chang et al. (2011), McGivern et al. (2013), Schwab and Ebert (2014), Boza-Morán et al. (2015), Demestre et al. (2015), Liu et al. (2015), Ng et al. (2015), Fuller et al. (2016), Heesen et al. (2016) and Patitucci and Ebert (2016)	Sareen et al. (2012), Ohuchi et al. (2016) and Xu et al. (2016)	Corti et al. (2012), Nizzardo et al. (2015) and Yoshida et al. (2015)

et al., 2012); oligodendrocytes (Nistor et al., 2005; Ogawa et al., 2011). Neuronal populations generated are typically heterogeneous, presenting both mature and immature cells, and thus need further technologies to achieve a high level of purity. Sorting techniques are often useful, but there are few neuronal subtype-specific surface markers available to select desired neural subpopulations (Pruszek et al., 2009; Yuan et al., 2011; Doi et al., 2014). To overcome this issue, sorting can sometimes be achieved by the expression of a selectable marker included as a reporter under expression of specific transcription factors or proteins (DeRosa et al., 2015; Toli et al., 2015).

IN VITRO DERIVED NEURAL CELLS: WHAT IS THEIR TRUE DEVELOPMENTAL STAGE?

During reprogramming into iPSCs, somatic cells return to a developmental stage similar to that of ESCs, independent of their original age. Indeed, age-related characteristics of the original cells, (such as nuclear abnormalities, telomere length, and mitochondrial activity) are lost during this re-set to an embryonic stage (Marion et al., 2009; Suhr et al., 2010). Differentiation protocols for the generation of neuronal subtypes from PSCs require a significant amount of time spanning from weeks to months (Srikanth and Young-Pearse, 2014) to produce neurons that show a relatively mature morphological, molecular and electrophysiological phenotype. Despite this maturation process, generated neurons are still reminiscent of human fetal neurons (Mariani et al., 2012; Lancaster et al., 2013; Miller et al., 2013;

Vera and Studer, 2015). It is therefore conceivable that such *in vitro* model systems could fail to recapitulate the disease phenotype especially for late-onset disorders.

Studer and colleagues (Miller et al., 2013) have addressed this issue, by developing a genetic strategy for introducing aging-related features in iPSC-derived neurons, specifically studying Parkinson disease (PD). Specifically, PD patient iPSC-derived midbrain dopaminergic neurons (mDA) recapitulate some PD disease features, including α -synuclein (α SYN) accumulation, oxidative stress, defects in neural outgrowth and mitochondrial dysfunction (Byers et al., 2011; Jiang et al., 2012; Reinhardt et al., 2013). However key late disease features of PD, such as neural degeneration, were only evident in model systems exposed to external stressors (Byers et al., 2011; Nguyen et al., 2011). Importantly, the accumulation of Lewy bodies and appearance of neuromelanin, a distinct feature of adult mDA neurons, have not been observed in iPSC-derived neurons. In this case, Studer and colleagues transiently overexpressed progerin, and showed restoration of aging features in both fibroblasts and mDA neurons derived from iPSCs. In particular, in iPSC-derived mDA neurons, they observed features of normal neural aging, with degeneration of dendrites *in vitro* and neuromelanin accumulation after grafting *in vivo* (Miller et al., 2013).

The relatively immature characteristics of iPSC-derived neurons should therefore always be a major consideration when modeling postnatal-, childhood- and adult-onset neurological diseases, where pathological features only manifest during postnatal development or the aging process.

VARIABLE GENETIC BACKGROUND: DEFINING GOOD CONTROLS

Using patient derived iPSCs guarantees a unique opportunity to study the phenotype associated with a specific mutation in the context of the genetic background in which the mutation leads to disease. However, genetic background and potential genetic modulators of disease could conceivably affect the phenotype of both healthy control and patient lines. This is a definite limiting factor in the study of both Mendelian and more complex multigenic/multifactorial disorders. One solution is to use iPSCs derived from un-affected relatives for comparison, or to compare several control and several different patient lines in the same study. However, both these methods can be costly and time consuming. In more recent times, gene-editing technologies have become a more robust method by which the effect of a specific genotype on the iPSC model system can be unequivocally validated. Indeed, for monogenic disorders, correction of the single mutation in an iPSC cell line allows development of a unique “isogenic” control which harbors the same genetic background of the patient, thereby decreasing any “background noise” that could mask or affect cell phenotype. Furthermore, the insertion of a specific mutation into a control line can be utilized to show that such mutagenesis can induce disease phenotypes into a control line, akin to those seen in patient lines. Such concepts have been elegantly illustrated by Reinhardt et al. (2013) in their study of *LRRK2*-related PD, where they generated and compared several control lines, from healthy age- and gender-matched individuals, vs. isogenic controls using gene editing tools. No significant difference in α SYN levels was observed when comparing mDA neurons from wild type to *LRRK2*-mutated patient derived iPSC lines. However, α SYN levels were markedly reduced in patient lines when compared to the corresponding corrected isogenic lines. Gene expression profiles after 30 days of differentiation revealed significant differences in the age- and gender-matched iPSC lines when compared to both patient and isogenic lines. It is therefore clear that genetic background can have effects on gene expression, and the comparison of patient lines with isogenic controls can help overcome such genetic variability.

A number of different techniques can be used to generate isogenic controls. Reinhardt et al. (2013) used Zinc Finger Nuclease (ZFNs) technology. Both ZFN and the similar Transcription Activator-Like Effector Nuclease (TALENs) have been used successfully for gene editing in iPSCs (Hockemeyer et al., 2009, 2011). Both methods rely on the generation of costumed DNA binding domains conjugated to FokI nuclease, which can induce double strand breaks in a non-specific manner. The landmark discovery of the Clustered Regularly Interspaced Short Palindromic Repeats (CRISPR)-Cas9 system has added a highly efficient tool to manipulate the iPSCs genome (Ding et al., 2013) using endonuclease Cas9 and a guide RNA, targeting a specific region. Due to the efficient, relatively fast and targeted approach of the CRISPR-Cas9 technique compared to ZFNs and TALENs, this newer technique appears to be the preferred genome editing methodology for many researchers.

Furthermore, the different commercial companies now offer generation of custom isogenic control lines using CRISPR-Cas9 technology (Baker, 2014).

NEURONAL CELLS IN A DISH: THE NEED FOR A 3D SYSTEM

Although iPSCs represent an advantageous tool to study molecular phenotypes in neurological disease, their two dimensional nature means that some of the environmental factors, regional identities and complex neural circuits are absent when compared to either an animal disease model or human patient. Different studies have shown the intrinsic ability of NSCs to spontaneously self-organize in 3-dimensional (3D) structures resembling whole organs (Lancaster and Knoblich, 2014). Lancaster et al. (2013) showed how simple cultivation of control iPSCs in suspension can give rise to organoids which display several brain regions along the rostral-caudal and dorso-ventral pathways of mainly the forebrain and mid-hindbrain areas. The degree of cellular organization was maximal in the dorsal cortical region of the generated organoid where they observed a layered organization typical of the developing human forebrain. The same group then generated organoids from iPSCs derived from patients with microcephaly. The patient-derived cortical organoids mimicked a number of the features seen in disease, including smaller neural tissues with few progenitors regions, and radial glial maturation and orientation abnormalities, which were not previously recapitulated in a murine model. Organoids therefore represent a powerful tool to study both human fetal neocortical development (Camp et al., 2015) and developmental disorders. The generation of organoids representing more caudal fetal regions, (such as the midbrain and hindbrain) is also no doubt useful for studying neurological disorders affecting these areas of the central nervous system. Indeed, midbrain-like organoids (MLOs) have recently been derived from human ESCs (Jo et al., 2016). Neural cells of such MLOs not only expressed midbrain markers and displayed characteristic dopaminergic electrical activity, but also produced neuromelanin, a characteristic not observed in bi-dimensional systems.

MOVING iPSCs INTO CLINICAL UTILITY: DRUGS, CELL AND GENE THERAPY FOR PHARMACORESISTANT CHILDHOOD NEUROLOGICAL DISORDERS

The development of new drugs to treat human disorders is a challenging field. Indeed, many drugs tested in animal models have failed in human clinical trials due to lack of efficacy or intolerability (Scannell et al., 2012). Overall, new drugs for pharmacoresistant disorders are an unmet need, and constitute a priority area for research. The development of new drugs is hindered by the lack of appropriate models. Human iPSCs offer a unique opportunity for high-throughput drug screening in patient derived cells to assess drug efficacy and toxicity. Despite being in the early stages, several studies have

demonstrated the feasibility and usefulness of this approach for childhood neurological disorders. For example, motor neurons derived from patients affected by Spinal Muscular Atrophy (SMA) have been used to test specific drugs (Xu et al., 2016). SMA is characterized by mutations in *SMN1*, which leads to degeneration of spinal motor neurons associated with mitochondrial dysfunction. Treatment of SMA human iPSCs derived motor neurons with N-acetylcysteine (NAC) improved mitochondrial functionality, thereby rescuing motor neuron degeneration *in vitro*.

In Rett syndrome (RTT) patient-derived iPSCs have been utilized to test the effect of IGF1 and gentamicin *in vitro* (Marchetto et al., 2010). RTT iPSCs derived glutamatergic neurons showed a decreased level of glutamatergic synapses when compared to controls, which was increased by IGF1 treatment. Gentamicin, administered at high dose acted as a suppressor of nonsense mutations which cause impaired function of MeCP2 in RTT. Furthermore, IGF1 has been used to rescue the phenotype observed in neurons differentiated from Phelan-McDermid syndrome (PMDS)-derived iPSCs (Shcheglovitov et al., 2013). PMDS neurons showed impairment in excitatory synaptic transmission and reduced number of excitatory synapses, which were restored after treatment with IGF1.

These and other studies (Table 1), have mainly tested small number of compounds on iPSC differentiated cells, thereby demonstrating the feasibility of using iPSCs for drug testing. In the future, high-throughput technologies allowing the screening of an extensive library of compounds will be useful. High-content imaging and analysis are likely to be helpful for such high-throughput approaches (Sirenko et al., 2014). High-content high-throughput assays have already been undertaken on iPSC-derived neural cells in 384-well assays, with analysis focusing on neurite outgrowth, cell number and viability, mitochondrial integrity and membrane potential.

Two studies have used high-throughput assays to screen large numbers of candidate drugs for Fragile X syndrome, a neurodevelopmental disorder characterized by learning problems, autism, and anxiety. This syndrome is associated with CGG repeat expansion in the 5'-untranslated region of *FMR1*, which leads to the absence of FMR protein. Both studies used patient derived iPSCs and differentiated them either in NSCs or neural precursors. In the first study 5000 compounds (both novel and approved drugs) were tested (Kumari et al., 2015), while the second study expanded drug screening to over 50,000 compounds (Kaufmann et al., 2015). In both studies *FMR1*-neural cells, treated with compounds as decanehydroxamate, deserpidine or tibrofam, showed increased mRNA levels, though not to clinically significant levels. Nevertheless, both studies show how promising high-throughput techniques can be in expanding the potential of drug testing using iPSCs derived cells.

In addition to the screening of new drugs, human iPSCs also offer other therapeutic possibilities that can be translated into clinical practice, as evident in the Phase I SMA study (Chiriboga et al., 2016). The antisense oligonucleotide nusinersen was designed to alter splicing of *SMN2* mRNA. *SMN1* motor neurons compensate with the paralogous gene *SMN2*. *SMN2* shows a

high sequence homology to *SMN1*, the only difference resides in the C-to-T base change inside exon 7. This mutation leads to abnormal *SMN2* splicing and to the generation of truncated highly unstable proteins that trigger neural degeneration of motor neurons. *SMN2* splicing correction with the use of oligonucleotides resulted in the production of a greater amount of full-length *SMN2*. This strategy has been tested on patient-derived iPSCs differentiated motor neurons (Corti et al., 2012) and showed the ability to convert SMA-differentiated motor neurons to a normal phenotype, both *in vitro* and after grafting into a mouse model of disease.

iPSC-derived neural cells can also be a patient-derived platform to test genetic therapies. Juvenile neuronal ceroid lipofuscinosis (NCL) disorder is caused by loss-of-function mutations in *CLN3*. Patient-derived iPSCs neurons showed abnormal lysosomal storage with abnormalities observed in mitochondria, Golgi apparatus and endoplasmic reticulum. After restoring the function of *CLN3* via AAVrh.10 virus bearing wild-type human *CLN3*, *in vitro* differentiated neurons showed a rescued phenotype, without excess accumulation of storage material (Lojewski et al., 2014). Similarly, a lentiviral approach was used for a genetic early onset form of PD. iPSC-derived mDA harboring mutations in *PINK1*, a gene encoding a mitochondrial kinase, showed dysfunctional mitochondrial function. Expression of the non-mutated *PINK1* via lentivirus in patient-derived mDA neurons restored normal recruitment of *PINK1* upon mitochondrial depolarization, and normalized mitochondrial number and biogenesis (Seibler et al., 2011).

The combination of genetic engineering techniques and the promise of human PSCs differentiated cells as a donor source for cell replacement therapies, could in the future lead to the generation of patient-derived "corrected" cells that could potentially be used in autologous transplantation to replace affected disease cells. Such use of patient derived, genetically corrected neural cells may also potentially overcome immune-mediated responses that might be triggered by using allogeneic neural cells. Overall, even though such approaches are extremely promising and although PSCs are already used in clinical trials (Kimbrel and Lanza, 2015), there remain many issues regarding the use of PSC as cell replacement therapy, particularly concerning cell identity, purity, safety and long term risks. For this reason, even though it remains an extremely promising approach, clinical translation of such a therapeutic approach is likely to take some time.

CONCLUSION

Patient derived iPSCs represent a unique and increasingly utilized tool for the study of human genetic neurological diseases of childhood. iPSCs are an extraordinary model that can facilitate new insight into the molecular basis of disease and aid the development of new therapies, especially for pharmacoresistant diseases where human tissue is inaccessible for research purposes. Like all other laboratory models, human iPSCs have some limitations, namely that the model can be time consuming and costly to establish, shows clonal variability and genetic background can influence phenotype. Despite this,

the ever-growing number of studies using human iPSCs to both model genetic disease and discover new therapies, render them an extremely promising tool, capturing the attention of researchers worldwide.

AUTHOR CONTRIBUTIONS

SB: conceptional design and writing of the manuscript. MAK: conceptional design and writing of the manuscript.

REFERENCES

- Amenduni, M., De Filippis, R., Cheung, A. Y., Disciglio, V., Epistolato, M. C., Ariani, F., et al. (2011). iPS cells to model CDKL5-related disorders. *Eur. J. Hum. Genet.* 19, 1246–1255. doi: 10.1038/ejhg.2011.131
- An, M. C., Zhang, N., Scott, G., Montoro, D., Wittkop, T., Mooney, S., et al. (2012). Genetic correction of Huntington's disease phenotypes in induced pluripotent stem cells. *Cell Stem Cell* 11, 253–263. doi: 10.1016/j.stem.2012.04.026
- Ananiev, G., Williams, E. C., Li, H., and Chang, Q. (2011). Isogenic pairs of wild type and mutant induced pluripotent stem cell (iPSC) lines from Rett syndrome patients as *in vitro* disease model. *PLoS One* 6:e25255. doi: 10.1371/journal.pone.0025255
- Andoh-Noda, T., Akamatsu, W., Miyake, K., Matsumoto, T., Yamaguchi, R., Sanosaka, T., et al. (2015). Differentiation of multipotent neural stem cells derived from Rett syndrome patients is biased toward the astrocytic lineage. *Mol. Brain* 8:31. doi: 10.1186/s13041-015-0121-2
- Awad, O., Sarkar, C., Panicker, L. M., Miller, D., Zeng, X., Sgambato, J. A., et al. (2015). Altered TFEB-mediated lysosomal biogenesis in Gaucher disease iPSC-derived neuronal cells. *Hum. Mol. Genet.* 24, 5775–5788. doi: 10.1093/hmg/ddv297
- Baarine, M., Khan, M., Singh, A., and Singh, I. (2015). Functional characterization of iPSC-derived brain cells as a model for X-linked Adrenoleukodystrophy. *PLoS One* 10:e0143238. doi: 10.1371/journal.pone.0143238
- Baker, M. (2014). Gene editing at CRISPR speed. *Nat. Biotechnol.* 32, 309–312. doi: 10.1038/nbt.2863
- Bar-Nur, O., Brumbaugh, J., Verheul, C., Apostolou, E., Pruteanu-Malinici, I., Walsh, R. M., et al. (2014). Small molecules facilitate rapid and synchronous iPSC generation. *Nat. Methods* 11, 1170–1176. doi: 10.1038/nmeth.3142
- Bird, M. J., Needham, K., Frazier, A. E., van Rooijen, J., Leung, J., Hough, S., et al. (2014). Functional characterization of Friedreich ataxia iPS-derived neuronal progenitors and their integration in the adult brain. *PLoS One* 9:e017178. doi: 10.1371/journal.pone.0101718
- Boza-Morán, M. G., Martínez-Hernández, R., Bernal, S., Wanisch, K., Also-Rallo, E., Le Heron, A., et al. (2015). Decay in survival motor neuron and plastin 3 levels during differentiation of iPSC-derived human motor neurons. *Sci. Rep.* 5:11696. doi: 10.1038/srep11696
- Byers, B., Cord, B., Nguyen, H. N., Schüle, B., Fenno, L., Lee, P. C., et al. (2011). SNCA triplication Parkinson's patient's iPSC-derived DA neurons accumulate α -synuclein and are susceptible to oxidative stress. *PLoS One* 6:e26159. doi: 10.1371/journal.pone.0026159
- Camnasio, S., Delli Carri, A., Lombardo, A., Grad, I., Mariotti, C., Castucci, A., et al. (2012). The first reported generation of several induced pluripotent stem cell lines from homozygous and heterozygous Huntington's disease patients demonstrates mutation related enhanced lysosomal activity. *Neurobiol. Dis.* 46, 41–51. doi: 10.1016/j.nbd.2011.12.042
- Camp, J. G., Badsha, F., Florio, M., Kanton, S., Gerber, T., Wilsch-Bräuninger, M., et al. (2015). Human cerebral organoids recapitulate gene expression programs of fetal neocortex development. *Proc. Natl. Acad. Sci. U S A* 112, 15672–15677. doi: 10.1073/pnas.1520760112
- Carlessi, L., Fusar Poli, E., Bechi, G., Mantegazza, M., Pascucci, B., Narciso, L., et al. (2014). Functional and molecular defects of hiPSC-derived neurons from patients with ATM deficiency. *Cell Death Dis.* 5:e1342. doi: 10.1038/cddis.2014.310
- Chae, J. I., Kim, D. W., Lee, N., Jeon, Y. J., Jeon, I., Kwon, J., et al. (2012). Quantitative proteomic analysis of induced pluripotent stem cells derived from a human Huntington's disease patient. *Biochem. J.* 446, 359–371. doi: 10.1042/bj20111495
- Chamberlain, S. J., Chen, P. F., Ng, K. Y., Bourgois-Rocha, F., Lemtiri-Chlieh, F., Levine, E. S., et al. (2010). Induced pluripotent stem cell models of the genomic imprinting disorders Angelman and Prader-Willi syndromes. *Proc. Natl. Acad. Sci. U S A* 107, 17668–17673. doi: 10.1073/pnas.1004487107
- Chang, T., Zheng, W., Tsark, W., Bates, S., Huang, H., Lin, R. J., et al. (2011). Brief report: phenotypic rescue of induced pluripotent stem cell-derived motoneurons of a spinal muscular atrophy patient. *Stem Cells* 29, 2090–2093. doi: 10.1002/stem.749
- Cheng, P. H., Li, C. L., Chang, Y. F., Tsai, S. J., Lai, Y. Y., Chan, A. W., et al. (2013). miR-196a ameliorates phenotypes of Huntington disease in cell, transgenic mouse and induced pluripotent stem cell models. *Am. J. Hum. Genet.* 93, 306–312. doi: 10.1016/j.ajhg.2013.05.025
- Cheung, A. Y., Horvath, L. M., Grafodatskaya, D., Pasceri, P., Weksberg, R., Hotta, A., et al. (2011). Isolation of MECP2-null Rett Syndrome patient hiPS cells and isogenic controls through X-chromosome inactivation. *Hum. Mol. Genet.* 20, 2103–2115. doi: 10.1093/hmg/ddr093
- Chiriboga, C. A., Swoboda, K. J., Darras, B. T., Iannaccone, S. T., Montes, J., De Vivo, D. C., et al. (2016). Results from a phase 1 study of nusinersen (ISIS-SMNR_{xx}) in children with spinal muscular atrophy. *Neurology* 86, 890–897. doi: 10.1212/wnl.00000000000002445
- Corti, S., Nizzardo, M., Simone, C., Falcone, M., Nardini, M., Ronchi, D., et al. (2012). Genetic correction of human induced pluripotent stem cells from patients with spinal muscular atrophy. *Sci. Transl. Med.* 4:165ra162. doi: 10.1126/scitranslmed.3004108
- Delli Carri, A., Onorati, M., Lelos, M. J., Castiglioni, V., Faedo, A., Menon, R., et al. (2013). Developmentally coordinated extrinsic signals drive human pluripotent stem cell differentiation toward authentic DARPP-32⁺ medium-sized spiny neurons. *Development* 140, 301–312. doi: 10.1242/dev.084608
- Demestre, M., Orth, M., Föhr, K. J., Achberger, K., Ludolph, A. C., Liebau, S., et al. (2015). Formation and characterisation of neuromuscular junctions between hiPSC derived motoneurons and myotubes. *Stem Cell Res.* 15, 328–336. doi: 10.1016/j.scr.2015.07.005
- Denton, K. R., Lei, L., Grenier, J., Rodionov, V., Blackstone, C., and Li, X. J. (2014). Loss of spastin function results in disease-specific axonal defects in human pluripotent stem cell-based models of hereditary spastic paraplegia. *Stem Cells* 32, 414–423. doi: 10.1002/stem.1569
- DeRosa, B. A., Belle, K. C., Thomas, B. J., Cukier, H. N., Pericak-Vance, M. A., Vance, J. M., et al. (2015). hVGAT-mCherry: a novel molecular tool for analysis of GABAergic neurons derived from human pluripotent stem cells. *Mol. Cell. Neurosci.* 68, 244–257. doi: 10.1016/j.mcn.2015.08.007
- Ding, Q., Regan, S. N., Xia, Y., Oostrom, L. A., Cowan, C. A., and Musunuru, K. (2013). Enhanced efficiency of human pluripotent stem cell genome editing through replacing TALENs with CRISPRs. *Cell Stem Cell* 12, 393–394. doi: 10.1016/j.stem.2013.03.006
- Djuric, J., Cheung, A. Y., Zhang, W., Mok, R. S., Lai, W., Piekna, A., et al. (2015). MECP2e1 isoform mutation affects the form and function of neurons derived from Rett syndrome patient iPS cells. *Neurobiol. Dis.* 76, 37–45. doi: 10.1016/j.nbd.2015.01.001
- Doerr, J., Böckenhoff, A., Ewald, B., Ladewig, J., Eckhardt, M., Gieselmann, V., et al. (2015). Arylsulfatase a overexpressing Human iPSC-derived neural cells reduce CNS sulfatide storage in a mouse model of Metachromatic Leukodystrophy. *Mol. Ther.* 23, 1519–1531. doi: 10.1038/mt.2015.106

ACKNOWLEDGMENTS

SB is funded by the Wellcome Trust (158065). MAK is funded by a Wellcome Trust Intermediate Clinical Fellowship and receives funding from GOSHCC, the Gracious Heart Charity Foundation, Rosetrees Trust, the AADC Research Trust, and supported by the National Institute for Health Research Biomedical Research Centre at Great Ormond Street Hospital for Children NHS Foundation Trust and University College London.

- Doers, M. E., Musser, M. T., Nichol, R., Berndt, E. R., Baker, M., Gomez, T. M., et al. (2014). iPSC-derived forebrain neurons from FXS individuals show defects in initial neurite outgrowth. *Stem Cells Dev.* 23, 1777–1787. doi: 10.1089/scd.2014.0030
- Doi, D., Samata, B., Katsukawa, M., Kikuchi, T., Morizane, A., Ono, Y., et al. (2014). Isolation of human induced pluripotent stem cell-derived dopaminergic progenitors by cell sorting for successful transplantation. *Stem Cell Reports* 2, 337–350. doi: 10.1016/j.stemcr.2014.01.013
- Ebert, A. D., Yu, J., Rose, F. F. Jr., Mattis, V. B., Lorson, C. L., Thomson, J. A., et al. (2009). Induced pluripotent stem cells from a spinal muscular atrophy patient. *Nature* 457, 277–280. doi: 10.1038/nature07677
- Efthymiou, A. G., Steiner, J., Pavan, W. J., Wincovitch, S., Larson, D. M., Porter, F. D., et al. (2015). Rescue of an *in vitro* neuron phenotype identified in Niemann-Pick disease, type C1 induced pluripotent stem cell-derived neurons by modulating the WNT pathway and calcium signaling. *Stem Cells Transl. Med.* 4, 230–238. doi: 10.5966/sctm.2014-0127
- Eigentler, A., Boesch, S., Schneider, R., Dechant, G., and Nat, R. (2013). Induced pluripotent stem cells from friedreich ataxia patients fail to upregulate frataxin during *in vitro* differentiation to peripheral sensory neurons. *Stem Cells Dev.* 22, 3271–3282. doi: 10.1089/scd.2013.0126
- Emdad, L., D'Souza, S. L., Kothari, H. P., Qadeer, Z. A., and Germano, I. M. (2012). Efficient differentiation of human embryonic and induced pluripotent stem cells into functional astrocytes. *Stem Cells Dev.* 21, 404–410. doi: 10.1089/scd.2010.0560
- Erceg, S., Láinez, S., Ronaghi, M., Stojkovic, P., Pérez-Aragó, M. A., Moreno-Manzano, V., et al. (2008). Differentiation of human embryonic stem cells to regional specific neural precursors in chemically defined medium conditions. *PLoS One* 3:e2122. doi: 10.1371/journal.pone.0002122
- Erceg, S., Ronaghi, M., Zipancic, I., Láinez, S., Roselló, M. G., Xiong, C., et al. (2010). Efficient differentiation of human embryonic stem cells into functional cerebellar-like cells. *Stem Cells Dev.* 19, 1745–1756. doi: 10.1089/scd.2009.0498
- Espuny-Camacho, I., Michelsen, K. A., Gall, D., Linaro, D., Hasche, A., Bonnefont, J., et al. (2013). Pyramidal neurons derived from human pluripotent stem cells integrate efficiently into mouse brain circuits *in vivo*. *Neuron* 77, 440–456. doi: 10.1016/j.neuron.2012.12.011
- Farra, N., Zhang, W. B., Pasceri, P., Eubanks, J. H., Salter, M. W., and Ellis, J. (2012). Rett syndrome induced pluripotent stem cell-derived neurons reveal novel neurophysiological alterations. *Mol. Psychiatry* 17, 1261–1271. doi: 10.1038/mp.2011.180
- Fernandes, T. G., Duarte, S. T., Ghazvini, M., Gaspar, C., Santos, D. C., Porteira, A. R., et al. (2015). Neural commitment of human pluripotent stem cells under defined conditions recapitulates neural development and generates patient-specific neural cells. *Biotechnol. J.* 10, 1578–1588. doi: 10.1002/biot.201400751
- Fuller, H. R., Mandefro, B., Shirran, S. L., Gross, A. R., Kaus, A. S., Botting, C. H., et al. (2016). Spinal muscular atrophy patient iPSC-derived motor neurons have reduced expression of proteins important in neuronal development. *Front. Cell. Neurosci.* 9:506. doi: 10.3389/fncel.2015.00506
- Fusaki, N., Ban, H., Nishiyama, A., Saeki, K., and Hasegawa, M. (2009). Efficient induction of transgene-free human pluripotent stem cells using a vector based on Sendai virus, an RNA virus that does not integrate into the host genome. *Proc. Jpn. Acad. Ser. B Phys. Biol. Sci.* 85, 348–362. doi: 10.2183/pjab.85.348
- Guo, X., Disatnik, M. H., Monbureau, M., Shamloo, M., Mochly-Rosen, D., and Qi, X. (2013). Inhibition of mitochondrial fragmentation diminishes Huntington's disease-associated neurodegeneration. *J. Clin. Invest.* 123, 5371–5388. doi: 10.1172/jci70911
- Halevy, T., Czech, C., and Benvenisty, N. (2015). Molecular mechanisms regulating the defects in fragile X syndrome neurons derived from human pluripotent stem cells. *Stem Cell Reports* 4, 37–46. doi: 10.1016/j.stemcr.2014.10.015
- Havlicek, S., Kohl, Z., Mishra, H. K., Prots, I., Eberhardt, E., Denguir, N., et al. (2014). Gene dosage-dependent rescue of HSP neurite defects in SPG4 patients' neurons. *Hum. Mol. Genet.* 23, 2527–2541. doi: 10.1093/hmg/ddt644
- HD iPSC Consortium. (2012). Induced pluripotent stem cells from patients with Huntington's disease show CAG-repeat-expansion-associated phenotypes. *Cell Stem Cell* 11, 264–278. doi: 10.1016/j.stem.2012.04.027
- Heesen, L., Peitz, M., Torres-Benito, L., Hölker, I., Hupperich, K., Dobrindt, K., et al. (2016). Platin 3 is upregulated in iPSC-derived motoneurons from asymptomatic SMN1-deleted individuals. *Cell. Mol. Life Sci.* 73, 2089–2104. doi: 10.1007/s00018-015-2084-y
- Hick, A., Wattenhofer-Donzé, M., Chintawar, S., Tropel, P., Simard, J. P., Vaucamps, N., et al. (2013). Neurons and cardiomyocytes derived from induced pluripotent stem cells as a model for mitochondrial defects in Friedreich's ataxia. *Dis. Model. Mech.* 6, 608–621. doi: 10.1242/dmm.010900
- Higurashi, N., Uchida, T., Lossin, C., Misumi, Y., Okada, Y., Akamatsu, W., et al. (2013). A human Dravet syndrome model from patient induced pluripotent stem cells. *Mol. Brain* 6:19. doi: 10.1186/1756-6606-6-19
- Hockemeyer, D., Soldner, F., Beard, C., Gao, Q., Mitalipova, M., DeKaveler, R. C., et al. (2009). Efficient targeting of expressed and silent genes in human ESCs and iPSCs using zinc-finger nucleases. *Nat. Biotechnol.* 27, 851–857. doi: 10.1038/nbt.1562
- Hockemeyer, D., Wang, H., Kiani, S., Lai, C. S., Gao, Q., Cassady, J. P., et al. (2011). Genetic engineering of human pluripotent cells using TALE nucleases. *Nat. Biotechnol.* 29, 731–744. doi: 10.1038/nbt.1927
- Hsiao, H. Y., Chiu, F. L., Chen, C. M., Wu, Y. R., Chen, H. M., Chen, Y. C., et al. (2014). Inhibition of soluble tumor necrosis factor is therapeutic in Huntington's disease. *Hum. Mol. Genet.* 23, 4328–4344. doi: 10.1093/hmg/ddu151
- Hu, Y., Qu, Z. Y., Cao, S. Y., Li, Q., Ma, L., Krencik, R., et al. (2016). Directed differentiation of basal forebrain cholinergic neurons from human pluripotent stem cells. *J. Neurosci. Methods* 266, 42–49. doi: 10.1016/j.jneumeth.2016.03.017
- Igoillo-Esteve, M., Gurgul-Convey, E., Hu, A., Romagueira Bichara Dos Santos, L., Abdulkarim, B., Chintawar, S., et al. (2015). Unveiling a common mechanism of apoptosis in β -cells and neurons in Friedreich's ataxia. *Hum. Mol. Genet.* 24, 2274–2286. doi: 10.1093/hmg/ddu745
- Jang, J., Kang, H. C., Kim, H. S., Kim, J. Y., Huh, Y. J., Kim, D. S., et al. (2011). Induced pluripotent stem cell models from X-linked adrenoleukodystrophy patients. *Ann. Neurol.* 70, 402–409. doi: 10.1002/ana.22486
- Jeon, I., Lee, N., Li, J. Y., Park, I. H., Park, K. S., Moon, J., et al. (2012). Neuronal properties, *in vivo* effects and pathology of a Huntington's disease patient-derived induced pluripotent stem cells. *Stem Cells* 30, 2054–2062. doi: 10.1002/stem.1245
- Jiang, H., Ren, Y., Yuen, E. Y., Zhong, P., Ghaedi, M., Hu, Z., et al. (2012). Parkin controls dopamine utilization in human midbrain dopaminergic neurons derived from induced pluripotent stem cells. *Nat. Commun.* 3:668. doi: 10.1038/ncomms1669
- Jiao, J., Yang, Y., Shi, Y., Chen, J., Gao, R., Fan, Y., et al. (2013). Modeling Dravet syndrome using induced pluripotent stem cells (iPSCs) and directly converted neurons. *Hum. Mol. Genet.* 22, 4241–4252. doi: 10.1093/hmg/ddt275
- Jo, J., Xiao, Y., Sun, A. X., Cukuroglu, E., Tran, H. D., Göke, J., et al. (2016). Midbrain-like organoids from human pluripotent stem cells contain functional dopaminergic and neuromelanin-producing neurons. *Cell Stem Cell* 19, 248–257. doi: 10.1016/j.stem.2016.07.005
- Juopperi, T. A., Kim, W. R., Chiang, C. H., Yu, H., Margolis, R. L., Ross, C. A., et al. (2012). Astrocytes generated from patient induced pluripotent stem cells recapitulate features of Huntington's disease patient cells. *Mol. Brain* 5:17. doi: 10.1186/1756-6606-5-17
- Kaufmann, M., Schuffenhauer, A., Fruh, I., Klein, J., Thiemeyer, A., Rigo, P., et al. (2015). High-throughput screening using iPSC-derived neuronal progenitors to identify compounds counteracting epigenetic gene silencing in Fragile X syndrome. *J. Biomol. Screen.* 20, 1101–1111. doi: 10.1177/1087057115588287
- Kim, K. Y., Hysolli, E., and Park, I. H. (2011). Neuronal maturation defect in induced pluripotent stem cells from patients with Rett syndrome. *Proc. Natl. Acad. Sci. U S A* 108, 14169–14174. doi: 10.1073/pnas.1018979108
- Kim, D., Kim, C. H., Moon, J. I., Chung, Y. G., Chang, M. Y., Han, B. S., et al. (2009). Generation of human induced pluripotent stem cells by direct delivery of reprogramming proteins. *Cell Stem Cell* 4, 472–476. doi: 10.1016/j.stem.2009.05.005
- Kimbrel, E. A., and Lanza, R. (2015). Current status of pluripotent stem cells: moving the first therapies to the clinic. *Nat. Rev. Drug Discov.* 14, 681–692. doi: 10.1038/nrd4738
- Kirkeby, A., Grealish, S., Wolf, D. A., Nelander, J., Wood, J., Lundblad, M., et al. (2012). Generation of regionally specified neural progenitors and functional neurons from human embryonic stem cells under defined conditions. *Cell Rep.* 1, 703–714. doi: 10.1016/j.celrep.2012.04.009

- Krey, J. F., Paşca, S. P., Shcheglovitov, A., Yazawa, M., Schwemberger, R., Rasmusson, R., et al. (2013). Timothy syndrome is associated with activity-dependent dendritic retraction in rodent and human neurons. *Nat. Neurosci.* 16, 201–209. doi: 10.1038/nn.3307
- Kriks, S., Shim, J. W., Piao, J., Ganat, Y. M., Wakeman, D. R., Xie, Z., et al. (2011). Dopamine neurons derived from human ES cells efficiently engraft in animal models of Parkinson's disease. *Nature* 480, 547–551. doi: 10.1038/nature10648
- Kumari, D., Swaroop, M., Southall, N., Huang, W., Zheng, W., and Usdin, K. (2015). High-throughput screening to identify compounds that increase fragile X mental retardation protein expression in neural stem cells differentiated from fragile X syndrome patient-derived induced pluripotent stem cells. *Stem Cells Transl. Med.* 4, 800–808. doi: 10.5966/sctm.2014-0278
- Lancaster, M. A., and Knoblich, J. A. (2014). Organogenesis in a dish: modeling development and disease using organoid technologies. *Science* 345:1247125. doi: 10.1126/science.1247125
- Lancaster, M. A., Renner, M., Martin, C. A., Wenzel, D., Bicknell, L. S., Hurler, M. E., et al. (2013). Cerebral organoids model human brain development and microcephaly. *Nature* 501, 373–379. doi: 10.1038/nature12517
- Larimore, J., Ryder, P. V., Kim, K. Y., Ambrose, L. A., Chapple, C., Calfa, G., et al. (2013). MeCP2 regulates the synaptic expression of a Dysbindin-BLOC-1 network component in mouse brain and human induced pluripotent stem cell-derived neurons. *PLoS One* 8:e65069. doi: 10.1371/journal.pone.0065069
- Lee, P., Martin, N. T., Nakamura, K., Azghadi, S., Amiri, M., Ben-David, U., et al. (2013). SMRT compounds abrogate cellular phenotypes of ataxia telangiectasia in neural derivatives of patient-specific hiPSCs. *Nat. Commun.* 4:1824. doi: 10.1038/ncomms2824
- Li, Y., Polak, U., Bhalla, A. D., Rozwadowska, N., Butler, J. S., Lynch, D. R., et al. (2015). Excision of expanded GAA repeats alleviates the molecular phenotype of Friedreich's ataxia. *Mol. Ther.* 23, 1055–1065. doi: 10.1038/mt.2015.41
- Liu, J., Gao, C., Chen, W., Ma, W., Li, X., Shi, Y., et al. (2016). CRISPR/Cas9 facilitates investigation of neural circuit disease using human iPSCs: mechanism of epilepsy caused by an SCN1A loss-of-function mutation. *Transl. Psychiatry* 6:e703. doi: 10.1038/tp.2015.203
- Liu, Y., Lopez-Santiago, L. F., Yuan, Y., Jones, J. M., Zhang, H., O'Malley, H. A., et al. (2013). Dravet syndrome patient-derived neurons suggest a novel epilepsy mechanism. *Ann. Neurol.* 74, 128–139. doi: 10.1002/ana.23897
- Liu, H., Lu, J., Chen, H., Du, Z., Li, X. J., and Zhang, S. C. (2015). Spinal muscular atrophy patient-derived motor neurons exhibit hyperexcitability. *Sci. Rep.* 5:12189. doi: 10.1038/srep12189
- Liu, J., Verma, P. J., Evans-Galea, M. V., Delatycki, M. B., Michalska, A., Leung, J., et al. (2011). Generation of induced pluripotent stem cell lines from Friedreich ataxia patients. *Stem Cell Rev.* 7, 703–713. doi: 10.1007/s12015-010-9210-x
- Livide, G., Patriarchi, T., Amenduni, M., Amabile, S., Yasui, D., Calcagno, E., et al. (2015). GluD1 is a common altered player in neuronal differentiation from both MECP2-mutated and CDKL5-mutated iPS cells. *Eur. J. Hum. Genet.* 23, 195–201. doi: 10.1038/ejhg.2014.81
- Lojewski, X., Staropoli, J. F., Biswas-Legrand, S., Simas, A. M., Haliu, L., Selig, M. K., et al. (2014). Human iPSC models of neuronal ceroid lipofuscinosis capture distinct effects of TPP1 and CLN3 mutations on the endocytic pathway. *Hum. Mol. Genet.* 23, 2005–2022. doi: 10.1093/hmg/ddt596
- Lu, X. H., Mattis, V. B., Wang, N., Al-Ramahi, I., Van den Berg, N., Frattantoni, S. A., et al. (2014). Targeting ATM ameliorates mutant Huntingtin toxicity in cell and animal models of Huntington's disease. *Sci. Transl. Med.* 6:268ra178. doi: 10.1126/scitranslmed.3010523
- Maeda, H., Chiyonobu, T., Yoshida, M., Yamashita, S., Zuiki, M., Kidowaki, S., et al. (2016). Establishment of isogenic iPSCs from an individual with SCN1A mutation mosaicism as a model for investigating neurocognitive impairment in Dravet syndrome. *J. Hum. Genet.* 61, 565–569. doi: 10.1038/jhg.2016.5
- Marchetto, M. C., Carroumeu, C., Acab, A., Yu, D., Yeo, G. W., Mu, Y., et al. (2010). A model for neural development and treatment of Rett syndrome using human induced pluripotent stem cells. *Cell* 143, 527–539. doi: 10.1016/j.cell.2010.10.016
- Mariani, J., Simonini, M. V., Palejev, D., Tomasini, L., Coppola, G., Szekely, A. M., et al. (2012). Modeling human cortical development *in vitro* using induced pluripotent stem cells. *Proc. Natl. Acad. Sci. U S A* 109, 12770–12775. doi: 10.1073/pnas.1202944109
- Marion, R. M., Strati, K., Li, H., Tejera, A., Schoeffner, S., Ortega, S., et al. (2009). Telomeres acquire embryonic stem cell characteristics in induced pluripotent stem cells. *Cell Stem Cell* 4, 141–154. doi: 10.1016/j.stem.2008.12.010
- Maroof, A. M., Keros, S., Tyson, J. A., Ying, S. W., Ganat, Y. M., Merkle, F. T., et al. (2013). Directed differentiation and functional maturation of cortical interneurons from human embryonic stem cells. *Cell Stem Cell* 12, 559–572. doi: 10.1016/j.stem.2013.04.008
- Mastrangelo, L., Kim, J. E., Miyano, A., Kang, T. H., and Friedmann, T. (2012). Purinergic signaling in human pluripotent stem cells is regulated by the housekeeping gene encoding hypoxanthine guanine phosphoribosyltransferase. *Proc. Natl. Acad. Sci. U S A* 109, 3377–3382. doi: 10.1073/pnas.1118067109
- Mattis, V. B., Tom, C., Akimov, S., Saeedian, J., Østergaard, M. E., Southwell, A. L., et al. (2015). HD iPSC-derived neural progenitors accumulate in culture and are susceptible to BDNF withdrawal due to glutamate toxicity. *Hum. Mol. Genet.* 24, 3257–3271. doi: 10.1093/hmg/ddv080
- McGivern, J. V., Patitucci, T. N., Nord, J. A., Barabas, M. E., Stucky, C. L., and Ebert, A. D. (2013). Spinal muscular atrophy astrocytes exhibit abnormal calcium regulation and reduced growth factor production. *Glia* 61, 1418–1428. doi: 10.1002/glia.22522
- Mekhoubad, S., Bock, C., de Boer, A. S., Kiskinis, E., Meissner, A., and Eggan, K. (2012). Erosion of dosage compensation impacts human iPSC disease modeling. *Cell Stem Cell* 10, 595–609. doi: 10.1016/j.stem.2012.02.014
- Miller, J. D., Ganat, Y. M., Kishinevsky, S., Bowman, R. L., Liu, B., Tu, E. Y., et al. (2013). Human iPSC-based modeling of late-onset disease via progerin-induced aging. *Cell Stem Cell* 13, 691–705. doi: 10.1016/j.stem.2013.11.006
- Mishra, H. K., Prots, I., Havlicek, S., Kohl, Z., Perez-Branguli, F., Boerstler, T., et al. (2016). GSK3β-dependent dysregulation of neurodevelopment in SPG11-patient iPSC model. *Ann. Neurol.* doi: 10.1002/ana.24633 [Epub ahead of print].
- Muotri, A. R., Marchetto, M. C., Coufal, N. G., Oefner, R., Yeo, G., Nakashima, K., et al. (2010). L1 retrotransposition in neurons is modulated by MeCP2. *Nature* 468, 443–446. doi: 10.1038/nature09544
- Naylor, S., Gatei, M., Kozlov, S., Gatti, R., Mar, J. C., Wells, C. A., et al. (2012). Induced pluripotent stem cells from ataxia-telangiectasia recapitulate the cellular phenotype. *Stem Cells Transl. Med.* 1, 523–535. doi: 10.5966/sctm.2012-0024
- Ng, S. Y., Soh, B. S., Rodriguez-Muela, N., Hendrickson, D. G., Price, F., Rinn, J. L., et al. (2015). Genome-wide RNA-seq of human motor neurons implicates selective ER stress activation in spinal muscular atrophy. *Cell Stem Cell* 17, 569–584. doi: 10.1016/j.stem.2015.08.003
- Nguyen, H. N., Byers, B., Cord, B., Shcheglovitov, A., Byrne, J., Gujar, P., et al. (2011). LRRK2 mutant iPSC-derived DA neurons demonstrate increased susceptibility to oxidative stress. *Cell Stem Cell* 8, 267–280. doi: 10.1016/j.stem.2011.01.013
- Nicholas, C. R., Chen, J., Tang, Y., Southwell, D. G., Chalmers, N., Vogt, D., et al. (2013). Functional maturation of hPSC-derived forebrain interneurons requires an extended timeline and mimics human neural development. *Cell Stem Cell* 12, 573–586. doi: 10.1016/j.stem.2013.04.005
- Nistor, G. I., Totoiu, M. O., Haque, N., Carpenter, M. K., and Keirstead, H. S. (2005). Human embryonic stem cells differentiate into oligodendrocytes in high purity and myelinate after spinal cord transplantation. *Glia* 49, 385–396. doi: 10.1002/glia.20127
- Nizzardo, M., Simone, C., Dametti, S., Salani, S., Ulzi, G., Pagliarini, S., et al. (2015). Spinal muscular atrophy phenotype is ameliorated in human motor neurons by SMN increase via different novel RNA therapeutic approaches. *Sci. Rep.* 5:11746. doi: 10.1038/srep11746
- Nizzardo, M., Simone, C., Falcone, M., Locatelli, F., Riboldi, G., Comi, G. P., et al. (2010). Human motor neuron generation from embryonic stem cells and induced pluripotent stem cells. *Cell. Mol. Life Sci.* 67, 3837–3847. doi: 10.1007/s00018-010-0463-y
- Ogawa, S., Tokumoto, Y., Miyake, J., and Nagamune, T. (2011). Induction of oligodendrocyte differentiation from adult human fibroblast-derived induced pluripotent stem cells. *In Vitro Cell. Dev. Biol. Anim.* 47, 464–469. doi: 10.1007/s11626-011-9435-2
- Ohuchi, K., Funato, M., Kato, Z., Seki, J., Kawase, C., Tamai, Y., et al. (2016). Established stem cell model of spinal muscular atrophy is applicable in the evaluation of the efficacy of thyrotropin-releasing hormone analog. *Stem Cells Transl. Med.* 5, 152–163. doi: 10.5966/sctm.2015-0059

- Okita, K., Matsumura, Y., Sato, Y., Okada, A., Morizane, A., Okamoto, S., et al. (2011). A more efficient method to generate integration-free human iPSC cells. *Nat. Methods* 8, 409–412. doi: 10.1038/nmeth.1591
- Park, C. Y., Halevy, T., Lee, D. R., Sung, J. J., Lee, J. S., Yanuka, O., et al. (2015). Reversion of FMR1 methylation and silencing by editing the triplet repeats in fragile X iPSC-derived. *Cell Rep.* 13, 234–241. doi: 10.1016/j.celrep.2015.break08.084
- Paşca, S. P., Portmann, T., Voineagu, I., Yazawa, M., Shcheglovitov, A., Paşca, A. M., et al. (2011). Using iPSC-derived neurons to uncover cellular phenotypes associated with Timothy syndrome. *Nat. Med.* 17, 1657–1662. doi: 10.1038/nm.2576
- Patitucci, T. N., and Ebert, A. D. (2016). SMN deficiency does not induce oxidative stress in SMA iPSC-derived astrocytes or motor neurons. *Hum. Mol. Genet.* 25, 514–523. doi: 10.1093/hmg/ddv489
- Pruszak, J., Ludwig, W., Blak, A., Alavian, K., and Isacson, O. (2009). CD15, CD24 and CD29 define a surface biomarker code for neural lineage differentiation of stem cells. *Stem Cells* 27, 2928–2940. doi: 10.1002/stem.211
- Reinhardt, P., Schmid, B., Burbulla, L. F., Schöndorf, D. C., Wagner, L., Glatza, M., et al. (2013). Genetic correction of a LRRK2 mutation in human iPSCs links parkinsonian neurodegeneration to ERK-dependent changes in gene expression. *Cell Stem Cell* 12, 354–367. doi: 10.1016/j.stem.2013.01.008
- Sareen, D., Ebert, A. D., Heins, B. M., McGivern, J. V., Ornelas, L., and Svendsen, C. N. (2012). Inhibition of apoptosis blocks human motor neuron cell death in a stem cell model of spinal muscular atrophy. *PLoS One* 7:e39113. doi: 10.1371/journal.pone.0039113
- Scannell, J. W., Blankley, A., Boldon, H., and Warrington, B. (2012). Diagnosing the decline in pharmaceutical RandD efficiency. *Nat. Rev. Drug Discov.* 11, 191–200. doi: 10.1038/nrd3681
- Schwab, A. J., and Ebert, A. D. (2014). Sensory neurons do not induce motor neuron loss in a human stem cell model of spinal muscular atrophy. *PLoS One* 9:e013112. doi: 10.1371/journal.pone.0103112
- Seibler, P., Graziotto, J., Jeong, H., Simunovic, F., Klein, C., and Krainc, D. (2011). Mitochondrial Parkin recruitment is impaired in neurons derived from mutant PINK1 induced pluripotent stem cells. *J. Neurosci.* 31, 5970–5976. doi: 10.1523/JNEUROSCI.4441-10.2011
- Shan, B., Xu, C., Zhang, Y., Xu, T., Gottesfeld, J. M., and Yates, J. R. (2014). Quantitative proteomic analysis identifies targets and pathways of a 2-aminobenzamide HDAC inhibitor in Friedreich's ataxia patient iPSC-derived neural stem cells. *J. Proteome Res.* 13, 4558–4566. doi: 10.1021/pr500514r
- Shcheglovitov, A., Shcheglovitova, O., Yazawa, M., Portmann, T., Shu, R., Sebastiao, V., et al. (2013). SHANK3 and IGF1 restore synaptic deficits in neurons from 22q13 deletion syndrome patients. *Nature* 503, 267–271. doi: 10.1038/nature12618
- Sheridan, S. D., Theriault, K. M., Reis, S. A., Zhou, F., Madison, J. M., Daheron, L., et al. (2011). Epigenetic characterization of the FMR1 gene and aberrant neurodevelopment in human induced pluripotent stem cell models of fragile X syndrome. *PLoS One* 6:e26203. doi: 10.1371/journal.pone.0026203
- Sirenko, O., Hesley, J., Rusyn, I., and Cromwell, E. F. (2014). High-content high-throughput assays for characterizing the viability and morphology of human iPSC-derived neuronal cultures. *Assay Drug Dev. Technol.* 12, 536–547. doi: 10.1089/adt.2014.592
- Soragni, E., Miao, W., Iudicello, M., Jacoby, D., De Mercanti, S., Clerico, M., et al. (2014). Epigenetic therapy for Friedreich ataxia. *Ann. Neurol.* 76, 489–508. doi: 10.1002/ana.24260
- Srikanth, P., and Young-Pearse, T. L. (2014). Stem cells on the brain: modeling neurodevelopmental and neurodegenerative diseases using human induced pluripotent stem cells. *J. Neurogenet.* 28, 5–29. doi: 10.1016/j.jneurogenet.2014.08.012
- Suhr, S. T., Chang, E. A., Tjong, J., Alcasid, N., Perkins, G. A., Goissis, M. D., et al. (2010). Mitochondrial rejuvenation after induced pluripotency. *PLoS One* 5:e14095. doi: 10.1371/journal.pone.0014095
- Sun, Y., Florer, J., Mayhew, C. N., Jia, Z., Zhao, Z., Xu, K., et al. (2015). Properties of neurons derived from induced pluripotent stem cells of Gaucher disease type 2 patient fibroblasts: potential role in neuropathology. *PLoS One* 10:e0118771. doi: 10.1371/journal.pone.0118771
- Szlachcic, W. J., Switonski, P. M., Krzyzosiak, W. J., Figlerowicz, M., and Figiel, M. (2015). Huntington disease iPSCs show early molecular changes in intracellular signaling, the expression of oxidative stress proteins and the p53 pathway. *Dis. Model. Mech.* 8, 1047–1057. doi: 10.1242/dmm.019406
- Takahashi, K., Tanabe, K., Ohnuki, M., Narita, M., Ichisaka, T., Tomoda, K., et al. (2007). Induction of pluripotent stem cells from adult human fibroblasts by defined factors. *Cell* 131, 861–872. doi: 10.1016/j.cell.2007.11.019
- Takahashi, K., and Yamanaka, S. (2016). A decade of transcription factor-mediated reprogramming to pluripotency. *Nat. Rev. Mol. Cell Biol.* 17, 183–193. doi: 10.1038/nrm.2016.8
- Tang, X., Kim, J., Zhou, L., Wengert, E., Zhang, L., Wu, Z., et al. (2016). KCC2 rescues functional deficits in human neurons derived from patients with Rett syndrome. *Proc. Natl. Acad. Sci. U S A* 113, 751–756. doi: 10.1073/pnas.1524013113
- Thomson, J. A., Itskovitz-Eldor, J., Shapiro, S. S., Waknitz, M. A., Swiergiel, J. J., Marshall, V. S., et al. (1998). Embryonic stem cell lines derived from human blastocysts. *Science* 282, 1145–1147. doi: 10.1126/science.282.5391.1145
- Tian, Y., Voineagu, I., Paşca, S. P., Won, H., Chandran, V., Horvath, S., et al. (2014). Alteration in basal and depolarization induced transcriptional network in iPSC derived neurons from Timothy syndrome. *Genome Med.* 6:75. doi: 10.1186/s13073-014-0075-5
- Tiscornia, G., Vivas, E. L., Matalonga, L., Berniakovich, I., Barragán Monasterio, M., Eguizabal, C., et al. (2013). Neuronopathic Gaucher's disease: induced pluripotent stem cells for disease modelling and testing chaperone activity of small compounds. *Hum. Mol. Genet.* 22, 633–645. doi: 10.1093/hmg/ddt471
- Toli, D., Buttigieg, D., Blanchard, S., Lemonnier, T., Lamotte d'Incamps, B., Bellouze, S., et al. (2015). Modeling amyotrophic lateral sclerosis in pure human iPSC-derived motor neurons isolated by a novel FACS double selection technique. *Neurobiol. Dis.* 82, 269–280. doi: 10.1016/j.nbd.2015.06.011
- Trilck, M., Hübner, R., and Frech, M. J. (2016). Generation and neuronal differentiation of patient-specific induced pluripotent stem cells derived from niemann-pick type C1 fibroblasts. *Methods Mol. Biol.* 1353, 233–259. doi: 10.1007/7651_2014_166
- Trilck, M., Hübner, R., Seibler, P., Klein, C., Rolfs, A., and Frech, M. J. (2013). Niemann-Pick type C1 patient-specific induced pluripotent stem cells display disease specific hallmarks. *Orphanet J. Rare Dis.* 8:144. doi: 10.1186/1750-1172-8-144
- Urbach, A., Bar-Nur, O., Daley, G. Q., and Benvenisty, N. (2010). Differential modeling of fragile X syndrome by human embryonic stem cells and induced pluripotent stem cells. *Cell Stem Cell* 6, 407–411. doi: 10.1016/j.stem.2010.04.005
- Vera, E., and Studer, L. (2015). When rejuvenation is a problem: challenges of modeling late-onset neurodegenerative disease. *Development* 142, 3085–3089. doi: 10.1242/dev.120667
- Vessoni, A. T., Herai, R. H., Karpiak, J. V., Leal, A. M., Trujillo, C. A., Quinet, A., et al. (2016). Cockayne syndrome-derived neurons display reduced synapse density and altered neural network synchrony. *Hum. Mol. Genet.* 25, 1271–1280. doi: 10.1093/hmg/ddw008
- Wada, T., Honda, M., Minami, I., Tooi, N., Amagai, Y., Nakatsuji, N., et al. (2009). Highly efficient differentiation and enrichment of spinal motor neurons derived from human and monkey embryonic stem cells. *PLoS One* 4:e6722. doi: 10.1371/journal.pone.0006722
- Warren, L., Manos, P. D., Ahfeldt, T., Loh, Y. H., Li, H., Lau, F., et al. (2010). Highly efficient reprogramming to pluripotency and directed differentiation of human cells with synthetic modified mRNA. *Cell Stem Cell* 7, 618–630. doi: 10.1016/j.stem.2010.08.012
- Wicklund, L., Leão, R. N., Strömberg, A. M., Mousavi, M., Hovatta, O., Nordberg, A., et al. (2010). β -amyloid 1–42 oligomers impair function of human embryonic stem cell-derived forebrain cholinergic neurons. *PLoS One* 5:e15600. doi: 10.1371/journal.pone.0015600
- Williams, E. C., Zhong, X., Mohamed, A., Li, R., Liu, Y., Dong, Q., et al. (2014). Mutant astrocytes differentiated from Rett syndrome patients-specific iPSCs have adverse effects on wild-type neurons. *Hum. Mol. Genet.* 23, 2968–2980. doi: 10.1093/hmg/ddu008

- Xu, C. C., Denton, K. R., Wang, Z. B., Zhang, X., and Li, X. J. (2016). Abnormal mitochondrial transport and morphology as early pathological changes in human models of spinal muscular atrophy. *Dis. Model. Mech.* 9, 39–49. doi: 10.1242/dmm.021766
- Yamashita, S., Chiyonobu, T., Yoshida, M., Maeda, H., Zuiki, M., Kidowaki, S., et al. (2016). Mislocalization of syntaxin-1 and impaired neurite growth observed in a human iPSC model for STXBP1-related epileptic encephalopathy. *Epilepsia* 57, e81–e86. doi: 10.1111/epi.13338
- Yoshida, M., Kitaoka, S., Egawa, N., Yamane, M., Ikeda, R., Tsukita, K., et al. (2015). Modeling the early phenotype at the neuromuscular junction of spinal muscular atrophy using patient-derived iPSCs. *Stem Cell Reports* 4, 561–568. doi: 10.1016/j.stemcr.2015.02.010
- Yuan, S. H., Martin, J., Elia, J., Flippin, J., Paramban, R. I., Hefferan, M. P., et al. (2011). Cell-surface marker signatures for the isolation of neural stem cells, glia and neurons derived from human pluripotent stem cells. *PLoS One* 6:e17540. doi: 10.1371/journal.pone.0017540
- Zhang, Z. N., Freitas, B. C., Qian, H., Lux, J., Acab, A., Trujillo, C. A., et al. (2016). Layered hydrogels accelerate iPSC-derived neuronal maturation and reveal migration defects caused by MeCP2 dysfunction. *Proc. Natl. Acad. Sci. U S A* 113, 3185–3190. doi: 10.1073/pnas.1521255113
- Zhou, W., and Freed, C. R. (2009). Adenoviral gene delivery can reprogram human fibroblasts to induced pluripotent stem cells. *Stem Cells* 27, 2667–2674. doi: 10.1002/stem.201
- Zhu, P. P., Denton, K. R., Pierson, T. M., Li, X. J., and Blackstone, C. (2014). Pharmacologic rescue of axon growth defects in a human iPSC model of hereditary spastic paraplegia SPG3A. *Hum. Mol. Genet.* 23, 5638–5648. doi: 10.1093/hmg/ddu280
- Conflict of Interest Statement:** The authors declare that the research was conducted in the absence of any commercial or financial relationships that could be construed as a potential conflict of interest.
- The handling Editor declared a shared affiliation, though no other collaboration, with the authors SB, MAK and states that the process nevertheless met the standards of a fair and objective review.
- Copyright © 2016 Barral and Kurian. This is an open-access article distributed under the terms of the Creative Commons Attribution License (CC BY). The use, distribution and reproduction in other forums is permitted, provided the original author(s) or licensor are credited and that the original publication in this journal is cited, in accordance with accepted academic practice. No use, distribution or reproduction is permitted which does not comply with these terms.



Precision Medicine in Multiple Sclerosis: Future of PET Imaging of Inflammation and Reactive Astrocytes

Pekka Poutiainen¹, Merja Jaronen², Francisco J. Quintana² and Anna-Liisa Brownell^{1*}

¹ Athinoula A Martinos Biomedical Imaging Center, Department of Radiology, Massachusetts General Hospital, Harvard Medical School, Charlestown, MA, USA, ² Ann Romney Center for Neurologic Diseases, Brigham and Women's Hospital, Harvard Medical School, Boston, MA, USA

OPEN ACCESS

Edited by:

Kirsten Harvey,
University College London, UK

Reviewed by:

Hartmut Lüddens,
University of Mainz, Germany
Samaneh Maysami,
University of Manchester, UK

*Correspondence:

Anna-Liisa Brownell
abrownell@mgh.harvard.edu

Received: 08 May 2016

Accepted: 30 August 2016

Published: 15 September 2016

Citation:

Poutiainen P, Jaronen M, Quintana FJ and Brownell A-L (2016) Precision Medicine in Multiple Sclerosis: Future of PET Imaging of Inflammation and Reactive Astrocytes. *Front. Mol. Neurosci.* 9:85. doi: 10.3389/fnmol.2016.00085

Non-invasive molecular imaging techniques can enhance diagnosis to achieve successful treatment, as well as reveal underlying pathogenic mechanisms in disorders such as multiple sclerosis (MS). The cooperation of advanced multimodal imaging techniques and increased knowledge of the MS disease mechanism allows both monitoring of neuronal network and therapeutic outcome as well as the tools to discover novel therapeutic targets. Diverse imaging modalities provide reliable diagnostic and prognostic platforms to better achieve precision medicine. Traditionally, magnetic resonance imaging (MRI) has been considered the golden standard in MS research and diagnosis. However, positron emission tomography (PET) imaging can provide functional information of molecular biology in detail even prior to anatomic changes, allowing close follow up of disease progression and treatment response. The recent findings support three major neuroinflammation components in MS: astrogliosis, cytokine elevation, and significant changes in specific proteins, which offer a great variety of specific targets for imaging purposes. Regardless of the fact that imaging of astrocyte function is still a young field and in need for development of suitable imaging ligands, recent studies have shown that inflammation and astrocyte activation are related to progression of MS. MS is a complex disease, which requires understanding of disease mechanisms for successful treatment. PET is a precise non-invasive imaging method for biochemical functions and has potential to enhance early and accurate diagnosis for precision therapy of MS. In this review we focus on modulation of different receptor systems and inflammatory aspect of MS, especially on activation of glial cells, and summarize the recent findings of PET imaging in MS and present the most potent targets for new biomarkers with the main focus on experimental MS research.

Keywords: multiple sclerosis, inflammation, neuroreceptors, positron emission tomography, precision medicine, microglia, astrocyte

INTRODUCTION

Multiple sclerosis (MS) is the most common disabling neurologic disease of young people, afflicting approximately a quarter of million Americans (Anderson et al., 1992; Islam et al., 2006; Brody, 2012; Ransohoff et al., 2015). It occurs more in women than in men by a ratio of nearly 2 to 1, and it strikes most often between the ages of 20 and 40 (Compston and Coles, 2008). MS results from the immune-driven demyelination of the central nervous system (CNS), which leads to axonal damage and progressive loss of neurological functions (Sofroniew and Vinters, 2010; Malpass, 2012; Sofroniew, 2015). Based on clinical characteristics, MS pathology can be divided into three different disease courses: relapsing-remitting (RR), secondary progressive (SP), and primary progressive (PP) (Goodin, 2014). Initially, most MS patients exhibit a RR-MS disease course (Morales et al., 2006), experiencing heterogeneous symptoms such as ataxia, visual disturbances, paresthesia, and muscle weakness (Ellwardt and Zipp, 2014). However, eventually the majority of these patients develop SP-MS characterized by the progressive and irreversible accumulation of neurological disability (Lublin and Reingold, 1996). PP-MS patients have continuous disease progression from onset, without relapses or remissions (Morales et al., 2006; Lopez-Diego and Weiner, 2008).

Recent findings of the innate and the adaptive immune system of CNS have shaken up the classical view of MS as being strictly an autoimmune disease of the white matter (Weiner, 2008; Gandhi et al., 2010; Hemmer et al., 2015). The studies have revealed the important role of infiltrating immune cells from the periphery as well as the role of resident activated glial cells leading ultimately to the T cells and macrophages reaction against myelin (see **Figure 1**) (Frohman et al., 2006; Compston and Coles, 2008). These advances have switched the focus of MS research toward neurodegenerative aspects of the disease, occurring early in the pathological process (Kiferle et al., 2011). Despite the recent progresses in the field of MS therapeutic strategies there is no curative treatment for progressive MS (Lopez-Diego and Weiner, 2008; Derwenskus and Lublin, 2014). Therefore, identifying new specific biomarkers for MS could reveal new potential drug targets and diagnostic markers. Moreover, there is an unmet clinical need for methods to monitor different mechanisms of disease pathogenesis in MS patients, therefore advanced non-invasive molecular imaging technologies are needed to expand our understanding of the controversial aspects of the MS pathology (Kiferle et al., 2011; Jacobs and Tavitian, 2012).

Historically, MRI has overruled other imaging technologies in the diagnosis of MS (Traboulsee and Li, 2006; Barkhof and Filippi, 2009). The classical McDonald criterion for MS diagnosis requires objective dissemination of lesions in time and space (Filippi and Rocca, 2011). The literature analysis has shown that the sensitivity of MRI has been between 35 and 100%, and specificity has been between 36 and 92% depending on the research protocol (Schäffler et al., 2011; Tillema and Pirko, 2013). Overall, T2-weighted MRI is effective way to detect MS lesions, but because the signal reflects the water content, it does not provide reliable information about the myelin content

(Ge, 2006; Poloni et al., 2011). T1-weighted imaging together with contrast agents such as gadolinium-DTPA has increased the lesion detection sensitivity, however, signal frequency is associated with the opening of the blood brain barrier (BBB; Lund et al., 2013). This leads to the problem that MRI can vary greatly in terms of sensitivity and specificity, especially in MS-related pathological pathways (Barkhof et al., 2009; Lövblad et al., 2010). Early diagnosis and treatment is effective for the therapy and decreases the financial burden of the disease (Noyes et al., 2011; Guo et al., 2014). The annual mean cost is around \$47,000 per MS patient, which arises to a national cost of about \$13 billion in US per year (Olek, 2012). The disease modifying treatments (DMTs, typically used first-line interferon betas and glatiramer acetate) have been available for the last 25 years and are estimated to account for one third of the total cost. Unfortunately, these treatments suppress the disease only for a few years (Hartung et al., 2015) and the spectrum of treatment options is narrow (Oh and O'Connor, 2015). Conventional MRI gives anatomical information from the progressed lesions in the brain of MS patients but lacks the power to provide target for drug discovery and more specific molecular markers when compared to imaging modalities like positron emission tomography (PET; Filippi et al., 2012; Matthews et al., 2012).

PET research field is emerging and the researchers have been successful in developing novel tracers for multiple different aspects of MS to enhance understanding the pathophysiology of the disease. In this review, we summarize PET imaging in MS research and introduce some of the most potent imaging targets and applications that have been successfully investigated in inflammation and which can be implemented especially to astrocyte activation related pathways, which are presently of high interest in MS research (Maragakis and Rothstein, 2006; Nair et al., 2008; Miljković et al., 2011; Nash et al., 2011; Mayo et al., 2014).

PET IMAGING TECHNIQUES

PET imaging is based on detection of isotope labeled tracers, which emit beta radiation (see **Table 1**). These tracers are administered into the subjects to monitor underlying biological processes (Kiferle et al., 2011). The radioisotope undergoes positron emission decay and emits positron, which travels into surrounding tissue until it interacts with an electron and the annihilation process takes part (see **Figure 2**). The formed two photons travel in approximately opposite directions and can be detected with the imaging device as a coincidence pair. Each detected coincident forms a line of response (LOR) where the point of origin is the location of annihilation event. The combination of LORs can be used for reconstruction of images to provide 3-dimensional (3D) distribution of the radiolabeled tracer (Gambhir, 2002).

The clinical history of positron emission techniques started in 1952 when Gordon Brownell was able to localize brain tumors from patients (Brownell and Sweet, 1953). Further technical progression led to 3D tomographical positron imaging by 1971 (Pizer et al., 1971). However, even today PET suffers

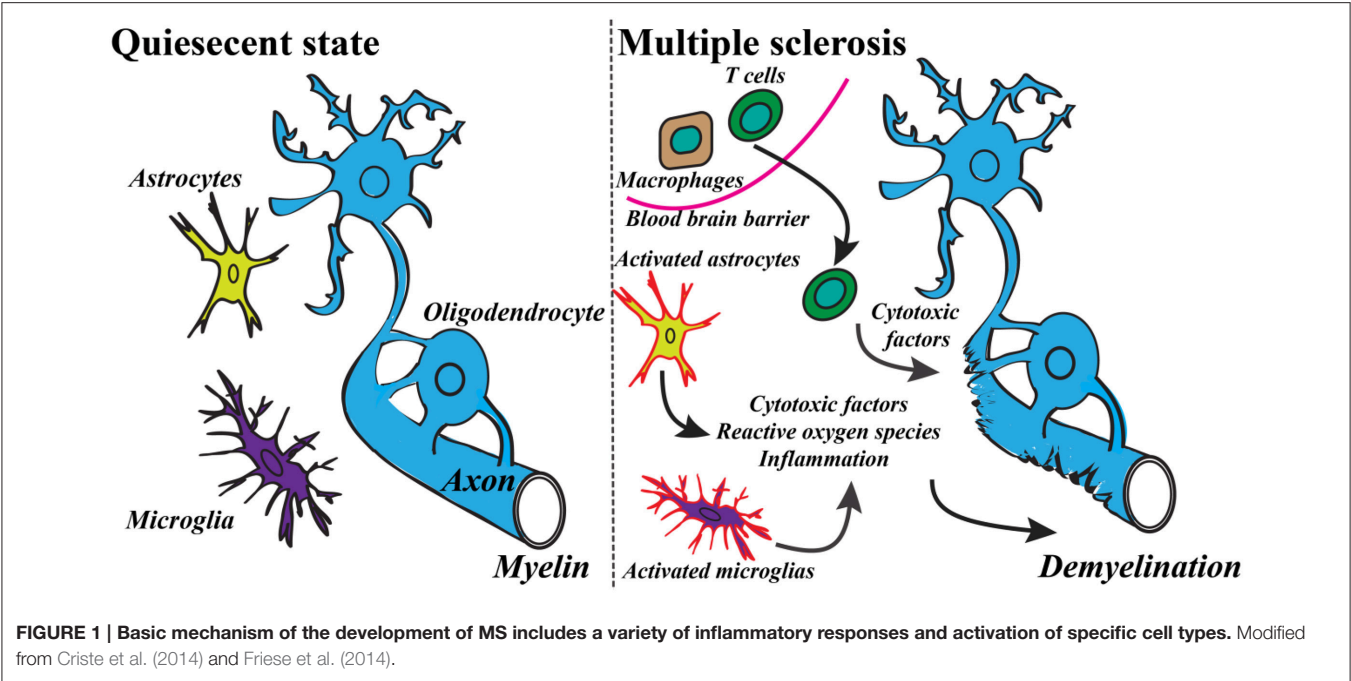


TABLE 1 | Properties of discussed positron emitting radio-isotopes.

Isotope	Half-life (min)	Production method	Positron range in (mm)	Maximum positron energy (MeV)
¹¹ C	20.3	Cyclotron	1.1	0.96
¹³ N	9.97	Cyclotron	1.5	1.19
¹⁸ F	109.8	Cyclotron	0.6	0.64
⁶⁴ Cu	764	Cyclotron	0.6	0.65
⁶⁸ Ga	67.8	Generator	2.9	1.89
⁸² Rb	1.26	Generator	5.9	3.15

Saha et al., 1994; Partridge et al., 2006; Miller et al., 2008; Jodal et al., 2012.

from high cost because the production of radiopharmaceutical agents increase the imaging cost compared to CT or MRI, both which became available later. After the development of [¹⁸F]fluorodeoxy glucose ([¹⁸F]FDG) PET imaging received more significant clinical role especially in oncological diagnosis (Portnow et al., 2013). In MS however, MRI has been regarded as the golden standard in assessing patients (Filippi et al., 2012; Miller et al., 2012). Combined PET/MRI imaging with high specificity to MS lesions, would have a potential to become a practical tool in clinics to follow up the treatment of MS patients and increase cost-effectiveness. This approach could reveal an optimized treatment regimen; increase the treatment effectiveness and safety of patients, especially in early stage and patients with aggressive disease (Catana et al., 2013). When comparing these two imaging techniques, PET imaging has at least four major advantages over conventional MR imaging: (Massoud, 2003; Kiferle et al., 2011; Poloni et al., 2011; Jacobs and Tavitian, 2012; Miller et al., 2012; Torigian et al., 2013; Faria Dde et al., 2014; Jadvar and Colletti, 2014; Bodini et al., 2015) (1) Specific information of disease mechanism

and molecular contributors, (2) Enhance development of new medicines and therapeutic targets, (3) Efficient allocation of new costly therapeutics and personalized medicine, and (4) Improved prognostic method for the MS patients.

Although the first clinical positron emission imaging studies were done over 60 years ago, the spectrum of applications of PET imaging is still limited due to the high cost and lack of validated traces and state-of-the-art facilities including availability of cyclotrons and automated radiopharmaceutical production laboratories (Jones et al., 2012). Complete knowledge about pharmacokinetic and pharmacodynamic properties of injected tracers can assure the correct interpretation of the images from preclinical and clinical studies. Overall, PET is an extremely powerful technology and the *in vivo* receptor occupancy can help answer many vital questions in the MS research (Matthews et al., 2012; Bodini et al., 2015). Furthermore, PET offers an opportunity for the detection of enzyme reactions, ligand-receptor interactions, cellular metabolism, cell proliferation, protein-protein interactions, as well as gene and cell therapy (Herschman, 2003; Ono, 2009; Thorek et al., 2013). The development of new PET tracers is challenging because the binding affinity and selectivity of the tracer have to be high and the dissociation must be fast enough to obtain the binding equilibrium in time frame of scan (1–2 h) (Hicks, 2006; Sharma et al., 2010). The tracer should penetrate the BBB, but too lipophilic compound might have strong non-specific binding (Liu et al., 2008). The optimal radiotracer should have minimum amount of unwanted metabolism and fast synthetic method (usually in single half-life of the radioisotope).

PET imaging systems have been developed also for small animals enhancing significantly basic research. Modern micro-PET instrumentation (resolution < 1 mm) is rapidly expanding the use of non-invasive PET imaging techniques in

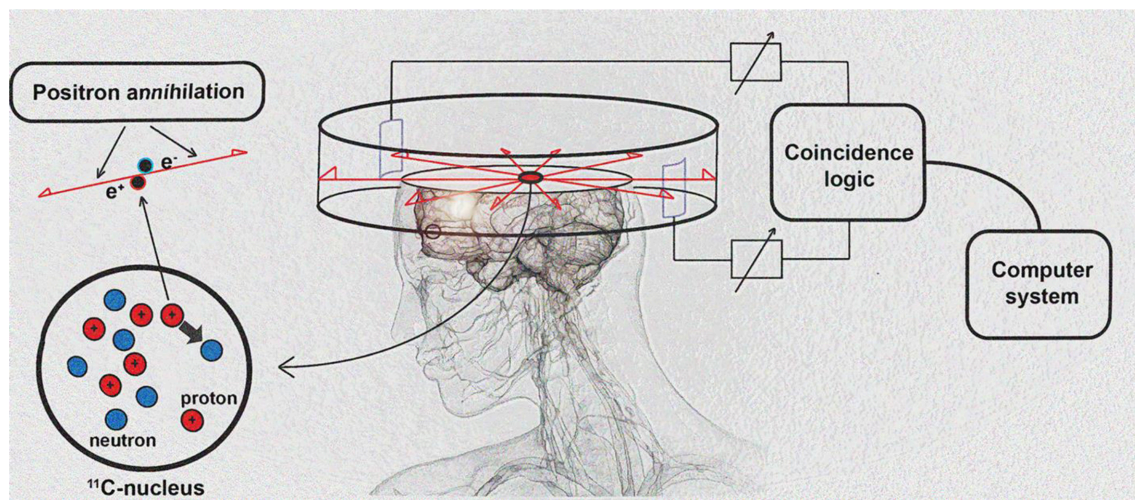


FIGURE 2 | Schematic diagram of positron detection. Modified from Brownell (2008).

basic research. These advances have been progressively translated to human studies (Herschman, 2003; Liang et al., 2007; Lancelot and Zimmer, 2010). PET imaging offers tools to evaluate a great variety of molecular aspects of MS and neurodegeneration in animal models as well as in clinics (see **Figures 3, 4**).

PRECLINICAL MODELS FOR MS

Several animal models are used to study mechanisms of disease pathogenesis relevant for MS (Furlan et al., 2009; Denic et al., 2011; Ransohoff, 2012). Experimental autoimmune encephalomyelitis (EAE) is the most vividly used animal model especially to study the inflammation aspects of MS. In this model, rodents are immunized with myelin antigens to activate peripheral antigen specific T-cells, which travel to CNS and induce formation of demyelinating lesion (Baxter, 2007; Constantinescu et al., 2011). Based on the hypothesis that viral infections may cause MS, virus-induced demyelination animal models are also used to study the disease (Gilden, 2005; Owens et al., 2011; Tselis, 2012). A disadvantage of this model is that the experimental disease manifests months after the initial infection (Olson et al., 2001; Fatima et al., 2010). Demyelination and spontaneous remyelination processes relevant to MS are predominantly studied using toxin-induced models (Blakemore and Franklin, 2008). The induction with copper chelating agent, Cuprizone [oxalic acid bis(cyclohexylidene hydrazide)], is one of the frequently used methods, since it is highly reproducible, relatively simple, induces fast demyelination, and the model has spontaneous remyelination after halting the toxin exposure (Torkildsen et al., 2008; Kipp et al., 2009). The focal demyelination lesions are commonly induced with ethidium bromide and lysolecithin (Woodruff and Franklin, 1999). The small size of the disease model increases the technical aspects for imaging technology. In the following chapters we will discuss the current tracers designed to detect the main pathological features of MS.

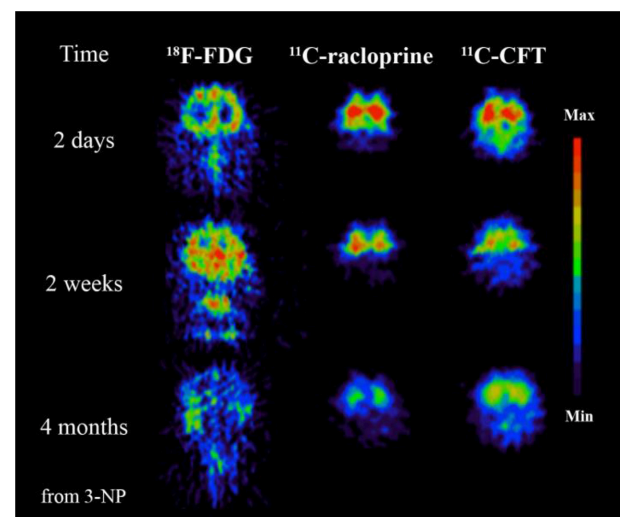


FIGURE 3 | 3-Nitropropionic acid (3-NP, a naturally occurring plant toxin and mycotoxin) could be involved to the development of MS. This study demonstrates the advantages of PET imaging where specific tracers can be used to reveal different time dependent neurochemical processes. In this case significant decrease of glucose metabolism imaged by ^{18}F -FDG, decrease of dopamine D2 receptor function imaged by ^{11}C -raclopride and decrease of dopamine transporter function imaged with ^{11}C -CFT follow after 3-NP administration. Modified from Brownell et al. (2004).

PET IMAGING OF AXONAL DEGENERATION

The complex network of conditions leading to neuroaxonal degeneration and neuronal loss contribute the permanent disability related to MS pathology (Frieze et al., 2014). Even though during the earlier days of MS research, axonal loss was considered to be late-occurring, it is now discovered to happen also in the early stages of MS (Trapp and Nave, 2008; Trapp

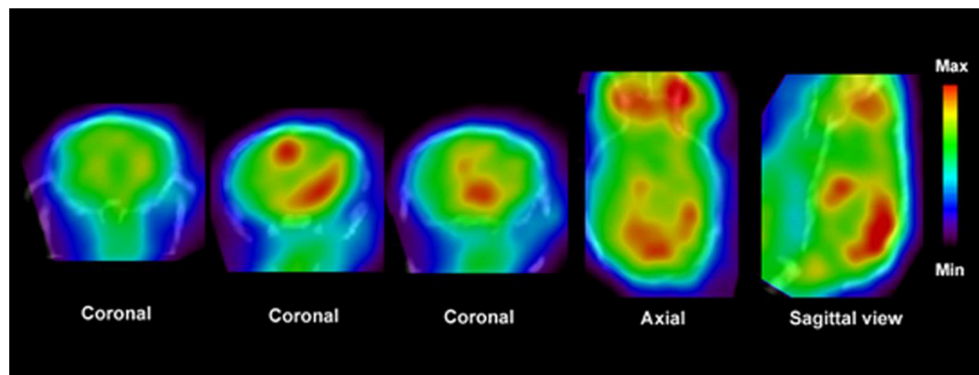


FIGURE 4 | PET images show distribution of $[^{11}\text{C}]\text{PBR28}$ in the brain of an EAE mouse model. Fused CT images show the boundaries of the skull. Enhanced accumulation of $[^{11}\text{C}]\text{PBR28}$ in the hind brain and cerebellum is an indication of regionally activated microglia. Modified from Radu et al. (2007) and Arsenault et al. (2014).

and Stys, 2009). In the earlier phases of the disease axonal damage can occur acutely in the new inflammatory lesions. Whereas later in the disease progression axonal damage is usually related to chronic and demyelinated regions and there is only little if any active inflammation present (Criste et al., 2014). In addition, there is growing amount of evidence from both MRI and histological studies proposing that the axonal degeneration contributes to the development of clinical disability (Edgar and Nave, 2009; Nave, 2010). These interesting facts further highlight the need of specific markers for imaging of disease stage.

Currently, the most promising marker for neuronal integrity is benzodiazepine site on the GABA_A receptor (Sigel and Buhr, 1997). Flumazenil, antagonist for benzodiazepine site, has been already labeled with ^{18}F and ^{11}C (Suzuki et al., 1985; The MICAD Research Team, 2004). Interestingly, in MS patients the axonal reduction has been demonstrated with the use of $[^{11}\text{C}]\text{flumazenil}$ (Barkhof et al., 2009). Furthermore, it has been shown that focal brain inflammation causes reduced GABA_A mediated inhibition in neurons (Rossi et al., 2012). In addition, the inhibition is also induced in gray matter in the acute relapsing phases of MS (Rossi et al., 2012). Rossi et al. suggest that neurodegeneration in white and gray matter lesions are accompanied by a loss of GABA_A receptors. PET could visualize this with radiolabeled flumazenil. However, this strategy remains yet to be tested.

Another cell type, which suffers from axonal loss during MS, is cholinergic neurons (D'Intino et al., 2005). Degradation of these neurons can, at least partly, contribute to the cognitive impairment of the MS patients (Kooi et al., 2011). Interestingly, when assessing the acetylcholinesterase (AChE) activity by $[^{11}\text{C}]\text{MP4A}$ (^{11}C -methyl-4-piper-idinylpropionate), an inverse correlation with the activity of AChE and cognitive impairment was observed in MS patients (Virta et al., 2011). This result is contradicting the demonstrated positive response seen in MS patients with AChE inhibitors (Krupp et al., 2004; Tsao and Heilman, 2005). However, it has been hypothesized that the controversial results with increased AChE expression might be due to induction by inflammatory response in glial cells (Virta et al., 2011).

In addition, the reduction of glucose metabolism in the degenerated regions has shown correlation between disease activity, hypo-metabolism and specific cognitive functions during the MS progression (Bakshi et al., 1998). $[^{18}\text{F}]\text{FDG}$ has some valuable characteristics for monitoring cognitive and mental dysfunctions associated with MS (Paulesu et al., 1996; Zarei, 2003; Buck et al., 2012; Colasanti et al., 2014).

PET IMAGING OF DEMYELINATION

Demyelination, the pathological removal of myelin sheaths surrounding the axons, has been thought to be an integral part of axonal degeneration, as chronic CNS demyelination has been demonstrated to lead to axonal pathology and degeneration (Wilkins et al., 2010). However, these two events can happen independently from one another as axonal degeneration has been demonstrated to occur without myelin loss (Nave, 2010) and recently it has been demonstrated that the loss of myelin does not necessarily lead to axonal degeneration (Smith et al., 2013).

Classically in MS, demyelination is thought to cause the axonal dysfunction and disease-related pathogen conditions (Lucchinetti et al., 2000). On the other hand, spontaneous remyelination, executed by oligodendrocytes that mature from oligodendrocyte precursor cells, may occur following demyelination, presumably allowing a partial, if not complete, recovery from disability (Brück, 2005; Compston and Coles, 2008). Both adaptive and innate immune systems control the fine balance between demyelination and remyelination during MS and determine the outcome of the disease (Zhang et al., 2013). However, recently researchers have demonstrated early loss of both neurons and oligodendrocytes, leading to the question whether inflammatory demyelination is primary or secondary in the disease process of MS (Trapp and Nave, 2008). Remyelination is usually seen to occur in the early phases of the disease, whereas in the later phases it fails to recover the demyelinated areas leading to chronic demyelinated lesions (Chang et al., 2002; Kuhlmann et al., 2008).

Several tracers have been developed to target the β -sheet structures of intact myelin (Wu et al., 2006; Mallik et al., 2014). The first tracer, [^{11}C]BMB (1,4-bis(p-aminostyryl)-[^{11}C]2-methoxy benzene), had significant off-target affinity toward white and gray matter (Stankoff et al., 2006). Some of these downsides have been overcome with Congo red derivatives (e.g. [^{11}C]CIC, Case Imaging Compound) and thioflavine-T derivatives (e.g. [^{11}C]PIB, N-methyl-[^{11}C]2-(4'-methylaminophenyl)-6-hydroxybenzothiazole). Moreover, these tracers have more reliable production and BBB penetration (Wang et al., 2009; Stankoff et al., 2011). Recent comparisons between these series and new [^{11}C]MeDAS, (N-[^{11}C]methyl-4,4'-diaminostilbene) tracers prefer the latter compound as the most promising ligand so far to detect MS-like lesions and spinal cord imaging (de Paula Faria et al., 2014b). [^{11}C]MeDAS has been successfully used to image acute focal neuroinflammation in the brain, lyso-phosphatidyl choline induced focal demyelination in the spinal cord and EAE rodent models of MS (Wu et al., 2013). Furthermore, [^{11}C]MeDAS was also able to highlight both demyelination and remyelination processes in cuprizone mouse model (de Paula Faria et al., 2014b). Interestingly, the uptake of [^{11}C]MeDAS was not interfered by inflammation (Wu et al., 2013). The current literature suggest that [^{11}C]MeDAS is the most preferred PET agent so far to highlight the lesions as well as the myelin content in the spinal cord in motor disability related MS (de Paula Faria et al., 2014a). To this point the only PET tracer used to image myelin in MS patients is [^{11}C]PIB, a tracer widely utilized to visualize β -amyloid plaques in Alzheimer's disease (Stankoff et al., 2011; Zhang et al., 2014).

Altogether, PET imaging of myelin integrity shows great potential in animal models of MS. It is interesting to validate these methods in patients, especially now that new remyelination therapies are introduced in clinical trials (Brugarolas and Popko, 2014).

PET IMAGING OF MICROGLIAL ACTIVATION

Neuroinflammation is a common characteristic of numerous neurodegenerative disorders, including MS (Glass et al., 2010). Reactive states of astrocytes (astrogliosis), and microglia (microgliosis), as well as the infiltration of the lymphocytes are the hallmarks of neuroinflammation (Carson et al., 2006). Although factors inducing inflammation vary between CNS related diseases, there is evidence that convergence mechanisms are accountable for the sensing, transduction, and amplification of inflammatory processes that eventually lead to the production of neurotoxic mediators (Glass et al., 2010). In fact, neuroinflammation is a highly dynamic and complex process combining local and systemic reactions of multiple cell types, chemical signals, and signaling pathways to adaptive response for restoring tissue homeostasis (Medzhitov, 2008; Aguzzi et al., 2013; Naegelé and Martin, 2014). In the following, we will discuss the PET tracers used to visualize microglial and astrocytic activation.

Microglia are of mesenchymal origin and constantly monitor the extracellular environment as well as interact closely with astrocytes and neurons (Yamasaki et al., 2014; Michell-Robinson et al., 2015). As macrophages in the periphery, microglia are the first line of defense against infections or insults in the CNS (Olson et al., 2001; Hanisch and Kettenmann, 2007; Nau et al., 2014). Upon activation, microglia acquire an amoeboid appearance and secrete pro-inflammatory molecules such as interleukin 1β , interferon γ , and tumor necrosis factor- α (TNF α) (Boche et al., 2013): a classically activated M1 state (Mills et al., 2000; Martinez and Gordon, 2014). The aim of the pro-inflammatory reaction is to clear the hazardous material and correct the inflicted damage (Gordon, 2003; Martinez et al., 2009). Usually, the pro-inflammatory reaction is down-regulated by the anti-inflammatory molecules (Tambuyzer et al., 2009; Scheller et al., 2011). In addition to pro-inflammatory molecules, microglia can release trophic and anti-inflammatory factors such as interleukins 4 and 10 as well as insulin-like growth factor 1 (Cherry et al., 2014). These factors are aimed to contribute to the repair and limitation of the inflammation (Mantovani et al., 2004; Hanisch and Kettenmann, 2007; Michelucci et al., 2009). Astrocytes and inflammatory T-cell subsets surrounding microglia influence the state of microglia, and determine whether they are releasing pro- or anti-inflammatory factors (Shih, 2006; Goverman, 2009; Mayo et al., 2012, 2014; Quintana et al., 2014).

The role of microglial activation in MS progression has remained enigmatic (Correale, 2014). However, several theories have been offered. The first theory suggests that inflammatory processes similar to those observed in RR-MS cause the brain damage (Kutzelnigg and Lassmann, 2014). However, during the progressive disease stages, a microenvironment is created within the brain favoring the homing and retention of inflammatory cells, finally resulting in the failure of disease-modifying therapies (Frischer et al., 2009). According to the second theory, MS starts out as an inflammatory disease and after several years, neurodegeneration, a process autonomous of inflammatory response, becomes the mechanism responsible for progression of the disease (Meuth et al., 2008; Kutzelnigg and Lassmann, 2014). Finally, MS could be seen primarily as a neurodegenerative disease, where inflammation occurs as a secondary response, augmenting and modifying progressive stages (Kassmann et al., 2007; Fitzner and Simons, 2010). Needless to say, these theories are not mutually exclusive. Furthermore, it has been postulated that the lack of understanding the exact microglial function during course of MS, has led to the absence of therapies for SP-MS (Correale, 2014). Altogether, this clearly demonstrates the need for a consensus and better understanding of microglial activation, which can only be achieved by using appropriate methodology.

Inflammation related PET studies in MS are traditionally focused on monitoring changes in glucose metabolism and the presence of activated microglia/macrophages in sclerotic lesions (Schiepers et al., 1997; Kiferle et al., 2011). [^{18}F]FDG was recently used to evaluate the inflammation in the spinal cord in the EAE rat model (Buck et al., 2012). However, the basal uptake of glucose is elevated in the brain reducing the usability of [^{18}F]FDG as a marker for brain lesions. Results of different stage patients indicate that [^{18}F]FDG could be used to classify white matter

lesions as either acute (hyper metabolism) or chronic (hypo metabolism) based on the glucose consumption (Paulesu et al., 1996; Dimitrakopoulou-Strauss et al., 2004; Buck et al., 2012). It is obvious that more specific markers are required to image the inflammation related metabolism in MS.

The majority of current PET tracers used to detect microglial activation utilize the expression of the peripheral benzodiazepine receptor (PBR), also known as the translocator protein TSPO (18 kDa) (Ryu et al., 2005; Ching et al., 2012). Translocator protein is expressed in the outer mitochondrial membrane. It was assumed to contribute through the cholesterol transportation into mitochondria regulating the rate of the synthesis of neurosteroids. However, these views have recently been challenged (Rupprecht et al., 2010; Selvaraj and Stocco, 2015). Gene-expression studies in the brain of rodents, primates, and humans have shown that TSPO expression is nearly absent in microglia patrolling the intact CNS parenchyma but rapidly increases in inflammation (Venneti et al., 2008; Ching et al., 2012). TSPO is highly expressed in activated microglia, in the choroid plexus and in reactive astrocytes, but its expression is globally low in the normal brain (Chauveau et al., 2008; Banati et al., 2014; Liu et al., 2014). These findings indicate that TSPO is a biomarker and an attractive target for the imaging microglial activation and reactive gliosis in cerebral inflammation (Rupprecht et al., 2010; Ching et al., 2012).

The isoquinoline carboxamide derivate PK11195 (N-butan-2-yl-1-(2-chlorophenyl)-N-methylisoquinoline-3-carboxamide), a nonbenzodiazepine ligand specifically binding to TSPO, has been widely used for its functional characterization and for the identification of its cellular origin in brain tissue (Banati et al., 1997, 2000; Chauveau et al., 2008). The issues regarding sensitivity and specificity of traditional PK11195 has been discussed (Venneti et al., 2008; Dickens et al., 2014; Boutin et al., 2015). Fortunately, recently developed radioligands such as DPA-714 (James et al., 2008; Chauveau et al., 2009), PBR28 (Imaizumi et al., 2007), PBR111 (Van Camp et al., 2010), SSR18075 (Chauveau et al., 2011), CLINME (Arlicot et al., 2008; Van Camp et al., 2010), and GE-180 (Dickens et al., 2014) have demonstrated better binding potency and bioavailability compared to the classical PK11195 and could overcome the problems of the classical tracers in MS and its models. A number of other TSPO targeting tracers have been developed to study the inflammation including but not limiting to DAA1106, FE-DAA1106, DPA-713, and vinpocetine, and reviewed by (Chauveau et al., 2008; James et al., 2008; Winkeler et al., 2010; Ciarmiello, 2011; Kiferle et al., 2011). Microglial activation was demonstrated in clinical MS studies with [^{11}C]PK11195, unfortunately only in a limited number of patients (Banati et al., 2000; Debruyne et al., 2003; Versijpt et al., 2005; Vas et al., 2008). Radiotracer binding was increased in areas of acute and relapse-associated inflammation detected by classical Gd-DTPA enhanced T1-weighted MRI imaging (Rissanen et al., 2014). Interestingly, a significant increase in [^{11}C]PK11195 binding was observed in activated microglia outside the histopathologically or MRI defined borders of MS plaques in both cerebral central gray-matter areas, which are not normally reported as sites of pathology in MS, as well as in normal appearing white matter (Banati et al.,

2000; Debruyne et al., 2003). Unfortunately, 2nd generation TSPO targeting agents suffer from unexpected low binding status in over 30% of the population, which limits their use in clinics and demands genetic testing of the TSPO polymorphism. However, clinical studies have shown increased uptake with ^{18}F -PBR111 and ^{11}C -PBR28 in white matter lesions but not with all 2nd generation compounds like ^{18}F -FEDAA1106. Additional studies are required to further investigate the specificity of these radiotracers for activated microglia over other activated glial cells. Overall, imaging of microglial activation in MS patients may serve as a complementary biomarker for disease progress (Abourbeh et al., 2012; Airas et al., 2015).

The type 2 cannabinoid receptor (CB2R) is part of the human endocannabinoid system and is involved in both central and peripheral inflammatory processes (Ehrhart et al., 2005; Pacher, 2006; Chiurchiù et al., 2014). CB2R can be found in immune cells, such as macrophages, perivascular T lymphocytes, astrocytes and reactive microglia, and it is thought to mediate anti-inflammatory as well as immunomodulatory effects (Docagne et al., 2008; Rodgers et al., 2013). 2-oxoquinoline and oxadiazolyle derivatives have been synthesized and radiolabeled with ^{11}C and ^{18}F , representing promising candidates for brain imaging in mice (Evens et al., 2009; Teodoro et al., 2013; Slavik et al., 2015). CB2R is almost undetectable in a healthy brain, whereas it is expressed in the activated glial cells (Stella, 2004; Cabral et al., 2008; Atwood and Mackie, 2010). This demonstrates that the effective PET ligands for CB receptors have the potential to act as biomarkers in the studies of pathophysiology of MS (Sanchez-Pernaute et al., 2008; Evens et al., 2009; Horti et al., 2010; Turkman et al., 2011; Vandeputte et al., 2011). In addition, new microglial targets, like P2X purinoceptor 7 (P2X7; Yiangou et al., 2006; Monif et al., 2009) and matrix metalloproteinases (Wagner et al., 2007; Iwama et al., 2011), have been explored for imaging of MS.

Overall, the benefits of PET contribute to the understanding of personalized status of MS patients, disease profiling, prognosis, and response, which are all combined in precision medicine. Specific biomarkers are the backbone for capturing the different aspects of MS heterogeneity, which could be useful for diagnosis, treatment stratification, and personalization of the therapeutic approach. Simplified, the precision medicine aims to provide the right drug with the right dose for the right indication in the right patient at the right time. Such as the case with the current 2nd generation TSPO markers, precision medicine relies on variability of genes, environment and life style of each person rather than on the data from large clinical trials. The customization of the treatment is based on the characterization of the genotype and phenotype induced effects on imaging in the individual patient. Biomedical imaging offers a great tool for mapping data from biomarkers, genomics, and physiology. There is a great interest for the monitoring of microglial activation in MS. However, the recent results with TSPO ligands suggest that the reactive astrocytes might increase the signal levels in MS (Lavisette et al., 2012). Since the role of reactive astrocytes in MS is recently of great interest, more specific markers are needed for reliable imaging of neuroinflammation (Rostami and Ciric, 2014; Zeis et al., 2015).

IMAGING ASTROCYTE ACTIVATION

Astrocytes are one of the most abundant cell types in the CNS. They have complex function ranging from supporting the surrounding neurons to the regulation of synaptic activity and BBB integrity (Sofroniew and Vinters, 2010). Although astrocytes are not immune cells *per-se* they can in specific conditions, such as in CNS inflammation, exert both pro- and anti-inflammatory effects on microglia (Min et al., 2006; Farina et al., 2007; Sofroniew, 2015).

Astrocytes were regarded to be non-participating bystanders in MS, responding secondarily to insults by undergoing astrogliosis and producing a glial scar (Brosnan and Raine, 2013). However, since the T-cell mediated immunity has been strongly associated with MS there are several plausible means by which astrocytes could contribute to autoimmunity. Astrocytes may facilitate immune cell extravasation into the CNS by releasing chemokines. They can modulate the activity of innate immune cells, such as microglia and inflammatory monocytes recruited to the CNS, by boosting their ability to promote neurodegeneration. Finally, astrocytes also have direct neurodegenerative functions mediated by the production of TNF α and nitric oxide (NO). However, these actions can also represent potential mechanisms by which astrocytes could reduce inflammation to promote remyelination (Claycomb et al., 2013).

Activation of glial cells is a common feature of MS as discussed earlier. Acetate is reported to accumulate into astrocytes and the [^{11}C]acetate accumulation is increased in MS lesions (Takata et al., 2014). However, brain uptake of [^{11}C]acetate is insufficient for obtaining a quantitative image of astrocytes' oxidative metabolism (Okada et al., 2013). To overcome this drawback benzyl [^{11}C]acetate has been synthesized (Okada et al., 2013). Although the quantitative measurement remains under development, acetate is specific for astrocyte lipid metabolism (Brekke et al., 2015) and could serve as a marker for activated astrocyte metabolism in MS (Takata et al., 2014). In addition, ^{18}F labeled derivative of acetate could increase the signal to noise ratio compared to ^{11}C analog. It is expected that this tracer will be used in MS (Ponde et al., 2007).

One critical function of astrocytes is acting as sentinels and monitoring the BBB, a complex barrier composed of endothelial cells, astrocytes, pericytes, and myeloid cells such as perivascular macrophages and mast cells (Abbott et al., 2006). BBB functions as an anatomical mechanism for the highly selective passage of water, ions, nutrients, and cells from peripheral circulation into and out of the brain parenchyma (Abbott et al., 2006; Daneman and Rescigno, 2009; Larochelle et al., 2011). Under inflammatory conditions the BBB opens and it enables higher leukocyte passage into the CNS (Claycomb et al., 2013). Astrocytes play a critical role in shielding and protecting the CNS under inflammatory conditions (Voskuhl et al., 2009). Furthermore, astrocyte ablation has been shown to cause enhanced monocyte, but not T-cell, migration into the CNS (Toft-Hansen et al., 2011). To date, there is no clinically relevant PET tracer for BBB integrity, although several candidates have been proposed [^{13}N]glutamate, [^{82}Rb]Cl, or ^{68}Ga Gallium-ethylene-diamine-tetra-acetic acid (EDTA) (Saha et al., 1994; Wunder et al., 2012).

Imaging of astrocyte function is still a young field and it needs development of suitable imaging ligands. Astrocytes are involved in several neurological diseases and the main obstacle using imaging techniques has been the lack of proper tracers.

TARGETS FOR PET IMAGING IN MS

The recent increased availability of PET tracers to assess activated glial cells, disease pathology, and signaling pathways give PET a promising role in MS research. Since the underlying mechanisms of neurodegeneration and regeneration are still poorly understood the non-invasive techniques will enhance understanding these processes to develop better drug candidates, early diagnosis, and reliable monitoring of the treatment response. Several possible targets for PET imaging in MS are discussed in this section. These candidates may serve as more specific targets and may reveal some of the missing links in MS treatment and pathology, especially in the glial cell mediated actions.

Neuroinflammation is a dynamic and complex adaptive response process, which involves multiple cell types and various signaling routes, pathways, and receptors (Singhal et al., 2014). As discussed earlier, neuroinflammation can be imaged in MS. However, new tracers are needed to gain practical importance in clinics. The greatest potential may lay in the imaging of the dynamic interplay between neuroinflammation and the molecular mechanisms that contributes to the disease progression. The recent findings support three major neuroinflammation components in MS: astrogliosis, cytokine elevation, and significant changes in specific proteins, which offer a great variety of specific targets for imaging purposes.

TNF- α is associated with self-propagation of neuroinflammation and the expression of TNF- α is elevated in MS patients (Rossi et al., 2014). Microglia, inflammatory monocytes recruited to the CNS and astrocytes are major sources of TNF- α in CNS, interestingly proposing TNF- α expression as a marker in MS (Welser-Alves and Milner, 2013). PET tracers, like [^{64}Cu]DOTA-etanercept and [^{64}Cu]pegylated dimeric c(RGDyK), have been developed to target TNF- α in both acute and chronic inflammation in mice (Cao et al., 2007). TNF- α may be a target for MS imaging in the future. Overall, cytokines are highly related to oxidative stress in the brain (Di Penta et al., 2013). The expression of inducible nitric oxide synthase (iNOS) is increased in MS lesions, increasing generation of NO as well as reactive nitrogen species like peroxynitrite (Kröncke et al., 1998; Ortiz et al., 2013). The accumulation of these molecules induces lipid peroxidation, resulting in damage to DNA and neuronal degeneration (Haider et al., 2011).

In the healthy CNS tissues, the expression levels of iNOS are low but become highly expressed in astrocytes and neurons during inflammation (Saha and Pahan, 2006). In chronic pathology the reactive nitrogen species produced by iNOS are not efficiently eliminated, which leads to cellular dysfunctions (Fulda et al., 2010). The number of tracers for iNOS is minimal and the current [^{18}F]NOS (6-(1/2)-(2-[^{18}F]fluoropropyl)-4-methylpyridin-2-amine) needs

further modification and improvement. Importantly, the feasibility of iNOS PET imaging has been demonstrated in human inflammation (Herrero et al., 2012; Huang et al., 2015). In addition, active iNOS enzyme has been demonstrated in astrocytes in both acute and chronic active MS lesions and might therefore be an interesting target for imaging purposes (Liu et al., 2001).

The expression of another proinflammatory cytokine mediator, cyclooxygenase-2 (COX-2), is extensively increased in MS lesions and it has been tightly linked to increased iNOS expression (Rose et al., 2004). Furthermore, COX-2 expression was found in the cells expressing microglial marker, highlighting the importance of immune-derived cells. COX-2 has also been suggested to act as a link between neuroinflammation and glutamate mediated neuronal excitotoxicity (Kelley et al., 1999). These facts clearly indicate a need for methods to detect COX-2 expression. PET tracers for COX-2 have been developed, but the *in vivo* imaging properties have not been very effective (de Vries et al., 2003, 2008; Takashima-Hirano et al., 2011; Ji et al., 2013). The most promising COX-2 tracer so far is [¹¹C]Rofecoxib (4-(4-methylsulfonylphenyl)-3-phenyl-5H-furan-2-one), demonstrating *in vitro* usability, but lacking necessary affinity for *in vivo* studies (Ji et al., 2013). Nevertheless, cyclooxygenases is presently an important target for PET tracer development.

Besides stimulating production of reactive oxygen species, cytokines are known to modulate the lipid metabolism and increase the production of neurodegeneration promoters such as eicosanoids and ceramides (Adibhatla and Hatcher, 2007). As previously mentioned, acetate is converted into fatty acid by acetyl-CoA synthase and [¹¹C]acetate PET has proven useful for imaging in several diseases (Grassi et al., 2012). In addition, acetate is preferentially absorbed into astrocytes by the monocarboxylate transporter, which is overexpressed in MS (Nijland et al., 2014). Moreover, bioactive lipids exert significant effects on inflammation during autoimmunity targets or regulators of the immune response (Rinaldi et al., 2009). In addition, the appearance of cytosolic lipid synthesis is one the corner stones of macrophage foam cell formation (Matthäus et al., 2012). The intracellular concentrations of different individual lipids or the receptors involved the synthesis of particular bioactive lipids could reveal novel aspects of the disease progression (Mayo et al., 2014). Recently β -1,4-galactosyltransferase 6 (B4GALT6) was found to promote astrocyte activation and neuroinflammation during chronic EAE. The lactosylceramide (LacCer) synthesized by B4GALT6 in astrocytes controls the production of chemokines and cytokines, such as CCL2 and GM-CSF, which regulates the recruitment and activation of inflammatory monocytes and microglia and clearly highlights the importance of a specific lipid profile for disease progression (Mayo et al., 2014).

In summary, comprehensive profiling of lipid metabolism and the BBB function are likely to reveal new targets for therapeutic intervention in MS as well as for other neurological disorders where astrocyte activation contributes to disease pathology (Neu and Woelk, 1982; Pannu et al., 2005; Adibhatla and Hatcher, 2007; Wheeler et al., 2008; Kooij et al., 2012; Prüss et al., 2013).

The imaging of specific bioactive lipids, receptors or enzymes that are involved in their synthesis may be novel targets for PET imaging.

BIOMARKERS FOR THE EARLY PHASES OF MS

In the search of better treatments for MS, cerebrospinal fluid (CSF) biomarkers have been used to identify high risk MS patients as well as patients with other neuronal disorders. Recently, high levels of astrocyte derived chitinase 3-like protein 1 (CHI3L1) were associated with the strong prediction of MS. This finding further demonstrates the increased importance of astrocyte activation and the specific role of astrocyte as a source for biomarkers in MS, already at the early disease phase.

The activated lipid metabolism in astrocytes demands increased acetate and lipid transportation (Lev, 2012). ATP and glutamate stimulation can significantly enhance the dynamin-independent endocytosis and their receptors control the microglial physiology and pathology (Jiang and Chen, 2009). For example ATP related purinergic receptors control microglial cytokine release among several other functions (Sperlágh and Illes, 2007). Moreover, purinergic pathways regulate neuroinflammation (Burnstock, 2008). The increasing evidence suggests that the P2X7 receptor is an interesting neuroinflammation associated molecular target (Lister et al., 2007; Monif et al., 2009; Gandelman et al., 2010). PET tracers have been developed to image P2X7 receptor, [¹¹C]A-740003 (N-[1-[(Cyanoamino)(5-quinolinylamino)methylene]amino]-2,2-dimethylpropyl]-3,4-dimethoxybenzeneacetamide) and [¹¹C]GSK1482160 ((S)-N-(2-chloro-3-(trifluoromethyl)benzyl)-1-[¹¹C]methyl-5-oxopyrro-lidine-2-carboxamide; Janssen et al., 2014; Gao et al., 2015). Purinergic system might serve as a sensitive target for MS imaging.

Furthermore, the adenosine receptors, whose expression is modulated by microglial activation, moderate immune function (Haskó et al., 2008; Orr et al., 2009; Domercq et al., 2013; Luongo et al., 2014). Especially A_{2A} receptors are up-regulated during inflammation (Rissanen et al., 2013). It is clear that adenosine signaling play a significant role in MS as a neuromodulator and the clinical studies with [¹¹C]TMSX (7-methyl-[¹¹C]-(E)-8-(3,4,5-Trimethoxystyryl)-1,3,7-trimethylxanthine) PET will likely open new perspective to develop new tracers to this target in the future (Rissanen et al., 2015).

In addition, the cholinergic system shows decreased function in MS patients (Kooij et al., 2011). PET imaging studies of cholinergic activity may define which patient will respond to the treatment which will further increase the knowledge of MS. A similar approach has been already used in Alzheimer's disease using radiolabeled choline derivatives and these techniques could be easily transferred to MS clinical research (Volkow et al., 2001; Rinne, 2003; Kooij et al., 2011).

The cannabinoid receptors CB2 are expressed in very low levels in a healthy brain, but the expression increases during microglial activation (Benito et al., 2007). CB2 is an interesting target for PET imaging in MS models especially

with [^{11}C]A836339 (2,2,3,3-Tetramethylcyclopropanecarboxylic acid [3-(2-[^{11}C]methoxyethyl)-4,5-dimethyl-3H-thiazol-(2Z)-ylidene]amide) and [^{11}C]NE40. Recently there has been great progress in developing new tracers for this target (Docagne et al., 2008; Horti et al., 2010; Evens et al., 2011, 2012; Slavik et al., 2015; Yrjölä et al., 2015).

During inflammation microglia will release glutamate in response to the production of reactive oxygen species (ROS; Bal-Price and Brown, 2001; Brown and Neher, 2010; Takaki et al., 2012). The cysteine-glutamate exchange modulates the release of ROS and cytokines which impairs the function of glutamate transporters and leads to increased extracellular glutamate levels as well as excitotoxicity (Rao et al., 2003; Matute et al., 2006). Metabotropic glutamate receptors (mGluRs) are transmembrane proteins that are expressed in glial cells and play a pivotal role in cell function and glial-neuronal co-operation (Kritik et al., 2015). Immunohistochemical analyses have revealed that mGluR5 is expressed in reactive astrocytes surrounding the MS lesion site and the expression is higher than in non-activated astrocytes (Geurts et al., 2003). In addition, the activation of mGluR5 reduced the microglial activation in an inflammation model (Byrnes et al., 2009; Loane et al., 2009). During the last 15 years the subtype selective allosteric modulators have been identified for different mGluRs (see Figure 5; Zhang and Brownell, 2012). Many PET tracers have been synthesized by radiolabeling the derivatives of MPEP and MTEP and to date over 15 mGluR5 targeting PET ligands have been reported (Mu et al., 2010; Zhang and Brownell, 2012). Tracers like [^{18}F]FPEB ((3-[^{18}F]Fluoro-5-(2-pyridinylethynyl)benzonitrile) have been already developed for automated synthesis and evaluated in humans (Lim et al., 2014).

Monoamine oxidase type B located in the outer membrane of mitochondria and is expressed in astrocytes, where its activity is increased in neurodegenerative diseases (Mallajosyula et al., 2008; Veitinger et al., 2014). It catalyzes the deamination reaction thus modulating neurotransmitter concentrations and has been

a major target for drug development, especially in movement related diseases (Talati et al., 2009; Deftereos et al., 2012). The [^{11}C]-L-deprenyl indicates increased monoamine oxidase type B content in reactive and proliferating astrocytes in AD (Gulyás et al., 2011). Results from the MS patients studies are likely to be published soon (Hurley, 2015).

The above exploration shows that the combined PET imaging of activated microglia and astrocytes is presently of special interest in MS research.

PET AS A TOOL FOR PRECISION MEDICINE IN MS

More specific features of MS lesions have been described in parallel with the identification of body fluid markers such as CHI3L1 and B4GALT6. Recent progress with biomarkers and imaging tracers suggests that precision medicine is becoming a reality in MS. The prevalence of MS is increasing and there is relatively little data available to personalize the treatments and increase the cost effectiveness. Sophisticated tools are needed to handle the complex data to obtain more detailed insight of the clinical status of the patient's condition. The combined information from various biomarkers and imaging studies can be used to predict the disease evolution individually. PET imaging can provide precise data for the cross-roads of multiple fields, like biomedical imaging, pharmacology, neurology, genomics etc. Achieving precision medicine in MS requires high quality data, large samples, and consistent interdisciplinary approach.

CONCLUSION

Inflammation and glial activation play an important role in numerous neurodegenerative diseases, such as Alzheimer's disease, Parkinson disease, amyotrophic lateral sclerosis and MS. Although factors inducing inflammation vary between diseases, there is evidence of greatly converging mechanisms for the sensing, transduction, and amplification of inflammatory processes that eventually lead to the production of neurotoxic mediators. PET imaging provides a powerful method for dynamic imaging of these events. The full potential of PET is not yet recognized, mainly due to the lack of validated tracers; the complicated and costly process of validating new tracers needs partnerships, human resources, expertise, funding, and access to patients, but it is something that needs to be focused on to obtain the essential information of the biological processes in disease pathology. This will ultimately produce more reliable diagnosis, better treatments and effective prevention methods for MS. The role of PET imaging will increase in clinics, when onsite cyclotrons, the development of new tracers, and imaging equipment become available.

[^{18}F]-FDG is still the most extensively used PET imaging tracer for inflammation even though it tends to produce controversial results. New imaging tracers for TSPO ([^{11}C]PK11195, [^{11}C]PBR28, etc.) have gained a great interest for detection of inflammation and evaluation of therapy. Using these new tracers, PET imaging has greatly improved our

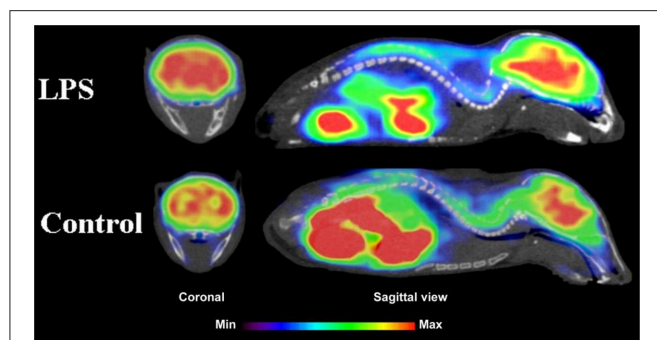
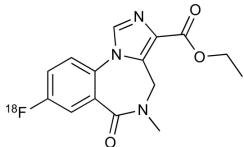
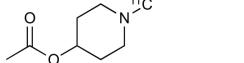
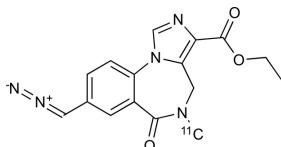
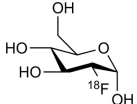
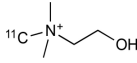
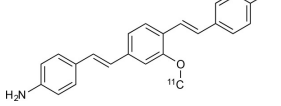
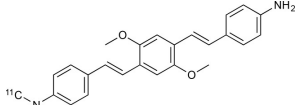
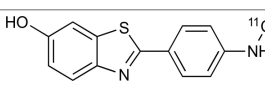
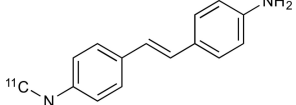
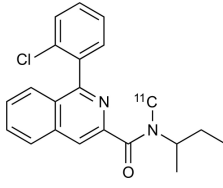
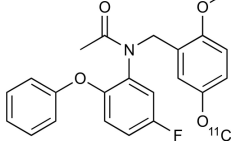


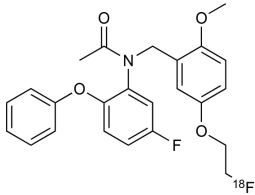
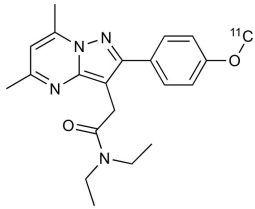
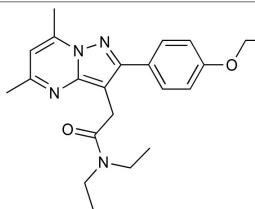
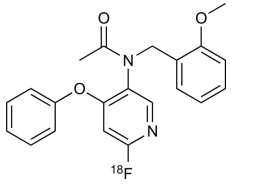
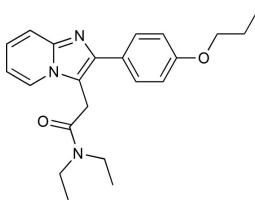
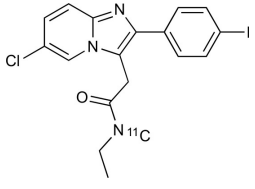
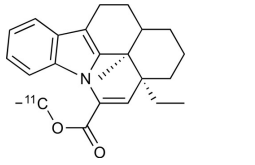
FIGURE 5 | Coronal and sagittal sections of fused PET and CT images in 10 days old pups of mice. PET studies using [^{18}F]FPEB show enhanced mGluR5 expression in the brain of the pups, whose mothers were injected with LPS compared to saline injection (control). Coronal slices show highest accumulation in the hippocampal area of the mouse, whose mother had LPS administration. Sagittal images show spine based on CT images and high accumulation of [^{18}F]FPEB in the brain and gut. Modified from Arseneault et al. (2014).

TABLE 2 | Examples of PET tracers in MS research.

MS characteristic	Target	Compound	Structure	Stage in MS imaging	References
Axonal degeneration	GABA _A receptor	¹⁸ F-flumazenil (K _i ~6.0 nM)		Clinical studies in MS patients are ongoing.	Banati et al., 1997, 2000; Ohyama et al., 1999; Barkhof et al., 2009; Pascual et al., 2012
		¹¹ C-MP4A		Clinical studies in AD patients.	Virta et al., 2011; Garibotto et al., 2013; Lund et al., 2013
		¹¹ C-Ro15-4513		Subtype specific ligand. No studies with MS patients.	Halldin et al., 1992; Quelch et al., 2015
Demyelination and remyelination	Glucose metabolism	¹⁸ F-FDG		Studies with MS patients conducted.	Kuhlmann, 2002; Buck et al., 2012; Maffione et al., 2014; Rudroff et al., 2014
	Choline metabolism	¹¹ C-Choline		Clinically approved for cancer imaging.	Stankoff et al., 2006, 2011
		¹¹ C-BMB		Studies with MS patients conducted.	Stankoff et al., 2006, 2011
		¹¹ C-CiC		Studies with preclinical MS rodent models.	Wang et al., 2009; de Paula Faria et al., 2014a,b; Ellwardt and Zipp, 2014
		¹¹ C-PIB (K _i ~1.9 nM)		Studies with MS patients.	de Paula Faria et al., 2014a,b
Glial activation	TSPO	¹¹ C-MeDAS		Studies with MS mouse models.	Wu et al., 2010, 2013; de Paula Faria et al., 2014a,b
		¹¹ C-PK11195 (K _i ~9.3 nM)		Studies with MS patients and early stage MS m patients conducted.	Debruyne et al., 2003; Versijpt et al., 2005; Politis et al., 2012; Rissanen et al., 2014; Giannetti et al., 2015
		¹¹ C-DAA1106 (K _i ~0.28 nM)		Preclinical models. Clinical studies have been conducted with healthy volunteers.	Maeda et al., 2004; Venneti et al., 2008; Brody et al., 2014

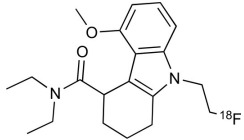
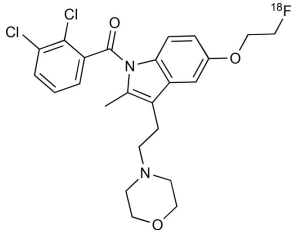
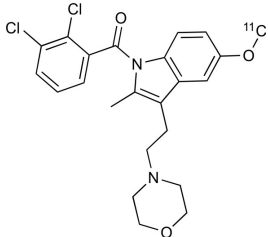
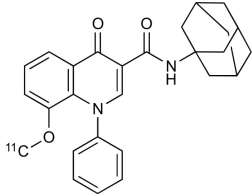
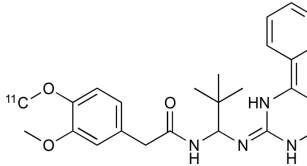
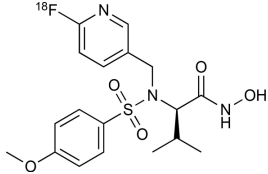
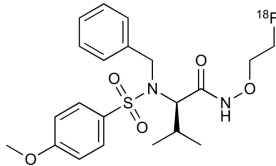
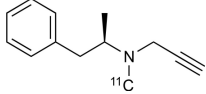
(Continued)

TABLE 2 | Continued

MS characteristic	Target	Compound	Structure	Stage in MS imaging	References
		¹⁸ F-FE-DAA1106 (K _i ~0.08 nM)		Clinical studies in MS patients conducted.	Ji et al., 2008; Takano et al., 2013
		¹¹ C-DPA-713 (K _i ~4.7 nM)		Preclinical models in MS. Clinical studies with healthy patients and patients with inflammation.	Boutin et al., 2007a; Endres et al., 2009; Coughlin et al., 2014
		¹⁸ F-DPA-714 (K _i ~7.0 nM)		Preclinical models in MS. Clinical studies in AD patients.	Peyronneau et al., 2013; Golla et al., 2015
		¹⁸ F-PBR28 (K _i ~4.6 nM)		Clinical studies in MS patients.	Oh et al., 2011; Moon et al., 2014; Park et al., 2015
		¹⁸ F-PBR111 (K _i ~4.5 nM)		Clinical studies in MS patients.	Mattner et al., 2013; Colasanti et al., 2014
		¹¹ C-CLINME (K _i ~8.5 nM)		Preclinical in MS. Clinical studies with acute neuroinflammation.	Boutin et al., 2007b; Van Camp et al., 2010
		¹¹ C-vinpocetine		Clinical studies in MS patients.	Vas et al., 2008; Oh et al., 2011

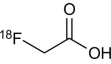
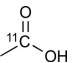
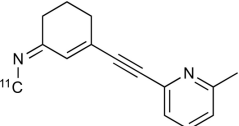
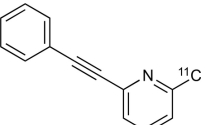
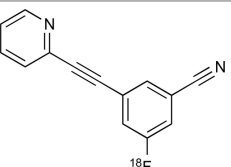
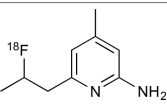
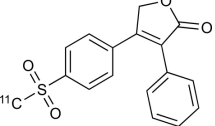
(Continued)

TABLE 2 | Continued

MS characteristic	Target	Compound	Structure	Stage in MS imaging	References
		¹⁸ F-GE180 (K _i ~0.87 nM)		Preclinical studies in MS models. Clinical studies with inflammation.	Wadsworth et al., 2012; Dickens et al., 2014; Airas et al., 2015
	CB2r	⁸ F-GW405833		Preclinical models.	Vandeputte et al., 2011
		¹¹ C-A-836339		Preclinical models.	Horti et al., 2010
		¹¹ C-KD2		Preclinical models.	Mu et al., 2013
	P2X7 receptor	¹¹ C-A-740003		Rodent baseline.	Janssen et al., 2014
	Matrix metalloproteinases	¹⁸ F- CGS27023A		Preclinical models.	Wagner et al., 2007, 2009
		¹⁸ F-CGS25966		Preclinical models.	Wagner et al., 2007
	Monoamine oxidase type B	¹¹ C-l-deprenyl		Preclinical models. Clinical studies in ALS patients.	Johansson et al., 2007; Gulyás et al., 2011

(Continued)

TABLE 2 | Continued

MS characteristic	Target	Compound	Structure	Stage in MS imaging	References
Lipid metabolism		¹⁸ F-Acetate		Preclinical models.	Marik et al., 2009
		¹¹ C-Acetate		Clinical studies in MS patients.	Takata et al., 2014
Metabotropic glutamate receptor subtype 5		¹¹ C-ABP688		Clinical studies. No MS studies.	Ametamey et al., 2006; DeLorenzo et al., 2015
		¹¹ C-MPEP		No MS imaging published.	Yu et al., 2005
		¹⁸ F-FBEP		Clinically validated. No MS imaging published.	Wang et al., 2007; Wong et al., 2013
Induced nitric oxide synthetase		¹⁸ F-NOS		No MS imaging published. Clinical studies with inflammation.	Herrero et al., 2012
Cyclooxygenase-2		¹¹ C-Rofecoxib		Preclinical evaluation with inflammation model.	de Vries et al., 2008

understanding of the mechanism of inflammation and increased the diagnostic specificity and accuracy of inflammation. As summarized in **Table 2**, various radiopharmaceutical approaches have been developed for PET imaging to detect inflammation, including biomarkers targeting to specific receptors and lipid metabolism.

So far, the clinical PET studies in MS are limited to evaluation of two biological processes: glucose metabolism and inflammation. It is clear that the use of combined PET/MR imaging is increasing also in MS research. One of the main interests is to develop combined imaging markers and methods for MS pathology to stage, cell type and record activity related changes in lesions. However, presently PET imaging is relatively expensive and it also requires sophisticated quantification, which demands special software and skilled operators. MS is a complex disease, which remains difficult to treat before more specific disease mechanisms are revealed. PET research community is looking for the first ligands to be recommended for routine clinical practice in MS diagnosis and follow up of therapy. PET has already shown to be one of the most sophisticated, sensitive, reliable, effective, and safest tools for

the monitoring of several cancers in clinics and there is no reason why it could not be same in the neurodegenerative disorders as well. Clinical imaging and research modalities should be combined to expand the knowledge of clinical findings, genetics, phenotyping, pharmacology, and drug targeting. Advanced imaging technologies, including PET, could be used to reveal the causes of MS rather than concentrating on correlations. MS is a complex and heterogeneous disease, which could benefit from precision medicine in the future. The genomic approach can be used to individualize the imaging data as presently done with 2nd generation TSPO markers ([¹¹C]PBR28 etc.). Astrocyte activation and their ability to modulate the complex neuronal network and inflammation related pathways have a great potential to reveal disease stage specific markers for personalized medicine. Despite the astrocyte related research in MS is still in early stages, and the recent promising results suggest new techniques to diagnose, monitor and treat this cruel disease. The combined pathogenic characteristics of MS are still unknown and the key to prevent and cure this devastating disease is still waiting for discovery.

AUTHOR CONTRIBUTIONS

PP did literature search, prepared tables and participated writing. MJ participated literature search, writing and composing the manuscript. FQ did critical evaluation of the manuscript. AB participated writing, preparation of figures, and final evaluation of the manuscript.

REFERENCES

- Abbott, N. J., Rönnbäck, L., and Hansson, E. (2006). Astrocyte-endothelial interactions at the blood-brain barrier. *Nat. Rev. Neurosci.* 7, 41–53. doi: 10.1038/nrn1824
- Abourbeh, G., Thézé, B., Maroy, R., Dubois, A., Brulon, V., Fontyn, Y., et al. (2012). Imaging microglial/macrophage activation in spinal cords of experimental autoimmune encephalomyelitis rats by positron emission tomography using the mitochondrial 18 kDa translocator protein radioligand [¹⁸F]DPA-714. *J. Neurosci.* 32, 5728–5736. doi: 10.1523/JNEUROSCI.2900-11.2012
- Adibhatla, R. M., and Hatcher, J. F. (2007). Role of lipids in brain injury and diseases. *Future Lipidol.* 2, 403–422. doi: 10.2217/17460875.2.4.403
- Aguzzi, A., Barres, B. A., and Bennett, M. L. (2013). Microglia: scapegoat, saboteur, or something else? *Science* 339, 156–161. doi: 10.1126/science.1227901
- Airas, L., Dickens, A. M., Elo, P., Marjamäki, P., Johansson, J., Eskola, O., et al. (2015). *In vivo* PET imaging demonstrates diminished microglial activation after fingolimod treatment in an animal model of multiple sclerosis. *J. Nucl. Med.* 56, 305–310. doi: 10.2967/jnumed.114.14955
- Ametamey, S. M., Kessler, L. J., Honer, M., Wyss, M. T., Buck, A., Hintermann, S., et al. (2006). Radiosynthesis and preclinical evaluation of 11C-ABP688 as a probe for imaging the metabotropic glutamate receptor subtype 5. *J. Nucl. Med.* 47, 698–705.
- Anderson, D. W., Ellenberg, J. H., Leventhal, C. M., Reingold, S. C., Rodriguez, M., and Silberberg, D. H. (1992). Revised estimate of the prevalence of multiple sclerosis in the United States. *Ann. Neurol.* 31, 333–336. doi: 10.1002/ana.410310317
- Arlicot, N., Katsifis, A., Garreau, L., Mattner, F., Vergote, J., Duval, S., et al. (2008). Evaluation of CLINDE as potent translocator protein (18 kDa) SPECT radiotracer reflecting the degree of neuroinflammation in a rat model of microglial activation. *Eur. J. Nucl. Med. Mol. Imaging* 35, 2203–2211. doi: 10.1007/s00259-008-0834-x
- Arsenault, D., Zhu, A., Gong, C., Kil, K.-E., Kura, S., Choi, J.-K., et al. (2014). Hypo-anxious phenotype of adolescent offspring prenatally exposed to LPS is associated with reduced mGluR5 expression in hippocampus. *Open J. Med. Psychol.* 3, 202–211. doi: 10.4236/ojmp.2014.33022
- Atwood, B. K., and Mackie, K. (2010). CB2: a cannabinoid receptor with an identity crisis. *Br. J. Pharmacol.* 160, 467–479. doi: 10.1111/j.1476-5381.2010.00729.x
- Bakshi, R., Miletich, R. S., Kinkel, P. R., Emmet, M. L., and Kinkel, W. R. (1998). High-resolution fluorodeoxyglucose positron emission tomography shows both global and regional cerebral hypometabolism in multiple sclerosis. *J. Neuroimaging* 8, 228–234. doi: 10.1111/jon199884228
- Bal-Price, A., and Brown, G. C. (2001). Inflammatory neurodegeneration mediated by nitric oxide from activated glia-inhibiting neuronal respiration, causing glutamate release and excitotoxicity. *J. Neurosci.* 21, 6480–6491.
- Banati, R. B., Middleton, R. J., Chan, R., Hatty, C. R., Wai-Ying Kam, W., Quin, C., et al. (2014). Positron emission tomography and functional characterization of a complete PBR/TSPO knockout. *Nat. Commun.* 5:5452. doi: 10.1038/ncomms6452
- Banati, R. B., Myers, R., and Kreutzberg, G. W. (1997). PK (‘peripheral benzodiazepine’)–binding sites in the CNS indicate early and discrete brain lesions: microautoradiographic detection of [3H]PK11195 binding to activated microglia. *J. Neurocytol.* 26, 77–82. doi: 10.1023/A:1018567510105
- Banati, R. B., Newcombe, J., Gunn, R. N., Cagnin, A., Turkheimer, F., Heppner, F., et al. (2000). The peripheral benzodiazepine binding site in the brain in multiple sclerosis: quantitative *in vivo* imaging of microglia as a measure of disease activity. *Brain J. Neurol.* 123 (Pt 11), 2321–2337. doi: 10.1093/brain/123.11.2321

ACKNOWLEDGMENTS

AB was supported by the grant NIBIB-R01EB012864. PP was supported by the Orion Farnos Research Foundation and Kuopio University Foundation, Finland. MJ was supported by the Sigrid Juselius Foundation, Finnish MS-Society, Orion Farnos Research Foundation and Saastamoinen Foundation, Finland.

- Barkhof, F., Calabresi, P. A., Miller, D. H., and Reingold, S. C. (2009). Imaging outcomes for neuroprotection and repair in multiple sclerosis trials. *Nat. Rev. Neurol.* 5, 256–266. doi: 10.1038/nrneuro.2009.41
- Barkhof, F., and Filippi, M. (2009). Multiple sclerosis: MRI—the perfect surrogate marker for multiple sclerosis? *Nat. Rev. Neurol.* 5, 182–183. doi: 10.1038/nrneuro.2009.31
- Baxter, A. G. (2007). The origin and application of experimental autoimmune encephalomyelitis. *Nat. Rev. Immunol.* 7, 904–912. doi: 10.1038/nri2190
- Benito, C., Romero, J. P., Tolón, R. M., Clemente, D., Docagne, F., Hillard, C. J., et al. (2007). Cannabinoid CB1 and CB2 receptors and fatty acid amide hydrolase are specific markers of plaque cell subtypes in human multiple sclerosis. *J. Neurosci.* 27, 2396–2402. doi: 10.1523/JNEUROSCI.4814-06.2007
- Blakemore, W. F., and Franklin, R. J. M. (2008). Remyelination in experimental models of toxin-induced demyelination. *Curr. Top. Microbiol. Immunol.* 318, 193–212. doi: 10.1007/978-3-540-73677-6_8
- Boche, D., Perry, V. H., and Nicoll, J. A. (2013). Review: activation patterns of microglia and their identification in the human brain. *Neuropathol. Appl. Neurobiol.* 39, 3–18. doi: 10.1111/nan.12011
- Bodini, B., Louapre, C., and Stankoff, B. (2015). Advanced imaging tools to investigate multiple sclerosis pathology. *Presse Medicale.* 44, e159–e167. doi: 10.1016/j.lpm.2015.02.011
- Boutin, H., Chauveau, F., Thominiaux, C., Grégoire, M.-C., James, M. L., Trebassen, R., et al. (2007a). 11C-DPA-713: a novel peripheral benzodiazepine receptor PET ligand for *in vivo* imaging of neuroinflammation. *J. Nucl. Med.* 48, 573–581. doi: 10.2967/jnumed.106.036764
- Boutin, H., Chauveau, F., Thominiaux, C., Kuhnast, B., Grégoire, M.-C., Jan, S., et al. (2007b). *In vivo* imaging of brain lesions with [(11)C]CLINME, a new PET radioligand of peripheral benzodiazepine receptors. *Glia* 55, 1459–1468. doi: 10.1002/glia.20562
- Boutin, H., Murray, K., Pradillo, J., Maroy, R., Smigova, A., Gerhard, A., et al. (2015). 18F-GE-180: a novel TSPO radiotracer compared to 11C-R-PK11195 in a preclinical model of stroke. *Eur. J. Nucl. Med. Mol. Imaging* 42, 503–511. doi: 10.1007/s00259-014-2939-8
- Brekke, E., Morken, T. S., and Sonnewald, U. (2015). Glucose metabolism and astrocyte-neuron interactions in the neonatal brain. *Neurochem. Int.* 82, 33–41. doi: 10.1016/j.neuint.2015.02.002
- Brody, A. L., Okita, K., Shieh, J., Liang, L., Hubert, R., Mamoun, M., et al. (2014). Radiation dosimetry and biodistribution of the translocator protein radiotracer [(11)C]DAA1106 determined with PET/CT in healthy human volunteers. *Nucl. Med. Biol.* 41, 871–875. doi: 10.1016/j.nucmedbio.2014.07.004
- Brody, H. (2012). Multiple sclerosis. *Nature* 484, S1. doi: 10.1038/nature11104
- Brosnan, C. F., and Raine, C. S. (2013). The astrocyte in multiple sclerosis revisited. *Glia* 61, 453–465. doi: 10.1002/glia.22443
- Brown, G. C., and Neher, J. J. (2010). Inflammatory neurodegeneration and mechanisms of microglial killing of neurons. *Mol. Neurobiol.* 41, 242–247. doi: 10.1007/s12035-010-8105-9
- Brownell, A.-L. (2008). “Positron emission tomography (PET),” in *Encyclopedia of Biomaterials and Biomedical Engineering*, 2nd Edn., eds G. E. Wnek and G. L. Bowlin (Boca Raton, FL: CRC Press), 2314–2325.
- Brownell, A.-L., Chen, Y. I., Yu, M., Wang, X., Dedeoglu, A., Cicchetti, C., et al. (2004). 3- Nitropropionic acid induced neurotoxicity – assessed by ultra high resolution PET with comparison to MRS. *J. Neurochem.* 89, 1206–1214. doi: 10.1111/j.1471-4159.2004.02408.x
- Brownell, G. L., and Sweet, W. H. (1953). Localization of brain tumors with positron emitters. *Nucleonics* 11, 40–45.

- Brück, W. (2005). Clinical implications of neuropathological findings in multiple sclerosis. *J. Neurol.* 252(Suppl. 3), iii10–iii14. doi: 10.1007/s00415-005-2011-5
- Brugarolas, P., and Popko, B. (2014). Remyelination therapy goes to trial for multiple sclerosis. *Neurol. Neuroimmunol. Neuroinflammation* 1:e26. doi: 10.1212/wnx.0000000000000026
- Buck, D., Forschler, A., Lapa, C., Schuster, T., Vollmar, P., Korn, T., et al. (2012). 18F-FDG PET detects inflammatory infiltrates in spinal cord experimental autoimmune encephalomyelitis lesions. *J. Nucl. Med.* 53, 1269–1276. doi: 10.2967/jnumed.111.102608
- Burnstock, G. (2008). Purinergic signalling and disorders of the central nervous system. *Nat. Rev. Drug Discov.* 7, 575–590. doi: 10.1038/nrd2605
- Byrnes, K. R., Stoica, B., Loane, D. J., Riccio, A., Davis, M. I., and Faden, A. I. (2009). Metabotropic glutamate receptor 5 activation inhibits microglial associated inflammation and neurotoxicity. *Glia* 57, 550–560. doi: 10.1002/glia.20783
- Cabral, G. A., Raborn, E. S., Griffin, L., Dennis, J., and Marciano-Cabral, F. (2008). CB₂ receptors in the brain: role in central immune function. *Br. J. Pharmacol.* 153, 240–251. doi: 10.1038/sj.bjp.0707584
- Cao, Q., Cai, W., Li, Z.-B., Chen, K., He, L., Li, H.-C., et al. (2007). PET imaging of acute and chronic inflammation in living mice. *Eur. J. Nucl. Med. Mol. Imaging* 34, 1832–1842. doi: 10.1007/s00259-007-0451-0
- Carson, M. J., Cameron Thrash, J., and Walter, B. (2006). The cellular response in neuroinflammation: the role of leukocytes, microglia and astrocytes in neuronal death and survival. *Clin. Neurosci. Res.* 6, 237–245. doi: 10.1016/j.cnr.2006.09.004
- Catana, C., Guimaraes, A. R., and Rosen, B. R. (2013). PET and MR imaging: the odd couple or a match made in heaven? *J. Nucl. Med.* 54, 815–824. doi: 10.2967/jnumed.112.112771
- Chang, A., Tourtellotte, W. W., Rudick, R., and Trapp, B. D. (2002). Premyelinating oligodendrocytes in chronic lesions of multiple sclerosis. *N. Engl. J. Med.* 346, 165–173. doi: 10.1056/NEJMoa010994
- Chauveau, F., Boutin, H., Van Camp, N., Dollé, F., and Tavitian, B. (2008). Nuclear imaging of neuroinflammation: a comprehensive review of [11C]PK11195 challengers. *Eur. J. Nucl. Med. Mol. Imaging* 35, 2304–2319. doi: 10.1007/s00259-008-0908-9
- Chauveau, F., Boutin, H., Van Camp, N., Thominaux, C., Hantraye, P., Rivron, L., et al. (2011). *In vivo* imaging of neuroinflammation in the rodent brain with [11C]SSR180575, a novel indoleacetamide radioligand of the translocator protein (18 kDa). *Eur. J. Nucl. Med. Mol. Imaging* 38, 509–514. doi: 10.1007/s00259-010-1628-5
- Chauveau, F., Van Camp, N., Dollé, F., Kuhnast, B., Hinnen, F., Damont, A., et al. (2009). Comparative evaluation of the translocator protein radioligands 11C-DPA-713, 18F-DPA-714, and 11C-PK11195 in a rat model of acute neuroinflammation. *J. Nucl. Med.* 50, 468–476. doi: 10.2967/jnumed.108.058669
- Cherry, J. D., Olschowka, J. A., and O'Banion, M. (2014). Neuroinflammation and M2 microglia: the good, the bad, and the inflamed. *J. Neuroinflammation* 11:98. doi: 10.1186/1742-2094-11-98
- Ching, A. S. C., Kuhnast, B., Damont, A., Roeda, D., Tavitian, B., and Dollé, F. (2012). Current paradigm of the 18-kDa translocator protein (TSPO) as a molecular target for PET imaging in neuroinflammation and neurodegenerative diseases. *Insights Imaging* 3, 111–119. doi: 10.1007/s13244-011-0128-x
- Chiurchiù, V., Lanuti, M., Catanzaro, G., Fezza, F., Rapino, C., and Maccarrone, M. (2014). Detailed characterization of the endocannabinoid system in human macrophages and foam cells, and anti-inflammatory role of type-2 cannabinoid receptor. *Atherosclerosis* 233, 55–63. doi: 10.1016/j.atherosclerosis.2013.12.042
- Ciarmiello, A. (2011). Imaging of neuroinflammation. *Eur. J. Nucl. Med. Mol. Imaging* 38, 2198–2201. doi: 10.1007/s00259-011-1959-x
- Claycomb, K. I., Johnson, K. M., Winokur, P. N., Sacino, A. V., and Crocker, S. J. (2013). Astrocyte regulation of CNS inflammation and remyelination. *Brain Sci.* 3, 1109–1127. doi: 10.3390/brainsci3031109
- Colasanti, A., Guo, Q., Muhlert, N., Giannetti, P., Onega, M., Newbould, R. D., et al. (2014). *In vivo* assessment of brain white matter inflammation in multiple sclerosis with 18F-PBR111 PET. *J. Nucl. Med.* 55, 1112–1118. doi: 10.2967/jnumed.113.135129
- Compston, A., and Coles, A. (2008). Multiple sclerosis. *Lancet* 372, 1502–1517. doi: 10.1016/S0140-6736(08)61620-7
- Constantinescu, C. S., Farooqi, N., O'Brien, K., and Gran, B. (2011). Experimental autoimmune encephalomyelitis (EAE) as a model for multiple sclerosis (MS): EAE as model for MS. *Br. J. Pharmacol.* 164, 1079–1106. doi: 10.1111/j.1476-5381.2011.01302.x
- Correale, J. (2014). The role of microglial activation in disease progression. *Mult. Scler. Houndmills Basingstoke Engl.* 20, 1288–1295. doi: 10.1177/1352458514533230
- Coughlin, J. M., Wang, Y., Ma, S., Yue, C., Kim, P. K., Adams, A. V., et al. (2014). Regional brain distribution of translocator protein using [(11)C]DPA-713 PET in individuals infected with HIV. *J. Neurovirol.* 20, 219–232. doi: 10.1007/s13365-014-0239-5
- Criste, G., Trapp, B., and Dutta, R. (2014). Axonal loss in multiple sclerosis: causes and mechanisms. *Handb. Clin. Neurol.* 122, 101–113. doi: 10.1016/B978-0-444-52001-2.00005-4
- D'Intino, G., Paradisi, M., Fernandez, M., Giuliani, A., Aloe, L., Giardino, L., et al. (2005). Cognitive deficit associated with cholinergic and nerve growth factor down-regulation in experimental allergic encephalomyelitis in rats. *Proc. Natl. Acad. Sci. U.S.A.* 102, 3070–3075. doi: 10.1073/pnas.0500073102
- Daneman, R., and Rescigno, M. (2009). The gut immune barrier and the blood-brain barrier: are they so different? *Immunity* 31, 722–735. doi: 10.1016/j.immuni.2009.09.012
- Debruyne, J. C., Versijpt, J., Van Laere, K. J., De Vos, F., Keppens, J., Strijckmans, K., et al. (2003). PET visualization of microglia in multiple sclerosis patients using [11C]PK11195. *Eur. J. Nucl. Med.* 10, 257–264. doi: 10.1046/j.1468-1331.2003.00571.x
- Defereros, S. N., Dodou, E., Andronis, C., and Persidis, A. (2012). From depression to neurodegeneration and heart failure: re-examining the potential of MAO inhibitors. *Expert Rev. Clin. Pharmacol.* 5, 413–425. doi: 10.1586/ecp.12.29
- DeLorenzo, C., DellaGioia, N., Bloch, M., Sanacora, G., Nabulsi, N., Abdallah, C., et al. (2015). *In vivo* ketamine-induced changes in [11C]ABP688 binding to metabotropic glutamate receptor subtype 5. *Biol. Psychiatry* 77, 266–275. doi: 10.1016/j.biopsych.2014.06.024
- Denic, A., Johnson, A. J., Bieber, A. J., Warrington, A. E., Rodriguez, M., and Pirko, I. (2011). The relevance of animal models in multiple sclerosis research. *Pathophysiology* 18, 21–29. doi: 10.1016/j.pathophys.2010.04.004
- de Paula Faria, D., Copray, S., Sijbesma, J. W. A., Willemsen, A. T. M., Buchpiguel, C. A., Dierckx, R. A. J. O., et al. (2014a). PET imaging of focal demyelination and remyelination in a rat model of multiple sclerosis: comparison of [11C]MeDAS, [11C]CIC and [11C]PIB. *Eur. J. Nucl. Med. Mol. Imaging* 41, 995–1003. doi: 10.1007/s00259-013-2682-6
- de Paula Faria, D., de Vries, E. F. J., Sijbesma, J. W. A., Dierckx, R. A. J. O., Buchpiguel, C. A., and Copray, S. (2014b). PET imaging of demyelination and remyelination in the cuprizone mouse model for multiple sclerosis: a comparison between [11C]CIC and [11C]MeDAS. *Neuroimage* 87, 395–402. doi: 10.1016/j.neuroimage.2013.10.057
- Derwenskus, J., and Lublin, F. D. (2014). Future treatment approaches to multiple sclerosis. *Handb. Clin. Neurol.* 122, 563–577. doi: 10.1016/B978-0-444-52001-2.00024-8
- de Vries, E. F. J., Doorduyn, J., Dierckx, R. A., and van Waarde, A. (2008). Evaluation of [(11)C]rofecoxib as PET tracer for cyclooxygenase 2 overexpression in rat models of inflammation. *Nucl. Med. Biol.* 35, 35–42. doi: 10.1016/j.nucmedbio.2007.07.015
- de Vries, E. F. J., van Waarde, A., Buursma, A. R., and Vaalburg, W. (2003). Synthesis and *in vivo* evaluation of 18F-desbromo-DuP-697 as a PET tracer for cyclooxygenase-2 expression. *J. Nucl. Med.* 44, 1700–1706.
- Dickens, A. M., Vainio, S., Marjamäki, P., Johansson, J., Lehtiniemi, P., Rokka, J., et al. (2014). Detection of microglial activation in an acute model of neuroinflammation using PET and radiotracers 11C-(R)-PK11195 and 18F-GE-180. *J. Nucl. Med.* 55, 466–472. doi: 10.2967/jnumed.113.125625
- Dimitrakopoulou-Strauss, A., Strauss, L. G., Burger, C., Rühl, A., Irngartinger, G., Stremmel, W., et al. (2004). Prognostic aspects of 18F-FDG PET kinetics in patients with metastatic colorectal carcinoma receiving FOLFOX chemotherapy. *J. Nucl. Med.* 45, 1480–1487.
- Di Penta, A., Moreno, B., Reix, S., Fernandez-Diez, B., Villanueva, M., Errea, O., et al. (2013). Oxidative stress and proinflammatory cytokines contribute to demyelination and axonal damage in a cerebellar culture

- model of neuroinflammation. *PLoS ONE* 8:e54722. doi: 10.1371/journal.pone.0054722
- Docagne, F., Mestre, L., Loria, F., Hernangómez, M., Correa, F., and Guaza, C. (2008). Therapeutic potential of CB2 targeting in multiple sclerosis. *Expert Opin. Ther. Targets* 12, 185–195. doi: 10.1517/14728222.12.2.185
- Domercq, M., Vázquez-Villoldo, N., and Matute, C. (2013). Neurotransmitter signaling in the pathophysiology of microglia. *Front. Cell. Neurosci.* 7:49. doi: 10.3389/fncel.2013.00049
- Edgar, J. M., and Nave, K.-A. (2009). The role of CNS glia in preserving axon function. *Curr. Opin. Neurobiol.* 19, 498–504. doi: 10.1016/j.conb.2009.08.003
- Ehrhart, J., Obregon, D., Mori, T., Hou, H., Sun, N., Bai, Y., et al. (2005). Stimulation of cannabinoid receptor 2 (CB2) suppresses microglial activation. *J. Neuroinflammation* 2:29. doi: 10.1186/1742-2094-2-29
- Ellwardt, E., and Zipp, F. (2014). Molecular mechanisms linking neuroinflammation and neurodegeneration in MS. *Exp. Neurol.* 262 (Pt A), 8–17. doi: 10.1016/j.expneurol.2014.02.006
- Endres, C. J., Pomper, M. G., James, M., Uzuner, O., Hammoud, D. A., Watkins, C. C., et al. (2009). Initial evaluation of 11C-DPA-713, a novel TSPO PET ligand, in humans. *J. Nucl. Med.* 50, 1276–1282. doi: 10.2967/jnumed.109.062265
- Evens, N., Muccioli, G. G., Houbrechts, N., Lambert, D. M., Verbruggen, A. M., Van Laere, K., et al. (2009). Synthesis and biological evaluation of carbon-11- and fluorine-18-labeled 2-oxoquinoline derivatives for type 2 cannabinoid receptor positron emission tomography imaging. *Nucl. Med. Biol.* 36, 455–465. doi: 10.1016/j.nucmedbio.2009.01.009
- Evens, N., Vandeputte, C., Coolen, C., Janssen, P., Sciort, R., Baekelandt, V., et al. (2012). Preclinical evaluation of [11C]NEA0, a type 2 cannabinoid receptor PET tracer. *Nucl. Med. Biol.* 39, 389–399. doi: 10.1016/j.nucmedbio.2011.09.005
- Evens, N., Vandeputte, C., Muccioli, G. G., Lambert, D. M., Baekelandt, V., Verbruggen, A. M., et al. (2011). Synthesis, *in vitro* and *in vivo* evaluation of fluorine-18 labelled FE-GW405833 as a PET tracer for type 2 cannabinoid receptor imaging. *Bioorg. Med. Chem.* 19, 4499–4505. doi: 10.1016/j.bmc.2011.06.033
- Faria Dde, P., Copray, S., Buchpiguel, C., Dierckx, R., and de Vries, E. (2014). PET imaging in multiple sclerosis. *J. Neuroimmune Pharmacol.* 9, 468–482. doi: 10.1007/s11481-014-9544-2
- Farina, C., Aloisi, F., and Meinl, E. (2007). Astrocytes are active players in cerebral innate immunity. *Trends Immunol.* 28, 138–145. doi: 10.1016/j.it.2007.01.005
- Fatima, N., Toscano, M. P., Hunter, S. B., and Cohen, C. (2010). Controversial Role of Epstein-Barr Virus in Multiple Sclerosis. *Appl. Immunohistochem. Mol. Morphol.* 19, 246–252. doi: 10.1097/PAI.0b013e3181f3b3b4
- Filippi, M., and Rocca, M. A. (2011). MR imaging of multiple sclerosis. *Radiology* 259, 659–681. doi: 10.1148/radiol.11101362
- Filippi, M., Rocca, M. A., Barkhof, F., Brück, W., Chen, J. T., Comi, G., et al. (2012). Association between pathological and MRI findings in multiple sclerosis. *Lancet Neurol.* 11, 349–360. doi: 10.1016/S1474-4422(12)70003-0
- Fitzner, D., and Simons, M. (2010). Chronic progressive multiple sclerosis – pathogenesis of neurodegeneration and therapeutic strategies. *Curr. Neuropharmacol.* 8, 305–315. doi: 10.2174/157015910792246218
- Friese, M. A., Schattling, B., and Fugger, L. (2014). Mechanisms of neurodegeneration and axonal dysfunction in multiple sclerosis. *Nat. Rev. Neurol.* 10, 225–238. doi: 10.1038/nrneurol.2014.37
- Frischer, J. M., Bramow, S., Dal-Bianco, A., Lucchinetti, C. F., Rauschka, H., Schmidbauer, M., et al. (2009). The relation between inflammation and neurodegeneration in multiple sclerosis brains. *Brain J. Neurol.* 132, 1175–1189. doi: 10.1093/brain/awp070
- Frohman, E. M., Racke, M. K., and Raine, C. S. (2006). Multiple sclerosis—the plaque and its pathogenesis. *N. Engl. J. Med.* 354, 942–955. doi: 10.1056/NEJMra052130
- Fulda, S., Gorman, A. M., Hori, O., and Samali, A. (2010). Cellular stress responses: cell survival and cell death. *Int. J. Cell Biol.* 2010, 1–23. doi: 10.1155/2010/214074
- Furlan, R., Cuomo, C., and Martino, G. (2009). “Animal models of multiple sclerosis,” in *Neural Cell Transplantation*, eds D. Gordon and N. J. Scolding (Totowa, NJ: Humana Press), 157–173. Available online at: http://link.springer.com/10.1007/978-1-60327-931-4_11 (Accessed May 14, 2015).
- Gambhir, S. S. (2002). Molecular imaging of cancer with positron emission tomography. *Nat. Rev. Cancer* 2, 683–693. doi: 10.1038/nrc882
- Gandelman, M., Peluffo, H., Beckman, J. S., Cassina, P., and Barbeito, L. (2010). Extracellular ATP and the P2X7 receptor in astrocyte-mediated motor neuron death: implications for amyotrophic lateral sclerosis. *J. Neuroinflammation* 7:33. doi: 10.1186/1742-2094-7-33
- Gandhi, R., Laroni, A., and Weiner, H. L. (2010). Role of the innate immune system in the pathogenesis of multiple sclerosis. *J. Neuroimmunol.* 221, 7–14. doi: 10.1016/j.jneuroim.2009.10.015
- Gao, M., Wang, M., Green, M. A., Hutchins, G. D., and Zheng, Q.-H. (2015). Synthesis of [11C]GSK1482160 as a new PET agent for targeting P2X7 receptor. *Bioorg. Med. Chem. Lett.* 25, 1965–1970. doi: 10.1016/j.bmcl.2015.03.021
- Garibotto, V., Tettamanti, M., Marcone, A., Florea, I., Panzacchi, A., Moresco, R., et al. (2013). Cholinergic activity correlates with reserve proxies in Alzheimer's disease. *Neurobiol. Aging* 34, 2694.e13–18. doi: 10.1016/j.neurobiolaging.2013.05.020
- Ge, Y. (2006). Multiple sclerosis: the role of MR imaging. *AJNR Am. J. Neuroradiol.* 27, 1165–1176.
- Geurts, J. J. G., Wolswijk, G., Bö, L., van der Valk, P., Polman, C. H., Troost, D., et al. (2003). Altered expression patterns of group I and II metabotropic glutamate receptors in multiple sclerosis. *Brain J. Neurol.* 126, 1755–1766. doi: 10.1093/brain/awg179
- Giannetti, P., Politis, M., Su, P., Turkheimer, F. E., Malik, O., Keihaninejad, S., et al. (2015). Increased PK11195-PET binding in normal-appearing white matter in clinically isolated syndrome. *Brain* 138, 110–119. doi: 10.1093/brain/awu331
- Gilden, D. H. (2005). Infectious causes of multiple sclerosis. *Lancet Neurol.* 4, 195–202. doi: 10.1016/S1474-4422(05)70023-5
- Glass, C. K., Saijo, K., Winner, B., Marchetto, M. C., and Gage, F. H. (2010). Mechanisms underlying inflammation in neurodegeneration. *Cell* 140, 918–934. doi: 10.1016/j.cell.2010.02.016
- Golla, S. S. V., Boellaard, R., Oikonen, V., Hoffmann, A., van Berckel, B. N. M., Windhorst, A. D., et al. (2015). Quantification of [18F]DPA-714 binding in the human brain: initial studies in healthy controls and Alzheimer's disease patients. *J. Cereb. Blood Flow Metab.* 35, 766–772. doi: 10.1038/jcbfm.2014.261
- Goodin, D. S. (2014). “Chapter 11 - The epidemiology of multiple sclerosis: insights to disease pathogenesis,” in *Handbook of Clinical Neurology Multiple Sclerosis and Related Disorders*, ed D. S. Goodin (Elsevier), 231–266. Available online at: <http://www.sciencedirect.com/science/article/pii/B9780444520012000108> (Accessed March 13, 2015).
- Gordon, S. (2003). Alternative activation of macrophages. *Nat. Rev. Immunol.* 3, 23–35. doi: 10.1038/nri978
- Goverman, J. (2009). Autoimmune T cell responses in the central nervous system. *Nat. Rev. Immunol.* 9, 393–407. doi: 10.1038/nri2550
- Grassi, I., Nanni, C., Allegri, V., Morigi, J. J., Montini, G. C., Castellucci, P., et al. (2012). The clinical use of PET with (11)C-acetate. *Am. J. Nucl. Med. Mol. Imaging* 2, 33–47.
- Gulyás, B., Pavlova, E., Kása, P., Gulya, K., Bakota, L., Várszegi, S., et al. (2011). Activated MAO-B in the brain of Alzheimer patients, demonstrated by [11C]-L-deprenyl using whole hemisphere autoradiography. *Neurochem. Int.* 58, 60–68. doi: 10.1016/j.neuint.2010.10.013
- Guo, S., Pelligra, C., Saint-Laurent Thibault, C., Hernandez, L., and Kansal, A. (2014). Cost-effectiveness analyses in multiple sclerosis: a review of modelling approaches. *Pharmacoeconomics* 32, 559–572. doi: 10.1007/s40273-014-0150-1
- Haider, L., Fischer, M. T., Frischer, J. M., Bauer, J., Hoftberger, R., Botond, G., et al. (2011). Oxidative damage in multiple sclerosis lesions. *Brain* 134, 1914–1924. doi: 10.1093/brain/awr128
- Halldin, C., Farde, L., Litton, J. E., Hall, H., and Sedvall, G. (1992). [11C]Ro 15-4513, a ligand for visualization of benzodiazepine receptor binding. Preparation, autoradiography and positron emission tomography. *Psychopharmacology (Berl.)* 108, 16–22. doi: 10.1007/BF02245279
- Hanisch, U.-K., and Kettenmann, H. (2007). Microglia: active sensor and versatile effector cells in the normal and pathologic brain. *Nat. Neurosci.* 10, 1387–1394. doi: 10.1038/nn1997
- Hartung, D. M., Bourdette, D. N., Ahmed, S. M., and Whitham, R. H. (2015). The cost of multiple sclerosis drugs in the US and the pharmaceutical industry: too big to fail? *Neurology* 84, 2185–2192. doi: 10.1212/WNL.0000000000001608
- Haskó, G., Linden, J., Cronstein, B., and Pacher, P. (2008). Adenosine receptors: therapeutic aspects for inflammatory and immune diseases. *Nat. Rev. Drug Discov.* 7, 759–770. doi: 10.1038/nrd2638

- Hemmer, B., Kerschensteiner, M., and Korn, T. (2015). Role of the innate and adaptive immune responses in the course of multiple sclerosis. *Lancet Neurol.* 14, 406–419. doi: 10.1016/S1474-4422(14)70305-9
- Herrero, P., Laforest, R., Shoghi, K., Zhou, D., Ewald, G., Pfeifer, J., et al. (2012). Feasibility and dosimetry studies for 18F-NOS as a potential PET radiopharmaceutical for inducible nitric oxide synthase in humans. *J. Nucl. Med.* 53, 994–1001. doi: 10.2967/jnumed.111.088518
- Herschman, H. R. (2003). Micro-PET imaging and small animal models of disease. *Curr. Opin. Immunol.* 15, 378–384. doi: 10.1016/S0952-7915(03)00066-9
- Hicks, R. J. (2006). PET tracer development - a tale of mice and men. *Cancer Imaging* 6, S102–S106. doi: 10.1102/1470-7330.2006.9098
- Horti, A. G., Gao, Y., Ravert, H. T., Finley, P., Valentine, H., Wong, D. F., et al. (2010). Synthesis and biodistribution of [11C]A-836339, a new potential radioligand for PET imaging of cannabinoid type 2 receptors (CB2). *Bioorg. Med. Chem.* 18, 5202–5207. doi: 10.1016/j.bmc.2010.05.058
- Huang, H. J., Isakow, W., Byers, D. E., Engle, J. T., Griffin, E. A., Kemp, D., et al. (2015). Imaging pulmonary inducible nitric oxide synthase expression with PET. *J. Nucl. Med.* 56, 76–81. doi: 10.2967/jnumed.114.146381
- Hurley, D. (2015). News from the annual meeting: multiple sclerosis. *Neurol. Today* 15, 21–22. doi: 10.1097/01.NT.0000465868.70272.0c
- Imaizumi, M., Kim, H.-J., Zoghbi, S. S., Briard, E., Hong, J., Musachio, J. L., et al. (2007). PET imaging with [11C]PBR28 can localize and quantify upregulated peripheral benzodiazepine receptors associated with cerebral ischemia in rat. *Neurosci. Lett.* 411, 200–205. doi: 10.1016/j.neulet.2006.09.093
- Islam, T., Gauderman, W. J., Cozen, W., Hamilton, A. S., Burnett, M. E., and Mack, T. M. (2006). Differential twin concordance for multiple sclerosis by latitude of birthplace. *Ann. Neurol.* 60, 56–64. doi: 10.1002/ana.20871
- Iwama, S., Sugimura, Y., Suzuki, H., Suzuki, H., Murase, T., Ozaki, N., et al. (2011). Time-dependent changes in proinflammatory and neurotrophic responses of microglia and astrocytes in a rat model of osmotic demyelination syndrome. *Glia* 59, 452–462. doi: 10.1002/glia.21114
- Jacobs, A. H., and Tavitian, B. (2012). Noninvasive molecular imaging of neuroinflammation. *J. Cereb. Blood Flow Metab.* 32, 1393–1415. doi: 10.1038/jcbfm.2012.53
- Jadvar, H., and Colletti, P. M. (2014). Competitive advantage of PET/MRI. *Eur. J. Radiol.* 83, 84–94. doi: 10.1016/j.ejrad.2013.05.028
- James, M. L., Fulton, R. R., Vercoullie, J., Henderson, D. J., Garreau, L., Chalou, S., et al. (2008). DPA-714, a new translocator protein-specific ligand: synthesis, radiofluorination, and pharmacologic characterization. *J. Nucl. Med.* 49, 814–822. doi: 10.2967/jnumed.107.046151
- Janssen, B., Vugts, D. J., Funke, U., Spaans, A., Schuit, R. C., Kooijman, E., et al. (2014). Synthesis and initial preclinical evaluation of the P2X7 receptor antagonist [¹¹C]A-740003 as a novel tracer of neuroinflammation. *J. Label. Compd. Radiopharm.* 57, 509–516. doi: 10.1002/jlcr.3206
- Ji, B., Kumata, K., Onoe, H., Kaneko, H., Zhang, M.-R., Seki, C., et al. (2013). Assessment of radioligands for PET imaging of cyclooxygenase-2 in an ischemic neuronal injury model. *Brain Res.* 1533, 152–162. doi: 10.1016/j.brainres.2013.08.026
- Ji, B., Maeda, J., Sawada, M., Ono, M., Okauchi, T., Inaji, M., et al. (2008). Imaging of peripheral benzodiazepine receptor expression as biomarkers of detrimental versus beneficial glial responses in mouse models of Alzheimer's and other CNS pathologies. *J. Neurosci.* 28, 12255–12267. doi: 10.1523/JNEUROSCI.2312-08.2008
- Jiang, M., and Chen, G. (2009). Ca²⁺ regulation of dynamin-independent endocytosis in cortical astrocytes. *J. Neurosci.* 29, 8063–8074. doi: 10.1523/JNEUROSCI.6139-08.2009
- Jødal, L., Le Loire, C., and Champion, C. (2012). Positron range in PET imaging: an alternative approach for assessing and correcting the blurring. *Phys. Med. Biol.* 57, 3931–3943. doi: 10.1088/0031-9155/57/12/3931
- Johansson, A., Engler, H., Blomquist, G., Scott, B., Wall, A., Aquilonius, S.-M., et al. (2007). Evidence for astrocytosis in ALS demonstrated by [11C](L)-deprenyl-D2 PET. *J. Neurol. Sci.* 255, 17–22. doi: 10.1016/j.jns.2007.01.057
- Jones, T., Rabiner, E. A., and PET Research Advisory Company (2012). The development, past achievements, and future directions of brain PET. *J. Cereb. Blood Flow Metab.* 32, 1426–1454. doi: 10.1038/jcbfm.2012.20
- Kassmann, C. M., Lappe-Siefke, C., Baes, M., Brügger, B., Mildner, A., Werner, H. B., et al. (2007). Axonal loss and neuroinflammation caused by peroxisome-deficient oligodendrocytes. *Nat. Genet.* 39, 969–976. doi: 10.1038/ng2070
- Kelley, K. A., Ho, L., Winger, D., Freire-Moar, J., Borelli, C. B., Aisen, P. S., et al. (1999). Potentiation of excitotoxicity in transgenic mice overexpressing neuronal cyclooxygenase-2. *Am. J. Pathol.* 155, 995–1004. doi: 10.1016/S0002-9440(10)65199-1
- Kiferle, L., Politis, M., Muraro, P. A., and Piccini, P. (2011). Positron emission tomography imaging in multiple sclerosis-current status and future applications. *Eur. J. Neurol.* 18, 226–231. doi: 10.1111/j.1468-1331.2010.03154.x
- Kipp, M., Clarner, T., Dang, J., Copray, S., and Beyer, C. (2009). The cuprizone animal model: new insights into an old story. *Acta Neuropathol. (Berl.)* 118, 723–736. doi: 10.1007/s00401-009-0591-3
- Kooi, E.-J., Prins, M., Bajic, N., Beliën, J. A. M., Gerritsen, W. H., van Horssen, J., et al. (2011). Cholinergic imbalance in the multiple sclerosis hippocampus. *Acta Neuropathol. (Berl.)* 122, 313–322. doi: 10.1007/s00401-011-0849-4
- Kooij, G., van Horssen, J., Bandaru, V. V. R., Haughey, N. J., and de Vries, H. E. (2012). The role of ATP-binding cassette transporters in neuroinflammation: relevance for bioactive lipids. *Front. Pharmacol.* 3:74. doi: 10.3389/fphar.2012.00074
- Kritis, A. A., Stamoula, E. G., Paniskaki, K. A., and Vavilis, T. D. (2015). Researching glutamate-induced cytotoxicity in different cell lines: a comparative/collective analysis/study. *Front. Cell. Neurosci.* 9:91. doi: 10.3389/fncel.2015.00091
- Kröncke, K.-D., Fehsel, K., and Kolb-Bachofen, V. (1998). Inducible nitric oxide synthase in human diseases. *Clin. Exp. Immunol.* 113, 147–156. doi: 10.1046/j.1365-2249.1998.00648.x
- Krupp, L. B., Christodoulou, C., Melville, P., Scherl, W. F., MacAllister, W. S., and Elkins, L. E. (2004). Donepezil improved memory in multiple sclerosis in a randomized clinical trial. *Neurology* 63, 1579–1585. doi: 10.1212/01.WNL.0000142989.09633.5A
- Kuhlmann, T. (2002). Acute axonal damage in multiple sclerosis is most extensive in early disease stages and decreases over time. *Brain* 125, 2202–2212. doi: 10.1093/brain/awf235
- Kuhlmann, T., Miron, V., Cui, Q., Cuo, Q., Wegner, C., Antel, J., et al. (2008). Differentiation block of oligodendroglial progenitor cells as a cause for remyelination failure in chronic multiple sclerosis. *Brain J. Neurol.* 131, 1749–1758. doi: 10.1093/brain/awn096
- Kutzelnigg, A., and Lassmann, H. (2014). "Pathology of multiple sclerosis and related inflammatory demyelinating diseases," in *Handbook of Clinical Neurology* (Elsevier), 15–58. Available online at: <http://linkinghub.elsevier.com/retrieve/pii/B9780444520012000029> (Accessed May 20, 2015).
- Lancelot, S., and Zimmer, L. (2010). Small-animal positron emission tomography as a tool for neuropharmacology. *Trends Pharmacol. Sci.* 31, 411–417. doi: 10.1016/j.tips.2010.06.002
- Laroche, C., Alvarez, J. I., and Prat, A. (2011). How do immune cells overcome the blood-brain barrier in multiple sclerosis? *FEBS Lett.* 585, 3770–3780. doi: 10.1016/j.febslet.2011.04.066
- Lavisse, S., Guillermier, M., Herard, A.-S., Petit, F., Delahaye, M., Van Camp, N., et al. (2012). Reactive astrocytes overexpress TSPO and are detected by TSPO positron emission tomography imaging. *J. Neurosci.* 32, 10809–10818. doi: 10.1523/JNEUROSCI.1487-12.2012
- Lev, S. (2012). Nonvesicular lipid transfer from the endoplasmic reticulum. *Cold Spring Harb. Perspect. Biol.* 4:a013300. doi: 10.1101/cshperspect.a013300
- Liang, H., Yang, Y., Yang, K., Wu, Y., Boone, J. M., and Cherry, S. R. (2007). A microPET/CT system for *in vivo* small animal imaging. *Phys. Med. Biol.* 52, 3881–3894. doi: 10.1088/0031-9155/52/13/015
- Lim, K., Labaree, D., Li, S., and Huang, Y. (2014). Preparation of the metabotropic glutamate receptor 5 (mGluR5) PET tracer [18F]FPFB for human use: an automated radiosynthesis and a novel one-pot synthesis of its radiolabeling precursor. *Appl. Radiat. Isot.* 94, 349–354. doi: 10.1016/j.apradiso.2014.09.006
- Lister, M. F., Sharkey, J., Sawatzky, D. A., Hodgkiss, J. P., Davidson, D. J., Rossi, A. G., et al. (2007). The role of the purinergic P2X7 receptor in inflammation. *J. Inflamm.* 4:5. doi: 10.1186/1476-9255-4-5
- Liu, G.-J., Middleton, R. J., Hatty, C. R., Kam, W. W.-Y., Chan, R., Pham, T., et al. (2014). The 18 kDa translocator protein, microglia and neuroinflammation: TSPO, microglia and neuroinflammation. *Brain Pathol.* 24, 631–653. doi: 10.1111/bpa.12196
- Liu, J. S.-H., Zhao, M.-L., Brosnan, C. F., and Lee, S. C. (2001). Expression of inducible nitric oxide synthase and nitrotyrosine in multiple sclerosis

- lesions. *Am. J. Pathol.* 158, 2057–2066. doi: 10.1016/S0002-9440(10)64677-9
- Liu, X., Chen, C., and Smith, B. J. (2008). Progress in brain penetration evaluation in drug discovery and development. *J. Pharmacol. Exp. Ther.* 325, 349–356. doi: 10.1124/jpet.107.130294
- Loane, D. J., Stoica, B. A., Pajoohesh-Ganji, A., Byrnes, K. R., and Faden, A. I. (2009). Activation of metabotropic glutamate receptor 5 modulates microglial reactivity and neurotoxicity by inhibiting NADPH oxidase. *J. Biol. Chem.* 284, 15629–15639. doi: 10.1074/jbc.M806139200
- Lopez-Diego, R. S., and Weiner, H. L. (2008). Novel therapeutic strategies for multiple sclerosis—a multifaceted adversary. *Nat. Rev. Drug Discov.* 7, 909–925. doi: 10.1038/nrd2358
- Lövlblad, K.-O., Anzalone, N., Dörfler, A., Essig, M., Hurwitz, B., Kappos, L., et al. (2010). MR imaging in multiple sclerosis: review and recommendations for current practice. *AJNR Am. J. Neuroradiol.* 31, 983–989. doi: 10.3174/ajnr.A1906
- Lublin, F. D., and Reingold, S. C. (1996). Defining the clinical course of multiple sclerosis results of an international survey. *Neurology* 46, 907–911. doi: 10.1212/WNL.46.4.907
- Lucchinetti, C., Brück, W., Parisi, J., Scheithauer, B., Rodriguez, M., and Lassmann, H. (2000). Heterogeneity of multiple sclerosis lesions: implications for the pathogenesis of demyelination. *Ann. Neurol.* 47, 707–717. doi: 10.1002/1531-8249(200006)47:6<707::AID-ANA3>3.0.CO;2-Q
- Lund, H., Krakauer, M., Skimminge, A., Sellebjerg, F., Garde, E., Siebner, H. R., et al. (2013). Blood-brain barrier permeability of normal appearing white matter in relapsing-remitting multiple sclerosis. *PLoS ONE* 8:e56375. doi: 10.1371/journal.pone.0056375
- Luongo, L., Guida, F., Imperatore, R., Napolitano, F., Gatta, L., Cristino, L., et al. (2014). The A1 adenosine receptor as a new player in microglia physiology: new player in microglia physiology. *Glia* 62, 122–132. doi: 10.1002/glia.22592
- Maeda, J., Suhara, T., Zhang, M.-R., Okauchi, T., Yasuno, F., Ikoma, Y., et al. (2004). Novel peripheral benzodiazepine receptor ligand [11C]DAA1106 for PET: an imaging tool for glial cells in the brain. *Synapse* 52, 283–291. doi: 10.1002/syn.20027
- Maffione, A. M., Rampin, L., Grassetto, G., L'Erario, R., Colletti, P. M., and Rubello, D. (2014). 18F-FDG PET/CT in tumefactive multiple sclerosis. *Clin. Nucl. Med.* 39, 750–751. doi: 10.1097/RLU.0000000000000427
- Mallajosyula, J. K., Kaur, D., Chinta, S. J., Rajagopalan, S., Rane, A., Nicholls, D. G., et al. (2008). MAO-B elevation in mouse brain astrocytes results in Parkinson's pathology. *PLoS ONE* 3:e1616. doi: 10.1371/journal.pone.0001616
- Mallik, S., Samson, R. S., Wheeler-Kingshott, C. A. M., and Miller, D. H. (2014). Imaging outcomes for trials of remyelination in multiple sclerosis. *J. Neurol. Neurosurg. Psychiatr.* 85, 1396–1404. doi: 10.1136/jnnp-2014-307650
- Malpass, K. (2012). Multiple sclerosis: “Outside-in” demyelination in MS. *Nat. Rev. Neurol.* 8, 61. doi: 10.1038/nrneurol.2011.217
- Mantovani, A., Sica, A., Sozzani, S., Allavena, P., Vecchi, A., and Locati, M. (2004). The chemokine system in diverse forms of macrophage activation and polarization. *Trends Immunol.* 25, 677–686. doi: 10.1016/j.it.2004.09.015
- Maragakis, N. J., and Rothstein, J. D. (2006). Mechanisms of disease: astrocytes in neurodegenerative disease. *Nat. Clin. Pract. Neurol.* 2, 679–689. doi: 10.1038/ncpneu0355
- Marik, J., Ogasawara, A., Martin-McNulty, B., Ross, J., Flores, J. E., Gill, H. S., et al. (2009). PET of glial metabolism using 2-18F-fluoroacetate. *J. Nucl. Med.* 50, 982–990. doi: 10.2967/jnumed.108.057356
- Martinez, F. O., and Gordon, S. (2014). The M1 and M2 paradigm of macrophage activation: time for reassessment. *F1000Prime Rep.* 6:13. doi: 10.12703/P6-13
- Martinez, F. O., Helming, L., and Gordon, S. (2009). Alternative activation of macrophages: an immunologic functional perspective. *Annu. Rev. Immunol.* 27, 451–483. doi: 10.1146/annurev.immunol.021908.132532
- Massoud, T. F. (2003). Molecular imaging in living subjects: seeing fundamental biological processes in a new light. *Genes Dev.* 17, 545–580. doi: 10.1101/gad.1047403
- Matthäus, C., Krafft, C., Dietzek, B., Brehm, B. R., Lorkowski, S., and Popp, J. (2012). Noninvasive imaging of intracellular lipid metabolism in macrophages by Raman microscopy in combination with stable isotopic labeling. *Anal. Chem.* 84, 8549–8556. doi: 10.1021/ac3012347
- Matthews, P. M., Rabiner, E. A., Passchier, J., and Gunn, R. N. (2012). Positron emission tomography molecular imaging for drug development. *Br. J. Clin. Pharmacol.* 73, 175–186. doi: 10.1111/j.1365-2125.2011.04085.x
- Mattner, F., Staykova, M., Berghofer, P., Wong, H. J., Fordham, S., Callaghan, P., et al. (2013). Central nervous system expression and PET imaging of the translocator protein in relapsing-remitting experimental autoimmune encephalomyelitis. *J. Nucl. Med.* 54, 291–298. doi: 10.2967/jnumed.112.108894
- Matute, C., Domercq, M., and Sánchez-Gómez, M.-V. (2006). Glutamate-mediated glial injury: mechanisms and clinical importance. *Glia* 53, 212–224. doi: 10.1002/glia.20275
- Mayo, L., Quintana, F. J., and Weiner, H. L. (2012). The innate immune system in demyelinating disease. *Immunol. Rev.* 248, 170–187. doi: 10.1111/j.1600-065X.2012.01135.x
- Mayo, L., Trauger, S. A., Blain, M., Nadeau, M., Patel, B., Alvarez, J. I., et al. (2014). Regulation of astrocyte activation by glycolipids drives chronic CNS inflammation. *Nat. Med.* 20, 1147–1156. doi: 10.1038/nm.3681
- Medzhitov, R. (2008). Origin and physiological roles of inflammation. *Nature* 454, 428–435. doi: 10.1038/nature07201
- Meuth, S. G., Simon, O. J., Grimm, A., Melzer, N., Herrmann, A. M., Spitzer, P., et al. (2008). CNS inflammation and neuronal degeneration is aggravated by impaired CD200-CD200R-mediated macrophage silencing. *J. Neuroimmunol.* 194, 62–69. doi: 10.1016/j.jneuroim.2007.11.013
- Micell-Robinson, M. A., Touil, H., Healy, L. M., Owen, D. R., Durafoort, B. A., Bar-Or, A., et al. (2015). Roles of microglia in brain development, tissue maintenance and repair. *Brain* 138, 1138–1159. doi: 10.1093/brain/aww066
- Michelucci, A., Heurtaux, T., Grandbarbe, L., Morga, E., and Heuschling, P. (2009). Characterization of the microglial phenotype under specific pro-inflammatory and anti-inflammatory conditions: effects of oligomeric and fibrillar amyloid-beta. *J. Neuroimmunol.* 210, 3–12. doi: 10.1016/j.jneuroim.2009.02.003
- Miljković, D., Timotijević, G., and Stojković, M. M. (2011). Astrocytes in the tempest of multiple sclerosis. *FEBS Lett.* 585, 3781–3788. doi: 10.1016/j.febslet.2011.03.047
- Miller, D. H., Altmann, D. R., and Chard, D. T. (2012). Advances in imaging to support the development of novel therapies for multiple sclerosis. *Clin. Pharmacol. Ther.* 91, 621–634. doi: 10.1038/clpt.2011.349
- Miller, P. W., Long, N. J., Vilar, R., and Gee, A. D. (2008). Synthesis of 11C, 18F, 15O, and 13N radiolabels for positron emission tomography. *Angew. Chem. Int. Ed. Engl.* 47, 8998–9033. doi: 10.1002/anie.200800222
- Mills, C. D., Kincaid, K., Alt, J. M., Heilman, M. J., and Hill, A. M. (2000). M-1/M-2 macrophages and the Th1/Th2 paradigm. *J. Immunol.* 164, 6166–6173. doi: 10.4049/jimmunol.164.12.6166
- Min, K.-J., Yang, M., Kim, S.-U., Jou, I., and Joe, E. (2006). Astrocytes induce hemeoxygenase-1 expression in microglia: a feasible mechanism for preventing excessive brain inflammation. *J. Neurosci.* 26, 1880–1887. doi: 10.1523/JNEUROSCI.3696-05.2006
- Monif, M., Reid, C. A., Powell, K. L., Smart, M. L., and Williams, D. A. (2009). The P2X7 receptor drives microglial activation and proliferation: a trophic role for P2X7R pore. *J. Neurosci.* 29, 3781–3791. doi: 10.1523/JNEUROSCI.5512-08.2009
- Moon, B. S., Kim, B. S., Park, C., Jung, J. H., Lee, Y. W., Lee, H.-Y., et al. (2014). [¹⁸F]Fluoromethyl-PBR28 as a potential radiotracer for TSPO: preclinical comparison with [¹¹C]PBR28 in a rat model of neuroinflammation. *Bioconjug. Chem.* 25, 442–450. doi: 10.1021/bc400556h
- Morales, Y., Parisi, J. E., and Lucchinetti, C. F. (2006). The pathology of multiple sclerosis: evidence for heterogeneity. *Adv. Neurol.* 98, 27–45.
- Mu, L., Bieri, D., Slavik, R., Drandarov, K., Müller, A., Cermak, S., et al. (2013). Radiolabeling and *in vitro/in vivo* evaluation of N-(1-adamantyl)-8-methoxy-4-oxo-1-phenyl-1,4-dihydroquinoline-3-carboxamide as a PET probe for imaging cannabinoid type 2 receptor. *J. Neurochem.* 126, 616–624. doi: 10.1111/jnc.12354
- Mu, L., Schubiger, P. A., and Ametamey, S. M. (2010). Radioligands for the PET imaging of metabotropic glutamate receptor subtype 5 (mGluR5). *Curr. Top. Med. Chem.* 10, 1558–1568. doi: 10.2174/156802610793176783
- Naegele, M., and Martin, R. (2014). “The good and the bad of neuroinflammation in multiple sclerosis,” in *Handbook of Clinical Neurology* (Elsevier), 59–87. Available online at: <http://linkinghub.elsevier.com/retrieve/pii/B9780444520012000030> (Accessed May 20, 2015).

- Nair, A., Frederick, T. J., and Miller, S. D. (2008). Astrocytes in multiple sclerosis: a product of their environment. *Cell. Mol. Life Sci.* 65, 2702–2720. doi: 10.1007/s00018-008-8059-5
- Nash, B., Thomson, C. E., Lington, A. T., McClure, J. D., McBride, M. W., et al. (2011). Functional duality of astrocytes in myelination. *J. Neurosci.* 31, 13028–13038. doi: 10.1523/JNEUROSCI.1449-11.2011
- Nau, R., Ribes, S., Djukic, M., and Eifert, H. (2014). Strategies to increase the activity of microglia as efficient protectors of the brain against infections. *Front. Cell. Neurosci.* 8:138. doi: 10.3389/fncel.2014.00138
- Nave, K.-A. (2010). Myelination and the trophic support of long axons. *Nat. Rev. Neurosci.* 11, 275–283. doi: 10.1038/nrn2797
- Neu, I., and Woelk, H. (1982). Investigations of the lipid metabolism of the white matter in multiple sclerosis: changes in glycerophosphatides and lipid-splitting enzymes. *Neurochem. Res.* 7, 727–735. doi: 10.1007/BF00965525
- Nijland, P. G., Michailidou, I., Witte, M. E., Mizee, M. R., van der Pol, S. M. A., van het Hof, B., et al. (2014). Cellular distribution of glucose and monocarboxylate transporters in human brain white matter and multiple sclerosis lesions: nutrient transporters in multiple sclerosis. *Glia* 62, 1125–1141. doi: 10.1002/glia.22667
- Noyes, K., Bajorska, A., Chappel, A., Schwid, S. R., Mehta, L. R., Weinstock-Guttman, B., et al. (2011). Cost-effectiveness of disease-modifying therapy for multiple sclerosis: a population-based study. *Neurology* 77, 355–363. doi: 10.1212/WNL.0b013e3182270402
- Oh, J., and O'Connor, P. W. (2015). Established disease-modifying treatments in relapsing-remitting multiple sclerosis. *Curr. Opin. Neurol.* 28, 220–229. doi: 10.1097/WCO.0000000000000202
- Oh, U., Fujita, M., Ikonomidou, V. N., Evangelou, I. E., Matsuura, E., Harberts, E., et al. (2011). Translocator protein PET imaging for glial activation in multiple sclerosis. *J. Neuroimmune Pharmacol.* 6, 354–361. doi: 10.1007/s11481-010-9243-6
- Ohshima, M., Senda, M., Ishiwata, K., Kitamura, S., Mishina, M., Ishii, K., et al. (1999). Preserved benzodiazepine receptors in Alzheimer's disease measured with C-11 flumazenil PET and I-123 iomazenil SPECT in comparison with CBF. *Ann. Nucl. Med.* 13, 309–315. doi: 10.1007/BF03164869
- Okada, M., Nakao, R., Momosaki, S., Yamamoto, K., Kikuchi, T., Okamura, T., et al. (2013). Improvement of brain uptake for *in vivo* PET imaging of astrocytic oxidative metabolism using benzyl [1-(11)C]acetate. *Appl. Radiat. Isot.* 78, 102–107. doi: 10.1016/j.apradiso.2013.04.025
- Olek, M. (2012). *Treatment of Relapsing-Remitting Multiple Sclerosis in Adults*. Available online at: <http://www.uptodate.com/contents/treatment-of-relapsing-remitting-multiple-sclerosis-in-adults>
- Olson, J. K., Croxford, J. L., Calenoff, M. A., Dal Canto, M. C., and Miller, S. D. (2001). A virus-induced molecular mimicry model of multiple sclerosis. *J. Clin. Invest.* 108, 311–318. doi: 10.1172/JCI200113032
- Ono, M. (2009). Development of positron-emission tomography/single-photon emission computed tomography imaging probes for *in vivo* detection of β -amyloid plaques in Alzheimer's brains. *Chem. Pharm. Bull. (Tokyo)* 57, 1029–1039. doi: 10.1248/cpb.57.1029
- Orr, A. G., Orr, A. L., Li, X.-J., Gross, R. E., and Traynelis, S. F. (2009). Adenosine A2A receptor mediates microglial process retraction. *Nat. Neurosci.* 12, 872–878. doi: 10.1038/nn.2341
- Ortiz, G. G., Pacheco-Moisés, F. P., Bitzer-Quintero, O. K., Ramírez-Anguiano, A. C., Flores-Alvarado, L. J., Ramírez-Ramírez, V., et al. (2013). Immunology and oxidative stress in multiple sclerosis: clinical and basic approach. *Clin. Dev. Immunol.* 2013, 1–14. doi: 10.1155/2013/708659
- Owens, G. P., Gilden, D., Burgoon, M. P., Yu, X., and Bennett, J. L. (2011). Viruses and multiple sclerosis. *Neuroscientist* 17, 659–676. doi: 10.1177/1073858410386615
- Pacher, P. (2006). The endocannabinoid system as an emerging target of pharmacotherapy. *Pharmacol. Rev.* 58, 389–462. doi: 10.1124/pr.58.3.2
- Pannu, R., Singh, A. K., and Singh, I. (2005). A novel role of lactosylceramide in the regulation of tumor necrosis factor α -mediated proliferation of rat primary astrocytes: Implications For Astroglial Proliferation Following Neurotrauma. *J. Biol. Chem.* 280, 13742–13751. doi: 10.1074/jbc.M411959200
- Park, E., Gallezot, J.-D., Delgado, A., Liu, S., Planeta, B., Lin, S.-F., et al. (2015). (11)C-PBR28 imaging in multiple sclerosis patients and healthy controls: test-retest reproducibility and focal visualization of active white matter areas. *Eur. J. Nucl. Med. Mol. Imaging* 42, 1081–1092. doi: 10.1007/s00259-015-3043-4
- Partridge, M., Spinelli, A., Ryder, W., and Hindorf, C. (2006). The effect of β -energy on performance of a small animal PET camera. *Nucl. Instrum. Methods Phys. Res. Sect. Accel. Spectrometers Detect. Assoc. Equip.* 568, 933–936. doi: 10.1016/j.nima.2006.09.035
- Pascual, B., Prieto, E., Arbizu, J., Marti-Climent, J. M., Peñuelas, I., Quincoces, G., et al. (2012). Decreased carbon-11-flumazenil binding in early Alzheimer's disease. *Brain J. Neurol.* 135, 2817–2825.
- Paulsen, E., Perani, D., Fazio, F., Comi, G., Pozzilli, C., Martinelli, V., et al. (1996). Functional basis of memory impairment in multiple sclerosis: a [18F]FDG PET study. *Neuroimage* 4, 87–96. doi: 10.1006/nimg.1996.0032
- Peyronneau, M.-A., Saba, W., Goutal, S., Damont, A., Dolle, F., Kassio, M., et al. (2013). Metabolism and quantification of [18F]DPA-714, a new TSPO positron emission tomography radioligand. *Drug Metab. Dispos.* 41, 122–131. doi: 10.1124/dmd.112.046342
- Pizer, S. M., Chesler, D. A., Clark, F. H., Maskewitz, B. F., Gurney, J., and Brownell, G. L. (1971). "Physics research Scan processing program," in *Sharing of Computer Programs and Technology in Nuclear Medicine USAEC Conf-710425* (Springfield, VA: US Department of Commerce), 92.
- Politis, M., Giannetti, P., Su, P., Turkheimer, F., Keihaninejad, S., Wu, K., et al. (2012). Increased PK11195 PET binding in the cortex of patients with MS correlates with disability. *Neurology* 79, 523–530. doi: 10.1212/WNL.0b013e3182635645
- Poloni, G., Minagar, A., Haacke, E. M., and Zivadinov, R. (2011). Recent developments in imaging of multiple sclerosis. *Neurologist* 17, 185–204. doi: 10.1097/NRL.0b013e31821a2643
- Ponde, D. E., Dence, C. S., Oyama, N., Kim, J., Tai, Y.-C., Laforest, R., et al. (2007). 18F-fluoroacetate: a potential acetate analog for prostate tumor imaging—*in vivo* evaluation of 18F-fluoroacetate versus 11C-acetate. *J. Nucl. Med.* 48, 420–428.
- Portnow, L. H., Vaillancourt, D. E., and Okun, M. S. (2013). The history of cerebral PET scanning: from physiology to cutting-edge technology. *Neurology* 80, 952–956. doi: 10.1212/WNL.0b013e318285c135
- Prüss, H., Rosche, B., Sullivan, A. B., Brommer, B., Wengert, O., Gronert, K., et al. (2013). Proresolution lipid mediators in multiple sclerosis — differential, disease severity-dependent synthesis — a clinical pilot trial. *PLoS ONE* 8:e55859. doi: 10.1371/journal.pone.0055859
- Quelch, D., De Santis, V., Strega, A., Myers, J., Wells, L., Nutt, D., et al. (2015). Influence of agonist induced internalization on [3 H]Ro15-4513 binding—an application to imaging fluctuations in endogenous GABA with positron emission tomography: influence of agonist induced internalization on [3 H]Ro15-4513 binding. *Synapse* 69, 60–65. doi: 10.1002/syn.21780
- Quintana, F. J., Yeste, A., and Mascanfroni, I. D. (2014). Role and therapeutic value of dendritic cells in central nervous system autoimmunity. *Cell Death Differ.* 22, 215–224. doi: 10.1038/cdd.2014.125
- Radu, C. G., Shu, C. J., Shelly, S. M., Phelps, M. E., and Witte, O. N. (2007). Positron emission tomography with computed tomography imaging of neuroinflammation in experimental autoimmune encephalomyelitis. *Proc. Natl. Acad. Sci. U.S.A.* 104, 1937–1942. doi: 10.1073/pnas.0610544104
- Ransohoff, R. M. (2012). Animal models of multiple sclerosis: the good, the bad and the bottom line. *Nat. Neurosci.* 15, 1074–1077. doi: 10.1038/nn.3168
- Ransohoff, R. M., Hafler, D. A., and Lucchinetti, C. F. (2015). Multiple sclerosis—a quiet revolution. *Nat. Rev. Neurol.* 11, 134–142. doi: 10.1038/nrneurol.2015.14
- Rao, S. D., Yin, H. Z., and Weiss, J. H. (2003). Disruption of glial glutamate transport by reactive oxygen species produced in motor neurons. *J. Neurosci.* 23, 2627–2633.
- Rinaldi, L., Grassi, F., and Gallo, P. (2009). "Lipids in Multiple Sclerosis," in *Handbook of Neurochemistry and Molecular Neurobiology*, eds A. Lajtha, G. Tettamanti, and G. Goracci (Boston, MA: Springer US), 593–602. Available online at: http://link.springer.com/10.1007/978-0-387-30378-9_24 (Accessed May 21, 2015).
- Rinne, J. O. (2003). Brain acetylcholinesterase activity in mild cognitive impairment and early Alzheimer's disease. *J. Neurol. Neurosurg. Psychiatr.* 74, 113–115. doi: 10.1136/jnnp.74.1.113
- Rissanen, E., Tuisku, J., Luoto, P., Arponen, E., Johansson, J., Oikonen, V., et al. (2015). Automated reference region extraction and population-based input function for brain [11C]TMSX PET image analyses. *J. Cereb. Blood Flow Metab.* 35, 157–165. doi: 10.1038/jcbfm.2014.194

- Rissanen, E., Tuisku, J., Rokka, J., Paavilainen, T., Parkkola, R., Rinne, J. O., et al. (2014). *In vivo* detection of diffuse inflammation in secondary progressive multiple sclerosis using PET imaging and the radioligand ¹¹C-PK11195. *J. Nucl. Med.* 55, 939–944. doi: 10.2967/jnumed.113.131698
- Rissanen, E., Virta, J. R., Paavilainen, T., Tuisku, J., Helin, S., Luoto, P., et al. (2013). Adenosine A2A receptors in secondary progressive multiple sclerosis: a [¹¹C]TMSX brain PET study. *J. Cereb. Blood Flow Metab.* 33, 1394–1401. doi: 10.1038/jcbfm.2013.85
- Rodgers, J. M., Robinson, A. P., and Miller, S. D. (2013). Strategies for protecting oligodendrocytes and enhancing remyelination in multiple sclerosis. *Discov. Med.* 16, 53–63.
- Rose, J. W., Hill, K. E., Watt, H. E., and Carlson, N. G. (2004). Inflammatory cell expression of cyclooxygenase-2 in the multiple sclerosis lesion. *J. Neuroimmunol.* 149, 40–49. doi: 10.1016/j.jneuroim.2003.12.021
- Rossi, S., Motta, C., Studer, V., Barbieri, F., Buttari, F., Bergami, A., et al. (2014). Tumor necrosis factor is elevated in progressive multiple sclerosis and causes excitotoxic neurodegeneration. *Mult. Scler. J.* 20, 304–312. doi: 10.1177/1352458513498128
- Rossi, S., Studer, V., Motta, C., De Chiara, V., Barbieri, F., Bernardi, G., et al. (2012). Inflammation inhibits GABA transmission in multiple sclerosis. *Mult. Scler. Houndmills Basingstoke Engl.* 18, 1633–1635. doi: 10.1177/1352458512440207
- Rostami, A., and Ciric, B. (2014). Astrocyte-derived lactosylceramide implicated in multiple sclerosis. *Nat. Med.* 20, 1092–1093. doi: 10.1038/nm.3719
- Rudroff, T., Kindred, J. H., Koo, P. J., Karki, R., and Hebert, J. R. (2014). Asymmetric glucose uptake in leg muscles of patients with multiple sclerosis during walking detected by [¹⁸F]-FDG PET/CT. *NeuroRehabilitation* 35, 813–823. doi: 10.3233/NRE-141179
- Rupprecht, R., Papadopoulos, V., Rammes, G., Baghai, T. C., Fan, J., Akula, N., et al. (2010). Translocator protein (18 kDa) (TSPO) as a therapeutic target for neurological and psychiatric disorders. *Nat. Rev. Drug Discov.* 9, 971–988. doi: 10.1038/nrd3295
- Ryu, J. K., Choi, H. B., and McLarnon, J. G. (2005). Peripheral benzodiazepine receptor ligand PK11195 reduces microglial activation and neuronal death in quinolinic acid-injected rat striatum. *Neurobiol. Dis.* 20, 550–561. doi: 10.1016/j.nbd.2005.04.010
- Saha, G. B., MacIntyre, W. J., and Go, R. T. (1994). Radiopharmaceuticals for brain imaging. *Semin. Nucl. Med.* 24, 324–349. doi: 10.1016/S0001-2998(05)80022-4
- Saha, R. N., and Pahan, K. (2006). Regulation of inducible nitric oxide synthase gene in glial cells. *Antioxid. Redox Signal.* 8, 929–947. doi: 10.1089/ars.2006.8.929
- Sanchez-Pernaute, R., Wang, J.-Q., Kuruppu, D., Cao, L., Tueckmantel, W., Kozikowski, A., et al. (2008). Enhanced binding of metabotropic glutamate receptor type 5 (mGluR5) PET tracers in the brain of parkinsonian primates. *Neuroimage* 42, 248–251. doi: 10.1016/j.neuroimage.2008.04.170
- Schäffler, N., Köpke, S., Winkler, L., Schipling, S., Ingles, M., Fischer, K., et al. (2011). Accuracy of diagnostic tests in multiple sclerosis—a systematic review. *Acta Neurol. Scand.* 124, 151–164. doi: 10.1111/j.1600-0404.2010.01454.x
- Scheller, J., Chalaris, A., Schmidt-Arras, D., and Rose-John, S. (2011). The pro- and anti-inflammatory properties of the cytokine interleukin-6. *Biochim. Biophys. Acta* 1813, 878–888. doi: 10.1016/j.bbamcr.2011.01.034
- Schiepers, C., Van Hecke, P., Vandenbergh, R., Van Oostende, S., Dupont, P., Demaerel, P., et al. (1997). Positron emission tomography, magnetic resonance imaging and proton NMR spectroscopy of white matter in multiple sclerosis. *Mult. Scler. Houndmills Basingstoke Engl.* 3, 8–17. doi: 10.1177/135245859700300102
- Selvaraj, V., and Stocco, D. M. (2015). The changing landscape in translocator protein (TSPO) function. *Trends Endocrinol. Metab.* 26, 341–348. doi: 10.1016/j.tem.2015.02.007
- Sharma, M. K., Seidlitz, E. P., and Singh, G. (2010). Cancer cells release glutamate via the cystine/glutamate antiporter. *Biochem. Biophys. Res. Commun.* 391, 91–95. doi: 10.1016/j.bbrc.2009.10.168
- Shih, A. Y. (2006). Policing the police: astrocytes modulate microglial activation. *J. Neurosci.* 26, 3887–3888. doi: 10.1523/JNEUROSCI.0936-06.2006
- Sigel, E., and Buhr, A. (1997). The benzodiazepine binding site of GABA_A receptors. *Trends Pharmacol. Sci.* 18, 425–429. doi: 10.1016/S0165-6147(97)90675-1
- Singhal, G., Jaehne, E. J., Corrigan, F., Toben, C., and Baune, B. T. (2014). Inflammasomes in neuroinflammation and changes in brain function: a focused review. *Front. Neurosci.* 8:315. doi: 10.3389/fnins.2014.00315
- Slavik, R., Herde, A. M., Bieri, D., Weber, M., Schibli, R., Krämer, S. D., et al. (2015). Synthesis, radiolabeling and evaluation of novel 4-oxo-quinoline derivatives as PET tracers for imaging cannabinoid type 2 receptor. *Eur. J. Med. Chem.* 92, 554–564. doi: 10.1016/j.ejmech.2015.01.028
- Smith, C. M., Cooksey, E., and Duncan, I. D. (2013). Myelin loss does not lead to axonal degeneration in a long-lived model of chronic demyelination. *J. Neurosci.* 33, 2718–2727. doi: 10.1523/JNEUROSCI.4627-12.2013
- Sofroniew, M. V. (2015). Astrocyte barriers to neurotoxic inflammation. *Nat. Rev. Neurosci.* 16, 249–263. doi: 10.1038/nrn3898
- Sofroniew, M. V., and Vinters, H. V. (2010). Astrocytes: biology and pathology. *Acta Neuropathol. (Berl.)* 119, 7–35. doi: 10.1007/s00401-009-0619-8
- Sperlágh, B., and Illes, P. (2007). Purinergic modulation of microglial cell activation. *Purinergic Signal.* 3, 117–127. doi: 10.1007/s11302-006-9043-x
- Stankoff, B., Freeman, L., Aigrot, M.-S., Chardain, A., Dollé, F., Williams, A., et al. (2011). Imaging central nervous system myelin by positron emission tomography in multiple sclerosis using [methyl-¹¹C]-2-(4'-methylaminophenyl)-6-hydroxybenzothiazole. *Ann. Neurol.* 69, 673–680. doi: 10.1002/ana.22320
- Stankoff, B., Wang, Y., Bottlaender, M., Aigrot, M.-S., Dollé, F., Wu, C., et al. (2006). Imaging of CNS myelin by positron-emission tomography. *Proc. Natl. Acad. Sci. U.S.A.* 103, 9304–9309. doi: 10.1073/pnas.0600769103
- Stella, N. (2004). Cannabinoid signaling in glial cells. *Glia* 48, 267–277. doi: 10.1002/glia.20084
- Suzuki, K., Inoue, O., Hashimoto, K., Yamasaki, T., Kuchiki, M., and Tamate, K. (1985). Computer-controlled large scale production of high specific activity [¹¹C]RO 15-1788 for PET studies of benzodiazepine receptors. *Int. J. Appl. Radiat. Isot.* 36, 971–976. doi: 10.1016/0020-708X(85)90258-3
- Takaki, J., Fujimori, K., Miura, M., Suzuki, T., Sekino, Y., and Sato, K. (2012). L-glutamate released from activated microglia downregulates astrocytic L-glutamate transporter expression in neuroinflammation: the “collusion” hypothesis for increased extracellular L-glutamate concentration in neuroinflammation. *J. Neuroinflammation* 9:275. doi: 10.1186/1742-2094-9-275
- Takano, A., Piehl, F., Hillert, J., Varrone, A., Nag, S., Gulyás, B., et al. (2013). *In vivo* TSPO imaging in patients with multiple sclerosis: a brain PET study with [¹⁸F]FEDAA1106. *EJNMMI Res.* 3:30. doi: 10.1186/2191-219X-3-30
- Takashima-Hirano, M., Takashima, T., Katayama, Y., Wada, Y., Sugiyama, Y., Watanabe, Y., et al. (2011). Efficient sequential synthesis of PET Probes of the COX-2 inhibitor [¹¹C]celecoxib and its major metabolite [¹¹C]SC-62807 and *in vivo* PET evaluation. *Bioorg. Med. Chem.* 19, 2997–3004. doi: 10.1016/j.bmc.2011.03.020
- Takata, K., Kato, H., Shimosegawa, E., Okuno, T., Koda, T., Sugimoto, T., et al. (2014). ¹¹C-Acetate PET imaging in patients with multiple sclerosis. *PLoS ONE* 9:e111598. doi: 10.1371/journal.pone.0111598
- Talati, R., Reinhart, K., Baker, W., White, C. M., and Coleman, C. I. (2009). Pharmacologic treatment of advanced Parkinson's disease: a meta-analysis of COMT inhibitors and MAO-B inhibitors. *Parkinsonism Relat. Disord.* 15, 500–505. doi: 10.1016/j.parkreldis.2008.12.007
- Tambuyzer, B. R., Ponsaerts, P., and Nouwen, E. J. (2009). Microglia: gatekeepers of central nervous system immunology. *J. Leukoc. Biol.* 85, 352–370. doi: 10.1189/jlb.0608385
- Teodoro, R., Moldovan, R.-P., Lueg, C., Günther, R., Donat, C. K., Ludwig, F.-A., et al. (2013). Radiofluorination and biological evaluation of N-aryl-oxadiazolyl-propionamides as potential radioligands for PET imaging of cannabinoid CB2 receptors. *Org. Med. Chem. Lett.* 3:11. doi: 10.1186/2191-2858-3-11
- The MICAD Research Team (2004). “2-[(18F)Fluoroflumazenil],” in *Molecular Imaging and Contrast Agent Database (MICAD)* (Bethesda, MD: National Center for Biotechnology Information US). (Accessed May 20, 2015).
- Thorek, D. L. J., Ogirala, A., Beattie, B. J., and Grimm, J. (2013). Quantitative imaging of disease signatures through radioactive decay signal conversion. *Nat. Med.* 19, 1345–1350. doi: 10.1038/nm.3323
- Tillema, J.-M., and Pirkko, I. (2013). Neuroradiological evaluation of demyelinating disease. *Ther. Adv. Neurol. Disord.* 6, 249–268. doi: 10.1177/1756285613478870

- Toft-Hansen, H., Füchtbauer, L., and Owens, T. (2011). Inhibition of reactive astrogliosis in established experimental autoimmune encephalomyelitis favors infiltration by myeloid cells over T cells and enhances severity of disease. *Glia* 59, 166–176. doi: 10.1002/glia.21088
- Torigian, D. A., Zaidi, H., Kwee, T. C., Saboury, B., Udupa, J. K., Cho, Z.-H., et al. (2013). PET/MR imaging: technical aspects and potential clinical applications. *Radiology* 267, 26–44. doi: 10.1148/radiol.13121038
- Torkildsen, Ø., Brunborg, L. A., Myhr, K.-M., and Bø, L. (2008). The cuprizone model for demyelination. *Acta Neurol. Scand.* 117, 72–76. doi: 10.1111/j.1600-0404.2008.01036.x
- Traboulsee, A. L., and Li, D. K. B. (2006). The role of MRI in the diagnosis of multiple sclerosis. *Adv. Neurol.* 98, 125–146.
- Trapp, B. D., and Nave, K.-A. (2008). Multiple sclerosis: an immune or neurodegenerative disorder? *Annu. Rev. Neurosci.* 31, 247–269. doi: 10.1146/annurev.neuro.30.051606.094313
- Trapp, B. D., and Stys, P. K. (2009). Virtual hypoxia and chronic necrosis of demyelinated axons in multiple sclerosis. *Lancet Neurol.* 8, 280–291. doi: 10.1016/S1474-4422(09)70043-2
- Tsao, J. W., and Heilman, K. M. (2005). Donepezil improved memory in multiple sclerosis in a randomized clinical trial. *Neurology* 64, 1823; author reply 1823. doi: 10.1212/wnl.64.10.1823
- Tselis, A. (2012). Epstein-Barr virus cause of multiple sclerosis. *Curr. Opin. Rheumatol.* 24, 424–428. doi: 10.1097/BOR.0b013e3283542cf8
- Turkman, N., Shavrin, A., Ivanov, R. A., Rabinovich, B., Volgin, A., Gelovani, J. G., et al. (2011). Fluorinated cannabinoid CB2 receptor ligands: synthesis and *in vitro* binding characteristics of 2-oxoquinoline derivatives. *Bioorg. Med. Chem.* 19, 5698–5707. doi: 10.1016/j.bmc.2011.07.062
- Van Camp, N., Boisgard, R., Kuhnast, B., Thézé, B., Viel, T., Grégoire, M.-C., et al. (2010). *In vivo* imaging of neuroinflammation: a comparative study between [(18F)PBR111], [(11C)CLINME] and [(11C)PK11195] in an acute rodent model. *Eur. J. Nucl. Med. Mol. Imaging* 37, 962–972. doi: 10.1007/s00259-009-1353-0
- Vandeputte, C., Evens, N., Toelen, J., Deroose, C. M., Bosier, B., Ibrahim, A., et al. (2011). A PET brain reporter gene system based on type 2 cannabinoid receptors. *J. Nucl. Med.* 52, 1102–1109. doi: 10.2967/jnumed.110.084426
- Vas, A., Shchukin, Y., Karrenbauer, V. D., Cselényi, Z., Kostulas, K., Hillert, J., et al. (2008). Functional neuroimaging in multiple sclerosis with radiolabelled glia markers: preliminary comparative PET studies with [(11C)vinpocetine] and [(11C)PK11195] in patients. *J. Neurol. Sci.* 264, 9–17. doi: 10.1016/j.jns.2007.07.018
- Veitinger, M., Varga, B., Guterres, S. B., and Zellner, M. (2014). Platelets, a reliable source for peripheral Alzheimer's disease biomarkers? *Acta Neuropathol. Commun.* 2:65. doi: 10.1186/2051-5960-2-65
- Venneti, S., Wang, G., Nguyen, J., and Wiley, C. A. (2008). The positron emission tomography ligand DAA1106 binds with high affinity to activated microglia in human neurological disorders. *J. Neuropathol. Exp. Neurol.* 67, 1001–1010. doi: 10.1097/NEN.0b013e318188b204
- Versijpt, J., Debruyne, J. C., Van Laere, K. J., De Vos, F., Keppens, J., Strijckmans, K., et al. (2005). Microglial imaging with positron emission tomography and atrophy measurements with magnetic resonance imaging in multiple sclerosis: a correlative study. *Mult. Scler. Houndmills Basingstoke Engl.* 11, 127–134. doi: 10.1191/1352458505ms11400a
- Virta, J. R., Laatu, S., Parkkola, R., Oikonen, V., Rinne, J. O., and Ruutinen, J. (2011). Cerebral acetylcholinesterase activity is not decreased in MS patients with cognitive impairment. *Mult. Scler. J.* 17, 931–938. doi: 10.1177/1352458511399613
- Volkow, N. D., Ding, Y. S., Fowler, J. S., and Gatley, S. J. (2001). Imaging brain cholinergic activity with positron emission tomography: its role in the evaluation of cholinergic treatments in Alzheimer's dementia. *Biol. Psychiatry* 49, 211–220. doi: 10.1016/S0006-3223(00)01112-4
- Voskuhl, R. R., Peterson, R. S., Song, B., Ao, Y., Morales, L. B. J., Tiwari-Woodruff, S., et al. (2009). Reactive astrocytes form scar-like perivascular barriers to leukocytes during adaptive immune inflammation of the CNS. *J. Neurosci.* 29, 11511–11522. doi: 10.1523/JNEUROSCI.1514-09.2009
- Wadsworth, H., Jones, P. A., Chau, W.-F., Durrant, C., Fouladi, N., Passmore, J., et al. (2012). [18F]GE-180: A novel fluorine-18 labelled PET tracer for imaging Translocator protein 18kDa (TSPO). *Bioorg. Med. Chem. Lett.* 22, 1308–1313. doi: 10.1016/j.bmcl.2011.12.084
- Wagner, S., Breyholz, H.-J., Hölte, C., Faust, A., Schober, O., Schäfers, M., et al. (2009). A new 18F-labelled derivative of the MMP inhibitor CGS 27023A for PET: radiosynthesis and initial small-animal PET studies. *Appl. Radiat. Isot. Data Instrum. Methods Use Agric. Ind. Med.* 67, 606–610. doi: 10.1016/j.apradiso.2008.12.009
- Wagner, S., Breyholz, H.-J., Law, M. P., Faust, A., Hölte, C., Schröder, S., et al. (2007). Novel fluorinated derivatives of the broad-spectrum MMP inhibitors N-hydroxy-2(R)-[[[(4-methoxyphenyl)sulfonyl](benzyl)- and (3-picolyl)-amino]-3-methyl-butanamide as potential tools for the molecular imaging of activated MMPs with PET. *J. Med. Chem.* 50, 5752–5764. doi: 10.1021/jm0708533
- Wang, J.-Q., Tueckmantel, W., Zhu, A., Pellegrino, D., and Brownell, A.-L. (2007). Synthesis and preliminary biological evaluation of 3-[(18F)fluoro-5-(2-pyridinylethynyl)benzonitrile] as a PET radiotracer for imaging metabotropic glutamate receptor subtype 5. *Synapse* 61, 951–961. doi: 10.1002/syn.20445
- Wang, Y., Wu, C., Capriarello, A. V., Somoza, E., Zhu, W., Wang, C., et al. (2009). *In vivo* quantification of myelin changes in the vertebrate nervous system. *J. Neurosci.* 29, 14663–14669. doi: 10.1523/JNEUROSCI.4082-08.2009
- Weiner, H. L. (2008). A shift from adaptive to innate immunity: a potential mechanism of disease progression in multiple sclerosis. *J. Neurol.* 255(Suppl. 1), 3–11. doi: 10.1007/s00415-008-1002-8
- Wesler-Alves, J. V., and Milner, R. (2013). Microglia are the major source of TNF- α and TGF- β 1 in postnatal glial cultures; regulation by cytokines, lipopolysaccharide, and vitronectin. *Neurochem. Int.* 63, 47–53. doi: 10.1016/j.neuint.2013.04.007
- Wheeler, D., Bandaru, V. V. R., Calabresi, P. A., Nath, A., and Haughey, N. J. (2008). A defect of sphingolipid metabolism modifies the properties of normal appearing white matter in multiple sclerosis. *Brain* 131, 3092–3102. doi: 10.1093/brain/awn190
- Wilkins, A., Kondo, Y., Song, J., Liu, S., Compston, A., Black, J. A., et al. (2010). Slowly progressive axonal degeneration in a rat model of chronic, nonimmune-mediated demyelination. *J. Neuropathol. Exp. Neurol.* 69, 1256–1269. doi: 10.1097/NEN.0b013e3181ff317
- Winkler, A., Boisgard, R., Martin, A., and Tavitian, B. (2010). Radioisotopic imaging of neuroinflammation. *J. Nucl. Med.* 51, 1–4. doi: 10.2967/jnumed.109.065680
- Wong, D. F., Waterhouse, R., Kuwabara, H., Kim, J., Brašić, J. R., Chamroonrat, W., et al. (2013). 18F-FPEB, a PET radiopharmaceutical for quantifying metabotropic glutamate 5 receptors: a first-in-human study of radiochemical safety, biokinetics, and radiation dosimetry. *J. Nucl. Med.* 54, 388–396. doi: 10.2967/jnumed.112.107995
- Woodruff, R. H., and Franklin, R. J. M. (1999). Demyelination and remyelination of the caudal cerebellar peduncle of adult rats following stereotaxic injections of lysolecithin, ethidium bromide, and complement/anti-galactocerebroside: a comparative study. *Glia* 25, 216–228.
- Wu, C., Tian, D., Feng, Y., Polak, P., Wei, J., Sharp, A., et al. (2006). A novel fluorescent probe that is brain permeable and selectively binds to myelin. *J. Histochem. Cytochem.* 54, 997–1004. doi: 10.1369/jhc.5A6901.2006
- Wu, C., Wang, C., Popescu, D., Zhu, W., Somoza, E., Zhu, J., et al. (2010). A novel PET marker for *in vivo* quantification of myelination. *Bioorg. Med. Chem.* 18, 8592–8599. doi: 10.1016/j.bmc.2010.10.018
- Wu, C., Zhu, J., Baeslack, J., Zaremba, A., Hecker, J., Kraso, J., et al. (2013). Longitudinal positron emission tomography imaging for monitoring myelin repair in the spinal cord. *Ann. Neurol.* 74, 688–698. doi: 10.1002/ana.23965
- Wunder, A., Schoknecht, K., Stanimirovic, D. B., Prager, O., and Chassidim, Y. (2012). Imaging blood-brain barrier dysfunction in animal disease models. *Epilepsia* 53(Suppl. 6), 14–21. doi: 10.1111/j.1528-1167.2012.03698.x
- Yamasaki, R., Lu, H., Butovsky, O., Ohno, N., Rietsch, A. M., Cialic, R., et al. (2014). Differential roles of microglia and monocytes in the inflamed central nervous system. *J. Exp. Med.* 211, 1533–1549. doi: 10.1084/jem.20132477
- Yiangou, Y., Facer, P., Durrenberger, P., Chessell, I. P., Naylor, A., Bountra, C., et al. (2006). COX-2, CB2 and P2X7-immunoreactivities are increased in activated microglial cells/macrophages of multiple sclerosis and amyotrophic lateral sclerosis spinal cord. *BMC Neurol.* 6:12. doi: 10.1186/1471-2377-6-12

- Yrjölä, S., Sarparanta, M., Airaksinen, A. J., Hytti, M., Kauppinen, A., Pasonen-Seppänen, S., et al. (2015). Synthesis, *in vitro* and *in vivo* evaluation of 1,3,5-triazines as cannabinoid CB2 receptor agonists. *Eur. J. Pharm. Sci.* 67, 85–96. doi: 10.1016/j.ejps.2014.11.003
- Yu, M., Tueckmantel, W., Wang, X., Zhu, A., Kozikowski, A. P., and Brownell, A.-L. (2005). Methoxyphenylethynyl, methoxypyridylethynyl and phenylethynyl derivatives of pyridine: synthesis, radiolabeling and evaluation of new PET ligands for metabotropic glutamate subtype 5 receptors. *Nucl. Med. Biol.* 32, 631–640. doi: 10.1016/j.nucmedbio.2005.05.004
- Zarei, M. (2003). Cognitive presentation of multiple sclerosis: evidence for a cortical variant. *J. Neurol. Neurosurg. Psychiatry* 74, 872–877. doi: 10.1136/jnnp.74.7.872
- Zeis, T., Allaman, I., Gentner, M., Schroder, K., Tschopp, J., Magistretti, P. J., et al. (2015). Metabolic gene expression changes in astrocytes in Multiple Sclerosis cerebral cortex are indicative of immune-mediated signaling. *Brain. Behav. Immun.* 48, 313–325. doi: 10.1016/j.bbi.2015.04.013
- Zhang, S., Smailagic, N., Hyde, C., Noel-Storr, A. H., Takwoingi, Y., McShane, R., et al. (2014). “¹¹C-PIB-PET for the early diagnosis of Alzheimer’s disease dementia and other dementias in people with mild cognitive impairment (MCI),” in *Cochrane Database of Systematic Reviews*, ed The Cochrane Collaboration (Chichester, UK: John Wiley and Sons, Ltd). Available online at: <http://doi.wiley.com/10.1002/14651858.CD010386.pub2> (Accessed May 20, 2015).
- Zhang, Y., Guo, T. B., and Lu, H. (2013). Promoting remyelination for the treatment of multiple sclerosis: opportunities and challenges. *Neurosci. Bull.* 29, 144–154. doi: 10.1007/s12264-013-1317-z
- Zhang, Z., and Brownell, A.-L. (2012). “Imaging of Metabotropic Glutamate Receptors (mGluRs),” in *Neuroimaging - Clinical Applications*, ed P. Bright (InTech). Available online at: <http://www.intechopen.com/books/neuroimaging-clinical-applications/imaging-of-metabotropic-glutamate-receptors-mglur-s> (Accessed May 4, 2015).

Conflict of Interest Statement: The authors declare that the research was conducted in the absence of any commercial or financial relationships that could be construed as a potential conflict of interest.

Copyright © 2016 Poutiainen, Jaronen, Quintana and Brownell. This is an open-access article distributed under the terms of the Creative Commons Attribution License (CC BY). The use, distribution or reproduction in other forums is permitted, provided the original author(s) or licensor are credited and that the original publication in this journal is cited, in accordance with accepted academic practice. No use, distribution or reproduction is permitted which does not comply with these terms.



Function Over Form: Modeling Groups of Inherited Neurological Conditions in Zebrafish

Robert A. Kozol^{1*}, Alexander J. Abrams², David M. James¹, Elena Buglo², Qing Yan¹ and Julia E. Dallman^{1*}

¹ Department of Biology, University of Miami, Coral Gables, FL, USA, ² Department of Human Genetics, John P. Hussman Institute for Human Genomics, Dr. John T. Macdonald Foundation, University of Miami, Miami, FL, USA

Zebrafish are a unique cell to behavior model for studying the basic biology of human inherited neurological conditions. Conserved vertebrate genetics and optical transparency provide *in vivo* access to the developing nervous system as well as high-throughput approaches for drug screens. Here we review zebrafish modeling for two broad groups of inherited conditions that each share genetic and molecular pathways and overlap phenotypically: neurodevelopmental disorders such as Autism Spectrum Disorders (ASD), Intellectual Disability (ID) and Schizophrenia (SCZ), and neurodegenerative diseases, such as Cerebellar Ataxia (CATX), Hereditary Spastic Paraplegia (HSP) and Charcot-Marie Tooth Disease (CMT). We also conduct a small meta-analysis of zebrafish orthologs of high confidence neurodevelopmental disorder and neurodegenerative disease genes by looking at duplication rates and relative protein sizes. In the past zebrafish genetic models of these neurodevelopmental disorders and neurodegenerative diseases have provided insight into cellular, circuit and behavioral level mechanisms contributing to these conditions. Moving forward, advances in genetic manipulation, live imaging of neuronal activity and automated high-throughput molecular screening promise to help delineate the mechanistic relationships between different types of neurological conditions and accelerate discovery of therapeutic strategies.

Keywords: zebrafish, disease modeling, autism spectrum disorder, intellectual disability, schizophrenia, ataxia, Charcot-Marie tooth, hereditary spastic paraplegia

OPEN ACCESS

Edited by:

Robert J. Harvey,
UCL School of Pharmacy, UK

Reviewed by:

Ellen J. Hoffman,
Yale University, USA
Hiromi Hirata,
Aoyama Gakuin University, Japan

*Correspondence:

Robert A. Kozol
robkozol@bio.miami.edu
Julia E. Dallman
jdallman@bio.miami.edu

Received: 05 April 2016

Accepted: 23 June 2016

Published: 07 July 2016

Citation:

Kozol RA, Abrams AJ, James DM, Buglo E, Yan Q and Dallman JE (2016) Function Over Form: Modeling Groups of Inherited Neurological Conditions in Zebrafish. *Front. Mol. Neurosci.* 9:55. doi: 10.3389/fnmol.2016.00055

INTRODUCTION

As genetically tractable vertebrates (Streisinger et al., 1981) that share with humans many pathways targeted by FDA approved pharmaceuticals (Renier et al., 2007; Rihel et al., 2010) zebrafish are a powerful model for inherited neurological conditions, both in terms of delineating underlying mechanisms and developing therapeutic strategies. Their small size and optical transparency enable *in vivo* visualization of cell- and systems-level processes throughout early developmental stages (McLean and Fetcho, 2011; Rasmussen and Sagasti, 2016) while, precocious development of quantifiable behaviors (Brustein et al., 2003) and reduced complexity of the zebrafish nervous system (Goulding, 2009) simplify functional studies of neural circuits. These advantages combined with conserved vertebrate genetics lend themselves to keeping pace with the extraordinary discovery rate of genetic mutations that cause inherited neurological conditions in humans. With the sequencing of the human genome, the formation of worldwide consortia of human geneticists and clinicians and ever-cheaper sequencing technologies, these discoveries have revealed that many

inherited disorders with related clinical diagnoses consist of large sets of rare molecular genetic variation (Buxbaum et al., 2012; Gonzalez et al., 2015). Here we focus on these parallel and synergistic frontiers of disease gene discovery and systems-level analyses in zebrafish that promise to yield insight into disease mechanisms and therapies.

To assess zebrafish as a model, we compare studies of two broad classes of inherited neurological conditions: developmental disorders and degenerative diseases, with each class presenting a spectrum of overlapping genotypes and phenotypes. For developmental disorders, we include Autism Spectrum Disorders (ASD), Intellectual Disability (ID) and Schizophrenia (SCZ) that can all affect executive functions, social and overall intellectual abilities (American Psychiatric Association, and DSM-5 Task Force, 2013). Such disorders can co-occur in the same individual (Amaral et al., 2011) supporting overlapping disease etiologies. The second general class we consider are a subset of degenerative diseases including Cerebellar Ataxia (CATX), Hereditary Spastic Paraplegia (HSP), spinal motor atrophy (SMA), amyotrophic lateral sclerosis (ALS) and Charcot-Marie Tooth Disease (CMT) that impair movement due to degeneration of long axon tracts (Züchner and Vance, 2005). In both developmental and degenerative cases there are examples of: (1) distinct clinical features within a given class that result from mutations in the same genes; and (2) shared clinical phenotypes produced by many different types of genetic mutation (Espinós and Palau, 2009; Kaufman et al., 2010; Timmerman et al., 2013; Vissers et al., 2016). For example, ASD affects roughly 1% of the population but even the most commonly mutated genes only account for 1–3% of ASD with hundreds of suspected causal loci (Miles, 2011; De Rubeis and Buxbaum, 2015; Geschwind and State, 2015). It is likely that these two groupings also have phenotypic overlap since age of onset and progression of symptoms varies within each grouping. For example, SCZ that we group with “developmental” disorders also shares symptoms with neurodegenerative conditions. None-the-less, by reviewing the literature on zebrafish models of these two groups of disorders, we hope to highlight the role we feel the zebrafish model has to play in revealing grouped mechanisms of shared clinical features that result from diverse genetic mutations.

COMPARING HUMAN AND ZEBRAFISH BRAINS AND GENETICS

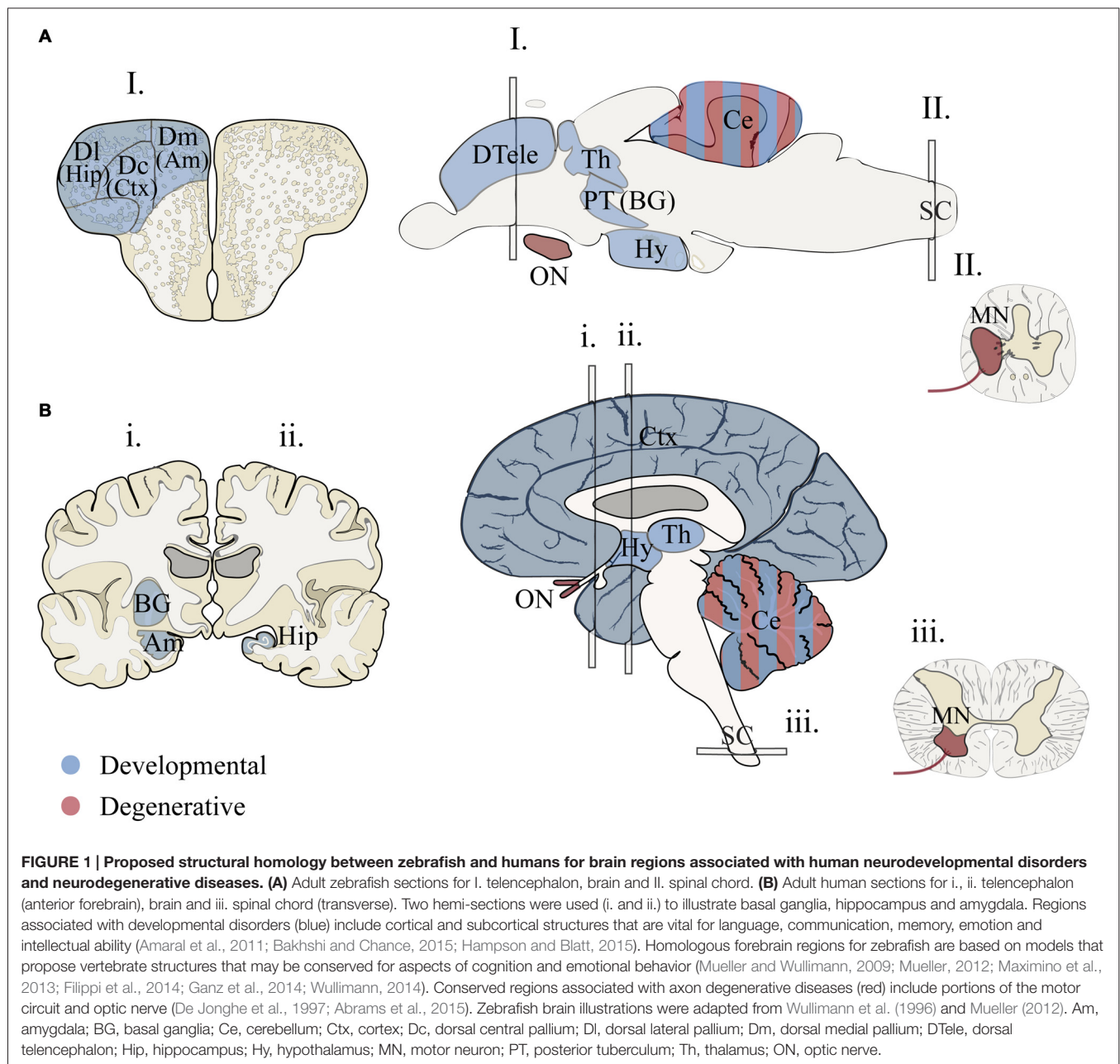
In addition to significant advantages of using zebrafish to model human disease, there are also challenges to modeling disease conditions in zebrafish. For example, in HSP symptoms are associated with degeneration of corticospinal tracts that have no clear homologous cell type in zebrafish. Moreover, for many human brain regions, the baseline studies to determine whether some of these brain regions function similarly to humans still need to be done. Finally, in terms of genetics, zebrafish have retained gene duplicates from a ray-finned fish whole genome duplication (Glasauer and Neuhauss, 2014) that likely provides both advantages (sub-functionalization of

pleiotropic phenotypes) and disadvantages (genetic redundancy) for generating disease models.

Conserved Brain Regions?

Many brain regions relevant to human disease show molecular and structural homology in zebrafish (**Figure 1**). Gene expression patterns that molecularly define large-scale regions of fore-, mid-, hindbrain and spinal cord of the central nervous system (CNS) are generally conserved in vertebrates (Myers et al., 1986; Lumsden and Krumlauf, 1996; Wurst and Bally-Cuif, 2001; McLean et al., 2007; Wullimann et al., 2011). These major regions exhibit both neurochemical identities (e.g., neurotransmitters and receptors; Higashijima et al., 2004; Renier et al., 2007; Jones et al., 2015) and regional connectivity of sub-structures, including the thalamus (Mueller, 2012), optic tectum (Wullimann, 1994), hypothalamic regulatory nuclei (Herget et al., 2014), cerebellum (Hashimoto and Hibi, 2012), medulla oblongata (Kinkhabwala et al., 2011; Koyama et al., 2011), and spinal cord (Higashijima et al., 2004; Wen and Brehm, 2005). Determining homology between human and zebrafish forebrain structures is more challenging because of developmental differences affecting telencephalon topology (eversion vs. invagination) and the elaboration of the mammalian cerebrum (Striedter, 2005). Recent studies have made headway supporting the existence of zebrafish basal ganglia- (Filippi et al., 2014; Wullimann, 2014), cortex- (Ganz et al., 2014), amygdala- (Maximino et al., 2013) and hippocampus-like circuits (O’Connell and Hofmann, 2011; Maximino et al., 2013; Ganz et al., 2014). While these studies support the existence of structurally homologous brain regions, work is still needed to resolve connectivity and functional homology among fore- and midbrain structures. Furthermore some structures in the human brain appear absent in zebrafish including the pons (Wullimann et al., 2011), cortico-thalamic (Mueller, 2012) and cortico-spinal tracts (Babin et al., 2014). With these detailed analyses, we have the necessary anatomical map needed for neurological disease research that is quickly being enriched by functional studies to test the relevance to these brain regions for both zebrafish behaviors and human disorders.

To address the involvement of brain regions in a particular behavior, advances in functional imaging have been critical. Importantly, these studies focus on larval stages, 5–7 post fertilization, when it is possible to image the entire brain and the larva has already acquired an impressive repertoire of behaviors (Haesemeyer and Schier, 2015). For example, recent studies support functional homology of the zebrafish cerebellum during visual-motor behaviors (Hsieh et al., 2014; Matsui et al., 2014). These findings were made possible by combining behavioral experiments with both genetically encoded calcium imaging to visualize neuronal activity (Matsui et al., 2014) and loose patch recordings from cerebellar Purkinje neurons (Hsieh et al., 2014). These pioneering studies now open the door to sophisticated functional modeling of cerebellar-based neuropathies that can manifest in both neurodevelopmental disorders and neurodegenerative diseases, particularly CATX. Extending these functional technologies



to forebrain circuits will be essential to support past studies suggesting similar cognitive and emotional functions exist in subdivisions of the zebrafish forebrain (Northcutt, 2006; O'Connell and Hofmann, 2011; Maximino et al., 2013).

Conserved Genomes?

Human and zebrafish genomes are highly conserved, with 76–82% of human disease genes present in zebrafish and an average of 20–24% of zebrafish genes duplicated (Howe et al., 2013). In some cases duplicates become sub-functionalized providing an advantage for studying pleiotropic phenotypes (Fleisch et al., 2008; Good et al., 2012; Lagman et al., 2015);

in other cases, duplicates have redundant functions providing phenotypic buffering and complicating the generation of disease models (Hinitz et al., 2012; Manoli and Driever, 2014). To determine if genes linked to a particular human neurological condition are enriched in gene duplicates we compared gene duplication rates in disease gene orthologs. Because past studies have shown duplicate enrichment in genes associated with neuronal development, signaling pathways and neuronal activity (Howe et al., 2013; Glasauer and Neuhaus, 2014), we hypothesized that neurodevelopmental duplicates would have a higher retention rate compared to neurodegenerative duplicates. Several gene sets showed a high duplicate retention frequency: over 60% (ASD-ID) and 45% (ASD and CMT;

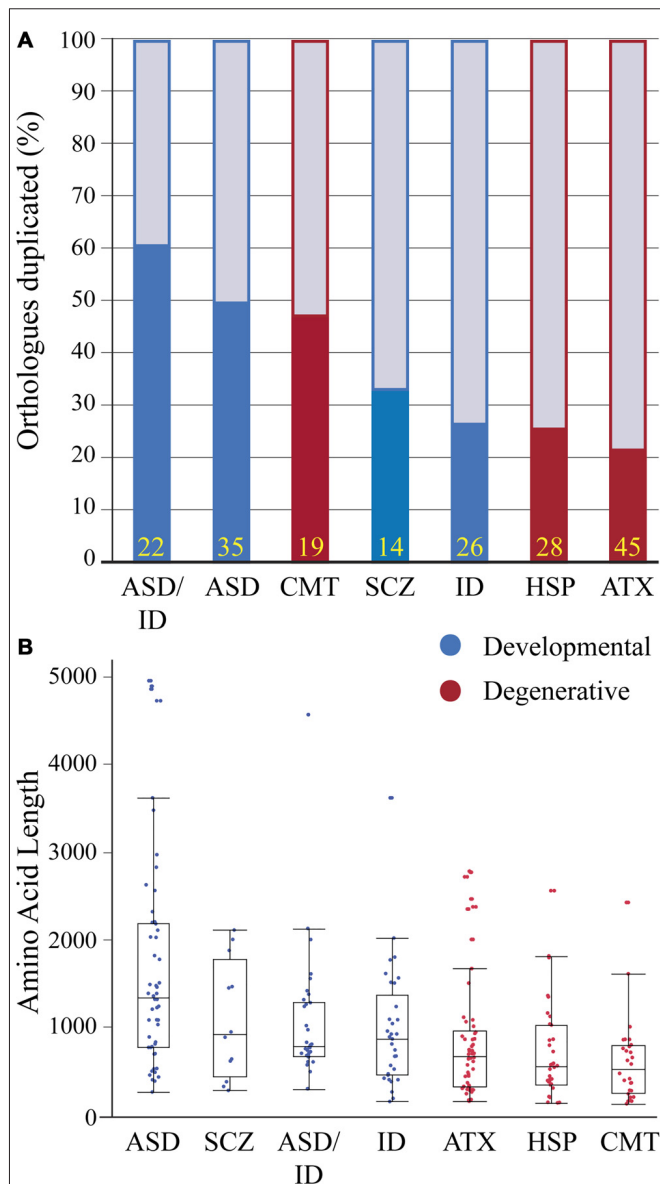


FIGURE 2 | Zebrafish orthologs of human neurological disease genes vary with respect to duplicate retention and average protein size. (A)

Gene duplicate retention rates in zebrafish are graphed for neurodevelopmental and neurodegenerative disease groups. Yellow numbers at the base of bars represent sample size. **(B)** Protein sizes of zebrafish orthologs of human disease genes with floating box plots (median with upper and lower quartile-box and range-whiskers). Note some larger proteins are outliers that fall outside of the calculated range. These gene sets for each human disease only incorporate a small percentage of associated genes and selection criteria varied because of the heterogeneity in genes linked to each disease and an emphasis on producing conservative lists. Each gene set was selected using data from research groups and review articles with the goal of including only the highest confidence disease genes based on either statistical thresholds and/or reoccurrence. Autism spectrum disorders (ASD) genes were chosen from the Simons Foundation Autism Initiative (SFARI.org) “high confidence” and “strong candidate” gene lists, which uses a multi-variable scoring analysis that includes sample size, statistical significance, replication, and functional analysis (Basu et al., 2009). ASD-intellectual disability (ID) genes were found in four separate reviews that provide evidence for reoccurrence in

(Continued)

FIGURE 2 | Continued

both ASD and ID (Kaufman et al., 2010; Krumm et al., 2014; Srivastava et al., 2014; Vissers et al., 2016). Schizophrenia (SCZ) genes were chosen from a SCZ genetics review, however this list is small and does not provide a confidence level for the disease contribution of each gene (Escudero and Johnstone, 2014). X-linked ID genes (Piton et al., 2013) and Charcot-Marie Tooth Disease (CMT; Timmerman et al., 2014) genes were chosen from recent meta-analyses to which we included a threshold of >5 cases per gene. Autosomal dominant and recessive and X-linked ataxia (ATX; Bird, 2016) and Hereditary Spastic Paraplegia (HSP; Fink, 2014) genes were chosen with well-known inheritance pedigrees. Human proteins for these gene lists were generated using BioMart (Kinsella et al., 2011) and the longest isoforms were used to identify zebrafish orthologs (Supplementary Material, Tables S1–7). Human proteins were then Blasted (Flicek et al., 2014) against the zebrafish proteome and ortholog information was recorded. Zebrafish proteins with low percent coverage, protein identity, e-value and ambiguous gene annotation (e.g., *gene-like*, *LOC1084*, etc.) were reciprocally blasted to confirm orthology.

Figure 2A). In comparison, ID, ATX and HSP zebrafish orthologs had duplicate retention frequencies of 22–26% similar to the estimated genome-wide (20–24%) duplicate retention rate (Postlethwait et al., 2004; Howe et al., 2013). To determine if neurodevelopmental processes were enriched in sets with high duplicate retention rates we compared gene ortholog Gene Ontology (GO) term enrichments within orthologs sets (Mi et al., 2013). This program compares the frequency of a biological term (e.g., neuron development) with the expected frequency calculated for the genome. ASD ($n = 35$) and ASD-ID ($n = 22$) orthologs showed enrichments for GO terms associated with nervous system and neuronal development that confirm large studies analyzing extensive data sets of ASD and ID genes (Parikshak et al., 2013; Pinto et al., 2014). By contrast, CMT orthologs ($n = 19$) did not show any GO term enrichments overall, but those retained zebrafish CMT duplicates were enriched in genes associated with neuronal development (7/9 genes; Supplementary Material, Table S12). Therefore these genes may be associated with earlier onset cases of CMT, which can occur anywhere between birth and adulthood (De Jonghe et al., 1997). Although these gene sets are small and not statistically powerful, these rates show a general trend for retaining duplicates associated with neural development.

To continue comparing these ortholog classes we looked at the length of the longest protein-coding isoform for each disease gene ortholog. This parameter impacts modeling due to numerous exons and complex splicing. For example SH3 and multiple ankyrin repeat domain 3 (*SHANK3*) is a large gene and mouse *Shank3* knockout models exhibit variable phenotypes depending on whether a mutation is expressed in a predominant isoform (Peça et al., 2011; Zhou et al., 2016). Therefore we compared protein sizes between disease gene orthologs (Figure 2B). Between groups developmental disorders all had larger median protein sizes when compared to degenerative disease orthologs (Figure 2B). However, most notably proteins encoded by ASD genes were more than twice as long when compared to all degenerative disease proteins (Figure 2B). Because ASD genes have been suggested to encompass relatively large genes this result was perhaps not surprising (King et al., 2013; Uddin et al., 2014). Together these

results on isoform length and duplicate enrichment suggests that ASD gene modeling in zebrafish will need to grapple with both extensive gene duplication and large complex genes that present challenges for knocking out all protein-coding isoforms and for generating rescue constructs.

NEURODEVELOPMENTAL AND NEURODEGENERATIVE ZEBRAFISH MODELS

Developmental Disorders

Zebrafish models of developmental disorders have benefitted from the accessible embryonic stages and simplified nervous system that reveal an important role for signaling that patterns in the early embryo. Developmental disorders including ASD, ID and SCZ start to manifest phenotypically early in development and include deficits in social, learning and occupational functions (DSM-V). Because brain regions mediating human cognitive symptoms may lack parallels in zebrafish, modeling has focused on embryonic development and disorder comorbidities (such as sensory hypo-/hyper-sensitivity, sleep disruptions, and epilepsy) that still allow testing of etiological theories for these developmental disorders. These studies have paved the way for comprehensive functional assessments that link cellular- and circuit-level phenotypes to changes in behavior.

Molecular to Cellular Mechanisms: Signaling Pathways and Head Size

Mounting evidence links the etiology of neurodevelopmental disorders to embryonic stages. For example, teratogen exposure during gestation can cause developmental disorders (Arndt et al., 2005; Levy, 2011) and embryonic phenotypes in knockout mouse models provide support for an embryonic component underlying neurodevelopmental disorders (Knuesel et al., 2005; Lee et al., 2011; Durak et al., 2015). Zebrafish knockdown models of ASD and ID genes suggest that disrupted patterning of presumptive neural tissue in developmental disorders can occur as early as blastula stages (Yimlamai et al., 2005) and during gastrulation (De Rienzo et al., 2011; Turner et al., 2015). At the molecular level, these disruptions in patterning are likely due to changes in conserved signaling pathways. Several ASD and SCZ zebrafish models have investigated disease genes associated with the Wnt pathway (De Rienzo et al., 2011; Bernier et al., 2014; Brooks et al., 2014). For example, the Wnt interacting protein Chromodomain Helicase DNA binding domain 8 (CHD8) directly affects brain development during gastrulation and increases the size of the optic tectum, mirroring macrocephaly seen in ASD patients carrying CHD8 mutations (Bernier et al., 2014; Sugathan et al., 2014). These genotype-specific features (e.g., macrocephaly) provide a phenotypic screen that can be used to investigate genetic classes within disorders. For example zebrafish *potassium channel tetramerization domain containing 13* (*kctd13*) was shown to have a dose-dependent affect in producing macrocephaly (knockdown) and microcephaly (overexpression) that supports a role for KCTD13 copy number variants causing head size phenotypes (Golzio et al., 2012).

Moreover, *Disrupted In Schizophrenia 1* (*DISC1*) interacts with canonical and non-canonical Wnt signaling and *zdisc1* morphants and mutants exhibit disorganized axon tracts at larval stages that can be rescued by activating Wnt signaling (De Rienzo et al., 2011). These studies provide clear examples of utilizing zebrafish as an embryonic model to determine molecular and cellular mechanisms that define morphological phenotypes seen in individuals with developmental disorders.

Systems-Level Mechanisms: Disrupting the Balance of Neuronal Activity

Mechanisms affecting neuronal activity can contribute to neurodevelopmental disorders and zebrafish have been used to relate circuit-level changes in activity to behavior (Rubenstein and Merzenich, 2003; Eichler and Meier, 2008; Nelson and Valakh, 2015; Scharf et al., 2015). Circuit-level changes include disrupting the excitatory and inhibitory (E/I) balance, an operational set-point of excitation and inhibition within neural circuits that maintains functional behaviors (Borodinsky et al., 2004; Gatto and Broadie, 2010; Turrigiano, 2012; Vituriera et al., 2012; Davis, 2013). Zebrafish ASD and ID models have looked at E/I balance using transgenic fish lines expressing fluorescent glutamatergic (excitatory) and GABAergic (inhibitory) neurons (Kozol et al., 2015; Hoffman et al., 2016). Recently, Hoffman et al. found that populations of GABAergic neurons were significantly decreased in *contactin associated protein-like 2* (*cntnap2ab*) mutants, recapitulating a mutant mouse *Cntnap2* model and suggesting that in the absence of *cntnap2ab* larvae fail to maintain inhibitory neuronal populations. This inhibitory decrease was shown to increase seizure susceptibility in *cntnap2ab*^{-/-} mutants by applying a GABA receptor antagonist (Hoffman et al., 2016). In addition to seizure susceptibility, *cntnap2ab*^{-/-} mutants had increased nighttime activity providing a circadian disruption for high-throughput drug screening. To identify potential therapies, they screened for drugs that reduced nighttime activity and identified a phytestrogen that restored wild type-like activity states. Like decreased inhibition, increased excitation is also known to contribute to developmental disorders. One well-studied example of this is augmented metabotropic glutamate receptor (mGluR) signaling in Fragile X Syndrome (Scharf et al., 2015). Similar to *Fragile x mental retardation 1* (*Fmr1*) knockout models in mice, a zebrafish *fmr1* knockdown model showed behavioral deficits that were ameliorated when treated with an mGluR inhibitor (Tucker et al., 2006). These studies demonstrate how zebrafish genetic models can be used to explore disorder etiology at multiple levels and efficiently test molecular theories for drug discovery.

Systems-Level Mechanisms: Comorbidities and Connecting Cells to Behavior

Individuals with developmental disorders are more likely to have accompanying medical conditions, or comorbidities, than typically developing individuals (Gurney et al., 2006; American Psychiatric Association, and DSM-5 Task Force, 2013; Chen et al., 2013a). Non-cognitive comorbidities such as sensory

hypo- or hyper-sensitivity, epilepsy and gastrointestinal (GI) discomfort have revealed cellular-level mechanisms that may underlie behavioral phenotypes in developmental disorders. Several zebrafish knockdowns models of ASD, ID and epilepsy genes have looked at impaired touch sensitivity. Knockdown models of the ASD genes *autism susceptibility candidate 2 (auts2)* and *shank3a* exhibit hyposensitivity with concomitant neuronal cell death and morphological changes in skin innervating sensory neurons (Oksenberg et al., 2013; Kozol et al., 2015). Also exploring sensitivity, *chromodomain helicase DNA binding protein 2 (chd2)* knockdowns and *sodium channel, voltage gated, type II, alpha (scn1lab)* knockouts display hyper-excitable phenotypes that are characterized by extended or disorganized swimming with epileptiform-like activity in the brain (Baraban et al., 2013; Suls et al., 2013; Galizia et al., 2015). These epileptic swimming bouts provide a stereotyped behavior for high-throughput drug screening. Such a screen in *scn1lab* mutants identified anti-histamine clemizole as a novel anti-epileptic drug (Baraban et al., 2013). Although more focus has been paid to conditions such as epilepsy, other comorbidities like GI distress in ASD have yet to be investigated comprehensively (Hsiao, 2014; Bresnahan et al., 2015). For instance, *chd8* morphants have a decrease in HuC/D positive enteric neurons innervating the gut and have impaired gut motility (Bernier et al., 2014). Again this example provided a cellular to systems level mechanism for GI distress seen in a majority of ASD patients carrying a *CHD8* mutation. These examples all show the utility of zebrafish for studying comorbidities that impact the quality of life of large cohorts of patients; therefore a better understanding of the basis for these comorbidities would likely improve patient care.

Hereditary Neurodegenerative Disorders

Some common cellular mechanisms underlying degenerative diseases have been elucidated through gene discovery and zebrafish modeling of rare hereditary diseases. The degeneration of axon tracts in the central and peripheral nervous system are a clinical feature in neurodegenerative disorders such as Charcot-Marie-Tooth disease type 2 (CMT2), HSP, SMA or spinal muscle atrophy (SMA), ALS, as well as some forms of CATX which have phenotypic and mechanistic overlap (Züchner and Vance, 2005; Timmerman et al., 2013; Bargiela et al., 2015; Burté et al., 2015). The early development of zebrafish peripheral, motor and sensory neurons provide a foundation that has been used to dissect molecular mechanisms at both the cellular and systems level especially in models of SMA and ALS (McGown et al., 2013; Wiley et al., 2014). Using an innovative strategy to develop SMA therapies, one study used a high-throughput synthetic genetic array (SGA) screen in fission yeast to identify gene networks that when targeted with drugs reversed motor axon outgrowth deficits in a zebrafish SMA model (Wiley et al., 2014). Zebrafish models of these neurodegenerative diseases have also focused on molecular mechanisms such as axonal transport, mitochondrial dynamics, and autophagy, while also measuring morphological changes at the systems level such as alterations at the neuromuscular junction, degeneration of motor

and sensory neurons, and disruptions of Purkinje cell (PC) development.

Cellular Level Mechanisms: Axonal Transport

A subset of the causative genes in these disorders are directly involved in axonal transport processes (Timmerman et al., 2013). The optical transparency of zebrafish and transgenic lines available make zebrafish an ideal model to study the relationship between axonal transport and axon degeneration *in vivo* (Plucińska et al., 2012; O'Donnell et al., 2014). Mutations in *Kinesin Family member 5A (KIF5A)*, a molecular motor for transporting microtubule-mediated cargo, have been reported in both CMT2 (Crimella et al., 2012), and HSP patients (Reid et al., 2002; Fichera et al., 2004). A *kif5a* mutant zebrafish shows decreased touch response, and defective sensory neuronal maintenance all within the larval stages of development (Campbell et al., 2014). Furthermore the authors found that *kif5a* specifically affects the transport and distribution of mitochondria in neurons, but not lysosomes or presynaptic vesicles. Dominant mutations in *Atlastin GTPase 1 (ATL1)* encoding atlastin-1 cause an early onset form of HSP (Dürr et al., 2004). Morpholino knockdown of *atl1* in zebrafish causes decreased mobility in larval fish and specifically disrupts axon tracts of spinal motor neurons (Fassier et al., 2010). Fassier et al. (2010) further demonstrated that the phenotype is the result of altered BMP signaling and that atlastin may play a role in BMP receptor trafficking. This link to BMP receptor trafficking suggested blocking BMP receptors as a therapeutic strategy that indeed ameliorated both cellular and behavioral phenotypes in the *atl1* morphant zebrafish model. These zebrafish models support axonal transport as a cellular mechanism that could explain why long axons in CMT2 and HSP are primarily affected by genetic mutations in genes associated with transport processes.

Cellular Level Mechanisms: Mitochondrial Neuropathies

Mitochondrial dysfunction is another common mechanism in neurodegeneration. Dominant mutations in *Mitofusin 2 (MFN2)* are the primary cause of axonal degeneration in Charcot-Marie-Tooth Neuropathy (CMT2), and MFN2 has been implicated in the fusion and transport of mitochondria in neurons (Chen et al., 2003; Züchner et al., 2004; Baloh et al., 2007). Murine *Mfn2* knockout and knock-in models are embryonic or postnatal lethal and do not develop a peripheral neuropathy, however a conditional knockout model did produce cerebellar degeneration and neonatal lethality (Chen et al., 2003, 2007; Strickland et al., 2014). In contrast, a stable *mfn2*^{L285X} loss-of-function zebrafish model does recapitulate the motor neuron degenerative phenotype showing progressive loss of swimming ability, loss of neuromuscular junctions (NMJs), and early lethality by 1 year of age (Chapman et al., 2013). The authors found that the transport of mitochondria is disrupted in cultured motor neurons from the homozygous *mfn2*^{L285X} at 24 hpf suggesting that a primary transport defect occurs before the onset of symptoms. In addition to axon degeneration of motor neurons a portion of patients with *MFN2* mutations also develop optic atrophy (Züchner

et al., 2006). The optic nerve seems to be particularly susceptible to mitochondrial dysfunction and is often affected in clinical spectrum phenotypes classified as mitochondrial optic neuropathies (Yu-Wai-Man et al., 2009). Recessive mutations in the nuclear encoded mitochondrial gene *Optic Atrophy 3* (*OPA3*) cause a spectrum disorder classified as Costeff syndrome and includes optic atrophy, ataxia, extra pyramidal dysfunction, and increased urinary excretion of 3-methylglutaconic acid (MGC; Costeff et al., 1989). Zebrafish *opa3* null mutants show increased MGC at both 5 dpf and at 2–5 months (Pei et al., 2010). At 1 year they show decreased optic nerve thickness and retinal ganglion cell density. Mutants have detectable changes in movement behaviors at larval stages and adults show loss of horizontal swimming. The authors speculate that the swimming phenotype can be attributed to ataxia, however TUNEL and histological staining of the cerebellum did not reveal any abnormalities. A third disease gene linked to mitochondrial dynamics and a spectrum of degenerative neurological conditions that include optic atrophy, CMT and cerebellar degeneration is *Solute Carrier family 25, member 46* *SLC25A46*; Abrams et al., 2015). Studies in zebrafish and patient stem cells linked disruption of *slc25a46* to reduced mitochondrial fission, altered distribution of mitochondria in motor neurons, and defective maintenance of neuronal processes. Even though cellular phenotypes were dramatic, swimming deficits in *slc25a46* morphants were mild.

Cellular Level Mechanisms: Cerebellar Purkinje Neurons

Ataxia and associated sensory and motor phenotypes result from genetic mutations that affect various cell types within the spinocerebellar circuit. Cerebellar PCs are commonly affected and appear especially sensitive to peroxisomal dysfunction associated with PC loss or cerebellar atrophy (Akbar and Ashizawa, 2015). Consistent with this, zebrafish ataxia models, such as *sorting nexin 14* (*snx14*) morphants show decreases in PC progenitors while *cowf19-like 1* (*cowf1911*) morphants show disruptions in overall hindbrain morphology (Burns et al., 2014; Akizu et al., 2015). Alternatively, one group has focused on primary motor neurons for functional studies of *Potassium Channel, voltage gated shaw related subfamily c, member 3* (*KCN3*) mutations that cause Spinocerebellar ataxia type 13 (Waters et al., 2006). They found that zebrafish *kcn3a* is expressed in the primary motor neurons and overexpression of a dominant negative version of this potassium channel decreases in neuronal excitability during fictive swimming (Issa et al., 2012). To follow up this study, Issa et al. also investigated the affect of *KCN3* mutations associated with infant onset ataxia. Overexpression of two human *KCN3* mutations demonstrated axonal defects that were only found in a mutation associated with infantile onset of SCA13. Given that neurodegenerative phenotypes become more severe with age, there has been doubt as to whether modeling these diseases in zebrafish larvae would be informative. The studies reviewed above indicate that indeed it is possible to gain functional insight into the basic biology of these disease genes from modeling in the larva. As a newer model, however, approaches in zebrafish are not quite as standardized

as those in longer established models like *Drosophila* and mouse resulting in the diversity of modeling strategies employed by different researchers to model these inherited neurological conditions.

LESSONS LEARNED FROM MODELING INHERITABLE DISEASE GENES

Homeostatic Plasticity: Unlinking Cellular and Systems Level Phenotypes

In some less common examples, genetic mutations cause cellular- and molecular-level phenotypes without leading to behavioral phenotypes. In zebrafish *where's waldo* and *strumpy* mutants, neuromuscular synaptogenesis is defected but the mutants exhibit normal motility (Hutson and Chien, 2002; Panzer et al., 2005). Similar phenomena have been observed in mouse hypoxanthine-guanine phosphoribosyltransferase (HPRT) and HPRT-adenine phosphoribosyltransferase (APRT) mutant models of Lesch-Nyhan syndrome genes that produced an expected drop in dopamine but lacked self mutilation behaviors (Kuehn et al., 1987; Engle et al., 1996; Jinnah et al., 1999). These observations indicate that molecular- and cellular-level phenotype does not always correspond to behavioral phenotype, suggesting the existence of compensatory mechanisms at the systems-level. Besides genetic compensation from other genes, the nervous system also has remarkable capacity to stabilize its functions via homeostatic plasticity. Compensatory homeostatic plasticity operates on multiple levels, regulating synaptogenesis, synaptic strength and intrinsic excitability to stabilize neural circuit output in the context of genetic and/or environmental perturbations (Turrigiano, 2012; Vitureira et al., 2012; Davis, 2013). In zebrafish *strumpy*^{p37er} mutants have enlarged NMJ acetylcholine receptor clusters are compared to wild-type (Panzer et al., 2005), but lack motor phenotypes, indicating homeostatic plasticity. In addition, defective homeostatic plasticity has been associated to a variety of human neurological diseases, including ASD, ID and Fragile X Syndrome (Rubenstein and Merzenich, 2003; Eichler and Meier, 2008; Gatto and Broadie, 2010; Yizhar et al., 2011; Wondolowski and Dickman, 2013; Nelson and Valakh, 2015). Mutant animal models with cellular but not behavioral phenotype have the potential to shed light on mechanisms of homeostatic plasticity at the systems-level. Given the diversity of molecular genetic pathways that contribute to developmental and degenerative disorders, a potential therapeutic target is to boost compensatory mechanisms that act to re-establish systems-level function.

Genetic Buffering: Molecular Compensation for Genetic Lesions

It is also common, though not necessarily well-represented in the literature, for knockout models to lack phenotypes. In a zebrafish study that generated mutant lines with 32 distinct lesions in 24 genes, most of the mutants exhibit a wild-type phenotype (Kok et al., 2015). Rather than a unique characteristic of zebrafish, such phenotypic buffering is found across single-celled to multi-cellular organisms. For example, >70% in fission

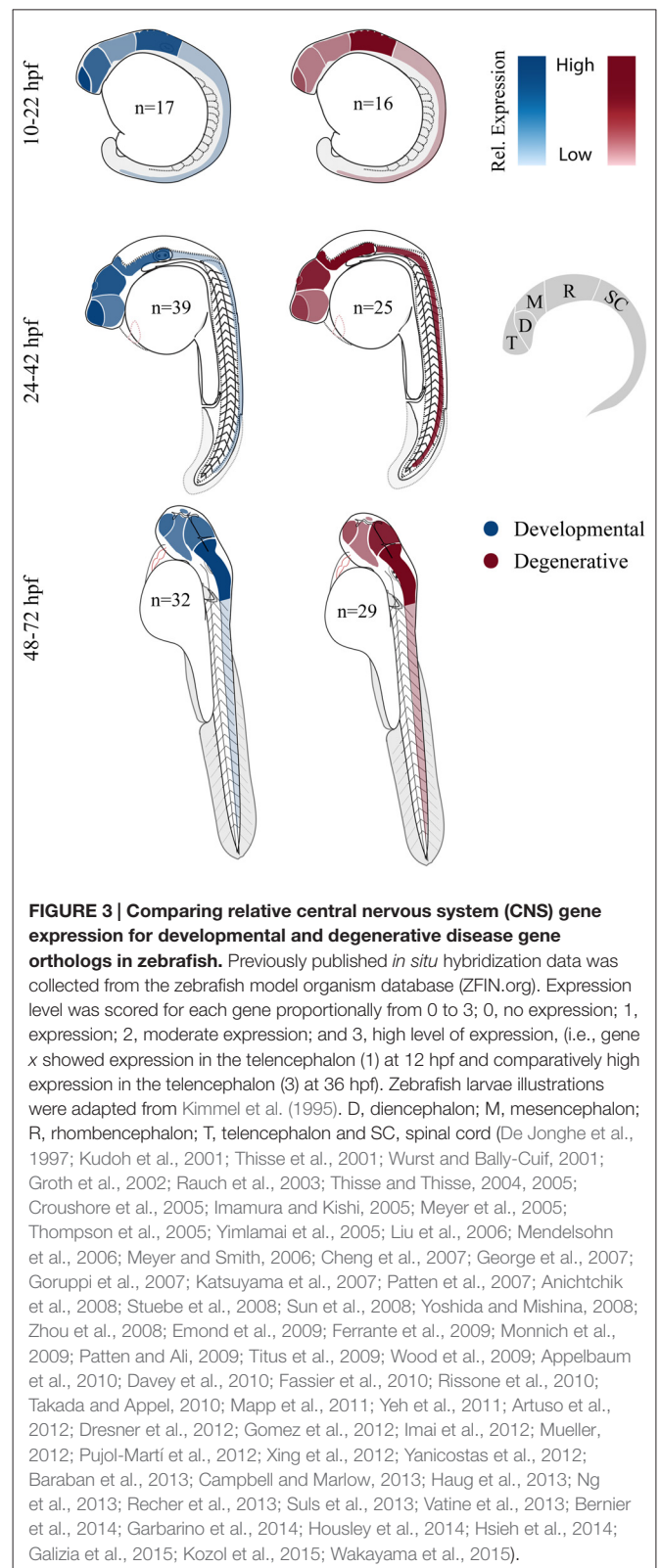
yeast and >80% in bakers yeast, of genes can be individually mutated with little effect on haploid viability in the laboratory setting (Kim et al., 2010)¹. Also in mice, though it is hard to accurately estimate the proportion of knockout mice without detectable phenotypes due to a lack of publications, the number is considerable (Barbaric et al., 2007). This phenomenon can be explained by the recent finding that other genes in a regulatory network can provide genetic compensation in mutants (Rossi et al., 2015). Such compensation can vary depending on genetic background (Gerlai, 1996; Pearson, 2002). Another recent study in zebrafish shows that the oncogenic *B-RAF* proto-oncogene (*BRAF*^{V600E}) mutations rarely convert carrier cells into cancer cells unless in a *p53* mutant background (Kaufman et al., 2016). The importance of genetic background for gene regulatory compensation likely contributes to disease penetrance and expressivity in humans as well (Zlotogora, 2003; Andersen and Al-Chalabi, 2011; Cooper et al., 2013; Persico and Napolioni, 2013), and suggests the importance to move from analyzing single gene to systems-level analysis of gene regulatory networks in disease models (Döhr et al., 2005; Barabási et al., 2011; Chen et al., 2014; Wiley et al., 2014; Marbach et al., 2016).

Broad Gene Expression; Local Pathology

Both developmental and degenerative diseases are associated with dysfunction in specific regions of the CNS (Figure 1). None-the-less most genes have heterogeneous spatial and temporal expression patterns that extend well beyond the windows of time and specific neural circuits associated with the disorder. Therefore we did a limited meta-analysis of mRNA expression of zebrafish disease orthologs. Unfortunately a zebrafish gene expression atlas does not exist and the most complete data sets only span embryonic development. Therefore we chose to compile previously published *in situ* hybridization data and determine the relative enrichment of gene expression in brain regions and spinal cord (Figure 3; Supplementary Material, Tables S13–18). During the first day of development, both gene sets show enriched expression in the hindbrain with the developmental set having enriched expression in the forebrain. By the second and third day, expression patterns become broader showing similar enrichment throughout the brain at these stages of morphogenesis and circuit formation. Broad CNS expression patterns suggest that genes play functional roles throughout development and across the nervous system despite being associated with symptoms that disrupt specific circuits during particular times of life.

LOOKING FORWARD: NEURAL CIRCUITS, BEHAVIOR, AND THERAPY

Because of the large number of rare mutations linked to inherited nervous system diseases, an important frontier for disease modeling is strategies that leverage to make stable F₀ mutant models of inherited neurological disorders (Jao et al.,



2013; Shah et al., 2015). Such models enable the rapid screening of candidate disease genes for whether they produce disease relevant phenotypes in the zebrafish model. To this end, many

¹<http://www.yeastgenome.org>

groups currently augment their MO studies by demonstrating similar phenotypes in F_0 mutants (Bernier et al., 2014; Aspatwar et al., 2015; Bögershausen et al., 2015; O'Rawe et al., 2015; Wheeler et al., 2015; Xing et al., 2015). Still others have found mismatches between morphant and stable mutant phenotypes (Kok et al., 2015; Rossi et al., 2015; Stainier et al., 2015). Clearly in some cases these mismatches ascribed to non-specific effects of the morpholino (Kok et al., 2015) can also be explained by compensatory mechanisms masking the phenotype in the stable mutant (Rossi et al., 2015). To address the challenges of gene duplicates and multiple mutation causes of disease (Shah et al., 2015), several labs have further pioneered a strategy to pool guides targeting multiple genes and inject them together to efficiently screen multiple mutations in the F_0 generation. Combined with a large repertoire of behaviors that develop within 5 days of fertilization and diverse transgenic lines for rapid screening of cellular phenotypes, F_0 CRISPR zebrafish mutagenesis promises to contribute significantly to our understanding of genetic variation linked to nervous system disorders.

To model specific patient missense mutations and to better understand the basic biology of disease genes by tagging them *in vivo* or create conditional mutant alleles, several groups have also recently pioneered the use CRISPR/Cas9 for more sophisticated genome engineering. One novel strategy effectively “enhancer traps” a gene of interest by replacing the last exon with an engineered last exon encoding the C-terminal end of the coding sequence in frame with a cleavable p2A sequence followed by a fluorescent reporter (Li et al., 2015). In this way, the spatial and temporal expression dynamics of the protein can be captured. Also recently, Hoshijima et al. (2016) have developed streamlined strategies to precisely edit the genome and generate conditional mutant alleles flanked by LoxP sites. Such conditional mutant alleles have been used to great effect in mouse models to test when the mutation acts to produce different disease phenotypes. For example, in a mouse *Shank3* autism model, rescuing the mutant Shank3 protein in the adult was sufficient to rescue social interactions and excessive grooming but not anxiety and repetitive motor behaviors (Mei et al., 2016).

The development of approaches that enable monitoring of behavior-relevant neural circuits in the intact larvae will be a boon for modeling inherited neurological disease (Ahrens et al., 2013; Fosque et al., 2015; Randlett et al., 2015; Dunn et al., 2016). Such approaches have the significant advantage of being unbiased. While many of these systems-level analyses use light-sheet or high-end microscopy to capture data (Ahrens et al., 2013; Fosque et al., 2015; Dunn et al., 2016), others use standard confocal microscopy to identify relevant brain circuits (Randlett et al., 2015) that are often spatially distributed across the nervous system. Several groups have also made concerted efforts towards establishing brain atlases to structurally and functionally annotate the brain (Ronneberger et al., 2012; Turner et al., 2014; Randlett et al., 2015) which is crucial since the ability to interpret imaging data is only as good as our understanding of brain regions (Arrenberg and Driever, 2013). Once these circuits are identified, they can then be studied in greater depth using *in vivo* calcium imaging with genetically

encoded calcium indicators- (GECIs; Chen et al., 2013b), laser or enzymatic ablation of parts of the circuit (Liu and Fetcho, 1999; Tabor et al., 2014; Chen et al., 2016), electrophysiological recordings (Koyama et al., 2011; Baraban, 2013; Johnston et al., 2013; Wen et al., 2013), and optogenetics (Wyart et al., 2009; Kimura et al., 2013) to dissect circuit properties. Most of these approaches have yet to be broadly applied to zebrafish models of disease but once applied more broadly they promise to significantly contribute to our understanding of systems-level neural circuit mechanisms that contribute to symptoms of inherited neurological disorders.

In addition to genetic screens, due to their small size and their tendency to absorb drugs added directly to the water, zebrafish larvae are uniquely amenable for high-throughput drug screens (Rihel et al., 2010; Rihel and Schier, 2013; Bruni et al., 2014). High-throughput behavioral screens in zebrafish have enabled the classification of neuro-active drugs with respect to their impact on whole organism behavior. The ability to screen compounds in this manner is crucial since neuroactive drug discovery is still more empirical—a matter of what works—rather than rational—a matter of what makes sense based on chemistry and known molecular targets (Bruni et al., 2014). As highlighted in neurodevelopmental and neurodegenerative sections above, several disease models have made great use of the ability to use drugs to enhance or suppress mutant phenotypes as a means to identify therapeutic strategies (Fassier et al., 2010; Baraban et al., 2013; Hoffman et al., 2016).

CONCLUSION

The continued expertise and innovations of zebrafish genetic and developmental tools will continue to make zebrafish an attractive neurological disease model. Going forward, combining standard assays that allow comparisons across models with newer approaches would be ideal to enable a better understanding of the molecular, cellular, and systems-level groupings of these neurological conditions. Finally, zebrafish will certainly contribute to consortia of research groups that use multiple animal models for discovering essential molecular to circuit level mechanisms underlying neurological disease.

AUTHOR CONTRIBUTIONS

RAK conducted all meta-analyses, made all figures and wrote introductory and developmental disorder sections and conducted extensive edits to coordinate sections. AJA wrote the bulk of the neurodegenerative section with the exception of the ataxia section that was written by EB. DMJ wrote comorbidity section that centered on GI distress in developmental disorders. QY wrote the lessons learned section. JED conceived the scope of the review, wrote frontiers section and helped RAK to conduct extensive edits to coordinate sections.

FUNDING

This work was supported by support from the National Institutes of Health Institute of Mental Health R03MH103857

to JED and from the Institute of General Medicine, an IMSD graduate fellowship from parent grant R25GM076419 to DMJ.

ACKNOWLEDGMENTS

We would like to acknowledge our human genetics colleagues Stephan Züchner, Rebecca Schüle, Margaret Pericak-Vance, and

Joseph Buxbaum without whom we would never have started modeling human genetic disorders and diseases in zebrafish.

SUPPLEMENTARY MATERIAL

The Supplementary Material for this article can be found online at: <http://journal.frontiersin.org/article/10.3389/fnmol.2016.00055/abstract>

REFERENCES

- Abrams, A. J., Hufnagel, R. B., Rebelo, A., Zanna, C., Patel, N., Gonzalez, M. A., et al. (2015). Mutations in SLC25A46, encoding a UGO1-like protein, cause an optic atrophy spectrum disorder. *Nat. Genet.* 47, 926–932. doi: 10.1038/ng.3354
- Ahrens, M. B., Orger, M. B., Robson, D. N., Li, J. M., and Keller, P. J. (2013). Whole-brain functional imaging at cellular resolution using light-sheet microscopy. *Nat. Methods* 10, 413–420. doi: 10.1038/nmeth.2434
- Akbar, U., and Ashizawa, T. (2015). Ataxia. *Neurol. Clin.* 33, 225–248. doi: 10.1016/j.ncl.2014.09.004
- Akizu, N., Cantagrel, V., Zaki, M. S., Al-Gazali, L., Wang, X., Rosti, R. O., et al. (2015). Biallelic mutations in SNX14 cause a syndromic form of cerebellar atrophy and lysosome-autophagosome dysfunction. *Nat. Genet.* 47, 528–534. doi: 10.1038/ng.3256
- Amaral, D. G., Dawson, G., and Geschwind, D. H. (2011). *Autism Spectrum Disorders*. New York, NY: Oxford University Press, Inc.
- American Psychiatric Association, and DSM-5 Task Force. (2013). *Diagnostic and Statistical Manual of Mental Disorders : DSM-5*. Washington, D.C.: American Psychiatric Association.
- Andersen, P. M., and Al-Chalabi, A. (2011). Clinical genetics of amyotrophic lateral sclerosis: what do we really know? *Nat. Rev. Neurol.* 7, 603–615. doi: 10.1038/nrneuro.2011.150
- Anichtchik, O., Diekmann, H., Fleming, A., Roach, A., Goldsmith, P., and Rubinstein, D. C. (2008). Loss of PINK1 function affects development and results in neurodegeneration in zebrafish. *J. Neurosci.* 28, 8199–8207. doi: 10.1523/jneurosci.0979-08.2008
- Appelbaum, L., Wang, G., Yokogawa, T., Skariah, G. M., Smith, S. J., Mourrain, P., et al. (2010). Circadian and homeostatic regulation of structural synaptic plasticity in hypocretin neurons. *Neuron* 68, 87–98. doi: 10.1016/j.neuron.2010.09.006
- Arndt, T. L., Stodgell, C. J., and Rodier, P. M. (2005). The teratology of autism. *Int. J. Dev. Neurosci.* 23, 189–199. doi: 10.1016/j.ijdevneu.2004.11.001
- Arrenberg, A. B., and Driever, W. (2013). Integrating anatomy and function for zebrafish circuit analysis. *Front. Neural Circuits* 7:74. doi: 10.3389/fncir.2013.00074
- Artuso, L., Romano, A., Verri, T., Domenichini, A., Argenton, F., Santorelli, F. M., et al. (2012). Mitochondrial DNA metabolism in early development of zebrafish (Danio rerio). *Biochim. Biophys. Acta* 1817, 1002–1011. doi: 10.1016/j.bbabi.2012.03.019
- Aspatwar, A., Tolvanen, M. E., Ojanen, M. J., Barker, H. R., Saralahti, A. K., Bäuerlein, C. A., et al. (2015). Inactivation of ca10a and ca10b genes leads to abnormal embryonic development and alters movement pattern in zebrafish. *PLoS One* 10:e0134263. doi: 10.1371/journal.pone.0134263
- Babin, P. J., Goizet, C., and Raldua, D. (2014). Zebrafish models of human motor neuron diseases: advantages and limitations. *Prog. Neurobiol.* 118, 36–58. doi: 10.1016/j.pneurobio.2014.03.001
- Bakshi, K., and Chance, S. A. (2015). The neuropathology of schizophrenia: a selective review of past studies and emerging themes in brain structure and cytoarchitecture. *Neuroscience* 303, 82–102. doi: 10.1016/j.neuroscience.2015.06.028
- Baloh, R. H., Schmidt, R. E., Pestronk, A., and Milbrandt, J. (2007). Altered axonal mitochondrial transport in the pathogenesis of Charcot-Marie-Tooth disease from mitofusin 2 mutations. *J. Neurosci.* 27, 422–430. doi: 10.1523/jneurosci.4798-06.2007
- Baraban, S. C. (2013). Forebrain electrophysiological recording in larval zebrafish. *J. Vis. Exp.* 17:50104. doi: 10.3791/50104
- Baraban, S. C., Dinday, M. T., and Hortopan, G. A. (2013). Drug screening in Scn1a zebrafish mutant identifies clemizole as a potential Dravet syndrome treatment. *Nat. Commun.* 4:2410. doi: 10.1038/ncomms3410
- Barabási, A. L., Gulbahce, N., and Loscalzo, J. (2011). Network medicine: a network-based approach to human disease. *Nat. Rev. Genet.* 12, 56–68. doi: 10.1038/nrg2918
- Barbaric, I., Miller, G., and Dear, T. N. (2007). Appearances can be deceiving: phenotypes of knockout mice. *Brief. Funct. Genomic. Proteomic.* 6, 91–103. doi: 10.1093/bfpg/elm008
- Bargiela, D., Shanmugarajah, P., Lo, C., Blakely, E. L., Taylor, R. W., Horvath, R., et al. (2015). Mitochondrial pathology in progressive cerebellar ataxia. *Cerebellum Ataxias* 2:16. doi: 10.1186/s40673-015-0035-x
- Basu, S. N., Kollu, R., and Banerjee-Basu, S. (2009). AutDB: a gene reference resource for autism research. *Nucleic Acids Res.* 37, D832–D836. doi: 10.1093/nar/gkn835
- Bernier, R., Golzio, C., Xiong, B., Stessman, H. A., Coe, B. P., Penn, O., et al. (2014). Disruptive CHD8 mutations define a subtype of autism early in development. *Cell* 158, 263–276. doi: 10.1016/j.cell.2014.06.017
- Bird, T. D. (2016). *Hereditary Ataxia Overview*. Gene Reviews. Seattle, WA: University of Washington.
- Bögershausen, N., Tsai, I. C., Pohl, E., Kiper, P. Ö., Beleggia, F., Percin, E. F., et al. (2015). RAP1-mediated MEK/ERK pathway defects in Kabuki syndrome. *J. Clin. Invest.* 125, 3585–3599. doi: 10.1172/jci80102
- Borodinsky, L. N., Root, C. M., Cronin, J. A., Sann, S. B., Gu, H. L., and Spitzer, N. C. (2004). Activity-dependent homeostatic specification of transmitter expression in embryonic neurons. *Nature* 429, 523–530. doi: 10.1038/nature02518
- Bresnahan, M., Hornig, M., Schultz, A. F., Gunnes, N., Hirtz, D., Lie, K. K., et al. (2015). Association of maternal report of infant and toddler gastrointestinal symptoms with autism: evidence from a prospective birth cohort. *JAMA Psychiatry* 72, 466–474. doi: 10.1001/jamapsychiatry.2014.3034
- Brooks, S. S., Wall, A. L., Golzio, C., Reid, D. W., Kondyles, A., Willer, J. R., et al. (2014). A novel ribosomopathy caused by dysfunction of RPL10 disrupts neurodevelopment and causes X-linked microcephaly in humans. *Genetics* 198, 723–733. doi: 10.1534/genetics.114.168211
- Bruni, G., Lakhani, P., and Kokel, D. (2014). Discovering novel neuroactive drugs through high-throughput behavior-based chemical screening in the zebrafish. *Front. Pharmacol.* 5:153. doi: 10.3389/fphar.2014.00153
- Brustein, E., Saint-Amant, L., Buss, R. R., Chong, M., McDermid, J. R., and Drapeau, P. (2003). Steps during the development of the zebrafish locomotor network. *J. Physiol. Paris* 97, 77–86. doi: 10.1016/j.jphysparis.2003.10.009
- Burns, R., Majcenko, K., Xu, J., Peng, W., Yapici, Z., Dowling, J. J., et al. (2014). Homozygous splice mutation in CWF19L1 in a Turkish family with recessive ataxia syndrome. *Neurology* 83, 2175–2182. doi: 10.1212/wnl.0000000000001053
- Burté, F., Carelli, V., Chinnery, P. F., and Yu-Wai-Man, P. (2015). Disturbed mitochondrial dynamics and neurodegenerative disorders. *Nat. Rev. Neurol.* 11, 11–24. doi: 10.1038/nrneuro.2014.228
- Buxbaum, J. D., Daly, M. J., Devlin, B., Lehner, T., Roeder, K., State, M. W., et al. (2012). The autism sequencing consortium: large-scale, high-throughput sequencing in autism spectrum disorders. *Neuron* 76, 1052–1056. doi: 10.1016/j.neuron.2012.12.008
- Campbell, P. D., and Marlow, F. L. (2013). Temporal and tissue specific gene expression patterns of the zebrafish kinesin-1 heavy chain family, kif5s, during development. *Gene Expr. Patterns* 13, 271–279. doi: 10.1016/j.gexp.2013.05.002

- Campbell, P. D., Shen, K., Sapio, M. R., Glenn, T. D., Talbot, W. S., and Marlow, F. L. (2014). Unique function of Kinesin Kif5A in localization of mitochondria in axons. *J. Neurosci.* 34, 14717–14732. doi: 10.1523/jneurosci.2770-14.2014
- Chapman, A. L., Bennett, E. J., Ramesh, T. M., De Vos, K. J., and Grierson, A. J. (2013). Axonal transport defects in a mitofusin 2 loss of function model of charcot-marie-tooth disease in zebrafish. *PLoS One* 8:e67276. doi: 10.1371/journal.pone.0067276
- Chen, H., Detmer, S. A., Ewald, A. J., Griffin, E. E., Fraser, S. E., and Chan, D. C. (2003). Mitofusins Mfn1 and Mfn2 coordinately regulate mitochondrial fusion and are essential for embryonic development. *J. Cell Biol.* 160, 189–200. doi: 10.1083/jcb.200211046
- Chen, H., McCaffery, J. M., and Chan, D. C. (2007). Mitochondrial fusion protects against neurodegeneration in the cerebellum. *Cell* 130, 548–562. doi: 10.1016/j.cell.2007.06.026
- Chen, J. C., Alvarez, M. J., Talos, F., Dhruv, H., Rieckhof, G. E., Iyer, A., et al. (2014). Identification of causal genetic drivers of human disease through systems-level analysis of regulatory networks. *Cell* 159, 402–414. doi: 10.1016/j.cell.2014.09.021
- Chen, M. H., Su, T. P., Chen, Y. S., Hsu, J. W., Huang, K. L., Chang, W. H., et al. (2013a). Comorbidity of allergic and autoimmune diseases among patients with ADHD: a nationwide population-based study. *J. Atten. Disord.* doi: 10.1177/1087054712474686 [Epub ahead of print].
- Chen, T. W., Wardill, T. J., Sun, Y., Pulver, S. R., Renninger, S. L., Baohan, A., et al. (2013b). Ultrasensitive fluorescent proteins for imaging neuronal activity. *Nature* 499, 295–300. doi: 10.1038/nature12354
- Chen, S., Chiu, C. N., McArthur, K. L., Fethco, J. R., and Prober, D. A. (2016). TRP channel mediated neuronal activation and ablation in freely behaving zebrafish. *Nat. Methods* 13, 147–150. doi: 10.1038/nmeth.3691
- Cheng, L., Chong, M., Fan, W., Guo, X., Zhang, W., Yang, X., et al. (2007). Molecular cloning, characterization and developmental expression of foxp1 in zebrafish. *Dev. Genes Evol.* 217, 699–707. doi: 10.1007/s00427-007-0177-9
- Cooper, D. N., Krawczak, M., Polychronakos, C., Tyler-Smith, C., and Kehrer-Sawatzki, H. (2013). Where genotype is not predictive of phenotype: towards an understanding of the molecular basis of reduced penetrance in human inherited disease. *Hum. Genet.* 132, 1077–1130. doi: 10.1007/s00439-013-1331-2
- Costeff, H., Gadoth, N., Apter, N., Prialnic, M., and Savir, H. (1989). A familial syndrome of infantile optic atrophy, movement disorder and spastic paraplegia. *Neurology* 39, 595–597. doi: 10.1212/wnl.39.4.595
- Crimella, C., Baschiroto, C., Arnoldi, A., Tonelli, A., Tenderini, E., Airoidi, G., et al. (2012). Mutations in the motor and stalk domains of KIF5A in spastic paraplegia type 10 and in axonal Charcot-Marie-Tooth type 2. *Clin. Genet.* 82, 157–164. doi: 10.1111/j.1399-0004.2011.01717.x
- Croushore, J. A., Blasiole, B., Riddle, R. C., Thisse, C., Thisse, B., Canfield, V. A., et al. (2005). Ptena and ptenb genes play distinct roles in zebrafish embryogenesis. *Dev. Dyn.* 234, 911–921. doi: 10.1002/dvdy.20576
- Davey, C., Tallafuss, A., and Washbourne, P. (2010). Differential expression of neurexin genes in the nervous system of zebrafish. *Dev. Dyn.* 239, 703–714. doi: 10.1002/dvdy.22195
- Davis, G. W. (2013). Homeostatic signaling and the stabilization of neural function. *Neuron* 80, 718–728. doi: 10.1016/j.neuron.2013.09.044
- De Jonghe, P., Timmerman, V., Nelis, E., Martin, J. J., and Van Broeckhoven, C. (1997). Charcot-Marie-Tooth disease and related peripheral neuropathies. *J. Peripher. Nerv. Syst.* 2, 370–387.
- De Rienzo, G., Bishop, J. A., Mao, Y., Pan, L., Ma, T. P., Moens, C. B., et al. (2011). Disc1 regulates both beta-catenin-mediated and noncanonical Wnt signaling during vertebrate embryogenesis. *FASEB J.* 25, 4184–4197. doi: 10.1096/fj.11-186239
- De Rubeis, S., and Buxbaum, J. D. (2015). Genetics and genomics of autism spectrum disorder: embracing complexity. *Hum. Mol. Genet.* 24, R24–R31. doi: 10.1093/hmg/ddv273
- Döhr, S., Klingenhoff, A., Maier, H., Hrabé de Angelis, M., Werner, T., and Schneider, R. (2005). Linking disease-associated genes to regulatory networks via promoter organization. *Nucleic Acids Res.* 33, 864–872. doi: 10.1093/nar/gki230
- Dresner, E., Malishkevich, A., Arviv, C., Leibman Barak, S., Alon, S., Ofir, R., et al. (2012). Novel evolutionary-conserved role for the activity-dependent neuroprotective protein (ADNP) family that is important for erythropoiesis. *J. Biol. Chem.* 287, 40173–40185. doi: 10.1074/jbc.m112.387027
- Dunn, T. W., Mu, Y., Narayan, S., Randlett, O., Naumann, E. A., Yang, C. T., et al. (2016). Brain-wide mapping of neural activity controlling zebrafish exploratory locomotion. *Elife* 5:e12741. doi: 10.7554/elifelife.12741
- Durak, O., de Anda, F. C., Singh, K. K., Leussis, M. P., Petryshen, T. L., Sklar, P., et al. (2015). Ankyrin-G regulates neurogenesis and Wnt signaling by altering the subcellular localization of beta-catenin. *Mol. Psychiatry* 20, 388–397. doi: 10.1038/mp.2014.42
- Dürr, A., Camuzat, A., Colin, E., Tallaksen, C., Hannequin, D., Coutinho, P., et al. (2004). Atlastin1 mutations are frequent in young-onset autosomal dominant spastic paraplegia. *Arch. Neurol.* 61, 1867–1872. doi: 10.1001/archneur.61.12.1867
- Eichler, S. A., and Meier, J. C. (2008). E-I balance and human diseases—from molecules to networking. *Front. Mol. Neurosci.* 1:2. doi: 10.3389/neuro.02.002.2008
- Emond, M. R., Biswas, S., and Jontes, J. D. (2009). Protocadherin-19 is essential for early steps in brain morphogenesis. *Dev. Biol.* 334, 72–83. doi: 10.1016/j.ydbio.2009.07.008
- Engle, S. J., Womer, D. E., Davies, P. M., Boivin, G., Sahota, A., Simmonds, H. A., et al. (1996). HPRT-APRT-deficient mice are not a model for lesch-nyhan syndrome. *Hum. Mol. Genet.* 5, 1607–1610. doi: 10.1093/hmg/5.10.1607
- Escudero, I., and Johnstone, M. (2014). Genetics of schizophrenia. *Curr. Psychiatry Rep.* 16:502. doi: 10.1007/s11920-014-0502-8
- Espinós, C., and Palau, F. (2009). Genetics and pathogenesis of inherited ataxias and spastic paraplegias. *Adv. Exp. Med. Biol.* 652, 263–296. doi: 10.1007/978-90-481-2813-6_18
- Fassier, C., Hutt, J. A., Scholpp, S., Lumsden, A., Giros, B., Nothias, F., et al. (2010). Zebrafish atlastin controls motility and spinal motor axon architecture via inhibition of the BMP pathway. *Nat. Neurosci.* 13, 1380–1387. doi: 10.1038/nn.2662
- Ferrante, M. I., Romio, L., Castro, S., Collins, J. E., Goulding, D. A., Stemple, D. L., et al. (2009). Convergent extension movements and ciliary function are mediated by ofd1, a zebrafish orthologue of the human oral-facial-digital type 1 syndrome gene. *Hum. Mol. Genet.* 18, 289–303. doi: 10.1093/hmg/ddn356
- Fichera, M., Lo Giudice, M., Falco, M., Sturnio, M., Amata, S., Calabrese, O., et al. (2004). Evidence of kinesin heavy chain (KIF5A) involvement in pure hereditary spastic paraplegia. *Neurology* 63, 1108–1110. doi: 10.1212/01.wnl.0000138731.60693.d2
- Filippi, A., Mueller, T., and Driever, W. (2014). vglut2 and gad expression reveal distinct patterns of dual GABAergic versus glutamatergic cotransmitter phenotypes of dopaminergic and noradrenergic neurons in the zebrafish brain. *J. Comp. Neurol.* 522, 2019–2037. doi: 10.1002/cne.23524
- Fink, J. K. (2014). *Hereditary Spastic Paraplegia Overview*. GeneReviews. Seattle, WA: University of Washington.
- Fleisch, V. C., Schonthal, H. B., von Lintig, J., and Neuhaus, S. C. (2008). Subfunctionalization of a retinoid-binding protein provides evidence for two parallel visual cycles in the cone-dominant zebrafish retina. *J. Neurosci.* 28, 8208–8216. doi: 10.1523/jneurosci.2367-08.2008
- Flicke, P., Amode, M. R., Barrell, D., Beal, K., Billis, K., Brent, S., et al. (2014). Ensembl 2014. *Nucleic Acids Res.* 42, D749–D755. doi: 10.1093/nar/gkt1196
- Fosque, B. F., Sun, Y., Dana, H., Yang, C. T., Ohya, T., Tadross, M. R., et al. (2015). Neural circuits. Labeling of active neural circuits *in vivo* with designed calcium integrators. *Science* 347, 755–760. doi: 10.1126/science.1260922
- Galizia, E. C., Myers, C. T., Leu, C., de Kovel, C. G., Afrikanova, T., Cordero-Maldonado, M. L., et al. (2015). CHD2 variants are a risk factor for photosensitivity in epilepsy. *Brain* 138, 1198–1207. doi: 10.1093/brain/awv052
- Ganz, J., Kroehne, V., Freudenreich, D., Machate, A., Gefarth, M., Braasch, I., et al. (2014). Subdivisions of the adult zebrafish pallidum based on molecular marker analysis. *F1000Res.* 3:308. doi: 10.12688/f1000research.5595.2
- Garbarino, G., Costa, S., Pestarino, M., and Candiani, S. (2014). Differential expression of synapsin genes during early zebrafish development. *Neuroscience* 280, 351–367. doi: 10.1016/j.neuroscience.2014.09.015
- Gatto, C. L., and Broadie, K. (2010). Genetic controls balancing excitatory and inhibitory synaptogenesis in neurodevelopmental disorder models. *Front. Synaptic Neurosci.* 2:4. doi: 10.3389/fnsyn.2010.00004
- George, B., Datar, R. H., Wu, L., Cai, J., Patten, N., Beil, S. J., et al. (2007). p53 gene and protein status: the role of p53 alterations in predicting outcome in patients with bladder cancer. *J. Clin. Oncol.* 25, 5352–5358. doi: 10.1200/jco.2006.10.4125

- Gerlai, R. (1996). Gene-targeting studies of mammalian behavior: is it the mutation or the background genotype? *Trends Neurosci.* 19, 177–181. doi: 10.1016/s0166-2236(96)20020-7
- Geschwind, D. H., and State, M. W. (2015). Gene hunting in autism spectrum disorder: on the path to precision medicine. *Lancet Neurol.* 14, 1109–1120. doi: 10.1016/S1474-4422(15)00044-7
- Glasauer, S. M., and Neuhauss, S. C. (2014). Whole-genome duplication in teleost fishes and its evolutionary consequences. *Mol. Genet. Genomics* 289, 1045–1060. doi: 10.1007/s00438-014-0889-2
- Golzio, C., Willer, J., Talkowski, M. E., Oh, E. C., Taniguchi, Y., Jacquemont, S., et al. (2012). KCTD13 is a major driver of mirrored neuroanatomical phenotypes of the 16p11.2 copy number variant. *Nature* 485, 363–367. doi: 10.1038/nature11091
- Gomez, G., Lee, J. H., Veldman, M. B., Lu, J., Xiao, X., and Lin, S. (2012). Identification of vascular and hematopoietic genes downstream of etsrp by deep sequencing in zebrafish. *PLoS One* 7:e31658. doi: 10.1371/journal.pone.0031658
- Gonzalez, M., Falk, M. J., Gai, X., Postrel, R., Schüle, R., and Zuchner, S. (2015). Innovative genomic collaboration using the GENESIS (GEM.app) platform. *Hum. Mutat.* 36, 950–956. doi: 10.1002/humu.22836
- Good, S., Yegorov, S., Martijn, J., Franck, J., and Bogerd, J. (2012). New insights into ligand-receptor pairing and coevolution of relaxin family peptides and their receptors in teleosts. *Int. J. Evol. Biol.* 2012:310278. doi: 10.1155/2012/310278
- Goruppi, S., Patten, R. D., Force, T., and Kyriakis, J. M. (2007). Helix-loop-helix protein p8, a transcriptional regulator required for cardiomyocyte hypertrophy and cardiac fibroblast matrix metalloproteinase induction. *Mol. Cell. Biol.* 27, 993–1006. doi: 10.1128/mcb.00996-06
- Goulding, M. (2009). Circuits controlling vertebrate locomotion: moving in a new direction. *Nat. Rev. Neurosci.* 10, 507–518. doi: 10.1038/nrn2608
- Groth, C., Nornes, S., McCarty, R., Tammé, R., and Lardelli, M. (2002). Identification of a second presenilin gene in zebrafish with similarity to the human Alzheimer's disease gene presenilin2. *Dev. Genes Evol.* 212, 486–490. doi: 10.1007/s00427-002-0269-5
- Gurney, J. G., McPheeters, M. L., and Davis, M. M. (2006). Parental report of health conditions and health care use among children with and without autism: national survey of children's health. *Arch. Pediatr. Adolesc. Med.* 160, 825–830. doi: 10.1001/archpedi.160.8.825
- Haesemeyer, M., and Schier, A. F. (2015). The study of psychiatric disease genes and drugs in zebrafish. *Curr. Opin. Neurobiol.* 30, 122–130. doi: 10.1016/j.conb.2014.12.002
- Hampson, D. R., and Blatt, G. J. (2015). Autism spectrum disorders and neuropathology of the cerebellum. *Front. Neurosci.* 9:420. doi: 10.3389/fnins.2015.00420
- Hashimoto, M., and Hibi, M. (2012). Development and evolution of cerebellar neural circuits. *Dev. Growth Differ.* 54, 373–389. doi: 10.1111/j.1440-169x.2012.01348.x
- Haug, M. F., Gesemann, M., Mueller, T., and Neuhauss, S. C. (2013). Phylogeny and expression divergence of metabotropic glutamate receptor genes in the brain of zebrafish (*Danio rerio*). *J. Comp. Neurol.* 521, 1533–1560. doi: 10.1002/cne.23240
- Herget, U., Wolf, A., Wullmann, M. F., and Ryu, S. (2014). Molecular neuroanatomy and chemoarchitecture of the neurosecretory preoptic-hypothalamic area in zebrafish larvae. *J. Comp. Neurol.* 522, 1542–1564. doi: 10.1002/cne.23480
- Higashijima, S., Masino, M. A., Mandel, G., and Fetcho, J. R. (2004). Engrailed-1 expression marks a primitive class of inhibitory spinal interneuron. *J. Neurosci.* 24, 5827–5839. doi: 10.1523/JNEUROSCI.5342-03.2004
- Hinitz, Y., Pan, L., Walker, C., Dowd, J., Moens, C. B., and Hughes, S. M. (2012). Zebrafish *Mef2ca* and *Mef2cb* are essential for both first and second heart field cardiomyocyte differentiation. *Dev. Biol.* 369, 199–210. doi: 10.1016/j.ydbio.2012.06.019
- Hoffman, E. J., Turner, K. J., Fernandez, J. M., Cifuentes, D., Ghosh, M., Ijaz, S., et al. (2016). Estrogens suppress a behavioral phenotype in zebrafish mutants of the autism risk gene, *CNTNAP2*. *Neuron* 89, 725–733. doi: 10.1016/j.neuron.2015.12.039
- Hoshijima, K., Juryneć, M. J., and Grunwald, D. J. (2016). Precise editing of the zebrafish genome made simple and efficient. *Dev. Cell* 36, 654–667. doi: 10.1016/j.devcel.2016.02.015
- Housley, M. P., Reischauer, S., Dieu, M., Raes, M., Stainier, D. Y., and Vanhollenbeke, B. (2014). Translational profiling through biotinylation of tagged ribosomes in zebrafish. *Development* 141, 3988–3993. doi: 10.1242/dev.111849
- Howe, K., Clark, M. D., Torroja, C. F., Torrance, J., Berthelot, C., Muffato, M., et al. (2013). The zebrafish reference genome sequence and its relationship to the human genome. *Nature* 496, 498–503. doi: 10.1038/nature12111
- Hsiao, E. Y. (2014). Gastrointestinal issues in autism spectrum disorder. *Harv. Rev. Psychiatry* 22, 104–111. doi: 10.1097/HRP.0000000000000029
- Hsieh, J. Y., Ulrich, B., Issa, F. A., Wan, J., and Papazian, D. M. (2014). Rapid development of Purkinje cell excitability, functional cerebellar circuit and afferent sensory input to cerebellum in zebrafish. *Front. Neural Circuits* 8:147. doi: 10.3389/fncir.2014.00147
- Hutson, L. D., and Chien, C. B. (2002). Wiring the zebrafish: axon guidance and synaptogenesis. *Curr. Opin. Neurobiol.* 12, 87–92. doi: 10.1016/s0959-4388(02)00294-5
- Imai, H., Oomiya, Y., Kikkawa, S., Shoji, W., Hibi, M., Terashima, T., et al. (2012). Dynamic changes in the gene expression of zebrafish Reelin receptors during embryogenesis and hatching period. *Dev. Growth Differ.* 54, 253–263. doi: 10.1111/j.1440-169x.2012.01327.x
- Imamura, S., and Kishi, S. (2005). Molecular cloning and functional characterization of zebrafish ATM. *Int. J. Biochem. Cell Biol.* 37, 1105–1116. doi: 10.1016/j.biocel.2004.10.015
- Issa, F. A., Mock, A. F., Sagasti, A., and Papazian, D. M. (2012). Spinocerebellar ataxia type 13 mutation that is associated with disease onset in infancy disrupts axonal pathfinding during neuronal development. *Dis. Model. Mech.* 5, 921–929. doi: 10.1242/dmm.010157
- Jao, L. E., Wente, S. R., and Chen, W. (2013). Efficient multiplex biallelic zebrafish genome editing using a CRISPR nuclease system. *Proc. Natl. Acad. Sci. U S A* 110, 13904–13909. doi: 10.1073/pnas.1308335110
- Jinnah, H. A., Jones, M. D., Wojcik, B. E., Rothstein, J. D., Hess, E. J., Friedmann, T., et al. (1999). Influence of age and strain on striatal dopamine loss in a genetic mouse model of Lesch-Nyhan disease. *J. Neurochem.* 72, 225–229. doi: 10.1046/j.1471-4159.1999.0720225.x
- Johnston, L., Ball, R. E., Acuff, S., Gaudet, J., Sornborger, A., and Lauderdale, J. D. (2013). Electrophysiological recording in the brain of intact adult zebrafish. *J. Vis. Exp.* 81:e51065. doi: 10.3791/51065
- Jones, L. J., McCutcheon, J. E., Young, A. M., and Norton, W. H. (2015). Neurochemical measurements in the zebrafish brain. *Front. Behav. Neurosci.* 9:246. doi: 10.3389/fnbeh.2015.00246
- Katsuyama, Y., Oomiya, Y., Dekimoto, H., Motooka, E., Takano, A., Kikkawa, S., et al. (2007). Expression of zebrafish ROR alpha gene in cerebellar-like structures. *Dev. Dyn.* 236, 2694–2701. doi: 10.1002/dvdy.21275
- Kaufman, L., Ayub, M., and Vincent, J. B. (2010). The genetic basis of non-syndromic intellectual disability: a review. *J. Neurodev. Disord.* 2, 182–209. doi: 10.1007/s11689-010-9055-2
- Kaufman, C. K., Mosimann, C., Fan, Z. P., Yang, S., Thomas, A. J., Ablain, J., et al. (2016). A zebrafish melanoma model reveals emergence of neural crest identity during melanoma initiation. *Science* 351:aad2197. doi: 10.1126/science.aad2197
- Kim, D. U., Hayles, J., Kim, D., Wood, V., Park, H. O., Won, M., et al. (2010). Analysis of a genome-wide set of gene deletions in the fission yeast *Schizosaccharomyces pombe*. *Nat. Biotechnol.* 28, 617–623. doi: 10.1038/nbt.1628
- Kimmel, C. B., Ballard, W. W., Kimmel, S. R., Ullmann, B., and Schilling, T. F. (1995). Stages of embryonic development of the zebrafish. *Dev. Dyn.* 203, 253–310. doi: 10.1002/aja.1002030302
- Kimura, Y., Satou, C., Fujioka, S., Shoji, W., Umeda, K., Ishizuka, T., et al. (2013). Hindbrain V2a neurons in the excitation of spinal locomotor circuits during zebrafish swimming. *Curr. Biol.* 23, 843–849. doi: 10.1016/j.cub.2013.03.066
- King, I. F., Yandava, C. N., Mabb, A. M., Hsiao, J. S., Huang, H. S., Pearson, B. L., et al. (2013). Topoisomerases facilitate transcription of long genes linked to autism. *Nature* 501, 58–62. doi: 10.1038/nature12504
- Kinkhabwala, A., Riley, M., Koyama, M., Monen, J., Satou, C., Kimura, Y., et al. (2011). A structural and functional ground plan for neurons in the hindbrain of zebrafish. *Proc. Natl. Acad. Sci. U S A* 108, 1164–1169. doi: 10.1073/pnas.1012185108
- Kinsella, R. J., Kähäri, A., Haider, S., Zamora, J., Proctor, G., Spudich, G., et al. (2011). Ensembl BioMart: a hub for data retrieval across taxonomic space. *Database (Oxford)* 2011:bar030. doi: 10.1093/database/bar030

- Knuesel, I., Elliott, A., Chen, H. J., Mansuy, I. M., and Kennedy, M. B. (2005). A role for synGAP in regulating neuronal apoptosis. *Eur. J. Neurosci.* 21, 611–621. doi: 10.1111/j.1460-9568.2005.03908.x
- Kok, F. O., Shin, M., Ni, C. W., Gupta, A., Grosse, A. S., van Impel, A., et al. (2015). Reverse genetic screening reveals poor correlation between morpholino-induced and mutant phenotypes in zebrafish. *Dev. Cell* 32, 97–108. doi: 10.1016/j.devcel.2014.11.018
- Koyama, M., Kinkhabwala, A., Satou, C., Higashijima, S., and Fetcho, J. (2011). Mapping a sensory-motor network onto a structural and functional ground plan in the hindbrain. *Proc. Natl. Acad. Sci. U S A* 108, 1170–1175. doi: 10.1073/pnas.1012189108
- Kozol, R. A., Cukier, H. N., Zou, B., Mayo, V., De Rubeis, S., Cai, G., et al. (2015). Two knockdown models of the autism genes SYNGAP1 and SHANK3 in zebrafish produce similar behavioral phenotypes associated with embryonic disruptions of brain morphogenesis. *Hum. Mol. Genet.* 24, 4006–4023. doi: 10.1093/hmg/ddv138
- Krumm, N., O’Roak, B. J., Shendure, J., and Eichler, E. E. (2014). A de novo convergence of autism genetics and molecular neuroscience. *Trends Neurosci.* 37, 95–105. doi: 10.1016/j.tins.2013.11.005
- Kudoh, T., Tsang, M., Hukriede, N. A., Chen, X., Dedekian, M., Clarke, C. J., et al. (2001). A gene expression screen in zebrafish embryogenesis. *Genome Res.* 11, 1979–1987. doi: 10.1101/gr.209601
- Kuehn, M. R., Bradley, A., Robertson, E. J., and Evans, M. J. (1987). A potential animal model for Lesch-Nyhan syndrome through introduction of HPRT mutations into mice. *Nature* 326, 295–298. doi: 10.1038/326295a0
- Lagman, D., Callado-Pérez, A., Franzén, I. E., Larhammar, D., and Abalo, X. M. (2015). Transducin duplicates in the zebrafish retina and pineal complex: differential specialisation after the teleost tetraploidisation. *PLoS One* 10:e0121330. doi: 10.1371/journal.pone.0121330
- Lee, F. H., Fadel, M. P., Preston-Maher, K., Cordes, S. P., Clapcote, S. J., Price, D. J., et al. (2011). Discl point mutations in mice affect development of the cerebral cortex. *J. Neurosci.* 31, 3197–3206. doi: 10.1523/JNEUROSCI.4219-10.2011
- Levy, Y. (2011). Developmental delay revisited. *Dev. Disabil. Res. Rev.* 17, 180–184. doi: 10.1002/ddrr.1112
- Li, J., Zhang, B. B., Ren, Y. G., Gu, S. Y., Xiang, Y. H., and Du, J. L. (2015). Intron targeting-mediated and endogenous gene integrity-maintaining knockin in zebrafish using the CRISPR/Cas9 system. *Cell Res.* 25, 634–637. doi: 10.1038/cr.2015.43
- Liu, Q., Duff, R. J., Liu, B., Wilson, A. L., Babb-Clendenon, S. G., Francl, J., et al. (2006). Expression of cadherin10, a type II classic cadherin gene, in the nervous system of the embryonic zebrafish. *Gene Expr. Patterns* 6, 703–710. doi: 10.1016/j.modgep.2005.12.009
- Liu, K. S., and Fetcho, J. R. (1999). Laser ablations reveal functional relationships of segmental hindbrain neurons in zebrafish. *Neuron* 23, 325–335. doi: 10.1016/s0896-6273(00)80783-7
- Lumsden, A., and Krumlauf, R. (1996). Patterning the vertebrate neuraxis. *Science* 274, 1109–1115. doi: 10.1126/science.274.5290.1109
- Manoli, M., and Driever, W. (2014). nkx2.1 and nkx2.4 genes function partially redundant during development of the zebrafish hypothalamus, preoptic region and pallidum. *Front. Neuroanat.* 8:145. doi: 10.3389/fnana.2014.00145
- Mapp, O. M., Walsh, G. S., Moens, C. B., Tada, M., and Prince, V. E. (2011). Zebrafish Prickle1b mediates facial branchiomotor neuron migration via a farnesylation-dependent nuclear activity. *Development* 138, 2121–2132. doi: 10.1242/dev.060442
- Marbach, D., Lamparter, D., Quon, G., Kellis, M., Kutalik, Z., and Bergmann, S. (2016). Tissue-specific regulatory circuits reveal variable modular perturbations across complex diseases. *Nat. Methods* 13, 366–370. doi: 10.1038/nmeth.3799
- Matsui, H., Namikawa, K., Babaryka, A., and Köster, R. W. (2014). Functional regionalization of the teleost cerebellum analyzed *in vivo*. *Proc. Natl. Acad. Sci. U S A* 111, 11846–11851. doi: 10.1073/pnas.1403105111
- Maximino, C., Lima, M. G., Oliveira, K. R., Batista Ede, J., and Herculano, A. M. (2013). “Limbic associative” and “autonomic” amygdala in teleosts: a review of the evidence. *J. Chem. Neuroanat.* 48–49, 1–13. doi: 10.1016/j.jchemneu.2012.10.001
- McGown, A., McDermid, J. R., Panagiotaki, N., Tong, H., Al Mashhadi, S., Redhead, N., et al. (2013). Early interneuron dysfunction in ALS: insights from a mutant sod1 zebrafish model. *Ann. Neurol.* 73, 246–258. doi: 10.1002/ana.23780
- McLean, D. L., Fan, J., Higashijima, S., Hale, M. E., and Fetcho, J. R. (2007). A topographic map of recruitment in spinal cord. *Nature* 446, 71–75. doi: 10.1038/nature05588
- McLean, D. L., and Fetcho, J. R. (2011). Movement, technology and discovery in the zebrafish. *Curr. Opin. Neurobiol.* 21, 110–115. doi: 10.1016/j.conb.2010.09.011
- Mei, Y., Monteiro, P., Zhou, Y., Kim, J. A., Gao, X., Fu, Z., et al. (2016). Adult restoration of Shank3 expression rescues selective autistic-like phenotypes. *Nature* 530, 481–484. doi: 10.1038/nature16971
- Mendelsohn, B. A., Yin, C., Johnson, S. L., Wilm, T. P., Solnica-Krezel, L., and Gitlin, J. D. (2006). Atp7a determines a hierarchy of copper metabolism essential for notochord development. *Cell Metab.* 4, 155–162. doi: 10.1016/j.cmet.2006.05.001
- Meyer, M. P., and Smith, S. J. (2006). Evidence from *in vivo* imaging that synaptogenesis guides the growth and branching of axonal arbors by two distinct mechanisms. *J. Neurosci.* 26, 3604–3614. doi: 10.1523/JNEUROSCI.0223-06.2006
- Meyer, M. P., Trimmer, J. S., Gilthorpe, J. D., and Smith, S. J. (2005). Characterization of zebrafish PSD-95 gene family members. *J. Neurobiol.* 63, 91–105. doi: 10.1002/neu.20118
- Mi, H., Muruganujan, A., Casagrande, J. T., and Thomas, P. D. (2013). Large-scale gene function analysis with the PANTHER classification system. *Nat. Protoc.* 8, 1551–1566. doi: 10.1038/nprot.2013.092
- Miles, J. H. (2011). Autism spectrum disorders—a genetics review. *Genet. Med.* 13, 278–294. doi: 10.1097/GIM.0b013e3181ff67ba
- Monnick, M., Banks, S., Eccles, M., Dickinson, E., and Horsfield, J. (2009). Expression of cohesin and condensin genes during zebrafish development supports a non-proliferative role for cohesin. *Gene Expr. Patterns* 9, 586–594. doi: 10.1016/j.gexp.2009.08.004
- Mueller, T., and Wullmann, M. F. (2009). An evolutionary interpretation of teleostean forebrain anatomy. *Brain Behav. Evol.* 74, 30–42. doi: 10.1159/000229011
- Mueller, T. (2012). What is the thalamus in zebrafish? *Front. Neurosci.* 6:64. doi: 10.3389/fnins.2012.00064
- Myers, P. Z., Eisen, J. S., and Westerfield, M. (1986). Development and axonal outgrowth of identified motoneurons in the zebrafish. *J. Neurosci.* 6, 2278–2289.
- Nelson, S. B., and Valakh, V. (2015). Excitatory/inhibitory balance and circuit homeostasis in autism spectrum disorders. *Neuron* 87, 684–698. doi: 10.1016/j.neuron.2015.07.033
- Ng, M. C., Yang, Y. L., and Lu, K. T. (2013). Behavioral and synaptic circuit features in a zebrafish model of fragile X syndrome. *PLoS One* 8:e51456. doi: 10.1371/journal.pone.0051456
- Northcutt, R. G. (2006). Connections of the lateral and medial divisions of the goldfish telencephalic pallium. *J. Comp. Neurol.* 494, 903–943. doi: 10.1002/cne.20853
- O’Connell, L. A., and Hofmann, H. A. (2011). The vertebrate mesolimbic reward system and social behavior network: a comparative synthesis. *J. Comp. Neurol.* 519, 3599–3639. doi: 10.1002/cne.22735
- O’Donnell, K. C., Lulla, A., Stahl, M. C., Wheat, N. D., Bronstein, J. M., and Sagasti, A. (2014). Axon degeneration and PGC-1 α -mediated protection in a zebrafish model of alpha-synuclein toxicity. *Dis. Model. Mech.* 7, 571–582. doi: 10.1242/dmm.013185
- Oksenberg, N., Stevison, L., Wall, J. D., and Ahituv, N. (2013). Function and regulation of APTS2, a gene implicated in autism and human evolution. *PLoS Genet.* 9:e1003221. doi: 10.1371/journal.pgen.1003221
- O’Rawe, J. A., Wu, Y., Dorfel, M. J., Rope, A. F., Au, P. Y., Parboosingh, J. S., et al. (2015). TAF1 variants are associated with dysmorphic features, intellectual disability and neurological manifestations. *Am. J. Hum. Genet.* 97, 922–932. doi: 10.1016/j.ajhg.2015.11.005
- Panzer, J. A., Gibbs, S. M., Dosch, R., Wagner, D., Mullins, M. C., Granato, M., et al. (2005). Neuromuscular synaptogenesis in wild-type and mutant zebrafish. *Dev. Biol.* 285, 340–357. doi: 10.1016/j.ydbio.2005.06.027
- Parikshak, N. N., Luo, R., Zhang, A., Won, H., Lowe, J. K., Chandran, V., et al. (2013). Integrative functional genomic analyses implicate specific molecular pathways and circuits in autism. *Cell* 155, 1008–1021. doi: 10.1016/j.cell.2013.10.031

- Patten, S. A., and Ali, D. W. (2009). PKCgamma-induced trafficking of AMPA receptors in embryonic zebrafish depends on NSF and PICK1. *Proc. Natl. Acad. Sci. U S A* 106, 6796–6801. doi: 10.1073/pnas.0811171106
- Patten, S. A., Sihra, R. K., Dhami, K. S., Coutts, C. A., and Ali, D. W. (2007). Differential expression of PKC isoforms in developing zebrafish. *Int. J. Dev. Neurosci.* 25, 155–164. doi: 10.1016/j.ijdevneu.2007.02.003
- Pearson, H. (2002). Surviving a knockout blow. *Nature* 415, 8–9. doi: 10.1038/415008a
- Peça, J., Feliciano, C., Ting, J. T., Wang, W., Wells, M. F., Venkatraman, T. N., et al. (2011). Shank3 mutant mice display autistic-like behaviours and striatal dysfunction. *Nature* 472, 437–442. doi: 10.1038/nature09965
- Pei, W., Kratz, L. E., Bernardini, I., Sood, R., Yokogawa, T., Dorward, H., et al. (2010). A model of Costeff Syndrome reveals metabolic and protective functions of mitochondrial OPA3. *Development* 137, 2587–2596. doi: 10.1242/dev.043745
- Persico, A. M., and Napolioni, V. (2013). Autism genetics. *Behav. Brain Res.* 251, 95–112. doi: 10.1016/j.bbr.2013.06.012
- Pinto, D., Delaby, E., Merico, D., Barbosa, M., Merikangas, A., Klei, L., et al. (2014). Convergence of genes and cellular pathways dysregulated in autism spectrum disorders. *Am. J. Hum. Genet.* 94, 677–694. doi: 10.1016/j.ajhg.2014.03.018
- Piton, A., Redin, C., and Mandel, J. L. (2013). XLID-causing mutations and associated genes challenged in light of data from large-scale human exome sequencing. *Am. J. Hum. Genet.* 93, 368–383. doi: 10.1016/j.ajhg.2013.06.013
- Plucińska, G., Paquet, D., Hruscha, A., Godinho, L., Haass, C., Schmid, B., et al. (2012). *In vivo* imaging of disease-related mitochondrial dynamics in a vertebrate model system. *J. Neurosci.* 32, 16203–16212. doi: 10.1523/JNEUROSCI.1327-12.2012
- Postlethwait, J., Amores, A., Cresko, W., Singer, A., and Yan, Y. L. (2004). Subfunction partitioning, the teleost radiation and the annotation of the human genome. *Trends Genet.* 20, 481–490. doi: 10.1016/j.tig.2004.08.001
- Pujol-Martí, J., Zecca, A., Baudoin, J. P., Faucherre, A., Asakawa, K., Kawakami, K., et al. (2012). Neuronal birth order identifies a dimorphic sensorineural map. *J. Neurosci.* 32, 2976–2987. doi: 10.1523/JNEUROSCI.5157-11.2012
- Randlett, O., Wee, C. L., Naumann, E. A., Nnaemeka, O., Schoppik, D., Fitzgerald, J. E., et al. (2015). Whole-brain activity mapping onto a zebrafish brain atlas. *Nat Methods* 12, 1039–1046. doi: 10.1038/nmeth.3581
- Rasmussen, J. P., and Sagasti, A. (2016). Learning to swim, again: axon regeneration in fish. *Exp. Neurol.* doi: 10.1016/j.expneurol.2016.02.022 [Epub ahead of print].
- Rauch, G. J., Lyons, D. A., Middendorf, I., Friedlander, B., Arana, N., Reyes, T., et al. (2003). Submission and curation of gene expression data. ZFIN Direct Data Submission. Available online at: <http://zfinfo.org>
- Recher, G., Jouralet, J., Brombin, A., Heuze, A., Mugniery, E., Hermel, J. M., et al. (2013). Zebrafish midbrain slow-amplifying progenitors exhibit high levels of transcripts for nucleotide and ribosome biogenesis. *Development* 140, 4860–4869. doi: 10.1242/dev.099010
- Reid, E., Kloos, M., Ashley-Koch, A., Hughes, L., Bevan, S., Svenson, I. K., et al. (2002). A kinesin heavy chain (KIF5A) mutation in hereditary spastic paraplegia (SPG10). *Am. J. Hum. Genet.* 71, 1189–1194. doi: 10.1086/344210
- Renier, C., Faraco, J. H., Bourgin, P., Motley, T., Bonaventure, P., Rosa, F., et al. (2007). Genomic and functional conservation of sedative-hypnotic targets in the zebrafish. *Pharmacogenet. Genomics* 17, 237–253. doi: 10.1097/fpc.0b013e3280119d62
- Rihel, J., Prober, D. A., Arvanites, A., Lam, K., Zimmerman, S., Jang, S., et al. (2010). Zebrafish behavioral profiling links drugs to biological targets and rest/wake regulation. *Science* 327, 348–351. doi: 10.1126/science.1183090
- Rihel, J., and Schier, A. F. (2013). Sites of action of sleep and wake drugs: insights from model organisms. *Curr. Opin. Neurobiol.* 23, 831–840. doi: 10.1016/j.conb.2013.04.010
- Rissone, A., Sangiorgio, L., Monopoli, M., Beltrame, M., Zucchi, I., Bussolino, F., et al. (2010). Characterization of the neurexin gene family expression and evolution in zebrafish. *Dev. Dyn.* 239, 688–702. doi: 10.1002/dvdy.22196
- Ronneberger, O., Liu, K., Rath, M., Rueß, D., Mueller, T., Skibbe, H., et al. (2012). ViBE-Z: a framework for 3D virtual colocalization analysis in zebrafish larval brains. *Nat. Methods* 9, 735–742. doi: 10.1038/nmeth.2076
- Rossi, A., Kontarakis, Z., Gerri, C., Nolte, H., Hölper, S., Krüger, M., et al. (2015). Genetic compensation induced by deleterious mutations but not gene knockdowns. *Nature* 524, 230–233. doi: 10.1038/nature14580
- Rubenstein, J. L., and Merzenich, M. M. (2003). Model of autism: increased ratio of excitation/inhibition in key neural systems. *Genes Brain Behav.* 2, 255–267. doi: 10.1034/j.1601-183x.2003.00037.x
- Scharf, S. H., Jaeschke, G., Wettstein, J. G., and Lindemann, L. (2015). Metabotropic glutamate receptor 5 as drug target for Fragile X syndrome. *Curr. Opin. Pharmacol.* 20, 124–134. doi: 10.1016/j.coph.2014.11.004
- Shah, A. N., Davey, C. F., Whitebitch, A. C., Miller, A. C., and Moens, C. B. (2015). Rapid reverse genetic screening using CRISPR in zebrafish. *Nat. Methods* 12, 535–540. doi: 10.1038/nmeth.3360
- Srivastava, S., Cohen, J., Pevsner, J., Aradhya, S., McKnight, D., Butler, E., et al. (2014). A novel variant in GABRB2 associated with intellectual disability and epilepsy. *Am. J. Med. Genet. A* 164A, 2914–2921. doi: 10.1002/ajmg.a.36714
- Stainier, D. Y., Kontarakis, Z., and Rossi, A. (2015). Making sense of anti-sense data. *Dev. Cell* 32, 7–8. doi: 10.1016/j.devcel.2014.12.012
- Streisinger, G., Walker, C., Dower, N., Knauber, D., and Singer, F. (1981). Production of clones of homozygous diploid zebra fish (*Brachydanio rerio*). *Nature* 291, 293–296. doi: 10.1038/291293a0
- Strickland, A. V., Rebelo, A. P., Zhang, F., Price, J., Bolon, B., Silva, J. P., et al. (2014). Characterization of the mitofusin 2 R94W mutation in a knock-in mouse model. *J. Peripher. Nerv. Syst.* 19, 152–164. doi: 10.1111/jns.12066
- Striedter, G. F. (2005). *Principles of Brain Evolution*. Sunderland, MA: Sinauer Associates.
- Stuebe, S., Wieland, T., Kraemer, E., Stritzky, A., Schroeder, D., Seekamp, S., et al. (2008). Sphingosine-1-phosphate and endothelin-1 induce the expression of rgs16 protein in cardiac myocytes by transcriptional activation of the rgs16 gene. *Naunyn Schmiedebergs Arch. Pharmacol.* 376, 363–373. doi: 10.1007/s00210-007-0214-2
- Sugathan, A., Biagioli, M., Golzio, C., Erdin, S., Blumenthal, I., Manavalan, P., et al. (2014). CHD8 regulates neurodevelopmental pathways associated with autism spectrum disorder in neural progenitors. *Proc. Natl. Acad. Sci. U S A* 111, E4468–E4477. doi: 10.1073/pnas.1405266111
- Suls, A., Jaehn, J. A., Kecskes, A., Weber, Y., Weckhuysen, S., Craiu, D. C., et al. (2013). De novo loss-of-function mutations in CHD2 cause a fever-sensitive myoclonic epileptic encephalopathy sharing features with Dravet syndrome. *Am. J. Hum. Genet.* 93, 967–975. doi: 10.1016/j.ajhg.2013.09.017
- Sun, X. J., Xu, P. F., Zhou, T., Hu, M., Fu, C. T., Zhang, Y., et al. (2008). Genome-wide survey and developmental expression mapping of zebrafish SET domain-containing genes. *PLoS One* 3:e1499. doi: 10.1371/journal.pone.0001499
- Tabor, K. M., Bergeron, S. A., Horstick, E. J., Jordan, D. C., Aho, V., Porkka-Heiskanen, T., et al. (2014). Direct activation of the Mauthner cell by electric field pulses drives ultrarapid escape responses. *J. Neurophysiol.* 112, 834–844. doi: 10.1152/jn.00228.2014
- Takada, N., and Appel, B. (2010). Identification of genes expressed by zebrafish oligodendrocytes using a differential microarray screen. *Dev. Dyn.* 239, 2041–2047. doi: 10.1002/dvdy.22338
- Thisse, B., Pflumio, S., Furthauer, M., Loppin, B., Heyer, V., Degraeve, A., et al. (2001). Expression of the zebrafish genome during embryogenesis. ZFIN Direct Data Submission. Available online at: <http://zfinfo.org>
- Thisse, B., and Thisse, C. (2004). Fast release clones: a high throughput expression analysis. ZFIN Direct Data Submission. Available online at: <http://zfinfo.org>
- Thisse, C., and Thisse, B. (2005). High throughput expression analysis of ZF models consortium clones. ZFIN Direct Data Submission. Available online at: <http://zfinfo.org>
- Thompson, C. M., Davis, E., Carrigan, C. N., Cox, H. D., Bridges, R. J., and Gerdes, J. M. (2005). Inhibitor of the glutamate vesicular transporter (VGLUT). *Curr. Med. Chem.* 12, 2041–2056. doi: 10.2174/0929867054637635
- Timmerman, V., Clowes, V. E., and Reid, E. (2013). Overlapping molecular pathological themes link Charcot-Marie-Tooth neuropathies and hereditary spastic paraplegias. *Exp. Neurol.* 246, 14–25. doi: 10.1016/j.expneurol.2012.01.010
- Timmerman, V., Strickland, A. V., and Zuchner, S. (2014). Genetics of Charcot-Marie-Tooth (CMT) disease within the frame of the human genome project success. *Genes (Basel)* 5, 13–32. doi: 10.3390/genes5010013
- Titus, T. A., Yan, Y. L., Wilson, C., Starks, A. M., Frohnmayer, J. D., Bremiller, R. A., et al. (2009). The fanconi anemia/BRCA gene network in zebrafish: embryonic expression and comparative genomics. *Mutat. Res.* 668, 117–132. doi: 10.1016/j.mrfmmm.2008.11.017

- Tucker, B., Richards, R. I., and Lardelli, M. (2006). Contribution of mGluR and Fmr1 functional pathways to neurite morphogenesis, craniofacial development and fragile X syndrome. *Hum. Mol. Genet.* 15, 3446–3458. doi: 10.1093/hmg/ddl422
- Turner, K. J., Bracewell, T. G., and Hawkins, T. A. (2014). Anatomical dissection of zebrafish brain development. *Methods Mol. Biol.* 1082, 197–214. doi: 10.1007/978-1-62703-655-9_14
- Turner, T. N., Sharma, K., Oh, E. C., Liu, Y. P., Collins, R. L., Sosa, M. X., et al. (2015). Loss of δ -catenin function in severe autism. *Nature* 520, 51–56. doi: 10.1038/nature14186
- Turrigiano, G. (2012). Homeostatic synaptic plasticity: local and global mechanisms for stabilizing neuronal function. *Cold Spring Harb. Perspect. Biol.* 4:a005736. doi: 10.1101/cshperspect.a005736
- Uddin, M., Tammimies, K., Pellicchia, G., Alipanahi, B., Hu, P., Wang, Z., et al. (2014). Brain-expressed exons under purifying selection are enriched for de novo mutations in autism spectrum disorder. *Nat. Genet.* 46, 742–747. doi: 10.1038/ng.2980
- Vatine, G. D., Zada, D., Lerer-Goldshtein, T., Toviv, A., Malkinson, G., Yaniv, K., et al. (2013). Zebrafish as a model for monocarboxyl transporter 8-deficiency. *J. Biol. Chem.* 288, 169–180. doi: 10.1074/jbc.M112.413831
- Visser, L. E., Gilissen, C., and Veltman, J. A. (2016). Genetic studies in intellectual disability and related disorders. *Nat. Rev. Genet.* 17, 9–18. doi: 10.1038/nrg3999
- Viturreira, N., Letellier, M., and Goda, Y. (2012). Homeostatic synaptic plasticity: from single synapses to neural circuits. *Curr. Opin. Neurobiol.* 22, 516–521. doi: 10.1016/j.conb.2011.09.006
- Wakayama, Y., Fukuhara, S., Ando, K., Matsuda, M., and Mochizuki, N. (2015). Cdc42 mediates Bmp-induced sprouting angiogenesis through Fmnl3-driven assembly of endothelial filopodia in zebrafish. *Dev. Cell* 32, 109–122. doi: 10.1016/j.devcel.2014.11.024
- Waters, B. M., Chu, H. H., Didonato, R. J., Roberts, L. A., Easley, R. B., Lahner, B., et al. (2006). Mutations in Arabidopsis yellow stripe-like1 and yellow stripe-like3 reveal their roles in metal ion homeostasis and loading of metal ions in seeds. *Plant Physiol.* 141, 1446–1458. doi: 10.1104/pp.106.082586
- Wen, H., and Brehm, P. (2005). Paired motor neuron-muscle recordings in zebrafish test the receptor blockade model for shaping synaptic current. *J. Neurosci.* 25, 8104–8111. doi: 10.1523/jneurosci.2611-05.2005
- Wen, H., Linhoff, M. W., Hubbard, J. M., Nelson, N. R., Stensland, D., Dallman, J., et al. (2013). Zebrafish calls for reinterpretation for the roles of P/Q calcium channels in neuromuscular transmission. *J. Neurosci.* 33, 7384–7392. doi: 10.1523/JNEUROSCI.5839-12.2013
- Wheeler, N. A., Lister, J. A., and Fuss, B. (2015). The autotaxin-lysophosphatidic acid axis modulates histone acetylation and gene expression during oligodendrocyte differentiation. *J. Neurosci.* 35, 11399–11414. doi: 10.1523/JNEUROSCI.0345-15.2015
- Wiley, D. J., Juan, I., Le, H., Cai, X., Baumbach, L., Beattie, C., et al. (2014). Yeast augmented network analysis (YANA): a new systems approach to identify therapeutic targets for human genetic diseases. *PLoS Res* 3:121. doi: 10.12688/f1000research.4188.1
- Wondolowski, J., and Dickman, D. (2013). Emerging links between homeostatic synaptic plasticity and neurological disease. *Front. Cell. Neurosci.* 7:223. doi: 10.3389/fncel.2013.00223
- Wood, J. D., Bonath, F., Kumar, S., Ross, C. A., and Cunliffe, V. T. (2009). Disrupted-in-schizophrenia 1 and neuregulin 1 are required for the specification of oligodendrocytes and neurones in the zebrafish brain. *Hum. Mol. Genet.* 18, 391–404. doi: 10.1093/hmg/ddn361
- Wullmann, M. F. (1994). The teleostean torus longitudinalis: a short review on its structure, histochemistry, connectivity, possible function and phylogeny. *Eur. J. Morphol.* 32, 235–242.
- Wullmann, M. F., Rupp, B., and Reichert, H. (1996). *Neuroanatomy of the Zebrafish Brain: A Topological Atlas*. Basel, CHE: Birkhauser.
- Wullmann, M. F. (2014). Ancestry of basal ganglia circuits: new evidence in teleosts. *J. Comp. Neurol.* 522, 2013–2018. doi: 10.1002/cne.23525
- Wullmann, M. F., Mueller, T., Distel, M., Babaryka, A., Grothe, B., and Koster, R. W. (2011). The long adventurous journey of rhombic lip cells in jawed vertebrates: a comparative developmental analysis. *Front. Neuroanat.* 5:27. doi: 10.3389/fnana.2011.00027
- Wurst, W., and Bally-Cuif, L. (2001). Neural plate patterning: upstream and downstream of the isthmic organizer. *Nat. Rev. Neurosci.* 2, 99–108. doi: 10.1038/35053516
- Wyart, C., Del Bene, F., Warp, E., Scott, E. K., Trauner, D., Baier, H., et al. (2009). Optogenetic dissection of a behavioural module in the vertebrate spinal cord. *Nature* 461, 407–410. doi: 10.1038/nature08323
- Xing, L., Hoshijima, K., Grunwald, D. J., Fujimoto, E., Quist, T. S., Sneddon, J., et al. (2012). Zebrafish foxP2 zinc finger nuclease mutant has normal axon pathfinding. *PLoS One* 7:e43968. doi: 10.1371/journal.pone.0043968
- Xing, L., Son, J. H., Stevenson, T. J., Lillesaar, C., Bally-Cuif, L., Dahl, T., et al. (2015). A serotonin circuit acts as an environmental sensor to mediate midline axon crossing through EphrinB2. *J. Neurosci.* 35, 14794–14808. doi: 10.1523/JNEUROSCI.1295-15.2015
- Yanicostas, C., Barbieri, E., Hibi, M., Brice, A., Stevanin, G., and Soussi-Yanicostas, N. (2012). Requirement for zebrafish ataxin-7 in differentiation of photoreceptors and cerebellar neurons. *PLoS One* 7:e50705. doi: 10.1371/journal.pone.0050705
- Yeh, C. M., Liu, Y. C., Chang, C. J., Lai, S. L., Hsiao, C. D., and Lee, S. J. (2011). Ptenb mediates gastrulation cell movements via Cdc42/AKT1 in zebrafish. *PLoS One* 6:e18702. doi: 10.1371/journal.pone.0018702
- Yimlamai, D., Konnikova, L., Moss, L. G., and Jay, D. G. (2005). The zebrafish down syndrome cell adhesion molecule is involved in cell movement during embryogenesis. *Dev. Biol.* 279, 44–57. doi: 10.1016/j.ydbio.2004.12.001
- Yizhar, O., Fenno, L. E., Prigge, M., Schneider, F., Davidson, T. J., O'Shea, D. J., et al. (2011). Neocortical excitation/inhibition balance in information processing and social dysfunction. *Nature* 477, 171–178. doi: 10.1038/nature10360
- Yoshida, T., and Mishina, M. (2008). Zebrafish orthologue of mental retardation protein IL1RAPL1 regulates presynaptic differentiation. *Mol. Cell Neurosci.* 39, 218–228. doi: 10.1016/j.mcn.2008.06.013
- Yu-Wai-Man, P., Griffiths, P. G., Hudson, G., and Chinnery, P. F. (2009). Inherited mitochondrial optic neuropathies. *J. Med. Genet.* 46, 145–158. doi: 10.1136/jmg.2007.054270
- Zhou, W., Horstlick, E. J., Hirata, H., and Kuwada, J. Y. (2008). Identification and expression of voltage-gated calcium channel beta subunits in Zebrafish. *Dev. Dyn.* 237, 3842–3852. doi: 10.1002/dvdy.21776
- Zhou, Y., Kaiser, T., Monteiro, P., Zhang, X., Van der Goes, M. S., Wang, D., et al. (2016). Mice with Shank3 Mutations associated with ASD and schizophrenia display both shared and distinct defects. *Neuron* 89, 147–162. doi: 10.1016/j.neuron.2015.11.023
- Zlotogora, J. (2003). Penetrance and expressivity in the molecular age. *Genet. Med.* 5, 347–352. doi: 10.1097/01.gim.0000086478.87623.69
- Züchner, S., De Jonghe, P., Jordanova, A., Claeys, K. G., Guergueltcheva, V., Cherninkova, S., et al. (2006). Axonal neuropathy with optic atrophy is caused by mutations in mitofusin 2. *Ann. Neurol.* 59, 276–281. doi: 10.1002/ana.20797
- Züchner, S., Mersianova, I. V., Muglia, M., Bissar-Tadmouri, N., Rochelle, J., Dadali, E. L., et al. (2004). Mutations in the mitochondrial GTPase mitofusin 2 cause Charcot-Marie-Tooth neuropathy type 2A. *Nat. Genet.* 36, 449–451. doi: 10.1038/ng1341
- Züchner, S., and Vance, J. M. (2005). Emerging pathways for hereditary axonopathies. *J. Mol. Med. (Berl)* 83, 935–943. doi: 10.1007/s00109-005-0694-9

Conflict of Interest Statement: The authors declare that the research was conducted in the absence of any commercial or financial relationships that could be construed as a potential conflict of interest.

Copyright © 2016 Kozol, Abrams, James, Buglo, Yan and Dallman. This is an open-access article distributed under the terms of the Creative Commons Attribution License (CC BY). The use, distribution and reproduction in other forums is permitted, provided the original author(s) or licensor are credited and that the original publication in this journal is cited, in accordance with accepted academic practice. No use, distribution or reproduction is permitted which does not comply with these terms.



Defects of the Glycinergic Synapse in Zebrafish

Kazutoyo Ogino* and Hiromi Hirata*

Department of Chemistry and Biological Science, College of Science and Engineering, Aoyama Gakuin University, Sagami-hara, Japan

Glycine mediates fast inhibitory synaptic transmission. Physiological importance of the glycinergic synapse is well established in the brainstem and the spinal cord. In humans, the loss of glycinergic function in the spinal cord and brainstem leads to hyperekplexia, which is characterized by an excess startle reflex to sudden acoustic or tactile stimulation. In addition, glycinergic synapses in this region are also involved in the regulation of respiration and locomotion, and in the nociceptive processing. The importance of the glycinergic synapse is conserved across vertebrate species. A teleost fish, the zebrafish, offers several advantages as a vertebrate model for research of glycinergic synapse. Mutagenesis screens in zebrafish have isolated two motor defective mutants that have pathogenic mutations in glycinergic synaptic transmission: *bandoneon* (*beo*) and *shocked* (*sho*). *Beo* mutants have a loss-of-function mutation of glycine receptor (GlyR) β -subunit b, alternatively, *sho* mutant is a glycinergic transporter 1 (GlyT1) defective mutant. These mutants are useful animal models for understanding of glycinergic synaptic transmission and for identification of novel therapeutic agents for human diseases arising from defect in glycinergic transmission, such as hyperekplexia or glycine encephalopathy. Recent advances in techniques for genome editing and for imaging and manipulating of a molecule or a physiological process make zebrafish more attractive model. In this review, we describe the glycinergic defective zebrafish mutants and the technical advances in both forward and reverse genetic approaches as well as *in vivo* visualization and manipulation approaches for the study of the glycinergic synapse in zebrafish.

Keywords: startle disease, glycine, receptor, synapse, transporter, zebrafish

OPEN ACCESS

Edited by:

Robert J. Harvey,
University College London, UK

Reviewed by:

Jochen C. Meier,
Technical University Braunschweig,
Germany

Julia Dallman,
University of Miami, USA

*Correspondence:

Kazutoyo Ogino
kogino@chem.aoyama.ac.jp;
Hiromi Hirata
hihirata@chem.aoyama.ac.jp

Received: 31 March 2016

Accepted: 13 June 2016

Published: 29 June 2016

Citation:

Ogino K and Hirata H (2016) Defects of the Glycinergic Synapse in Zebrafish.
Front. Mol. Neurosci. 9:50.
doi: 10.3389/fnmol.2016.00050

OVERVIEW OF GLYCINERGIC NEUROTRANSMISSION IN THE MAMMALIAN NERVOUS SYSTEM

Glycine is a major inhibitory neurotransmitter in the brainstem and spinal cord. The glycinergic transmission plays important roles in the reflex and the control of rhythmic motor behaviors such as locomotion and breathing (Schmid et al., 1991, 1996; Gomeza et al., 2003a; Grillner, 2003; Callister and Graham, 2010), as well as nociceptive processing (Baba et al., 2001; Ahmadi et al., 2002; Harvey et al., 2004; Zeilhofer, 2005). Glycine receptors (GlyRs) are also expressed in the retina (Sassòè-Pognetto et al., 1994; Haverkamp et al., 2003, 2004; Jusuf et al., 2005; Heinze et al., 2007) and various regions of the brain, such as amygdala (McCool and Botting, 2000; McCool and Farroni, 2001), hippocampus (Malosio et al., 1991; Chattipakorn and McMahon, 2002, 2003; Brackmann et al., 2004; Danglot et al., 2004; Eichler et al., 2009; Jonsson et al., 2012;

Chen et al., 2014; Winkelmann et al., 2014; Çalişkan et al., 2016), midbrain (Malosio et al., 1991; Mangin et al., 2002; Jonsson et al., 2012), neocortex (Malosio et al., 1991; Jonsson et al., 2012; Salling and Harrison, 2014), to regulate neuronal network excitability. GlyRs are pentameric ligand-gated chloride channels taking the form of α -subunit homopentamers or $\alpha\beta$ -subunit heteropentamers. The α -subunit is ligand-binding subunit (Becker et al., 1988; Grenningloh et al., 1990a,b; Kuhse et al., 1990), whereas the β -subunit binds to synaptic gephyrin scaffold consisting of tens to hundreds gephyrin molecules, thereby the $\alpha\beta$ heteromeric GlyRs can be accumulated at postsynaptic sites (Kirsch et al., 1993; Meyer et al., 1995; Feng et al., 1998; Hanus et al., 2004; Sola et al., 2004; Grudzinska et al., 2005; Kim et al., 2006; Calamai et al., 2009; Herweg and Schwarz, 2012; Specht et al., 2013). However, the postsynaptic localization of GlyR is not permanent. GlyRs are constantly exchanged between synaptic sites and extrasynaptic plasma-membrane by means of lateral diffusion, and alterations of the diffusion properties have been considered to be mechanisms involved in the synaptic plasticity (Meier et al., 2001; Dahan et al., 2003; Ehrensperger et al., 2007; Lévi et al., 2008; Calamai et al., 2009; Specht et al., 2011). Furthermore, the postsynaptic gephyrin scaffold is involved in regulation of the properties for synaptic plasticity in both glycinergic synapses and GABAergic synapses through interactions with various proteins (Fritschy et al., 2008; Tyagarajan and Fritschy, 2014).

Two possible stoichiometric models of the heteromeric GlyR have been proposed from research using purified GlyR subunits: $3\alpha 2\beta$ and $2\alpha 3\beta$ (Langosch et al., 1988; Burzomato et al., 2003; Grudzinska et al., 2005). Durisic et al. (2012) published data supporting $3\alpha 2\beta$ stoichiometry by single-molecule stepwise photo-bleaching: whereas a homomeric channel of fluorescent protein-tagged α subunits exhibited bleaching by a five-step reduction of fluorescence, a heteromeric channel containing the fluorescent protein-tagged α -subunits exhibited bleaching by a three-step reduction (Durisic et al., 2012). However, another group proposed the likelihood of the $2\alpha 3\beta$ stoichiometry based on the observation of antibody bounded receptor consisting of FLAG-tagged α -subunit and His-tagged β -subunit using single-molecule resolution atomic force microscopy (Yang et al., 2012). The single-molecular imaging showed that the maximum binding number of antibodies to each of the tag, anti-FLAG antibodies and anti-His antibodies could bind to the receptor up to two and three, respectively. The exact stoichiometry of the $\alpha\beta$ GlyR heteromer thus remains a point of contention, and requires further investigation. Although the formation of a homomeric β GlyR has also been hypothesized, biochemical evidence has indicated that β subunits do not form pentamers (Griffon et al., 1999), and an electrophysiological analysis showed that recombinant expression of only the β subunit in HEK-293 cells does not result in glycine-gated currents (Bormann et al., 1993).

In contrast to heteromeric GlyR, homomeric GlyRs are mainly distributed in the extrasynaptic area or presynaptic terminal in the brain and spinal cord (Turecek and Trussell, 2001; Jeong et al., 2003; Ye et al., 2004; Wang et al., 2005; Deleuze et al., 2005; Eichler et al., 2008; Kubota et al., 2010; Hruskova et al., 2012; Kunz et al., 2012; Avila et al., 2013; Chen et al., 2014;

Salling and Harrison, 2014; Winkelmann et al., 2014). The extrasynaptic homomeric GlyRs are activated by ambient glycine or taurine, thereby tonic glycinergic current that contributed to regulation of neuronal excitability both in mature and immature neural tissue is evoked (Chattipakorn and McMahon, 2003; Wang et al., 2005; Eichler et al., 2008; Chen et al., 2014; Maguire et al., 2014; Salling and Harrison, 2014). In contrast to the GlyRs on mature neurons, GlyRs on immature neurons typically induce depolarizing chloride efflux in accordance with the chloride gradient that is opposite to that of mature neurons (Reichling et al., 1994; Flint et al., 1998; Ben-Ari, 2002). The inverted chloride gradient is formed and maintained by Na^+ - K^+ - 2Cl^- cotransporter (NKCC1), which import chloride ions into the cell. On immature neurons, presynaptic GlyRs facilitate neurotransmitter release through activation of voltage gated calcium channel (VGCC) (Turecek and Trussell, 2001; Jeong et al., 2003; Ye et al., 2004; Eichler et al., 2009; Kunz et al., 2012; Winkelmann et al., 2014). Similarly, tonic activation of the extrasynaptic GlyR on the developing immature neurons induced Ca^{2+} transients through VGCCs. The activation of VGCCs have been considered to promote the synaptic accumulation of GlyRs (Kirsch and Betz, 1998; Kneussel and Betz, 2000) or to regulate the development of cortical neurons by promoting migration (Avila et al., 2013, 2014). The Ca^{2+} transients may also be involved in the K^+ - Cl^- cotransporter type 2 (KCC2) expression (Brustein et al., 2013; Allain et al., 2015). It is generally accepted, the activity of NKCC1 declines with progress of development, whereas activity of KCC2, which establishes the chloride gradient of mature neurons by extrusion of chloride ions, becomes predominant (Kanaka et al., 2001; Ben-Ari, 2002; Mikawa et al., 2002; Wang et al., 2002; Delpy et al., 2008). The KCC2 activity is necessary for glycinergic synapse maturation. Knockdown of KCC2 impaired cluster formation of GlyR $\alpha 1$ subunit (adult-type subunit) and gephyrin in cultured spinal neurons, whereas $\alpha 2$ subunit (neonatal type subunit) cluster formation was not affected by the KCC2 knockdown (Schwale et al., 2016). In addition to the developmental role, the tonic depolarizing current contributes to regulate the neuronal excitability in immature hippocampus (Chattipakorn and McMahon, 2003; Eichler et al., 2008; Chen et al., 2014).

The α homomeric GlyR current can be pharmacologically distinguished from that of the $\alpha\beta$ heteromeric GlyR by picrotoxin, a GlyR inhibitor: picrotoxin has a 100-fold greater affinity for the α homomeric GlyR than the $\alpha\beta$ heteromeric GlyR, such that the α homomeric GlyR is specifically blocked by picrotoxin at low concentrations (Pribilla et al., 1992; Mangin et al., 2002). These currents can also be distinguished by electrophysiological analysis, because the conductance mediated by $\alpha 1$ or $\alpha 3$ homomeric GlyR is larger than that of $\alpha 1\beta$ or $\alpha 3\beta$ heteromeric GlyR (Takahashi et al., 1992; Bormann et al., 1993; Rajendra et al., 1995; Beato et al., 2002; Burzomato et al., 2004; Zhang et al., 2015).

In addition to the GlyR agonist, glycine acts as co-agonist of N-methyl-D-aspartate receptor (NMDAR) (Johnson and Ascher, 1987). The simultaneous binding of glutamate and the co-agonist is required to activate the NMDAR (Johnson and Ascher, 1987; Furukawa et al., 2005; Paoletti and Neyton, 2007). Although the

physiological significance of co-agonist glycine is unclear, the recent works have reported the involvement in induction of LTD (Papouin et al., 2012), morphogenesis of dopaminergic neurons (Schmitz et al., 2009, 2013).

Mammalian Glycine Receptor Subunits

There exist four GlyR α subunit genes (*GLRA1*, *GLRA2*, *GLRA3*, *GLRA4*) and one β subunit gene (*GLRB*) in humans and rodents (Grenningloh et al., 1987, 1990b; Kuhse et al., 1990, 1991; Harvey et al., 2000), although the human *GLRA4* is not expressed due to a premature stop codon in this gene, thus human *GLRA4* is pseudogene (Simon et al., 2004). Electrophysiological studies on cultured cells expressing mammalian GlyR subunits have shown that the difference in conductance and kinetics between $\alpha1\beta/\alpha3\beta$ and $\alpha2\beta$, the conductance of $\alpha2\beta$ is larger than that of the former, activation kinetics of $\alpha2$ homomeric and $\alpha2\beta$ heteromeric is slower than $\alpha1/\alpha3$ containing receptor (Takahashi et al., 1992; Bormann et al., 1993; Rajendra et al., 1995; Beato et al., 2002; Mangin et al., 2003; Burzomato et al., 2004; Zhang et al., 2015). The adult mammalian hindbrain and spinal cord predominantly expresses the $\alpha1$ (*GLRA1*) and β (*GLRB*) GlyR subunits (Malosio et al., 1991; Singer et al., 1998; Jonsson et al., 2012; Weltzien et al., 2012). Hence, it is assumed that heteromeric $\alpha1\beta$ GlyRs mediate a majority of glycinergic neurotransmission in these matured neural tissues. In this physiological context, it has been shown that glycinergic synaptic transmission is important for the generation of rhythmic motor behaviors. Functional loss of human *GLRA1* due to missense, nonsense, or frame-shift mutation leads to the development of a hyperekplexia syndrome that is characterized by various exaggerated startle responses to unexpected acoustic or tactile stimuli, as well as neonatal apnea (Harvey et al., 2008a; Davies et al., 2010; Bode and Lynch, 2014). In addition, mutations that are associated with hyperekplexia syndrome have been identified in the GlyR β subunit gene (Rees et al., 2002; Al-Owain et al., 2012; Chung et al., 2013; James et al., 2013; Mine et al., 2013; Rizk and Mahmoud, 2014), the gephyrin gene (Rees et al., 2003), and the collybistin gene (Harvey et al., 2004). Furthermore, mutation of the glycine transporter 2 (GlyT2) gene (*slc5a6*) leads to a reduction in presynaptic glycine release and also produces hyperekplexia (Harvey et al., 2008a).

Also $\alpha3$ subunits are expressed in the spinal cord as heteromeric GlyRs. The $\alpha3$ subunit distribution is restricted to the superficial layer of the adult dorsal horn of the spinal cord (Harvey et al., 2004), and the $\alpha3$ subunit is involved in nociceptive processing by modulating the excitability of projection neurons that relay nociceptive input from peripheral afferents (Harvey et al., 2004, 2009; Zeilhofer, 2005). Prostaglandin E2, an important inflammatory mediator, induces protein kinase A-dependent phosphorylation at Ser346 of the $\alpha3$ subunit to depress glycinergic synaptic transmission and facilitate inflammatory pain (Ahmadi et al., 2002; Harvey et al., 2004; Zeilhofer, 2005). Although the $\alpha3$ knockout mice exhibited neither morphological abnormality nor neuro-motor phenotype, the prostaglandin E2 induced pain sensitization was abolished in the $\alpha3$ knockout mice (Harvey et al., 2004). Hence the $\alpha3$ subunit may therefore be a promising target for the regulation of inflammatory pain. In fact, cannabinoids that potentiate $\alpha3$

subunit exhibited analgesic effect to chronic inflammatory pain without psychoactive side effect (Xiong et al., 2012). The $\alpha3$ phosphorylation induced conformational change specifically on glycine binding site of the $\alpha3$ subunit, because the serine residues is not conserved at the equivalent position of the $\alpha1$ subunit (Harvey et al., 2004; Han et al., 2013). The specific conformational change may be a help to develop other type specific drugs potentiating the phosphorylated $\alpha3$ subunit. Thus, the glycinergic synaptic transmission in spinal cord is mediated by the $\alpha1\beta$ and $\alpha3\beta$ heteromeric receptor, and synaptic transmission is an attractive for the development effective remedies. In addition to the pain regulation in spinal cord, changes in the activity of hippocampal $\alpha3$ subunit are also associated with temporal lobe epilepsy (Eichler et al., 2008; Legendre et al., 2009; Winkelmann et al., 2014).

The $\alpha2$ subunit mRNA encoded by *GLRA2* gene is predominantly expressed in the developing spinal cord, and then the $\alpha2$ subunit is largely replaced by the $\alpha1$ subunit in this regions within 2 weeks after birth in mice (Kuhse et al., 1990; Malosio et al., 1991; Watanabe and Akagi, 1995; Singer et al., 1998; Liu and Wong-Riley, 2013). Functional $\alpha2$ homomeric GlyRs also found in embryonic immature cortex neurons (Flint et al., 1998; Young-Pearse et al., 2006). Although a previous study using $\alpha2$ knockout mice showed no morphological or molecular alterations in nervous system development (Young-Pearse et al., 2006), recent analysis in newly established $\alpha2$ knockout mice indicated that the $\alpha2$ subunit contributes to several neural development process, such as tangential migration in developing cortex (Avila et al., 2013), cerebral cortical neurogenesis (Avila et al., 2014), morphogenesis and synaptogenesis of somatosensory cortical neuron (Morelli et al., 2016). The importance of $\alpha2$ subunit in development and maturation of brain was also underscored by the recent identification of a micro-deletion and two mutations in *GLRA2* gene from patients with autism spectrum disorder (Pinto et al., 2010; Pilorge et al., 2015).

After the developmental switching in the spinal cord, $\alpha2$ and $\alpha3$ subunits are still expressed as the predominant subunits in some regions of adult brain such as hippocampus and frontal cortex; in these regions the GlyRs contribute to regulation of neural excitability and synaptic plasticity (Chattipakorn and McMahon, 2002; Song et al., 2006; Zhang et al., 2006, 2008; Eichler et al., 2009; Kubota et al., 2010; Aroeira et al., 2011; Jonsson et al., 2012). GlyR β subunit mRNA was abundantly detected throughout the embryonic and adult brain, from olfactory bulb to spinal cord (Fujita et al., 1991; Malosio et al., 1991). However, a recent immunohistochemical study using a novel monoclonal antibody to the GlyR β subunit exhibited distinctive punctate staining of the β subunit at synaptic sites only in spinal cord, brainstem, midbrain, olfactory bulb, and retina of adult mice (Weltzien et al., 2012). In contrast to these regions, only weak diffuse immunostaining signals were detected in the hypothalamus, the cerebellum, the hippocampus and the neocortex of adult mice (Weltzien et al., 2012). These observations suggest that most of GlyRs in adult brain are extrasynaptic homopentamer, as presented in previous studies about hippocampal GlyR (Chattipakorn and McMahon, 2002; Zhang et al., 2008; Aroeira et al., 2011). It has been suggested

that the tonic inhibition by the neocortex GlyRs have antiepileptic effect (Chattipakorn and McMahon, 2003; Kirchner et al., 2003; Zhang et al., 2008; Shen et al., 2015). Epilepsy upregulated the expression of high-affinity GlyR through RNA editing in GlyR mRNA; this high-affinity GlyR may facilitate tonic inhibition to suppress the epileptic activity (Eichler et al., 2008).

In other region of adult brain, GlyRs are considered to participate in drug addiction. Studies using rodent models have revealed that some of the cortex GlyRs are involved in the behavioral effect of ethanol, such as a motor incoordination or a hypnosis (Quinlan et al., 2002; Ye et al., 2009; Blednov et al., 2012; McCracken et al., 2013a,b; Aguayo et al., 2014), and in the ethanol preference (Blednov et al., 2015). Ethanol increases extracellular dopamine levels in nucleus accumbens of the brain reward system through enhancement of the accumbal GlyR activity (Molander and Söderpalm, 2005; Molander et al., 2005; Maguire et al., 2014). The accumbal GlyRs are also involved in the dopamine-elevating effects of tetrahydrocannabinol and nicotine in the nucleus accumbens (Jonsson et al., 2014). Since dopamine elevation is a basis of drug addiction, the accumbal GlyR could be therapeutic targets of the addiction of ethanol or nicotine.

In addition to the expression within the brain, immunolabeling studies have demonstrated that all α subunits are also expressed in retina, especially in inner plexiform layer (IPL), with subunit-specific expression patterns (Sassoè-Pognetto et al., 1994; Haverkamp et al., 2003, 2004; Jusuf et al., 2005; Heinze et al., 2007; Weiss et al., 2008; Zhang et al., 2014), suggesting that different GlyR α subunits may be involved in different levels of visual processing (Wässle et al., 2009). Monoclonal antibody against the GlyR β subunit revealed that the β subunits were almost completely colocalized with GlyR α 1-3 subunits and gephyrin in the IPL of mouse retina, however, GlyR α 4 subunit did not show the highly colocalization with the β subunits (Weltzien et al., 2012). Thus, most of the retinal GlyR are $\alpha\beta$ heteromeric receptor. The physiological role of these glycinergic synapses have been investigated by pharmacological and genetic approaches. For example, strychnine, a specific GlyR blocker, mediated blockade of glycinergic feedback pathway that from neuron in IPL to photoreceptor cell reduced the amplitudes of light-evoked response in both ON and OFF bipolar cells, indicating that the feedback pathway regulates signal propagation in the distal retina (Jiang et al., 2014). Genetic manipulations of GlyR α subunits *in vivo* have informed the significance of GlyR α subunit expression in the retina. Inhibitory glycinergic transmission between amacrine and bipolar cells of the retina is absent in *GLRA1*-deficient mice (Ivanova et al., 2006), and the frequency of spontaneous glycinergic input to A-type ganglion cells is also significantly reduced in the *GLRA1*-deficient retina (Majumdar et al., 2007). A study of *GLRA2* knockout mice revealed that α 2-containing GlyRs are involved in glycinergic input to group II wide-field amacrine cells (Majumdar et al., 2009). In the *GLRA2*-deficient retina, glycine-evoked currents are also reduced in MA-S5 and ON-starburst amacrine cells, suggesting that the α 2 subunit is also involved in information processing by the amacrine cells. In *GLRA3* deficient mice, spontaneous glycinergic currents are absent in AII amacrine

cells (Weiss et al., 2008), additionally suggesting a role for the α 3 subunit in these cells. In addition, α 2 and α 3 subunits enhance the excitatory center response of retinal receptive fields through modulation of local receptive field interactions (Nobles et al., 2012). Since the kinetics of glycinergic transmission differ according to α subunit type, signaling via different GlyRs may facilitate the complex regulation of retinal neuronal networks in visual processing.

Mammalian Glycine Transporters

Two glycine transporters have been identified in the mammalian CNS: glycine transporter 1 (GlyT1) and 2 (GlyT2). Both of these transporters belong to the Na^+/Cl^- dependent transporter family and mediate the uptake of glycine from the extracellular space into the cytosol (Eulenburg et al., 2005; Betz et al., 2006). GlyT1 is primarily expressed in glial cells throughout the CNS (Eulenburg et al., 2005; Betz et al., 2006). Glycinergic transporter 1 regulates glycine concentrations in the synaptic cleft of glycinergic synapses and glutamatergic synapses, where glycine acts as an essential co-agonist of NMDAR (Eulenburg et al., 2005; Betz et al., 2006). GlyT1 knockout mice display respiratory insufficiency as a result of elevated synaptic glycine and over-activation of GlyRs in the respiratory pathway (Gomez et al., 2003a). Alternatively, GlyT2 is expressed in glycinergic neurons and mainly localizes to the presynaptic terminal. GlyT2 facilitates the uptake of glycine released into the presynaptic terminal in order to limit the extent of neurotransmission and allow the recycling of glycine for future synaptic transmission. Accordingly, GlyT2 knockout mice display attenuated glycinergic synaptic transmission (Gomez et al., 2003b).

GLYCINERGIC NEUROTRANSMISSION IN NON-MAMMALIAN SYSTEMS

Many investigations to reveal the physiological role of glycinergic synapse have been conducted in the mammalian model animals or human; however, non-mammalian vertebrates have been used for investigation the physiological roles of glycinergic synapse in locomotive behaviors (Drapeau et al., 2002; Grillner, 2003; Korn and Faber, 2005; Roberts et al., 2008). Most teleosts have Mauthner cells (M-cells), which are paired large neurons found in their hindbrain (Eaton et al., 1977; Zottoli, 1977). The M-cell is activated by auditory input, and the M-cell firing triggers fast escape behaviors (Kohashi and Oda, 2008; Kohashi et al., 2012). Both excitatory (e.g., glutamatergic) and inhibitory (e.g., glycinergic and GABAergic) synapses are formed on dendrites and soma of the M-cell (Korn and Faber, 2005). In goldfish, glycinergic input to M-cells was enhanced by tetanization of the auditory pathway (Korn et al., 1992) or repeated sound stimulation (Oda et al., 1998). Glycinergic synaptic transmission reduces M-cell excitability by countering concurrent excitatory synaptic input (Korn and Faber, 2005; Curtin and Preuss, 2015). Thus, the plasticity of the glycinergic synapse has been shown to regulate auditory conditioning of the escape response (Oda et al., 1998). Recently, zebrafish (*Danio rerio*) have also been used as a model for investigating the physiological roles of glycinergic

neurotransmission (Cui et al., 2005; Hirata et al., 2005; Downes and Granato, 2006; Rigo and Legendre, 2006; Mongeon et al., 2008). In this review, we will describe advances in both forward and reverse genetic approaches as well as visualization techniques that have proven helpful for the study of the glycinergic synapse in zebrafish.

Zebrafish Glycine Receptors

In total, zebrafish express five α subunits (*glra1*, *glra2*, *glra3*, *glra4a* and *glra4b*) and two β subunits (*glrba* and *glrbb*) (Hirata et al., 2010). Four GlyR α subunits ($\alpha Z1$, $\alpha Z2$, $\alpha Z3$, and $\alpha Z4$) and two β subunits ($\beta a/\beta Z$ and βb) were initially reported in zebrafish (David-Watine et al., 1999; Imboden et al., 2001a,b,c; Hirata et al., 2005). Although $\alpha Z2$ was originally thought to encode a GlyR $\alpha 2$ subunit (Imboden et al., 2001a), the gene was subsequently reclassified as a second $\alpha 4$ subunit in a more detailed phylogenetic analysis (Imboden et al., 2001b). Thus, $\alpha Z2$ was designated *glra4a*. Phylogenetic analyses have suggested that $\alpha Z1$, $\alpha Z3$, and $\alpha Z4$ subunits are orthologs of the mammalian $\alpha 1$, $\alpha 3$, and $\alpha 4$ GlyR subunits, respectively (Imboden et al., 2001b); thus, these subunits have been referred to as the zebrafish GlyR $\alpha 1$, GlyR $\alpha 3$, and GlyR $\alpha 4b$. Of note, the existence of distinct orthologs of a mammalian gene is common in the zebrafish genome due to suspected whole genome duplication during fish evolution (Amores et al., 1998). The spatial expression of GlyR genes has been examined using *in situ* hybridization (Table 1). Although the spatial expression patterns of *glra2* and *glra3* remain to be determined, quantitative PCR analysis of developing zebrafish embryos (24–72 hpf) has revealed the temporal expression patterns for these genes: *glra1*, *glra3*, and *glra4a* were observed at 24 hpf, whereas *glra2* expression was not induced until 32 hpf (Ganser et al., 2013). Moreover, the expression levels of *glra1*, *glra2*, and *glra4a* were noted to steadily increase during development, while the expression of *glra3* subsided after 48 hpf (Ganser et al., 2013). Knock down experiments using antisense morpholino

oligo (MO) have reported the specific involvement of *glra4a* in the differentiation of spinal interneurons (McDermid et al., 2006).

The Advantages of Zebrafish as a Vertebrate Model

Zebrafish offer several advantages as a model for vertebrate development. First, zebrafish quickly reach sexual maturity (within 3 months), and the adult zebrafish lay 100–200 eggs twice a week, such that fertilized eggs are readily available throughout the year with a relatively low cost, because a large number of zebrafish can be maintained in smaller space compared to model mammals. Second, zebrafish embryos are optically transparent, and their development progresses rapidly at 28.5°C (Kimmel et al., 1995). These characteristics are helpful for developmental studies *in vivo*. Indeed, *in vivo* imaging of events such as synapse formation and subcellular CaMKII translocation has been achieved through the use of green fluorescent protein tagging in zebrafish embryos (Gleason et al., 2003; Niell et al., 2004). Moreover, the transparency of early zebrafish embryos has enabled the *in vivo* study and manipulation of neural activity (Douglass et al., 2008; Arrenberg et al., 2009; Zhu et al., 2009; Schoonheim et al., 2010; Muto et al., 2011). While the transparency of the zebrafish embryo is progressively diminished by the formation of melanophores after 24 hpf, 1-phenyl 2-thiourea (PTU) is a widely used agent to prevent the pigment formation (Karlsson et al., 2001). Alternatively, because it is not feasible to grow zebrafish into adulthood in the presence of PTU, a pigment-deficient mutant known as *casper* is now available, and facilitates the *in vivo* visualization and manipulation of neural activity in adult zebrafish (White et al., 2008). Third, zebrafish are suitable for electrophysiological analyses. The activity of neurons and muscles can be recorded using standard patch-clamp and extracellular recording techniques during most stages of zebrafish development (Grunwald et al., 1988; Legendre and Korn, 1994, 1995; Ribera and Nüsslein-Volhard, 1998; Drapeau et al., 1999;

TABLE 1 | Spatial expression pattern of glycine receptor subunits

Gene	Stage	Expressing tissue	Reference
<i>glra1</i>	24 hpf	Telencephalon, posterior part of midbrain midbrain-hindbrain boundary reticular neurons of hindbrain, spinal neurons, eye primordium	Devignot et al., 2003
	48 hpf	Spinal neurons	Hirata et al., 2005
	52 hpf	Telencephalon, Diencephalon, Midbrain, Hindbrain, Spinal cord	McDermid et al., 2006
<i>glra2</i>		Remain to be determined	Devignot et al., 2003
<i>glra3</i>		Remain to be determined	
<i>glra4a</i>	24 hpf	Subset of cells in the telencephalon, rhombic lip, midbrain-hindbrain boundary region, reticular neurons of hindbrain, spinal neuron, somite	Imboden et al., 2001b
	52 hpf	Olfactory pit, midbrain, reticular neurons of hindbrain, somite	McDermid et al., 2006
<i>glra4b</i>	24 hpf	Rhombensephalic lip, midbrain hindbrain boundary region	Imboden et al., 2001b
	52 hpf	Ganglion cell layer of retina	Imboden et al., 2001b; Hensley et al., 2011
<i>glrba</i>		Remain to be determined	
<i>glrbb</i>	24 hpf	Reticular neurons of hindbrain, spinal neuron	Hirata et al., 2005

Saint-Amant and Drapeau, 2001; Sidi et al., 2003; Higashijima et al., 2004; Kimura et al., 2006; Fetcho, 2007; McLean et al., 2007; Tanimoto et al., 2009). Finally, the high-efficient mutagenesis and transgenesis are available in zebrafish, as discussed in a later section of this review.

In addition to the usefulness in developmental study, zebrafish is also valuable model for high-throughput screening of novel drugs (Peterson et al., 2000; Goldsmith, 2004; Love et al., 2004). The high-throughput screening using mutant zebrafish model of human disease have identified novel compound that potentially ameliorate the phenotype associated with the mutation (Peterson et al., 2004; Cao et al., 2009; Paik et al., 2010; Kawahara et al., 2011; Peal et al., 2011; Baraban et al., 2013).

The Development of Locomotive Behavior

Zebrafish exhibit three distinct behaviors during embryogenesis: spontaneous coiling, touch-evoked escape contractions, and swimming. Spontaneous coiling appears after 17 hpf, and consists of side-to-side alternating contractions of the axial muscles (Saint-Amant and Drapeau, 1998; Downes and Granato, 2006; Pietri et al., 2009). The frequency of spontaneous coiling reaches a peak of 0.3–1 Hz at 19 hpf and gradually declines to less than 0.1 Hz by 26 hpf. After 21 hpf, zebrafish embryos respond to tactile stimuli with escape contractions that typically consists of two-to-three rapid, alternating contractions of the axial muscles (Saint-Amant and Drapeau, 1998; Hirata et al., 2005). By 28 hpf, tactile stimuli initiate swimming (Saint-Amant and Drapeau, 1998). The frequency of swimming contractions reaches 30 Hz at 36 hpf, which is comparable to the frequency of tail contraction in adult zebrafish (Buss and Drapeau, 2001). Thus, the neural network regulating swimming is functionally matured within 1.5 days of development. Interestingly, head-removed embryos transected at somites 5–7 are capable of responding to touch with an initial tail flip, although swimming fails to follow in most cases (Downes and Granato, 2006). Indeed, detailed observations suggest that the spinal cord can initiate touch responses, while supraspinal input is necessary for swimming. The spinal cord region located between somites 5–10 somite appears to be responsible for spontaneous coiling (Pietri et al., 2009). Given this knowledge, a variety of *in vivo* and *ex vivo* manipulations are possible in zebrafish.

Mutagenesis and Transgenesis in Zebrafish

Mutagenesis for the forward genetic screening of zebrafish mutants was first established in the early 1990's (Mullins et al., 1994), and two large-scale *N*-ethyl-*N*-nitrosourea (ENU)-based mutagenesis projects were completed in Tübingen, Germany and Boston, USA by 1996. These screens identified more than 4,000 mutants, including motility defective mutants, caused by the dysfunction of glycinergic neurotransmission.

Additionally, more comprehensive ENU-based mutagenesis project named “Zebrafish Mutation Project (ZMP)” was launched in 2011. ZMP identified potentially disruptive mutations in

more than 38% of all known zebrafish protein-coding genes (Kettleborough et al., 2013). The forward genetic approach provides an opportunity to identify novel genes participating in the investigating subject. The growing list of disruptive mutated alleles will be a valuable resource both for fundamental and clinical research to reveal the interested gene function.

On the other hand, reverse genetic approaches has also been applied to zebrafish biology. Targeting-induced local lesions in genomes (TILLING) has been introduced to zebrafish as the first available reverse genetics method (Wienholds et al., 2002). TILLING is a combinational method of chemical-induced mutagenesis and high-throughput screening; accordingly, TILLING can generate not only loss of function mutations, but also unexpected mutations due to non-directional missense mutagenesis (Wienholds et al., 2002, 2003; Moens et al., 2008). However, TILLING is time-consuming and less effective for intron-rich genes due to a decreased chance of obtaining null or hypomorphic alleles (Stemple, 2004). Subsequently, Zinc finger nucleases (ZFNs) (Doyon et al., 2008; Meng et al., 2008; Foley et al., 2009; Sander et al., 2011a) and transcription activator-like effector nucleases (TALEN) (Sander et al., 2011b; Bedell et al., 2012; Cade et al., 2012; Dahlem et al., 2012) were introduced to zebrafish genetics as targeted mutagenesis methods. ZFNs utilize an array of zinc finger DNA-binding motifs that bind to specific DNA triplet sequences (Urnov et al., 2005; Carroll, 2011). However, the exact DNA binding specificity of ZFNs has not been completely resolved (Carroll, 2011) and thus each ZFN construct requires careful design and screening of its target DNA-binding zinc finger motifs. Alternatively, TALEN DNA binding specificity is more predictable (Miller et al., 2011). The DNA-binding motif of TALEN is composed of repeated modules, where each module independently binds to a specific single nucleotide through repeat variable di-residues in a 1:1 manner. Thus, each module is a functional unit for the recognition of DNA sequences (Boch et al., 2009; Moscou and Bogdanove, 2009). This simple rule of nucleotide recognition has made TALEN more popular than ZFN for zebrafish genetics.

More recently, the clustered regularly interspaced palindromic repeats/CRISPR-associated 9 (CRISPER/Cas9) method was applied to zebrafish as a surprisingly simple and effective method. CRISPR and Cas are involved in bacterial adaptive immunity against the invasion of foreign nucleic acids derived from exogenous plasmids or bacteriophages (Barrangou et al., 2007; Garneau et al., 2010; Horvath and Barrangou, 2010). In type II CRISPR/Cas systems, Cas9 nuclease is guided to the target site by two RNA molecules, tracrRNA and crRNA. Alternatively, the use of a single chimeric guide RNA, generated by fusing the 3' end of a crRNA to the 5' end of a tracrRNA, has been used to guide Cas9 to its target site (Jinek et al., 2012). Thus, instead of the need to design a DNA binding domain consisting of several 10–100s amino acids as in the case of ZFN and TALEN, a single small guide RNA can be used in CRISPR/Cas9. Codon-optimized Cas9 with guide RNA efficiently induces target sequence-specific genome modification in humans and mammals (Cong et al., 2013; Li D. et al., 2013; Li W. et al., 2013; Mali et al., 2013). In zebrafish, CRISPR/Cas9 produces targeted gene

lesion with a similar efficiency to that of TALENs (Chang et al., 2013; Hwang et al., 2013). Furthermore, the mutagenesis efficiency was improved with zebrafish codon optimized Cas9 (Jao et al., 2013; Liu et al., 2014). The off-target effects of the CRISPR/Cas9 method are reported to be quite limited (Chang et al., 2013; Hruscha et al., 2013; Hwang et al., 2013; Jao et al., 2013), although some studies in cultured cells have reported high off-target mutagenesis (Fu et al., 2013; Hsu et al., 2013). This complication can be resolved through back-crossing with wild-type zebrafish. CRISPR/Cas9 system is able to introduce not only an in-del mutation leading to gene knockout, but also exogenous coding DNA in site specific manner (Auer et al., 2014; Kimura et al., 2014; Hisano et al., 2015). The site specific insertion allows researchers to substitute any nucleotides or amino acids, or to tagging any protein with fluorescent protein or epitope tag.

Other than the knockout technologies, MO injection into fertilized eggs has been widely used as gene knockdown method (Nasevicius and Ekker, 2000). However, in some cases MO-induced phenotypes (morphant) were not observed to correspond with equivalent mutants generated by ZFN and TALEN (Kok et al., 2015). Phenotypic discrepancies between morphants and mutants may be due to the off-target effects of MO (Kok et al., 2015). Alternatively, genetic compensation induced by deleterious mutation has also been reported as a cause of phenotype variation between morphants and mutants, as compensatory gene upregulation is not typically observed in MO-injected embryos (Rossi et al., 2015). Regardless of the cause of phenotypic discrepancy, antisense MOs should be used with meticulous care, and consider dose dependency as well as the implementation of proper positive and negative controls.

Transposon or retroviral methods have also been used to generate transgenic zebrafish (Davidson et al., 2003; Kawakami et al., 2004; Ellingsen et al., 2005; Villefranc et al., 2007; Asakawa et al., 2008) with improved efficiency (Davidson et al., 2003; Kawakami et al., 2004; Ellingsen et al., 2005; Sivasubbu et al., 2006; Villefranc et al., 2007). This increased efficiency has facilitated the use of the yeast GAL4/UAS system (Scheer and Campos-Ortega, 1999; Inbal et al., 2006; Scott et al., 2007; Asakawa et al., 2008; Halpern et al., 2008). GAL4, a yeast transcriptional activator, is capable of binding UAS sequences and driving the expression of downstream genes (Brand and Perrimon, 1993; Asakawa and Kawakami, 2008). Thus, a gene of interest can be expressed in any tissue by crossing UAS transgenic zebrafish with tissue-specific GAL4 driver transgenic zebrafish. Recently, various GAL4 driver transgenic zebrafish have been established using the Tol2 transposon-mediated enhancer trap method (Asakawa and Kawakami, 2008; Kawakami et al., 2010). In fact, the GAL4/UAS system has proven to have great utility for *in vivo* imaging and the manipulation of neural activity in zebrafish (Douglass et al., 2008; Arrenberg et al., 2009; Zhu et al., 2009; Schoonheim et al., 2010; Muto et al., 2011, 2013). However, GAL4/UAS systems also have a disadvantage. It has been reported that the methylation at CpG nucleotides in the UAS sequences could silence the transgene expression in zebrafish that is offspring of the

founder (Goll et al., 2009; Akitake et al., 2011; Pang et al., 2015). Although tryptophan repressor (TrpR) and its upstream activation sequence (tUAS) was proposed as an alternative gene expression system to overcome the silencing effect of Gal4/UAS, TrpR/tUAS system gave toxic effect to developing zebrafish may be due to strong transcriptional activity or toxic effect of TrpR protein (Suli et al., 2014). Four distinct Gal4 binding sites that placed in tandem (4x nr UAS) drove high levels of reporter expression with significantly less susceptible to the methylation compare to fourteen tandem copies of UAS (Akitake et al., 2011). Therefore, the fewer non-repetitive UAS sequence could be useful to circumvent the silencing by the methylation.

The Non-invasive Imaging of Neuronal Excitability

Inhibitory glycinergic and GABAergic synaptic inputs critically regulate neuronal excitability. Electrophysiological techniques are available for the monitoring of single neuron excitability through membrane potential and synaptic current recordings; however, it is difficult to investigate network excitability using this approach. An alternative approach is the monitoring of Ca^{2+} transients as a surrogate of excitability. To this end, genetically encoded calcium indicators have been used for Ca^{2+} imaging in zebrafish (Muto et al., 2011). GCaMP, the most widely used genetically encoded calcium indicator, is a fusion protein of circularly permuted EGFP, calmodulin, and calmodulin-interacting M13 peptide (Baird et al., 1999; Nakai et al., 2001). Although the fluorescence intensity of circularly permuted EGFP is very low, conformational changes induced by Ca^{2+} binding to calmodulin lead to the enhancement of fluorescence intensity and improved detection. The sensitivity of this method has been improved by the generation of GCaMP variants, which are now available for research use (Ohkura et al., 2005; Tallini et al., 2006; Tian et al., 2009; Akerboom et al., 2012; Chen et al., 2013; Muto et al., 2013). Muto et al. (2011) have successfully used this technique to visualize the alternating activation of spinal motor neurons during spontaneous coiling, and neural activity in the optic tectum during prey capture behavior (Muto et al., 2013).

ZEBRAFISH MOTILITY DEFECT MUTANTS

In the Tübingen screen, 166 mutants showing motility defects between 48 and 60 hpf were identified (Granato et al., 1996). Among them, 63 mutants were assumed to be muscle-defective based on the simple observation of actin-myosin organization (birefringence intensity) under polarized light (Felsenfeld et al., 1990). Mutations in dystrophin, laminin, titin, Hsp90 and the cognate co-chaperone Unc45b were identified in this manner (Bassett et al., 2003; Etard et al., 2007; Hall et al., 2007; Steffen et al., 2007; Hawkins et al., 2008; Guyon et al., 2009). The other 103 mutants with normal muscle structure were divided into two groups: locomotion abnormal and reduced motility (Granato et al., 1996), and assumed to have impairments

in the nervous system, neuromuscular junction (NMJ), or muscular functional components. Electrophysiological analyses have been useful in delineating the exact cause of each abnormality. For example, electrophysiological recordings from the *accordion* (*acc*) mutant, a locomotion abnormal mutant, revealed normal neuronal outputs and thus implicated deficits in the functional components of the muscle (Hirata et al., 2004). In the *atp2a1* mutant, it was determined that the simultaneous contraction of the bilateral trunk muscles results from the impaired clearance of cytosolic Ca^{2+} by the sarcoplasmic reticulum Ca^{2+} -ATPase SERCA1 (Gleason et al., 2004; Hirata et al., 2004). Several other muscle mutants (*relaxed*, *relatively relaxed*) have exhibited defects in excitation-contraction coupling (Schredelseker et al., 2005, 2009; Zhou et al., 2006; Hirata et al., 2007).

Six abnormal locomotive mutants (*bandoneon*, *ziehharmonika*, *bajan*, *diwanka*, *quetschkommode*, and *expander*) were previously compared with the *acc* mutant (Granato et al., 1996). In contrast to *acc*, electrophysiological recordings from

the *bandoneon* (*beo*) mutant showed aberrant, arrhythmic fluctuations in response to tactile stimulation, indicating a defect in CNS output (Hirata et al., 2005). As will be described in detail, a molecular genetic study revealed that alteration of the *glrb* gene is responsible for the *beo* mutant, and thus *beo* exhibits defects in glycinergic synaptic transmission (Hirata et al., 2005). Of note, *beo* is the only known *acc* subgroup mutant with dysfunctional glycinergic transmission (Table 2).

In addition to *beo*, the *shocked* (*sho*) mutant also shows reduced mobility due to a defect in glycinergic synaptic transmission. The *sho* gene encodes the glycine transporter GlyT1 (Cui et al., 2005; Mongeon et al., 2008). Based on its function, the loss-of-function mutation of GlyT1 should increase the availability of extracellular glycine in the CNS. Over-activation of the glycinergic synapse by elevated extracellular glycine can suppress the neural network responsible for motility, and therefore result in a phenotype of reduced mobility. Of note, strychnine, a specific inhibitor of GlyR, partially restores normal neuronal activity in *sho* mutants (Cui et al., 2005). Other

TABLE 2 | Accordion mutants.

Mutant	Responsible gene	Alleles	Substitutions	Cause of defective behavior	References
<i>accordion</i> <i>acc</i>	Sarcoplasmic reticulum Ca^{2+} -ATPase SERCA1 gene (<i>atp2a1</i>) on chromosome 3	dta5 mi25i mi289a tc249a ti284a tm286 tn218b tp72x tq206 ty20	G598V I97N T848I Unknown Unknown Unknown Unknown Unknown S766F Unknown	Impaired clearance of cytosolic Ca^{2+} in muscle cells.	Granato et al., 1996; Gleason et al., 2004; Hirata et al., 2004; Masino and Fetcho, 2005; Olson et al., 2010
<i>bajan</i> <i>baj</i>	Choline acetyltransferase gene (<i>chat</i>) on chromosome 13	tf247	IVS2-2A > C	Attenuated transmission at neuromuscular junction	Granato et al., 1996; Wang et al., 2008
<i>bandoneon</i> <i>beo</i>	GlyR β subunit gene (<i>glrb</i>) on chromosome 14	tp221 tw38f ta86d ta92 tm115 tf242 tu230 mi106a	Y79X L255R Y79X K343X Q87X Y79D Allele lost R275H	Dysfunction of glycinergic synaptic transmission on spinal motor neurons due to defect in clustering formation of glycine receptor at synapses	Granato et al., 1996; Hirata et al., 2005; Ganser et al., 2013
<i>diwanka</i> <i>diw</i>	Procollagen lysin 2-oxoglutarate 5-dioxygenase 3 gene (<i>plod3</i>) on chromosome 23	ts286 tv205a tz290	Q608X IVS4-2A > G W447X	Defect in primary motoneuron projection. All primary motor axons fail to exit the spinal cord	Granato et al., 1996; Zeller and Granato, 1999; Zeller et al., 2002; Schneider and Granato, 2006
<i>expander</i> <i>exp</i>	Unknown	tu12	Unknown	Unknown	Granato et al., 1996
<i>quetschkommode</i> <i>que</i>	Dihydrolipoamide branched chain transacylase E2 (<i>dbt</i>) gene on chromosome 22	ti274	IVS6 + 1G > A	Abnormal output from CNS. The abnormality may be result of decrease in neurotransmitter glutamate level within CNS due to dysfunction of amino acid metabolism	Granato et al., 1996; Friedrich et al., 2012
<i>ziehharmonika</i> <i>zim</i>	Acetylcholine-esterase gene (<i>ache</i>) on chromosome 7	sb55 tf222a tm205 tm206	S226N G198R Y139X Allele lost	Reduction of acetylcholine receptor clustering at neuromuscular junction	Granato et al., 1996; Behra et al., 2002; Downes and Granato, 2004

mutants with reduced mobility have gene mutations unrelated to glycinergic transmission (Table 3).

Defective GlyR Clustering in the *bandoneon* Mutant

The tubingen mutant screen identified seven mutant alleles (tp221 = Y79X, tw38f = L255R, ta86d = Y79X, ta92 = K343X, tm115 = Q87X, tf242 = Y79D, and tu230 = lost) of *glrbb* (Granato et al., 1996; Ganser et al., 2013). In addition, we have isolated an eighth allele (mi106a = R275H) in a previous mutagenesis screen (Hirata et al., 2005). These

zebrafish *glrbb* mutants were named *bandoneon* after the South American accordion-like instrument. Phenotypically, the *bandoneon* mutations show simultaneous contraction of both axial muscles instead of alternating in response to touch stimuli; therefore, the mutant body length is shortened by tactile stimuli, similar to the movement of an accordion (Hirata et al., 2005). Since axial muscle contractions are controlled by the reciprocal inhibition of the left and right sides of the spinal cord, inhibitory synaptic transmission is required to produce alternating contractions for swimming (Grillner, 2003; Roberts et al., 2008). As abovementioned, GlyR clustering at synaptic

TABLE 3 | Mutants with reduced locomotion.

Mutant	Responsible gene	Alleles	Substitutions	Cause of defective behavior	References
<i>sofa potato sop</i>	Acetylcholine receptor δ subunit gene on chromosome 24	tj19d ts29 tf207c	L28P Unknown Unknown	Loss of neuromuscular transmission due to defect in acetylcholine receptor clustering	Granato et al., 1996; Ono et al., 2001, 2004
<i>relaxed red</i>	Dihydropyridine receptor β_{1a} subunit gene (<i>CACNB1</i>) on chromosome 3	ts25 mi90	W451X Y283X	Defect in excitation-contraction coupling	Granato et al., 1996; Zhou et al., 2006; Schredelseker et al., 2009
<i>nicotinic receptor nic</i>	Acetylcholine receptor α subunit gene on chromosome 6	tk48d	Unknown	Loss of neuromuscular transmission due to defect in acetylcholine receptor clustering	Granato et al., 1996
<i>heart attack hat</i>	Unknown	te313	Unknown	Unknown	Granato et al., 1996
<i>herzschlag hel</i>	Titin gene (<i>ttna</i>) on chromosome 9	tg287	Unknown	Unknown	Granato et al., 1996; Myhre et al., 2014
<i>unplugged unp</i>	Muscle specific receptor tyrosine kinase gene on chromosome 10	te314b	Unknown	Defect in initial outgrowth of motor axons	Granato et al., 1996; Lefebvre et al., 2007; Jing et al., 2009
<i>shocked sho</i>	Glycine transporter 1 gene (<i>slc6a9</i>) on chromosome 2	ta51e te301 ta229g	Unknown C893Y G81D	Over-activation of glycinergic synapse by elevated extracellular glycine level	Granato et al., 1996; Luna et al., 2004; Cui et al., 2005; Mongeon et al., 2008
<i>twitch once two</i>	Acetylcholine receptor clustering factor rapsyn gene (<i>rapsn</i>) on chromosome 18	th26e tm335 tq265b	G130E Unknown Unknown	Loss of neuromuscular transmission due to defect in acetylcholine receptor clustering	Granato et al., 1996; Ono et al., 2002, 2004
<i>alligator ali</i>	RING finger protein 121 gene (<i>mf121</i>) on chromosome 21	tm342 mi500	L39X V232A	Defect in the excitability of sensory Rohon-Beard neurons	Granato et al., 1996; Ogino et al., 2015
<i>fakir far</i>	α subunit of voltage-gated calcium channel 2.1b gene (<i>CACNA1Ab</i>) on chromosome 11	tm154	L356V	Reduced synaptic transmission between Rohon-Beard neuron and interneuron	Granato et al., 1996; Low et al., 2012
<i>macho mao</i>	Pigk gene (<i>pigk</i>) on chromosome 2	tt261	M1T	Defect in the excitability of sensory Rohon-Beard neurons	Granato et al., 1996; Carnean et al., 2015
<i>steiff tier ste</i>	Unknown	tf220	Unknown	Defect in the excitability of sensory Rohon-Beard neurons	Granato et al., 1996
<i>crocodile cro</i>	Unknown	tw212d m148 s3556	Unknown Unknown Unknown	Unknown	Granato et al., 1996
<i>schlaffi sla</i>	Unknown	ty112 th239 tg230	Unknown Unknown Unknown	Unknown	Granato et al., 1996
<i>slumber slm</i>	Unknown	tt208 tm221 tm132c	Unknown Unknown Unknown	Unknown	Granato et al., 1996

sites is necessary for effective glycinergic transmission and motor pattern generation. In *bandoneon* mutants, GlyR cluster immunostaining in the spinal cord has a diffuse appearance rather than a clustered appearance, suggesting that GlyRb is necessary for the synaptic aggregation of $\alpha\beta$ GlyRs in zebrafish (Kirsch et al., 1993; Meyer et al., 1995; Feng et al., 1998; Kim et al., 2006).

Defective GlyT1 in the *shocked* Mutant

Shocked (*sho*) carries a mutation in *slc6a9*, which encodes GlyT1. Three mutant alleles of *slc6a9* were identified in the Tübingen screen (ta229g = G81D, te301 = C305Y and ta51e = unknown), and these *sho* mutants exhibit trunk twitching instead of swimming in response to tactile stimuli at 2 dpf (Granato et al., 1996; Luna et al., 2004; Cui et al., 2005; Mongeon et al., 2008). In addition, the frequency of spontaneous coiling is reduced and the escape contraction at 1 dpf is abolished in *sho* mutants. An electrophysiological analysis revealed that tactile stimuli induces arrhythmic muscle activation in *sho* mutants rather than the rhythmic depolarization observed in wild-type muscle (Cui et al., 2004). The ta229g allele, which produces the strongest phenotype, results from a G81D missense mutation that disrupts GlyT1 function (Cui et al., 2005). Increased extracellular glycine is thought to be the cause of the *sho* mutant phenotype. This presumption is supported by the following observations. First, the perfusion of glycine-free cerebrospinal fluid following the removal of the dorsal roof of the fourth ventricle recovers touch-evoked swimming in *sho* mutants, and this effect is lost when glycine is added to the perfusate (Cui et al., 2005; Mongeon et al., 2008). Second, the application of low concentrations of strychnine to *sho* mutants leads to partial motor recovery, similar to observations in GlyT1 knockout mice (Gomez et al., 2003a; Cui et al., 2005). Thus, a lack of functional GlyT1 and elevated extracellular glycine are likely to underlie the potentiation of glycinergic transmission in the *sho* phenotype.

The GlyT1 knockout mice exhibited severe motor and respiratory defects and die at birth due to the respiratory defect (Gomez et al., 2003a), whereas the GlyT1 defective zebrafishes exhibit a motility recovery by 4–5 dpf and survive thereafter (Mongeon et al., 2008). The motility recovery was accompanied by a reduction in GlyR expression that leads to a decrease in the amplitude of inhibitory potentials enhanced by the GlyT1 mutant (Mongeon et al., 2008). Although the alteration of GlyR expression may represent compensatory mechanisms, the molecular basis for this compensation is not revealed.

Glycinergic transporter 1 dysfunction has been posited in the pathogenesis of glycine encephalopathy, which is characterized by respiratory impairment (Gomez et al., 2003a; Applegarth and Toone, 2004, 2006; Harvey et al., 2008b), and schizophrenia which may be arose from hypofunction of NMDAR (Krystal et al., 1994; Lahti et al., 2001; Tsai et al., 2004; Dalmau et al., 2007). Animal models are clearly required to investigate the biological roles of GlyT1 in the context of human disorders, and zebrafish may provide particular advantages in future efforts. For example, while GlyT1 knockout mice die on the first postnatal day due to severe respiratory deficits (Gomez et al., 2003a; Tsai et al., 2004), zebrafish *sho* mutants can survive well into adulthood through

careful feeding and are thus useful as a physiologically relevant animal model for GlyT1 dysfunction.

CONCLUSION

Functional GlyRs are α homomeric or $\alpha\beta$ heteromeric pentamers. Electrophysiological studies of α subunits in cultured cells have shown the difference in conductance and kinetics of each α subunit (Takahashi et al., 1992; Bormann et al., 1993; Rajendra et al., 1995; Beato et al., 2002; Mangin et al., 2003; Burzomato et al., 2004; Zhang et al., 2015). Moreover, both in zebrafish and in mammals, each α subunit exhibits a distinct pattern of temporal and spatial expression in the CNS. This diversity of the α subunits suggests that GlyRs play various roles in physiological functions. However, the details of these physiological roles are not well understood. Several studies have identified GlyR subunit selective modulator in Cannabinoids and endocannabinoid (Hejazi et al., 2006; Yang et al., 2008; Xiong et al., 2012), in compounds isolated from ginkgo and Australian marine sponges (Balansa et al., 2010, 2013a,b; Maleeva et al., 2015). Furthermore, recent publications have reported that heptapeptide exhibit the subunit selective modulating effects on $\alpha1\beta$ and $\alpha3\beta$ heteromeric receptor with zinc ion dependence (Cornelison et al., 2016). These subunit-selective modulators would be useful tool to investigate the physiological roles of GlyR subunits in CNS. Together with the selective modulator, losses of function mutants of each GlyR subunit are powerful tools for uncovering the specific functions of each GlyR subunit. Now, zebrafish provide a cheaper, more convenient and highly useful alternative animal model for the study of GlyRs and glycinergic transmission. So far, the *glrb* and *slc6a9* mutants have been used to investigate the glycinergic synapse. Future work can further utilize CRISPR/Cas9-mediated gene disruption in zebrafish. In addition, *in vivo* observations of the glycinergic synapse in living zebrafish are a powerful method for the study of glycinergic synapse formation and plasticity. Taken together, a combination of readily available genetic mutants and innovative imaging techniques in zebrafish is sure to accelerate our understanding of glycinergic neurotransmission in the future.

AUTHOR CONTRIBUTIONS

All authors listed, have made substantial, direct and intellectual contribution to the work, and approved it for publication.

ACKNOWLEDGMENTS

We apologize to investigators whose work could not be cited in this manuscript owing to space limitations. This work was supported by a Grant-in-Aid for Young Scientists (B) from the Ministry of Education, Culture, Sports, Science, and Technology of Japan (MEXT) to KO and Grant-in-Aid for Scientific Research (B) from the MEXT, the Takeda Science Foundation, the Mochida Memorial Foundation for Medical and Pharmaceutical Research, the Naito Foundation, and the Suzuken Memorial Foundation and the Japan Epilepsy Research Foundation to HH.

REFERENCES

- Aguayo, L. G., Castro, P., Mariqueo, T., Muñoz, B., Xiong, W., Zhang, L., et al. (2014). Altered sedative effects of ethanol in mice with $\alpha 1$ glycine receptor subunits that are insensitive to Gbg modulation. *Neuropsychopharmacology* 39, 2538–2548. doi: 10.1038/npp.2014.100
- Ahmadi, S., Lippross, S., Neuhuber, W. L., and Zeilhofer, H. U. (2002). PGE2 selectively blocks inhibitory glycinergic neurotransmission onto rat superficial dorsal horn neurons. *Nat. Neurosci.* 5, 34–40. doi: 10.1038/nn778
- Akerboom, J., Chen, T. W., Wardill, T. J., Tian, L., Marvin, J. S., Mutlu, S., et al. (2012). Optimization of a GCaMP calcium indicator for neural activity imaging. *J. Neurosci.* 32, 13819–13840. doi: 10.1523/JNEUROSCI.2601-12.2012
- Akitake, C. M., Macurak, M., Halpern, M. E., and Goll, M. G. (2011). Transgenerational analysis of transcriptional silencing in zebrafish. *Dev. Biol.* 352, 191–201. doi: 10.1016/j.ydbio.2011.01.002
- Allain, A. E., Cazenave, W., Delpy, A., Exertier, P., Barthe, C., Meyrand, P., et al. (2015–2016). Nonsynaptic glycine release is involved in the early KCC2 expression. *Dev. Neurobiol.* 76, 764–779. doi: 10.1002/dneu.22358
- Al-Owain, M., Colak, D., Al-Bakheet, A., Al-Hashmi, N., Shuaib, T., Al-Hemidan, A., et al. (2012). Novel mutation in GLRB in a large family with hereditary hyperekplexia. *Clin. Genet.* 81, 479–484. doi: 10.1111/j.1399-0004.2011.01661.x
- Amores, A., Force, A., Yan, Y.-L., Joly, L., Amemiya, C., Fritz, A., et al. (1998). Zebrafish *hox* clusters and vertebrate genome evolution. *Science* 282, 1711–1714. doi: 10.1126/science.282.5394.1711
- Appelgarth, D. A., and Toone, J. R. (2004). Glycine encephalopathy (nonketotic hyperglycinaemia): review and update. *J. Inher. Metab. Dis.* 27, 417–422. doi: 10.1023/B:BOLI.0000031222.38328.59
- Appelgarth, D. A., and Toone, J. R. (2006). Glycine encephalopathy (nonketotic hyperglycinemia): comments and speculations. *Am. J. Med. Genet. Part A* 140, 186–188. doi: 10.1002/ajmg.a.31030
- Aroeira, R. I., Ribeiro, J. A., Sebastião, A. M., and Valente, C. A. (2011). Age-related changes of glycine receptor at the rat hippocampus: from the embryo to the adult. *J. Neurochem.* 118, 339–353. doi: 10.1111/j.1471-4159.2011.07197.x
- Arrenberg, A. B., Del Bene, F., and Baier, H. (2009). Optical control of zebrafish behavior with halorhodopsin. *Proc. Natl. Acad. Sci. U.S.A.* 106, 17968–17973. doi: 10.1073/pnas.0906252106
- Asakawa, K., and Kawakami, K. (2008). Targeted gene expression by the Gal4-UAS system in zebrafish. *Dev. Growth Differ.* 50, 391–399. doi: 10.1111/j.1440-169X.2008.01044.x
- Asakawa, K., Suster, M. L., Mizusawa, K., Nagayoshi, S., Kotani, T., Urasaki, A., et al. (2008). Genetic dissection of neural circuits by Tol2 transposon-mediated Gal4 gene and enhancer trapping in zebrafish. *Proc. Natl. Acad. Sci. U.S.A.* 105, 1255–1260. doi: 10.1073/pnas.0704963105
- Auer, T. O., Durore, K., De Cian, A., Concordet, J. P., and Del Bene, F. (2014). Highly efficient CRISPR/Cas9-mediated knock-in in zebrafish by homology-independent DNA repair. *Genome Res.* 24, 142–153. doi: 10.1101/gr.161638.113
- Avila, A., Vidal, P. M., Dear, T. N., Harvey, R. J., Rigo, J. M., and Nguyen, L. (2013). Glycine receptor $\alpha 2$ subunit activation promotes cortical interneuron migration. *Cell Rep.* 4, 738–750. doi: 10.1016/j.celrep.2013.07.016
- Avila, A., Vidal, P. M., Tielens, S., Morelli, G., Laguesse, S., Harvey, R. J., et al. (2014). Glycine receptors control the generation of projection neurons in the developing cerebral cortex. *Cell Death Differ.* 21, 1696–1708. doi: 10.1038/cdd.2014.75
- Baba, H., Kohno, T., Moore, K. A., and Woolf, C. J. (2001). Direct activation of rat spinal dorsal horn neurons by prostaglandin E2. *J. Neurosci.* 21, 1750–1756.
- Baird, G. S., Zacharias, D. A., and Tsien, R. Y. (1999). Circular permutation and receptor insertion within green fluorescent proteins. *Proc. Natl. Acad. Sci. U.S.A.* 96, 11241–11246. doi: 10.1073/pnas.96.20.11241
- Balansa, W., Islam, R., Fontaine, F., Piggott, A. M., Zhang, H., Webb, T. I., et al. (2010). Incinialactams: subunit-selective glycine receptor modulators from Australian sponges of the family Inciniidae. *Bioorg. Med. Chem.* 18, 2912–2919. doi: 10.1016/j.bmc.2010.03.002
- Balansa, W., Islam, R., Gilbert, D. F., Fontaine, F., Xiao, X., Zhang, H., et al. (2013a). Australian marine sponge alkaloids as a new class of glycine-gated chloride channel receptor modulator. *Bioorg. Med. Chem.* 21, 4420–4425. doi: 10.1016/j.bmc.2013.04.061
- Balansa, W., Islam, R., Fontaine, F., Piggott, A. M., Zhang, H., Xiao, X., et al. (2013b). Sesterterpene glycyl-lactams: a new class of glycine receptor modulator from Australian marine sponges of the genus *Psammocinia*. *Org. Biomol. Chem.* 11, 4695–4701. doi: 10.1039/C3OB40861B
- Baraban, S. C., Dinday, M. T., and Hortopan, G. A. (2013). Drug screening in *Scn1a* zebrafish mutant identifies clemizole as a potential Dravet syndrome treatment. *Nat. Commun.* 4:2410. doi: 10.1038/ncomms3410
- Barrangou, R., Fremaux, C., Deveau, H., Richards, M., Boyaval, P., Moineau, S., et al. (2007). CRISPR provides acquired resistance against viruses in prokaryotes. *Science* 315, 1709–1712. doi: 10.1126/science.1138140
- Bassett, D. I., Bryson-Richardson, R. J., Daggett, D. F., Gautier, P., Keenan, D. G., and Currie, P. D. (2003). Dystrophin is required for the formation of stable muscle attachments in the zebrafish embryos. *Development* 130, 5851–5860. doi: 10.1242/dev.00799
- Beato, M., Groot-Kormelink, P. J., Colquhoun, D., and Sivilotti, L. G. (2002). Openings of the rat recombinant $\alpha 1$ homomeric glycine receptor as a function of the number of agonist molecules bound. *J. Gen. Physiol.* 119, 443–466. doi: 10.1085/jgp.20028530
- Becker, C. M., Hoch, W., and Betz, H. (1988). Glycine receptor heterogeneity in rat spinal cord during postnatal development. *EMBO J.* 7, 3717.
- Bedell, V. M., Wang, Y., Campbell, J. M., Poshusta, T. L., Starker, C. G., Krug, R. G. II, et al. (2012). In vivo genome editing using a high-efficiency TALEN system. *Nature* 491, 114–118. doi: 10.1038/nature11537
- Behra, M., Cousin, X., Bertrand, C., Vonesch, J. L., Biellmann, D., Chatonnet, A., et al. (2002). Acetylcholinesterase is required for neuronal and muscular development in the zebrafish embryo. *Nat. Neurosci.* 5, 111–118. doi: 10.1038/nn788
- Ben-Ari, Y. (2002). Excitatory actions of GABA during development: the nature of the nurture. *Nat. Rev. Neurosci.* 3, 728–739. doi: 10.1038/nrn920
- Betz, H., Gomez, J., Armsen, W., Scholze, P., and Eulenburg, V. (2006). Glycine transporters: essential regulators of synaptic transmission. *Biochem. Soc. Trans.* 34, 55–58. doi: 10.1042/BST0340055
- Blednov, Y. A., Benavidez, J. M., Homanics, G. E., and Harris, R. A. (2012). Behavioral characterization of knockin mice with mutations M287L and Q266I in the glycine receptor $\alpha 1$ subunit. *J. Pharmacol. Exp. Ther.* 340, 317–329. doi: 10.1124/jpet.111.185124
- Blednov, Y. A., Benavidez, J. M., Black, M., Leiter, C. R., Osterndorff-Kahanek, E., and Harris, R. A. (2015). Glycine receptors containing $\alpha 2$ or $\alpha 3$ subunits regulate specific ethanol-mediated behaviors. *J. Pharm. Exp. Ther.* 353, 181–191. doi: 10.1124/jpet.114.221895
- Boch, J., Scholze, H., Schornack, S., Landgraf, A., Hahn, S., Kay, S., et al. (2009). Breaking the code of DNA binding specificity of TAL-type III effectors. *Science* 326, 1509–1512. doi: 10.1126/science.1178811
- Bode, A., and Lynch, J. W. (2014). The impact of human hyperekplexia mutations on glycine receptor structure and function. *Mol. Brain* 7:1. doi: 10.1186/1756-6606-7-2
- Bormann, J., Rundström, N., Betz, H., and Langosch, D. (1993). Residues within transmembrane segment M2 determine chloride conductance of glycine receptor homo- and hetero-oligomers. *EMBO J.* 12, 3729–3737.
- Brackmann, M., Zhao, C., Schmieden, V., and Braunewell, K. H. (2004). Cellular and subcellular localization of the inhibitory glycine receptor in hippocampal neurons. *Biochem. Biophys. Res. Commun.* 324, 1137–1142. doi: 10.1016/j.bbrc.2004.09.172
- Brand, A. H., and Perrimon, N. (1993). Targeted gene expression as a means of altering cell fates and generating dominant phenotypes. *Development* 118, 401–415.
- Brustein, E., Côté, S., Ghislain, J., and Drapeau, P. (2013). Spontaneous glycine-induced calcium transients in spinal cord progenitors promote neurogenesis. *Dev. Neurobiol.* 73, 168–175. doi: 10.1002/dneu.22050
- Burzomato, V., Beato, M., Groot-Kormelink, P. J., Colquhoun, D., and Sivilotti, L. G. (2004). Single-channel behavior of heteromeric $\alpha 1\beta$ glycine receptors: an attempt to detect a conformational change before the channel opens. *J. Neurosci.* 24, 10924–10940. doi: 10.1523/JNEUROSCI.3424-04.2004
- Burzomato, V., Groot-Kormelink, P. J., Sivilotti, L. G., and Beato, M. (2003). Stoichiometry of recombinant heteromeric glycine receptors revealed by a pore-lining region point mutation. *Receptors Channels* 9, 353–361. doi: 10.3109/714041016

- Buss, R. R., and Drapeau, P. (2001). Synaptic drive to motoneurons during fictive swimming in the developing zebrafish. *J. Neurophysiol.* 86, 197–210.
- Cade, L., Reyon, D., Hwang, W. Y., Tsai, S. Q., Patel, S., Khayter, C., et al. (2012). Highly efficient generation of heritable zebrafish gene mutations using homo- and heterodimeric TALENs. *Nucleic Acids Res.* 40, 8001–8010. doi: 10.1093/nar/gks518
- Calamai, M., Specht, C. G., Heller, J., Alcor, D., Machado, P., Vannier, C., et al. (2009). Gephyrin oligomerization controls GlyR mobility and synaptic clustering. *J. Neurosci.* 29, 7639–7648. doi: 10.1523/JNEUROSCI.5711-08.2009
- Çalışkan, G., Müller, I., Semtner, M., Winkelmann, A., Raza, A. S., Hollnagel, J. O., et al. (2016). Identification of parvalbumin interneurons as cellular substrate of fear memory persistence. *Cereb. Cortex* 26, 2325–2340. doi: 10.1093/cercor/bhw001
- Callister, R. J., and Graham, B. A. (2010). Early history of glycine receptor biology in mammalian spinal cord circuits. *Front. Mol. Neurosci.* 3:13. doi: 10.3389/fnmol.2010.00013
- Cao, Y., Semanchik, N., Lee, S. H., Somlo, S., Barbano, P. E., Coifman, R., et al. (2009). Chemical modifier screen identifies HDAC inhibitors as suppressors of PKD models. *Proc. Natl. Acad. Sci. U.S.A.* 106, 21819–21824. doi: 10.1073/pnas.0911987106
- Carmean, V., Yonkers, M. A., Tellez, M. B., Willer, J. R., Willer, G. B., Gregg, R. G., et al. (2015). pigk Mutation underlies macho behavior and affects Rohon-Beard cell excitability. *J. Neurophysiol.* 114, 1146–1157. doi: 10.1152/jn.00355.2015
- Carroll, D. (2011). Genome engineering with zinc-finger nucleases. *Genetics* 188, 773–782. doi: 10.1534/genetics.111.131433
- Chang, N., Sun, C., Gao, L., Zhu, D., Xu, X., Zhu, X., et al. (2013). Genome editing with RNA-guided Cas9 nuclease in zebrafish embryos. *Cell Res.* 23, 465–472. doi: 10.1038/cr.2013.45
- Chattipakorn, S. C., and McMahon, L. L. (2002). Pharmacological characterization of glycine-gated chloride currents recorded in rat hippocampal slices. *J. Neurophysiol.* 87, 1515–1525.
- Chattipakorn, S. C., and McMahon, L. L. (2003). Strychnine-sensitive glycine receptors depress hyperexcitability in rat dentate gyrus. *J. Neurophysiol.* 89, 1339–1342. doi: 10.1152/jn.00908.2002
- Chen, R., Okabe, A., Sun, H., Sharopov, S., Hanganu-Opatz, I. L., Kolbaev, S. N., et al. (2014). Activation of glycine receptors modulates spontaneous epileptiform activity in the immature rat hippocampus. *J. Physiol.* 592, 2153–2168. doi: 10.1113/jphysiol.2014.271700
- Chen, T. W., Wardill, T. J., Sun, Y., Pulver, S. R., Renninger, S. L., Baohuan, A., et al. (2013). Ultrasensitive fluorescent proteins for imaging neuronal activity. *Nature* 499, 295–300. doi: 10.1038/nature12354
- Chung, S. K., Bode, A., Cushion, T. D., Thomas, R. H., Hunt, C., Wood, S. E., et al. (2013). GLRB is the third major gene of effect in hyperekplexia. *Hum. Mol. Genet.* 22, 927–940. doi: 10.1093/hmg/ddt498
- Cong, L., Ran, F. A., Cox, D., Lin, S., Barretto, R., Habib, N., et al. (2013). Multiplex genome engineering using CRISPR/Cas systems. *Science* 339, 819–823. doi: 10.1126/science.1231143
- Cornelison, G. L., Pflanz, N. C., Tipps, M. E., and Mihic, S. J. (2016). Identification and characterization of heptapeptide modulators of the glycine receptor. *Eur. J. Pharmacol.* 780, 252–259. doi: 10.1016/j.ejphar.2016.03.058
- Cui, W. W., Low, S. E., Hirata, H., Saint-Amant, L., Geisler, R., Hume, R. I., et al. (2005). The zebrafish shocked gene encodes a glycine transporter and is essential for the function of early neural circuits in the CNS. *J. Neurosci.* 25, 6610–6620. doi: 10.1523/JNEUROSCI.5009-04.2005
- Cui, W. W., Saint-Amant, L., and Kuwada, J. Y. (2004). shocked Gene is required for the function of a premotor network in the zebrafish CNS. *J. Neurophysiol.* 92, 2898–2908. doi: 10.1152/jn.00419.2004
- Curtin, P. C., and Preuss, T. (2015). Glycine and GABAA receptors mediate tonic and phasic inhibitory processes that contribute to prepulse inhibition in the goldfish startle network. *Front. Neural Circuits* 9:12. doi: 10.3389/fncir.2015.00012
- Dahan, M., Lévi, S., Luccardini, C., Rostaing, P., Riveau, B., and Triller, A. (2003). Diffusion dynamics of glycine receptors revealed by single-quantum dot tracking. *Science* 302, 442–445. doi: 10.1126/science.1088525
- Dahlem, T. J., Hoshijima, K., Jurynek, M. J., Gunther, D., Starker, C. G., Locke, A. S., et al. (2012). Simple methods for generating and detecting locus-specific mutations induced with TALENs in the zebrafish genome. *PLoS Genet.* 8:e1002861. doi: 10.1371/journal.pgen.1002861
- Dalmau, J., Tüzün, E., Wu, H. Y., Masjuan, J., Rossi, J. E., Voloschin, A., et al. (2007). Paraneoplastic anti-N-methyl-D-aspartate receptor encephalitis associated with ovarian teratoma. *Ann. Neurol.* 61, 25–36. doi: 10.1002/ana.21050
- Danglot, L., Rostaing, P., Triller, A., and Bessis, A. (2004). Morphologically identified glycinergic synapses in the hippocampus. *Mol. Cell. Neurosci.* 27, 394–403. doi: 10.1016/j.mcn.2004.05.007
- Davidson, A. E., Balciunas, D., Mohn, D., Shaffer, J., Hermanson, S., Sivasubbu, S., et al. (2003). Efficient gene delivery and gene expression in zebrafish using the sleeping beauty transposon. *Dev. Biol.* 263, 191–202. doi: 10.1016/j.ydbio.2003.07.013
- David-Watine, B., Goblet, C., de Saint Jan, D., Fucile, S., Devignot, V., Bregestovski, P., et al. (1999). Cloning, expression and electrophysiological characterization of glycine receptor alpha subunit from zebrafish. *Neuroscience* 90, 303–317. doi: 10.1016/S0306-4522(98)00430-8
- Davies, J. S., Chung, S. K., Thomas, R. H., Robinson, A., Hammond, C. L., Mullins, J. G., et al. (2010). The glycinergic system in human startle disease: a genetic screening approach. *Front. Mol. Neurosci.* 3:8. doi: 10.3389/fnmol.2010.00008
- Deleuze, C., Runquist, M., Orcel, H., Rabie, A., Dayanithi, G., Alonso, G., et al. (2005). Structural difference between heteromeric somatic and homomeric axonal glycine receptors in the hypothalamo-neurohypophyseal system. *Neuroscience* 135, 475–483. doi: 10.1016/j.neuroscience.2005.05.024
- Delpy, A., Allain, A. E., Meyrand, P., and Branchereau, P. (2008). NKCC1 cotransporter inactivation underlies embryonic development of chloride-mediated inhibition in mouse spinal motoneuron. *J. Physiol.* 586, 1059–1075. doi: 10.1113/jphysiol.2007.146993
- Devignot, V., De Carvalho, L. P., Bregestovski, P., and Goblet, C. (2003). A novel glycine receptor $\alpha 1$ subunit variant in the zebrafish brain. *Neuroscience* 122, 449–457. doi: 10.1016/S0306-4522(03)00171-4
- Douglass, A. D., Kraves, S., Deisseroth, K., Schier, A. F., and Engert, F. (2008). Escape behavior elicited by single, channelrhodopsin-2-evoked spikes in zebrafish somatosensory neurons. *Curr. Biol.* 18, 1133–1137. doi: 10.1016/j.cub.2008.06.077
- Downes, G. B., and Granato, M. (2004). Acetylcholinesterase function is dispensable for sensory neurite growth but is critical for neuromuscular synapse stability. *Dev. Biol.* 270, 232–245. doi: 10.1016/j.ydbio.2004.02.027
- Downes, G. B., and Granato, M. (2006). Supraspinal input is dispensable to generate glycine-mediated locomotive behaviors in the zebrafish embryo. *J. Neurobiol.* 66, 437–451. doi: 10.1002/neu.20226
- Doyon, Y., McCammon, J. M., Miller, J. C., Faraji, F., Ngo, C., Katibah, G. E., et al. (2008). Heritable targeted gene disruption in zebrafish using designed zinc-finger nucleases. *Nat. Biotechnol.* 26, 702–708. doi: 10.1038/nbt1409
- Drapeau, P., Ali, D. W., Buss, R. R., and Saint-Amant, L. (1999). In vivo recording from identifiable neurons of the locomotor network in the developing zebrafish. *J. Neurosci. Methods* 88, 1–13. doi: 10.1016/S0165-0270(99)00008-4
- Drapeau, P., Saint-Amant, L., Buss, R. R., Chong, M., McDermid, J. R., and Brustein, E. (2002). Development of the locomotor network in zebrafish. *Prog. Neurobiol.* 68, 85–111. doi: 10.1016/S0301-0082(02)00075-8
- Duricic, N., Godin, A. G., Wever, C. M., Heyes, C. D., Lakadamyali, M., and Dent, J. A. (2012). Stoichiometry of the human glycine receptor revealed by direct subunit counting. *J. Neurosci.* 32, 12915–12920. doi: 10.1523/JNEUROSCI.2050-12.2012
- Eaton, R. C., Bombardieri, R. A., and Meyer, D. L. (1977). The Mauthner-initiated startle response in teleost fish. *J. Exp. Biol.* 66, 65–81.
- Ehrensperger, M. V., Hanus, C., Vannier, C., Triller, A., and Dahan, M. (2007). Multiple association states between glycine receptors and gephyrin identified by SPT analysis. *Biophys. J.* 92, 3706–3718. doi: 10.1529/biophysj.106.095596
- Eichler, S. A., Förstera, B., Smolinsky, B., Jüttner, R., Lehmann, T. N., Fähring, M., et al. (2009). Splice-specific roles of glycine receptor $\alpha 3$ in the hippocampus. *Eur. J. Neurosci.* 30, 1077–1091. doi: 10.1111/j.1460-9568.2009.06903.x
- Eichler, S. A., Kirischuk, S., Jüttner, R., Schafermeier, P. K., Legendre, P., Lehmann, T. N., et al. (2008). Glycinergic tonic inhibition of hippocampal neurons with depolarizing GABAergic transmission elicits histopathological signs of temporal lobe epilepsy. *J. Cell. Mol. Med.* 12, 2848–2866. doi: 10.1111/j.1582-4934.2008.00357.x
- Ellingsen, S., Laplante, M. A., König, M., Kikuta, H., Furmanek, T., Hoivik, E. A., et al. (2005). Large-scale enhancer detection in the zebrafish genome. *Development* 132, 3799–3811. doi: 10.1242/dev.01951

- Etard, C., Behra, M., Fisher, N., Hutcheson, D., Geisler, R., and Strähle, U. (2007). The UCS factor Steif/Unc-45b interacts with the heat shock protein Hsp90a during myofibrillogenesis. *Dev. Biol.* 308, 133–143. doi: 10.1016/j.ydbio.2007.05.014
- Eulenburg, V., Armsen, W., Betz, H., and Gomez, J. (2005). Glycine transporters: essential regulators of neurotransmission. *Trends Biochem. Sci.* 30, 325–333. doi: 10.1016/j.tibs.2005.04.004
- Felsenfeld, A. L., Walker, C., Westerfield, M., Kimmel, C., and Streisinger, G. (1990). Mutations affecting skeletal muscle myofibril structure in the zebrafish. *Development* 108, 443–459.
- Feng, G., Tintrup, H., Kirsch, J., Nichol, M. C., Kuhse, J., Betz, H., et al. (1998). Dual requirement for gephyrin in glycine receptor clustering and molybdoenzyme activity. *Science* 282, 1321–1324. doi: 10.1126/science.282.5392.1321
- Fetcho, J. R. (2007). The utility of zebrafish for studies of the comparative biology of motor systems. *J. Exp. Zool. B Mol. Dev. Evol.* 308, 550–562. doi: 10.1002/jez.b.21127
- Flint, A. C., Liu, X., and Kriegstein, A. R. (1998). Nonsynaptic glycine receptor activation during early neocortical development. *Neuron* 20, 43–53. doi: 10.1016/S0896-6273(00)80433-X
- Foley, J. E., Yeh, J. R. J., Maeder, M. L., Reyon, D., Sander, J. D., Peterson, R. T., et al. (2009). Rapid mutation of endogenous zebrafish genes using zinc finger nucleases made by Oligomerized Pool ENgineering (OPEN). *PLoS ONE* 4:e4348. doi: 10.1371/journal.pone.0004348
- Friedrich, T., Lambert, A. M., Masino, M. A., and Downes, G. B. (2012). Mutation of zebrafish dihydrolipoamide branched-chain transacylase E2 results in motor dysfunction and models maple syrup urine disease. *Dis. Model. Mech.* 5, 248–258. doi: 10.1242/dmm.008383
- Fritschy, J. M., Harvey, R. J., and Schwarz, G. (2008). Gephyrin: where do we stand, where do we go? *Trends Neurosci.* 31, 257–264. doi: 10.1016/j.tins.2008.02.006
- Fu, Y., Foden, J. A., Khayter, C., Maeder, M. L., Reyon, D., Joung, J. K., et al. (2013). High-frequency off-target mutagenesis induced by CRISPR-Cas nucleases in human cells. *Nat. Biotechnol.* 31, 822–826. doi: 10.1038/nbt.2623
- Fujita, M., Sato, K., Sato, M., Inoue, T., Kozuka, T., and Tohyama, M. (1991). Regional distribution of the cells expressing glycine receptor β subunit mRNA in the rat brain. *Brain Res.* 560, 23–37. doi: 10.1016/0006-8993(91)91210-R
- Furukawa, H., Singh, S. K., Mancusso, R., and Gouaux, E. (2005). Subunit arrangement and function in NMDA receptors. *Nature* 438, 185–192. doi: 10.1038/nature04089
- Ganser, L. R., Yan, Q., James, V. M., Kozol, R., Topf, M., Harvey, R. J., et al. (2013). Distinct phenotypes in zebrafish models of human startle disease. *Neurobiol. Dis.* 60, 139–151. doi: 10.1016/j.nbd.2013.09.002
- Garneau, J. E., Dupuis, M. E., Villion, M., Romero, D. A., Barrangou, R., Boyaval, P., et al. (2010). The CRISPR/Cas bacterial immune system cleaves bacteriophage and plasmid DNA. *Nature* 468, 67–71. doi: 10.1038/nature09523
- Gleason, M. R., Armisen, R., Verdecia, M. A., Sirotkin, H., Brehm, P., and Mandel, G. (2004). A mutation in *serca* underlies motility dysfunction in accordion zebrafish. *Dev. Biol.* 276, 441–451. doi: 10.1016/j.ydbio.2004.09.008
- Gleason, M. R., Higashijima, S. I., Dallman, J., Liu, K., Mandel, G., and Fetcho, J. R. (2003). Translocation of CaM kinase II to synaptic sites in vivo. *Nat. Neurosci.* 6, 217–218. doi: 10.1038/nn1011
- Goldsmith, P. (2004). Zebrafish as a pharmacological tool: the how, why and when. *Curr. Opin. Pharmacol.* 4, 504–512. doi: 10.1016/j.coph.2004.04.005
- Goll, M. G., Anderson, R., Stainier, D. Y., Spradling, A. C., and Halpern, M. E. (2009). Transcriptional silencing and reactivation in transgenic zebrafish. *Genetics* 182, 747–755. doi: 10.1534/genetics.109.102079
- Gomez, J., Hülsmann, S., Ohno, K., Eulenburg, V., Szöke, K., Richter, D., et al. (2003a). Inactivation of the glycine transporter 1 gene discloses vital role of glial glycine uptake in glycinergic inhibition. *Neuron* 40, 785–796. doi: 10.1016/S0896-6273(03)00672-X
- Gomez, J., Ohno, K., Hülsmann, S., Armsen, W., Eulenburg, V., Richter, D. W., et al. (2003b). Deletion of the mouse glycine transporter 2 results in a hyperekplexia phenotype and postnatal lethality. *Neuron* 40, 797–806. doi: 10.1016/S0896-6273(03)00673-1
- Granato, M., Van Eeden, F. J., Schach, U., Trowe, T., Brand, M., Furutani-Seiki, M., et al. (1996). Genes controlling and mediating locomotion behavior of the zebrafish embryo and larva. *Development* 123, 399–413.
- Grenningloh, G., Pribilla, I., Prior, P., Multhaup, G., Beyreuther, K., Taleb, O., et al. (1990b). Cloning and expression of the 58 kd β subunit of the inhibitory glycine receptor. *Neuron* 4, 963–970. doi: 10.1016/0896-6273(90)90149-A
- Grenningloh, G., Rienitz, A., Schmitt, B., Methfessel, C., Zensen, M., Beyreuther, K., et al. (1987). The strychnine-binding subunit of the glycine receptor shows homology with nicotinic acetylcholine receptors. *Nature* 328, 215–220. doi: 10.1038/328215a0
- Grenningloh, G., Schmieden, V., Schofield, P. R., Seeburg, P. H., Siddique, T., Mohandas, T. K., et al. (1990a). Alpha subunit variants of the human glycine receptor: primary structures, functional expression and chromosomal localization of the corresponding genes. *EMBO J.* 9, 771–776.
- Griffon, N., Büttner, C., Nicke, A., Kuhse, J., Schmalzing, G., and Betz, H. (1999). Molecular determinants of glycine receptor subunit assembly. *EMBO J.* 18, 4711–4721. doi: 10.1093/emboj/18.17.4711
- Grillner, S. (2003). The motor infrastructure: from ion channels to neuronal networks. *Nat. Rev. Neurosci.* 4, 573–586. doi: 10.1038/nrn1137
- Grudzinska, J., Schemm, R., Haeger, S., Nicke, A., Schmalzing, G., Betz, H., et al. (2005). The β subunit determines the ligand binding properties of synaptic glycine receptors. *Neuron* 45, 727–739. doi: 10.1016/j.neuron.2005.01.028
- Grunwald, D. J., Kimmel, C. B., Westerfield, M., Walker, C., and Streisinger, G. (1988). A neural degeneration mutation that spares primary neurons in the zebrafish. *Dev. Biol.* 126, 115–128. doi: 10.1016/0012-1606(88)90245-X
- Guyon, J. R., Goswami, J., Jun, S. J., Thorne, M., Howell, M., Pusack, T., et al. (2009). Genetic isolation and characterization of a splicing mutant of zebrafish dystrophin. *Hum. Mol. Genet.* 18, 202–211. doi: 10.1093/hmg/ddn337
- Hall, T. E., Bryson-Richardson, R. J., Berger, S., Jacoby, A. S., Cole, N. J., Hollway, G. E., et al. (2007). The zebrafish candyfloss mutant implicates extracellular matrix adhesion failure in laminin $\alpha 2$ -deficient congenital muscular dystrophy. *Proc. Natl. Acad. Sci. U.S.A.* 104, 7092–7097. doi: 10.1073/pnas.0700942104
- Halpern, M. E., Rhee, J., Goll, M. G., Akitake, C. M., Parsons, M., and Leach, S. D. (2008). Gal4/UAS transgenic tools and their application to zebrafish. *Zebrafish* 5, 97–110. doi: 10.1089/zeb.2008.0530
- Han, L., Talwar, S., Wang, Q., Shan, Q., and Lynch, J. W. (2013). Phosphorylation of $\alpha 3$ glycine receptors induces a conformational change in the glycine-binding site. *ACS Chem. Neurosci.* 4, 1361–1370. doi: 10.1021/cn400097j
- Hanus, C., Vannier, C., and Triller, A. (2004). Intracellular association of glycine receptor with gephyrin increases its plasma membrane accumulation rate. *J. Neurosci.* 24, 1119–1128. doi: 10.1523/JNEUROSCI.4380-03.2004
- Harvey, R. J., Depner, U. B., Wässle, H., Ahmadi, S., Heindl, C., Reinold, H., et al. (2004). GlyR $\alpha 3$: an essential target for spinal PGE2-mediated inflammatory pain sensitization. *Science* 304, 884–887. doi: 10.1126/science.1094925
- Harvey, R. J., Schmieden, V., Von Holst, A., Laube, B., Rohrer, H., and Betz, H. (2000). Glycine receptors containing the $\alpha 4$ subunit in the embryonic sympathetic nervous system, spinal cord and male genital ridge. *Eur. J. Neurosci.* 12, 994–1001. doi: 10.1046/j.1460-9568.2000.00993.x
- Harvey, R. J., Topf, M., Harvey, K., and Rees, M. I. (2008a). The genetics of hyperekplexia: more than startle! *Trends Genet.* 24, 439–447. doi: 10.1016/j.tig.2008.06.005
- Harvey, R. J., Carta, E., Pearce, B. R., Chung, S. K., Supplisson, S., Rees, M. I., et al. (2008b). A critical role for glycine transporters in hyperexcitability disorders. *Front. Mol. Neurosci.* 1:1. doi: 10.3389/neuro.02.001.2008
- Harvey, V. L., Caley, A., Müller, U. C., Harvey, R. J., and Dickinson, A. H. (2009). A selective role for $\alpha 3$ subunit glycine receptors in inflammatory pain. *Front. Mol. Neurosci.* 2:14. doi: 10.3389/neuro.02.014.2009
- Haverkamp, S., Müller, U., Harvey, K., Harvey, R. J., Betz, H., and Wässle, H. (2003). Diversity of glycine receptors in the mouse retina: localization of the $\alpha 3$ subunit. *J. Comp. Neurol.* 465, 524–539. doi: 10.1002/cne.10852
- Haverkamp, S., Müller, U., Zeilhofer, H. U., Harvey, R. J., and Wässle, H. (2004). Diversity of glycine receptors in the mouse retina: localization of the $\alpha 2$ subunit. *J. Comp. Neurol.* 477, 399–411. doi: 10.1002/cne.20267
- Hawkins, T. A., Haramis, A.-P., Etard, C., Prodromou, C., Vaughan, C. K., Ashworth, R., et al. (2008). The ATPase-dependent chaperoning activity of Hsp90a regulates thick filament formation and integration during skeletal muscle myofibrillogenesis. *Development* 135, 1147–1156. doi: 10.1242/dev.018150
- Heinze, L., Harvey, R. J., Haverkamp, S., and Wässle, H. (2007). Diversity of glycine receptors in the mouse retina: localization of the $\alpha 4$ subunit. *J. Comp. Neurol.* 500, 693–707. doi: 10.1002/cne.21201

- Hejazi, N., Zhou, C., Oz, M., Sun, H., Ye, J. H., and Zhang, L. (2006). Δ^9 -Tetrahydrocannabinol and endogenous cannabinoid anandamide directly potentiate the function of glycine receptors. *Mol. Pharmacol.* 69, 991–997. doi: 10.1124/mol.105.019174
- Hensley, M. R., Emman, F., Bonilla, S., Zhang, L., Zhong, W., Grosu, P., et al. (2011). Cellular expression of Smarca4 (Brg1)-regulated genes in zebrafish retinas. *BMC Dev. Biol.* 11:45. doi: 10.1186/1471-213X-11-45
- Herweg, J., and Schwarz, G. (2012). Splice-specific glycine receptor binding, folding, and phosphorylation of the scaffolding protein gephyrin. *J. Biol. Chem.* 287, 12645–12656. doi: 10.1074/jbc.M112.341826
- Higashijima, S. I., Masino, M. A., Mandel, G., and Fetcho, J. R. (2004). Engrailed-1 expression marks a primitive class of inhibitory spinal interneuron. *J. Neurosci.* 24, 5827–5839. doi: 10.1523/JNEUROSCI.5342-03.2004
- Hirata, H., Carta, E., Yamanaka, I., Harvey, R. J., and Kuwada, J. Y. (2010). Defective glycinergic synaptic transmission in zebrafish motility mutants. *Front. Mol. Neurosci.* 2:26. doi: 10.3389/fnro.02.026.2009
- Hirata, H., Saint-Amant, L., Downes, G. B., Cui, W. W., Zhou, W., Granato, M., et al. (2005). Zebrafish bandoneon mutants display behavioral defects due to a mutation in the glycine receptor β -subunit. *Proc. Natl. Acad. Sci. U.S.A.* 102, 8345–8350. doi: 10.1073/pnas.0500862102
- Hirata, H., Saint-Amant, L., Waterbury, J., Cui, W. W., Zhou, W., Li, Q., et al. (2004). accordion, a zebrafish behavioral mutant, has a muscle relaxation defect due to a mutation in the ATPase Ca^{2+} pump SERCA1. *Development* 131, 5457–5468. doi: 10.1242/dev.01410
- Hirata, H., Watanabe, T., Hatakeyama, J., Sprague, S. M., Saint-Amant, L., Nagashima, A., et al. (2007). Zebrafish relatively relaxed mutants have a ryanodine receptor defect, show slow swimming and provide a model of multi-minicore disease. *Development* 134, 2771–2781. doi: 10.1242/dev.004531
- Hisano, Y., Sakuma, T., Nakade, S., Ohga, R., Ota, S., Okamoto, H., et al. (2015). Precise in-frame integration of exogenous DNA mediated by CRISPR/Cas9 system in zebrafish. *Sci. Rep.* 5:8841. doi: 10.1038/srep08841
- Horvath, P., and Barrangou, R. (2010). CRISPR/Cas, the immune system of bacteria and archaea. *Science* 327, 167–170. doi: 10.1126/science.1179555
- Hruscha, A., Krawitz, P., Rechenberg, A., Heinrich, V., Hecht, J., Haass, C., et al. (2013). Efficient CRISPR/Cas9 genome editing with low off-target effects in zebrafish. *Development* 140, 4982–4987. doi: 10.1242/dev.099085
- Hruskova, B., Trojanova, J., Kulik, A., Kralikova, M., Pysanenko, K., Bures, Z., et al. (2012). Differential distribution of glycine receptor subtypes at the rat calyx of held synapse. *J. Neurosci.* 32, 17012–17024. doi: 10.1523/JNEUROSCI.1547-12.2012
- Hsu, P. D., Scott, D. A., Weinstein, J. A., Ran, F. A., Konermann, S., Agarwala, V., et al. (2013). DNA targeting specificity of RNA-guided Cas9 nucleases. *Nat. Biotechnol.* 31, 827–832. doi: 10.1038/nbt.2647
- Hwang, W. Y., Fu, Y., Reyon, D., Maeder, M. L., Tsai, S. Q., Sander, J. D., et al. (2013). Efficient genome editing in zebrafish using a CRISPR-Cas system. *Nat. Biotechnol.* 31, 227–229. doi: 10.1038/nbt.2501
- Imboden, M., de Saint Jan, D., Leulier, F., Korn, H., Goblet, C., and Bregestovski, P. (2001a). Isolation and characterization of an α 2-type zebrafish glycine receptor subunit. *Neuroscience* 103, 799–810. doi: 10.1016/S0306-4522(00)00575-3
- Imboden, M., Devignot, V., and Goblet, C. (2001b). Phylogenetic relationships and chromosomal location of five distinct glycine receptor subunit genes in the teleost *Danio rerio*. *Dev. Genes. Evol.* 211, 415–422. doi: 10.1007/s004270100164
- Imboden, M., Devignot, V., Korn, H., and Goblet, C. (2001c). Regional distribution of glycine receptor messenger RNA in the central nervous system of zebrafish. *Neuroscience* 103, 811–830. doi: 10.1016/S0306-4522(00)00576-5
- Inbal, A., Topczewski, J., and Solnica-Krezel, L. (2006). Targeted gene expression in the zebrafish prechordal plate. *Genesis* 44, 584–588. doi: 10.1002/dvg.20253
- Ivanova, E., Müller, U., and Wässle, H. (2006). Characterization of the glycinergic input to bipolar cells of the mouse retina. *Eur. J. Neurosci.* 23, 350–364. doi: 10.1111/j.1460-9568.2005.04557.x
- James, V. M., Bode, A., Chung, S. K., Gill, J. L., Nielsen, M., Cowan, F. M., et al. (2013). Novel missense mutations in the glycine receptor β subunit gene (GLRB) in startle disease. *Neurobiol. Dis.* 52, 137–149. doi: 10.1016/j.nbd.2012.12.001
- Jao, L. E., Wente, S. R., and Chen, W. (2013). Efficient multiplex biallelic zebrafish genome editing using a CRISPR nuclease system. *Proc. Natl. Acad. Sci. U.S.A.* 110, 13904–13909. doi: 10.1073/pnas.1308335110
- Jeong, H. J., Jang, I. S., Moorhouse, A. J., and Akaike, N. (2003). Activation of presynaptic glycine receptors facilitates glycine release from presynaptic terminals synapsing onto rat spinal sacral dorsal commissural nucleus neurons. *J. Physiol.* 550, 373–383. doi: 10.1113/jphysiol.2003.041053
- Jiang, Z., Yang, J., Purpura, L. A., Liu, Y., Rippes, H., and Shen, W. (2014). Glycinergic feedback enhances synaptic gain in the distal retina. *J. Physiol.* 592, 1479–1492. doi: 10.1113/jphysiol.2013.265785
- Jinek, M., Chylinski, K., Fonfara, I., Hauer, M., Doudna, J. A., and Charpentier, E. (2012). A programmable dual-RNA-guided DNA endonuclease in adaptive bacterial immunity. *Science* 337, 816–821. doi: 10.1126/science.1225829
- Jing, L., Lefebvre, J. L., Gordon, L. R., and Granato, M. (2009). Wnt signals organize synaptic prepattern and axon guidance through the zebrafish unplugged/MuSK receptor. *Neuron* 61, 721–733. doi: 10.1016/j.neuron.2008.12.025
- Johnson, J. W., and Ascher, P. (1987). Glycine potentiates the NMDA response in cultured mouse brain neurons. *Nature* 325, 529–531. doi: 10.1038/325529a0
- Jonsson, S., Adermark, L., Ericson, M., and Söderpalm, B. (2014). The involvement of accumbal glycine receptors in the dopamine-elevating effects of addictive drugs. *Neuropharmacol.* 82, 69–75. doi: 10.1016/j.neuropharm.2014.03.010
- Jonsson, S., Morud, J., Pickering, C., Adermark, L., Ericson, M., and Söderpalm, B. (2012). Changes in glycine receptor subunit expression in forebrain regions of the Wistar rat over development. *Brain Res.* 1446, 12–21. doi: 10.1016/j.brainres.2012.01.050
- Jusuf, P. R., Haverkamp, S., and Grünert, U. (2005). Localization of glycine receptor α subunits on bipolar and amacrine cells in primate retina. *J. Comp. Neurol.* 488, 113–128. doi: 10.1002/cne.20555
- Kanaka, C., Ohno, K., Okabe, A., Kuriyama, K., Itoh, T., Fukuda, A., et al. (2001). The differential expression patterns of messenger RNAs encoding K-Cl cotransporters (KCC1, 2) and Na-K-2Cl cotransporter (NKCC1) in the rat nervous system. *Neuroscience* 104, 933–946. doi: 10.1016/S0306-4522(01)00149-X
- Karlsson, J., von Hofsten, J., and Olsson, P. E. (2001). Generating transparent zebrafish: a refined method to improve detection of gene expression during embryonic development. *Mar. Biotechnol.* 3, 522–527. doi: 10.1007/s1012601-0053-4
- Kawahara, G., Karpf, J. A., Myers, J. A., Alexander, M. S., Guyon, J. R., and Kunkel, L. M. (2011). Drug screening in a zebrafish model of Duchenne muscular dystrophy. *Proc. Natl. Acad. Sci. U.S.A.* 108, 5331–5336. doi: 10.1073/pnas.1102116108
- Kawakami, K., Abe, G., Asada, T., Asakawa, K., Fukuda, R., Ito, A., et al. (2010). z Trap: zebrafish gene trap and enhancer trap database. *BMC Dev. Biol.* 10:105. doi: 10.1186/1471-213X-10-105
- Kawakami, K., Takeda, H., Kawakami, N., Kobayashi, M., Matsuda, N., and Mishina, M. (2004). A transposon-mediated gene trap approach identifies developmentally regulated genes in zebrafish. *Dev. Cell* 7, 133–144. doi: 10.1016/j.devcel.2004.06.005
- Kettleborough, R. N., Busch-Nentwich, E. M., Harvey, S. A., Dooley, C. M., de Bruijn, E., van Eeden, F., et al. (2013). A systematic genome-wide analysis of zebrafish protein-coding gene function. *Nature* 496, 494–497. doi: 10.1038/nature11992
- Kim, E. Y., Schrader, N., Smolinsky, B., Bedet, C., Vannier, C., Schwarz, G., et al. (2006). Deciphering the structural framework of glycine receptor anchoring by gephyrin. *EMBO J.* 25, 1385–1395. doi: 10.1038/sj.emboj.7601029
- Kimmel, C. B., Ballard, W. W., Kimmel, S. R., Ullmann, B., and Schilling, T. F. (1995). Stages of embryonic development of the zebrafish. *Dev. Dyn.* 203, 253–310. doi: 10.1002/aja.1002030302
- Kimura, Y., Hisano, Y., Kawahara, A., and Higashijima, S. I. (2014). Efficient generation of knock-in transgenic zebrafish carrying reporter/driver genes by CRISPR/Cas9-mediated genome engineering. *Sci. Rep.* 4:6545. doi: 10.1038/srep06545
- Kimura, Y., Okamura, Y., and Higashijima, S. I. (2006). α lx, a zebrafish homolog of Chx10, marks ipsilateral descending excitatory interneurons that participate in the regulation of spinal locomotor circuits. *J. Neurosci.* 26, 5684–5697. doi: 10.1523/JNEUROSCI.4993-05.2006
- Kirchner, A., Breustedt, J., Rosche, B., Heinemann, U. F., and Schmieden, V. (2003). Effects of taurine and glycine on epileptiform activity induced by removal of Mg^{2+} in combined rat entorhinal cortex–hippocampal slices. *Epilepsia* 44, 1145–1152. doi: 10.1046/j.1528-1157.2003.01603.x

- Kirsch, J., and Betz, H. (1998). Glycine-receptor activation is required for receptor clustering in spinal neurons. *Nature* 392, 717–720. doi: 10.1038/33694
- Kirsch, J., Wolters, I., Triller, A., and Betz, H. (1993). Gephyrin antisense oligonucleotides prevent glycine receptor clustering in spinal neurons. *Nature* 366, 745–748. doi: 10.1038/366745a0
- Kneussel, M., and Betz, H. (2000). Clustering of inhibitory neurotransmitter receptors at developing postsynaptic sites: the membrane activation model. *Trends Neurosci.* 23, 429–435. doi: 10.1016/S0166-2236(00)01627-1
- Kohashi, T., Nakata, N., and Oda, Y. (2012). Effective sensory modality activating an escape triggering neuron switches during early development in zebrafish. *J. Neurosci.* 32, 5810–5820. doi: 10.1523/JNEUROSCI.6169-11.2012
- Kohashi, T., and Oda, Y. (2008). Initiation of Mauthner-or non-Mauthner-mediated fast escape evoked by different modes of sensory input. *J. Neurosci.* 28, 10641–10653. doi: 10.1523/JNEUROSCI.1435-08.2008
- Kok, F. O., Shin, M., Ni, C. W., Gupta, A., Grosse, A. S., van Impel, A., et al. (2015). Reverse genetic screening reveals poor correlation between morpholino-induced and mutant phenotypes in zebrafish. *Dev. Cell* 32, 97–108. doi: 10.1016/j.devcel.2014.11.018
- Korn, H., and Faber, D. S. (2005). The Mauthner cell half a century later: a neurobiological model for decision-making? *Neuron* 47, 13–28. doi: 10.1016/j.neuron.2005.05.019
- Korn, H., Oda, Y., and Faber, D. S. (1992). Long-term potentiation of inhibitory circuits and synapses in the central nervous system. *Proc. Natl. Acad. Sci. U.S.A.* 89, 440–443. doi: 10.1073/pnas.89.1.440
- Krystal, J. H., Karper, L. P., Seibyl, J. P., Freeman, G. K., Delaney, R., Bremner, J. D., et al. (1994). Subanesthetic effects of the noncompetitive NMDA antagonist, ketamine, in humans: psychotomimetic, perceptual, cognitive, and neuroendocrine responses. *Arch. Gen. Psychiatry* 51, 199–214. doi: 10.1001/archpsyc.1994.03950030035004
- Kubota, H., Alle, H., Betz, H., and Geiger, J. R. (2010). Presynaptic glycine receptors on hippocampal mossy fibers. *Biochem. Biophys. Res. Commun.* 393, 587–591. doi: 10.1016/j.bbrc.2010.02.019
- Kuhse, J., Kuryatov, A., Maule, Y., Malosio, M. L., Schmieden, V., and Betz, H. (1991). Alternative splicing generates two isoforms of the $\alpha 2$ subunit of the inhibitory glycine receptor. *FEBS Lett.* 283, 73–77. doi: 10.1016/0014-5793(91)80557
- Kuhse, J., Schmieden, V., and Betz, H. (1990). Identification and functional expression of a novel ligand binding subunit of the inhibitory glycine receptor. *J. Biol. Chem.* 265, 22317–22320.
- Kunz, P. A., Burette, A. C., Weinberg, R. J., and Philpot, B. D. (2012). Glycine receptors support excitatory neurotransmitter release in developing mouse visual cortex. *J. Physiol.* 590, 5749–5764. doi: 10.1113/jphysiol.2012.241299
- Lahti, A. C., Weiler, M. A., Tamara, M., Parwani, A., and Tamminga, C. A. (2001). Effects of ketamine in normal and schizophrenic volunteers. *Neuropsychopharmacology* 25, 455–467. doi: 10.1016/S0893-133X(01)00243-3
- Langosch, D., Thomas, L., and Betz, H. (1988). Conserved quaternary structure of ligand-gated ion channels: the postsynaptic glycine receptor is a pentamer. *Proc. Natl. Acad. Sci. U.S.A.* 85, 7394–7398. doi: 10.1073/pnas.85.19.7394
- Lefebvre, J. L., Jing, L., Becafigo, S., Franzini-Armstrong, C., and Granato, M. (2007). Differential requirement for MuSK and dystroglycan in generating patterns of neuromuscular innervation. *Proc. Natl. Acad. Sci. U.S.A.* 104, 2483–2488. doi: 10.1073/pnas.0610822104
- Legendre, P., Förster, B., Jüttner, R., and Meier, J. C. (2009). Glycine receptors caught between genome and proteome—functional implications of RNA editing and splicing. *Front. Mol. Neurosci.* 2:23. doi: 10.3389/fnmo.2009.02.023
- Legendre, P., and Korn, H. (1994). Glycinergic inhibitory synaptic currents and related receptor channels in the zebrafish brain. *Eur. J. Neurosci.* 6, 1544–1557. doi: 10.1111/j.1460-9568.1994.tb00545.x
- Legendre, P., and Korn, H. (1995). Voltage dependence of conductance changes evoked by glycine release in the zebrafish brain. *J. Neurophysiol.* 73, 2404–2412.
- Lévi, S., Schweizer, C., Bannai, H., Pascual, O., Charrier, C., and Triller, A. (2008). Homeostatic regulation of synaptic GlyR numbers driven by lateral diffusion. *Neuron* 59, 261–273. doi: 10.1016/j.neuron.2008.05.030
- Li, D., Qiu, Z., Shao, Y., Chen, Y., Guan, Y., Liu, M., et al. (2013). Heritable gene targeting in the mouse and rat using a CRISPR-Cas system. *Nat. Biotechnol.* 31, 681–683. doi: 10.1038/nbt.2661
- Li, W., Teng, F., Li, T., and Zhou, Q. (2013). Simultaneous generation and germline transmission of multiple gene mutations in rat using CRISPR-Cas systems. *Nat. Biotechnol.* 31, 684–686. doi: 10.1038/nbt.2652
- Liu, D., Wang, Z., Xiao, A., Zhang, Y., Li, W., Zu, Y., et al. (2014). Efficient gene targeting in zebrafish mediated by a zebrafish-codon-optimized cas9 and evaluation of off-targeting effect. *J. Genet. Genomics.* 41, 43–46. doi: 10.1016/j.jgg.2013.11.004
- Liu, Q., and Wong-Riley, M. T. (2013). Postnatal development of glycine receptor subunits $\alpha 1$, $\alpha 2$, $\alpha 3$, and β immunoreactivity in multiple brain stem respiratory-related nuclear groups of the rat. *Brain Res.* 1538, 1–16. doi: 10.1016/j.brainres.2013.09.028
- Love, D. R., Pichler, F. B., Dodd, A., Copp, B. R., and Greenwood, D. R. (2004). Technology for high-throughput screens: the present and future using zebrafish. *Curr. Opin. Biotechnol.* 15, 564–571. doi: 10.1016/j.copbio.2004.09.004
- Low, S. E., Woods, I. G., Lachance, M., Ryan, J., Schier, A. F., and Saint-Amant, L. (2012). Touch responsiveness in zebrafish requires voltage-gated calcium channel 2.1 b. *J. Neurophysiol.* 108, 148–159. doi: 10.1152/jn.00839.2011
- Luna, V. M., Wang, M., Ono, F., Gleason, M. R., Dallman, J. E., Mandel, G., et al. (2004). Persistent electrical coupling and locomotory dysfunction in the zebrafish mutant shocked. *J. Neurophysiol.* 92, 2003–2009. doi: 10.1152/jn.00454.2004
- Maguire, E. P., Mitchell, E. A., Greig, S. J., Corteen, N., Balfour, D. J., Swinny, J. D., et al. (2014). Extrasynaptic glycine receptors of rodent dorsal raphe serotonergic neurons: a sensitive target for ethanol. *Neuropsychopharmacology* 39, 1232–1244. doi: 10.1038/npp.2013.326
- Majumdar, S., Heinze, L., Haverkamp, S., Ivanova, E., and Wässle, H. (2007). Glycine receptors of A-type ganglion cells of the mouse retina. *Vis. Neurosci.* 24, 471–487. doi: 10.1017/S0952523807070174
- Majumdar, S., Weiss, J., and Wässle, H. (2009). Glycinergic input of widefield, displaced amacrine cells of the mouse retina. *J. Physiol.* 587, 3831–3849. doi: 10.1113/jphysiol.2009.171207
- Maleeva, G., Buldakova, S., and Bregestovski, P. (2015). Selective potentiation of alpha 1 glycine receptors by ginkgolic acid. *Front. Mol. Neurosci.* 8:64. doi: 10.3389/fnmo.2015.00064
- Mali, P., Yang, L., Esvelt, K. M., Aach, J., Guell, M., DiCarlo, J. E., et al. (2013). RNA-guided human genome engineering via Cas9. *Science* 339, 823–826. doi: 10.1126/science.1232033
- Malosio, M. L., Marqueze-Pouey, B., Kuhse, J., and Betz, H. (1991). Widespread expression of glycine receptor subunit mRNAs in the adult and developing rat brain. *EMBO J.* 10, 2401–2409.
- Mangin, J. M., Baloul, M., Carvalho, L., Rogister, B., Rigo, J. M., and Legendre, P. (2003). Kinetic properties of the $\alpha 2$ homo-oligomeric glycine receptor impairs a proper synaptic functioning. *J. Physiol.* 553, 369–386. doi: 10.1113/jphysiol.2003.052142
- Mangin, J. M., Guyon, A., Eugene, D., Paupardin-Tritsch, D., and Legendre, P. (2002). Functional glycine receptor maturation in the absence of glycinergic input in dopaminergic neurones of the rat substantia nigra. *J. Physiol.* 542, 685–697. doi: 10.1113/jphysiol.2002.018978
- Masino, M. A., and Fetcho, J. R. (2005). Fictive swimming motor patterns in wild type and mutant larval zebrafish. *J. Neurophysiol.* 93, 3177–3188. doi: 10.1152/jn.01248.2004
- McCool, B. A., and Botting, S. K. (2000). Characterization of strychnine-sensitive glycine receptors in acutely isolated adult rat basolateral amygdala neurons. *Brain Res.* 859, 341–351. doi: 10.1016/S0006-8993(00)02026-6
- McCool, B. A., and Farroni, J. S. (2001). Subunit composition of strychnine-sensitive glycine receptors expressed by adult rat basolateral amygdala neurons. *Eur. J. Neurosci.* 14, 1082–1090. doi: 10.1046/j.0953-816x.2001.01730.x
- McCracken, L. M., Blednov, Y. A., Trudell, J. R., Benavidez, J. M., Betz, H., and Harris, R. A. (2013a). Mutation of a zinc-binding residue in the glycine receptor $\alpha 1$ subunit changes ethanol sensitivity in vitro and alcohol consumption in vivo. *J. Pharmacol. Exp. Ther.* 344, 489–500. doi: 10.1124/jpet.112.197707
- McCracken, L. M., Trudell, J. R., McCracken, M. L., and Harris, R. A. (2013b). Zinc-dependent modulation of $\alpha 2$ - and $\alpha 3$ -glycine receptor subunits by ethanol. *Alcohol Clin. Exp. Res.* 37, 2002–2010. doi: 10.1111/acer.12192
- McDearmid, J. R., Liao, M., and Drapeau, P. (2006). Glycine receptors regulate interneuron differentiation during spinal network development. *Proc. Natl. Acad. Sci. U.S.A.* 103, 9679–9684. doi: 10.1073/pnas.0504871103

- McLean, D. L., Fan, J., Higashijima, S. I., Hale, M. E., and Fetcho, J. R. (2007). A topographic map of recruitment in spinal cord. *Nature* 446, 71–75. doi: 10.1038/nature05588
- Meier, J., Vannier, C., Serge, A., Triller, A., and Choquet, D. (2001). Fast and reversible trapping of surface glycine receptors by gephyrin. *Nat. Neurosci.* 4, 253–260. doi: 10.1038/85099
- Meng, X., Noyes, M. B., Zhu, L. J., Lawson, N. D., and Wolfe, S. A. (2008). Targeted gene inactivation in zebrafish using engineered zinc-finger nucleases. *Nat. Biotechnol.* 26, 695–701. doi: 10.1038/nbt1398
- Meyer, G., Kirsch, J., Betz, H., and Langosch, D. (1995). Identification of a gephyrin binding motif on the glycine receptor β subunit. *Neuron* 15, 563–572. doi: 10.1016/0896-6273(95)90145-0
- Mikawa, S., Wang, C., Shu, F., Wang, T., Fukuda, A., and Sato, K. (2002). Developmental changes in KCC1, KCC2 and NKCC1 mRNAs in the rat cerebellum. *Dev. Brain Res.* 136, 93–100. doi: 10.1016/S0165-3806(02)00345-0
- Miller, J. C., Tan, S., Qiao, G., Barlow, K. A., Wang, J., Xia, D. F., et al. (2011). A TALE nuclease architecture for efficient genome editing. *Nat. Biotechnol.* 29, 143–148. doi: 10.1038/nbt1755
- Mine, J., Taketani, T., Otsubo, S., Kishi, K., and Yamaguchi, S. (2013). A 14-year-old girl with hyperekplexia having GLRB mutations. *Brain Dev.* 35, 660–663. doi: 10.1016/j.braindev.2012.10.013
- Moens, C. B., Donn, T. M., Wolf-Saxon, E. R., and Ma, T. P. (2008). Reverse genetics in zebrafish by TILLING. *Brief. Funct. Genomic. Proteomic.* 7, 454–459. doi: 10.1093/bfpg/eln046
- Molander, A., Löf, E., Stomberg, R., Ericson, M., and Söderpalm, B. (2005). Involvement of accumbal glycine receptors in the regulation of voluntary ethanol intake in the rat. *Alcohol. Clin. Exp. Res.* 29, 38–45. doi: 10.1097/01.ALC.0000150009.78622.E0
- Molander, A., and Söderpalm, B. (2005). Accumbal strychnine-sensitive glycine receptors: an access point for ethanol to the brain reward system. *Alcohol. Clin. Exp. Res.* 29, 27–37. doi: 10.1097/01.ALC.0000150012.09608.81
- Mongeon, R., Gleason, M. R., Masino, M. A., Fetcho, J. R., Mandel, G., Brehm, P., et al. (2008). Synaptic homeostasis in a zebrafish glial glycine transporter mutant. *J. Neurophysiol.* 100, 1716–1723. doi: 10.1152/jn.90596.2008
- Morelli, G., Avila, A., Ravanidis, S., Aourz, N., Neve, R. L., Smolders, I., et al. (2016). Cerebral cortical circuitry formation requires functional glycine receptors. *Cereb. Cortex* doi: 10.1093/cercor/bhw025 [Epub ahead of print].
- Moscou, M. J., and Bogdanove, A. J. (2009). A simple cipher governs DNA recognition by TAL effectors. *Science* 326, 1501–1501. doi: 10.1126/science.1178817
- Mullins, M. C., Hammerschmidt, M., Haffter, P., and Nüsslein-Volhard, C. (1994). Large-scale mutagenesis in the zebrafish: in search of genes controlling development in a vertebrate. *Curr. Biol.* 4, 189–202. doi: 10.1016/S0960-9822(00)00048-8
- Muto, A., Ohkura, M., Abe, G., Nakai, J., and Kawakami, K. (2013). Real-time visualization of neuronal activity during perception. *Curr. Biol.* 23, 307–311. doi: 10.1016/j.cub.2012.12.040
- Muto, A., Ohkura, M., Kotani, T., Higashijima, S. I., Nakai, J., and Kawakami, K. (2011). Genetic visualization with an improved GCaMP calcium indicator reveals spatiotemporal activation of the spinal motor neurons in zebrafish. *Proc. Natl. Acad. Sci. U.S.A.* 108, 5425–5430. doi: 10.1073/pnas.1000887108
- Myhre, J. L., Hills, J. A., Prill, K., Wohlgemuth, S. L., and Pilgrim, D. B. (2014). The titin A-band rod domain is dispensable for initial thick filament assembly in zebrafish. *Dev. Biol.* 387, 93–108. doi: 10.1016/j.ydbio.2013.12.020
- Nakai, J., Ohkura, M., and Imoto, K. (2001). A high signal-to-noise Ca²⁺ probe composed of a single green fluorescent protein. *Nat. Biotechnol.* 19, 137–141. doi: 10.1038/84397
- Nasevicius, A., and Ekker, S. C. (2000). Effective targeted gene 'knockdown' in zebrafish. *Nat. Genet.* 26, 216–220. doi: 10.1038/79951
- Niell, C. M., Meyer, M. P., and Smith, S. J. (2004). In vivo imaging of synapse formation on a growing dendritic arbor. *Nat. Neurosci.* 7, 254–260. doi: 10.1038/nn1191
- Nobles, R. D., Zhang, C., Müller, U., Betz, H., and McCall, M. A. (2012). Selective glycine receptor $\alpha 2$ subunit control of crossover inhibition between the on and off retinal pathways. *J. Neurosci.* 32, 3321–3332. doi: 10.1523/JNEUROSCI.5341-11.2012
- Oda, Y., Kawasaki, K., Morita, M., Korn, H., and Matsui, H. (1998). Inhibitory long-term potentiation underlies auditory conditioning of goldfish escape behaviour. *Nature* 394, 182–185. doi: 10.1038/28172
- Ogino, K., Low, S. E., Yamada, K., Saint-Amant, L., Zhou, W., Muto, A., et al. (2015). RING finger protein 121 facilitates the degradation and membrane localization of voltage-gated sodium channels. *Proc. Natl. Acad. Sci. U.S.A.* 112, 2859–2864. doi: 10.1073/pnas.1414002112
- Ohkura, M., Matsuzaki, M., Kasai, H., Imoto, K., and Nakai, J. (2005). Genetically encoded bright Ca²⁺ probe applicable for dynamic Ca²⁺ imaging of dendritic spines. *Anal. Chem.* 77, 5861–5869. doi: 10.1021/ac0506837
- Olson, B. D., Sgourdou, P., and Downes, G. B. (2010). Analysis of a zebrafish behavioral mutant reveals a dominant mutation in atp2a1/SERCA1. *Genesis* 48, 354–361. doi: 10.1002/dvg.20631
- Ono, F., Higashijima, S. I., Scherbatko, A., Fetcho, J. R., and Brehm, P. (2001). Paralytic zebrafish lacking acetylcholine receptors fail to localize rapsyn clusters to the synapse. *J. Neurosci.* 21, 5439–5448.
- Ono, F., Mandel, G., and Brehm, P. (2004). Acetylcholine receptors direct rapsyn clusters to the neuromuscular synapse in zebrafish. *J. Neurosci.* 24, 5475–5481. doi: 10.1523/JNEUROSCI.0851-04.2004
- Ono, F., Scherbatko, A., Higashijima, S. I., Mandel, G., and Brehm, P. (2002). The zebrafish motility mutant twitch once reveals new roles for rapsyn in synaptic function. *J. Neurosci.* 22, 6491–6498.
- Paik, E. J., de Jong, J. L., Pugach, E., Opara, P., and Zon, L. I. (2010). A chemical genetic screen in zebrafish for pathways interacting with cdx4 in primitive hematopoiesis. *Zebrafish* 7, 61–68. doi: 10.1089/zeb.2009.0643
- Pang, S. C., Wang, H. P., Zhu, Z. Y., and Sun, Y. H. (2015). Transcriptional Activity and DNA Methylation Dynamics of the Gal4/UAS System in Zebrafish. *Mar. Biotechnol.* 17, 593–603. doi: 10.1007/s10126-015-9641-0
- Paoletti, P., and Neyton, J. (2007). NMDA receptor subunits: function and pharmacology. *Curr. Opin. Pharmacol.* 7, 39–47. doi: 10.1016/j.coph.2006.08.011
- Papouin, T., Ladépêche, L., Ruel, J., Sacchi, S., Labasque, M., Hanini, M., et al. (2012). Synaptic and extrasynaptic NMDA receptors are gated by different endogenous coagonists. *Cell* 150, 633–646. doi: 10.1016/j.cell.2012.06.029
- Peal, D. S., Mills, R. W., Lynch, S. N., Mosley, J. M., Lim, E., Ellinor, P. T., et al. (2011). Novel chemical suppressors of long QT syndrome identified by an in vivo functional screen. *Circulation* 123, 23–30. doi: 10.1161/CIRCULATIONAHA.110.003
- Peterson, R. T., Link, B. A., Dowling, J. E., and Schreiber, S. L. (2000). Small molecule developmental screens reveal the logic and timing of vertebrate development. *Proc. Natl. Acad. Sci. U.S.A.* 97, 12965–12969. doi: 10.1073/pnas.97.24.12965
- Peterson, R. T., Shaw, S. Y., Peterson, T. A., Milan, D. J., Zhong, T. P., Schreiber, S. L., et al. (2004). Chemical suppression of a genetic mutation in a zebrafish model of aortic coarctation. *Nat. Biotechnol.* 22, 595–599. doi: 10.1038/nbt963
- Pietri, T., Manalo, E., Ryan, J., Saint-Amant, L., and Washbourne, P. (2009). Glutamate drives the touch response through a rostral loop in the spinal cord of zebrafish embryos. *Dev. Neurobiol.* 69, 780–795. doi: 10.1002/dneu.20741
- Pilorge, M., Fassier, C., Le Corrion, H., Potey, A., Bai, J., De Gois, S., et al. (2015). Genetic and functional analyses demonstrate a role for abnormal glycinergic signaling in autism. *Mol. Psychiatry* doi: 10.1038/mp.2015.139 [Epub ahead of print].
- Pinto, D., Pagnamenta, A. T., Klei, L., Anney, R., Merico, D., Regan, R., et al. (2010). Functional impact of global rare copy number variation in autism spectrum disorders. *Nature* 466, 368–372. doi: 10.1038/nature09146
- Pribilla, I., Takagi, T., Langosch, D., Bormann, J., and Betz, H. (1992). The atypical M2 segment of the beta subunit confers picrotoxinin resistance to inhibitory glycine receptor channels. *EMBO J.* 11, 4305–4311.
- Quinlan, J. J., Ferguson, C., Jester, K., Firestone, L. L., and Homanics, G. E. (2002). Mice with glycine receptor subunit mutations are both sensitive and resistant to volatile anesthetics. *Anesth. Analg.* 95, 578–582. doi: 10.1213/0000539-200209000-00016
- Rajendra, S., Lynch, J. W., Pierce, K. D., French, C. R., Barry, P. H., and Schofield, P. R. (1995). Mutation of an arginine residue in the human glycine receptor transforms β -alanine and taurine from agonists into competitive antagonists. *Neuron* 14, 169–175. doi: 10.1016/0896-6273(95)90251-1

- Rees, M. I., Harvey, K., Ward, H., White, J. H., Evans, L., Duguid, I. C., et al. (2003). Isoform heterogeneity of the human gephyrin gene (GPHN), binding domains to the glycine receptor, and mutation analysis in hyperekplexia. *J. Biol. Chem.* 278, 24688–24696. doi: 10.1074/jbc.M301070200
- Rees, M. I., Lewis, T. M., Kwok, J. B., Mortier, G. R., Govaert, P., Snell, R. G., et al. (2002). Hyperekplexia associated with compound heterozygote mutations in the β subunit of the human inhibitory glycine receptor (GLRB). *Hum. Mol. Genet.* 11, 853–860. doi: 10.1093/hmg/11.7.853
- Reichling, D. B., Kyzozis, A., Wang, J., and MacDermott, A. B. (1994). Mechanisms of GABA and glycine depolarization-induced calcium transients in rat dorsal horn neurons. *J. Physiol.* 476, 411–421. doi: 10.1113/jphysiol.1994.sp020142
- Ribera, A. B., and Nüsslein-Volhard, C. (1998). Zebrafish touch-insensitive mutants reveal an essential role for the developmental regulation of sodium current. *J. Neurosci.* 18, 9181–9191.
- Rigo, J. M., and Legendre, P. (2006). Frequency-dependent modulation of glycine receptor activation recorded from the zebrafish larvae hindbrain. *Neuroscience* 140, 389–402. doi: 10.1016/j.neuroscience.2006.01.057
- Rizk, T. M., and Mahmoud, A. A. H. (2014). Novel GLRB gene mutation in a Saudi baby with hyperekplexia. *Pediatr. Neurol.* 53, 54.
- Roberts, A., Li, W. C., Soffe, S. R., and Wolf, E. (2008). Origin of excitatory drive to a spinal locomotor network. *Brain Res. Rev.* 57, 22–28. doi: 10.1016/j.brainresrev.2007.06.015
- Rossi, A., Kontarakis, Z., Gerri, C., Nolte, H., Hölper, S., Krüger, M., et al. (2015). Genetic compensation induced by deleterious mutations but not gene knockdowns. *Nature* 524, 230–233. doi: 10.1038/nature14580
- Saint-Amant, L., and Drapeau, P. (1998). Time course of the development of motor behaviors in the zebrafish embryo. *J. Neurobiol.* 37, 622–632. doi: 10.1002/(SICI)1097-4695(199812)37:4<622::AID-NEU10>3.0.CO;2-S
- Saint-Amant, L., and Drapeau, P. (2001). Synchronization of an embryonic network of identified spinal interneurons solely by electrical coupling. *Neuron* 31, 1035–1046. doi: 10.1016/S0896-6273(01)00416-0
- Salling, M. C., and Harrison, N. L. (2014). Strychnine-sensitive glycine receptors on pyramidal neurons in layers II/III of the mouse prefrontal cortex are tonically activated. *J. Neurophysiol.* 112, 1169–1178. doi: 10.1152/jn.00714.2013
- Sander, J. D., Dahlborg, E. J., Goodwin, M. J., Cade, L., Zhang, F., Cifuentes, D., et al. (2011a). Selection-free zinc-finger-nuclease engineering by context-dependent assembly (CoDA). *Nat. Methods* 8, 67–69. doi: 10.1038/nmeth.1542
- Sander, J. D., Cade, L., Khayter, C., Reyon, D., Peterson, R. T., Joung, J. K., et al. (2011b). Targeted gene disruption in somatic zebrafish cells using engineered TALENs. *Nat. Biotechnol.* 29, 697–698. doi: 10.1038/nbt.1934
- Sassò-Pognetto, M., Wässle, H., and Grünert, U. (1994). Glycinergic synapses in the rod pathway of the rat retina: cone bipolar cells express the $\alpha 1$ subunit of the glycine receptor. *J. Neurosci.* 14, 5131–5146.
- Scheer, N., and Campos-Ortega, J. A. (1999). Use of the Gal4-UAS technique for targeted gene expression in the zebrafish. *Mech. Dev.* 80, 153–158. doi: 10.1016/S0925-4773(98)00209-3
- Schmid, K., Böhrer, G., and Gebauer, K. (1991). Glycine receptor-mediated fast synaptic inhibition in the brainstem respiratory system. *Respir. Physiol.* 84, 351–361. doi: 10.1016/0034-5687(91)90129-7
- Schmid, K., Foutz, A. S., and Denavit-Saubié, M. (1996). Inhibitions mediated by glycine and GABA A receptors shape the discharge pattern of bulbar respiratory neurons. *Brain Res.* 710, 150–160. doi: 10.1016/0006-8993(95)01380-6
- Schmitz, Y., Castagna, C., Mrejeru, A., Lizardi-Ortiz, J. E., Klein, Z., Lindsley, C. W., et al. (2013). Glycine transporter-1 inhibition promotes striatal axon sprouting via NMDA receptors in dopamine neurons. *J. Neurosci.* 33, 16778–16789. doi: 10.1523/JNEUROSCI.3041-12.2013
- Schmitz, Y., Luccarelli, J., Kim, M., Wang, M., and Sulzer, D. (2009). Glutamate controls growth rate and branching of dopaminergic axons. *J. Neurosci.* 29, 11973–11981. doi: 10.1523/JNEUROSCI.2927-09.2009
- Schneider, V. A., and Granato, M. (2006). The myotomal diwanka (lh3) glycosyltransferase and type XVIII collagen are critical for motor growth cone migration. *Neuron* 50, 683–695. doi: 10.1016/j.neuron.2006.04.024
- Schoonheim, P. J., Arrenberg, A. B., Del Bene, F., and Baier, H. (2010). Optogenetic localization and genetic perturbation of saccade-generating neurons in zebrafish. *J. Neurosci.* 30, 7111–7120. doi: 10.1523/JNEUROSCI.5193-09.2010
- Schredelseker, J., Dayal, A., Schwerte, T., Franzini-Armstrong, C., and Grabner, M. (2009). Proper restoration of excitation-contraction coupling in the dihydropyridine receptor $\beta 1$ -null zebrafish relaxed is an exclusive function of the $\beta 1a$ subunit. *J. Biol. Chem.* 284, 1242–1251. doi: 10.1074/jbc.M807767200
- Schredelseker, J., Di Biase, V., Obermair, G. J., Felder, E. T., Flucher, B. E., Franzini-Armstrong, C., et al. (2005). The $\beta 1a$ subunit is essential for the assembly of dihydropyridine-receptor arrays in skeletal muscle. *Proc. Natl. Acad. Sci. U.S.A.* 102, 17219–17224. doi: 10.1073/pnas.0508710102
- Schwale, C., Schumacher, S., Bruehl, C., Titz, S., Schlicksupp, A., Kokocinska, M., et al. (2016). KCC2 knockdown impairs glycinergic synapse maturation in cultured spinal cord neurons. *Histochem. Cell Biol.* 45, 637–646. doi: 10.1007/s00418-015-1397-0
- Scott, E. K., Mason, L., Arrenberg, A. B., Ziv, L., Gosse, N. J., Xiao, T., et al. (2007). Targeting neural circuitry in zebrafish using GAL4 enhancer trapping. *Nat. Methods* 4, 323–326. doi: 10.1038/nmeth1033
- Shen, H. Y., van Vliet, E. A., Bright, K. A., Hanthorn, M., Lytle, N. K., Gorter, J., et al. (2015). Glycine transporter 1 is a target for the treatment of epilepsy. *Neuropharmacology* 99, 554–565. doi: 10.1016/j.neuropharm.2015.08.031
- Sidi, S., Friedrich, R. W., and Nicolson, T. (2003). NompC TRP channel required for vertebrate sensory hair cell mechanotransduction. *Science* 301, 96–99. doi: 10.1126/science.1084370
- Simon, J., Wakimoto, H., Fujita, N., Lalande, M., and Barnard, E. A. (2004). Analysis of the set of GABAA receptor genes in the human genome. *J. Biol. Chem.* 279, 41422–41435. doi: 10.1074/jbc.M401354200
- Singer, J. H., Talley, E. M., Bayliss, D. A., and Berger, A. J. (1998). Development of glycinergic synaptic transmission to rat brain stem motoneurons. *J. Neurophysiol.* 80, 2608–2620.
- Sivasubbu, S., Balciunas, D., Davidson, A. E., Pickart, M. A., Hermanson, S. B., Wangenstein, K. J., et al. (2006). Gene-breaking transposon mutagenesis reveals an essential role for histone H2afza in zebrafish larval development. *Mech. Dev.* 123, 513–529. doi: 10.1016/j.mod.2006.06.002
- Sola, M., Bavro, V. N., Timmins, J., Franz, T., Ricard-Blum, S., Schoehn, G., et al. (2004). Structural basis of dynamic glycine receptor clustering by gephyrin. *EMBO J.* 23, 2510–2519. doi: 10.1038/sj.emboj.7600256
- Song, W., Chattipakorn, S. C., and McMahon, L. L. (2006). Glycine-gated chloride channels depress synaptic transmission in rat hippocampus. *J. Neurophysiol.* 95, 2366–2379. doi: 10.1152/jn.00386.2005
- Specht, C. G., Grünwald, N., Pascual, O., Rostgaard, N., Schwarz, G., and Triller, A. (2011). Regulation of glycine receptor diffusion properties and gephyrin interactions by protein kinase C. *EMBO J.* 30, 3842–3853. doi: 10.1038/emboj.2011.276
- Specht, C. G., Izeddin, I., Rodriguez, P. C., El Beheiry, M., Rostaing, P., Darzacq, X., et al. (2013). Quantitative nanoscopy of inhibitory synapses: counting gephyrin molecules and receptor binding sites. *Neuron* 79, 308–321. doi: 10.1016/j.neuron.2013.05.013
- Steffen, L. S., Guyon, J. R., Vogel, E. D., Howell, M. H., Zhou, Y., Weber, G. J., et al. (2007). The zebrafish runzel muscular dystrophy is linked to the titin gene. *Dev. Biol.* 309, 180–192. doi: 10.1016/j.ydbio.2007.06.015
- Stemple, D. L. (2004). TILLING—a high-throughput harvest for functional genomics. *Nat. Rev. Genet.* 5, 145–150. doi: 10.1038/nrg1273
- Suli, A., Guler, A. D., Raible, D. W., and Kimelman, D. (2014). A targeted gene expression system using the tryptophan repressor in zebrafish shows no silencing in subsequent generations. *Development* 141, 1167–1174. doi: 10.1242/dev.100057
- Takahashi, T., Momiyama, A., Hirai, K., Hishinuma, F., and Akagi, H. (1992). Functional correlation of fetal and adult forms of glycine receptors with developmental changes in inhibitory synaptic receptor channels. *Neuron* 9, 1155–1161. doi: 10.1016/0896-6273(92)90073-M
- Tallini, Y. N., Ohkura, M., Choi, B. R., Ji, G., Imoto, K., Doran, R., et al. (2006). Imaging cellular signals in the heart in vivo: cardiac expression of the high-signal Ca^{2+} indicator GCaMP2. *Proc. Natl. Acad. Sci. U.S.A.* 103, 4753–4758. doi: 10.1073/pnas.0509378103
- Tanimoto, M., Ota, Y., Horikawa, K., and Oda, Y. (2009). Auditory input to CNS is acquired coincidentally with development of inner ear after formation of functional afferent pathway in zebrafish. *J. Neurosci.* 29, 2762–2767. doi: 10.1523/JNEUROSCI.5530-08.2009
- Tian, L., Hires, S. A., Mao, T., Huber, D., Chiappe, M. E., Chalasani, S. H., et al. (2009). Imaging neural activity in worms, flies and mice with improved GCaMP calcium indicators. *Nat. Methods* 6, 875–881. doi: 10.1038/nmeth.1398

- Tsai, G., Ralph-Williams, R. J., Martina, M., Bergeron, R., Berger-Sweeney, J., Dunham, K. S., et al. (2004). Gene knockout of glycine transporter 1: characterization of the behavioral phenotype. *Proc. Natl. Acad. Sci. U.S.A.* 101, 8485–8490. doi: 10.1073/pnas.0402662101
- Turecek, R., and Trussell, L. O. (2001). Presynaptic glycine receptors enhance transmitter release at a mammalian central synapse. *Nature* 411, 587–590. doi: 10.1038/35079084
- Tyagarajan, S. K., and Fritschy, J. M. (2014). Gephyrin: a master regulator of neuronal function. *Nat. Rev. Neurosci.* 15, 141–156. doi: 10.1038/nrn3670
- Urnov, F. D., Miller, J. C., Lee, Y. L., Beausejour, C. M., Rock, J. M., Augustus, S., et al. (2005). Highly efficient endogenous human gene correction using designed zinc-finger nucleases. *Nature* 435, 646–651. doi: 10.1038/nature03556
- Villefranc, J. A., Amigo, J., and Lawson, N. D. (2007). Gateway compatible vectors for analysis of gene function in the zebrafish. *Dev. Dyn.* 236, 3077–3087. doi: 10.1002/dvdy.21354
- Wang, C., Shimizu-Okabe, C., Watanabe, K., Okabe, A., Matsuzaki, H., Ogawa, T., et al. (2002). Developmental changes in KCC1, KCC2, and NKCC1 mRNA expressions in the rat brain. *Dev. Brain Res.* 139, 59–66. doi: 10.1016/S0165-3806(02)00536-9
- Wang, F., Xiao, C., and Ye, J. H. (2005). Taurine activates excitatory non-synaptic glycine receptors on dopamine neurones in ventral tegmental area of young rats. *J. Physiol.* 565, 503–516. doi: 10.1113/jphysiol.2005.085423
- Wang, M., Wen, H., and Brehm, P. (2008). Function of neuromuscular synapses in the zebrafish choline-acetyltransferase mutant bajan. *J. Neurophysiol.* 100, 1995–2004. doi: 10.1152/jn.90517.2008
- Wässle, H., Heinze, L., Ivanova, E., Majumdar, S., Weiss, J., Harvey, R. J., et al. (2009). Glycinergic transmission in the Mammalian retina. *Front. Mol. Neurosci.* 2:6. doi: 10.3389/neuro.02.006.2009
- Watanabe, E., and Akagi, H. (1995). Distribution patterns of mRNAs encoding glycine receptor channels in the developing rat spinal cord. *Neurosci. Res.* 23, 377–382. doi: 10.1016/0168-0102(95)00972-V
- Weiss, J., O'sullivan, G. A., Heinze, L., Chen, H. X., Betz, H., and Wässle, H. (2008). Glycinergic input of small-field amacrine cells in the retinas of wildtype and glycine receptor deficient mice. *Mol. Cell. Neurosci.* 37, 40–55. doi: 10.1016/j.mcn.2007.08.012
- Weltzien, F., Puller, C., O'Sullivan, G. A., Paarmann, I., and Betz, H. (2012). Distribution of the glycine receptor β -subunit in the mouse CNS as revealed by a novel monoclonal antibody. *J. Comp. Neurol.* 520, 3962–3981. doi: 10.1002/cne.23139
- White, R. M., Sessa, A., Burke, C., Bowman, T., LeBlanc, J., Ceol, C., et al. (2008). Transparent adult zebrafish as a tool for in vivo transplantation analysis. *Cell Stem Cell* 2, 183–189. doi: 10.1016/j.stem.2007.11.002
- Wienholds, E., Schulte-Merker, S., Walderich, B., and Plasterk, R. H. (2002). Target-selected inactivation of the zebrafish *rag1* gene. *Science* 297, 99–102. doi: 10.1126/science.1071762
- Wienholds, E., Van Eeden, F., Kusters, M., Mudde, J., Plasterk, R. H., and Cuppen, E. (2003). Efficient target-selected mutagenesis in zebrafish. *Genome Res.* 13, 2700–2707. doi: 10.1101/gr.1725103
- Winkelmann, A., Maggio, N., Eller, J., Caliskan, G., Semtner, M., Häussler, U., et al. (2014). Changes in neural network homeostasis trigger neuropsychiatric symptoms. *J. Clin. Invest.* 124, 696–711. doi: 10.1172/JCI71472
- Xiong, W., Cui, T., Cheng, K., Yang, F., Chen, S. R., Willenbring, D., et al. (2012). Cannabinoids suppress inflammatory and neuropathic pain by targeting $\alpha 3$ glycine receptors. *J. Exp. Med.* 209, 1121–1134.
- Yang, Z., Aubrey, K. R., Alroy, I., Harvey, R. J., Vandenberg, R. J., and Lynch, J. W. (2008). Subunit-specific modulation of glycine receptors by cannabinoids and N-arachidonyl-glycine. *Biochem. Pharmacol.* 76, 1014–1023. doi: 10.1016/j.bcp.2008.07.037
- Yang, Z., Taran, E., Webb, T. I., and Lynch, J. W. (2012). Stoichiometry and subunit arrangement of $\alpha 1\beta$ glycine receptors as determined by atomic force microscopy. *Biochemistry* 51, 5229–5231. doi: 10.1021/bi300063m
- Ye, J. H., Sokol, K. A., and Bhavsar, U. (2009). Glycine receptors contribute to hypnosis induced by ethanol. *Alcohol. Clin. Exp. Res.* 33, 1069–1074. doi: 10.1111/j.1530-0277.2009.00928.x
- Ye, J. H., Wang, F., Krnjević, K., Wang, W., Xiong, Z. G., and Zhang, J. (2004). Presynaptic glycine receptors on GABAergic terminals facilitate discharge of dopaminergic neurons in ventral tegmental area. *J. Neurosci.* 24, 8961–8974. doi: 10.1523/JNEUROSCI.2016-04.2004
- Young-Pearse, T. L., Ivic, L., Kriegstein, A. R., and Cepko, C. L. (2006). Characterization of mice with targeted deletion of glycine receptor $\alpha 2$. *Mol. Cell. Biol.* 26, 5728–5734. doi: 10.1128/MCB.00237-06
- Zeilhofer, H. U. (2005). The glycinergic control of spinal pain processing. *Cell. Mol. Life Sci.* 62, 2027–2035. doi: 10.1007/s00018-005-5107-2
- Zeller, J., and Granato, M. (1999). The zebrafish *diwanka* gene controls an early step of motor growth cone migration. *Development* 126, 3461–3472.
- Zeller, J., Schneider, V., Malayaman, S., Higashijima, S., Okamoto, H., Gui, J., et al. (2002). Migration of zebrafish spinal motor nerves into the periphery requires multiple myotome-derived cues. *Dev. Biol.* 252, 241–256. doi: 10.1006/dbio.2002.0852
- Zhang, C., Rompani, S. B., Roska, B., and McCall, M. A. (2014). Adeno-associated virus-RNAi of GlyR $\alpha 1$ and characterization of its synapse-specific inhibition in OFF alpha transient retinal ganglion cells. *J. Neurophysiol.* 112, 3125–3137. doi: 10.1152/jn.00505.2014
- Zhang, L. H., Gong, N., Fei, D., Xu, L., and Xu, T. L. (2008). Glycine uptake regulates hippocampal network activity via glycine receptor-mediated tonic inhibition. *Neuropsychopharmacology* 33, 701–711. doi: 10.1038/sj.npp.1301449
- Zhang, L. H., Xu, L., and Xu, T. L. (2006). Glycine receptor activation regulates short-term plasticity in CA1 area of hippocampal slices of rats. *Biochem. Biophys. Res. Commun.* 344, 721–726. doi: 10.1016/j.bbrc.2006.03.198
- Zhang, Y., Dixon, C. L., Keramidas, A., and Lynch, J. W. (2015). Functional reconstitution of glycinergic synapses incorporating defined glycine receptor subunit combinations. *Neuropharmacology* 89, 391–397. doi: 10.1016/j.neuropharm.2014.10.026
- Zhou, W., Saint-Amant, L., Hirata, H., Cui, W. W., Sprague, S. M., and Kuwada, J. Y. (2006). Non-sense mutations in the dihydropyridine receptor $\beta 1$ gene, CACNB1, paralyze zebrafish relaxed mutants. *Cell Calcium* 39, 227–236. doi: 10.1016/j.ceca.2005.10.015
- Zhu, P., Narita, Y., Bundschuh, S. T., Fajardo, O., Zhang Schäfer, Y. P., Chattopadhyaya, B., et al. (2009). Optogenetic dissection of neuronal circuits in zebrafish using viral gene transfer and the Tet system. *Front. Neural Circuits* 3:21. doi: 10.3389/neuro.04.021.2009
- Zottoli, S. J. (1977). Correlation of the startle reflex and Mauthner cell auditory responses in unrestrained goldfish. *J. Exp. Biol.* 66, 243–254.

Conflict of Interest Statement: The authors declare that the research was conducted in the absence of any commercial or financial relationships that could be construed as a potential conflict of interest.

Copyright © 2016 Ogino and Hirata. This is an open-access article distributed under the terms of the Creative Commons Attribution License (CC BY). The use, distribution or reproduction in other forums is permitted, provided the original author(s) or licensor are credited and that the original publication in this journal is cited, in accordance with accepted academic practice. No use, distribution or reproduction is permitted which does not comply with these terms.



Age-Dependent Degeneration of Mature Dentate Gyrus Granule Cells Following NMDA Receptor Ablation

Yasuhito Watanabe¹, Michaela K. Müller^{2,3}, Jakob von Engelhardt^{2,3}, Rolf Sprengel⁴, Peter H. Seeburg⁴ and Hannah Monyer^{1*}

¹ Department of Clinical Neurobiology, University Hospital and German Cancer Research Center Heidelberg, Heidelberg, Germany, ² Synaptic Signalling and Neurodegeneration, German Center for Neurodegenerative Diseases, Bonn, Germany, ³ Synaptic Signalling and Neurodegeneration, German Cancer Research Center Heidelberg, Heidelberg, Germany, ⁴ Department of Molecular Neurobiology, Max Planck Institute for Medical Research, Heidelberg, Germany

N-methyl-*D*-aspartate receptors (NMDARs) in all hippocampal areas play an essential role in distinct processes of memory formation as well as in sustaining cell survival of postnatally generated neurons in the dentate gyrus (DG). In contrast to the beneficial effects, over-activation of NMDARs has been implicated in many acute and chronic neurological diseases, reason why therapeutic approaches and clinical trials involving receptor blockade have been envisaged for decades. Here we employed genetically engineered mice to study the long-term effect of NMDAR ablation on selective hippocampal neuronal populations. Ablation of either GluN1 or GluN2B causes degeneration of the DG. The neuronal demise affects mature neurons specifically in the dorsal DG and is NMDAR subunit-dependent. Most importantly, the degenerative process exacerbates with increasing age of the animals. These results lead us to conclude that mature granule cells in the dorsal DG undergo neurodegeneration following NMDAR ablation in aged mouse. Thus, caution needs to be exerted when considering long-term administration of NMDAR antagonists for therapeutic purposes.

Keywords: NMDA receptors, aging, neurodegeneration, hippocampus, dentate gyrus, mouse

OPEN ACCESS

Edited by:

Robert J. Harvey,
UCL School of Pharmacy, UK

Reviewed by:

Hansjürgen Volkmer,
Universität Tübingen, Germany
Hansen Wang,
University of Toronto, Canada

*Correspondence:

Hannah Monyer
h.monyer@dkfz-heidelberg.de

Received: 06 November 2015

Accepted: 18 December 2015

Published: 12 January 2016

Citation:

Watanabe Y, Müller MK, von Engelhardt J, Sprengel R, Seeburg PH and Monyer H (2016) Age-Dependent Degeneration of Mature Dentate Gyrus Granule Cells Following NMDA Receptor Ablation. *Front. Mol. Neurosci.* 8:87. doi: 10.3389/fnmol.2015.00087

INTRODUCTION

The dentate gyrus (DG) in the hippocampus has been the focus of numerous studies for two main reasons. Firstly, the DG is a major station in the trisynaptic pathway that conveys input from the cortex to the hippocampus. DG granule cells excite CA3 neurons, which in turn project to CA1 neurons. All hippocampal subregions have been much investigated in the context of distinct forms of plasticity, learning, and memory (e.g., McHugh et al., 2007; Niewoehner et al., 2007; Gu et al., 2012; Nakashiba et al., 2012). Secondly, the DG is one of the two principal neurogenic niches in the postnatal brain, and has been therefore frequently studied in the context of neurogenesis (reviewed in Jessberger and Gage, 2014). Some studies addressed questions that link these two research areas. Thus, young DG granule cells support pattern separation, whereas mature granule cells facilitate pattern completion (Nakashiba et al., 2012). The DG comprises a dorsal and a ventral part that can be distinguished on anatomical grounds, and also based on distinct functions that the two areas support. Thus, the dorsal DG is involved in cognitive functions such as spatial memory, whilst the ventral DG supports brain functions related to stress, emotion, and affect (reviewed in Fanselow and Dong, 2010).

Several decades of pharmacological and genetic research have taught us that *N*-methyl-*D*-aspartate receptors (NMDARs) are intricately linked to hippocampus-dependent memory (reviewed in Bannerman et al., 2014). Mouse genetics was fundamental to correlate subregions of the hippocampus, including the DG, with distinct functions supporting spatial memory (McHugh et al., 2007; Niewoehner et al., 2007). Thus, NMDARs in the DG are required for pattern separation (McHugh et al., 2007) and spatial working memory (Niewoehner et al., 2007). Furthermore, studies based on mouse mutants were instrumental in helping delineate the differential functions of NMDAR subunits. DG granule cells, like most neurons in the hippocampus, harbor NMDARs built from the obligatory GluN1 subunit (encoded by *Grin1*) and the developmentally regulated GluN2A and GluN2B subunits (encoded by *Grin2a* and *Grin2b*, respectively; Monyer et al., 1994; Rodenas-Ruano et al., 2012; Paoletti et al., 2013). NMDARs have been much discussed with respect to their function in postnatal neurogenesis. Thus, NMDARs in postnatally generated DG granule cells are a prerequisite for the survival of newborn neurons (Tashiro et al., 2006).

In mature neurons, over-activation or suppression of NMDARs are detrimental for cell function and survival. Thus, enhanced receptor activity as it occurs in many pathophysiological neurological diseases, e.g., stroke, epilepsy, induces excitotoxic cell death (reviewed in Choi, 1992; Paoletti et al., 2013). Conversely, pharmacological blockade of NMDARs for hours and days also has an adverse effect, as it induces cellular vacuolization in pyramidal neurons in many cortical brain areas (e.g., Ikonomidou et al., 1999). The effect of prolonged or even permanent NMDAR blockade on the survival of mature neurons has not yet been tested systematically. Moreover, a potential role of NMDARs for cell survival in aged animals has not been investigated. This is surprising, given that the NMDAR has been a key candidate when considering therapeutic strategies for stroke.

Here we took advantage of genetically modified mice and addressed the question whether the survival of mature and aged neurons depends on NMDARs. We demonstrate that in the hippocampus, mature neurons in the DG, but not in the CA1 region, require intact NMDAR function for survival.

MATERIALS AND METHODS

Animals

Animals were housed and handled according to the respected animal welfare guidelines and rules of the Max Planck Society and the Germany government animal welfare office in Karlsruhe, Germany. The following genetically modified male and female C57Bl/6N mice were used in this study: DG and CA1 selective *Grin1* knockout (*Grin1*^{ΔDGCAl}) mice (Bannerman et al., 2012), DG selective *Grin1* knockout (*Grin1*^{ΔDG}, previously called *NR1*^{ΔDG}) mice (Niewoehner et al., 2007), *Grin2a* knockout (*Grin2a*^{-/-}, previously called homozygous *GluR1* mutant) mice (Sakimura et al., 1995), and DG and CA1 selective *Grin2b* knockout (*Grin2b*^{ΔDGCAl}, previously called *NR2B*^{ΔHPC}) mice (von Engelhardt et al., 2008).

Grin1^{ΔDGCAl} mice are homozygous for the floxed *Grin1* and carry two transgenes, *Tg*^{LC1} and *Tg*^{CN12}, which enable doxycycline-sensitive, Cre-mediated gene ablation in CA1 and DG excitatory neurons and piriform cortex in the adult brain by use of a *CamKIIa/Grin2c* hybrid promoter (Bannerman et al., 2012). *Grin1*^{ΔDG} mice are homozygous for *Grin1* and carry the transgenes *Tg*^{LC1} and *Tg*^{CN10-itTA}, which are the same transgenes as in *Tg*^{CN12}, but yield differential expression in the two transgenic mouse lines. In *Grin1*^{ΔDG} mice, Cre is specifically expressed in the DG granule cells and some CA1 pyramidal neurons (Niewoehner et al., 2007) which express calbindin (CB; data not shown). *Grin2b*^{ΔDGCAl} mice are homozygous for the floxed *Grin2b* and carry *Tg*^{LC1} and *Tg*^{CN12}. For the selective expression of Cre in *Grin1*^{ΔDGCAl}, *Grin1*^{ΔDG} and *Grin2b*^{ΔDGCAl} mice, doxycycline was given via the drinking water to pregnant mice to suppress Cre expression of the offspring during embryonic development, and was withdrawn after birth (Bannerman et al., 2012). Doxycycline treatment was performed under the license 35-9185.81/G71/10 of the governmental council in the Karlsruhe, Germany. In *Grin1*^{ΔDGCAl} mice, Cre expression becomes detectable as early as postnatal day P28 (Bannerman et al., 2012). Control mice (i.e., mice with no Cre expression) to be compared with *Grin1*^{ΔDGCAl} and *Grin1*^{ΔDG} mice were homozygous for floxed *Grin1* and carried one or none of the transgenes. Control mice for the *Grin2a* knockout mice are wild-type mice. Control mice for *Grin2b*^{ΔDGCAl} mice were homozygous for floxed *Grin2b* and carried one or none of the transgene. As control mice for Cre expressing mice (carrying only *Tg*^{LC1} and *Tg*^{CN12} but no floxed gene) we used either wild-type mice or carriers of one of the transgenes. Following mice are available at EMMA (<https://www.infrafrontier.eu>) with respective EMMA ID: Floxed *Grin1* mice (EM: 09220), mice carrying *Tg*^{LC1} and *Tg*^{CN12} transgenes (EM: 09256), and mice carrying *Tg*^{CN10-itTA} transgene (EM: 09255). All animal experiments were performed according to the regulations of Heidelberg University/German Cancer Research Center/Max Planck Institute.

Immunohistochemistry

Mice were perfused with phosphate buffered saline (PBS, pH 7.4) followed by 4% paraformaldehyde (PFA). Brains were removed and postfixed with 2% PFA at 4°C overnight. Coronal sections were prepared at 50 μm using a vibratome. Sections were blocked and permeabilized with 5% bovine serum albumin (BSA) in PBS containing 0.5% Triton X-100, incubated with primary antibodies overnight at 4°C, then incubated with appropriate secondary antibodies. Primary and secondary antibodies were diluted in PBS containing 0.2% Triton X-100 before incubation. Sections were washed three times with PBS after every antibody incubation step. Sections were counterstained with DAPI (Invitrogen, Carlsbad, CA, USA) after the secondary antibody incubation step. For GluN1 staining, before blocking the sections, antigen retrieval was performed as follows. Sections were immersed in 10 mM sodium citrate (pH 6.0) and heated in a microwave oven for 5 min at 650 W twice with a 5 min break in between, kept for 20 min at room temperature, and washed twice with PBS. The following

primary antibodies were used: rabbit active caspase-3 (catalog # AF835; 1:2000; polyclonal; R&D systems, Minneapolis, MN, USA), mouse CB D-28k (300; 1:2000; monoclonal; Swant, Switzerland), goat DCX (sc-8066; 1:500; polyclonal; Santa Cruz Biotechnology, Santa Cruz, CA, USA), goat Sox-2 (sc-17320; 1:500; polyclonal; Santa Cruz Biotechnology), mouse GFAP (G3893; 1:10000; monoclonal; Sigma-Aldrich, Saint Louis, MO, USA), rabbit S100 β (721; 1:2000; polyclonal; Swant), rabbit NMDAR1 (for GluN1; AB9864R; 1:250; monoclonal; Millipore, Billerica, MA, USA), rabbit Cre [1:2000; polyclonal; a generous gift from Dr. Günther Schütz (Kellendonk et al., 1999)], mouse Mineralocorticoid receptor [6G1; 1:100; monoclonal; a generous gift from Dr. Elise P. Gomez-Sanchez (Gomez-Sanchez et al., 2006)].

Nissl Staining

Sections were mounted on microscope slides, air dried, immersed in 0.1% thionin, washed with water, dehydrated in 70, 95, and 100% ethanol for several minutes, cleared in xylene for 5 min twice. The slides were subsequently covered with Eukitt mounting medium, and mounted with coverslips.

Image Processing and Quantification

Fluorescent images were acquired using a LSM 700 confocal microscope (Zeiss, Oberkochen, Germany). A single focal plane picture of the whole DG area from one hemisphere was taken from each brain section using a tile scan function of the confocal microscope. Bright field images were acquired using a BX51W microscope (Olympus, Tokyo, Japan). All quantification analyses were done using ImageJ software. The DG thickness was measured from both dorsal/suprapyramidal blade and ventral/infrapyramidal blade. Care was taken to minimize variations in choosing sections in the rostrocaudal axis. Several, typically three, DG images from one animal were used for the analysis whenever possible. Measured values were averaged to create one representative value for each animal. To calculate DG thickness, a part of the DG with uniform thickness was selected as rectangular area of interest, and the area was then divided by the base length of the rectangular area. Dorsal DG thickness was calculated from the proximal areas to the crest where the two blades connect. Ventral DG thickness was calculated from the most ventral area close to the end of the blade. Degenerating cells were counted using the green channel after staining with antibody against active caspase-3. A cell was considered DCX-positive when the signal outlined the shape of a cell body with processes. To confirm that active caspase-3 (stained in green fluorescence) is expressed in CB-positive (stained in red fluorescence) cells, images of active caspase-3 positive cells were taken when there was no auto-fluorescence signal from degenerating cells in an unstained (far-red fluorescence) channel. Degenerating cells were counted as follows. The DG area to be examined was selected with selection tools. Putative degenerating cells were selected by MaxEntropy method of the autothreshold function, and signals bigger than 3 μm^2 were counted using “Analyze particles” function. We confirmed that this counting method matches manual counting. This method enabled us to quantify degenerating cells more objectively than manual

counting. Except for degenerating cells, all other fluorescently labeled cells were counted manually using cell counter function of ImageJ. Three to six images of the DG were used for counting fluorescent positive cells, and the obtained values were pooled to obtain one value for each mouse.

Statistical Analysis

Quantifications were carried out without referring to the genotype information. Differences or correlations between groups were examined using the statistical tests indicated in the figure legends. Statistical analyses were performed using R 3.1.3. Values were expressed as mean \pm standard deviation unless otherwise mentioned in the figure legends. Values of $p < 0.05$ were considered statically significant (* $p < 0.05$, ** $p < 0.005$, *** $p < 0.0005$).

RESULTS

GluN1 Ablation Causes Progressive Degeneration of Granule Cells in the Dorsal DG

In 6 months old *Grin1* ^{ΔDGCA1} mice, in which *Grin1* is deleted in both the DG and CA1, we found a reduced thickness of the DG granule cell layer (**Figures 1A,B,H**). This phenotype could be readily detected by eye after DAPI staining, and was more pronounced in 18 months old mice (**Figures 1C,D,H**). In contrast, there was no apparent abnormality in the CA1 region in 18 months old *Grin1* ^{ΔDGCA1} mice (**Figures 1E,F,I**). Expression of active caspase-3 in CB-positive granule cells was indicative of mature granule cell demise (**Figure 1G**). The alteration in the granule cell layer was restricted to the dorsal DG. In 18 months old mice, the ventral DG in *Grin1* ^{ΔDGCA1} mice was comparable to that of controls (Supplementary Figures S1A–C). We confirmed GluN1 ablation in the CA1 region and in both the dorsal and ventral DG of 6 months old *Grin1* ^{ΔDGCA1} mice by immunohistochemistry (Supplementary Figures S1D–G). Neuronal degeneration did not result from Cre expression itself, but was a consequence of *Grin1* deletion via Cre-mediated recombination, as the DG was normal in Cre expressing mice with wild-type *Grin1* alleles (Supplementary Figure S2). Thus, ablation of NMDARs in CA1 and DG causes selective degeneration of granule cells in the dorsal DG.

Neuronal Degeneration in *Grin1* ^{ΔDGCA1} Mice Affects Mature DG Granule Cells

To corroborate that NMDAR deletion causes cell death of mature DG granule cells, we compared the distribution of immature doublecortin (DCX) expressing cells (**Figure 2A**) and of degenerating cells visualized by active caspase-3 immunostaining (**Figure 2B**) within the DG granule cell layer (**Figure 2C**). If degeneration affected primarily immature DG granule cells, degenerating cells should be confined to the innermost rim of the DG granule cell layer that harbors DCX expressing neurons. This, however, was not the case. Degenerating cells were found throughout the entire DG granule cell layer (**Figure 2D**). We next

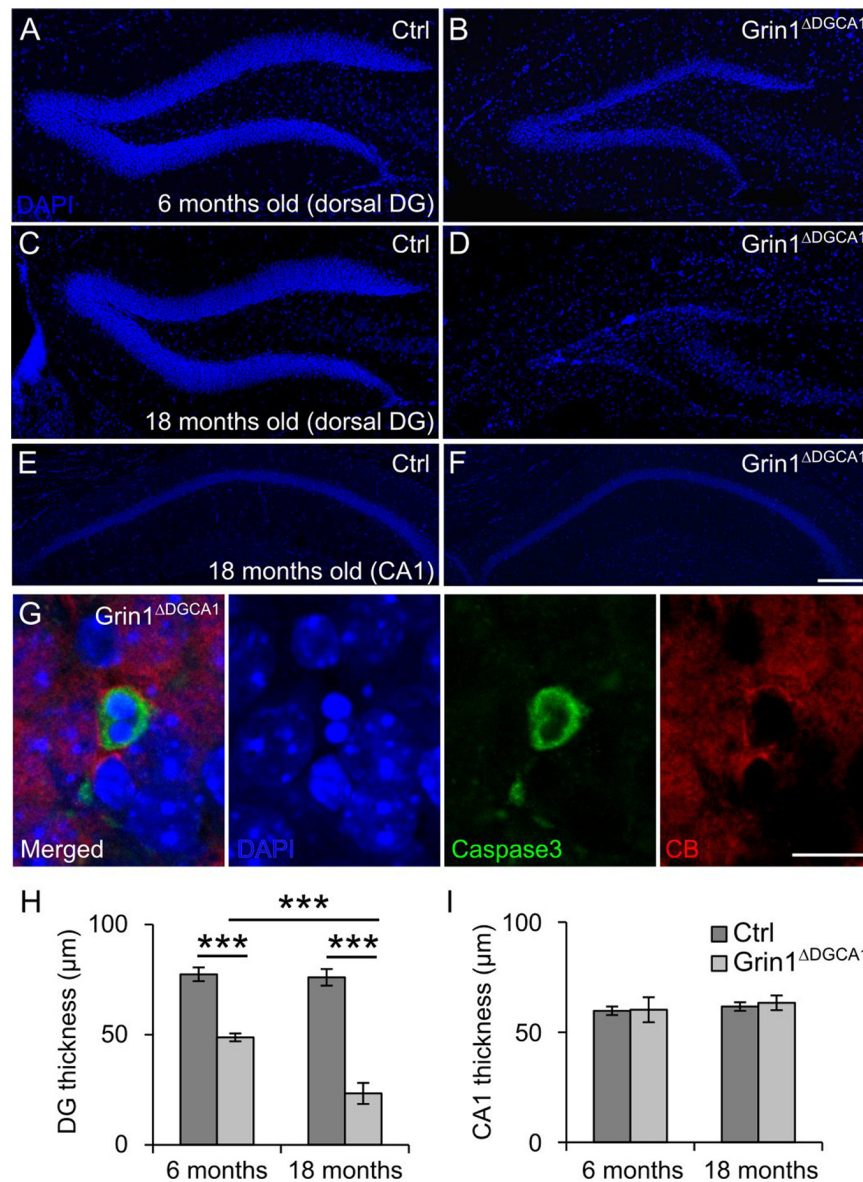


FIGURE 1 | GluN1 deletion causes age-dependent neurodegeneration in the dorsal dentate gyrus (DG). (A) DAPI staining illustrating a section of a dorsal DG from a 6 months old control (Ctrl) mouse. (B) DAPI staining of a dorsal DG from a 6 months old *Grin1*^{ΔDGCA1} mouse. Note the thinning of the dentate granule cell layer. (C) DAPI staining illustrating a section of a dorsal DG from an 18 months old control mouse. (D) DAPI staining of a dorsal DG from an 18 months old *Grin1*^{ΔDGCA1} mouse. Note the thinning of the dentate granule cell layer following profound neurodegeneration. (E) DAPI staining illustrating a section of a dorsal CA1 from an 18 months old control mouse. (F) DAPI staining of a dorsal DG from an 18 months old *Grin1*^{ΔDGCA1} mouse. There is no difference between the two genotypes. (G) Representative image from the DG showing an apoptotic, i.e., caspase-3-positive, CB-positive neuron in a 6 months old *Grin1*^{ΔDGCA1} mouse. The section is counterstained with DAPI. (H) Quantitative evaluation of dorsal DG thickness in 6 and 18 months old control and *Grin1*^{ΔDGCA1} mice. The thickness of the DG was analyzed by two-factor ANOVA, followed by pairwise comparison test with *p*-value modification by Holm's method, ****p* < 0.0005. The DG is thinner in *Grin1*^{ΔDGCA1} mice [*F*(1,16) = 662.39, *p* < 0.0005], and the difference increases with aging [*F*(1,16) = 59.92, *p* < 0.0005]. There is a significant interaction between genotype and age [*F*(1,16) = 53.99, *p* < 0.005]. (I) Quantitative evaluation of CA1 thickness in the dorsal hippocampus in 6 and 18 months old control and *Grin1*^{ΔDGCA1} mice. There is no difference in the thickness of the CA1 layer (two-factor ANOVA, no significant effect of genotype [*F*(1,16) = 0.594], no significant effect of age [*F*(1,16) = 2.793], and no significant interaction between age and genotype [*F*(1,16) = 0.168]. Scale bars, in (F), which applies to (A–E), and (G), 200 and 10 μm, respectively. Five and four mice for 6 months old control and *Grin1*^{ΔDGCA1}, and six and five mice for 18 months old control and *Grin1*^{ΔDGCA1} were used, respectively.

examined whether there was a correlation between the number of immature and degenerating DG granule cells. Since the number of immature DG granule cells decreases with age, both

populations would have to decrease in parallel, if degenerating cells were primarily immature DG granule cells. However, while the number of immature DG granule cells decreased with age

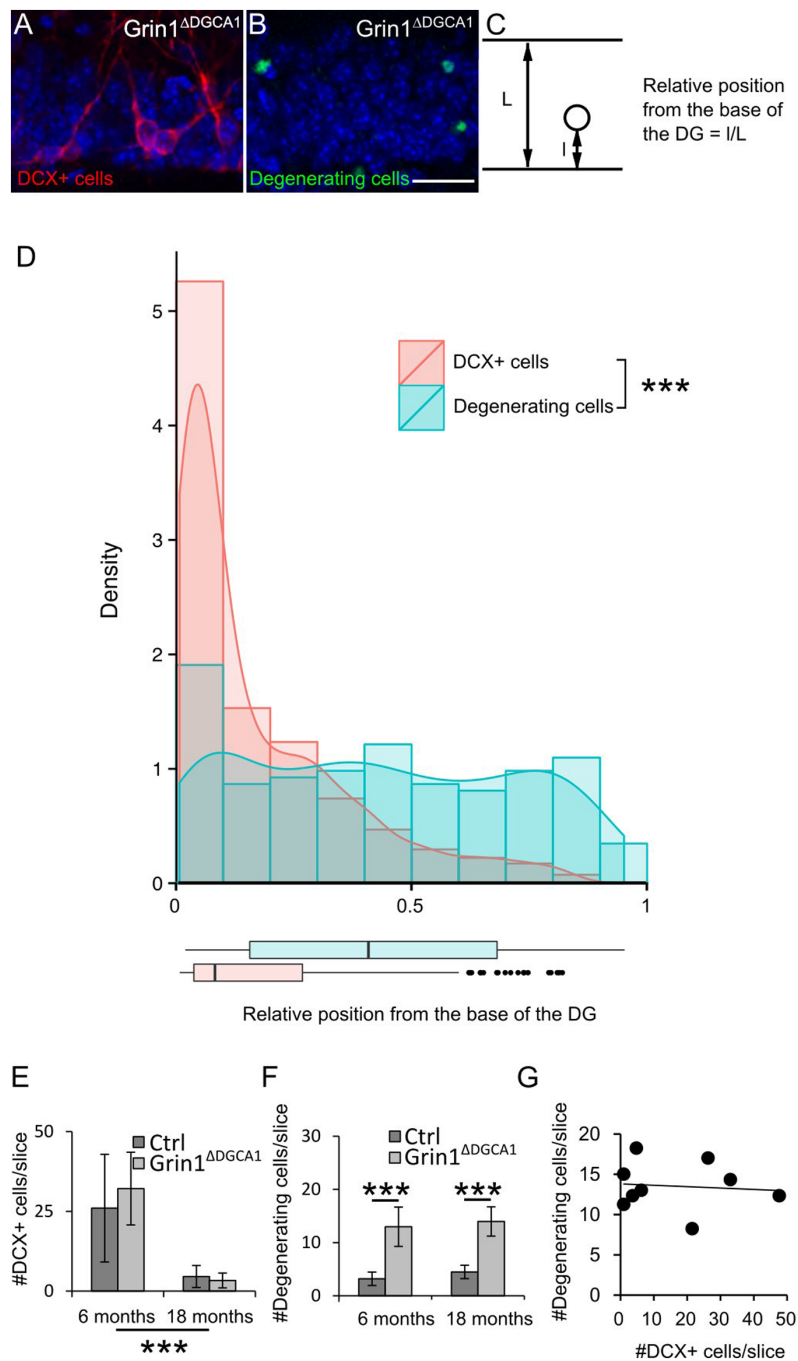


FIGURE 2 | N-methyl-D-aspartate receptor (NMDAR) depletion in *Grin1*^{ΔDGCA1} mice causes age-dependent degeneration of mature DG granule cells.

(A) DAPI stained section (blue) from a 6 months old *Grin1*^{ΔDGCA1} mouse brain showing DCX-positive (abbreviated DCX+ in the figure) neurons (red) located in the inner DG granule cell layer. (B) DAPI stained section (blue) from a 6 months old *Grin1*^{ΔDGCA1} mouse with degenerating neurons (green) dispersed throughout the layer. (C) Diagram indicating the parameters that were used to calculate the relative position of individual DG granule cells. (D) Histogram, density plot (curved line), and boxplot (bottom) of the relative position of DCX-positive cells (pink) and degenerating cells (blue) showing the differential distribution within the DG granule cell layer (significant difference in both Kolmogorov–Smirnov Tests and Mann–Whitney–Wilcoxon Test, *** $p < 0.0005$). Whiskers extending from the boxes in the boxplot indicate the maximum and minimum value within the 1.5-fold of the interquartile range from the higher (75th percentile) and the lower quartile (25th percentile). Dots in the boxplot are outliers. This analysis comprised 405 DCX-positive cells and 173 degenerating cells. (E) The number of DCX-positive cells in the DG decreases with age both in control and *Grin1*^{ΔDGCA1} mice [two-factor ANOVA, $F(1,16) = 30.090$, $p < 0.00005$]. There is neither a significant difference between genotypes [$F(1,16) = 0.653$], nor a significant interaction between age and genotype [$F(1,16) = 0.423$]. (F) The number of degenerating neurons in the DG is higher in *Grin1*^{ΔDGCA1} mice [two-factor ANOVA, $F(1,16) = 85.593$, $p < 0.00005$, followed by *post hoc* analysis with Holm's p -value modification, *** $p < 0.0005$]. There is neither an effect of age [$F(1,16) = 0.247$, ns], nor a significant interaction between age and genotype [$F(1,16) = 0.888$]. (G) There is no correlation between the number of degenerating and newborn neurons in the DG of *Grin1*^{ΔDGCA1} mice (Spearman's rank correlation coefficient test). The same animals were used as in Figure 1. Scale bar in (B), 25 μ m.

both in control and *Grin1*^{ΔDGCAl} mice (Figure 2E), the number of degenerating cells was higher in *Grin1*^{ΔDGCAl} mice than in controls both at 6 and 18 months of age (Figure 2F). Furthermore, in *Grin1*^{ΔDGCAl} mice, there was no correlation between the number of immature DG granule cells and the number of degenerating cells, suggesting that degenerating cells were not immature cells (Figure 2G). Together these results indicate that degenerating DG granule cells are primarily mature DG granule cells.

NMDAR Dependent Survival is a Cell Type-Specific Property of Mature DG Granule Cells

In *Grin1*^{ΔDGCAl} mice, DG granule cell degeneration might be a complex phenotype that results from changed interactions between CA1 and DG network activities, and might reflect, at least in part, altered output activity from CA1 neurons, in which NMDARs were also deleted. To directly test whether the observed degeneration of mature DG granule cells following GluN1 depletion is indicative of a specific DG granule cell vulnerability, we investigated the effect of NMDAR depletion in genetically modified mice (*Grin1*^{ΔDG}), in which the manipulation was restricted to the DG. Indeed, a reduction in the thickness of the dentate granule cell layer with degenerating cells was seen also in 6 months old *Grin1*^{ΔDG} mice (Figures 3A–D,G,H), indicating that adult granule cells require NMDAR-mediated activity for their survival.

Similarly to *Grin1*^{ΔDGCAl} mice, also in *Grin1*^{ΔDG} mice the number of immature DG granule cells was not reduced (Figures 3E,I), suggesting that GluN1 depletion was restricted to mature DG granule cells. Hence we determined Cre expression in mature and immature DG granule cells, and found that indeed, Cre expression was detected in CB-positive, but not DCX-positive neurons both in *Grin1*^{ΔDG} (Figures 3J–O) and in *Grin1*^{ΔDGCAl} mice (data not shown). Accordingly, GluN1 expression was present in immature DG granule cells (Supplementary Figures S3A–D). Together, these data provide evidence that GluN1 ablation was restricted to mature DG granule cells.

We wondered whether DG granule cell degeneration following NMDAR ablation was noticeable already at earlier developmental stages, and thus investigated 2 months old *Grin1*^{ΔDG} mice. Despite of the GluN1 ablation, the number of immature and degenerating DG granule cells, and the overall thickness of the granule cell layer were comparable between control and mutant mice (Supplementary Figures S3E–I). It thus appears that the phenotype of DG granule cell degeneration following NMDAR ablation worsens in an age-dependent fashion.

Next we examined whether the genetic manipulation altered the number of stem cells in the DG of 6 months old *Grin1*^{ΔDG} mice. The number of stem cells, i.e., GFAP/Sox2 positive cells, was not different between the two genotypes. The increased number of GFAP/Sox2/S100β positive cells in *Grin1*^{ΔDG} mice (Supplementary Figure S4), reflects enhanced proliferation of astrocytes as often reported in brain areas with

neurodegeneration. Hence NMDAR depletion in mature DG granule cells does not affect stem cell proliferation.

Survival of Mature DG Granule Cells Requires GluN2B Expression

Finally, to examine the composition of the NMDARs involved in the degeneration of DG granule cells, we investigated the survival of mature DG granule cells in mice with either GluN2A or GluN2B receptor ablation. To this end we took recourse to 18 months old *Grin2a*^{−/−} and *Grin2b*^{ΔDGCAl} mice. In *Grin2a*^{−/−} mice, the overall appearance and thickness of the DG granule cell layer was not different from that in control mice (Figures 4A,B,E). In contrast, the DG of *Grin2b*^{ΔDGCAl} mice was reminiscent of the above-described phenotype in *Grin1*^{ΔDGCAl} and *Grin1*^{ΔDG} mice (Figures 4C,D,F). These data demonstrate that GluN2B-containing NMDARs support the survival of aged dorsal DG granule cells.

DISCUSSION

Here we demonstrate that NMDAR ablation causes neurodegeneration of the DG. This phenotype derives from the demise of mature DG granule cells and not from altered neurogenesis for the following reasons: First, enhanced caspase-3 expression and degenerating neurons were detected in the outer DG granule cell layer in the mutant mice. Second, the number of stem cells in the DG did not differ between control and mutant mice. Third, neurogenesis in the DG is known to decrease with age. Thus, if NMDAR ablation affected newborn cells, one would expect a progressive age-dependent decline of degenerating neurons. This, however, was not the case. Fourth, GluN1 was depleted primarily in mature DG granule cells as evidenced both by Cre expression and GluN1 immunohistochemistry in *Grin1*^{ΔDG} mice. In addition, previous studies indicated that in several mouse mutants with reduced adult or absent adult neurogenesis the size or thickness of the DG granule cell layer was not visibly altered (Ansorg et al., 2012; Ouchi et al., 2013).

As evidenced in *Grin1*^{ΔDGCAl} mice, neurodegeneration following NMDAR ablation was region- and cell type-specific. Thus, dorsal but not ventral DG granule cell or CA1 pyramidal neurons were affected. A similar phenotype as the one detected in *Grin1*^{ΔDGCAl} and *Grin1*^{ΔDG} mice was also reported in two other animal models of neurodegeneration. Thus, in rats, adrenalectomy causes degeneration of granule cells in the dorsal DG. The ventral DG is much less affected, and CA1 neurons or other hippocampal regions not at all (e.g., Sloviter et al., 1993). The pro-survival effect of corticosterone appears to be mediated by mineralocorticoid receptors (Gass et al., 2000). We do not think, however, that altered downstream signaling in mice with NMDAR ablation in DG granule cell involves signaling via mineralocorticoid receptors as their expression was not affected in our mutants (data not shown).

Notably, transgenic mice overexpressing Gsk3β also exhibit degeneration of granule cells preferentially in the dorsal DG

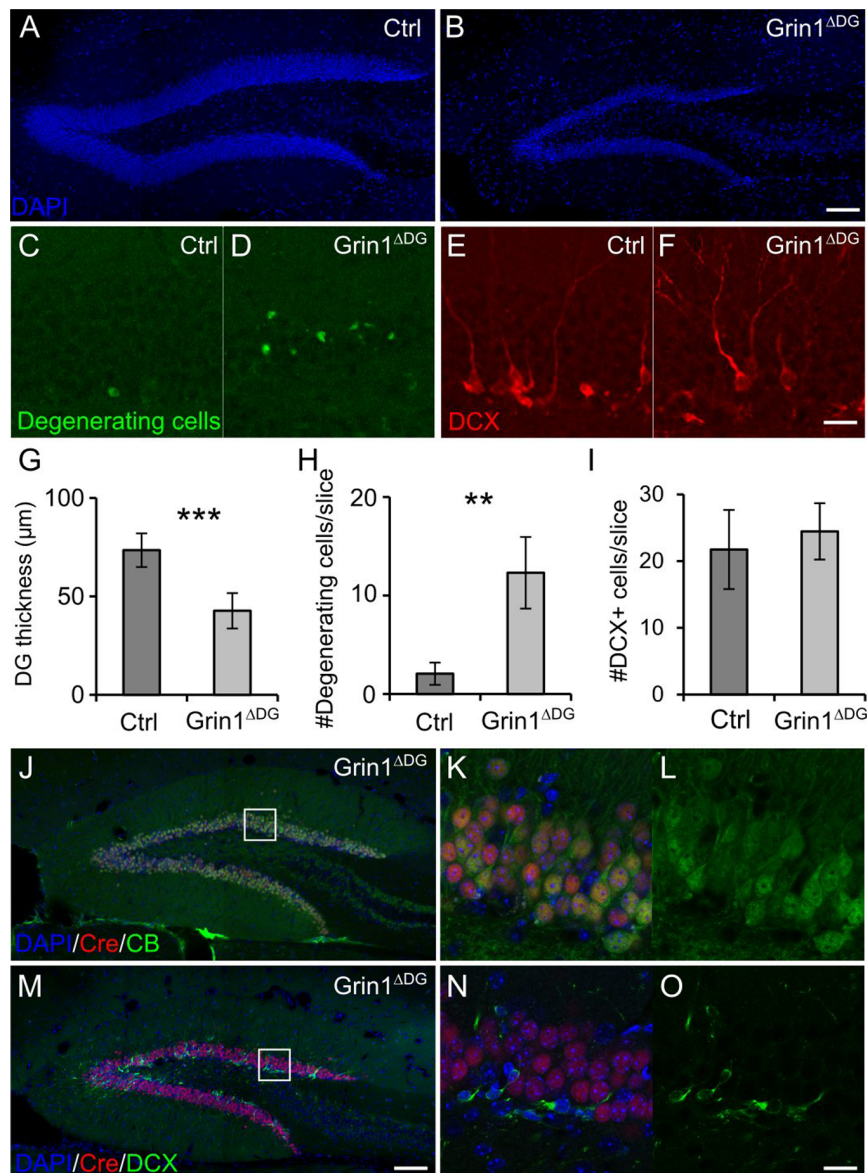


FIGURE 3 | DG selective deletion of GluN1 in *Grin1*^{ΔDG} recapitulates the phenotype observed in *Grin1*^{ΔDGCA1} mice. (A) DAPI stained section showing the DG of a 6 months old control mouse. (B) DAPI stained section from a 6 months old *Grin1*^{ΔDG} mouse brain showing thinning of the DG. (C–F) Degenerating cells [green in (C,D)] and DCX-positive cells [red in (E,F)] in the DG of a 6 months old control and *Grin1*^{ΔDG} mouse. (G) DG thickness is reduced in *Grin1*^{ΔDG} mice (Welch's *t*-test, ****p* < 0.0005). (H) The number of degenerating cells is increased in the DG of *Grin1*^{ΔDG} mice (Welch's *t*-test, ***p* < 0.005). (I) The number of DCX-positive immature cells is comparable between genotypes (Welch's *t*-test). (J–O) In the DG of *Grin1*^{ΔDG} mice, Cre (red) is expressed in CB-positive [green in (J–L)] mature neurons, but not in DCX-positive [green in (M–O)] immature neurons. Right panels (K,L,N,O) show a magnified view of the indicated area [white boxes in (J,M)]. Scale bars in (B,F,M,O), 100, 20, 100, and 20 μm, respectively. Five and seven mice were used for control and *Grin1*^{ΔDG}, respectively.

(Fuster-Matanzo et al., 2011), and the alteration is accompanied by activated astrocytes (e.g., Fuster-Matanzo et al., 2011). Interestingly, Gsk3β is more active in the dorsal, whilst Akt, an inhibitor of Gsk3β, is more active in the ventral hippocampus (Fuster-Matanzo et al., 2011). Conversely, chronic application of lithium, an inhibitor of Gsk3β, ameliorates DG neurodegeneration induced by injection of amyloid-β fibrils (De Ferrari et al., 2003). Notably, there is evidence that β-catenin, a substrate of Gsk3β, directly interacts with

the NMDAR (Al-Hallaq et al., 2007). Accordingly, GluN2B-containing NMDARs suppress apoptosis induced by Gsk3β overexpression in cultured neurons (Habas et al., 2006).

It was surprising that GluN2B, but not GluN2A, was required for the survival of DG granule cells, as several studies provided ample evidence that GluN2B-containing receptors mediate excitotoxic neuronal cell death (reviewed in Hardingham and Bading, 2010). There are nevertheless reports proposing that under certain conditions GluN2B

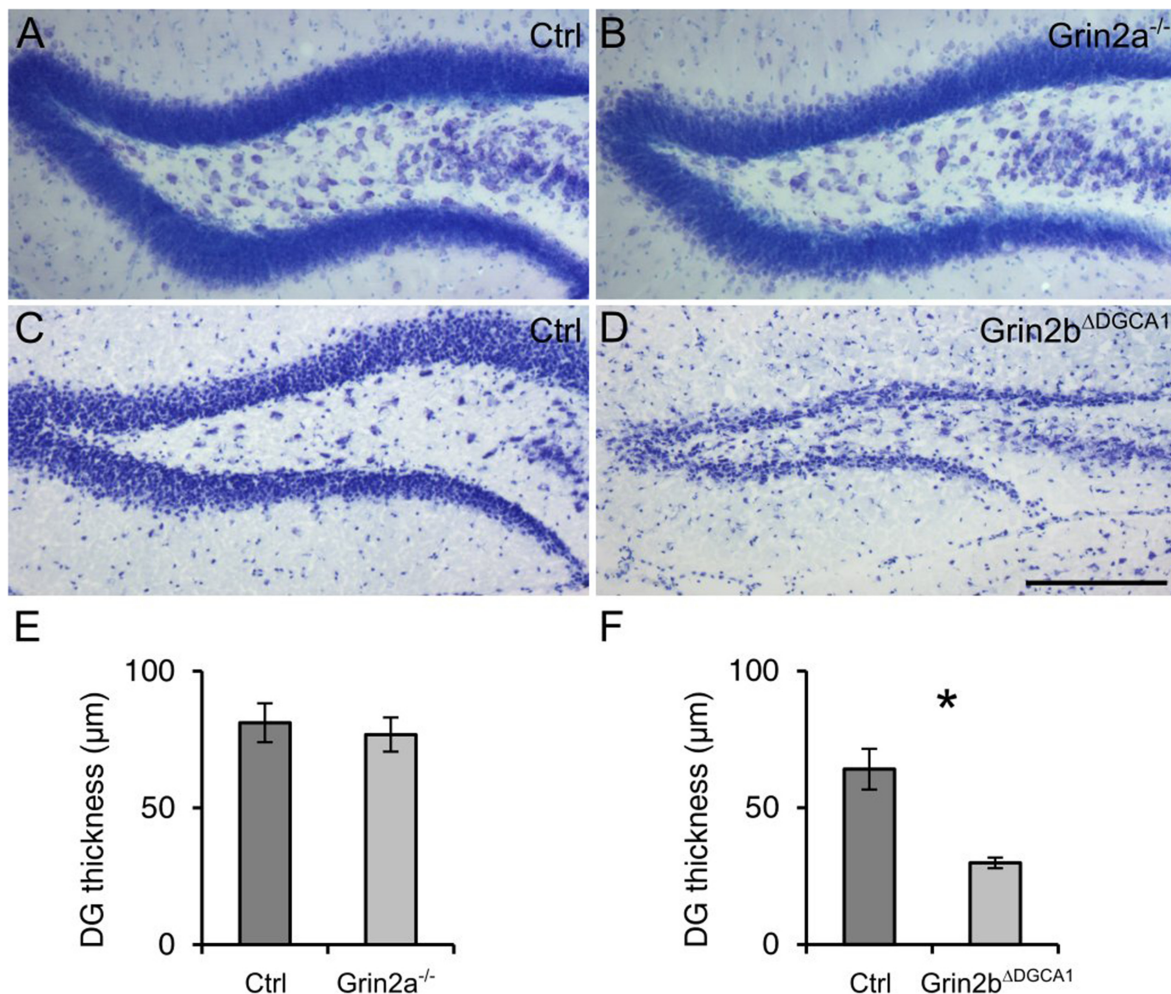


FIGURE 4 | Absence of GluN2B-, but not GluN2A-containing NMDARs causes age-associated neurodegeneration of granule cells in the dorsal DG. (A) Nissl staining of the DG from an 18 months old control mouse. (B) Nissl staining of the DG from an 18 months old *Grin2a*^{-/-} mouse. (C) Nissl staining of the DG from an 18 months old control mouse. (D) Nissl staining of the DG from an 18 months old control mouse (*Grin2b*^{ΔDGCA1}). (E) Quantitative evaluation of the granule cell layer thickness in the DG of control and *Grin2a*^{-/-} mice (Student's *t*-test, ns). (F) Quantitative evaluation of the granule cell layer thickness in the DG of control and *Grin2b*^{ΔDGCA1} mice (Welch's *t*-test, **p* < 0.05). Scale bar in (D), 200 μm. Four and three mice for control and *Grin2a*^{-/-}, and three and three mice for control and *Grin2b*^{ΔDGCA1} were used, respectively.

activation provides also pro-survival signals (Habas et al., 2006).

Our findings have implications for therapeutic approaches in which chronic NMDAR antagonist treatment is envisaged. Thus, NMDAR antagonists have been considered for treatment of many neurological diseases, including cerebral ischemia, traumatic brain injury, pain, Alzheimer's disease, Huntington's disease, Parkinson's disease, autism spectrum disorders, and depression (reviewed in Paoletti et al., 2013). In some cases, treatment appeared promising, at least in animal models (Paoletti et al., 2013; Patrizi et al., 2015). In humans, the NMDAR antagonist ketamine shows promising effects in patients with neuropathic pain and depression (reviewed in Niesters et al., 2014; Iadarola et al., 2015). Surveillance of the literature, however, indicates that in most studies the treatment was short, ranging from 1 day to few weeks. Importantly, ketamine, is also used for

recreational purposes, and the longest period of drug intake exceeds 10 years (Liao et al., 2010). Chronic use of ketamine has long-lasting devastating effects on brain function, including working memory and episodic memory deficits (reviewed in Morgan and Curran, 2012). Based on our results, we propose that NMDAR antagonists, whilst potentially beneficial for acute treatment, bear the risk of causing DG degeneration following chronic administration, which would contribute to the worsening of cognitive functions, considering the crucial role of the DG in memory processes. It is not clear, however, to which extent the results that we obtained in mice following genetic receptor ablation can be transferred to humans, and in particular whether chronic NMDAR antagonist administration mimics the results reported here. Finally, the results warrant further investigations as to the downstream cellular signal cascade that eventually leads to the region-specific cell death. It is tempting to propose a

putative involvement of Gsk3 β , but so far this hypothesis remains speculative.

In summary, mature granule cells in the dorsal DG undergo neurodegeneration following NMDAR ablation in aged mice. The study provides evidence that caution must be exerted, especially in aged patients, when long-term administration of NMDAR antagonists is considered for therapeutic purposes. Identification of downstream pathways leading to neurodegeneration following NMDAR ablation is warranted to eventually establish safe clinical administration of NMDAR antagonists.

AUTHOR CONTRIBUTIONS

YW and HM designed the experiments and wrote the manuscript. YW performed the experiments. YW and MM evaluated the data and performed the statistical analysis. All authors provided critical input for the generation of the final version of the manuscript. RS and PS provided the *Grin1* ^{Δ DGCA1},

Grin1 ^{Δ DG}, and *Grin2a* ^{$-/-$} mice. All authors read and approved the final manuscript.

ACKNOWLEDGMENTS

We thank R. Hinz-Herkommer, I. Preugschat-Gumprecht, and U. Amtmann for technical assistance, M. Higuchi and A. Herb for animal management. This study was supported in part by a Postdoctoral Fellowship from the Uehara Memorial Foundation to YW.

SUPPLEMENTARY MATERIAL

The Supplementary Material for this article can be found online at: <http://journal.frontiersin.org/article/10.3389/fnmol.2015.00087>

REFERENCES

- Al-Hallaq, R. A., Conrads, T. P., Veenstra, T. D., and Wenthold, R. J. (2007). NMDA di-heteromeric receptor populations and associated proteins in rat hippocampus. *J. Neurosci.* 27, 8334–8343. doi: 10.1523/JNEUROSCI.2155-07.2007
- Ansorg, A., Witte, O. W., and Urbach, A. (2012). Age-dependent kinetics of dentate gyrus neurogenesis in the absence of cyclin D2. *BMC Neurosci.* 13:46. doi: 10.1186/1471-2202-13-46
- Bannerman, D. M., Bus, T., Taylor, A., Sanderson, D. J., Schwarz, I., Jensen, V., et al. (2012). Dissecting spatial knowledge from spatial choice by hippocampal NMDA receptor deletion. *Nat. Neurosci.* 15, 1153–1159. doi: 10.1038/nn.3166
- Bannerman, D. M., Sprengel, R., Sanderson, D. J., McHugh, S. B., Rawlins, J. N. P., Monyer, H., et al. (2014). Hippocampal synaptic plasticity, spatial memory and anxiety. *Nat. Rev. Neurosci.* 15, 181–192. doi: 10.1038/nrn3677
- Choi, D. W. (1992). Excitotoxic cell death. *J. Neurobiol.* 23, 1261–1276. doi: 10.1002/neu.480230915
- De Ferrari, G. V., Chacón, M. A., Barria, M. I., Garrido, J. L., Godoy, J. A., Olivares, G., et al. (2003). Activation of Wnt signaling rescues neurodegeneration and behavioral impairments induced by β -amyloid fibrils. *Mol. Psychiatry* 8, 195–208. doi: 10.1038/sj.mp.4001208
- Fanselow, M. S., and Dong, H.-W. (2010). Are the dorsal and ventral hippocampus functionally distinct structures? *Neuron* 65, 7–19. doi: 10.1016/j.neuron.2009.11.031
- Fuster-Matanzo, A., Llorens-Martin, M., de Barreda, E. G., Ávila, J., and Hernández, F. (2011). Different susceptibility to neurodegeneration of dorsal and ventral hippocampal dentate gyrus: a study with transgenic mice overexpressing GSK3 β . *PLoS ONE* 6:e27262. doi: 10.1371/journal.pone.0027262
- Gass, P., Kretz, O., Wolfer, D. P., Berger, S., Tronche, F., Reichardt, H. M., et al. (2000). Genetic disruption of mineralocorticoid receptor leads to impaired neurogenesis and granule cell degeneration in the hippocampus of adult mice. *EMBO Rep.* 1, 447–451. doi: 10.1093/embo-reports/kvd088
- Gomez-Sanchez, C. E., de Rodriguez, A. F., Romero, D. G., Estess, J., Warden, M. P., Gomez-Sanchez, M. T., et al. (2006). Development of a panel of monoclonal antibodies against the mineralocorticoid receptor. *Endocrinology* 147, 1343–1348. doi: 10.1210/en.2005-0860
- Gu, Y., Arruda-Carvalho, M., Wang, J., Janoschka, S. R., Josselyn, S. A., Frankland, P. W., et al. (2012). Optical controlling reveals time-dependent roles for adult-born dentate granule cells. *Nat. Neurosci.* 15, 1700–1706. doi: 10.1038/nn.3260
- Habas, A., Kharebava, G., Szatmari, E., and Hetman, M. (2006). NMDA neuroprotection against a phosphatidylinositol-3 kinase inhibitor, LY294002 by NR2B-mediated suppression of glycogen synthase kinase-3 β -induced apoptosis. *J. Neurochem.* 96, 335–348. doi: 10.1111/j.1471-4159.2005.03543.x
- Hardingham, G. E., and Bading, H. (2010). Synaptic versus extrasynaptic NMDA receptor signalling: implications for neurodegenerative disorders. *Nat. Rev. Neurosci.* 11, 682–696. doi: 10.1038/nrn2911
- Iadarola, N. D., Niciu, M. J., Richards, E. M., Vande Voort, J. L., Ballard, E. D., Lundin, N. B., et al. (2015). Ketamine and other N-methyl-D-aspartate receptor antagonists in the treatment of depression: a perspective review. *Ther. Adv. Chronic Dis.* 6, 97–114. doi: 10.1177/2040622315579059
- Ikonomidou, C., Bosch, F., Miksa, M., Bittigau, P., Vöckler, J., Dikranian, K., et al. (1999). Blockade of NMDA receptors and apoptotic neurodegeneration in the developing brain. *Science* 283, 70–74. doi: 10.1126/science.283.5398.70
- Jessberger, S., and Gage, F. H. (2014). Adult neurogenesis: bridging the gap between mice and humans. *Trends Cell Biol.* 24, 558–563. doi: 10.1016/j.tcb.2014.07.003
- Kellendonk, C., Tronche, F., Casanova, E., Anlag, K., Opherk, C., and Schütz, G. (1999). Inducible site-specific recombination in the brain. *J. Mol. Biol.* 285, 175–182. doi: 10.1006/jmbi.1998.2307
- Liao, Y., Tang, J., Ma, M., Wu, Z., Yang, M., Wang, X., et al. (2010). Frontal white matter abnormalities following chronic ketamine use: a diffusion tensor imaging study. *Brain J. Neurol.* 133, 2115–2122. doi: 10.1093/brain/awq131
- McHugh, T. J., Jones, M. W., Quinn, J. J., Balthasar, N., Coppari, R., Elmquist, J. K., et al. (2007). Dentate gyrus NMDA receptors mediate rapid pattern separation in the hippocampal network. *Science* 317, 94–99. doi: 10.1126/science.1140263
- Monyer, H., Burnashev, N., Laurie, D. J., Sakmann, B., and Seeburg, P. H. (1994). Developmental and regional expression in the rat brain and functional properties of four NMDA receptors. *Neuron* 12, 529–540. doi: 10.1016/0896-6273(94)90210-0
- Morgan, C. J. A., and Curran, H. V. (2012). Independent scientific committee on drugs. Ketamine use: a review. *Addict. Abingdon Engl.* 107, 27–38. doi: 10.1111/j.1360-0443.2011.03576.x
- Nakashiba, T., Cushman, J. D., Pelkey, K. A., Renaudineau, S., Buhl, D. L., McHugh, T. J., et al. (2012). Young dentate granule cells mediate pattern separation, whereas old granule cells facilitate pattern completion. *Cell* 149, 188–201. doi: 10.1016/j.cell.2012.01.046
- Niesters, M., Martini, C., and Dahan, A. (2014). Ketamine for chronic pain: risks and benefits. *Br. J. Clin. Pharmacol.* 77, 357–367. doi: 10.1111/bcp.12094
- Niewoehner, B., Single, F. N., Hvalby, Ø., Jensen, V., Meyer zum Alten Borgloh, S., Seeburg, P. H., et al. (2007). Impaired spatial working memory but spared spatial reference memory following functional loss of NMDA receptors in the dentate gyrus. *Eur. J. Neurosci.* 25, 837–846. doi: 10.1111/j.1460-9568.2007.05312.x
- Ouchi, Y., Banno, Y., Shimizu, Y., Ando, S., Hasegawa, H., Adachi, K., et al. (2013). Reduced adult hippocampal neurogenesis and working memory deficits in the Dgcr8-deficient mouse model of 22q11.2 deletion-associated schizophrenia can be rescued by IGF2. *J. Neurosci.* 33, 9408–9419. doi: 10.1523/JNEUROSCI.2700-12.2013

- Paoletti, P., Bellone, C., and Zhou, Q. (2013). NMDA receptor subunit diversity: impact on receptor properties, synaptic plasticity and disease. *Nat. Rev. Neurosci.* 14, 383–400. doi: 10.1038/nrn3504
- Patrizi, A., Picard, N., Simon, A. J., Gunner, G., Centofante, E., Andrews, N. A., et al. (2015). Chronic administration of the N-methyl-D-aspartate receptor antagonist ketamine improves Rett syndrome phenotype. *Biol. Psychiatry* doi: 10.1016/j.biopsych.2015.08.018 [Epub ahead of print].
- Rodenas-Ruano, A., Chavez, A. E., Cossio, M. J., Castillo, P. E., and Zukin, R. S. (2012). REST-dependent epigenetic remodeling promotes the developmental switch in synaptic NMDA receptors. *Nat. Neurosci.* 15, 1382–1390. doi: 10.1038/nn.3214
- Sakimura, K., Kutsuwada, T., Ito, I., Manabe, T., Takayama, C., Kushiya, E., et al. (1995). Reduced hippocampal LTP and spatial learning in mice lacking NMDA receptor epsilon 1 subunit. *Nature* 373, 151–155. doi: 10.1038/373151a0
- Sloviter, R. S., Sollas, A. L., Dean, E., and Neubort, S. (1993). Adrenalectomy-induced granule cell degeneration in the rat hippocampal dentate gyrus: characterization of an in vivo model of controlled neuronal death. *J. Comp. Neurol.* 330, 324–336. doi: 10.1002/cne.903300304
- Tashiro, A., Sandler, V. M., Toni, N., Zhao, C., and Gage, F. H. (2006). NMDA-receptor-mediated, cell-specific integration of new neurons in adult dentate gyrus. *Nature* 442, 929–933. doi: 10.1038/nature05028
- von Engelhardt, J., Doganci, B., Jensen, V., Hvalby, Ø, Göngrich, C., Taylor, A., et al. (2008). Contribution of hippocampal and extra-hippocampal NR2B-containing NMDA receptors to performance on spatial learning tasks. *Neuron* 60, 846–860. doi: 10.1016/j.neuron.2008.09.039

Conflict of Interest Statement: The authors declare that the research was conducted in the absence of any commercial or financial relationships that could be construed as a potential conflict of interest.

Copyright © 2016 Watanabe, Müller, von Engelhardt, Sprengel, Seeburg and Monyer. This is an open-access article distributed under the terms of the Creative Commons Attribution License (CC BY). The use, distribution or reproduction in other forums is permitted, provided the original author(s) or licensor are credited and that the original publication in this journal is cited, in accordance with accepted academic practice. No use, distribution or reproduction is permitted which does not comply with these terms.



Molecular Mechanisms Regulating LPS-Induced Inflammation in the Brain

Olena Lykhmus¹, Nibha Mishra², Lyudmyla Koval¹, Olena Kalashnyk¹, Galyna Gergalova¹, Kateryna Uspenska¹, Serghiy Komisarenko¹, Hermona Soreq² and Maryna Skok^{1*}

¹ Laboratory of Cell Receptors Immunology, O. V. Palladin Institute of Biochemistry, Kyiv, Ukraine, ² The Edmond and Lily Safra Center of Brain Science and The Alexander Silberman Institute of Life Sciences, The Hebrew University of Jerusalem, Jerusalem, Israel

OPEN ACCESS

Edited by:

Kirsten Harvey,
University College London, UK

Reviewed by:

Changiz Geula,
Northwestern University, USA
Julie A. Saugstad,
Oregon Health & Science University,
USA

*Correspondence:

Maryna Skok
skok@biochem.kiev.ua

Received: 11 December 2015

Accepted: 23 February 2016

Published: 08 March 2016

Citation:

Lykhmus O, Mishra N, Koval L,
Kalashnyk O, Gergalova G,
Uspenska K, Komisarenko S,
Soreq H and Skok M (2016)
Molecular Mechanisms Regulating
LPS-Induced Inflammation
in the Brain.
Front. Mol. Neurosci. 9:19.
doi: 10.3389/fnmol.2016.00019

Neuro-inflammation, one of the pathogenic causes of neurodegenerative diseases, is regulated through the cholinergic anti-inflammatory pathway via the $\alpha 7$ nicotinic acetylcholine receptor ($\alpha 7$ nAChR). We previously showed that either bacterial lipopolysaccharide (LPS) or immunization with the $\alpha 7(1-208)$ nAChR fragment decrease $\alpha 7$ nAChRs density in the mouse brain, exacerbating chronic inflammation, beta-amyloid accumulation and episodic memory decline, which mimic the early stages of Alzheimer's disease (AD). To study the molecular mechanisms underlying the LPS and antibody effects in the brain, we employed an *in vivo* model of acute LPS-induced inflammation and an *in vitro* model of cultured glioblastoma U373 cells. Here, we report that LPS challenge decreased the levels of $\alpha 7$ nAChR RNA and protein and of acetylcholinesterase (AChE) RNA and activity in distinct mouse brain regions, sensitized brain mitochondria to the apoptogenic effect of Ca^{2+} and modified brain microRNA profiles, including the cholinergic-regulatory CholinomiRs-132/212, in favor of anti-inflammatory and pro-apoptotic ones. Adding $\alpha 7(1-208)$ -specific antibodies to the LPS challenge prevented elevation of both the anti-inflammatory and pro-apoptotic miRNAs while supporting the resistance of brain mitochondria to Ca^{2+} and maintaining $\alpha 7$ nAChR/AChE decreases. In U373 cells, $\alpha 7$ -specific antibodies and LPS both stimulated interleukin-6 production through the p38/Src-dependent pathway. Our findings demonstrate that acute LPS-induced inflammation induces the cholinergic anti-inflammatory pathway in the brain, that $\alpha 7$ nAChR down-regulation limits this pathway, and that $\alpha 7$ -specific antibodies aggravate neuroinflammation by inducing the pro-inflammatory interleukin-6 and dampening anti-inflammatory miRNAs; however, these antibodies may protect brain mitochondria and decrease the levels of pro-apoptotic miRNAs, preventing LPS-induced neurodegeneration.

Keywords: inflammation, brain, $\alpha 7$ nicotinic acetylcholine receptor, acetylcholine esterase, microRNA, antibody

INTRODUCTION

Neuro-inflammation accompanies and often precedes the development of neurodegenerative pathologies such as Parkinson's and Alzheimer's diseases (AD; Wee Yong, 2010) and might be one of the pathogenic factors for neurodegeneration (Chung et al., 2010; Heppner et al., 2015). However, the molecular mechanisms linking inflammatory reaction to degeneration in the brain are poorly understood. One of the cross-points may include nicotinic acetylcholine receptors of the $\alpha 7$ subtype ($\alpha 7$ nAChRs), which are involved in both cholinergic anti-inflammatory and pro-survival intracellular pathways (Ji et al., 2014; Báez-Pagán et al., 2015; Terrando et al., 2015; Truong et al., 2015).

A number of studies point out the involvement of $\alpha 7$ nAChRs in pro-survival cell signaling, engaging the PI3K/Akt signaling pathway (Parada et al., 2010; Yu et al., 2011; Cucina et al., 2012; Huang et al., 2012; Cui et al., 2013). Such signaling was shown to protect cultured brain cells from apoptosis induced by various apoptogenic agents (Parada et al., 2010). Moreover, $\alpha 7$ nAChRs were found to regulate mitochondrial permeability transition pore formation and release of apoptogenic factors like cytochrome (cyt *c*) and therefore, to control the mitochondrial-mediated pathway of apoptosis (Gergalova et al., 2012, 2014).

In addition, $\alpha 7$ nAChR directly interacts with the amyloid-beta ($A\beta$) precursor protein (Ikonomovic et al., 2009), which favors its normal processing by α -secretase (Kim et al., 1997; Qi et al., 2007) and promotes internalization of processed $A\beta$ forms (Wang et al., 2000; Parri and Dineley, 2010). Consequently, the decrease of $\alpha 7$ nAChR density on the plasma membrane impairs $A\beta$ metabolism and favors accumulation of extracellular $A\beta$ (1–42) (Gouras et al., 2005; Dziejczapolski et al., 2009).

Previously, we found that regular injections of bacterial lipopolysaccharide (LPS) decreased the density of $\alpha 7$ nAChRs in the brain and brain mitochondria of mice and reduced nucleated cell numbers in the hippocampus and striatum, while stimulating astrogliosis, accumulation of $A\beta$ (1–42) peptides and episodic memory decline—symptoms characteristic of the early stages of AD (Lykhmus et al., 2015). Antibodies, generated *in vivo* by immunization of mice with recombinant extracellular domain of $\alpha 7$ nAChR subunit, $\alpha 7(1-208)$, facilitated symptoms similar to those induced by LPS but did not cause degeneration in the brain of mice (Lykhmus et al., 2015), indicating the involvement of specific regulatory processes.

Another important regulator of cholinergic signaling is acetylcholinesterase (AChE), the levels of which decrease during inflammation, increasing acetylcholine levels and stimulating the anti-inflammatory pathway (Soreq, 2015). Acetylcholine was shown to attenuate the release of pro-inflammatory cytokines, like IL-1 or TNF α , by peritoneal monocytes and macrophages in response to bacterial endotoxin—LPS through $\alpha 7$ nAChRs (Borovikova et al., 2000). This phenomenon, first described in 2000 and called “Cholinergic Anti-Inflammatory Pathway”, was further observed in many organs and tissues including the brain

(de Jonge and Ulloa, 2007; Tyagi et al., 2010; Thomsen and Mikkelsen, 2012; Ji et al., 2014; Báez-Pagán et al., 2015; Egea et al., 2015; Truong et al., 2015). AChE expression has been shown to be regulated by microRNAs (miRNAs), small non coding RNAs suppressors of entire pathways of gene expression (Chen et al., 2004; Soreq and Wolf, 2011). MiRNA-132 is reported to increase during inflammation in many tissues (Maharshak et al., 2013; Shaltiel et al., 2013; Nadorp and Soreq, 2015) and is validated to target AChE further to potentiate cholinergic anti-inflammatory pathway (Shaked et al., 2009; Soreq and Wolf, 2011).

The present study was aimed to reveal the molecular mechanisms underlying the LPS and antibody effects in the brain, using a model of acute LPS-induced inflammation with or without $\alpha 7$ -specific antibody injections. Specifically, we studied the involvement of $\alpha 7$ nAChRs in brain inflammation and mitochondrial apoptosis, measured changes in AChE levels with inflammation and profiled brain miRNAs under exposure to LPS, LPS and $\alpha 7$ -specific antibody (Ab $\alpha 7$) or nicotine. Our findings indicate that LPS down-regulates $\alpha 7$ nAChR and AChE in the brain; exacerbates the mitochondrial pathway of apoptosis and changes brain miRNAs in favor of pro-apoptotic and anti-inflammatory ones. Inversely, the antibody supports the integrity of brain mitochondria and attenuates the LPS-induced pro-apoptotic miRNAs up-regulation while stimulating pro-inflammatory signaling and preventing the LPS-induced elevation of the anti-inflammatory miRNA-132/212 (Shaked et al., 2009; Shaltiel et al., 2013; Soreq, 2015).

MATERIALS AND METHODS

Animals and Reagents

Female 3 months old C57BL/6J mice were housed in a quiet, temperature-controlled room (22–23°C) in the animal facility of the O.V. Palladin Institute of Biochemistry and were provided with water and dry food pellets *ad libitum*. Mice were sacrificed by cervical dislocation to remove the brain. All procedures of this study conformed to the guidelines of the Animal Care and Use Committee of Palladin Institute and were approved by the IACUC Protocol 1/7–421.

All reagents were of chemical grade and were purchased from Sigma-Aldrich unless specially indicated. Antibodies against $\alpha 7(1-208)$, $\alpha 7(179-190)$, $\alpha 3(181-192)$, $\alpha 4(181-192)$, $\beta 2(190-200)$ and $\beta 4(190-200)$ nAChR fragments were obtained and characterized by us previously (Skok et al., 1999; Koval et al., 2004; Lykhmus et al., 2011).

Glioblastoma U373 cells (ATCC HTB17–1055) were a kind gift of Prof. A.V. Ryndich from the Institute of Molecular Biology and Genetics in Kyiv.

Animal Treatment and Samples Preparation

Mice were intra-peritoneally injected with LPS (30 μ g/mouse in PBS) on days 0 and 2 (groups 1 and 2). Group 2 mice were additionally intravenously injected with $\alpha 7(1-208)$ -specific

antibodies (200 µg/per mouse in saline) on days 0, 1 and 2. Group 3 mice received nicotine in the drinking water (200 µl/l) for either 3 days or 1 month and the 4th group was intact (Ctrl).

On the 3rd day of each treatment, mice were sacrificed; their brains were removed, homogenized and fractionated into primary pellets (nuclei, cell debris) and mitochondria (additionally pelleted from the supernatant) by a standard procedure of differential centrifugation (Gergalova et al., 2012). To quantify nAChR subunits, both mitochondria and primary pellets were lysed in detergent-containing buffer. Live mitochondria were further examined for functional activities.

In another set of experiments, the brains of similarly treated mice were divided into two halves (hemispheres) and each half was dissected into Hippocampus, Striatum/Thalamus, Cerebellum and Frontal cortex. The one half sections were homogenized under liquid nitrogen and used for RNA extraction. Sections of the 2nd half were homogenized; lysed in detergent-containing buffer (0.01 M Tris-HCl, pH 7.4, 1 M NaCl, 1 mM EGTA, 1% Triton X-100) for 45 min on ice and centrifuged at 13,000 rpm. The resulting supernatant was used for quantifying AChE activity and $\alpha 7$ nAChR protein. Protein content was measured with the BCA kit (Thermo Scientific, France).

Cytochrome c (cyt c) Release Assay with Live Mitochondria

Cyt c release from isolated mitochondria was measured as described previously (Gergalova et al., 2012). Briefly, purified mitochondria (120 µg of protein per ml) were incubated with different doses of CaCl_2 with or without the $\alpha 7$ nAChR agonist PNU282987 (30 nM) for 2 min at room temperature and were immediately pelleted by centrifugation. The supernatants were tested for the presence of cyt c by a sandwich ELISA assay.

Quantifying nAChR Subunits in the Brain or Mitochondria Preparations

The assay was performed as described Lykhmus et al. (2015). Briefly, immunoplates (NUNC, MaxiSorp) were coated with rabbit $\alpha 7$ (1–208)-specific antibody (20 µg/ml), blocked with 1% BSA, and the tested preparations were applied into the wells (1 µg of protein per 0.05 ml per well) for 2 h at 37°C. The plates were washed with water and the second biotinylated $\alpha 3$ (181–192), $\alpha 4$ (181–192), $\alpha 7$ (179–190), $\beta 2$ (190–200) or $\beta 4$ (190–200)-specific antibody was applied for additional 2 h being revealed with Streptavidin-peroxidase conjugate and o-phenyldiamine-containing substrate solution.

RT-PCR for $\alpha 7$, AChE and microRNA Transcripts

RNA extraction from tissue samples was carried out using Trizol (Sigma, NY, USA) as described Shaked et al. (2009). RNA concentration and integrity were determined spectrophotometrically and by electrophoresis, respectively.

RNA samples (500 ng) were reverse transcribed using the Quanta cDNA synthesis kit for mRNA and miRNA as per the manufacturer's (Quanta Biosciences) protocol. Real-time RT-PCR was performed using the ABI prism 7900 HT and SYBR green master mix (Quanta Biosciences). For miRNA transcripts, PerfeCTa microRNA assay primers (Quanta Biosciences) were used. Results were normalized to the expression of snoRD47 and actin for miRNA and mRNA respectively. Further all the results were normalized to respective regional control. The following primers were used for: AChE-S Forward (F): CTGAACCTGAAGCCCTTAGAG, Reverse (R): CCGCCTCG TCCAGAGTAT; nAChR7, F: CACATTCCACACAACGTCTT, R: AAAAGGGAACCAGCGTACATC; actin F: CCACACCCG CCACCAGTT, R: TACAGCCCGGGGAGCAT. Fold change values for both miRNAs and mRNAs were calculated using the $\Delta\Delta\text{Ct}$ method.

RNA-seq Library Preparation and Sequencing

Libraries for next generation sequencing (NGS) were prepared from whole brain RNA using TruSeq Small RNA Library Prep Kit as per the manufacturer's protocol. A total of four libraries (pooled from four animals of each group) were prepared from RNA of four groups. Briefly, the total 600 ng of RNA samples were hybridized with TruSeq Adaptor Mix which is a set of oligonucleotides with a single-stranded degenerate sequence at one end and a defined sequence required for Miseq sequencing at the other end. The Adaptor Mix constrains the orientation of the RNA in the ligation reaction such that hybridization with it yields template for sequencing from the 5' end of the sense strand. After hybridization, the adaptors are ligated to the small RNA molecules using the Ligation Enzyme Mix, which is a mixture of an RNA Ligase and other components. Ligation requires an RNA molecule with a 5'-monophosphate and a 3-hydroxyl end; therefore, most small RNAs can participate in this reaction, and intact mRNA molecules with a 5'-cap structure are excluded. Next, the small RNA population with ligated adaptors of each sample was reverse transcribed, to generate cDNA libraries. Treatment with RNaseH followed, to digest the RNA from RNA/cDNA duplexes and to reduce the concentration of un-ligated adaptors and adaptor by-products. The cDNA libraries were amplified using bar coded primer sets and 15–18 cycles of PCR. The amplified cDNA libraries were cleaned up and size selected from gel—PCR products of 105–150 bp were isolated, corresponding to inserts derived from the small RNA population. The amplified cDNA libraries generated were there after used for Miseq sequencing.

miRNA pathway analysis was performed using the microT-CDS tool available through Diana Tools¹.

Determination of AChE Activity

The acetylcholine hydrolyzing activity of AChE was measured by the Ellman's assay (Ellman et al., 1961) as described

¹<http://diana.imis.athena-innovation.gr/DianaTools/index.php?r=mirpath/index>

Arbel et al. (2014). Briefly, samples were diluted 1:5 with 0.2 M phosphate buffer pH 7.4. Ellman's reagent was added to each sample, the mixture was incubated at RT for 20 min under darkness, acetylthiocholine iodide was added and absorbance of the corresponding plate wells at 405 nm was monitored with Stat-Fax 2000 ELISA Reader (Advanced Technologies, IL, USA) at 15 time points with 2 min intervals. AChE activity was calculated based on the concentration of the resultant 5-thio-2-nitrobenzoate anion ($\epsilon_{405} = 13.6 \text{ M}^{-1} \text{ cm}^{-1}$); taking into account the average OD increment per minute and protein concentration in the sample.

U373 Culturing, Staining and Imaging

Glioblastoma U373 cells were cultured in RPMI 1640 medium supplemented with 20 mM L-glutamine, 20 mM HEPES, penicillin-streptomycin mixture and 10% fetal calf serum. For microscopy studies, the cells were attached onto glass slides, 3×10^4 per slide, in complete medium for 3 h and were incubated with biotinylated $\alpha 7(179-190)$ -specific antibody (0.06 mg/ml) and MitoTracker Green (Invitrogen, USA) for 100 min at 37°C. Cells were fixed with 4% paraformaldehyde and treated with Streptavidin-CyChrome3 conjugate to visualize the biotinylated antibody, followed by washes with PBS and water, embedding in MOWIOL-DABCO and examination in a Zeiss LSM 510 Meta confocal laser scanning microscope.

Measuring IL-6 Produced by U373 Cells

U373 cells (3×10^5 per ml) seeded into the wells of 96-well plates were cultured with LPS (clone 055 B5; 1 $\mu\text{g}/\text{ml}$) or $\alpha 7(179-190)$ -specific antibody (10 $\mu\text{g}/\text{ml}$) in the presence

or absence of the following kinase inhibitors: SB202190 (10 μM , p38 inhibitor), KN62 (1 μM , CaMKII inhibitor), PP1 (10 μM , Src kinase inhibitor), bisindolylmaleimide (50 nM, protein kinase C inhibitor) and Wortmaninn (1 μM , phosphatidylinositol-3-kinase inhibitor) for 24 h. The IL-6 concentration in the supernatants was detected using Diaclone test system as per the manufacturer's instructions.

Statistical Analysis

Each experiment has been performed in minimum 7 mice and ELISA assays for each mouse have been performed in triplicates. The mean values for individual mice were used for statistical analysis using Student's *t*-test. The data are presented as $M \pm SE$; * $p < 0.05$; ** $p < 0.005$.

RESULTS

Both LPS and $\alpha 7(1-208)$ -Specific Antibodies Modulate nAChR Composition in the Brain

Sandwich ELISA performed with whole brain preparations demonstrated that LPS treatment decreased the level of $\alpha 7$ nAChR subunits while increasing the $\alpha 3$ and $\beta 4$ subunits. Injections of $\alpha 7(1-208)$ -specific antibodies additionally decreased the $\alpha 4$ and $\beta 2$ subunits (Figure 1A). Nicotine (3 days) up-regulated both $\alpha 7$ and $\alpha 4\beta 2$ nAChRs and did not influence $\alpha 3\beta 4$ ones. LPS and LPS plus $\alpha 7(1-208)$ -specific antibody, but not nicotine, decreased $\alpha 7$ and $\alpha 4\beta 2$ nAChRs and non-significantly increased $\alpha 3\beta 4$ ones in mitochondria preparations (Figure 1B). LPS treatment decreased both $\alpha 7$ RNA and protein in the frontal cortex, striatum, hippocampus and cerebellum. The $\alpha 7(1-208)$ -specific

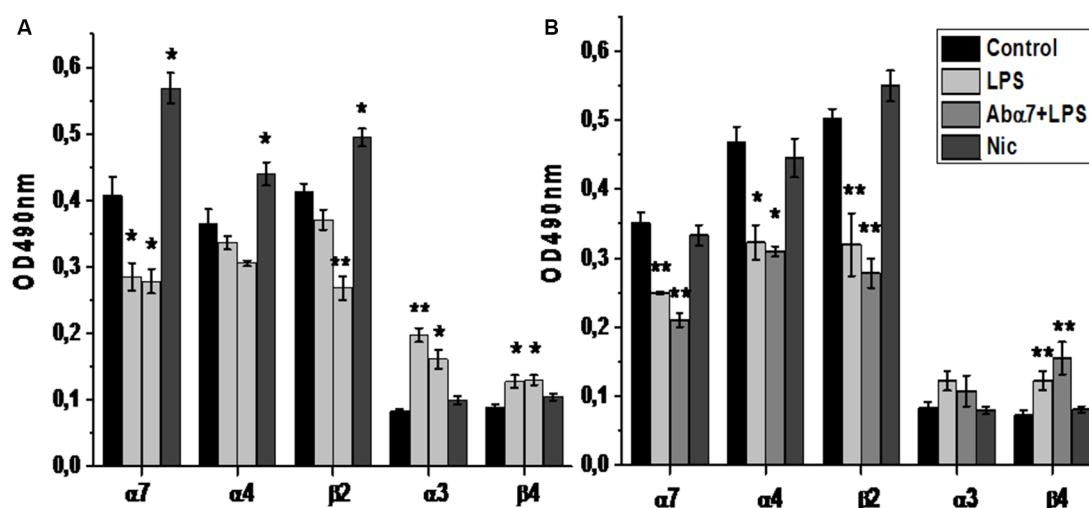


FIGURE 1 | The level of $\alpha 3$, $\alpha 4$, $\alpha 7$, $\beta 2$ and $\beta 4$ nAChR subunits in the whole brain preparations (A) or brain mitochondria (B) of mice treated with lipopolysaccharide (LPS), $\alpha 7(1-208)$ -specific antibody + LPS (Ab $\alpha 7$ + LPS) or nicotine (1 month, Nic) compared to non-treated mice (Control).

* $p < 0.05$; ** $p < 0.005$ compared to Control ($n = 4$).

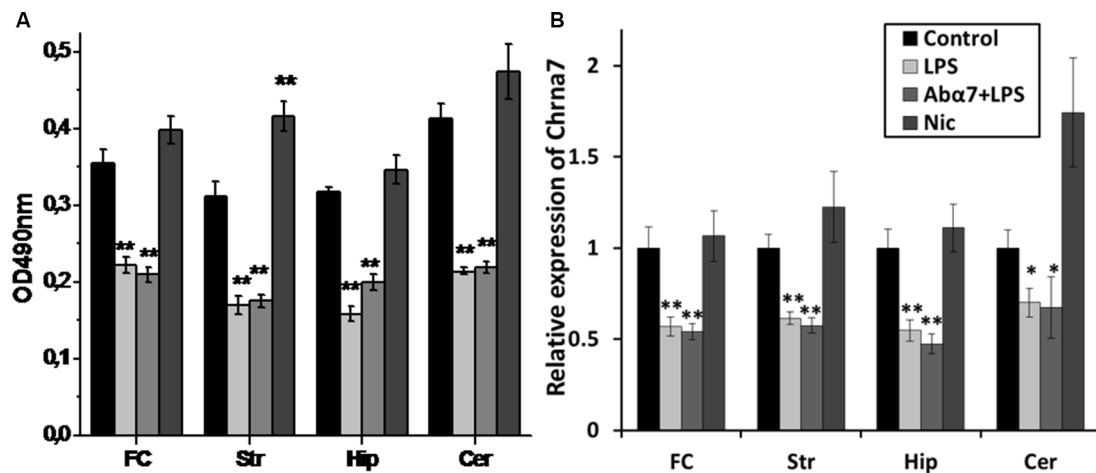


FIGURE 2 | Modified levels of $\alpha 7$ nAChR protein (A) or RNA (B) in various brain regions of mice treated with LPS, $\alpha 7(1-208)$ -specific antibody + LPS (Ab $\alpha 7$ + LPS) or nicotine (Nic) compared to non-treated mice (Control). FC—frontal cortex, Str—striatum, Hip—hippocampus, Cer—cerebellum * $p < 0.05$; ** $p < 0.005$ compared to Control ($n = 8$).

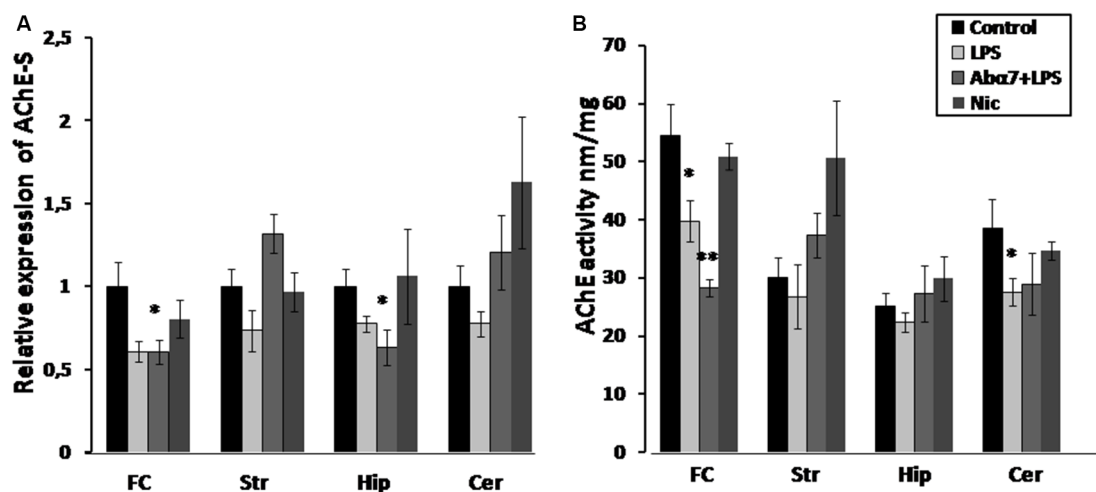


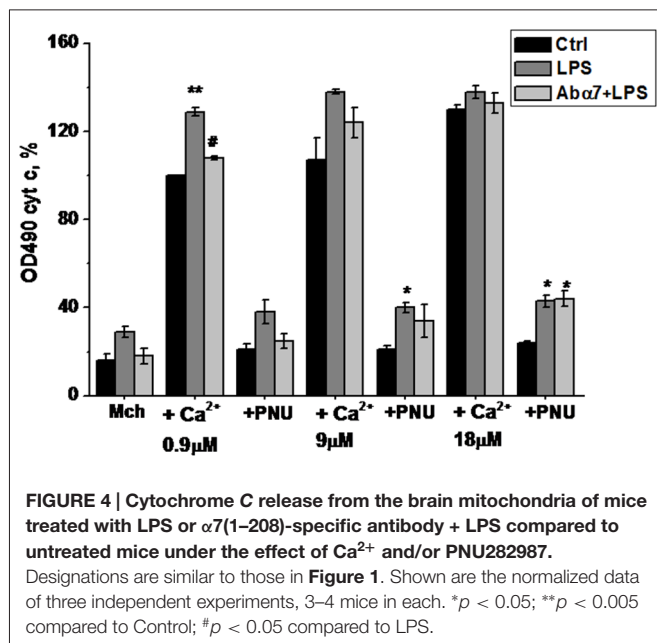
FIGURE 3 | Transcript levels (A) and enzyme activity (B) of acetylcholinesterase-S (AChE-S) in various brain regions of mice treated with LPS, $\alpha 7(1-208)$ -specific antibody + LPS or nicotine (3 days) compared to non-treated mice. Designations are similar to those in Figure 2. * $p < 0.05$; ** $p < 0.005$ compared to Control ($n = 8$).

antibody did not modify the effect of LPS on $\alpha 7$ nAChR RNA or protein expression. Nicotine slightly increased the $\alpha 7$ protein in the striatum but did not affect its RNA level (Figures 2A,B).

LPS and $\alpha 7(1-208)$ -Specific Antibodies Modulate Brain AChE Expression and Activity

LPS exposure significantly decreased the levels of the “synaptic” AChE-S variant (Soreq and Seidman, 2001) in the frontal cortex and non-significantly in the striatum, hippocampus and cerebellum that was interpreted as a tendency to decrease.

The antibody additionally decreased AChE-S RNA in the hippocampus. Nicotine (3 days) caused non-significant up-regulation of AChE-S in the striatum (Figure 3A). Enzyme activity measurements demonstrated decreased AChE activity in the frontal cortex and cerebellum and a tendency to decrease in the striatum and hippocampus under the effect of LPS. The antibody accentuated the LPS effect in the frontal cortex, while nicotine tended to increase AChE activity in striatum (Figure 3B). A correlation between AChE-S expression and activity was observed in the frontal cortex, cerebellum and striatum of individual mice (Pearson coefficient being from 0.80–0.99; data not shown).



LPS and α7(1–208)-Specific Antibodies Modify the Reaction of Brain Mitochondria to Apoptotic Stimuli

Live mitochondria isolated from the brains of LPS-treated mice released more cyt *c* in response to 0.9 and 9.0 μM Ca²⁺ and became less sensitive to the normalizing effect of the α7-specific agonist PNU282987 than mitochondria of non-treated animals (Figure 4). Moreover, mitochondria of LPS-treated mice released some cyt *c* without any Ca²⁺, reflecting their unstable (pre-apoptotic) state. The α7(1–208)-specific antibodies decreased the LPS-induced cyt *c* release from mitochondria at low Ca²⁺ doses and facilitated the normalizing effect of PNU282987.

The Effect of LPS and α7(1–208)-Specific Antibody on the microRNA Spectrum in the Brain

To delineate the differentially expressed miRs in brain during inflammation we performed whole brain miR-deep sequencing analysis. A total of 24, 249, 523 sequencing reads were obtained. All the reads (50 bp long) were subjected to trimming of the tag end terminal base pairs and P1 start adapter (Miseq miRNA reverse primer sequences) using CLC genomics workbench V7.0 (CLC Inc, Aarhus, Denmark). The remaining reads (1, 88, 986) obtained were aligned against the mouse miRNA genome (miRBase release 20) and Ensemble mouse database (GRCm38) for non coding RNA. Through the annotation and merge counts, only reads longer than 15 bases were analyzed. Match parameters included for mature length variants (IsomiRs)-additional two upstream and downstream bases, and two missing upstream and downstream bases, and maximum allowed mismatches two using standard specific alignment protocol. On average, 70% (range 76.6–50.6%) of the sequences of all annotated reads were mapped and 85% (range 90.4–76.7%) of miRBase genes were detected.

Of the mapped reads, on average 11% (range 12.2–10.8%) had perfect match to the aligned genes, 54% (range 54.5–55.2%) one mismatch, 23% and (range 21.7–24.7%) two mismatches. Mapping to Ensemble mouse database (GRCm38) yielded mapping to 10.5% (10–11%) of all annotated database sequences on average across libraries. Preference was given to miRBase, so the database which was not mapped to miRBase is mapped to this. Of them, 55.6% (range 55.6–37.3%) exhibited perfect match to the reference sequences, 39.6% (range 39.6–51.5%) with one mismatch, and 8.3 (8.3–11.2%) two mismatches. These alignments yielded an average of 2.06% aligned reads of the total number of reads (with a minimum of 0.2% and a maximum of 3.16%). Annotated samples were grouped by both precursor and mature sequence identity. Overall, a top 44 mature miRs that exhibited count of at least 30 per million reads in at least one sample were analyzed for differential expression between the different experimental conditions. For fold change analysis the above identified miRs of different groups were normalized to control group and that were 1.5 up-regulated or 0.5 fold down-regulated were identified as uniquely regulated miRs.

The wide screening of the brain RNA for the expression of 44 miRs demonstrated that the cluster of the highest expression contained miRs-99a, let7g and 9, that the cluster of medium expression included miRs-26a and let-7f, and that other miRs were of quite low or very low expression. The miR-21 and miR-434 were observed twofold up-regulated and let-7a-1 0.5 fold down-regulated. As shown in Figure 5A, all types of treatment (LPS, LPS + α7(1–208)-specific antibody or nicotine) influenced the level of many of them. MiR-99a was obviously up-regulated by both nicotine and LPS and the effect of LPS was withdrawn by the antibody. In contrast, miR-let7g was down-regulated by LPS and, less, nicotine but the effect of LPS was again withdrawn by the antibody. MiR-9 was up-regulated by nicotine and much less affected by the LPS; however, again, the antibody effect was opposite to that of LPS. MiRs-26a and let-7f were down-regulated in all groups of treated mice; the antibody obviously aggravated the LPS effect for miR-26a. Among other miRs, of considerable interest are miR-21a and miR-434: both of them were up-regulated in all treated mice, mostly by LPS, and the antibody prevented this effect more or less efficiently. In whole, the antibody obviously attenuated the LPS effect in 16 miRs tested and aggravated its effect in six miRs. The effects of nicotine and LPS were of similar direction for six miRs (miR-26, let-7f, let-7c, miR-30, miR-21a and miR-434) and showed an opposite impact for other four miRs (miR-9, let-7j, miR-218 and miR-125).

After miRNA differential expression analysis, we performed KEGG pathways analysis of differentially regulated miRNA of each group exposed to either LPS or LPS and Ab α7 or nicotine (Figure 5B). After removing redundant terms, our findings pointed that all pathways involved in LPS exposure were included in LPS and Ab α7 exposure group. In addition, this group was also associated with Notch signaling, apoptosis, mRNA surveillance, bacterial invasion and calcium signaling pathways. Similarly, nicotine group included all pathways involved in LPS inflammation; in addition it was associated

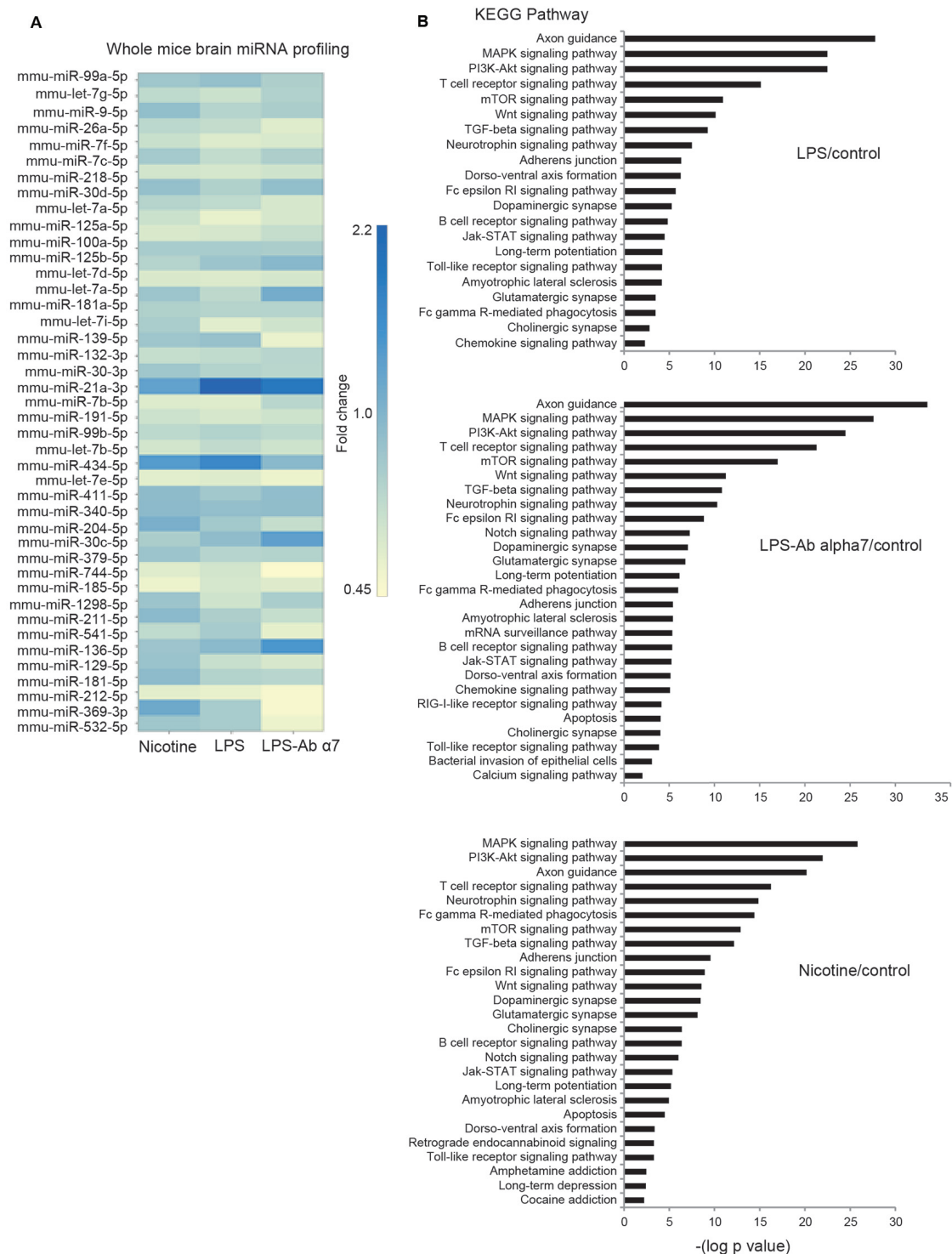


FIGURE 5 | (A) Fold changes in the levels of 44 differentially expressed miRs in the whole brain preparations of mice treated with LPS, $\alpha 7(1-208)$ -specific antibody + LPS or nicotine (1 month) compared to untreated mice (Control), **(B)** KEGG pathway analysis of predicted signaling pathways involved.

with addiction pathways like Cocaine, Amphetamine, Retrograde endocannabinoid signaling, apoptosis and Notch signaling. Common KEGG pathways found in all treatment groups are

either neuronal or inflammatory pathways which included axon guidance, MAPK signaling pathway, PI3K-Akt signaling pathway, T cell receptor signaling pathway, Neurotrophin

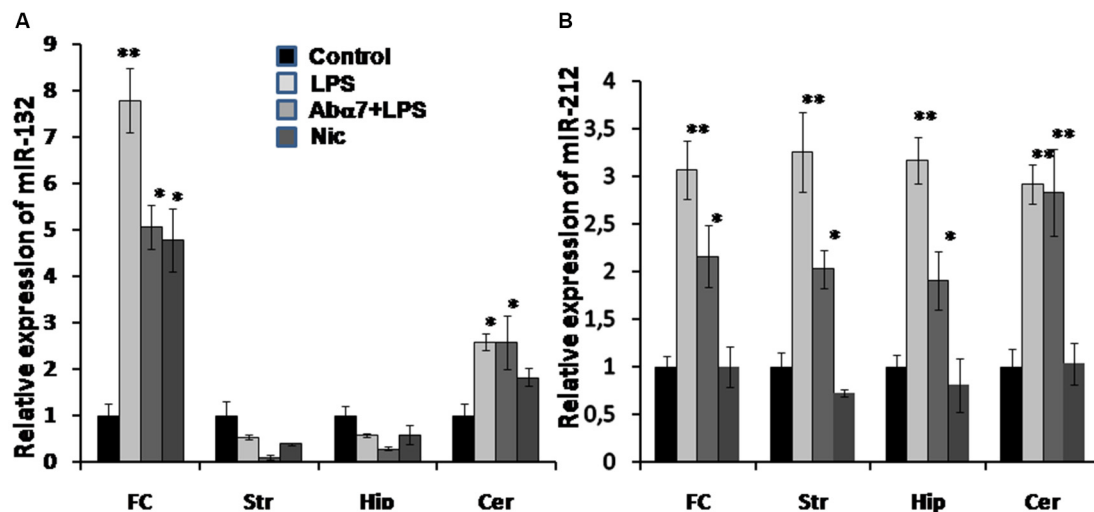


FIGURE 6 | Transcript levels of miR-132 (A) and miR-212 (B) in various brain regions of mice treated with LPS, $\alpha 7(1-208)$ -specific antibody + LPS or nicotine (3 days) compared to untreated mice. Designations are similar to those in Figures 1–5. $N = 5-8/\text{group}$. * $p < 0.05$; ** $p < 0.005$ compared to Control.

signaling pathway, mTOR signaling pathway, TGF-beta signaling pathway, Wnt signaling pathway, Fc gamma R-mediated phagocytosis, Adherence junction, Glutamatergic synapse, Long-term potentiation, Dopaminergic synapse, Amyotrophic lateral sclerosis (ALS), Fc epsilon RI signaling pathway, Dorso-ventral axis formation, Cholinergic synapse, B cell receptor signaling pathway, Jak-STAT signaling pathway, Toll-like receptor signaling pathway, chemokine signaling pathway.

qRT PCR Analysis of miRNA-132/212 in Different Regions of the Brain

To further understand the down-regulation in expression of the cholinergic $\alpha 7$ nAChR (global) and AChE-S (brain region specific) genes, we performed qRT PCR analysis for quantifying the expression of AChE-S targeting miRs: miR-132 and its co-clustered miR-212 in the above mentioned four brain regions. We observed significant LPS-induced increases in the expression levels of miR-212 in all of the tested brain regions, whereas miR-132 showed region-specific (frontal cortex and cerebellum) increases in its expression, correlating to AChE-S expression (Figures 3A,B vs. Figure 6). The antibody tended to cause decreases in miR-132 expression that was up-regulated by LPS in the frontal cortex, hippocampus and striatum. In comparison, the antibody treatment clearly prevented LPS-induced miR-212 up-regulation in all brain regions except cerebellum (Figure 6B). Nicotine (3 days) failed to significantly affect either miR-132 or miR-212 expression.

LPS and $\alpha 7(1-208)$ -Specific Antibodies Stimulate IL-6 Production by U373 Cells through a Similar Signaling Pathway

Previously we demonstrated that $\alpha 7(1-208)$ -specific antibodies and even more, $\alpha 7(179-190)$ -specific antibodies stimulated

IL-6 production in U373 cells via a p38-dependent pathway (Kalashnyk et al., 2014). To test if similar or different mechanisms are involved in LPS- or antibody-stimulated IL-6 production, we tested the effect of various kinase inhibitors on these consequences. As shown in Figure 7A, the antibody stimulated much weaker IL-6 production compared to LPS in U373 cells; however, both LPS-stimulated and antibody-stimulated IL-6 levels were significantly decreased in the presence of p38 and Src kinase inhibitors, suggesting the involvement of a similar Src/p38-dependent signaling pathway.

To study if internalized $\alpha 7$ -specific antibodies can bind mitochondria, we allowed their internalization by U373 cells for 100 min, followed by MitoTracker Green staining. Confocal microscopy showed no overlapping staining for the antibody and MitoTracker (Figure 7B); therefore, the internalized antibody seemed not to bind mitochondria.

DISCUSSION

The influence of $\alpha 7$ nAChR signaling on pro-inflammatory cytokines production is well documented (de Jonge and Ulloa, 2007; Kalashnyk et al., 2014). Our data support, deepen and extend these findings, showing that inflammation regulates $\alpha 7$ nAChR and AChE-S expression and changes miRNA profiles in the brain. Intraperitoneal LPS injections resulted in down-regulation of brain $\alpha 7$ nAChR and AChE-S RNAs and protein levels. AChE down-regulation was accompanied by up-regulation of its targeting miRNA-132 (Shaked et al., 2009; Shaltiel et al., 2013) in the frontal cortex and cerebellum of LPS-treated mice. This region-specific inter-related regulation of miRNA-132/AChE is compatible with the involvement of the cluster harboring miRNA-132/212 in the resolution of inflammation (Nahid et al., 2011; Rao et al., 2015). The

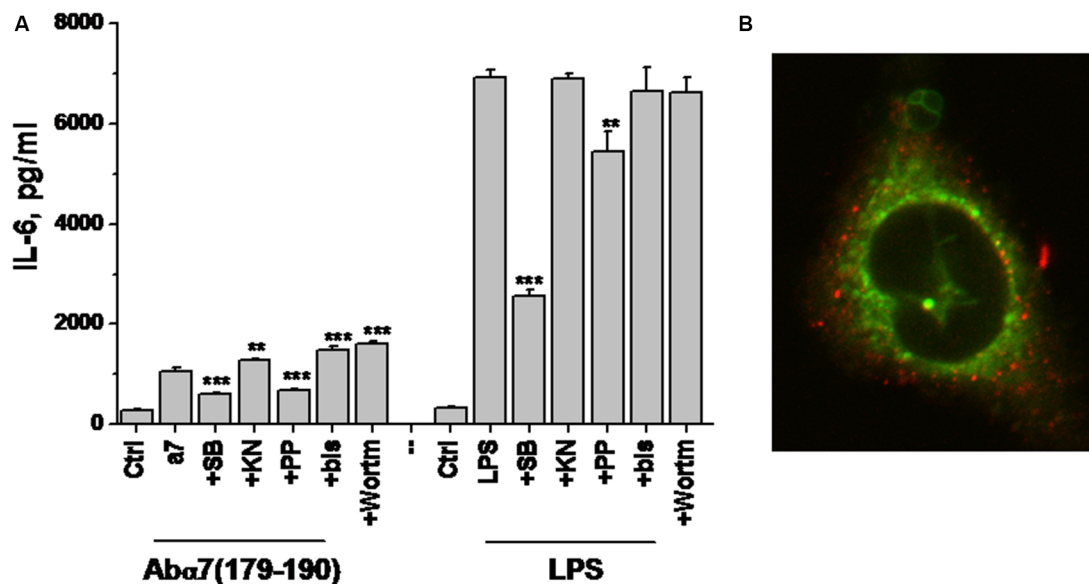


FIGURE 7 | IL-6 production by U373 cells stimulated with either $\alpha 7(179-190)$ -specific antibody or LPS in the presence or absence of various kinase inhibitors (A) and confocal image of U373 cell with internalized $\alpha 7$ -specific antibody (red) additionally stained with MitoTracker (green; B). SB—SB202190 (p38 inhibitor), KN—KN62 (CaMKII inhibitor), PP—PP1 (Src kinase inhibitor), bis—bisindolylmaleimide (protein kinase C inhibitor), Wortm—Wortmaninn (phosphatidylinositol-3-kinase inhibitor). ** $p < 0.005$; * $p < 0.0005$ compared to the effect of LPS or $\alpha 7$ -specific antibody alone.**

general up-regulation of miRNA-212 in all studied brain areas and its significant inhibition by the $\alpha 7$ -specific antibody in the frontal cortex, striatum and hippocampus suggests its specific involvement in inflammation-related mechanisms, different from those regulated by miRNA-132. In general, this data indicates that the LPS-induced inflammatory reaction also stimulated the anti-inflammatory cholinergic pathway by leading to consequent increases in ACh levels due to down-regulated AChE expression and activity. However, inhibiting the expression of $\alpha 7$ nAChRs (which presumably mediate the anti-inflammatory effect of ACh) makes inefficient this LPS-stimulated anti-inflammatory response.

Down-regulation of $\alpha 7$ nAChRs was accompanied by the increase of $\alpha 3\beta 4$ nAChRs, similarly to what we observed in $\alpha 7^{-/-}$ mice or in mice chronically treated with LPS (Lykhmus et al., 2011, 2015). This means that $\alpha 7$ to $\alpha 3\beta 4$ nAChRs substitution is an established mechanism, which could possibly be due to the chromosomal arrangement of nAChR subunit genes; and that a rather short LPS influence (3 days) is sufficient to stimulate this gene expression exchange. The antibody additionally decreased $\alpha 4$ and $\beta 2$ protein in the brain, possibly due to the cross-reactivity of $\alpha 7(1-208)$ -specific antibodies with the homologous $\alpha 4$ subunit, resulting in $\alpha 4\beta 2$ receptors internalization and degradation. Nicotine treatment did not cause significant changes in the nAChR or AChE expression but up-regulated $\alpha 4$, $\alpha 7$ and $\beta 2$ proteins in the whole brain that is in accordance with the suggested chaperon-like activity of nicotine (Sallette et al., 2005). We conclude that LPS and $\alpha 7(1-208)$ -specific antibodies manipulate the molecular components of the brain's cholinergic anti-inflammatory pathway.

Similarly to the chronic LPS treatment (Lykhmus et al., 2015), short-term LPS exposure decreased the level of mitochondrial $\alpha 7$ nAChRs and made the brain mitochondria more sensitive to Ca^{2+} . The $\alpha 7$ -specific antibody prevented the additional cyt *c* release from mitochondria and, therefore, supported their resistance to apoptogenic influence. Since $\alpha 7(1-208)$ -specific antibodies attenuated Ca^{2+} -stimulated cyt *c* release from isolated mitochondria (Gergalova et al., 2014), we hypothesized that the antibody could penetrate the brain cells to directly affect mitochondria, as it was recently suggested for anti-mitochondrial antibodies in patients with *Pemfigus vulgaris* (Chernyavsky et al., 2015). However, in our experiments, no binding of internalized antibody with mitochondria was observed in U373 cells (**Figure 7B**) assuming the involvement of indirect molecular mechanism, possibly, including miRNAs.

Over a decade many miRNAs showed functional involvement in neuro-inflammatory mechanisms (Soreq and Wolf, 2011; Maharshak et al., 2013; Nadorp and Soreq, 2015). Analysis of the present data suggests the involvement of miRNAs in regulating the brain cell survival under the effect of LPS and $\alpha 7$ -specific antibodies. The brain-abundant miRNA-9, which was down-regulated by LPS exposure, inhibits the expression of a proapoptotic Bcl-2L11 found in the outer mitochondrial membrane (Li et al., 2014); its potential pro-apoptotic effect was largely avoided by the antibody. Another brain-abundant miRNA-99 regulates pro-survival Akt/mTOR signaling (Jin et al., 2013); its up-regulation with LPS was expected to decrease the brain cell viability; whereas the $\alpha 7(1-208)$ -specific antibody limited this effect. Likewise, let-7g suppresses the expression of the anti-apoptotic protein Bcl-xL (Wu et al., 2015);

therefore, its down-regulation by LPS might be pro-apoptotic, whereas the antibody treatment inhibited this effect. In whole, LPS exerted anti-survival changes in multiple brain miRNAs, and the $\alpha 7$ -specific antibody could antagonize part of them, providing a tentative explanation for the protective antibody effect in mitochondria found here. According to our previously published data, $\alpha 7$ nAChR is located in the outer mitochondria membrane and its activation stimulates intramitochondrial PI3K/Akt signaling pathway (Gergalova et al., 2012, 2014), that is in good agreement with the present results. The pro-survival antibody effect also explains the data of Kamynina et al. (2013) and Lykhmus et al. (2015), where $\alpha 7$ -specific antibodies exerted neuroprotection in certain models of AD.

In addition to their involvement in inflammation-related processes, both miRNA-132 and miRNA-212 protect neurons against H_2O_2 -mediated cell death, and their loss causes neuronal apoptosis via elevated levels of the cell death-associated proteins PTEN, FOXO3 and P300 that antagonize Akt pro-survival signaling (Wong et al., 2013). Knockdown of miRNA-132 in the hippocampus impairs memory acquisition (Wang et al., 2013), which can be regarded as a marker for cognitive impairment (Xie et al., 2015). The brains of Alzheimer patients demonstrated decreased miR-132/212 level already at stages Braak III and IV of the disease and in a manner related to Tau pathology (Lau et al., 2014). Regarding our data, it may be suggested that neuro-inflammation up-regulates miRNA-132/212 as an anti-inflammatory reaction, which also protects the brain cells from excessive reactive oxygen species toxicity. The $\alpha 7(1-208)$ -specific antibodies weaken this reaction but do not decrease miRNA-132/212 below the control level. Obviously, the final pro- or anti-survival antibody effect is an integral interplay of multiple miRNAs and their targets.

The KEGG pathways analysis allowed deeper understanding of miRNA regulating activity in the brain under the effects of LPS, LPS and antibody or nicotine. According to the probability of engagement, the predicted signaling pathways could be classified into three groups (**Figure 5A**): extremely probable ($-\log p > 20$: Axon guidance, MAPK and PI3K/Akt pathways); highly probable ($20 > -\log p > 10$: TcR, mTOR, Wnt, TGF β and Neurotrophin pathways) and probable ($10 > -\log p > 2$: all other predicted pathways).

The first group includes pathways found under many different receptors; therefore, it is impossible to identify any definite one. However, comparison of $-\log p$ values found for LPS and LPS + Ab treatments allows suggesting that the antibody contributes additional signaling through these pathways. This is in accord with our experimental data on the ability of $\alpha 7$ -specific antibody to stimulate IL-6 production in U373 cells through p38-dependent pathway (**Figure 7A**). The involvement of both MAPK and PI3K/Akt pathways in $\alpha 7$ nAChR signaling is well documented (Parada et al., 2010; Yu et al., 2011; Cucina et al., 2012; Huang et al., 2012; Cui et al., 2013). Previously we reported that signaling of $\alpha 7$ nAChRs expressed in mitochondria can be triggered by $\alpha 7$ -specific antibody (Gergalova et al., 2014), therefore, the antibody could engage PI3K/Akt pathway in the brain.

The second group contains signaling pathways of TcR, TGF β , Wnt and Trk (neurotrophin) receptors, as well as mTOR pathway. Again, the antibody contributes to these pathways compared to LPS alone. The maximal increase of $-\log p$ was observed for TcR (22 vs. 15), mTOR (17 vs. 12) and neurotrophin (10.5 vs. 7.7) signaling pathways. Neurotrophins acting through Trk receptors activate PI3K/Akt and MAPK pathways, and the mTOR functions downstream of PI3K/Akt signaling pathway in response to cytokines and growth factors (LoPiccolo et al., 2008; Longo and Massa, 2013); therefore, their engagement by the antibody may be explained by the antibody effect found in group 1. Neurotrophin signaling is strongly stimulated by nicotine (14 (Nic) vs. 7.5 (LPS) vs. 10.5 (LPS + Ab)) that also assumes the involvement of nicotinic receptors and, possibly, their cross-talk with Trk receptors. T lymphocytes are normally not found in the brain parenchyma but can penetrate there under neuroinflammation when the blood-brain barrier is disrupted (Engelhardt, 2006). In addition, they could be found in the brain capillaries (since the brains had not been perfused before RNA extraction). The antibodies significantly contributed to this pathway; therefore, they could facilitate T lymphocyte migration to or penetration into the brain and subsequent activation resulting in TcR signaling pathway involvement. The Wnt and TGF β signaling pathways are engaged by all three treatments; however, there is no significant difference between nicotine, LPS or LPS + Ab-treated mice.

Among other signaling pathways of interest are the Notch and apoptosis signaling, which are found in nicotine- and LPS + Ab- but not LPS-treated mice and, therefore, relate to nicotinic receptors. The Notch signaling pathway components expressed in the brain were shown to be involved in the pathogenesis of AD (Woo et al., 2009) and, therefore, this pathway may contribute to the memory impairment found in $\alpha 7(1-208)$ -immunized mice (Lykhmus et al., 2015). The involvement of nAChRs in regulating cell survival and apoptosis has already been discussed. The data of KEGG analysis predict the miRNA-mediated regulation of apoptosis pathway by $\alpha 7(1-208)$ -specific antibodies that is in accord with the analysis of molecular targets of miRs 9, 99 and let-7g described above.

LPS notably stimulates pro-inflammatory cytokines production via toll-like receptor type 4 (TLR-4)/CD14 receptor complex, resulting in MAP kinases activation and a nuclear localization of NF- κ B (Kawai and Akira, 2010; Nadorp and Soreq, 2015) also engaging TLR-4 to Src activation (Liu et al., 2012). Here, we show that similar enzymes (Src kinases and p38) are involved in the signal transduction pathway from either LPS or $\alpha 7$ -specific antibodies, suggesting that the $\alpha 7$ nAChR can directly influence TLR-4 signaling. Together with the parallel TLR9/ACh interaction (Nadorp and Soreq, 2015), these findings explain how ACh may attenuate the LPS-induced pro-inflammatory cytokine production through $\alpha 7$ nAChR. Inversely, $\alpha 7$ -specific antibodies stimulate TLR-4 pro-inflammatory signaling, predicting close TLR-4 and $\alpha 7$ nAChR proximity in the plasma membrane. Although LPS failed to prevent binding of the $\alpha 7$ -specific antibodies to U373 cells in flow cytometry (data not shown), one might predict an

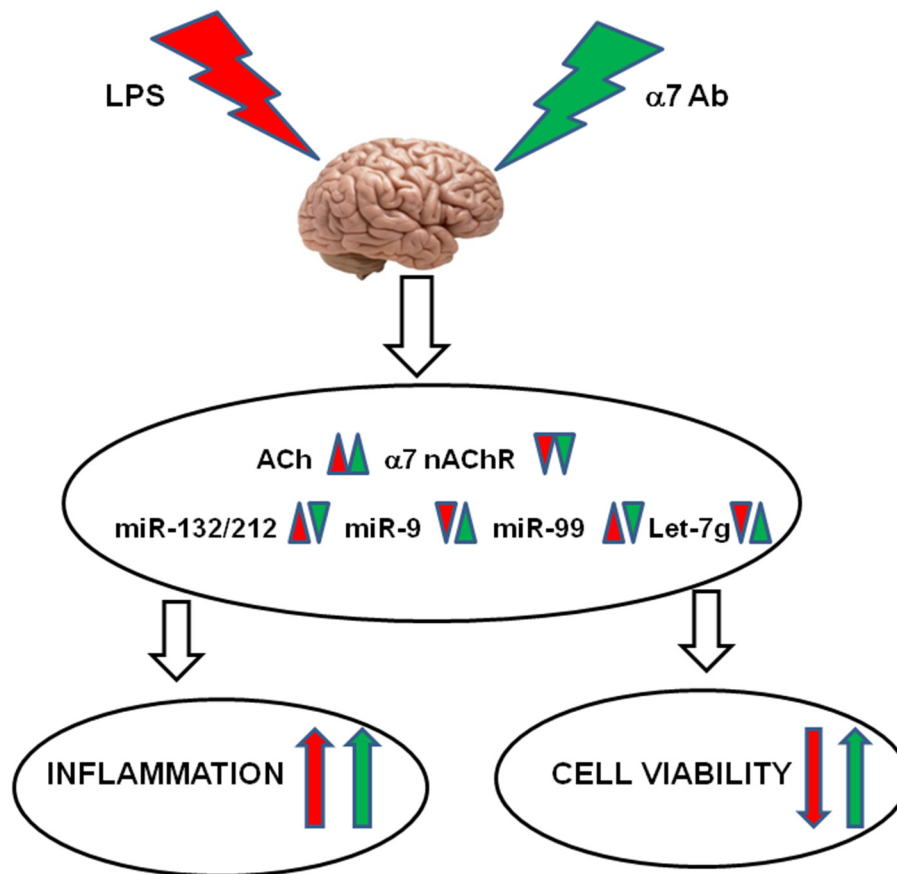


FIGURE 8 | Schematic diagram demonstrating the effects of LPS and $\alpha 7$ (1–208)-specific antibodies ($\alpha 7$ Ab) in the brain. LPS down-regulates AChR expression resulting in acetylcholine increase, down-regulates $\alpha 7$ nAChR expression and changes the levels of miR-132/212, miR-9, miR-99 and let-7g. The $\alpha 7$ Ab further decrease AChE and $\alpha 7$ nAChRs but antagonize LPS effects on miRNAs. As a result, the $\alpha 7$ Ab aggravates the LPS-induced inflammation but may support the brain cell viability.

intersection of $\alpha 7$ nAChR signaling with TLR-4 at the level of adaptor proteins or Src-kinases, i.e., at the very upstream, plasma membrane-proximal stage.

Taken together, our current findings, summarized in **Figure 8**, demonstrate that:

1. LPS-induced inflammation stimulates the ACh-mediated and miRNA-regulated anti-inflammatory pathway in the brain; however, down-regulation of the $\alpha 7$ nAChRs makes this pathway ineffective;
2. Inflammation dampens the mitochondrial cholinergic anti-apoptotic pathway and stimulates miRNAs assumed to decrease the brain cells viability;
3. The $\alpha 7$ -specific antibody aggravates LPS-induced inflammation by preventing the expression of anti-inflammatory miR-212 and stimulates the LPS-like signaling by itself;
4. The $\alpha 7$ -specific antibody dampens the excessive up-regulation of pro-apoptotic miRNAs upon inflammation and maintains mitochondrial integrity that may support the brain cells viability.

This data support the idea that excessive inflammation is an important pathogenic factor stimulating neurodegenerative processes. In this context, $\alpha 7$ nAChR-specific antibodies may play a dual role: potentiating a certain level of inflammation but preventing its neurodegenerative consequences.

AUTHOR CONTRIBUTIONS

MS, SK, and HS: substantial contributions to the conception and design of the work; OL, NM, LK, OK, GG, and KU: the acquisition, analysis, and interpretation of data for the work; MS, NM, and HS: drafting the work; OL, LK, OK, GG, KU, and SK: revising it critically for important intellectual content; OL, NM, LK, OK, GG, KU, SK, HS, and MS: final approval of the version to be published. Agreement to be accountable for all aspects of the work in ensuring that questions related to the accuracy or integrity of any part of the work are appropriately investigated and resolved (OL, NM, LK, OK, GG, KU, SK, HS, and MS).

FUNDING

Support of this study by the European Research Council under the European Union's Seventh Framework Programme (FP7/2007–2013)/ERC Advanced Award 321501 and the Israel Science Foundation grant no.817/13 (to HS) is acknowledged. NM was a recipient of post-doctoral

fellowships from the ELSC Brain Center and The Israeli Government.

ACKNOWLEDGMENTS

We are grateful to Dr S. Karakhim for the help in confocal microscopy studies.

REFERENCES

- Arbel, Y., Shenhar-Tsarfaty, S., Waikopf, N., Finkelstein, A., Halkin, A., Revivo, M., et al. (2014). Copyright and license information decline in serum cholinesterase activities predicts 2-year major adverse cardiac events. *Mol. Med.* 20, 38–45. doi: 10.2119/molmed.2013.00139
- Báez-Pagán, C. A., Delgado-Vélez, M., and Lasalde-Dominicci, J. A. (2015). Activation of the macrophage $\alpha 7$ nicotinic acetylcholine receptor and control of inflammation. *J. Neuroimmune Pharmacol.* 10, 468–476. doi: 10.1007/s11481-015-9601-5
- Borovikova, L. V., Ivanova, S., Zhang, M., Yang, H., Botchkina, G. I., Watkins, L. R., et al. (2000). Vagus nerve stimulation attenuates the systemic inflammatory response to endotoxin. *Nature* 405, 458–462. doi: 10.1038/35013070
- Chen, C. Z., Li, L., Lodish, F. H., and Bartel, D. P. (2004). MicroRNAs modulate hematopoietic lineage differentiation. *Science* 203, 83–86. doi: 10.1126/science.1091903
- Chernyavsky, A., Chen, Y., Wang, P. H., and Grando, S. A. (2015). Pemphigus vulgaris antibodies target the mitochondrial nicotinic acetylcholine receptors that protect keratinocytes from apoptosis. *Int. Immunopharmacol.* 29, 76–80. doi: 10.1016/j.intimp.2015.04.046
- Chung, Y. C., Ko, H. W., Bok, E., Park, E. S., Huh, S. H., Nam, J. H., et al. (2010). The role of neuroinflammation on the pathogenesis of Parkinson's disease. *BMB Rep.* 43, 225–232. doi: 10.5483/BMBRep.2010.43.4.225
- Cucina, A., Dinicola, S., Coluccia, P., Proietti, S., D'Anselmi, F., Pasqualato, A., et al. (2012). Nicotine stimulates proliferation and inhibits apoptosis in colon cancer cell lines through activation of survival pathways. *J. Surg. Res.* 178, 233–241. doi: 10.1016/j.jss.2011.12.029
- Cui, W., Hu, S., Chan, H. H., Luo, J., Li, W., Mak, S., et al. (2013). Bis(12)-huprydone, a novel acetylcholinesterase inhibitor, protects against glutamate-induced neuronal excitotoxicity via activating $\alpha 7$ nicotinic acetylcholine receptor/phosphoinositide 3-kinase/Akt cascade. *Chem. Biol. Interact.* 203, 365–370. doi: 10.1016/j.cbi.2012.10.003
- de Jonge, W. J., and Ulloa, L. (2007). The $\alpha 7$ nicotinic acetylcholine receptor as a pharmacological target for inflammation. *Br. J. Pharmacol.* 151, 915–929. doi: 10.1038/sj.bjp.0707264
- Dziewczapolski, G., Glogowski, C. M., Masliah, E., and Heinemann, S. F. (2009). Deletion of the $\alpha 7$ nicotinic acetylcholine receptor gene improves cognitive deficits and synaptic pathology in a mouse model of Alzheimer's disease. *J. Neurosci.* 29, 8805–8815. doi: 10.1523/JNEUROSCI.6159-08.2009
- Egea, J., Buendia, I., Parada, E., Navarro, E., León, R., and Lopez, M. G. (2015). Anti-inflammatory role of microglial $\alpha 7$ nAChRs and its role in neuroprotection. *Biochem. Pharmacol.* 97, 463–472. doi: 10.1016/j.bcp.2015.07.032
- Ellman, G. L., Courtney, K. D., Andres, V. Jr., and Feather-Stone, R. M. (1961). A new and rapid colorimetric determination of acetylcholinesterase activity. *Biochem. Pharmacol.* 7, 88–95. doi: 10.1016/0006-2952(61)90145-9
- Engelhardt, B. (2006). Molecular mechanisms involved in T cell migration across the blood-brain barrier. *J. Neural Transm. (Vienna)* 113, 477–485. doi: 10.1007/s00702-005-0409-y
- Gergalova, G., Lykhmus, O., Kalashnyk, O., Koval, L. M., Chernyshov, V. O., Kryukova, E. A., et al. (2012). Mitochondria express $\alpha 7$ nicotinic acetylcholine receptors to regulate Ca^{2+} accumulation and cytochrome c release: study on isolated mitochondria. *PLoS One* 7:e31361. doi: 10.1364/oe.15.010562
- Gergalova, G., Lykhmus, O., Komisarenko, S., and Skok, M. (2014). $\alpha 7$ Nicotinic acetylcholine receptors control cytochrome c release from isolated mitochondria through kinase-mediated pathways. *Int. J. Biochem. Cell Biol.* 49, 26–31. doi: 10.1016/j.biocel.2014.01.001
- Gouras, G. K., Almeida, C. G., and Takahashi, R. H. (2005). Intraneuronal A β accumulation and origin of plaques in Alzheimer's disease. *Neurobiol. Aging* 26, 1235–1244. doi: 10.1016/j.neurobiolaging.2005.05.022
- Heppner, F. L., Ransohoff, R. M., and Becher, B. (2015). Immune attack: the role of inflammation in Alzheimer disease. *Nat. Rev. Neurosci.* 16, 358–372. doi: 10.1038/nrn3880
- Huang, X., Cheng, Z., Su, Q., Zhu, X., Wang, Q., Chen, R., et al. (2012). Neuroprotection by nicotine against colchicine-induced apoptosis is mediated by PI3-kinase-Akt pathways. *Int. J. Neurosci.* 122, 324–332. doi: 10.3109/00207454.2012.657377
- Ikonomic, M. D., Wecker, L., Abrahamson, E. E., Wu, J., Counts, S. E., Ginsberg, S. D., et al. (2009). Cortical $\alpha 7$ nicotinic acetylcholine receptor and β -amyloid levels in early Alzheimer disease. *Arch. Neurol.* 66, 646–651. doi: 10.1001/archneurol.2009.46
- Ji, H., Rabbi, M. F., Labis, B., Pavlov, V. A., Tracey, K. J., and Ghia, J. E. (2014). Central cholinergic activation of a vagus nerve-to-spleen circuit alleviates experimental colitis. *Mucosal Immunol.* 7, 335–347. doi: 10.1038/mi.2013.52
- Jin, Y., Tymen, S. D., Chen, D., Fang, Z. J., Zhao, Y., Dragas, D., et al. (2013). MicroRNA-99 family targets AKT/mTOR signaling pathway in dermal wound healing. *PLoS One* 8:e64434. doi: 10.1371/journal.pone.0064434
- Kalashnyk, O. M., Lykhmus, O., Oliynyk, O. A., Komisarenko, S. V., and Skok, M. V. (2014). $\alpha 7$ nAChR-specific antibodies stimulate pro-inflammatory reaction in human astrocytes through p38-dependent pathway. *Int. Immunopharmacol.* 23, 475–479. doi: 10.1016/j.intimp.2014.09.022
- Kamynina, A. V., Holmström, K. M., Koroed, D. O., Volpina, O. M., and Abramov, A. Y. (2013). Acetylcholine and antibodies against the acetylcholine receptor protect neurons and astrocytes against β -amyloid toxicity. *Int. J. Biochem. Cell Biol.* 45, 899–907. doi: 10.1016/j.biocel.2013.01.011
- Kawai, T., and Akira, S. (2010). The role of pattern-recognition receptors in innate immunity: update on toll-like receptors. *Nat. Immunol.* 11, 373–384. doi: 10.1038/ni.1863
- Kim, S. H., Kim, Y. K., Jeong, S. J., Haass, C., Kim, Y. H., and Suh, Y. H. (1997). Enhanced release of secreted form of Alzheimer's amyloid precursor protein from PC12 cells by nicotine. *Mol. Pharmacol.* 52, 430–436.
- Koval, O. M., Voitenko, L. P., Skok, M. V., Lykhmus, E. Y., Tsetlin, V. I., Zhmak, M. N., et al. (2004). The β -subunit composition of nicotinic acetylcholine receptors in the neurons of the guinea pig inferior mesenteric ganglion. *Neurosci. Lett.* 365, 143–146. doi: 10.1016/j.neulet.2004.04.071
- Lau, P., Frigerio, C. S., and De Strooper, B. (2014). Variance in the identification of microRNAs deregulated in Alzheimer's disease and possible role of lincRNAs in the pathology: the need of larger datasets. *Ageing Res. Rev.* 17, 43–53. doi: 10.1016/j.arr.2014.02.006
- Li, Y., Peng, T., Li, L., Wang, X., Duan, R., Gao, H., et al. (2014). MicroRNA-9 regulates neuronal apoptosis in methylmalonic acidemia via targeting BCL2L1. *Int. J. Dev. Neurosci.* 36, 19–24. doi: 10.1016/j.jidvneu.2014.04.005
- Liu, A., Gong, P., Hyun, S. W., Wang, K. Z., Cates, E. A., Perkins, D., et al. (2012). TRAF6 protein couples Toll-like receptor 4 signaling to Src family kinase activation and opening of paracellular pathway in human lung microvascular endothelia. *J. Biol. Chem.* 287, 16132–16145. doi: 10.1074/jbc.M111.310102
- Longo, F. M., and Massa, S. M. (2013). Small-molecule modulation of neurotrophin receptors: a strategy for the treatment of neurological disease. *Nat. Rev. Drug Discov.* 12, 507–525. doi: 10.1038/nrd4024
- LoPiccolo, J., Blumenthal, G. M., Bernstein, W. B., and Dennis, P. A. (2008). Targeting the PI3K/Akt/mTOR pathway: effective combinations and clinical considerations. *Drug Resist. Updat.* 11, 32–50. doi: 10.1016/j.drug.2007.11.003

- Lykhmus, O., Koval, L. M., Skok, M. V., Zouridakis, M., Zisimopoulou, P., Tzartos, S. J., et al. (2011). Antibodies against extracellular domains of $\alpha 4$ and $\alpha 7$ subunits alter the levels of nicotinic receptors in the mouse brain and affect memory: possible relevance to Alzheimer pathology. *J. Alzheimers Dis.* 24, 693–704. doi: 10.3233/JAD-2011-101842
- Lykhmus, O., Voytenko, L., Koval, L., Mykhalskiy, S., Kholin, V., Peschana, K., et al. (2015). $\alpha 7$ Nicotinic acetylcholine receptor-specific antibody induces inflammation and amyloid $\beta 42$ accumulation in the mouse brain to impair memory. *PLoS One* 10:e0122706. doi: 10.1371/journal.pone.0122706
- Maharshak, N., Shenhar-Tsarfaty, S., Aroyo, N., Orpaz, N., Guberman, I., Canaani, J., et al. (2013). MicroRNA-132 modulates cholinergic signaling and inflammation in human inflammatory bowel disease. *Inflamm. Bowel Dis.* 19, 1346–1353. doi: 10.1097/MIB.0b013e318281f47d
- Nadorp, B., and Soreq, H. (2015). Gut feeling: MicroRNA discriminators of the intestinal TLR9-cholinergic links. *Int. Immunopharmacol.* 9, 8–14. doi: 10.1016/j.intimp.2015.04.058
- Nahid, M. A., Satoh, M., and Chan, E. K. (2011). MicroRNA in TLR signaling and endotoxin tolerance. *Cell Mol. Immunol.* 8, 388–403. doi: 10.1038/cmi.2011.26
- Parada, E., Egea, J., Romero, A., del Barrio, L., García, A. G., and López, M. G. (2010). Poststress treatment with PNU282987 can rescue SH-SY5Y cells undergoing apoptosis via $\alpha 7$ nicotinic receptors linked to a Jak2/Akt/HO-1 signaling pathway. *Free Radic. Biol. Med.* 49, 1815–1821. doi: 10.1016/j.freeradbiomed.2010.09.017
- Parri, H. R., and Dineley, K. T. (2010). Nicotinic acetylcholine receptor interaction with β -amyloid: molecular, cellular and physiological consequences. *Curr. Alzheimer Res.* 7, 27–39. doi: 10.2174/156720510790274464
- Qi, X. L., Nordberg, A., Xiu, J., and Guan, Z. Z. (2007). The consequences of reducing expression of the $\alpha 7$ nicotinic receptor by RNA interference and of stimulating its activity with an $\alpha 7$ agonist in SH-SY5Y cells indicate that this receptor plays a neuroprotective role in connection with the pathogenesis of Alzheimer's disease. *Neurochem. Int.* 51, 377–383. doi: 10.1016/j.neuint.2007.04.002
- Rao, R., Nagarkatti, P., and Nagarkatti, M. (2015). Role of miRNA in the regulation of inflammatory genes in staphylococcal enterotoxin B-induced acute inflammatory lung injury and mortality. *Toxicol. Sci.* 144, 284–297. doi: 10.1093/toxsci/kfu315
- Sallette, J., Pons, S., Devillers-Thiery, A., Soudant, M., Prado de Carvalho, L., Changeux, J. P., et al. (2005). Nicotine upregulates its own receptors through enhanced intracellular maturation. *Neuron* 46, 595–607. doi: 10.1016/j.neuron.2005.03.029
- Shaked, I., Meerson, A., Wolf, Y., Avni, R., Greenberg, D., Gilboa-Geffen, A., et al. (2009). MicroRNA-132 potentiates cholinergic anti-inflammatory signaling by targeting acetylcholinesterase. *Immunity* 31, 965–973. doi: 10.1016/j.immuni.2009.09.019
- Shaltiel, G., Hanan, M., Wolf, Y., Barbash, S., Kovalev, E., Shoham, S., et al. (2013). Hippocampal microRNA-132 mediates stress-inducible cognitive deficits through its acetylcholinesterase target. *Brain Struct. Funct.* 218, 59–72. doi: 10.1007/s00429-011-0376-z
- Skok, M. V., Voitenko, L. P., Voitenko, S. V., Lykhmus, E. Y., Kalashnik, E. N., Litvin, T., et al. (1999). Study of α subunit composition of nicotinic acetylcholine receptor in the neurons of autonomic ganglia of the rat with subunit-specific anti- $\alpha(181-192)$ peptide antibodies. *Neuroscience* 93, 1437–1446. doi: 10.1016/s0306-4522(99)00160-8
- Soreq, H. (2015). Checks and balances on cholinergic signaling in brain and body function. *Trends Neurosci.* 38, 448–458. doi: 10.1016/j.tins.2015.05.007
- Soreq, H., and Seidman, S. (2001). Acetylcholinesterase--new roles for an old actor. *Nat. Rev. Neurosci.* 2, 294–302. doi: 10.1038/35067589
- Soreq, H., and Wolf, Y. (2011). NeurimmiRs: microRNAs in the neuroimmune interface. *Trends Mol. Med.* 17, 548–555. doi: 10.1016/j.molmed.2011.06.009
- Terrando, N., Yang, T., Ryu, J. K., Newton, P. T., Monaco, C., Feldmann, M., et al. (2015). Stimulation of the $\alpha 7$ nicotinic acetylcholine receptor protects against neuroinflammation after tibia fracture and endotoxemia in mice. *Mol. Med.* 20, 667–675. doi: 10.2119/molmed.2014.00143
- Thomsen, M. S., and Mikkelsen, J. D. (2012). The $\alpha 7$ nicotinic acetylcholine receptor ligands methyllycaconitine, NS6740 and GTS-21 reduce lipopolysaccharide-induced TNF- α release from microglia. *J. Neuroimmunol.* 251, 65–72. doi: 10.1016/j.jneuroim.2012.07.006
- Truong, L. D., Trostel, J., and Garcia, G. E. (2015). Absence of nicotinic acetylcholine receptor $\alpha 7$ subunit amplifies inflammation and accelerates onset of fibrosis: an inflammatory kidney model. *FASEB J.* 29, 3558–3570. doi: 10.1096/fj.14-262493
- Tyagi, E., Agrawal, R., Nath, C., and Shukla, R. (2010). Cholinergic protection via $\alpha 7$ nicotinic acetylcholine receptors and PI3K-Akt pathway in LPS-induced neuroinflammation. *Neurochem. Int.* 56, 135–142. doi: 10.1016/j.neuint.2009.09.011
- Wang, H. Y., Lee, D. H., D'Andrea, M. R., Peterson, P. A., Shank, R. P., and Reitz, A. B. (2000). β -Amyloid 1–42 binds to $\alpha 7$ nicotinic acetylcholine receptor with high affinity. Implications for Alzheimer's disease pathology. *J. Biol. Chem.* 275, 5626–5632. doi: 10.1074/jbc.275.8.5626
- Wang, R. Y., Phang, R. Z., Hsu, P. H., Wang, W. H., Huang, H. T., and Liu, I. Y. (2013). *In vivo* knockdown of hippocampal miR-132 expression impairs memory acquisition of trace fear conditioning. *Hippocampus* 23, 625–633. doi: 10.1002/hipo.22123
- Wee Yong, V. (2010). Inflammation in neurological disorders: a help or a hindrance? *Neuroscientist* 16, 408–420. doi: 10.1177/1073858410371379
- Wong, H. K., Veremeyko, T., Patel, N., Lemere, C. A., Walsh, D. M., Esau, C., et al. (2013). De-repression of FOXO3a death axis by microRNA-132 and -212 causes neuronal apoptosis in Alzheimer's disease. *Hum. Mol. Genet.* 22, 3077–3092. doi: 10.1093/hmg/ddt164
- Woo, H.-N., Park, J.-S., Gwon, A.-R., Arumugam, T. V., and Jo, D.-G. (2009). Alzheimer's disease and Notch signaling. *Biochem. Biophys. Res. Commun.* 390, 1093–1097. doi: 10.1016/j.bbrc.2009.10.093
- Wu, L., Wang, Q., Yao, J., Jiang, H., Xiao, C., and Wu, F. (2015). MicroRNA let-7g and let-7i inhibit hepatoma cell growth concurrently via downregulation of the anti-apoptotic protein B-cell lymphoma-extra large. *Oncol. Lett.* 9, 213–218. doi: 10.3892/ol.2014.2706
- Xie, B., Zhou, H., Zhang, R., Song, M., Yu, L., Wang, L., et al. (2015). Serum mir-206 and mir-132 as potential circulating biomarkers for mild cognitive impairment. *J. Alzheimers Dis.* 45, 721–731. doi: 10.3233/JAD-142847
- Yu, W., Mechawar, N., Krantic, S., and Quirion, R. (2011). $\alpha 7$ Nicotinic receptor activation reduces β -amyloid-induced apoptosis by inhibiting caspase-independent death through phosphatidylinositol 3-kinase signaling. *J. Neurochem.* 119, 848–858. doi: 10.1111/j.1471-4159.2011.07466.x

Conflict of Interest Statement: The authors declare that the research was conducted in the absence of any commercial or financial relationships that could be construed as a potential conflict of interest.

Copyright © 2016 Lykhmus, Mishra, Koval, Kalashnyk, Gergalova, Uspenska, Komisarenko, Soreq and Skok. This is an open-access article distributed under the terms of the Creative Commons Attribution License (CC BY). The use, distribution and reproduction in other forums is permitted, provided the original author(s) or licensor are credited and that the original publication in this journal is cited, in accordance with accepted academic practice. No use, distribution or reproduction is permitted which does not comply with these terms.

Advantages of publishing in Frontiers



OPEN ACCESS

Articles are free to read,
for greatest visibility



COLLABORATIVE PEER-REVIEW

Designed to be rigorous
– yet also collaborative,
fair and constructive



FAST PUBLICATION

Average 85 days from
submission to publication
(across all journals)



COPYRIGHT TO AUTHORS

No limit to article
distribution and re-use



TRANSPARENT

Editors and reviewers
acknowledged by name
on published articles



SUPPORT

By our Swiss-based
editorial team



IMPACT METRICS

Advanced metrics
track your article's impact



GLOBAL SPREAD

5'100'000+ monthly
article views
and downloads



LOOP RESEARCH NETWORK

Our network
increases readership
for your article

Frontiers

EPFL Innovation Park, Building I • 1015 Lausanne • Switzerland
Tel +41 21 510 17 00 • Fax +41 21 510 17 01 • info@frontiersin.org
www.frontiersin.org

Find us on

